

**DEPARTMENT OF WATER RESOURCES**

DIVISION OF FLOOD MANAGEMENT  
P.O. BOX 219000  
SACRAMENTO, CA 95821-9000



November 24, 2015

Janis Cooke, Ph. D.  
Environmental Scientist  
Central Valley Regional Water Quality Control Board  
11020 Sun Center Drive, Suite 200  
Rancho Cordova, California 95670

Department of Water Resources: Mercury Control Studies for the  
Cache Creek Settling Basin - Report of Findings

Dear Ms. Cooke:

In fulfillment of the requirements of the Delta Mercury Control Program, which identified the Cache Creek Settling Basin (CCSB) as a source of mercury and methylmercury to the Yolo Bypass, the Department of Water Resources (DWR) is submitting this *Report of Findings* on Mercury Control Studies conducted in accordance with your November 10, 2011, letter requiring studies for the CCSB. This Report of Findings includes:

- A description of the long-term environmental benefits and costs of sustaining the CCSB mercury trapping abilities indefinitely,
- An evaluation of the trapping efficiency of the CCSB, and
- An evaluation of potential feasible alternatives for mercury reduction from the Basin (up to and including a 50% reduction from existing loads).

The studies summarized in the *Report of Findings* are the result of cumulative efforts by DWR, the United States Geological Survey (USGS), and the University of California Davis (UCD) since 2009. The USGS and UCD have provided contracted support to DWR for collecting and analyzing flow, sediment, surface-water and soil samples, and developing and performing numeric and physical models associated with the CCSB. These models and data provide the basis for considering benefits and consequences in evaluating potential feasible alternatives for extending the trapping capabilities of the Cache Creek Settling Basin.

The data collected for these studies and the results of the evaluations highlight the complexities associated with mercury methylation and bioaccumulation in an environment with diverse habitat and complex water interactions. The study results demonstrate that habitat, more than any other biogeochemical factor, is the primary driver for these processes. The *Report of Findings* also documents further complexities with regard to multiple stakeholder interest, and the importance of developing multi-benefit solutions that support all of the interests in this area, including providing increased levels of flood protection for the City of Woodland and nearby rural

Janis Cooke, Ph.D.  
November 24, 2015  
Page 2

communities, meeting the flood risk reduction needs and requirements of the United States Army Corps of Engineers and the Central Valley Flood Protection Board by increasing the life-span of the Basin, and complying with Delta Mercury Control Program water quality requirements established for the CCSB.

Consistent with the submittal of this document, DWR is committed to complying with the Delta Mercury Control Program total maximum daily load (TMDL) requirements established for the CCSB within the resource and funding limitations that exist. The studies described in the *Report of Findings* will continue through the remainder of the existing contracts. However, DWR has no current source of long-term funding to implement the large-scale remedies likely required to comply with the Delta Mercury Control Program requirements. Any solution to these long standing, natural and anthropogenic conditions should not be the responsibility of a single resource agency to fund and implement. As evident by the multiple interactions and complexities in this area, any solution must consider far more than simply mercury and methylmercury conditions. Multiple funding sources, provided by appropriate beneficiaries of any proposed solution, will be required to successfully resolve the complex issues of the Cache Creek watershed. The established TMDL for the CCSB cannot be met without an aggressive approach to reduce total mercury loads entering the Cache Creek Settling Basin from the upstream watershed, and significant land-use changes within the Basin, which have significant flood risk reduction implications.

Thank you for considering the data and conclusions presented in the attached *Report of Findings* on the Mercury Control Studies for the Cache Creek Settling Basin. If you have any questions or comments regarding the report, please contact Mr. Kevin Brown at (916) 572.2739 or [kevin.brown@water.ca.gov](mailto:kevin.brown@water.ca.gov).

Sincerely,

  
Mark R. List, CEG, CHG  
Supervising Engineering Geologist  
Acting Flood Maintenance Office Chief  
Division of Flood Management

cc: Colonel Michael Farrell, USACE  
Mr. William Edgar, CVFPB



# **Report of Findings: Mercury Control Studies for the Cache Creek Settling Basin, Yolo County, California**

**Prepared By: Kevin J. Brown, PG; John Nosacka, PE; Joy Nishida**

**California Department of Water Resources, Division of Flood Management, Flood  
Maintenance Office**

**3310 El Camino Ave., Rm. 110, Sacramento, CA**

**Prepared For:**

**Central Valley Regional Water Quality Control Board**

**11020 Sun Center Drive # 200, Rancho Cordova, CA**

**November 24, 2015**

# Report of Findings: Mercury Control Studies for the Cache Creek Settling Basin, Yolo County, CA

## Table of Contents

EXECUTIVE SUMMARY .....	xiv
1 INTRODUCTION.....	1
1.1 History of the Cache Creek Settling Basin.....	1
1.2 Regulatory Requirements .....	5
1.2.1 USACE O&M Manual.....	5
1.2.2 CVRWQCB TMDL .....	7
1.2.2.1 Summary of Deliverables and Schedule.....	8
1.3 Coordination with Stakeholders .....	8
1.4 Current and Proposed Studies and Schedule .....	10
1.4.1 Trapping Efficiency Study (UCD, USGS).....	10
1.4.2 Mercury Load Determination Study (USGS) .....	11
1.4.3 Cache Creek Watershed Study (UCD, USGS).....	11
1.4.4 Mercury Cycling Modeling (Reed Harris, USGS, UCD) .....	12
2 TRAPPING EFFICIENCY STUDY (UCD, USGS).....	13
2.1 Sensitivity Analysis of Trapping Efficiency by HEC-6 Model .....	14
2.2 Phase II Trapping Efficiency Study .....	17
2.2.1 CCHE2D Model Simulation Results .....	19
2.2.1.1 Calibration by 18-22 March 2011 Event at Road 102 .....	19
2.2.1.2 Sediment Transport Simulation Results.....	23
2.3 Basin Modification Simulations.....	25
2.3.1 Alternative A – Baseline Condition .....	25
2.3.2 Alternative B – Weir Raise Condition.....	26
2.3.3 Alternative C – Training Levee Notching Condition .....	26
2.3.4 Alternative D – Weir Raise and Training Levee Notching Condition.....	26
3 MERCURY LOAD DETERMINATION STUDY (USGS).....	27
3.1 Sediment Loading Calculations .....	28
3.1.1 Inflows and Outflows .....	28
3.2 Summary of Within-Basin Surficial Processes.....	31

3.3	Subsurface Properties .....	35
3.4	Constituent Loads .....	39
3.4.1	Suspended Sediment Loads .....	42
3.4.2	Total Mercury Loads .....	42
3.4.3	Methylmercury and Reactive Mercury Loads.....	43
3.5	Trapping Efficiency.....	46
3.5.1	Suspended Sediment .....	46
3.5.2	Total Mercury.....	46
3.5.3	Methylmercury and Reactive Mercury .....	50
3.6	Within-Basin Processes: Habitat, Sediment, Biota, and Water-Quality .....	54
3.6.1	Habitat Mapping .....	54
3.6.2	Sediment .....	54
3.6.2.1	Sediment Total Mercury .....	54
3.6.2.2	Sediment Methylmercury .....	55
3.6.2.3	Sediment Reactive Mercury.....	55
3.6.2.4	Ancillary Sediment Parameters.....	56
3.6.2.5	Sequential Extractions for Mercury Speciation .....	56
3.6.3	Biological Sampling .....	57
3.6.3.1	Mercury in Caged Mosquitofish.....	57
3.6.3.2	Mercury in Wild Mosquitofish .....	58
3.6.3.3	Mercury in Bird Eggs .....	58
3.6.4	Water-Quality Sampling Paired with Fish Cages.....	59
3.6.5	Water-Fish Relationships .....	62
3.7	Subsurface Conditions .....	63
3.7.1	Historical Sedimentation Rates.....	63
3.7.2	Vertical Profiles of Total Mercury and Methylmercury .....	66
3.8	Grain-Size Distribution .....	69
3.9	Discussion of USGS Findings .....	70
3.9.1	Surface Water .....	70
3.9.1.1	Total Mercury Loads .....	70
3.9.1.2	Methylmercury Loads .....	73
3.9.1.3	Comparison of THg and MeHg Loads to Regulatory Allocations .....	74

3.9.1.4	Within-Basin Water Quality .....	74
3.9.2	Sediment .....	74
3.9.2.1	Land Use and Organic Content are Key Drivers of Mercury Speciation .....	75
3.9.2.2	Hydrology is a Key Factor Affecting Reactive Mercury Trends .....	76
3.9.2.3	Methylmercury as the Focus.....	77
3.9.2.4	Controls on Methylmercury Production .....	77
3.9.3	Biota .....	80
3.9.3.1	Mercury Increased with Creek Distance into the Settling Basin.....	80
3.9.3.2	Mercury was Highest in Floodplain Habitats .....	80
3.9.3.3	Mercury Exposure Risk to Fish .....	81
3.9.3.4	Mercury Exposure Risk to Birds .....	81
4	Long-term Environmental Benefits and Costs of Sustaining TrapPING Efficiency.....	82
4.1	Summary of in-Basin Sample Analytical Results and Trends .....	82
4.2	Summary of Possible Management Actions to Increase Trapping Efficiency.....	83
4.3	Environmental Implications .....	87
5	CACHE CREEK WATERSHED STUDY (UCD, USGS) .....	88
5.1	Methodology.....	88
5.2	Results and Discussion .....	89
6	CACHE CREEK FEASIBILITY STUDIES .....	90
6.1	Lower Cache Creek Feasibility Study (USACE) .....	90
6.2	Cache Creek Settling Basin Feasibility Study (CVFPB).....	90
6.3	City of Woodland UFRR Grant.....	92
6.4	CCSB Control Alternatives to Decrease Mercury Loads from the Basin .....	92
6.4.1	Alternatives Constraints.....	93
6.4.2	Descriptions of Alternatives.....	93
6.4.3	Common Elements Among the Alternatives.....	93
6.4.4	No Action.....	95
6.4.5	Modify the Basin per O&M Manual Requirements .....	96
6.4.6	Sediment Stockpile – Modifying Land Use Practices .....	98
6.4.7	Enlarge Basin.....	99
6.4.8	Others.....	103
6.5	Comparison of Alternatives .....	104

7	LONG-TERM FUNDING SOURCES.....	108
8	CONCLUSIONS AND RECOMMENDATIONS.....	109
9	REFERENCES .....	112

## LIST OF TABLES, FIGURES AND APPENDICES

### **TABLES**

Table 2.1 - Grain Size Distributions Applied with Wu and Wang (1999) Roughness Simulations

Table 2.2 – Sediment Trap Efficiency under the Current Bathymetric Condition for Three Scenarios of CCHE2D Parameter Definition

Table 3.1 - Summary of Load Calculations for Suspended Sediment and Total Mercury, Cache Creek Settling Basin, California, Water Years 2010-14

Table 3.2 - Summary of Load Calculations for Total Mercury, Standard Error of the Mean, Cache Creek Settling Basin, California, Water Years 2010-14

Table 3.3 - Summary of Load Calculations for Methylmercury, Cache Creek Settling Basin, California, Water Years 2010-14

Table 3.4 - Summary of Load Calculations for Methylmercury, Standard Error of the Mean, Cache Creek Settling Basin, California, Water Years 2010-14

Table 3.5 - Trap Efficiency Calculations for Total Mercury, Cache Creek Settling Basin, California, Water Years 2010-14

Table 3.6 - Trap Efficiency Standard Error Calculations for Total Mercury, Cache Creek Settling Basin, California, Water Years 2010-14

Table 3.7 - Trap Efficiency Calculations for Methylmercury, Cache Creek Settling Basin, California, Water Years 2010-14

Table 3.8 - Trap Efficiency Standard Error Calculations for Methylmercury, Cache Creek Settling Basin, California, Water Years 2010-14

Table 6.1 - Summary Comparison of Alternatives

Table 6.2 - CCSB Alternatives: Dimensions, Quantities, and Extended Life Expectancy

Table 6.3 - Comparison of CCSB Alternatives

### **FIGURES**

Figure 1 – Site Vicinity Map

Figure 2 – Site Plan

Figure 3 - Comparison Plots of 18-22 March 2011 Simulation

Figure 4 - Comparison Plots of 23-27 March 2011, Validation Simulation

Figure 5 - Upstream Sediment Boundary Condition for all Modeled Sediment Transport Scenarios

Figure A – CCSB Hydrograph – 2010

Figure B – CCSB Hydrograph – 2011

Figure C – CCSB Hydrograph – 2012

Figure D – CCSB Hydrograph – 2013

Figure 6A – Surface Soil Sampling Locations: 2010-2012

Figure 6B – Surface Soil Sampling Locations: 2012-2015

Figure 7 – Fish Cage Locations

Figure 8 – Bird Nest Locations

Figure 9 – Deep Core Locations

Figure 10 – Plot of Particulate Total Mercury TE Estimates

Figure 11 – Plot of Particulate Methylmercury TE Estimates

Figure 12 – Profile for Soil Core 10b

Figure 13 – Plot of Projected Depth of 1937 Basin Horizon

Figure 14 – Vertical Profiles of THg in Soil Cores

Figure 15 – Vertical Profiles of MeHg in Soil Cores

Figure 16 – Summary Plot of Sand, Silt, and Clay Percentages for 20-cm Composite Samples

Figure 17 – Time-Series Plots of Streamflow Data for Yolo Gage

Figure 18 – Plot of %MeHg Versus THg/LOI

Figure 19 - Outline of Cache Creek Watershed

Figure 20 – Proposed Large Basin Expansion Alternative

## **APPENDICES**

Appendix A – UCD TE Reports: 2014 Annual Progress Report, 2015 Annual Progress Report

Appendix B – USGS Report: 2015 Scientific Investigation Report with Appendices 1 through 6



Appendix C – UCD 2015 Final Watershed Report

## LIST OF ACRONYMS

ADCP	Acoustic Doppler Current Profiler
Basin	Cache Creek Settling Basin aka CCSB
Basin Plan	Sacramento River and San Joaquin River Basin Plan
BiOps	Biological Opinions for CVP and SWP (NMFS)
BWFS	Basin Wide Feasibility Study (Sacramento River)
CCHE2D	National Center for Computational Hydroscience and Engineering Flow and Sediment Transport Model
CCSB	Cache Creek Settling Basin
CDM	Camp Dresser McGee
CS	Central Valley Conservation Strategy
Cs-137	Cesium 137
CVFPB	Central Valley Flood Protection Board
CVFPP	Central Valley Flood Protection Plan
CVP	Central Valley Project
CVRWQCB	Central Valley Regional Water Quality Control Board
DMCP	Delta Mercury Control Program
DOC	Dissolved Organic Carbon
DOM	Dissolved Organic Matter –measured as SUVA <sub>254</sub>
dw	dry weight
DWR	Department of Water Resources
EEM	Excitation-Emission Matrix
Fe	Iron
Fe(II) <sub>AE</sub>	Acid-extractable Ferrous Iron
Fe(III) <sub>a</sub>	Amorphous to Poorly-crystalline Ferric Iron
Fe(III) <sub>c</sub>	Crystalline Ferric Iron

Fe <sub>T</sub>	Total Iron
FESWMS	Finite Element Surface Water Modeling Systems (Flow and Sediment Transport Model)
fMeHg	Filtered Methylmercury
fTHg	Filtered Total Mercury
fw	fresh wet-weight
fw MeHg	fresh wet-weight Methylmercury
GCM	Global Climate Change Modeling
GIS	Geographical Information System
GPS	Global Positioning System
GRR	General Reevaluation Report
HgS	Cinnabar
Hg <sub>SE</sub>	Mercury analyzed by sequential extraction
HIX	humic index
LCCFS	Lower Cache Creek Feasibility Study
LOI	Loss on Ignition (measure of organic content)
MeHg	Methylmercury
m-HgS	Meta-cinnabar
nfMeHg	Non-filtered Methylmercury
NMFS	National Marine Fisheries Service
NSE	Nash-Sutcliffe Model Efficiency
O&M	Operations and Maintenance
PDT	Project Development Team
pMeHg	Particulate Methylmercury
pMeHg-g	gravimetric values for pMeHg
POC	Particulate Organic Carbon
pRHg(II)	Particulate Reactive Mercury

pTHg	Particulate Total Mercury
pTHg-g	gravimetric values for pTHg
pwCl <sup>-</sup>	pore-water Chloride
pwDOC	pore-water Dissolved Organic Carbon
pwH <sub>2</sub> S	pore-water Hydrogen Sulfide
pwMeHg	pore-water Methylmercury
pwTHg	pore-water Total Mercury
pwSO <sub>4</sub> <sup>2-</sup>	pore-water Sulfate
RCC	Roller Compacted Concrete
RFMP	Regional Flood Management Plan
RHg(II)	“reactive”-reducible (stannous-chloride) Mercury
SPFC	State Plan of Flood Control
SS	Suspended Sediment
SSC	Suspended Sediment Concentration
SSIA	State Systemwide Investment Approach
STCC	Sediment Transport Capacity Coefficient
SUVA <sub>254</sub>	Ultraviolet Absorbance at 254 Nanometers
SWP	State Water Project
TE	Trapping Efficiency
THg	Total Mercury (includes organic Hg and MeHg)
TMDL	Total Maximum Daily Load
TPN	Total Particulate Nitrogen
TRS	Total Reduced Sulfur
TSP	Tentatively Selected Plan (USACE, LCCFS)
UCD	University of California, Davis
UCDJAHL	UC Davis J. Amorocho Hydraulics Laboratory

UFRR	Urban Flood Risk Reduction (DWR Grant Program)
USACE	U.S. Army Corps of Engineers
USEPA	U.S. Environmental Protection Agency
USGS	U.S. Geological Survey
WEHY	Watershed Environmental Hydrology Modeling
ww	whole water
wwTHg	whole water Total Mercury
WY	Water Year (USGS)

## UNITS OF MEASURE

cfs	cubic feet per second
cm	centimeter
cm/yr	centimeters per year
ft	feet
ft/s	feet per second
g/yr	grams per year
ha	hectare
in/yr	inches per year
kg	kilogram
kg/yr	kilograms per year
km	kilometer
L	liter
m	meter
mm	millimeter
ng/g	nanograms per gram (ppb equivalent)
ng/L	nanograms per liter
nm	nanometer
ppm	parts per million
ppb	parts per billion
$\mu\text{g/g}$	micrograms per gram (ppm equivalent)
$\mu\text{m}$	micrometer

## **EXECUTIVE SUMMARY**

On November 10, 2011, the Central Valley Regional Water Quality Control Board (CVRWQCB) issued the Department of Water Resources (DWR) a letter because the Delta Mercury Control Program (DMCP) identified the Cache Creek Settling Basin (Basin) as a source of mercury and methylmercury (MeHg) to the Yolo Bypass. The November 10, 2011, CVRWQCB letter further identified DWR, the United States Army Corps of Engineers (USACE), and the Central Valley Flood Protection Board (CVFPB) as agencies required to develop and implement a plan to manage mercury and sediment in the Basin. The letter specifies requirements and deliverables necessary for these agencies to comply with the DMCP total maximum daily load (TMDL) requirements specified for the Basin. Specifically, these requirements include submitting a report that:

- Evaluates the trapping efficiency (TE) of the Basin
- Proposes, evaluates, and recommends potential feasible alternatives for mercury reduction from the Basin
- Evaluates the feasibility of decreasing mercury loads from the Basin, up to and including a 50% reduction from existing loads.
- Describes the long-term environmental benefits of sustaining the Basin's mercury trapping abilities indefinitely
- Describes the costs of sustaining the Basin's mercury trapping abilities indefinitely

In response to the November 10, 2011, CVRWQCB directive, DWR implemented several studies designed to: assess the Basin's TE; measure the Basin's annual sediment, total mercury (THg) and MeHg loads; assess in-basin processes that are associated with mercury methylation; and evaluate potential Basin modifications to improve the TE and decrease the release of THg and MeHg from the Basin. The development, methodology, and findings from these studies are presented in this report.

### **Trapping Efficiency Calculations**

The studies summarized herein are based on a five-year data set (Water Years (WY's) 2010 through 2014) with a maximum observed Basin inflow of approximately 14,000 cubic feet per second (cfs); noting that WY's 2012 and 2014 were essentially dry years with little to no flow into or out of the Basin and that the Basin is designed for a maximum flow of 30,000 cfs. Based

on these data, models developed on behalf of DWR by the United States Geological Survey (USGS) have calculated an overall five-year suspended sediment TE of 70%. Using the same five-year data set, a TE model (calibrated up to a flow of 15,900 cfs) developed on behalf of DWR by the University of California Davis (UCD) conservatively estimated the suspended sediment TE for this period at 49%. Other models by UCD for current conditions indicate a range of suspended sediment TE from 47% to 66%. This range of suspended sediment TE values for the Basin is consistent with historical estimates (CVRWQCB, 2004, 2010).

Utilizing multiple statistical analysis approaches for whole-water THg in surface water (THg in non-filtered samples as well as filtered (fTHg) plus particulate (pTHg) THg), the USGS reported an overall five-year THg TE of 59% for WY's 2010-2014. Of all mercury species evaluated, filtered MeHg (fMeHg) is the only constituent to demonstrate an increase in load leaving the Basin. The percentage fMeHg increase was calculated by the USGS at 20% when summing the two outfall loads (low-flow structure and weir) and at 34% when using an outfall load computed using discharge-weighted average concentrations of the two outfalls.

### **Suspended Sediment and Mercury Load Calculations**

Using the same five-year data set (WY's 2010 through 2014) as for the TE calculations, the USGS calculated a five-year annual average suspended sediment load into the Basin of  $145 \times 10^6$  kilograms per year (kg/yr). The USGS reported the five-year annual average THg load into the Basin to be 32 kg/yr. The USGS calculated the five-year annual average THg load leaving the Basin and flowing into the Yolo Bypass for this same data set at 13 kg/yr when using the sum of the total flows. When using the combined discharge-weighted-average outfall concentrations, the five-year annual average THg load out of the Basin for this same five-year data set is 14 kg/yr. It should be noted that both THg outflow quantification scenarios yield annual averages nearly an order of magnitude less than the 118 kg/yr estimated by the CVRWQCB in their 2010 Staff Report (CVRWQCB, 2010).

The same five-year data set yielded a five-year annual average MeHg load exiting the Basin of 183 grams per year (g/yr). Although the same order of magnitude, this MeHg load is greater than the 137 g/yr estimated by the CVRWQCB in their Staff Report (CVRWQCB, 2010) and supports historical conclusions that the Basin, in its current bathymetric condition and operational status, is a net producer of MeHg during low-flow conditions. This finding also supports that the CVRWQCB-mandated annual MeHg load allocation (reduction of 78.5%, to a maximum of 30 g/yr) exiting the Basin will be unachievable without the necessary load reductions from upstream sources as well as significant Basin land-use and flow-dynamic modifications that would limit MeHg production in the Basin. Planning of future Basin

modifications must strongly consider that annual THg loads entering the Basin should decrease with time as upstream mercury sources in the watershed are remediated.

Using cesium-137 (Cs-137) dating of deep soil cores penetrating about 30 feet, the USGS calculated an average annual aggradation rate of 0.89 inches per year for the years 1963 to 2012. Applying this average deposition rate to the entire Basin equates to approximately 267 acre-feet per year (acre-ft/yr); approximately 25% less than the 340 acre-ft/year accumulation rate estimated by USACE when designing the 1993 expansion for the Basin.

### **In-Basin Processes and Trends**

Robust statistical temporal and spatial analyses of shallow sediment (top 0.8-inches) data collected for these studies show that there is not a significant correlation between elevated THg concentrations and elevated MeHg concentrations within the Basin sediments and no significant correlation between either THg or MeHg concentration and sediment grain size (% less than 0.063 millimeter). Because of the large surface-area-to-volume ratio of small particles, it is common in many environments where mercury occurs adsorbed onto particle surfaces or associated with fine-grained organic matter, to observe increasing THg concentration with decreasing grain size; that was not found to be the case for the current data set (although more detailed grain-size analyses are pending). The lack of a significant grain-size effect on THg, together with sequential extraction results is interpreted to reflect mercury speciation dominated by particulate cinnabar and meta-cinnabar of various size classes, originating in the areas of historical mercury mining and active geothermal springs in the upper Cache Creek watershed. Elevated MeHg concentration was most closely correlated with habitat, specifically non-agricultural, seasonally flooded wetland habitats with elevated organic carbon. A significant increase in MeHg sediment concentration was observed from west to east, in the direction of flow within the Basin. Sediment MeHg concentrations also decreased with time during dry periods. Although it is difficult to assess the implications to MeHg loads if the objective of the TMDL to improve THg TE is achieved, it seems likely that MeHg loads exiting the Basin will not decrease without significant alteration of in-basin habitat and land use.

The USGS conducted in-basin sampling activities that included the analyses of fish tissue, bird eggs, and surface water to support the evaluation of in-basin biochemical processes. When results were compared to relative toxicity benchmarks, the Basin has relatively high THg and MeHg concentrations in fish and wildlife. Mercury concentrations in birds and fish also differed by habitat type (similar to shallow sediment) as well as with creek distance within the Basin. Fish THg concentrations were highest in mixed non-woody floodplain habitat, followed by mixed woody floodplain habitat, irrigation canals, tule wetland habitat, and creek habitat;

whereas THg concentrations in house wren eggs increased with the amount of mixed non-woody floodplain habitat located within 328 feet (100 m) of the nest box. Based on these results, it is apparent that the Basin floodplain habitats which experience a high frequency of wetting and drying and which have the highest organic content in soil, have the highest potential for THg bioaccumulation in fish and wildlife. Because the Basin receives various amounts of water flow among years, it is expected that MeHg concentrations will be highest in fish and wildlife during years with the most flooding for short periods of time during the spring breeding season. For both caged and wild mosquitofish, THg concentrations increased with creek distance into the Basin. THg and MeHg concentrations in surface water collected during the March-April 2013 caged-fish experiment also increased with creek distance.

### **Cache Creek Watershed Study**

A Cache Creek Watershed Study was conducted by UCD to investigate water, sediment, and mercury inflows to the Basin based on Cache Creek watershed hydrology and future climate conditions. The Study was intended to provide concurrent flow, sediment, and mercury information in the Cache Creek watershed and to provide more refined sediment and mercury loading estimates. The UCD watershed model was developed to simulate sediment and mercury TE under different climate-change projections such that development of a range of predictions on sediment loads entering the Basin for an anticipated flow regime, up to a 200-year event could be evaluated and serve as an inlet boundary condition for the flow and sediment transport model developed for the TE study. For model calibration, simulated flows were compared against the observed flow data collected at Rumsey and Yolo stations for the years 1950-2011. These comparisons yielded very satisfactory results with a correlation coefficient of 0.87. However, due to the lack of concurrent flow, sediment, and mercury data collected from within the watershed, the sediment and mercury conditions are quite uncertain. A consequence of the lack of concurrent flow with sediment data is that the sediment rating curve necessary for the estimation of sediment inflows into the Basin has substantial uncertainty for flows above 13,000 cfs. One way to fill the gap in the sediment rating curve is to develop a comprehensive field sampling program for collecting concurrent flow, sediment and mercury data at several sites within the watershed. However, the costs to initiate and manage this comprehensive of a field program are prohibitive. In lieu of these data, DWR will continue collecting concurrent flow-sediment-mercury field data that cover a range of flow conditions at the Rumsey station through June 2016.

## **Evaluation of Remedial Alternatives to Increase Trapping Efficiency**

Federal and state agencies as well as the local community are engaged in several independent feasibility studies that potentially impact the current operation and maintenance activities and thus, the functionality of the Basin. These studies include USACE and their evaluation of the lower leveed section of Cache Creek; the CVFPB in their evaluation of the Basin and other proposed improvements to the Yolo Bypass as part of the Basin Wide Feasibility Study (BWFS) for the Sacramento River Basin; and the City of Woodland in their recently awarded Urban Flood Risk Reduction grant. Each of these studies involves consideration of alternatives that could impact the Basin. In light of these on-going studies, DWR has considered basin TE solutions that are consistent with the CVFPB objectives while staying cognizant of USACE flood protection evaluations. Although DWR, CVFPB, and USACE are not responsible for the high concentrations of Hg or MeHg in Cache Creek as mercury is naturally occurring in the watershed as well as from past mining operations in the upstream portions of the Cache Creek watershed, the agencies along with local interests must work together to find solutions for sediment and mercury management in the Basin. These management solutions must be developed through engagement of USACE and the CVRWQCB as the project and alternative assessments are evaluated. As part of the BWFS, DWR evaluated the following alternatives to improve sediment, THg and MeHg TE in the Basin.

- Alternative 1 - Baseline (existing) conditions
- Alternative 2 – Raise outlet weir with phased notching of training levee (USACE Draft O&M Manual option)
- Alternative 3 - Sediment stockpile within existing Basin footprint
- Alternative 4 - Sediment stockpile within existing Basin footprint and Basin expansion
- Alternative 5 - Basin expansion for sediment stockpile, enlarge Basin, and additional weir

Activities that will likely be needed in conjunction with a Basin modification approach to reduce the mercury methylation process may include periodic re-grading of the Basin; modification of land use practices that would improve basin draining and minimize the formation of non-agricultural wetted floodplains; focused aeration or chemical oxidation; use of chemical amendments to promote settling of fine-grained mercury-containing sediments; lengthening the primary channel to increase open water habitat; and/or adding gates to increase or decrease water holding times. A cursory evaluation of these other options, much like the above evaluated

alternatives suggests both potential advantages and disadvantages to TE and in-basin MeHg production associated with these options.

The evaluation of potential remedial alternatives for the Basin presented in the BWFS and summarized in Section 6.0 of this report revealed a projected remaining basin life (basin filled to capacity) of 10 to 15 years based on current bathymetric conditions and the annual average estimated suspended sediment load of 340 acre-feet/yr stated in the USACE Draft O&M Manual. Implementation of the USACE Draft O&M Manual requirements (weir raise, training levee notching) is projected to extend the Basin lifespan for an additional 25 years and also improve TE up to 10%. However, neither the current condition nor the Draft O&M improvement condition is expected to decrease MeHg production within the Basin as neither of these approaches includes control of upstream mercury sources or land-use alterations that would substantially change land area used for non-agricultural wetted floodplain and riparian habitats. Each of the other proposed basin modifications includes enlargement or land-use modifications to decrease the area of non-agricultural wetted floodplain and riparian habitats. While it is apparent that any of these other potential basin modifications will provide basin lifespan expansion of up to 60 years and improvements in overall TE by as much as 15%, the effect on MeHg production within the Basin remains largely uncertain. Based on the data collected to date, it is clear that basin enlargements alone or basin capacity improvements through periodic sediment removal will be insufficient to decrease the MeHg loads exiting the Basin and may actually increase the MeHg loads by increasing inundation times or exposing sediment with higher concentrations of THg to methylation. Changes to the Basin's current water stilling and movement practices as well as the elimination of non-agricultural floodplain habitats will be required to alter the current mercury methylation processes occurring within the Basin

### **Long-term Environmental Benefits of Sustaining the Basin's Trapping Efficiency**

In assessing the long-term environmental benefits and costs of sustaining the Basin's mercury trapping abilities indefinitely, it is apparent that any mercury control measure implemented for the Basin that provides the benefit of decreased mercury loads entering the Yolo Bypass could also result in local or regional adverse impacts to humans, wildlife, and the environment. Generally, floodplain habitats are effective in trapping sediment. Based on the studies performed to date, it is apparent that, as sediment is settling out in the floodplain habitats within the Basin, there is increased MeHg production due to the breakdown of organic matter within the non-agricultural floodplains, which fuels methylation of mercury within the sediment during relatively wet conditions. The non-agricultural floodplain habitats also tend to have a longer period of floodwater inundation than the agricultural fields which also favors increased MeHg

production in the non-agricultural areas. Any management activity that increases the acreage of non-agricultural floodplains within the Basin will likely increase in-basin mercury accumulation by particle settling, but also increase MeHg formation and bioaccumulation in the biota.

Although increasing sediment and pTHg TE within the Basin would decrease the mercury load that would potentially go into the Delta, the trade-off is having localized effects of greater MeHg production and bioaccumulation within the Basin. Based on the historical estimated aggradation rate, the remaining basin life (TE > 30%) is estimated at approximately 15-years. DWR's historical annual operation and maintenance costs for the Basin (depending on the severity of the flood season) are approximately \$200,000 to \$1,300,000. Thus, the anticipated cost to maintain the Basin as is for its estimated remaining lifespan would be in the neighborhood of \$3 to \$20 million without a single basin improvement.

The eventual basin improvement plan must consider an alteration that can provide substantial flood risk reduction and water-quality improvements while also meeting the multiple concerns of the diverse regulatory and community interests as well as being fiscally responsible such that it can be funded. This is a challenge not likely to be easily met without aggressive pursuit of the elimination of mercury sources in the upstream watershed; including possible structures to entrain mercury-laden-sediment within the watershed, as well as significant habitat alterations within the Basin. Additionally, any project designed to provide the multiple benefits to be achieved by this type of infrastructure improvement must include regional coordination, be mutually funded by all beneficiaries, and not relegated solely to any one managing entity.

### **What's Next**

Further hydraulic and sediment transport modeling is necessary to evaluate possible flood inundation areas as well as the TE and mercury load effects that may result from implementation of the evaluated potential remedial alternatives. DWR has a contract with USGS to continue to collect flow measurements, and sediment and water-quality sampling through June 2016 but, has no funding mechanisms or contracts to continue the mercury-control studies and related modeling efforts beyond WY 2016. There is an approximate 2-year lag between when the USGS collects their data and when it has been peer-reviewed and released for public use. While these data are collected and reviewed, DWR will continue to have UCD and the USGS update their TE models as the data become available. A more statistically supported model output will provide less uncertainty to the Basin's TE and load estimates and help support informed decision making regarding appropriate modifications for the Basin.

# **Report of Findings: Mercury Control Studies for the Cache Creek Settling Basin, Yolo County, CA**

## **1 INTRODUCTION**

The Department of Water Resources (DWR) is pleased to submit this report of findings documenting our compliance with the Delta Mercury Control Program (DMCP) total maximum daily load (TMDL) requirements regarding the Cache Creek Settling Basin (Basin). On November 10, 2011, the Central Valley Regional Water Quality Control Board (CVRWQCB) issued DWR a letter because the DMCP identified that the Basin is a source of mercury and methylmercury (MeHg) to the Yolo Bypass. The November 10, 2011, CVRWQCB letter further identified DWR, the United States Army Corps of Engineers (USACE) and the Central Valley Flood Protection Board (CVFPB) as agencies required to develop and implement a plan to manage mercury sediment in the Basin. The letter specifies requirements and deliverables necessary for these agencies to comply with the DMCP TMDL requirements specified for the Basin. Specifically, these requirements include submitting a report that:

- Evaluates the trapping efficiency (TE) of the Basin;
- Proposes, evaluates, and recommends potential feasible alternatives for mercury reduction from the Basin;
- Evaluates the feasibility of decreasing mercury loads from the Basin, up to and including a 50% reduction from existing loads;
- Describes the long-term environmental benefits of sustaining the Basin's mercury trapping abilities indefinitely; and
- Describes the costs of sustaining the Basin's mercury trapping abilities indefinitely.

### **1.1 History of the Cache Creek Settling Basin**

The Basin is located in Yolo County, California, about 2 miles (3.2 kilometers (km)) east of the City of Woodland, is bound by levees on all sides and covers approximately 3,600 acres (1,457 hectares). The location of the Basin is shown on the Site Vicinity Map, Figure 1 and the Basin boundaries and adjoining land features are shown on the Site Plan, Figure 2. The Basin's fundamental purpose is to preserve the flood-way capacity of the Yolo Bypass by entrapping a portion of the heavy sediment load carried by Cache Creek. The Basin was built by USACE as part of the Sacramento River Flood Control Project authorized by the Flood Control Act of 1917 and State Plan of Flood Control (SPFC) in 1937.

The original Basin was built in 1937 within the alluvial flood plain of the Yolo Bypass to about 11 miles (17.7 km) west of the bypass and about 3 miles (4.8 km) north of the City of Woodland (Figure 2). This basin provided direct protection to nearby agricultural land in addition to Highway 99 and Highway 40, two railroad lines and the town of Yolo. Throughout the life of the project, the Basin's levees were

CCSB Mercury Control Studies  
Report of Findings



Division of Flood Management  
Flood Maintenance Office

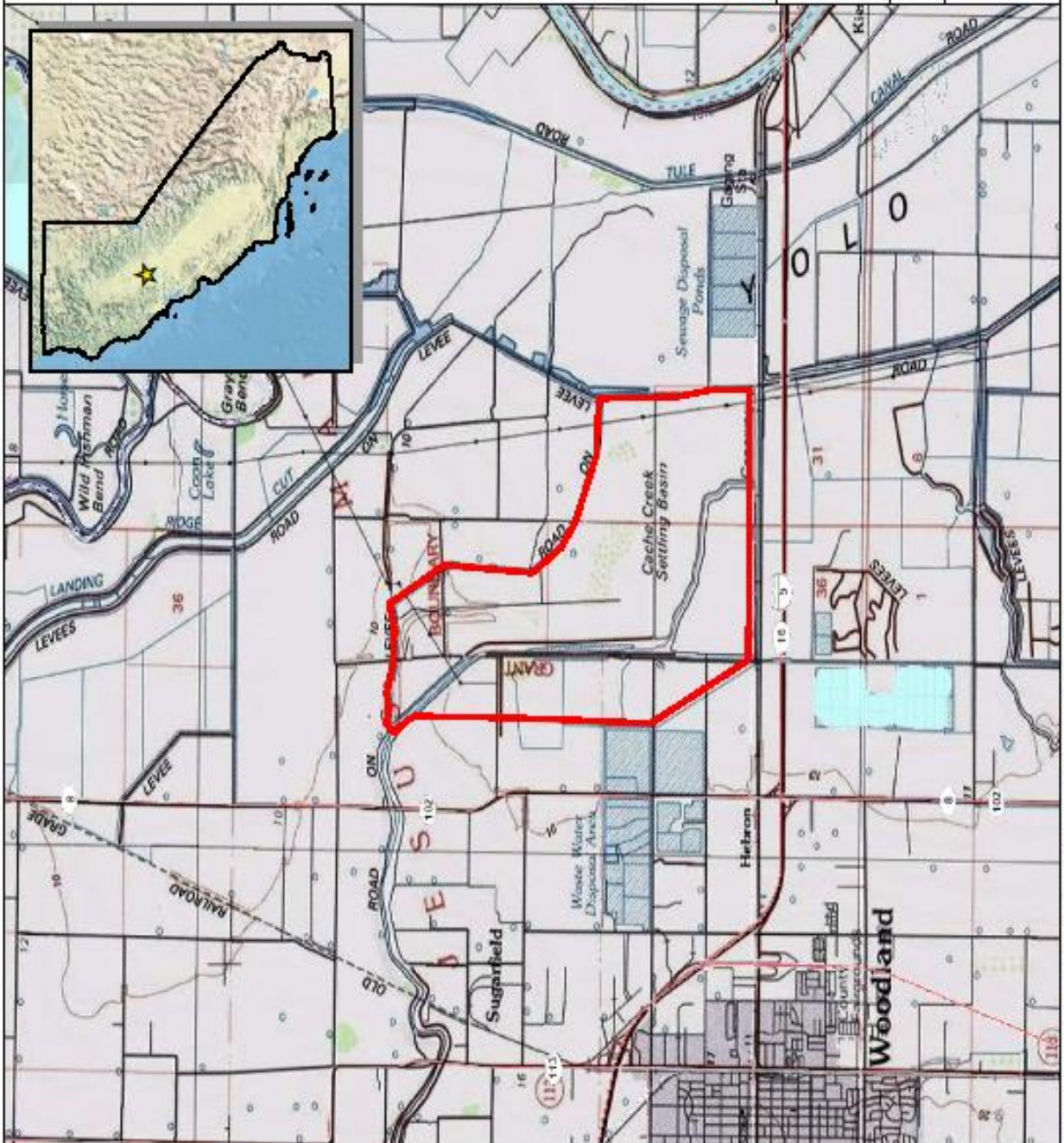


 Project Footprint

**SITE VICINITY MAP**  
Figure 1  
Cache Creek Settling Basin  
Yolo County, CA



Date: November 20, 2015  
Prepared By: Kristin Jacobs  
Document Path: G:\Projects\Cache\_Creek\_Setting\_Basin\Mercury\_Study\2015\_CCBB\_1\_VicinityMap.mxd



Service Layer Credits: Copyright © 2013 National Geographic Society. I-Loaded

CCSB Mercury  
Control Studies  
Report of Findings



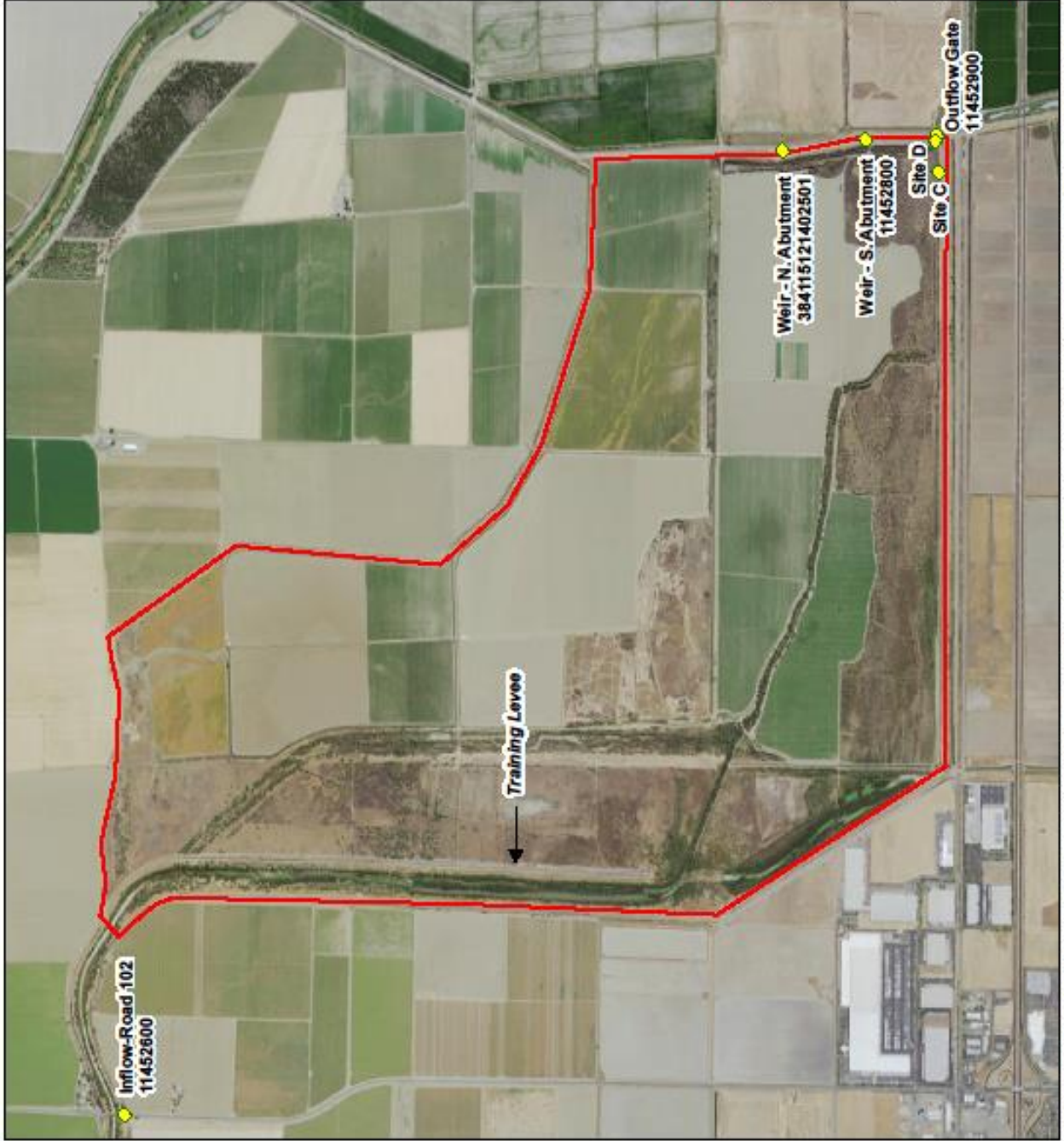
Division of Flood  
Management  
Flood Maintenance  
Office

- Project Footprint
- ◆ Stream Gauge

**SITE PLAN**  
Figure 2  
Cache Creek Settling Basin  
Yolo County, CA



Date: November 20, 2015  
Prepared By: Kaitlin Jacobs  
Document Path: G:\Project\Cache  
Creek\_Setting\_Basin\Mercury\_Study\  
2015\_CCBB\_2\_SitePlan.mxd



Service Layer Credits: Source: Esri, DigitalGlobe, GeoEye, Earthstar Geographics, CNES/Airbus DS, USDA, USGS, AEX, Getmapping, Aerogrid, IGN, IGP, swisstopo, and the GIS User Community

upgraded to increase the capacity of the Basin as well as bring them into SPFC compliance. A large scale modification took place in 1993 to upgrade the Basin's capacity and extend its life.

The objective of the 1993 basin modification was to augment the Basin to provide an additional 50 years of sediment storage capacity. The improved Basin collects up to 340 acre-feet of sediment per year which represents a TE of 50 percent (USACE, 2007). The upgraded basin was designed to safely contain and pass a design flow of 30,000 cubic feet per second (cfs) which is the stated limited capacity of the upstream channel system. This 30,000 cfs flow has an estimated rate of return of 15 to 25 years. The 1993 basin modifications consisted of raised and new levees; a fixed-elevation Roller Compacted Concrete (RCC) outlet weir to upgrade an old cobblestone weir; a low-flow outlet structure; low flow channels; an inlet training channel and levees, and patrol roads and access ramps.

The improved levee system consists of a raised north, west, and east levee and a new south levee. The levees have a 12 foot crown width, 3H to 1V basin side slopes, and 2H to 1V landside slopes, except for the east levee which has a 3H to 1V landside slope.

The fixed-elevation outlet weir is 1,740 feet (ft.) (530.5 meters (m)) in length and made of RCC. The weir was designed to pass flood flows exceeding the 400 cfs design capacity (with Yolo Bypass full) of the low-flow structure up to 30,000 cfs. The weir height is constructed to 12 ft (elevation 32.5 ft) and has been proposed by USACE to be converted to 18 ft (elevation 38.5 ft) at year 25 of the project life (2018), or if the Basin's TE drops below 30 percent.

The low-flow outlet structure, designed to convey 400 cfs when the Basin is full, consists of two 5 ft.(1.5 m) wide by 4 ft. (1.2 m) high flap-gated box culverts controlled by a dual sluice gate system which is fully accessible from the top of the east levee through a gate riser unit. The structure inlet is uncontrolled and equipped with trash collecting facilities. A two channel system carries low flows from the training channel to the outlet culverts. The main low-flow channel carries flows from the training channel to the outlet structure. The low-flow subreach channel carries flows from the area behind the RCC weir to the outlet structure. The main channel has a bottom width of 25 feet (7.6 m) and cut slopes of 3H to 1V. The subreach has a bottom width of 15 feet (4.6 m) and cut slopes of 3H to 1V.

The training channel has a 300 ft (91.5 m) bottom width and 3H on 1V cut-slopes, and ties into the existing channel approximately 350 ft (137.8 m) downstream of County Road 102. The training levee is offset 100 ft. (30.5 m) from the channel left bank and has 3H on 1V side-slopes. This system is designed to convey the design flow of 30,000 cfs. Between years 25-45 of the project life, USACE has proposed that along with the 6 ft. (1.8 m) weir raise, that 400-foot-long (122 m) sections of the training levee be systematically removed from south to north to encourage settlement in the northern portions of the Basin.

There are all-weather patrol roads on the crown of the training levee and perimeter levees for maintenance, inspection, and flood fighting purposes. These roads are accessible by six access roads and eight interior basin ramps (USACE, 2007).

## 1.2 Regulatory Requirements

On February 22, 1994, the State of California assumed operation and maintenance (O&M) responsibility for the Basin from USACE. USACE has provided DWR with O&M manuals outlining project features which are subject to flood control regulations as well as actions to take as the facility ages that will be outlined later in this report (USACE 1961, USACE 2007).

On April 22, 2010, the CVRWQCB adopted amendments to the Sacramento River and San Joaquin River Basin Plan (Basin Plan) to establish the DMCP to address Hg and MeHg impairments in the Delta (CVRWQCB, 2010). The DMCP includes fish-tissue objectives for the Delta and numerical MeHg allocations that affect the Basin. The DMCP lays out a strategy for implementing measures for controlling MeHg and total mercury (THg) in the Basin that will be covered in a following section.

### 1.2.1 USACE O&M Manual

USACE has issued two O&M Manuals for the Basin that outline the requirements and responsibilities for properly operating and maintaining the Basin. The first manual was issued in 1961 but due to the comprehensive modifications made to the Basin in 1993 a second updated draft manual was issued in 2007 (USACE, 1961, 2007). These manuals, while not outlining environmental requirements, will affect the way DWR is able to conduct required O&M activities and attempt to meet MeHg load allocations and TE requirements outlined in the TMDL.

The O&M manuals explicitly require that at all times maintenance as may be required shall be provided to insure serviceability of the structures in time of flood and that immediate steps will be taken to correct dangerous conditions disclosed by inspections. Regular maintenance repair measures are accomplished during the appropriate season and include maintenance to levee's, access roads and the low-flow and weir structures. Other Basin O&M activities include: exterminating burrowing animals and repair of rodent holes, routine mowing of the grass and weeds, removing wild growth and drift deposits, and repair of damage caused by erosion or other forces.

Other required O&M activities include routine inspections to ensure no unusual settlement, sloughing, or material loss of grade has taken place and that no seepage, saturated areas, or sand boils are occurring. In cases where the levee grade settles below the design elevations, the O&M manuals require that the crown grade be raised to the original designed grade. The surfaces of levee roads are also required to be maintained in original condition.

Our inspections must also confirm that there is no unauthorized grazing or vehicular traffic on the levees and that encroachments are not being made on the levee rights-of-way which might endanger the structure or hinder its proper and efficient functioning during times of emergency.

Our inspections are made prior to the beginning of the flood season; following each major high water period, and otherwise at intervals not exceeding 90 days; and such intermediate times as may be

necessary to insure the best possible care of the levee, channels and floodways. During flood periods the levee is patrolled continuously to locate possible sand boils or unusual wetness of the landward slope and to be certain that there are no indications of slides or sloughs developing; wave wash or scouring action occurring; low reaches of levee exist which may be overtopped and that no other conditions exist which might endanger the structures.

Improved channels and floodways are inspected to be certain that the channel or floodway is clear of debris, weeds, and wild growth and is not being restricted by the depositing of waste materials, building of unauthorized structures or other encroachments; the capacity of the channel or floodway is not being reduced by the formation of shoals; banks are not being damaged by rain or wave wash, and that no sloughing of banks has occurred; riprap sections and deflection dikes and walls are in good condition; and that approach and egress channels adjacent to the improved channel or floodway are sufficiently clear of obstructions and debris to permit proper functioning of the project works. Both banks of the channel are patrolled during periods of high water, and measures are taken to protect those reaches being attacked by the current or by wave wash. Appropriate measures are taken to prevent the formation of jams of debris and large objects which become lodged against the bank are removed. As soon as practicable thereafter, snags and other debris are removed and damage to banks, riprap, deflection dikes and walls, drainage outlets, or other flood control structures repaired.

Our inspections further implement measures to insure that inlet and outlet channels are kept open, that trash, drift, or other debris is not allowed to accumulate near drainage structures and that erosion is not occurring adjacent to the structure which might endanger its water tightness or stability. Flap gates and manually operated gates and valves on drainage structures are routinely examined, oiled, and trial operated. Eroded concrete is repaired as soon as erosion reaches a depth of 4 inches (10 centimeters (cm)) or any reinforcing steel is exposed.

The outlet weir is inspected prior to each flood season and subsequent to each major flood event. DWR checks the concrete surfaces for unevenness, settlement, tilting, cracking or spalling and monitors the contraction joints. They further investigate the weir for evidence of erosion; hand railings for indications of corrosion or other damage and look for the accumulation of trash and debris near the structure.

The outlet weir has been constructed to a crest elevation of 32.5 ft. The 2007 Draft O&M Manual states that at year 25 of the project life, or when a measured TE of less than 30% is realized, the weir shall be raised 6 ft, (1.8 m) to a crest elevation of 38.5 ft, the final weir height. USACE estimates the average TE for the life of the project is approximately 55%, based on increasing the weir height at year 25 (2018).

USACE designed the training channel and training levee to direct flood flows down into the greater Basin area thereby releasing sediment away from the upper channel region. The training channel and levee extends the “effective” Cache Creek down into the Basin. The Draft O&M Manual also requires that in years 25-45 of the project life, sections of the training levee be removed. Starting at year 25 of the project life, 400-foot-sections (122 m) of the training levee are proposed to be removed at 5 year intervals and

located at 1,100-foot (335 m) intervals along the training levee. The first 400-foot section (122 m) to be removed shall be located at the bottom of the training levee with each additional 400-foot section (122 m) removed 1,100 feet (335 m) upstream of the preceding section removed.

The Draft O&M Manual further includes a sediment monitoring plan to provide a means for checking the effectiveness of the outlet weir and the training channel and training levee in keeping sediment out of the bypass. The sediment monitoring plan requires that ground surveys be taken every five years with enough detail to generate topographic contours of one foot intervals and that sediment samples be taken near the inlet to the Cache Creek Basin so that total load discharge into the Basin can be determined. Sediment data are used to verify and adjust the assumed sediment discharge curve, and to compute the TE of the Basin.

### 1.2.2 CVRWQCB TMDL

On April 22, 2010, the CVRWQCB adopted amendments to the Basin Plan to establish the DMCP to address Hg and MeHg impairments in the Delta. The DMCP includes fish-tissue objectives for the Delta in the form of numerical MeHg allocations for NPDES facilities, municipal storm water, agricultural lands, wetlands, and open water in the Delta and Yolo Bypass. The DMCP lays out an implementation strategy for the control of MeHg and Hg in the Delta and Yolo Bypass designed to reduce MeHg levels in Delta fish tissue by using an adaptive management approach that contains two phases. Phase 1, which will last through approximately 2020, is primarily a study period when MeHg control measures will be developed and evaluated. At the end of Phase 1, the CVRWQCB will review the study results and will consider revising the fish tissue objectives and numerical MeHg allocations. Phase 2, which begins after the CVRWQCB conducts its reevaluation of the fish-tissue objectives and waste load and load allocations, will require implementation of the MeHg controls identified by the Phase 1 studies. On October 20, 2011, the United States Environmental Protection Agency (USEPA) approved the Basin Plan amendments, thus establishing the “effective date” of the DMCP and the start of the schedule for requirements.

The Basin Plan includes numeric MeHg load and waste load allocations for multiple sources to be used to inform the type and magnitude of management practices that should be evaluated in the control studies. In establishing the TMDLs for the Basin, the CVRWQCB evaluated available data for loads of THg, MeHg, and suspended sediment entering and exiting the Basin for two efforts: (1) the Cache Creek, Bear Creek, and Harley Gulch TMDL for mercury (Cooke et al., 2004 aka “Staff Report”, approved as a Basin Plan Amendment in 2006); and (2) the Sacramento-San Joaquin Delta TMDL for mercury and methylmercury (Wood et al., 2010a, approved as a Basin Plan Amendment in 2011). The MeHg load allocation in the Basin Plan is a reduction to 21.5% of “existing” loads, with a cap of 30 grams per year (g/yr). The “existing” MeHg load for Basin outflow in the Delta TMDL Staff Report was 137 g/yr (Wood et al., 2010b). The Basin specific TMDL further requires a THg load reduction of 50%; based on the “existing” load of 118 kilograms per year (kg/yr), the target THg load would be 59 kg/yr.

### 1.2.2.1 Summary of Deliverables and Schedule

In a letter dated November 10, 2011, the CVRWQCB notified DWR, the CVFPB and USACE that the DMCP/TMDL has identified the CCSB as a source of THg and MeHg to the Yolo Bypass. The letter requires these named agencies to comply with the applicable TMDL requirements contained in the Basin Plan and outlines the deliverable and schedule requirements necessary for the agencies to comply. The specified requirements for the CCSB include:

- By October 20, 2012, take all necessary actions to initiate the process for Congressional authorization to modify the Basin, or other actions as appropriate, including coordinating with USACE. DWR provided a Congressional Authorization/Project Update letter to the CVRWQCB on March 8, 2013.
- By October 20, 2013, develop a strategy to reduce total mercury from the Basin for the next 20 years. The strategy shall include a description of, and schedule for, potential studies and control alternatives, and an evaluation of funding options. The Agencies shall work with the landowners within the Basin and local communities affected by basin improvements. DWR submitted our Strategy to Reduce Total Mercury (from the Basin) in a letter to the CVRWQCB dated December 9, 2013. This letter provided the scope for control studies to be performed by DWR; the initial results of which are summarized in subsequent sections of this document.
- By October 20, 2015, submit a report describing the long-term environmental benefits and costs of sustaining the Basin's mercury trapping abilities indefinitely. These requirements are addressed in Section 4.0 of this report of findings, with additional cost information provided in Section 6.0.
- By October 20, 2015, submit a report that evaluates the TE of the CCSB and proposes, evaluates, and recommends potentially feasible alternative(s) for mercury reduction from the Basin. The report shall evaluate the feasibility of decreasing mercury loads from the Basin, up to and including a 50% reduction from existing loads. This evaluation is presented in Sections 3.0 and 6.0 of this report.
- By October 20, 2017, submit a detailed plan for improvements to the Basin to decrease mercury loads from the Basin.
- Submit the strategy and planning documents described above to the Regional Water Board for approval by the Executive Officer. During Phase 1, the agencies should consider implementing actions to reduce mercury loads from the Basin. Beginning in Phase 2, the agencies shall implement a mercury reduction plan.

DWR is conducting three major studies to collect information on the Basin to comply with the above Basin TMDL requirements: a study of the Cache Creek watershed and a TE study of the Basin, both conducted by UC Davis (UCD), and a mercury load study conducted by the United States Geological Survey (USGS). The current progress and results of these studies are summarized in subsequent sections of this report.

### 1.3 Coordination with Stakeholders

Throughout the initiation of the control studies, DWR has organized and participated in dozens of meetings with a wide range of stakeholders including: USACE; the City of Woodland and their respective Consultants; the CVFPB; the Water Resources Association of Yolo County, the Open Water

Workgroup, the Delta Tributaries Mercury Council and landowners within the Basin and adjacent Conaway Ranch.

The miscellaneous stakeholder meetings have typically been attended by a wide variety of interested parties including regulatory agencies, land owners/managers, technical experts, and local community representatives. The focus of these meetings has been on presenting updates on the various mercury control studies being performed by DWR and their technical experts; identifying concerns related to potential flood hazards resulting from proposed modifications to the Basin; and on how to cooperate in complying with the requirements of the DMCP.

Stakeholder participation in these meetings has also been critical for coordinating property access, data collection activities, resource management and funding mechanisms necessary to progress the control studies.

In addition, DWR is supporting the development of the Lower Cache Creek Feasibility Study (LCCFS) being prepared by USACE, the Sacramento River Basin Wide Feasibility Studies (BWFS) being prepared by the CVFPB, as well as the recently awarded Urban Flood Risk Reduction (UFRR) grant awarded to the City of Woodland to address increased urban flood protection for the City.

The LCCFS is investigating the feasibility of increasing the level of flood protection for the City of Woodland, Town of Yolo, and adjacent communities. While the study is considering whether or not the Basin is contributing to flood risk in the City of Woodland, the intent of the LCCFS is to be independent of specific issues related to the Basin. The LCCFS was originally scheduled to develop a tentatively selected plan (TSP) by November 30, 2015. However, DWR and the City of Woodland, the two non-federal sponsors for the project have recently requested the project be stalled for 6-months so that concerns regarding potential water-quality impacts associated with the selected alternative can be evaluated. The TSP developed through the LCCFS will be a critical flood improvement structure to consider when evaluating mercury control alternatives for the Basin.

The CVFPB is preparing an Administrative Draft Technical Memorandum for the BWFS that includes a feasibility study for the Basin evaluating alternatives for extending its functional life for an additional 50 years. While the document is still being prepared, the alternatives evaluated for the Basin in this Technical Memorandum are consistent with those identified by DWR in their December 9, 2013, response to the November 10, 2011, CVRWQCB directive for control studies. The BWFS is discussed further in Section 6.4.

Scoping for the services to be performed by the City of Woodland under the UFRR Grant are still being developed and how this work will align with the City's and USACE objectives under the LCCFS remain to be identified. However, based on the City's UFRR Grant Application it is apparent that modifications to the Basin are being considered in developing their preferred urban flood risk reduction alternative.

Based on the on-going efforts by the respective stakeholders, the large scale flood risk reduction plan and associated modification to the Basin will need to be identified and proposed for congressional approval before alternatives for the Basin beyond baseline conditions can fully evaluated. As such this uncertainty restrains the analysis presented in Section 6.0 of this report to a conceptual level.

#### **1.4 Current and Proposed Studies and Schedule**

In a letter dated November 10, 2011, the CVRWQCB notified DWR of its need to comply with applicable DMCP requirements contained in amendments to the Basin Plan. In anticipation of these requirements, DWR contracted with the USGS and UCD in 2008 to conduct studies to evaluate the Basin's TE and characterize sediment and mercury loads for the inflow to and the outflows from the Basin. The approach to the studies employs both standard monitoring activities and supporting research efforts. The monitoring activities were designed to address the need for high quality flow, velocity, and mercury and sediment load data whereas the research efforts were designed to address data gaps that may affect DWR's ability to manage the Basin and to effectively reduce loads of THg and MeHg.

DWR is currently conducting or plans to conduct the following studies associated with the Basin:

- Trapping Efficiency Study
- Mercury Load Determination Study
- Cache Creek Watershed Study
- Mercury Cycling Modeling

Additionally, DWR has used the initial findings from these studies to evaluate potential Basin, overland floodwater and sediment transport impacts under the requirements of the USACE March 2007 Draft O&M Manual. Further continuance or initiation of these studies will be dependent on providing value to DWR and the availability of funding.

A summary of each of the studies follows with more detailed description of these studies presented in subsequent sections of this report.

##### 1.4.1 Trapping Efficiency Study (UCD, USGS)

Determination of the sedimentation rate is critical for evaluating the lifespan of the Basin. The purpose of this study is to evaluate TE and sedimentation rate in the Basin and sediment load into the Yolo Bypass. In 2008, UC Davis began evaluating the Basin's TE with respect to current and future Basin design by utilizing field measurements of suspended sediment, high-resolution digital elevation data, discharge hydrographs of high water events and mean-daily discharge, scaled physical modeling, and numerical modeling.

The USGS collaborates with UCD by collecting continuous flow rates, suspended sediment loads into and out of the Basin, velocity profiling data, and continuous discharge data and mass loading rates for the

Basin. The calibrated and validated model was used to run simulations for evaluating flood inundation and sediment loading effects related to modifications made to the Basin, including those scripted in the Draft O&M Manual.

At the termination of the original Phase I study in 2012, field measurements of suspended sediment and flow were too scarce to calibrate and validate the numerical model, with substantial information gaps regarding the behavior of flow within the interior of the Basin, leaving uncertainty in the model results. The Study has been authorized to continue through April 2016 in an attempt to address these data gaps.

UC Davis submitted to DWR a Phase I Draft Final Report on June 30, 2012 (UCD, 2012), outlining preliminary findings pertaining to TE and sedimentation rate. The results of this Phase I study were preliminary due to prior collection effort limitations and because dry conditions during WY 2012 and 2014 prohibited sufficient data collection. UCD implemented Phase II studies in April 2013 and submitted to DWR Annual Progress Reports in 2014 and 2015 (UCD, 2014, 2015). The significant findings from these UCD Annual Progress Reports are discussed in Section 2.0 of this report and the 2014 and 2015 reports are included in entirety as Appendix A. By April 15, 2016, UC Davis will submit to DWR a Final Report presenting TE estimates.

#### 1.4.2 Mercury Load Determination Study (USGS)

USGS has developed a conceptual model describing transport of THg and MeHg in and out of the Basin and transformation of THg to MeHg within the Basin. USGS has further evaluated factors and hydrogeochemical processes that are most strongly associated with the transport of higher concentrations or loads of THg and MeHg from the Basin. The USGS collected and arranged for the analyses of abundant water quality and sediment samples to calculate daily, monthly, and annual loads. The USGS further evaluated the relationships between land management, geographic location, biogeochemical status, and mercury speciation and the potential linking of geographic features with mercury methylation and bioaccumulation. The contract for this study was initiated in 2009 and runs through June 30, 2017.

The USGS provided DWR with Annual Progress Reports for 2013 and 2014 and on November 16, 2015, USGS provided DWR with detailed descriptions of the scientific approach, basic data analyses and methods and results of trapping efficiency and sediment load calculations in a draft report titled *Mercury Studies in the Cache Creek Settling Basin, Yolo County, California: Preliminary Results, 2010-2014 (aka Scientific Investigations Report SIR)* (USGS, 2013, 2014, 2015). The significant findings from the USGS SIR are discussed in Section 3.0 and the draft 2015 USGS Report included in its entirety in Appendix B.

#### 1.4.3 Cache Creek Watershed Study (UCD, USGS)

The purpose of this study is to investigate water, sediment, and mercury inflows to the Basin based on Cache Creek watershed hydrology and future climate conditions. This Study was intended to provide concurrent flow, sediment, and mercury information in the Cache Creek watershed and to provide more refined sediment and mercury loading estimates. The intent of the model is to simulate sediment and

mercury TE under different climate change projections such that development of a range of predictions on sediment loads entering the Basin for an anticipated flow regime, up to a 200 year event could be evaluated. The predicted sediment loads can then serve as an inlet boundary condition for the flow and sediment transport model developed for the TE study.

On September 25, 2015, UCD submitted to DWR a Final Report (revised) describing the watershed study protocols, analyses performed, results and recommendations (UCD, 2015a). The substantive findings from this report are described in Section 5.0 and a copy of the entire report is presented as Appendix C. This report was preceded by 2013 and 2014 annual progress reports.

#### 1.4.4 Mercury Cycling Modeling (Reed Harris, USGS, UCD)

DWR has considered a scope of work for Reed Harris Environmental to model the Basin with the primary objective to develop a process-based model of mercury cycling and bioaccumulation to help assess options to achieve reduced mercury loads from the Basin. Concepts of the study considered the use of a conceptual model, numerical models, hypothesis testing, and possibly data collection to complement the results from the UCD and USGS studies. DWR has not proceeded with this work pending evaluation of the in-basin data collected and analyzed during the UCD and USGS studies and pending available funding.

## 2 TRAPPING EFFICIENCY STUDY (UCD, USGS)

To evaluate whether the TE and sedimentation rate in the Basin are meeting design requirements set forth by USACE, DWR contracted with UC Davis J. Amorocho Hydraulics Laboratory (UCDJAHL) to evaluate the Basin TE. The overall objective of this study is to evaluate the Basin TE with respect to current and future Basin design, utilizing field measurements of flow and suspended sediment in Cache Creek and the Basin, high-resolution digital elevation data of the Basin, experimental laboratory study, and numerical modeling. The following paragraphs summarize the methodology and results of this study. Further details regarding this study can be found in UCD's 2014 and 2015 trap efficiency annual progress reports (UCD, 2014, 2015); both of which are included in their entirety in Appendix A.

UCDJAHL identified several factors that are crucial to the success of the TE estimation: a) accurate representation of the Basin's training channel which has changed significantly since its construction due to deposition of sediment, b) calibration and validation of a 2-dimensional model with well-timed and well-placed measurements of flow and sediment properties, c) long-term simulations that encompass the full range of flows historically observed in the Basin as well as future predictions which incorporate climatic uncertainty, and d) simulations of flow which represent the transience of both sediment loads and flows entering the Basin. Once UCDJAHL selected a model, the TE evaluation was performed with reference to the current Basin geometry as defined by 2006 and 2008 surveys of the Basin, utilizing field measurements of suspended sediment and flow into, within, and out of the Basin as provided by USGS, and by physical sedimentation modeling performed at the UCDJAHL. To estimate the Basin's TE, UCDJAHL originally selected the Finite Element Surface Water Modeling Systems, 2-D Depth-averaged Flow and Sediment Transport Model (FESWMS) but, subsequently identified the National Center for Computational Hydroscience and Engineering's model of two-dimensional depth averaged flow and sediment transport model (CCHE2D) as more appropriate for the Basin. UCDJAHL further performed laboratory experiments to understand the sediment transport and deposition processes in the Basin. The laboratory experiments were performed in a large laboratory-based flume constructed at the UCDJAHL. Details of the flume construction and experiment methodologies are included in the 2012 UCD Final Progress Report (UCD, 2012) and briefly summarized in the following paragraphs.

Using only sediment collected from the Basin, UCDJAHL performed two sets of laboratory tests to assess the sediment transport and deposition processes. The first set of tests was performed to mimic the combined sediment transport and deposition processes. The second set of tests was performed to understand the settling process and the ensemble behavior of settling velocities. UCDJAHL performed nine sediment transport and deposition tests under various sweeping velocity, water depth and inlet sediment concentration conditions.

For the laboratory experiments at UCDJAHL, they measured the mean settling velocities using a methodology explained by McLaughlin (1959). This method involves taking sets of simultaneous concentration samples at several levels of a still water column. To measure the settling velocity, the suspended sediment concentration samples were taken at three depth intervals simultaneously. Tests were

conducted at 3 ft (0.9 m) and 5 ft (1.5 m) water depths. UCDJAHL calculated the cumulative settling velocity distributions from the cumulative particle size distributions of suspended particles (Julien, 2002). Cumulative settling velocity distributions were then superimposed on the measured mean settling velocities. The settling velocity experiments are described step by step in the UCD 2012 Annual Progress Report (UCD, 2012).

## **2.1 Sensitivity Analysis of Trapping Efficiency by HEC-6 Model**

In 2004, Camp Dresser McGee (CDM) initiated a Basin Mercury Study to assess the potential of modifying the function of the Basin to increase sediment and mercury deposition while improving the quality of Cache Creek outflows (CDM, 2004a, 2004b, 2007). Conclusions about the sediment and mercury TE of the Basin in the 2007 CDM study were based on the HEC-6 model (CDM, 2004b) developed by USACE in 1997. The original USACE model only covered the training channel portion of Basin. CDM (2004b) extended the USACE model from the outlet of the training channel to the greater Basin area based on a 2D hydraulic model that was also developed by USACE in their General Design Memorandum (USACE, 1987). The model input was based on 1983 survey data.

Using the HEC-6 model described in CDM (2004b), UCDJAHL identified the sensitivities to the sediment rating curve and the inlet flow conditions on the sediment TE of the Basin. The sensitivity analyses showed that the TE is very dependent on the sediment rating curve (sediment load-stream discharge relationship) and the inlet flow conditions. As such UCDJAHL initiated a rigorous approach to determine the sediment rating curve and the inlet flow conditions.

Daily average stream discharge observations at Cache Creek at Yolo station are available since the early 20th century. USACE constructed a computational hydrograph for simulating the 50-year project life of the Basin using the USGS daily flows at the Yolo stream gage during the period 1980-1989. This 10-year period was copied and repeated five times to generate a 50-year simulation period (CDM, 2004b). Using only a 10-year historical flow record and repeating it may not be representative of the statistical characteristics of the century long flow record. However, utilizing a longer historical period requires intense computations. The 30,000 cfs discharge, which is the design capacity of the upstream Cache Creek levee system, has approximately a 10-year return period. For the sensitivity analysis purposes, UCDJAHL added this 30,000 cfs discharge every 10-years.

USACE developed the inflowing sediment load estimate as described in the 1997 HEC-6 analysis (USACE, 1997). The sediment inflow is input into the model as a relationship between streamflow discharge rate with respect to total sediment load (in tons/day), which includes both bedload and suspended load. This relationship was based primarily on a sediment-discharge curve documented in the General Design Memorandum (USACE, 1987), which was ultimately derived from long-term instantaneous samples collected by the USGS between 1943 and 1971 (CDM, 2004b). Three regression equations were used to fit the suspended sediment load-stream discharge data. For this fit, uncertainties

exist in the suspended sediment load-stream discharge relationship for discharges greater than 12,000 cfs due to limited measurements.

The bed load was measured to be 7.3% of the suspended sediment load at Cache Creek Yolo gage for the water years 1960-1963 in Lustig and Busch (1967). Total sediment load at Cache Creek Yolo gage was measured and a regression curve was developed in Lustig and Busch (1967). However, this regression equation also is non-representative for flows larger than 13,000 cfs.

For UCDJAHL's sensitivity analyses, three sediment load-stream discharge relationships were used at the upstream boundary of the computations: 1) the same as the one used in CDM (2004b) study, 2) based on three regression equations described above, and 3) the same as the one suggested by Lustig and Busch (1967). For the first approach, using the assumptions described in CDM (2004b), the average TE values in the Basin were estimated as 51%, 30%, 60% and 60% during the periods 2008-2043, 2008-2018, 2018-2028, and 2028-2043, respectively. For the second approach (referred to as "New Estimate"), the same assumptions as of the HEC-6 model described in CDM (2004b) were used in this study except that 30,000 cfs flow was added every 10 years, and a new sediment-discharge relationship, composed of three regression equations for suspended sediment, was considered. By the "New Estimate" approach, the average TE values in the Basin were estimated as 43%, 11%, 60% and 57% during the periods 2008-2043, 2008-2018, 2018-2028, and 2028-2043, respectively. The third approach in this study was the same as the second approach, except that the sediment rating curve of Lustig and Busch (1967) was used. More conservative TE values were obtained in this study using the third approach; yielding 38%, 8%, 60% and 44% for the same periods. Lustig and Busch (1967) developed their sediment rating curve for flows that were less than 13,000 cfs. When extrapolated, their total sediment load estimate is close to five times that of CDM (2004b) and that of the "New Estimate" at 30,000 cfs.

CDM (2004b) extended the Corps model from the outlet of the training channel to the greater Basin area based on a 2-D hydraulic model that was developed by USACE (USACE, 1987) that is based on 1983 survey data. Therefore, UCDJAHL also started the HEC-6 model at 1983 instead of 1993. Using the assumptions described in CDM (2004b), the average TE values in the Basin were estimated as 47%, 17%, 60% and 60% during the periods 2008-2043, 2008-2018, 2018-2028, and 2028-2043, respectively. By the "New Estimate" approach, the average TE values in the Basin were estimated as 43%, 9%, 60% and 56% during the periods 2008-2043, 2008-2018, 2018-2028, and 2028-2043, respectively. By the third approach the average TE were estimated as 35%, 9%, 60% and 36% during the same periods.

UCDJAHL further determined that the TE of the training channel is considerably lower when compared to that of the Basin. The average TE in the training channel during 2008-2043 is between 5% and 6% by the three approaches. Based on this analysis, UCDJAHL opined that the sediment TE of the Basin is very dependent on the streamflow conditions and sediment load-streamflow relationship (sediment rating curve) at the upstream boundary of the computational model and that high uncertainties exist in the sediment-discharge curve for discharges that are greater than 12,000 cfs due to limited concurrent flow and sediment load measurements.

At the initiation of the project, the numerical modeling of flow and sediment transport at the Basin was to be performed by the USACE-sanctioned RMA2 and SED2D models. RMA2 and SED2D were models sold in a package with a graphical user interface, SMS, The Surface Water Modeling System. SMS is used for pre-processing and post-processing of model data. Software purchasing and training for numerical modeling of sediment transport with the SMS package were initiated in April of 2008. The packaged models offered in SMS were altered at that time, and SED2D was eradicated from the package in favor of FESWMS. FESWMS developed by David C. Froehlich, Ph.D. (Froehlich, 1989) was initially seen as a more complete model of sediment transport as the hydrodynamic and sediment modeling in this system are semi-coupled such that sediment transport for each time-step is taken into consideration when evaluating the next time-step of the hydrodynamic simulation. FESWMS simulates the movement of water and non-cohesive sediment in rivers, estuaries and coastal waters. UCDJAHL subsequently evaluated the suitability of FESWMS software for application to the Basin and its accuracy through the modeling of a number of physical experiments that were previously conducted at the UCDJAHL.

Testing of FESWMS sediment transport capabilities began with the comparison of modeled and measured results of a roughness study that was completed in the large outdoor flume of the UCDJAHL (Chen, 2009). Predicted water surface elevation values were extremely accurate with no additional calibration. FESWMS was able to fairly accurately model the sediment transport during the experiments, capturing well the magnitude and location of erosion in the flume. The results were considered encouraging given the uncertainty in grain size, which was assigned solely by visual observation. Isolated discrepancies between the real and model sediment surface were attributed to the movement of hard-packed, clumped soil which FESWMS cannot easily predict, but was observed during experiments. While these results were encouraging, they are for clear water over a bed of homogeneously sized sediment, and therefore represent a very special case. The ability of FESWMS to model the sediment transport process in the very diverse setting of the Basin was enhanced through calibration by using results of the previously described physical experiments. Calibrated Manning's Roughness values ranged from bare soil channel values to extremely dense vegetation values, as outlined in Arcement and Schneider (1989); all values that may be observed in the Basin. These calibrated results, while good, are again the result of simulating a special case. In this instance, the special case is steady state upstream flow over a short time period (less than 1 hour). Furthermore, an intense roughness value calibration was required for the flume experiment simulations, showing that the application of FESWMS to sediment transport and deposition processes in the field setting of the Basin may be challenging and impractical due to limited observed flow and sediment data for 2-dimensional model calibration. In the Basin, roughness values, while varying spatially, vary seasonally, as well as with inundation of the Basin. As water depths increase, roughness can change from shear roughness to form roughness, and can therefore change in magnitude as depths of inundation change. The above-reported results for FESWMS were used for model calibration due to the lack of sufficient field data. However, to support the model credibility for long-term simulations, it was necessary to validate the model performance by field observations of flow and sediment transport completed during Phase II of this study.

After an intense calibration process utilizing observed flow and sediment data, FESWMS quasi-steady state sediment transport module was successfully applied iteratively to replicate the deposition under unsteady sediment inflow conditions for the flume experiments. FESWMS was run in a quasi-steady state fashion; updating the input concentrations and bed geometry according to simulated steady state results every 12 minutes according to measured suspended sediment concentrations. These measured upstream concentrations vary through the experiment, while the discharge does not. While the application of a quasi-steady state approach was possible in the short time period of the sediment transport and deposition tests, through calibration, it was challenging to follow such an approach when modeling the Basin over the long durations required to estimate TE under limited observed flow and sediment data for calibration. Therefore, UCDJ AHL investigated possible other model alternatives that can simulate unsteady flow and sediment transport conditions under long durations efficiently.

## **2.2 Phase II Trapping Efficiency Study**

UCDJ AHL implemented Phase II of the TE Study in April 2013 (UCD, 2014). For Phase II, UCDJ AHL switched to evaluating the Basin TE through application of the CCHE2D model of two-dimensional depth averaged flow and sediment transport. The Phase II evaluation is being conducted consistent with prior modeling efforts in that it was conducted with respect to the current Basin design as defined by 2006 and 2008 surveys of the Basin, and utilizes the field measurements of suspended sediment and flow into, within, and out of the Basin as provided by USGS, as well as by the physical sedimentation modeling performed at the UCDJ AHL in 2009.

The major objectives of the Phase II study are to 1) perform field measurements by UCDJ AHL staff of 2-D velocities and flow within the Basin to be incorporated in calibration and validation of 2-D flow and sediment transport models; 2) to incorporate flow and suspended sediment measurements provided by USGS in order to calibrate and validate the 2-D flow and sediment transport models; and 3) to provide DWR with a method of reevaluating sedimentation for any further basin augmentation proposals.

Upon completion of Phase 1, UCD selected two-dimensional modeling for representation of the Basin, as vertical velocities and accelerations are believed to be small when compared with the significant 2-D horizontal velocities and accelerations. Developed at the National Center for Computation Hydroscience and Engineering at the University of Mississippi, CCHE2D is a two-dimensional depth averaged unsteady flow and sediment transport model. CCHE2D simulates the movement of water, and both cohesive and non-cohesive sediment. Flow modeling is based on depth-averaged Navier-Stokes equations, while sediment transport is modeled as total load by solving the depth-averaged convection-diffusion equation of the suspended sediment load, and the continuity equation of bed load. The system of equations is discretized using the Efficient Element Method, a finite element method described by Wang and Hu (1992). Detailed description of the solution method can be found in the CCHE2D Technical Manual (Jia and Wang, 2001a). The model provides user options in the sediment transport description. Five sediment transport formulas are available; Wu et al. (2000) bed-load formula, Wu et al., (2000) bed-material load formula, Modified Ackers–White bed-material formula (Proffit and Sutherland, 1983), Modified

Engelund–Hansen bed-material load formula (Engelund and Hansen, 1967) and SEDTRA module (Garbrecht et al., 1995) for bed-material load. The SEDTRA module (Garbrecht et al., 1995) uses three transport relations for different size classes. The Laursen (1958) formula is used for size classes 0.010 millimeter (mm) to 0.25 mm, the Yang (1973) formula for size classes from 0.25 mm to 2.0 mm, and the Meyer-Peter and Mueller’s (1948) formula for size classes from 2.0 mm to 50.0 mm. There are three methods for estimating Manning’s roughness coefficient: users defined value, movable bed roughness formula of Wu and Wang (1999) and that of Van Rijn (1986). The formulas can be applied to steady or unsteady flow boundary conditions. The developers of CCHE2D state that the model is developed for application to the study of unsteady, turbulent, free surface open channel flow and sediment transport problems in channels with highly irregular topography (Jia and Wang, 2001b). CCHE2D is well suited to application to the Basin for a number of reasons:

1. the model strictly enforces mass conservation, a property that leads to more reliable and accurate results.
2. the model is capable of representing transience in the flow and sediment boundary conditions for multiple inlets and outlets.
3. wetting and drying of the simulated domain is represented.
4. the model can simulate mixed flow, representing both subcritical and supercritical flow in a channel reach.
5. secondary flow in bends affects direction of bed shear and mean flow; the sediment module includes the curvature effects for enhanced representation of sediment transport in bends.
6. bed roughness is updated within the model as simulations progress, to account for the effect of sediment grain size and bed form on bed roughness.

UCDJ AHL reports that calibration and validation simulations performed by numerous authors reinforce the applicability of the CCHE2D model to the Basin (Jia and Wang, 2001b; De Vriend, 1999; Rajaratnam and Ahmadi, 1981; Soni, 1981; Newton, 1951; Jia and Wang, 2001a; Xu et al., 2001). UCDJ AHL further identified a number of investigations performed by parties unaffiliated with the development of CCHE2D to verify use of CCHE2D as a 2-dimensional flow and sediment transport model and the application of CCHE2D to the Basin (Kantoush et al., 2008; Mohanty et al., 2012; Huang, 2007; Negm et al., 2010). Summaries of these simulations and investigations are provided in UCDJ AHL’s 2014 Progress Report (UCD, 2014).

To calibrate and validate the 2-dimensional flow and sediment conditions within the Basin, a flow measurement campaign was initiated by the UCDJ AHL. Dr. Ali Ercan and Dr. Kara Carr attended the formal USGS training course, “Streamflow Measurement using ADCP’s in November 2013 and UCD purchased a StreamPro Acoustic Doppler Current Profiler (ADCP) with all necessary components and

software, boat and boating equipment, trailer, and suitable laptop. UCD performed trial measurements utilizing the equipment in December 2013, but the lack of large storms following these trials prevented the collection of any additional flow and sediment measurements in the Basin in 2013. When flow is present in the Basin, north of the low flow channel, flow velocity will be measured by UCDJ AHL with the ADCP. UCDJ AHL personnel will determine the number and route of sampling transect locations based on existing flow and inundation conditions. A global positioning system (GPS) mounted on the ADCP unit will allow for recognition of sampling locations and application of collected data to calibration and validation of the two-dimensional flow and sediment discharge model.

### 2.2.1 CCHE2D Model Simulation Results

UCD performed CCHE2D numerical flow simulations of the creek and Basin from Cache Creek at Yolo to the outlets of the Basin. Simulations were initiated, calibrated and validated for observed flows up to 15,000 cfs. Mesh generation is the initial step in simulating flow and sediment transport, and is an integral and time consuming component of successful numerical simulation. To adequately describe the topography, and accurately represent the hydrodynamics of the Basin a dense mesh was created, which optimized accuracy without sacrificing computational time required for each simulation. UCD opined that the Yolo gauge represented a better upstream boundary condition for the Basin simulations than Road 102 based on a more robust historical record and a considerable number of sediment measurements with concurrent flow measurements for Cache Creek at Yolo. Therefore, UCD extended the simulation area of the CCHE2D Basin model to include Cache Creek at Yolo. The computational domain is composed of about 15,400 computational nodes from Cache Creek at Yolo to Road 102 and about 60,013 computational nodes from Road 102 to the overflow weir. More than 75,000 nodes comprise the entire computational domain. The complex bathymetry and the flow dynamics in the training channel and in the Basin make it necessary to have such dense computational nodes.

The simulations utilized inflow boundary data taken from instantaneous flow data at the Cache Creek at Yolo gauge (source: <http://nwis.waterdata.usgs.gov>, USGS 11452500) from March 18, 2011, through March 22, 2011. The simulations also utilized rating table boundary conditions at the overflow weir, as provided by USGS (Brazelton, W. 2010 "Rating Curve for Cache Creek Settling Basin Weir") and at the low-flow outlet culvert box of the low-flow channel (source: <http://nwis.waterdata.usgs.gov>, USGS 11452900).

#### 2.2.1.1 Calibration by 18-22 March 2011 Event at Road 102

Correct specification of parameters such as; time step, turbulence model, wall slipness, bed roughness and bed sediment grain size are essential to accurate representation of field conditions. CCHE2D requires that bed grain size distribution be defined by specifying the D16, D50 and D90 sediment sizes. The model also allows either user specified bed roughness, or to select one of two bed roughness formulae (Wu and Wang, 1999 and van Rijn 1986) which calculate roughness as a function of the grain size distribution.

UCD performed sensitivity analyses to assess what bed roughness method and sediment grain size distribution should be applied when simulating the Basin. Simulations were run for each of the two bed roughness formulae, and different specified values of bed roughness. Results of the simulations at Road 102 were compared to measured water surface elevation values provided by USGS (B. Brazelton, personal communication, November 4, 2011). Based on these simulations, UCDJ AHL selected the Wu and Wang (1999) solution of bed roughness for application to the Basin as it provided the highest level of agreement between the simulated and measured water data. Using a constant roughness value for all flow conditions is not realistic for the Basin’s dynamic flow conditions. Moreover, bed elevation is changing due to deposition and erosion in the Basin. The roughness formula of Wu and Wang (1999) considers flow and bed elevation change and utilizes a more realistic roughness value considering the Froude number at each grid node.

Once identified as the most suitable bed roughness method, UCDJ AHL tested the Wu and Wang (1999) formula with three different grain size specifications, to identify sensitivity to grain size and to calibrate model roughness. The three different distributions of grain size, denoted A, B and C, are presented in Table 2.1 below. UCDJ AHL determined that distribution B performs the best.

**Table 2.1 Grain Size Distributions Applied with Wu and Wang (1999) Roughness Simulations.**

Grain Size Distribution	A	B	C
D16 (mm)	0.127	0.254	1.270
D50 (mm)	0.286	0.572	2.861
D90 (mm)	2.293	4.585	22.926

UCDJ AHL selected the CCHE2D model utilizing Wu and Wang (1999) bed roughness method with grain size distribution B as the best solution through the calibration process. This combination was validated for the March 18-22, 2011, flow event by observed water elevations at internal basin station Site C and at the overflow weir (Fig. 2). Moreover, UCDJ AHL validated the entire CCHE2D model of Basin for the March 23-27, 2011, flow event by the observed water elevations at three locations: Road 102, Site C and the overflow weir.

After calibration of the roughness formula by observed water elevations at Road 102 for 18-22 March 2011, simulated water elevations at the overflow weir and at Site C were validated by the observed counterparts.

For the 18-22 March 2011, validation the Basin inlet boundary flow data was taken from instantaneous flow data at the Cache Creek at Yolo gauge (source: <http://nwis.waterdata.usgs.gov>, USGS 11452500) which provides 15-minute flow data. The validation simulation ran from March 18, 2011, 16:45 through March 22, 2011, 20:45 and had recorded discharges up to 15,900 cfs (exceedance probability 41.4-percent). The simulation results along with water surface elevation data provided by USGS (B.

Brazelton, personal communication, November, 4, 2011) at Road 102, Site C in the interior of the Basin, and at the overflow weir are plotted in Figure 3, presented below.

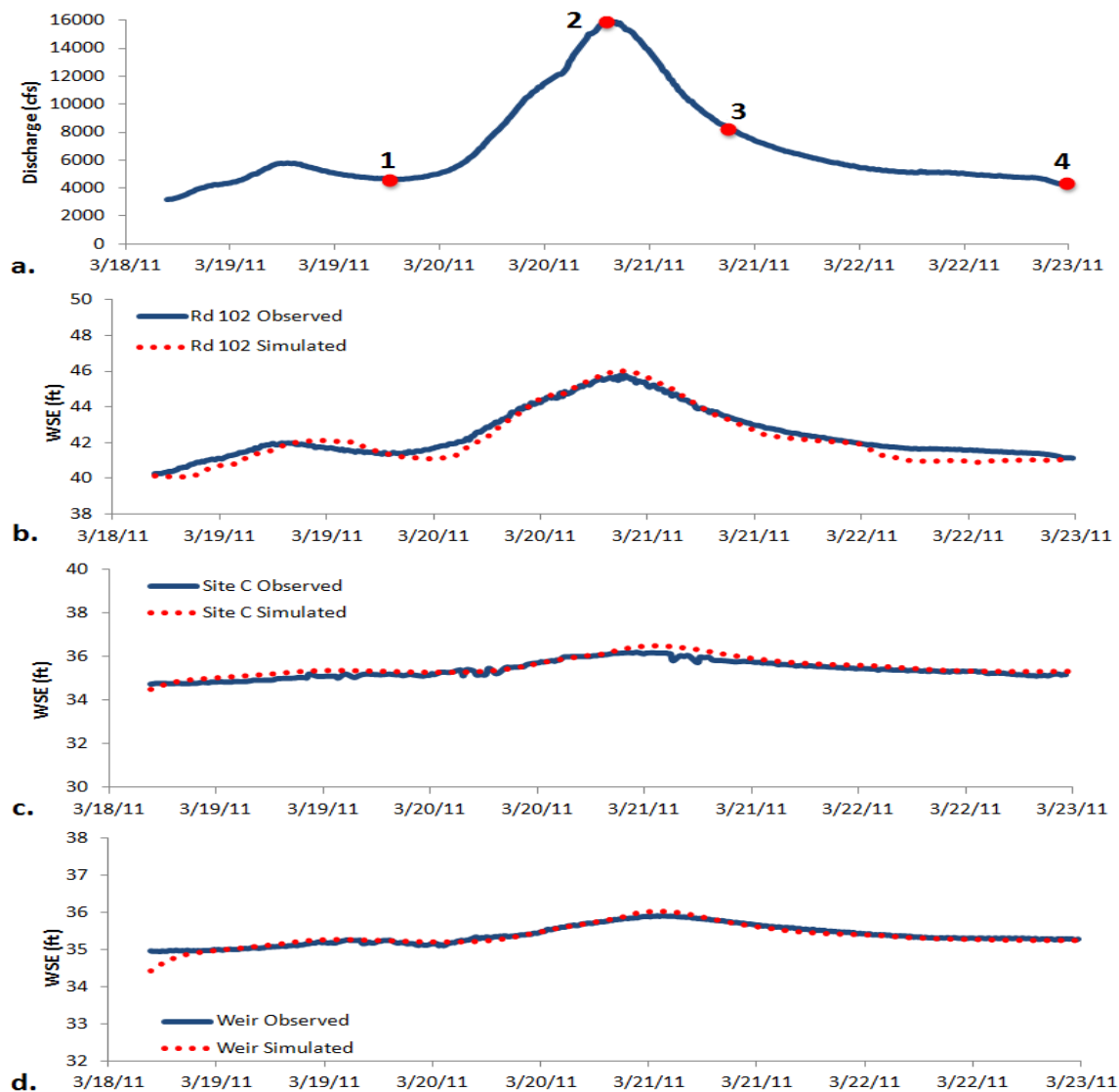


**Figure 3. Comparison Plots of 18-22 March 2011 Simulation:**

(a) Inflow discharge at Cache Creek at Yolo with time steps for results display, (b) Calibrated water surface elevation at Road 102 for entire simulation duration, (c) Water Surface Elevation validation at Site C for entire simulation duration, (d) Water Surface Elevation validation at Overflow Weir for entire simulation duration.

The inflow boundary flow hydrograph is also provided in Figure 3. As shown, there is good agreement between the water surface elevation simulated by CCHE2D and the measured data provided by USGS for each of the validation points: Road 102, Site C, and the overflow weir (Fig.2).

UCD further performed a validation simulation for the full extent of the simulation mesh previously described and for an inflow boundary condition for flow set as discharge at Yolo from March 23, 2011, 04:15 through March 27, 2011, 23:45. This event had a peak flow discharge of 14,300 cfs, a flow with an exceedance probability of 50%. The inflow hydrograph presented in Figure 4 is a storm hydrograph with multiple peaks, the largest of which occurs near the mid-point of the nearly 5-day hydrograph duration (labeled time selection 3). The simulation results are plotted, along with water surface elevation data collected during the storm event at Road 102, Site C and the Overflow Weir. There is good agreement between modeled and measured water surface elevation data, illustrating that the model is capable of simulating transient flows, and can handle wetting and drying of the Basin as inundation area directly relates to water surface elevation.



**Figure 4. Comparison Plots of 23-27 March 2011, Validation Simulation:**

(a) Inflow discharge at Cache Creek at Yolo with time steps for results display, (b) Water surface elevation validation at Road 102 for entire simulation duration, (c) Water Surface Elevation validation at Site C for entire simulation duration, (d) Water Surface Elevation validation at Overflow Weir for entire simulation duration

In Phase II, the 2-D flow and sediment transport models results were analyzed by UCDJ AHL utilizing the available flow and sediment data available to date, and further data gaps were noted including the observation that further sediment grain size distribution and sediment concentration at the inlet and outlet of the Basin are necessary to support the sediment transport model. As such, the TE values presented in the following text are estimated based on the available sediment rating curve at Cache Creek at Yolo and under the default sediment transport model settings, which will be calibrated and validated when the 2015 Basin survey data (currently being collected) is available. A detailed elevation survey of the Basin is required for calibration of the sediment transport model parameters.

Due to lack of storm events during this study period, UCDJ AHL completed only one visit to collect transects of ADCP flow velocity measurements in which they chose eight transect locations based on accessibility and flow conditions. Simulations of the corresponding flow event are ongoing and these velocity measurements may be utilized in the subsequent modeling efforts.

#### 2.2.1.2 Sediment Transport Simulation Results

Each numerical simulation presented herein was performed by UCDJ AHL using the CCHE2D model. The validated flow model, used in the numerical simulations presented below was briefly described above and is described in detail in the UCD's CCSB Trap Efficiency Study Progress Report dated June 15, 2015 (UCD, 2015). Sediment transport simulations were performed utilizing upstream flow boundary data taken from instantaneous flow data at the Cache Creek at Yolo gauge from March 18, 2011, through March 22, 2011. These data correspond to the flow validation simulation that has the highest available flow magnitude fully simulated by the model. The simulations are not calibrated with respect to sediment transport, and therefore results summarized herein are preliminary, and subject to change following sediment transport calibration and validation.

Sediment loading conditions for the simulations were assigned using the total sediment load rating curve developed by USACE and described in the 1997 HEC-6 Analysis Technical Memorandum (USACE, 1997). Because of limited available sediment data at higher flow rate, there is inherent uncertainty in the rating curve regression for flows larger than 10,000 cfs. Also, the USACE curve provides a single sediment load per discharge magnitude, without reference to time of occurrence (rising or falling limb), introducing additional uncertainty. Typically sediment loads are higher on the rising limb of a hydrograph than for sediment loads for an equivalent discharge on the falling limb. The averaging effect of disregarding the time-signature for data used in the curve introduces error, especially in simulations of Cache Creek where duration of the storm event is short, and the flow changes rapidly. Long-term simulations are less sensitive to this averaging effect.

The resulting sediment load hydrograph for the numerical simulations is provided below in Figure 5.

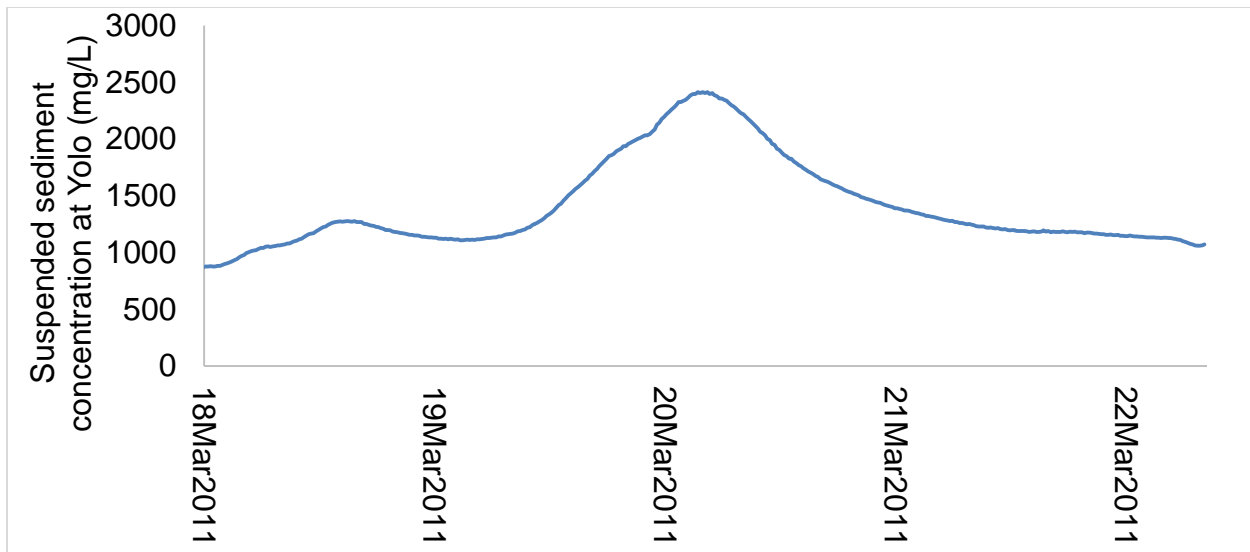


**Figure 5. Upstream Sediment Boundary Condition for all Modeled Sediment Transport Scenarios.**

Utilizing the CCHE2D model under the upstream boundary conditions described above, UCDJAHL ran simulations for the “current” bathymetric conditions of Cache Creek from Cache Creek at Yolo through the Basin for 18-22 March 2011 period. The current condition is defined by surveys taken in 2006 and 2008.

A sensitivity analysis was run on the uncalibrated model to assess the reaction of CCHE2D to sediment transport parameters. The TE was calculated under three different scenarios. Scenario A uses the default sediment transport parameters of CCHE2D. The model defaults the suspended transport capacity coefficient (STCC) to 1.0, and the sediment transport capacity equation to that described by the Wu, Wang, Jia method (Wu, 2001). Scenario B sets the STCC to 0.9, and as Scenario A, uses the Wu, Wang, Jia method. Scenario B therefore has a sediment transport capacity that is 90% of that for Scenario A. Scenario C was run with the STCC set to 1.0, and the SEDTRA sediment transport capacity equation was assigned. For each simulation, the sediment bed grain size, and roughness solution method were set as outlined previously. Trapping efficiencies for the three different simulated scenarios of sediment transport under the current condition are provided in Table 2.2.

**Table 2.2 Sediment Trapping Efficiency under the Current Bathymetric Condition for Three Scenarios of CCHE2D Parameter Definition.**

Scenario	Suspended Transport Capacity Coefficient	Sediment Transport Equation	Sediment Trapping Efficiency
A	1.0	Wu, Wang, Jia method	47.0%
B	0.9	Wu, Wang, Jia method	62.6%
C	1.0	SEDTRA	65.8%

UCDJAHL calculated the TE by determining the difference in the sediment inflow volume entering the Basin at Road 102 and that exiting the Basin, over the entire simulation duration. When the STCC was altered from the default of 1.0 to 0.9, the TE changed; increasing by 15.6%. When the SEDTRA sediment transport equation was utilized instead of the default equation, the TE increased by 18.8%. The sensitivity analysis to select the STCC and the sediment transport equation demonstrate the significance of the calibration and validation of the sediment transport modeling. The uncertainty and variability of the sediment TE estimates can be limited by calibration and validation of the sediment transport module of the CCHE2D model.

### **2.3 Basin Modification Simulations**

UCDJAHL ran simulations for the current condition, and three additional bathymetric conditions within the Basin. The current bathymetry, as defined by 2006 and 2008 surveys of the Basin, is denoted Alternative A. Alternative B raises the weir 6 ft (1.8 m), from its current elevation of 32.5 feet, to 38.5 feet, but does not otherwise change the bathymetry of the Basin. Alternative C removes a 400-foot (122 m) section from the terminus of the training levee, but does not otherwise change the bathymetry of the Basin. Alternative D is the combination of Alternatives B and C, such that the weir is raised 6 ft (1.8 m), and the lower 400-foot (122 m) section of training levee is removed. Each alteration scenario was run with the default parameters of the model (SSTC of 1.0; sediment transport capacity equation of Wu, Wang, Jia method (Wu, 2001)) such that they may be compared relative to each other.

#### **2.3.1 Alternative A – Baseline Condition**

As noted above, the simulated TE of the Basin for Alternative A, was most conservatively found to be 47%.

### 2.3.2 Alternative B – Weir Raise Condition

UCDJAHL reported the simulated TE of Alternative B, in which the overflow weir is raised 6 ft (1.8 m) at 72.8%. The relative increase in TE, for this basin modification compared to the current condition is nearly 26%. The simulation showed that this condition will result in higher bed load transport across the southern portion of the Basin. Based on this simulation the suspended sediment concentration is low in the northern portion of the Basin for the duration of the flow event. The simulation suggests that relative to the current bathymetry, raising the weir will enhance sediment TE, but less sediment will be transported to the northern portion of the Basin.

### 2.3.3 Alternative C – Training Levee Notching Condition

The simulated TE for Alternative C, in which 400 ft (122 m) of training levee is removed from the downstream end, was reported by UCDJAHL to be 48.6%. The 1.6% increase from the current condition suggests that notching just this initial section of training levee will not significantly alter sediment dynamics and sediment retention within the Basin. The simulation showed that both the bedload and suspended sediment concentration are altered when compared to the current condition. The slight increase in bedload transport rate in the northern portion of the Basin is more obvious than that in the southern portion; however, there is a slight increase in bedload transport over the entire simulation domain. The same pattern of increase is seen for suspended sediment concentration.

### 2.3.4 Alternative D – Weir Raise and Training Levee Notching Condition

UCDJAHL reported the simulated TE for Alternative D, in which 400 ft (122 m) of training levee are removed from the downstream end and the weir is raised 6 ft (1.8 m), to be 75.3%. Again the alteration of the weir elevation has a significant effect on sediment retention. Comparison of Alternative D and Alternative B (raised weir alone) shows that there is a 2.5% increase in sediment retention when the terminus of the training levee is notched in addition to the weir being raised. Comparing Alternative D to the current condition shows a 28.3% increase in TE. As with Alternative B, there is a clear band of bed load transport across the southern portion of the Basin, whereas the suspended sediment concentration is more uniformly distributed.

### 3 MERCURY LOAD DETERMINATION STUDY (USGS)

Under contract to DWR, the USGS has monitored the streamgages at the inflow, low-flow outflow gate, and overflow weir of the Basin for discharge and suspended sediment (SS) concentration since January 2009. The USGS initiated water-quality sampling and analysis of THg, MeHg, “reactive” (stannous-chloride-reducible) mercury (RHg(II)), dissolved organic carbon (DOC) concentration, and grain-size distribution in SS of Basin inflows and outflows in January 2010 and further initiated continuous monitoring of turbidity with in-situ probes to provide data on temporal variation in SS concentration, especially during storm events. The USGS further assessed spatial and temporal variations in bed-sediment THg, MeHg, and RHg(II) concentrations at selected riparian and agricultural sites within the Basin beginning in 2010. The streamgages at Rumsey were added to the monitoring program in October 2014. Streamgage and surface water sampling locations are shown on Figure 2. Streamflow and sediment data are available at: <http://waterdata.usgs.gov>.

The USGS water year extends from October through September thus, for example the 2010 water year (WY2010) represents the months October 2009 through September 2010, etc. Since May 2011, the USGS has provided DWR with Annual Progress Reports summarizing their data collection and analyses activities performed in association with the Basin and in November 2015, the USGS provided DWR with the draft USGS Scientific Investigations Report (SIR) titled *Mercury Studies in the Cache Creek Settling Basin, Yolo County, California: Preliminary Results, 2010-14* (USGS, 2015). The report includes preliminary results of the USGS Hg investigations at the Basin during Water Years 2010–14 and a discussion of the implications of the results with regard to management of the Basin. The significant methodology and findings presented in the USGS SIR are summarized in the following paragraphs and the report is included in its entirety as Appendix B.

The objectives of the USGS Hg studies at the Basin are described in three categories: (1) Inflows and Outflows: Determine concentrations and loads of THg and MeHg in water flowing into and out of the Basin and compute TE of the Basin with regard to these and other constituents; (2) In-basin Surficial Processes: Assess the spatial variability of THg and MeHg in sediment, biota, and surface water among dominant habitat types within the Basin, with the goal of improving the understanding of Hg methylation and MeHg bioaccumulation; and (3) Subsurface Properties: Determine the vertical variability of THg concentration in deep sediment cores (to a depth of about 30 feet (9.1 meters) below land surface) and identify potential layers of high concentration that could be affected by future excavation.

Mercury sampling of the inflow and outflows of the Basin began in January 2010 with the first flows of Water Year 2010 and is ongoing. For this Report of Findings, the USGS has provided data from five water years, WY2010 through WY2014. However, because WY2014 was critically dry, there was essentially no surface water flow into or out of the Basin. This report also contains data for surficial sediment (0–2 cm depth) that was sampled on a reconnaissance basis at approximately 8 locations within the Basin on six occasions during 2010–12, followed by more detailed sampling at 90 locations on two occasions during 2013. Results of Hg bioaccumulation studies of fish and bird eggs that were sampled

during 2012 and 2013 are also provided, along with results of water-quality sampling within the Basin that was done during March–April 2013 in conjunction with a caged-fish experiment.

### **3.1 Sediment Loading Calculations**

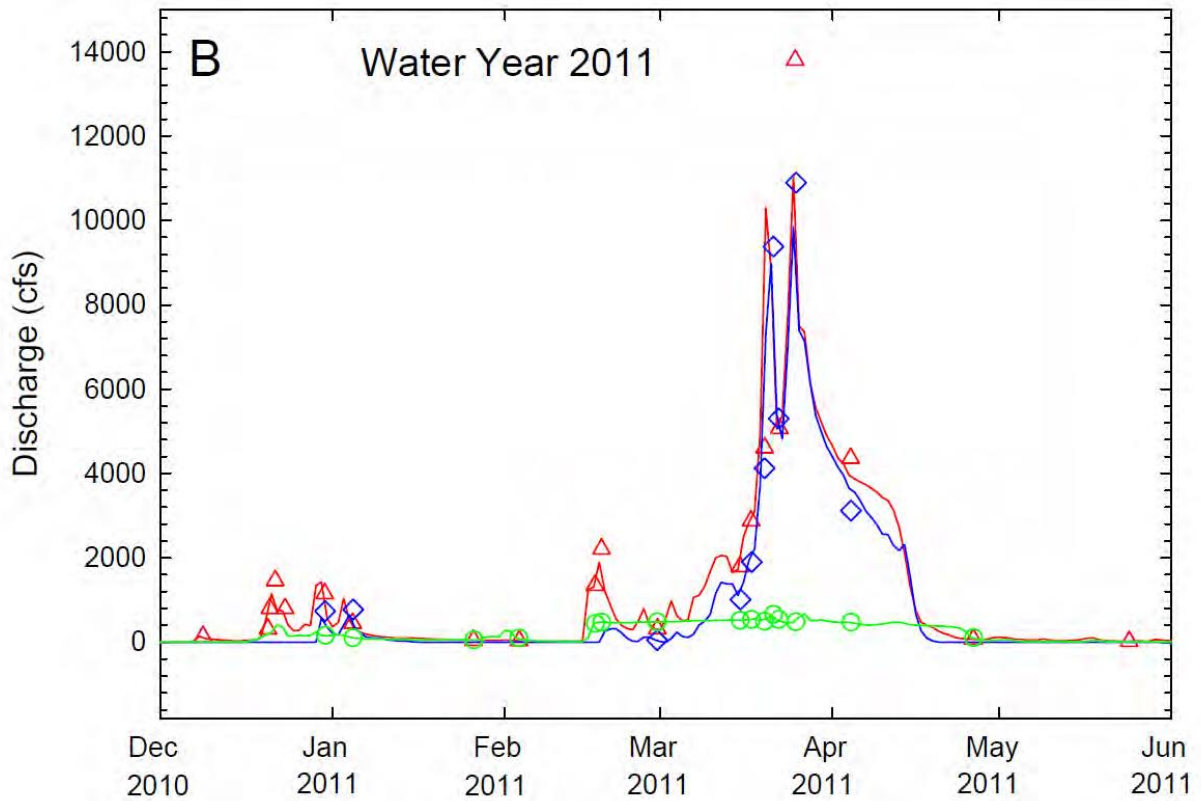
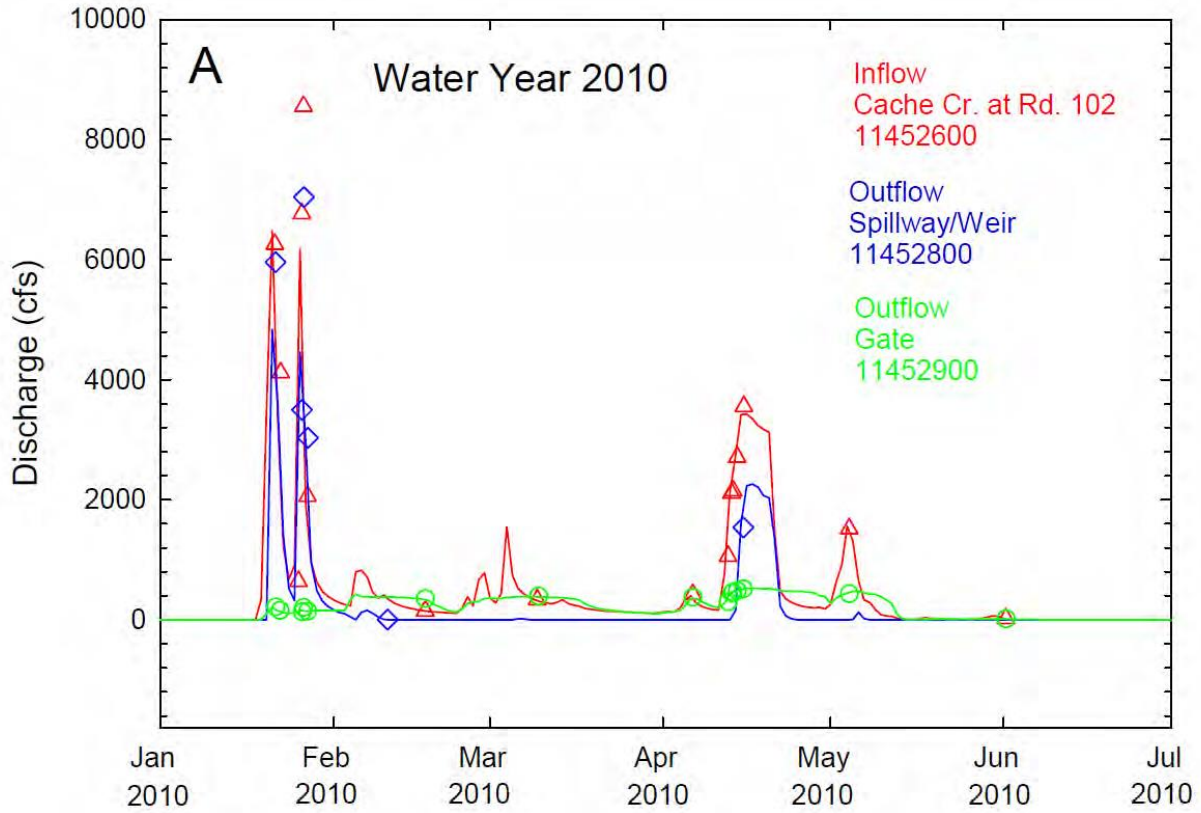
The USGS study was designed to address the objectives described above. As such, the following paragraphs are organized into three subsections to reflect the main objective categories: 1) Inflows and Outflows, (2) In-basin Surficial Processes, and (3) Subsurface Properties. Additional details regarding sampling and analytical methodology, quality assurance protocol and statistical approaches for data analysis are presented in the draft USGS SIR (USGS, 2015) included as Appendix B.

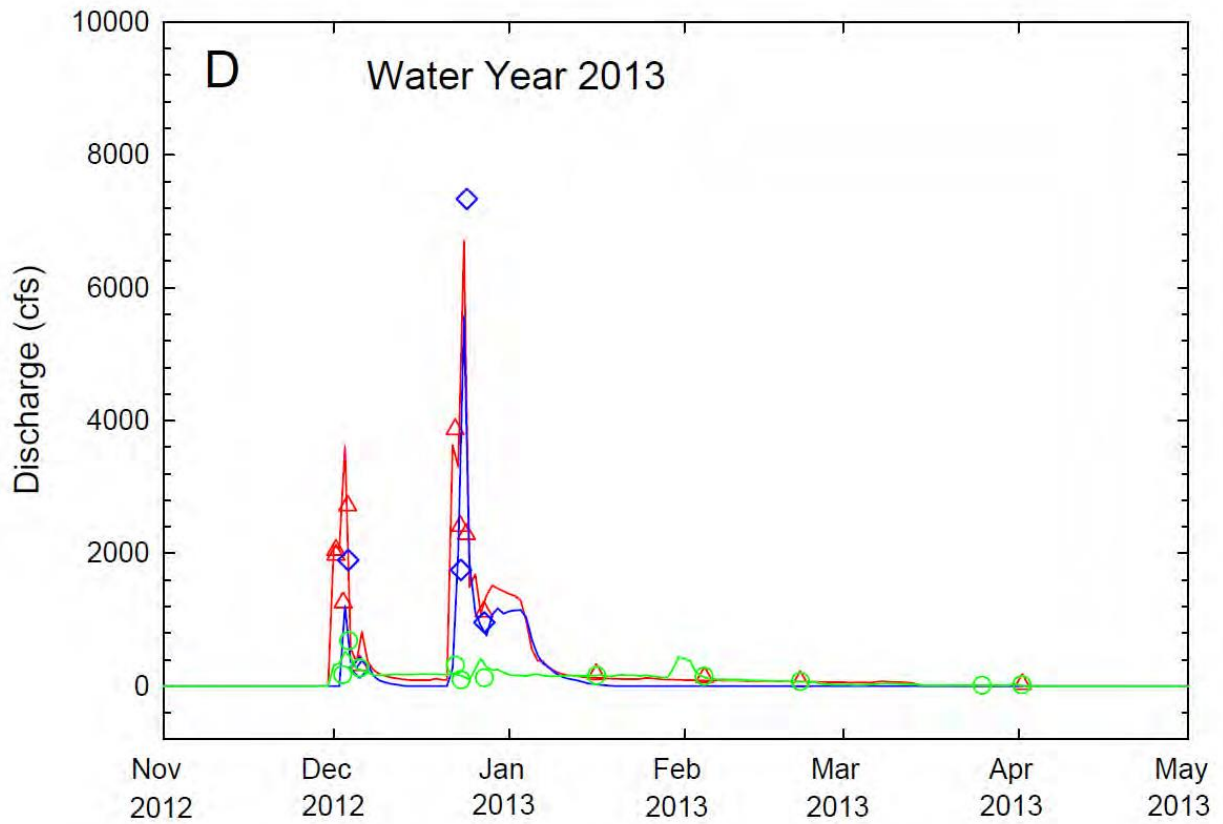
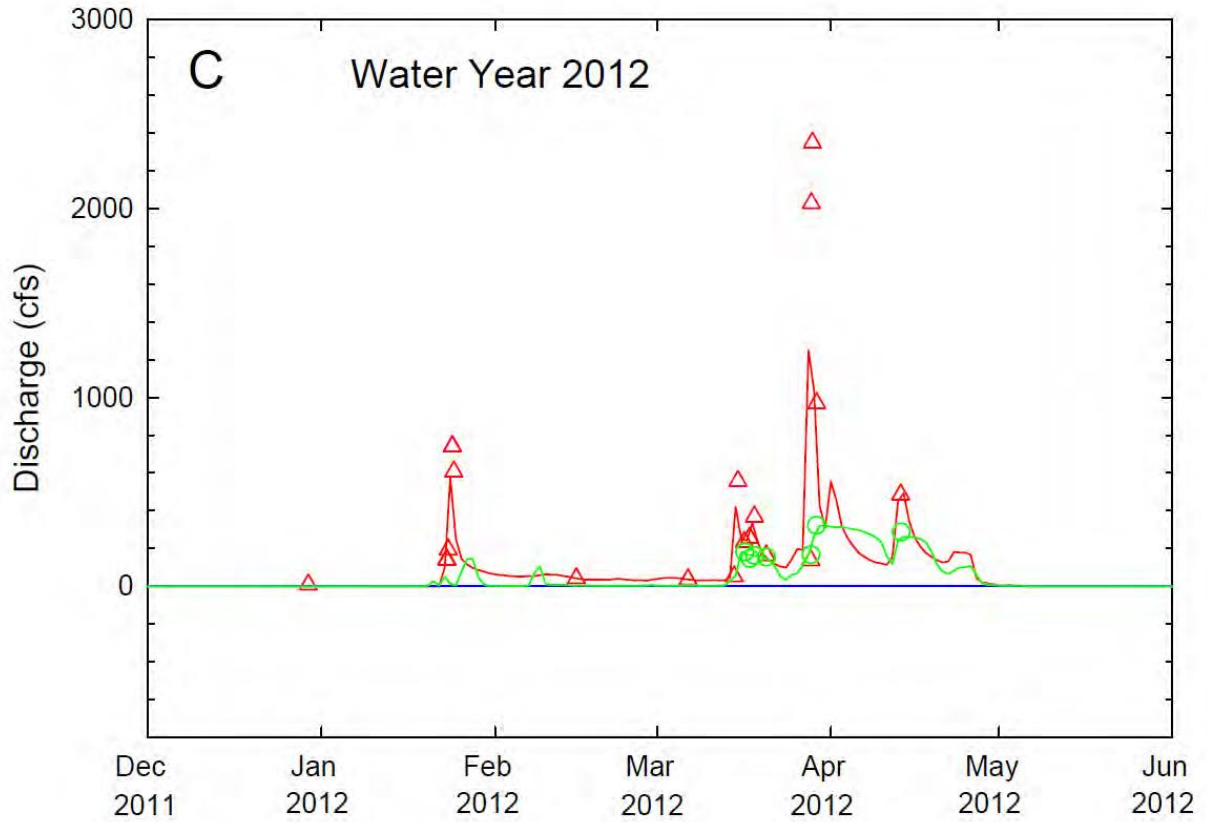
#### **3.1.1 Inflows and Outflows**

The USGS sampled inflows to the Basin from Cache Creek at the Road 102 Bridge, approximately 3 miles (4.8 kilometers (km)) north of Woodland, California (Fig. 2). The USGS sampled outflows from the Basin at three locations: (1) the low-flow outlet gate (station 11452900), (2) the south abutment of the outflow weir (station 11452800), and (3) the north abutment of the outflow weir (station 384115121402501) (Fig. 2). Typically the low-flow outlet gate is closed during duck season (December and January) and is open during the rest of the wet season (M. Hall, Conaway Ranch, oral communication). Discharge over the outflow weir is uncontrolled, and consists of outflows that exceed the capacity of the low-flow outlet gate.

Flows of Cache Creek into and out of the Basin are intermittent. During the study period described in this Report (Water Years 2010–14), inflows to the Basin typically ran for about five months per year during the winter and spring seasons with the exception of Water Year 2013, which had very little flow into or out the Basin after February 2013, and critically dry Water Year 2014, when there was essentially no flow into or out of the Basin. In Hydrographs (Figures A through D below) showing the inflows and outflows of the Basin it can be seen that the storm flows into the Basin typically have higher peaks than the outflows, which have somewhat broader peaks.

The USGS collected water-quality samples during baseline conditions (between storm events) at an interval of about three weeks. During storm events, an effort was made to collect samples on the rising limb, peak, and falling limb of each major storm pulse. Sampling at the Inflow station (11452600) was limited to daylight hours because of safety concerns. It was not feasible to install an autosampler at this location because of the slope of the bank and a restriction imposed by Yolo County on modifying the Road 102 bridge; resulting in some peaks not being sampled. The distribution of water-quality samples relative to the hydrograph at the Inflow and Outflow sites for Water Years 2010-13 is shown in Figures A through D.





The USGS reported that the values of particulate total mercury (pTHg) in Basin inflows span three orders of magnitude, ranging from 0.65 nanograms per liter (ng/L) to 707 ng/L (Table 6, USGS, 2015). Values of particulate methylmercury (pMeHg) in the inflows ranged from 0.02 to 4.4 ng/L, approximately two and one-half orders of magnitude. There is a systematic shift in values of %pMeHg (percent particulate MeHg relative to THg) from values greater than 1% at lower pTHg and pMeHg concentrations to values less than 1% at higher concentrations. Similar trends are evident for the outflow sampling locations. Samples from the within-basin locations tended to have higher values of %pMeHg than either the inflows or the outflows. Filtered water samples had a narrower range of concentration, less than two orders of magnitude for both filtered total mercury (fTHg) and filtered methyl mercury (fMeHg). Values of %fMeHg (percent filtered MeHg relative to THg) spanned a similar range as those for %pMeHg, from less than 1% to greater than 10%. Similarly, the water samples taken within the Basin had higher values of %fMeHg than those from the inflow or the outflow sites.

The USGS also concluded that the pTHg concentrations correlate well with suspended sediment concentration (SSC). There was little to no change apparent in the concentration of THg on suspended particles as a function of either SSC or pTHg. Average concentrations of gravimetric values for pTHg (pTHg-g) were 255 nanograms per gram (ng/g) dry weight (dw) (equivalent parts per billion, (ppb) for the Inflow and 284 ng/g for the Combined Outflow (Table 6, USGS, 2015).

The relationship between pMeHg and SSC is somewhat less robust than that between pTHg and SSC, but nevertheless the correlations are nearly as strong for the Inflow and Combined Outflow data. The values of pMeHg were higher for a given value of SSC at the low-flow Outflow Gate than the other sampling locations. This is consistent with a higher mean value of gravimetric values for pMeHg (pMeHg-g) at the low-flow Outflow Gate (8.3 ng/g, Table 6, USGS, 2015) compared with values of 4.3 ng/g at the Outflow Weir and 5.3 ng/g for the Inflow. The USGS reported that higher concentrations of pMeHg (for example, greater than 10 ng/g) are favored at lower SSC and lower flow conditions.

### **3.2 Summary of Within-Basin Surficial Processes**

Habitats within the Basin include main-channel streambed habitat, woody riparian zones along the stream channels, floodplains (woody, non-woody, and tule wetland), irrigation canals, and various agricultural fields. The study is designed to examine the influence of habitat features on mercury methylation and bioaccumulation by analyzing samples of sediment, surface water, caged fish, wild fish, and bird eggs. The USGS sampled sediment from different habitats within the Basin over several different seasons, whereas surface-water sampling was done primarily during a single sampling event, coincident with a caged-fish experiment during March–April 2013.

During 2010–12, the USGS collected surface sediment samples (0–2 cm depth) during six sampling events. Each sampling event accessed 7 to 8 of the 10 selected locations. Four of the sites were located in the western part of the Basin (sites WT-1 through WT-4, Figure 6A) and six of the sites were located in the eastern part of the Basin (sites ET-1A through ET-5). These sites were sampled during a variety of

CCSB Mercury  
Control Studies  
Report of Findings



Division of Flood  
Management  
Flood Maintenance  
Office

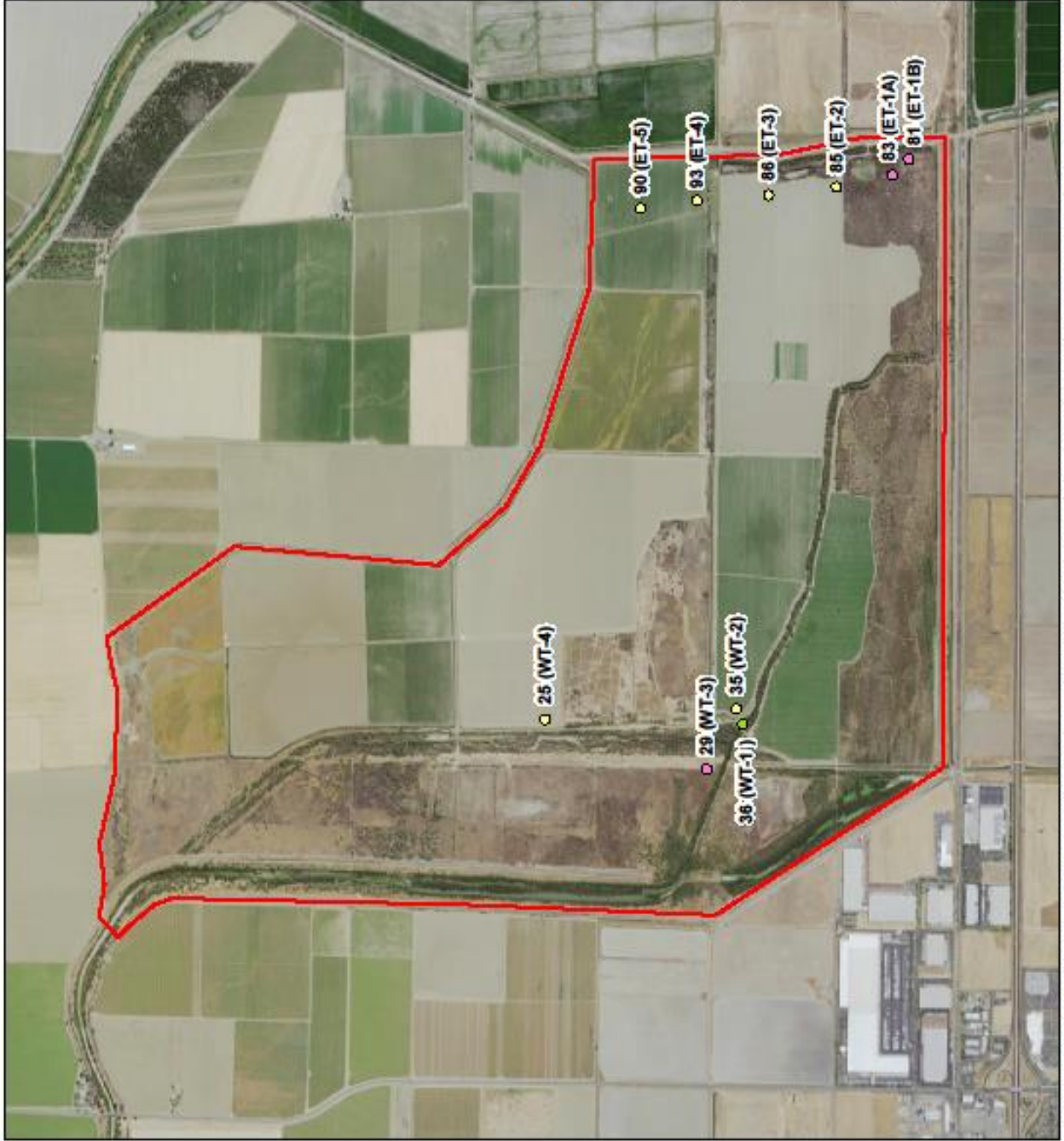
- Project Footprint
- Land Use - Sub-Habitat**
- Agriculture - corn
- Floodplain - mixed non-woody
- Riparian - mixed woody

**USGS SURFACE SEDIMENT  
SAMPLE LOCATIONS  
2010 - 2012**

Figure 6A  
Cache Creek Settling Basin  
Yolo County, CA



Date: November 20, 2015  
Prepared By: Kristin Jacobs  
Document Path: G:\Projects\Cache  
Creek\_Setting\_Basin\Mercury\_Study\2015\_CCBB\_6A\_Sediment10\_12.mxd



seasonal conditions as a reconnaissance effort to investigate whether difference would be observed in various chemical parameters between agricultural and non-agricultural soils, and between the western and eastern parts of the Basin. The shallow sediment samples were analyzed for THg, MeHg, RHg(II), loss on ignition (LOI, a measure of organic content), total reduced sulfur (TRS), iron (Fe) species, bulk density, and porosity. The Fe species included acid-extractable ferrous iron [(FeII)<sub>AE</sub>], amorphous to poorly crystalline ferric iron [Fe(III)a], and crystalline ferric iron [Fe(III)c]; the sum of these analyses is considered to represent total iron (Fe<sub>T</sub>). Water content was determined so that constituents could be reported on a dry weight basis.

The data from 2010–12 showed that there were strong differences between agricultural and non-agricultural land uses for many of the parameters measured, as well as some east-west differences. As a result, the USGS initiated a more comprehensive sediment sampling effort starting in early 2013 utilizing 90 sites representing the principal habitats within the Basin and providing better spatial coverage (Figure 6B). The 90 sites include: 18 sites in the Cache Creek streambed (9 locations, each duplicated); 22 riparian sites (most in pairs on left and right banks, adjacent to the stream channel); 13 woody floodplain sites; 9 non-woody floodplain sites; 6 mowed floodplain sites (adjacent to levees); 8 tule floodplain sites; and 14 agricultural sites. Most of the agricultural sites were planted in forage corn during 2010-13. During 2013, two of the 14 fields were planted in tomatoes, the other 12 in corn or mixed corn and pumpkins. The 90 sites were first sampled for shallow sediment (0–2 cm depth) during February–March 2013 and then again during May 2013. The same constituents were analyzed as during the 2010–12 shallow sediment sampling events. Selected sites were also sampled for sediment pore water, which was analyzed for THg, MeHg, TRS, major anions, and DOC. The February–March 2013 sampling period followed a wet period during December 2012 – January 2013, during which time the Basin was flooded. Inflows stopped during late March 2013, and diversion of nearly all flow in Cache Creek at the Capay Dam for irrigation deliveries began on April 1, 2013, earlier in the year than typical because of dry conditions (T. O’Halloran, Yolo County Flood Control and Water Conservation District, oral communication, April, 2013). The same 90 sites were also sampled for shallow sediment (and selected sites for pore water) during October–November 2014 and January through March 2015; results from the 2014 and 2015 sampling events will be reported separately.

During the period from April 2010 thru May 2013, the USGS collected 224 surface sediment (0–2 cm depth) samples from within the Basin, plus 27 field duplicates (at a rate of approximately 10% of environmental samples). The number of samples among the four identified primary land-use categories was as follows: Agricultural (n=58); Floodplain (n= 101); Open Water (n=40); Riparian (n=52). Considering the east-west spatial distribution, the number of samples from the east and west sides of the Basin were n=144 and n=107, respectively.

The USGS also collected pore-water samples over the same sampling period, with the total number varying by analyte as follows: pore-water total mercury (pw[THg]) (n=17, May 2013 only); pore-water methyl mercury (pw[ MeHg]) (n=17, May 2013 only); pore-water hydrogen sulfide (pw[H<sub>2</sub>S]); pore-

CCSB Mercury  
Control Studies  
Report of Findings



Division of Flood  
Management  
Flood Maintenance  
Office

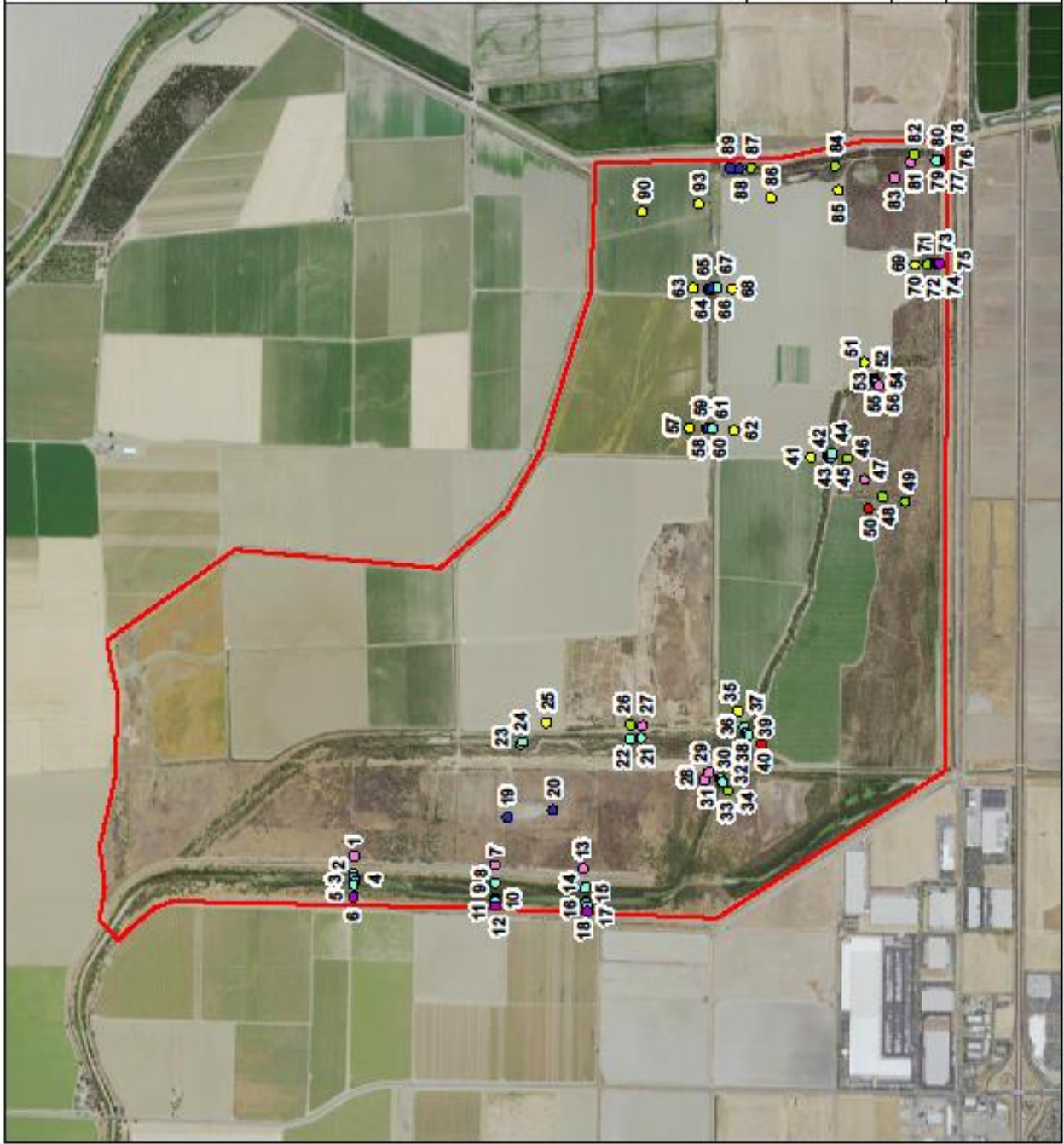
- Project Footprint**
- Land Use - Sub-Habitat**
- Agriculture - corn
  - Agriculture - tomato
  - ◇ Floodplain - mixed non-woody
  - Floodplain - mixed woody
  - Floodplain - mowed
  - Floodplain - tule
  - Open Water - stream
  - Riparian - mixed woody

**USGS SURFACE SEDIMENT  
SAMPLE LOCATIONS  
2013**

Figure 6B  
Cache Creek Settling Basin  
Yolo County, CA



Date: November 20, 2015  
Prepared By: Kristin Jacobs  
Document Path: G:\Project\Cache  
Creek\_Setting\_Basin\Mercury\_Study\2015\_CC\_SB\_6B\_Sediment13.mxd



water sulfate (pw[SO<sub>4</sub><sup>2-</sup>]) and pore-water chloride (pw[Cl<sup>-</sup>]) (each, n=44, February-March and May 2013); and pore-water dissolved organic carbon (pw[DOC]) (n=90, April 2010 thru May 2013). Of the 90 pore-water samples analyzed for DOC, 38 samples (those collected between September 2010 and March 2012) were elutriated (water was added to dry sediment) and 52 (collected during 2013) consisted of naturally occurring pore water.

The USGS utilized a five-step sequential extraction method (Bloom et al., 2003) on surface sediment sampled during May 2013 from 33 sites selected among the four land-use types (Agricultural (n=9), Floodplain (n=8), Open Water (n=8), Riparian (n=8)). This approach was used to assess if the dominant Hg species and the relative availability of the THg pool varied among habitat types.

The USGS designed and conducted a caged fish experiment in the Basin during March-April 2013. Forty cages were deployed (Figure 7) for 31 days, with 30 mosquitofish (*Gambusia affini*) in each cage; four cages were lost to vandalism. Up to 15 fish were analyzed for THg from each of the remaining 36 cages, resulting in 531 caged mosquitofish analyzed for THg. Wild fish were also caught and analyzed for THg at selected sites within the Basin (104 mosquitofish at 13 locations).

The USGS collected bird eggs during 2012–13 from nest boxes that were deployed throughout the Basin (although not in agricultural fields), plus some natural nests. The sampled bird nest locations are shown on Figure 8. Eggs from the following bird species were sampled: house wren (*Troglodytes aedon*); tree swallow (*Tachycineta bicolor*); Bewick's wren (*Thryomanes bewickii*); ash-throated flycatcher (*Myiarchus cinerascens*); marsh wren (*Cistothorus palustris*); and mourning dove (*Zenaida macroura*). Three-hundred-twenty-seven bird eggs were sampled during 2012–13 and analyzed for THg by the USGS laboratory in Dixon, California. Additional bird eggs were collected by USGS within the Basin during 2014 and 2015; results of THg analyses will be reported separately.

During Water Years 2010–12, the USGS collected 28 water-quality samples at selected sites within the Basin to evaluate spatial variability of chlorophyll-a and water quality within the Basin. Each collected sample was analyzed for DOC; selected samples were analyzed for fMeHg, non-filtered MeHg (nfMeHg), and/or chlorophyll-a.

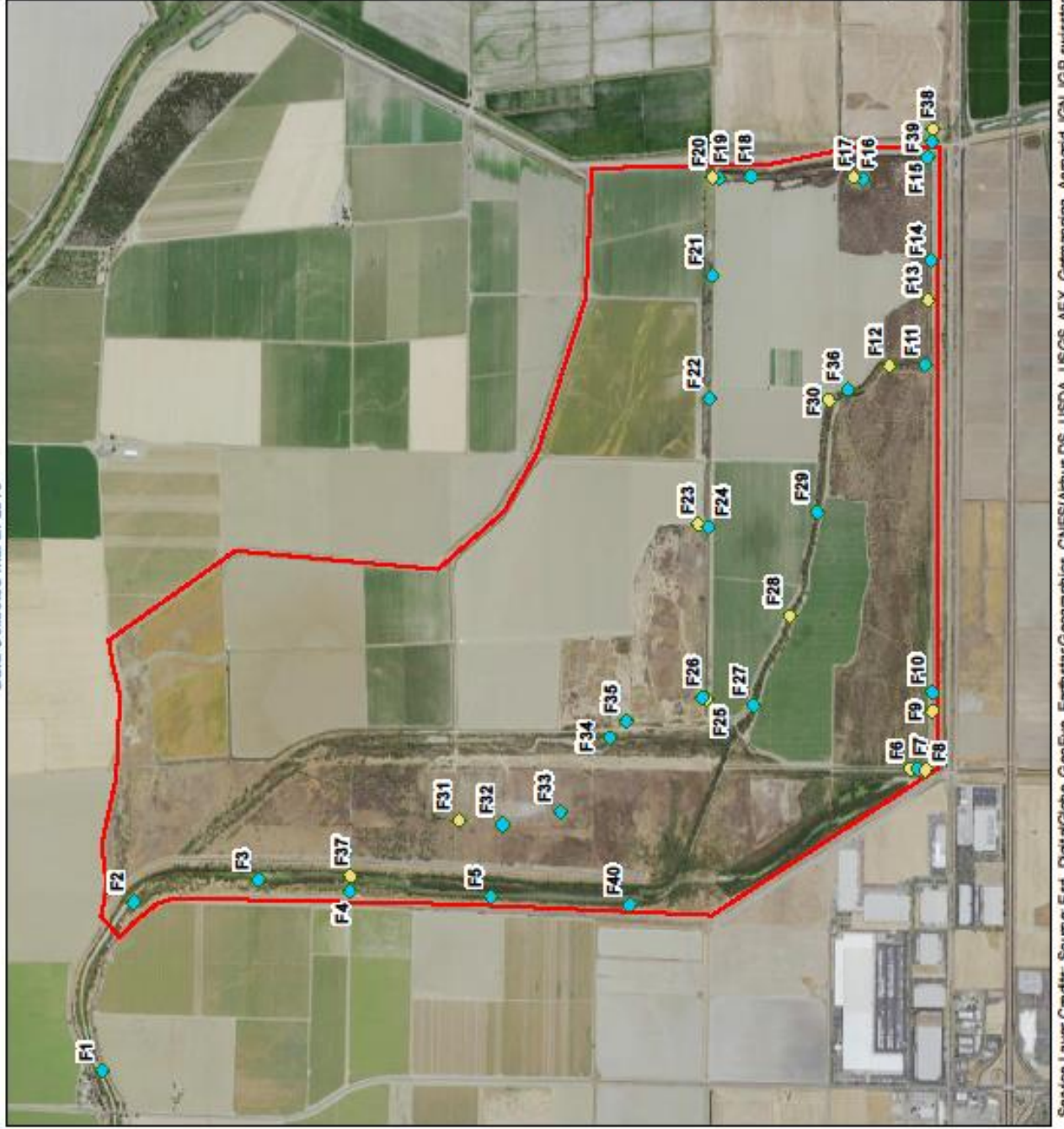
During March–April 2013, the USGS collected water-quality samples at 28 of the 40 fish cages deployed throughout the Basin. These samples were analyzed for fTHg, pTHg, fMeHg, pMeHg, particulate reactive mercury (pRHg(II)), DOC, SS, major anions, and alkalinity.

### **3.3 Subsurface Properties**

The USGS conducted two separate coring campaigns within the Basin, one during 2011 and the other in 2012, resulting in 15 drill sites. The soil core locations are shown on Figure 9. A truck-mounted, hollow-stem auger drill rig was used, to collect intact soil cores in segments up to five ft (152 cm) in length.

During the first coring campaign in September and October 2011, ten locations (sites 1-10, fig. 9) were cored to a depth of about 30 feet (9 meters). Typically, two complete vertical profiles were made at each

Data Collected March 2013



CCSB Mercury  
Control Studies  
Report of Findings



Division of Flood  
Management  
Flood Maintenance  
Office

- Project Footprint
- ◆ Fish Cage
- ◆ Fish Cage with  
Water Sample

**FISH CAGE LOCATION MAP**  
Figure 7  
Cache Creek Settling Basin  
Yolo County, CA



Date: November 20, 2015  
Prepared By: Kristin Jacobs  
Document Path: G:\Projects\Cache  
Creek\_Setting\_Basin\Mercury\_Study\  
2015\_CC88\_7\_FishCageMap.mxd

CCSB Mercury  
Control Studies  
Report of Findings



Division of Flood  
Management  
Flood Maintenance  
Office

Project Footprint

**Habitat**

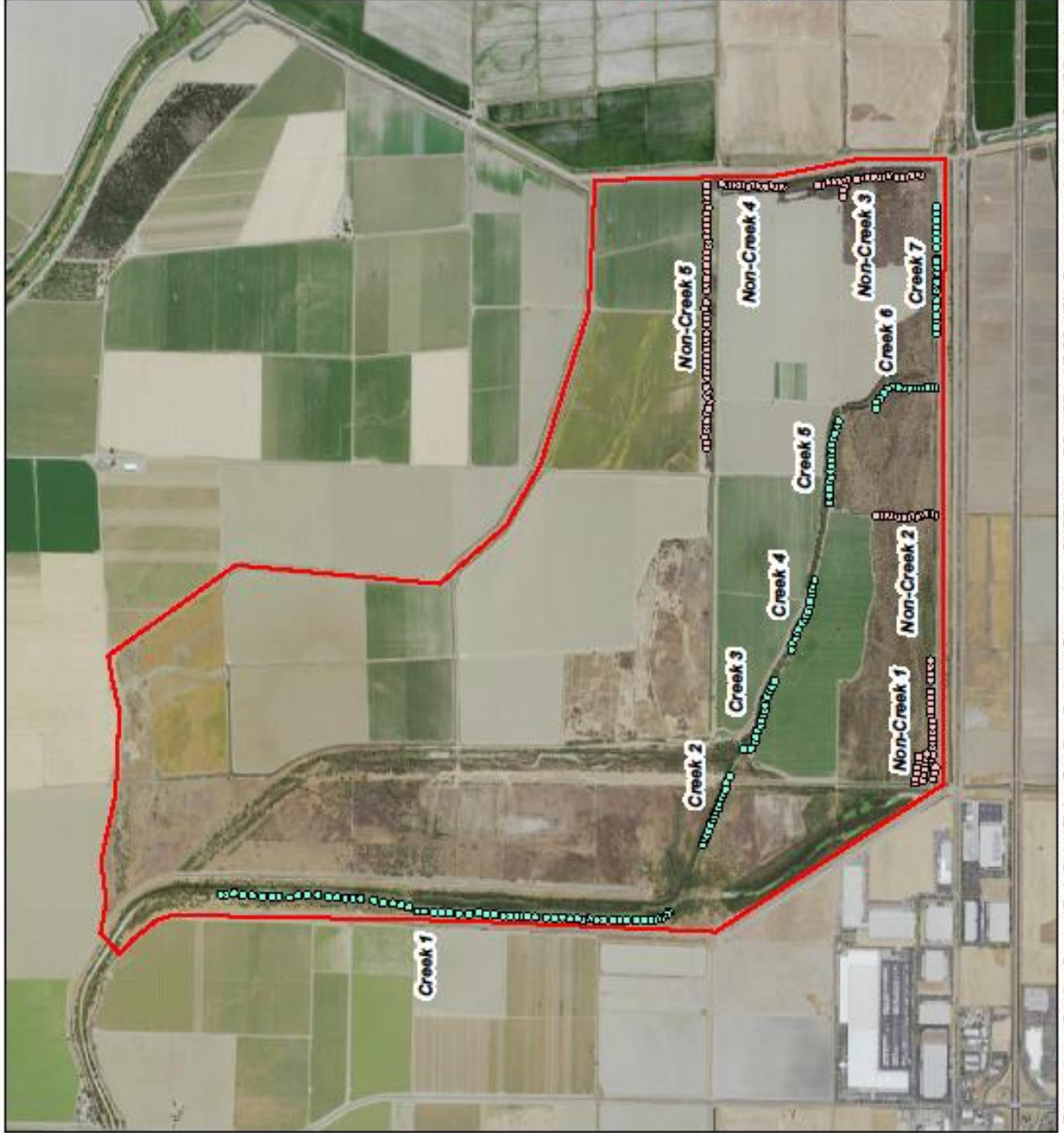
- Non-creek (n=131)
- Creek (n=155)

**BIRD NEST LOCATION MAP**

Figure 8  
Cache Creek Settling Basin  
Yolo County, CA



Date: November 20, 2015  
Prepared By: Kristin Jacobs  
Document Path: G:\Project\Ca che  
Creek\_Setting\_Basin\Mercury\_Study\  
2015\_CC SB\_8\_BirdNestMap.mxd



CCSB Mercury  
Control Studies  
Report of Findings



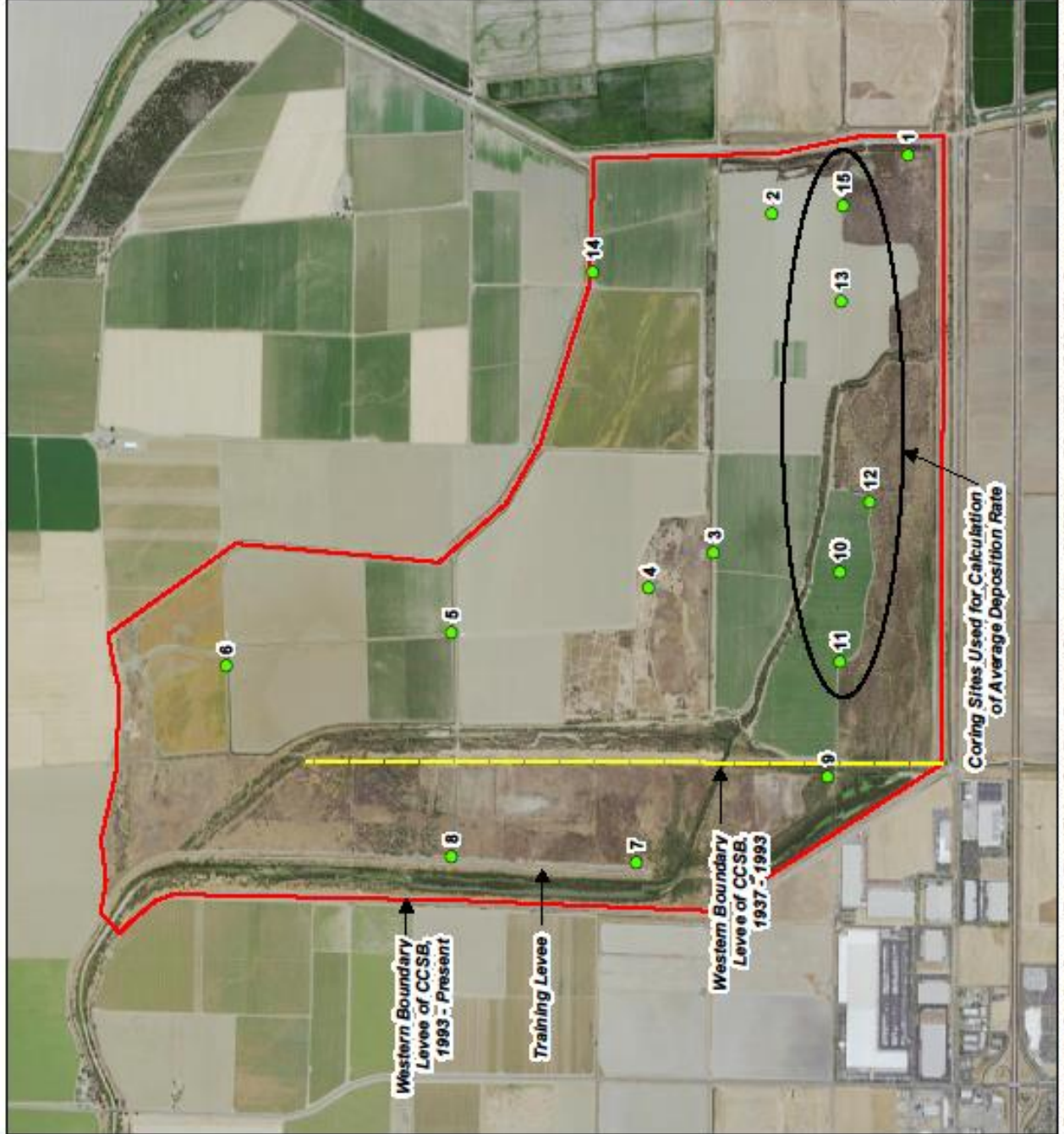
Division of Flood  
Management  
Flood Maintenance  
Office

- Project Footprint
- Borehole

**IN-BASIN DEEP SOIL  
CORE LOCATION MAP**  
Figure 9  
Cache Creek Settling Basin  
Yuba County, CA



Date: November 20, 2015  
Prepared By: Kaitlin Jacobs  
Document Path: G:\Projects\Cache  
Creek\_Setting\_Basin\Mercury\_Study\  
2015\_CC\_SB\_9\_CoreMap.mxd



**Coring Sites Used for Calculation  
of Average Deposition Rate**

site with staggered starting position so that gaps typically associated with the bottom of each cored interval would be covered by continuous sampling in the adjacent core. At drill site 8, only 17 ft (5.2 meters) of core were recovered because of equipment failure. The second coring campaign in August 2012 had five additional locations (sites 11-15, fig. 9). At site, 11, core was recovered to a total depth of 47 ft (14 meters); the other four sites had a total depth of 30 ft (9 meters) as in the 2011 campaign.

Each core was analyzed (prior to splitting) for geophysical properties (density, gamma log, magnetic susceptibility). Selected cores from each site were split, then photographed, described, and subsampled, as described by Arias et al., (in review). At each of the 15 locations, 5 depths were sampled in 8-in (20-cm) composites corresponding to approximately 1, 3, 5, 15, and 25 ft below land surface: approximately 10-30 cm; 70-90 cm; 150-170 cm; 450-470 cm; and 750-750 cm. The 20-cm composite samples were analyzed for THg, MeHg, LOI, TRS, Fe species, and grain-size distribution (by laser-scattering). Seventy six 20-cm composite samples were analyzed.

Detailed sampling was done at 7 of the 15 drill locations by taking 1.2-in (3-cm) subsamples and analyzing them for Cesium-137 (Cs-137), THg, and LOI. The Cs-137 analyses were for the purpose of age dating. The detailed sampling was done at first in an exploratory fashion, with samples taken at various depths to see where Cs-137 was detectable. Once a depth range with detectable Cs-137 was found, detailed samples were filled in to determine the depth of the highest Cs-137 concentration, which is interpreted as corresponding to 1963, the year with maximum fallout of Cs-137 from atmospheric testing of atomic weapons (Ritchie and McHenry, 1990). Three-hundred-five 1.2-in (3-cm) subsamples were analyzed.

### **3.4 Constituent Loads**

The USGS calculated loads into and out of the Basin for nine constituents using the LOADEST program (Runkel et al., 2004). In their SIR (USGS, 2015) they present the diagnostic results for the model that was chosen to compute loads for each constituent at each location considered. Typically the chosen model was the one with the value of the Nash-Sutcliffe model Efficiency (NSE) closest to 1.0 and Bias Percentage (BP) closest to zero. For most constituent-site combinations, a model was found with  $NSE > 0.8$ . There were only two constituent-site combinations for which no acceptable model ( $NSE > 0.5$ ) was found: fMeHg at the low-flow Outflow Gate (station 11452900) and pRHg(II) at the Outflow Weir (station 11452800). At each site other than the low-flow Outflow Gate, 7 or 8 of the 9 constituents analyzed had  $NSE > 0.8$  in the selected model, whereas at the low-flow Outflow Gate, only 2 of 9 constituents had models that met that standard. This relationship provides evidence that the nature of the hydrologic setting at the low-flow Outflow Gate makes it a difficult site for making accurate predictions. To improve load models for the Outlet locations, Combined Outflow (Outflow Gate plus Outflow Weir) was used in the calibration file for this site, resulting in more acceptable models. The USGS estimated loads for the nine constituents modeled are presented in detail in their SIR (USGS, 2015). The USGS load estimates for SSC, THg and MeHg are summarized in the following sections.

**Table 3.1.** Summary of Load Calculations for Suspended Sediment and Total Mercury Cache Creek Settling Basin, California, Water Years 2010-14

[THg, total mercury; pTHg, particulate total mercury; fTHg, filtered total mercury; p+fTHg, particulate plus filtered total mercury; wwTHg, whole water total mercury; SS-L, suspended sediment load from LOADEST model; SS-G, suspended sediment load from GLCAS model; pTHg-L, particulate total mercury load from multiplying median gravimetric pTHg concentration times SS-L; pTHg-G, particulate total mercury load from multiplying median gravimetric pTHg concentration times SS-G; conc., concentration; light gray shading indicates particulate total mercury load; dark gray shading indicates whole water total mercury load]

	Total flow	pTHg	fTHg	p+fTHg	wwTHg	pTHg	SS-L	pTHg-L	SS-G	pTHg-G	
	volume	load	load	load	load	conc.	load	load	load	load	
	10 <sup>9</sup> L	kg	kg	kg	kg	(median) ng/g	10 <sup>6</sup> kg	kg	10 <sup>6</sup> kg	kg	
<b>Inflow 11452600</b>											
WY 2010	205	19	0.85	19	21	237	137	33	181	43	
WY 2011	487	98	2.0	100	105	208	562	117	377	79	
WY 2012	37	1	0.1	1	1	252	3	1	5	1	
WY 2013	117	16	1.0	17	17	242	106	26	82	20	
WY 2014	0	0	0	0	0	na	0	0	0	0	
WY 2010-2014 sum	846	133	3.9	137	144		sum	809	176	645	142
WY 2010-2014						240	5-yr	809	194	645	155
<b>Outflow Weir (Spillway) 11452800</b>											
WY 2010	86	8.0	0.02	8.0	6.2	298	35	10	36	11	
WY 2011	364	46	1.1	47	50	252	95	24	88	22	
WY 2012	0	0	0	0	0	336	0.0	0.0	0.0	0.0	
WY 2013	63	4.7	0.57	5.2	7.2	291	29	8.5	34	9.8	
WY 2014	0	0	0	0	0	na	0	0	0	0	
WY 2010-2014	513	59	1.7	61	64		sum	159	43	158	43
WY 2010-2014						280	5-yr	159	45	158	44
<b>Outflow Gate 11452900</b>											
WY 2010	86	2.5	0.30	2.8	6.7	298	8.7	2.6	6.1	1.8	
WY 2011	96	6.6	0.42	7.0	14	252	25	6.2	20	5.1	
WY 2012	22	0.3	0.06	0.4	0.6	336	0.9	0.32	1.3	0.5	
WY 2013	39	1.9	0.25	2.2	5.2	291	9.4	2.7	9.2	2.7	
WY 2014	0	0	0	0	0	na	0	0	0	0	
WY 2010-2014	243	11	1.0	12	26		sum	44	12	37	10
WY 2010-2014						280	5-yr	44	12	37	10
<b>Total Outflow (11452901) - sum of 11452800 and 11452900</b>											
WY 2010	172	10	0.33	11	13	298	43	13	42	13	
WY 2011	460	53	1.6	54	64	252	120	30	108	27	
WY 2012	22	0.3	0.06	0.4	0.6	336	0.9	0.3	1.3	0.5	
WY 2013	103	6.6	0.83	7.4	12	291	39	11	43	12	
WY 2014		0	0	0	0	na	0	0	0	0	
WY 2010-2014	756	70	2.78	73	90		sum	203	55	195	53
WY 2010-2014						280	5-yr	203	57	195	55
<b>Combined Outflow (11452901) - weighted average of 11452800 and 11452900</b>											
WY 2010	172	9.3	0.82	10	11	298	35	10	42	13	
WY 2011	460	44	1.9	46	55	252	216	54	108	27	
WY 2012	22	0.5	0.06	0.6	0.6	336	2.5	0.8	1.3	0.5	
WY 2013	103	5.1	0.79	5.9	6.0	291	37	11	43	12	
WY 2014		0	0	0	0	na	0	0	0	0	
WY 2010-2014	756	59	3.6	63	73		sum	289	76	195	53
WY 2010-2014						280	5-yr	289	81	195	55

**Table 3.2.** Summary of Load Calculations for Total Mercury, Standard Error of the Mean, Cache Creek Settling Basin, California, Water Years 2010-14

[THg, total mercury; pTHg, particulate total mercury; fTHg, filtered total mercury; p+fTHg, particulate plus filtered total mercury; wwTHg, whole water total mercury; SS-L, suspended sediment load from LOADEST model; SS-G, suspended sediment load from GLCAS model; pTHg-L, particulate total mercury load from multiplying median gravimetric pTHg concentration times SS-L; pTHg-G, particulate total mercury load from multiplying median gravimetric pTHg concentration times SS-G; conc., concentration; SE, standard error of the mean; light gray shading indicates particulate total mercury load; dark gray shading indicates whole water total mercury load]

	Total flow volume	pTHg load (SE)	fTHg load (SE)	p+fTHg load (SE)	wwTHg load (SE)	pTHg conc. (median) ng/g		SS-L load (SE)	pTHg-L load (SE)	SS-G load (SE)	pTHg-G load (SE)
	10 <sup>9</sup> L	kg	kg	kg	kg			10 <sup>6</sup> kg	kg	10 <sup>6</sup> kg	kg
<b>Inflow 11452600</b>											
WY 2010	205	5.1	0.23	5.3	3.8	237		35.9	8.5	nd	nd
WY 2011	487	22	0.36	22	17	208		185	38	nd	nd
WY 2012	37	0.12	0.02	0.14	0.12	252		0.83	0.21	nd	nd
WY 2013	117	4.0	0.19	4.2	3.7	242		36.5	8.8	nd	nd
WY 2014	0	0	0	0	0	na		0	0	nd	nd
WY 2010-2014 sum	846	31	0.80	32	25			258	56	nd	nd
WY 2010-2014						240		258	62	nd	nd
<b>Outflow Weir (Spillway) 11452800</b>											
WY 2010	86	4.1	0.043	4.1	3.0	298		15.8	4.7	nd	nd
WY 2011	364	27	0.16	27	19	252		35.3	8.9	nd	nd
WY 2012	0	0	0	0	0	336		0	0	nd	nd
WY 2013	63	2.3	0.092	2.4	4.1	291		13.8	4.0	nd	nd
WY 2014	0	0	0	0	0	na		0	0	nd	nd
WY 2010-2014	513	34	0.29	34	26		sum	65.0	18	nd	nd
WY 2010-2014						280	5-yr	65.0	18	nd	nd
<b>Outflow Gate 11452900</b>											
WY 2010	86	1.0	0.082	1.1	16	298		2.4	0.72	nd	nd
WY 2011	96	2.3	0.082	2.4	190	252		8.2	2.1	nd	nd
WY 2012	22	0.11	0.012	0.13	0.3	336		0.23	0.08	nd	nd
WY 2013	39	0.74	0.059	0.80	12	291		3.2	0.92	nd	nd
WY 2014	0	0	0	0	0	na		0	0.0	nd	nd
WY 2010-2014	243	4.2	0.23	4.4	218		sum	14	3.8	nd	nd
WY 2010-2014						280	5-yr	14	3.9	nd	nd
<b>Total Outflow (11452901) - sum of 11452800 and 11452900</b>											
WY 2010	172	5.1	0.12	5.2	19	298		18	5.4	nd	nd
WY 2011	460	30	0.24	30	209	252		43	11	nd	nd
WY 2012	22	0.11	0.012	0.13	0.29	336		0	0	nd	nd
WY 2013	103	3.1	0.15	3.2	16	291		17	4.9	nd	nd
WY 2014	0	0	0	0	0	na		0	0	nd	nd
WY 2010-2014	756	38	0.53	38	244		sum	79	21	nd	nd
WY 2010-2014						280	5-yr	79	22	nd	nd
<b>Combined Outflow (11452901) - weighted average of 11452800 and 11452900</b>											
WY 2010	172	2.5	0.15	2.6	2.2	298		11	3	nd	nd
WY 2011	460	17	0.24	17	15	252		65	16	nd	nd
WY 2012	22	0.13	0.0077	0.14	0.11	336		0.7	0.2	nd	nd
WY 2013	103	1.3	0.12	1.4	1.1	291		15	4	nd	nd
WY 2014	0	0	0	0	0	na		0	0	nd	nd
WY 2010-2014	756	21	0.52	21	19		sum	91	24	nd	nd
WY 2010-2014						280	5-yr	91	26	nd	nd

### 3.4.1 Suspended Sediment Loads

The USGS reported that flow versus SSC showed a strong correlation for the Inflow site, a weaker correlation for the Combined Outflow data and no significant correlation for the low-flow Outflow Gate data.

Suspended sediment loads computed with LOADEST are shown in Table 3.1 (column labelled “SS-L”). Total sediment load at the Inflow site for WYs 2010–14 was  $809 \times 10^6$  kilograms (kg). Total sediment load for WYs 2010–14 for the Combined Outflow (using flow-weighted average concentrations) was  $289 \times 10^6$  kg. Sediment load was also computed separately for the Outflow Gate and Outflow Weir sites using LOADEST — the sum of those loads for WYs 2010–14 was  $203 \times 10^6$  kg.

The USGS Sacramento Field Office (SFO) independently estimated suspended sediment loads for the same period using samples taken separately at the same locations. The two SSC data sets have minimal overlap, although some samples were taken concurrently to cross-check slight differences in sample collection methodology. The loads published by the SFO for the Basin inflow and outflows (<http://waterdata.usgs.gov/ca/nwis/>) were computed using GCLAS (Koltun et al., 2006). Using this methodology, the total sediment load for the WYs 2010–14 was  $645 \times 10^6$  kg for the Basin Inflow (station 11452600) and  $195 \times 10^6$  kg for the Combined Outflow (station 11452901) (Table 3.1, column labelled “SS-G”).

Standard error on LOADEST computations of suspended sediment loads are given in Table 3.2. The Inflow sediment load with standard error (indicated as  $\pm$  SE) is  $809 \pm 258 \times 10^6$  kg, and the combined outflow sediment load is  $289 \pm 91 \times 10^6$  kg. Error estimates are not available for GCLAS because the program works by interpolation between known data points and synthetic data points that are estimated using the relationship between flow and the constituent being analyzed. The differences between the SS-L and SS-G load totals for WY’s 2010-14 are approximately 20% for the Inflow and 33% for the Combined Outflow; these are similar to the percentages of SE on the LOADEST estimates, so the GCLAS estimates are approximately within the error of the LOADEST model results. The computed LOADEST sediment loads for the two outflow sites computed separately are in much closer agreement; the sum of the sediment loads at these two sites was  $203 \pm 79 \times 10^6$  kg, compared with  $195 \times 10^6$  kg for GCLAS, a difference of only 4%.

### 3.4.2 Total Mercury Loads

Computed loads of pTHg for the Inflow site for WYs 2010-14 totaled 133 kg (Table 3.1) with SE of  $\pm$  31 kg (Table 3.2). The Inflow fTHg loads were more than two orders of magnitude lower,  $3.9 \pm 0.8$  kg for the same 5-year period. The sum of the pTHg and fTHg loads ( $137 \pm 32$  kg) compares favorably with the whole-water total mercury (wwTHg) load of  $144 \pm 25$  kg for the same time frame at the same location (the wwTHg loads were computed in LOADEST using non-filtered samples and the sum of pTHg and fTHg concentrations for individual samples). Similarly, for the Combined Outflow, the computed pTHg

load of  $59 \pm 21$  kg and fTHg load of  $3.6 \pm 0.52$  kg sum to  $63 \pm 21$  kg, which is in the same range as the wwTHg load of  $73 \pm 19$  kg.

The strong correlations between pTHg and SSC at each of the inflow and outflow sites allows another approach to estimating pTHg loads, by using the suspended sediment load multiplied by a representative concentration of THg on suspended sediment. The gravimetric values of pTHg (pTHg-g) represent direct measurement of the THg concentration of suspended sediment particles. The median values for pTHg for each Water Year are compiled in Table 3.1 for each of the sites modeled, and the median value for the five-year period (WYs 2010-14) is also provided. The pTHg values were multiplied by the sediment loads computed by GCLAS (“SS-L” column on Table 3.1) and also by the GCLAS sediment loads (“SS-G” column) to derive two additional estimates of pTHg load. The initial estimates were made by computing an estimated annual load for each of the water years for which data are available. Loads of pTHg using the 5-year median concentration value of pTHg-g were also used, in addition to the annual values. The four additional estimates of pTHg loads for the Basin Inflow are:  $176 \pm 56$  kg (pTHg-L, combining the SS-L sediment load with the median value of pTHg-g for each WY and then summing the years);  $194 \pm 62$  kg (pTHg-L5, combining SS-L with the median value of pTHg-g for the 5-year period, 240 ng/g);  $142$  kg (pTHg-G, combining the SS-G sediment load with the median value of pTHg-g for each WY and then summing the years), and  $155$  kg (pTHg-G5, combining SS-G with the median value of pTHg-g for the 5-year period, 240 ng/g). Similarly, four additional estimates of pTHg load were made for each of the other sites considered using the sediment loads and the pTHg-g values (Table 3.1), with standard error estimates for all except the SS-G loads derived using GCLAS (Table 3.2). These various estimates are used later in this report to help evaluate uncertainty in TE, as described in a later section.

### 3.4.3 Methylmercury and Reactive Mercury Loads

The USGS reported that the computed loads of pMeHg for the Inflow site for WYs 2010-14 totaled 1.08 kg (Table 3.3) with SE of  $\pm 0.21$  kg (Table 3.4). The Inflow fMeHg loads were lower by approximately a factor of three:  $0.078 \pm 0.009$  kg for the same 5-year period. The sum of the pMeHg and fMeHg loads ( $1.16 \pm 0.22$  kg) compares favorably with the wwMeHg load of  $1.00 \pm 0.14$  kg for the same time frame at the same location. Similarly, for the Combined Outflow, the computed pMeHg load of  $0.53 \pm 0.13$  kg and fMeHg load of  $0.11 \pm 0.012$  kg sum to  $0.64 \pm 0.14$  kg, which is very similar to the 5-year wwMeHg load of  $0.62 \pm 0.13$  kg.

In a similar manner to that described above for pTHg-g, the gravimetric values of pMeHg (pMeHg-g) data were combined with the SS-L and SS-G sediment loads from LOADEST and GCLAS, respectively, to derive additional estimates of pMeHg loads, as shown in Table 3.3, with corresponding SE estimates in Table 3.4.

The USGS also used the ratios of MeHg loads to THg loads to compute %pMeHg, %fMeHg, and %wwMeHg, and SE values were propagated using the “square root of the sum of the squares” method. This analysis showed that there was no significant change in %pMeHg from the Basin Inflow to the

**Table 3.3.** Summary of Load Calculations for Methylmercury, Cache Creek Settling Basin, California, Water Years 2010-14

[MeHg, methylmercury; pMeHg, particulate methylmercury; fMeHg, filtered methylmercury; p+fMeHg, particulate plus filtered methylmercury; wwMeHg, whole water methylmercury; SS-L, suspended sediment load from LOADEST model; SS-G, suspended sediment load from GLCAS model; pMeHg-L, particulate methylmercury load from multiplying median gravimetric pMeHg concentration times SS-L; pMeHg-G, particulate methylmercury load from multiplying median gravimetric pMeHg concentration times SS-G; kg, kilogram; ng/g, nanogram per gram; conc., concentration; light gray shading indicates particulate methylmercury load; dark gray shading indicates whole water methylmercury load]

	Total flow volume	pMeHg load	fMeHg load	p+fMeHg load	wwMeHg load	pMeHg conc. (median) ng/g		SS-L load	pMeHg-L load	SS-G load	pMeHg-G load
	10 <sup>9</sup> L	kg	kg	kg	kg			10 <sup>6</sup> kg	kg	10 <sup>6</sup> kg	kg
<b>Inflow 11452600</b>											
WY 2010	205	0.19	0.023	0.21	0.18	4.1		137	0.57	181	0.75
WY 2011	487	0.76	0.042	0.80	0.67	2.3		562	1.3	377	0.88
WY 2012	37	0.011	0.0037	0.015	0.015	7.2		3.5	0.025	4.7	0.034
WY 2013	117	0.12	0.010	0.13	0.12	1.9		106	0.21	82	0.16
WY 2014	0	0	0	0	0	na		0	0	0	0
WY 2010-2014	846	1.08	0.078	1.16	1.00		sum	809	2.1	645	1.83
WY 2010-2014						4.0	5-yr	809	3.2	645	2.59
<b>Outflow Weir (Spillway) 11452800</b>											
WY 2010	86	0.024	0.0081	0.032	0.043	11		35	0.38	36	0.39
WY 2011	364	0.27	0.034	0.30	0.32	3.0		95	0.28	88	0.26
WY 2012	0	0	0	0	0	7.0		0	0	0	0
WY 2013	63	0.048	0.0082	0.056	0.049	2.4		29	0.070	34	0.081
WY 2014	0	0	0	0	0	na		0	0	0	0
WY 2010-2014	513	0.34	0.051	0.39	0.41		sum	159	0.73	158	0.74
WY 2010-2014						4.5	5-yr	159	0.71	158	0.71
<b>Outflow Gate 11452900</b>											
WY 2010	86	0.039	0.020	0.060	0.033	11		8.7	0.094	6.1	0.066
WY 2011	96	0.080	0.015	0.095	0.10	3.0		25	0.073	20	0.060
WY 2012	22	0.0074	0.0038	0.011	0.014	7.0		0.9	0.0066	1.3	0.0094
WY 2013	39	0.015	0.0049	0.020	0.018	2.4		9.4	0.023	9.2	0.022
WY 2014	0	0	0	0	0	na		0	0	0	0
WY 2010-2014	243	0.14	0.044	0.19	0.16		sum	44	0.20	37	0.16
WY 2010-2014						4.5	5-yr	44	0.20	37	0.17
<b>Total Outflow 11452901 - sum of 11452800 and 11452900</b>											
WY 2010	172	0.064	0.028	0.092	0.077	11		43	0.47	42.2	0.46
WY 2011	460	0.35	0.049	0.40	0.42	3.0		120	0.36	108.3	0.32
WY 2012	22	0.0074	0.0038	0.011	0.014	7.0		0.95	0.0066	1.3	0.0094
WY 2013	103	0.063	0.013	0.076	0.067	2.4		39	0.093	42.9	0.10
WY 2014		0	0	0	0	na		0	0	0	0
WY 2010-2014	756	0.48	0.094	0.58	0.58		sum	203	0.93	195	0.89
WY 2010-2014						4.5	5-yr	203	0.91	195	0.87
<b>Combined Outflow 11452901 - flow-weighted average of 11452800 and 11452900</b>											
WY 2010	172	0.102	0.028	0.13	0.13	11		35	0.38	42.2	0.46
WY 2011	460	0.34	0.056	0.39	0.38	3.0		216	0.64	108.3	0.32
WY 2012	22	0.0089	0.0047	0.014	0.012	7.0		2.5	0.017	1.3	0.0094
WY 2013	103	0.084	0.017	0.10	0.10	2.4		37	0.088	42.9	0.10
WY 2014		0	0	0	0	na		0	0	0	0
WY 2010-2014	756	0.53	0.11	0.64	0.62		sum	289	1.1	195	0.89
WY 2010-2014						4.5	5-yr	289	1.3	195	0.87

**Table 3.4.** Summary of Load Calculations for Methylmercury, Standard Error of the Mean, Cache Creek Settling Basin, California, Water Years 2010-14

[MeHg, methylmercury; pMeHg, particulate methylmercury; fMeHg, filtered methylmercury; p+fMeHg, particulate plus filtered methylmercury; wwMeHg, whole water methylmercury; SS-L, suspended sediment load from LOADEST model; SS-G, suspended sediment load from GLCAS model; pMeHg-L, particulate methylmercury load from multiplying median gravimetric pMeHg concentration times SS-L; pMeHg-G, particulate methylmercury load from multiplying median gravimetric pMeHg concentration times SS-G; SE, standard error of the mean; kg, kilogram; ng/g, nanogram per gram; conc., concentration; light gray shading indicates particulate methylmercury load; dark gray shading indicates whole water total methylmercury load]

	Total flow	pMeHg	fMeHg	p+fMeHg	wwMeHg	pMeHg	SS-L	pMeHg-L	SS-G	pMeHg-G
	volume	load (SE)	load (SE)	load (SE)	load (SE)	conc.	load (SE)	load (SE)	load (SE)	load (SE)
	10 <sup>9</sup> L	kg	kg	kg	kg	(median) ng/g	10 <sup>6</sup> kg	kg	10 <sup>6</sup> kg	kg
<b>Inflow 11452600</b>										
WY 2010	205	0.044	0.0030	0.047	0.028	4.1	35.9	0.15	nd	nd
WY 2011	487	0.14	0.0046	0.148	0.088	2.3	185	0.43	nd	nd
WY 2012	37	0.0014	0.00032	0.002	0.0015	7.2	0.83	0.0059	nd	nd
WY 2013	117	0.026	0.0011	0.027	0.020	1.9	36.5	0.071	nd	nd
WY 2014	0	0	0	0	0	na	0	0	nd	nd
WY 2010-2014	846	0.21	0.0090	0.22	0.14		sum	258	0.66	nd
WY 2010-2014						4.0	5-yr	258	1.0	nd
<b>Outflow Weir (Spillway) 11452800</b>										
WY 2010	86	0.42	0.0030	0.42	nd	11	16	0.17	nd	nd
WY 2011	364	0.21	0.0058	0.22	0.15	3.0	35	0.10	nd	nd
WY 2012	0	0	0	0	0	7.0	0	0	nd	nd
WY 2013	63	nd	0.0022	nd	0.017	2.4	14	0.033	nd	nd
WY 2014	0	0	0	0	0	na	0	0	nd	nd
WY 2010-2014	513	nd	0.011	nd	nd		sum	65	0.31	nd
WY 2010-2014						4.5	5-yr	65	0.29	nd
<b>Outflow Gate 11452900</b>										
WY 2010	86	0.017	0.0041	0.021	0.012	11	2.4	0.026	nd	nd
WY 2011	96	0.025	0.0022	0.027	0.0286	3.0	8.2	0.024	nd	nd
WY 2012	22	0.0025	0.00058	0.0031	0.0043	7.0	0.23	0.0016	nd	nd
WY 2013	39	0.0056	0.0010	0.0065	0.0061	2.4	3.2	0.0075	nd	nd
WY 2014	0	0	0	0	0	na	0	0	nd	nd
WY 2010-2014	243	0.050	0.0078	0.058	0.051		sum	14	0.060	nd
WY 2010-2014						4.5	5-yr	14	0.063	nd
<b>Total Outflow 11452901 - sum of 11452800 and 11452900</b>										
WY 2010	172	0.43	0.0071	0.44	nd	11	18	0.20	nd	nd
WY 2011	460	0.24	0.0079	0.24	0.183	3.0	43	0.13	nd	nd
WY 2012	22	0.0025	0.00058	0.0031	0.0043	7.0	0	0.0016	nd	nd
WY 2013	103	nd	0.0031	nd	0.023	2.4	17	0.041	nd	nd
WY 2014	0	0	0	0	0	na	0	0	nd	nd
WY 2010-2014	756	nd	0.019	nd	nd		sum	79	0.37	nd
WY 2010-2014						4.5	5-yr	79	0.35	nd
<b>Combined Outflow 11452901 - flow-weighted average of 11452800 and 11452900</b>										
WY 2010	172	0.018	0.0027	0.021	0.019	11	21	0.23	nd	nd
WY 2011	460	0.089	0.0072	0.097	0.084	3.0	52	0.15	nd	nd
WY 2012	22	0.0019	0.0005	0.0024	0.0021	7.0	0	0.0032	nd	nd
WY 2013	103	0.021	0.0016	0.022	0.022	2.4	20	0.048	nd	nd
WY 2014	0	0	0	0	0	na	0	0	nd	nd
WY 2010-2014	756	0.13	0.012	0.14	0.13		sum	93	0.43	nd
WY 2010-2014						4.5	5-yr	93	0.42	nd



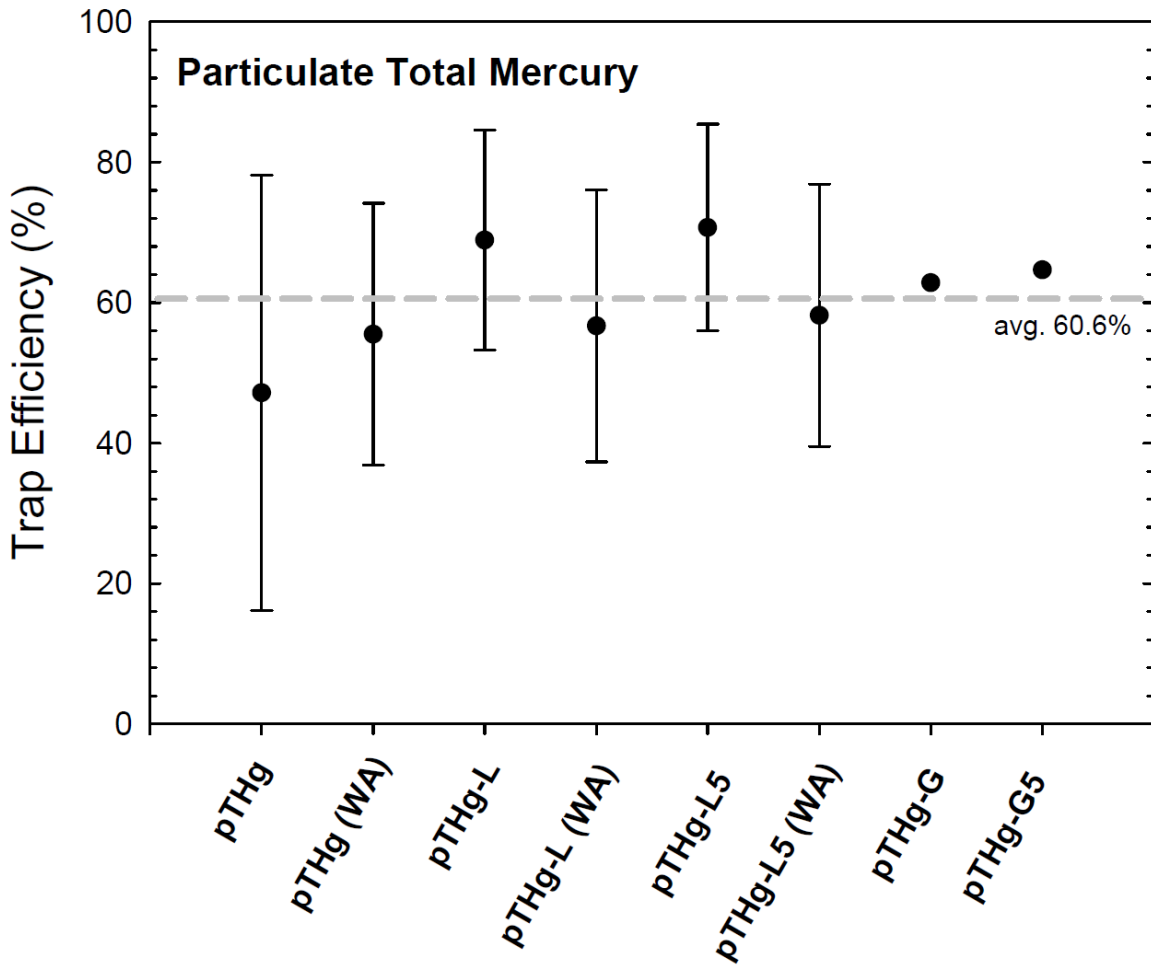


**Figure 10. Plot of Particulate Total Mercury TE Estimates**

The TE value labelled “pTHg” represents the combination of the LOADEST pTHg load and the sum of the two outflow sites; this TE ± SE value is 47 ± 31%, a relatively large error bar reflecting relatively large SE values for the various loads. The entry labelled “pTHg (WA)” uses the pTHg load and the Combined Outflow (weighted average) pTHg loads resulting in TE ± SE of 56 ± 19%. The entry “pTHg-L” represents the pTHg loads computed using LOADEST sediment loads for the inflow and the sum of the two outflow sites (69 ± 16%); and “pTHg-L (WA)” represents the same Inflow load combined with the Combined Outflow (weighted average) (57 ± 19%). The “pTHg-L5” entry represents the pTHg loads computed using LOADEST sediment loads (SS-L) with the 5-year median value of pTHg-g and the sum of the loads from the two outflow sites (71 ± 15%), and the pTHg-L5 (WA) entry is the same Inflow load combined with the Combined Outflow (weighted average) (58 ± 19%). The two final entries are for the pTHg loads computed using GCLAS sediment loads, for which there are no SE values available, TE values of 63% (entry pTHg-g) for the sum of the 5 years using separate pTHg-g values for each year, and

**Table 3.5.** Trap Efficiency Calculations for Total Mercury, Cache Creek Settling Basin, California, Water Years 2010-14

[THg, total mercury; pTHg, particulate total mercury; fTHg, filtered total mercury; p+fTHg, particulate plus filtered total mercury; wwTHg, whole water total mercury; SS-L, suspended sediment load from LOADEST model; SS-G, suspended sediment load from GLCAS model; pTHg-L, particulate total mercury load from multiplying median gravimetric pTHg concentration times SS-L; pTHg-G, particulate total mercury load from multiplying median gravimetric pTHg concentration times SS-G; TE, Trap Efficiency; TE computed as (LoadIn-LoadOut)/(LoadIn) using load data in table 3.1, as indicated]

Total flow	pTHg	fTHg	p+fTHg	wwTHg
TE	TE	TE	TE	TE

SS-L	pTHg-L	SS-G	pTHg-G
TE	TE	TE	TE

**Inflow (11452600) vs. Total Outflow (11452901) - sum of 11452800 and 11452900**

WY 2010	16%	44%	62%	44%	39%
WY 2011	6%	46%	21%	45%	39%
WY 2012	40%	60%	43%	58%	43%
WY 2013	12%	58%	17%	56%	28%
WY 2014	nd	nd	nd	nd	nd
WY 2010-2014 sum	11%	47%	29%	47%	38%
WY 2010-2014 sum					

sum  
5-yr

69%	60%	77%	71%
79%	74%	71%	65%
73%	64%	71%	62%
63%	56%	47%	37%
nd	nd	nd	nd
75%	69%	70%	63%
75%	71%	70%	65%

**Inflow (11452600) vs. Combined Outflow (11452901) - weighted average of 11452800 and 11452900**

WY 2010	16%	50%	4%	48%	48%
WY 2011	6%	55%	4%	54%	47%
WY 2012	40%	36%	46%	37%	44%
WY 2013	12%	68%	21%	65%	65%
WY 2014	nd	nd	nd	nd	nd
WY 2010-2014 sum	11%	56%	10%	54%	50%
WY 2010-2014 sum					

sum  
5-yr

75%	68%	77%	71%
62%	53%	71%	65%
29%	6%	71%	62%
65%	59%	47%	37%
nd	nd	nd	nd
64%	57%	70%	63%
64%	58%	70%	65%

**Table 3.6.** Trap Efficiency Standard Error Calculations for Total Mercury, Cache Creek Settling Basin, California, Water Years 2010-14

[THg, total mercury; pTHg, particulate total mercury; fTHg, filtered total mercury; p+fTHg, particulate plus filtered total mercury; wwTHg, whole water total mercury; SS-L, suspended sediment load from LOADEST model; SS-G, suspended sediment load from GLCAS model; pTHg-L, particulate total mercury load from multiplying median gravimetric pTHg concentration times SS-L; pTHg-G, particulate total mercury load from multiplying median gravimetric pTHg concentration times SS-G; TE, Trap Efficiency; SE, standard error; TE data in Table 3.2]

	pTHg	fTHg	p+fTHg	wwTHg		SS-L	pTHg-L	SS-G	pTHg-G
	TE (SE)	TE (SE)	TE (SE)	TE (SE)		TE (SE)	TE (SE)	TE (SE)	TE (SE)
<b>Inflow (11452600) vs. Total Outflow (11452901) - sum of 11452800 and 11452900</b>									
WY 2010	31%	18%	31%	91%		16%	20%	nd	nd
WY 2011	33%	19%	32%	199%		10%	13%	nd	nd
WY 2012	15%	14%	15%	31%		9%	12%	nd	nd
WY 2013	22%	22%	22%	92%		20%	24%	nd	nd
WY 2014	nd	nd	nd	nd		nd	nd	nd	nd
WY 2010-2014 sum	31%	20%	31%	169%	sum	13%	16%	nd	nd
WY 2010-2014 sum					5-yr	13%	15%	nd	nd
<b>Inflow (11452600) vs. Combined Outflow (11452901) - weighted average of 11452800 and 11452900</b>									
WY 2010	19%	31%	20%	14%		10%	13%	nd	nd
WY 2011	20%	21%	20%	17%		17%	21%	nd	nd
WY 2012	19%	11%	18%	13%		25%	34%	nd	nd
WY 2013	12%	20%	12%	10%		18%	22%	nd	nd
WY 2014	nd	nd	nd	nd		nd	nd	nd	nd
WY 2010-2014 sum	19%	23%	19%	16%		16%	19%	nd	nd
WY 2010-2014 sum					sum	16%	19%	nd	nd
					5-yr				

65% (entry pTHg-G4) for the median pTHg-g value for all 5 years. The average value for the eight estimates of TE for pTHg is 60.6%

The physical process of particle settling that results in trapping of suspended sediment and particulate forms of mercury does not directly affect dissolved constituents. This is illustrated by results for fTHg, which shows an apparent TE of  $10 \pm 23\%$ . The water balance for WYs 2010–14 shows a similar net loss (apparent trapping) of 11% (Table 3.5). Although fTHg appears to behave conservatively, various processes affecting fTHg concentration may be cancelling each other out, resulting in this net behavior. The TE for whole-water mercury (wwTHg) was calculated at  $50 \pm 16\%$ . As expected this value is between the values for pTHg and fTHg. Additional estimates of wwTHg loads (Table 3.1) were made by adding fTHg loads to pTHg load estimates made using SS-L and SS-G loads combined with gravimetric pTHg-g concentrations. The TE was computed for each of these load estimates, with outflows considered alternately as two separate sites and as a single Combined Outflow site with flow-weighted average concentrations (Table 3.1). The average TE value for 12 estimates of wwTHg loads was 57% (Table 3.5).

### 3.5.3 Methylmercury and Reactive Mercury

The USGS made several estimates of TE for pMeHg in a similar manner to those made for pTHg. The TE results are shown in Table 3.7, with standard errors in Table 3.8. The average TE for pMeHg based on eight estimates is 57.3% as shown on Figure 11 below.

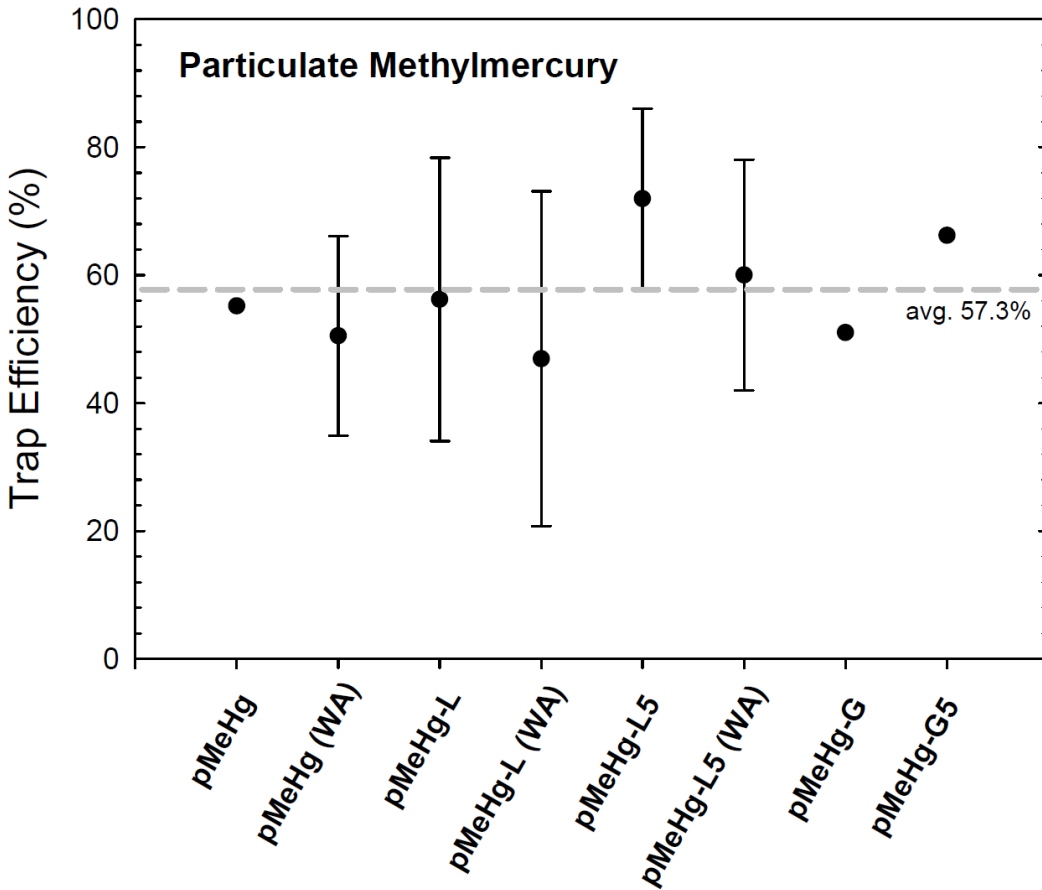


**Figure 11. Plot of Particulate Methylmercury TE Estimates**

A significant finding of the USGS TE calculations is that the only constituent studied that shows a negative value for TE is fMeHg ( $-34 \pm 16\%$ , weighted-average) (Tables 3.7 and 3.8). Flow versus fMeHg shows that fMeHg concentrations are consistently higher in the Basin outflows compared to Basin inflow, except at the very highest flow; while flow versus wwMeHg indicates an intermediate degree of trapping, consistent with the computed TE value of  $37 \pm 15\%$ . When considering each of the six methods the USGS employed for estimating wwMeHg loads using SS-L, SS-G, and pMeHg-g values and the two different ways of dealing with outflows (sum of two sites and flow-weighted average concentrations, Table 3.3), the average TE value for the 12 different sets of load estimates for wwMeHg was 50% (Table 3.7).

The USGS further reported that the TE for pRHg(II) is similar to that for pTHg and pMeHg; and that plots of flow versus pRHg(II) are similar to those for SSC, pTHg and pMeHg, with the line representing high outflows plotting below the regression line representing inflows; a pattern consistent with particle trapping within the Basin. The average TE value for pRHg(II) based on 7 estimates was 73.3%. Values

**Table 3.7. Trap Efficiency Calculations for Methylmercury, Cache Creek Settling Basin, California, Water Years 2010-14**

[MeHg, methylmercury; pMeHg, particulate methylmercury; fMeHg, filtered methylmercury; p+fMeHg, particulate plus filtered methylmercury; wwMeHg, whole water methylmercury; SS-L, suspended sediment load from LOADEST model; SS-G, suspended sediment load from GLCAS model; pMeHg-L, particulate methylmercury load from multiplying median gravimetric pMeHg concentration times SS-L; pMeHg-G, particulate methylmercury load from multiplying median gravimetric pMeHg concentration times SS-G; TE, Trap Efficiency; TE computed as (LoadIn-LoadOut)/(LoadIn) using load data in table 3.3, as indicated; nd, not determined]

	Total flow	pMeHg	fMeHg	p+fMeHg	wwMeHg		SS-L	pMeHg-L	SS-G	pMeHg-G
	TE	TE	TE	TE	TE		TE	TE	TE	TE
<b>Inflow (11452600) vs. Total Outflow (11452901) - sum of 11452800 and 11452900</b>										
WY 2010	16%	66%	-25%	57%	58%		69%	17%	77%	39%
WY 2011	6%	54%	-15%	50%	37%		79%	73%	71%	64%
WY 2012	40%	33%	-3%	24%	11%	min	73%	74%	71%	72%
WY 2013	12%	48%	-35%	42%	46%		63%	55%	47%	35%
WY 2014	nd	nd	nd	nd	nd		nd	nd	nd	nd
WY 2010-2014 sum	11%	55%	-20%	50%	42%	sum	75%	56%	70%	51%
WY 2010-2014 sum						5-yr	75%	72%	70%	66%
<b>Inflow (11452600) vs. Combined Outflow (11452901) - weighted average of 11452800 and 11452900</b>										
WY 2010	16%	46%	-22%	38%	31%		75%	34%	77%	39%
WY 2011	6%	55%	-32%	51%	43%		62%	51%	71%	64%
WY 2012	40%	20%	-26%	8%	19%		29%	31%	71%	72%
WY 2013	12%	30%	-76%	22%	18%		65%	57%	47%	35%
WY 2014	nd	nd	nd	nd	nd		nd	nd	nd	nd
WY 2010-2014 sum	11%	51%	-34%	45%	37%	sum	64%	47%	70%	51%
WY 2010-2014 sum						5-yr	64%	60%	70%	66%

**Table 3.8.** Trap Efficiency Standard Error Calculations for Methylmercury, Cache Creek Settling Basin, California, Water Years 2010-14

[MeHg, methylmercury; pMeHg, particulate methylmercury; fMeHg, filtered methylmercury; p+fMeHg, particulate plus filtered methylmercury; wwMeHg, whole water methylmercury; SS-L, suspended sediment load from LOADEST model; SS-G, suspended sediment load from GLCAS model; pMeHg-L, particulate methylmercury load from multiplying median gravimetric pMeHg concentration times SS-L; pMeHg-G, particulate methylmercury load from multiplying median gravimetric pMeHg concentration times SS-G; TE, Trap Efficiency; SE, standard error; TE data in Table 3.4]

Total flow	pMeHg	fMeHg	p+fMeHg	wwMeHg
TE (SE)	TE (SE)	TE (SE)	TE (SE)	TE (SE)

SS-L	pMeHg-L	SS-G	pMeHg-G
TE (SE)	TE (SE)	TE (SE)	TE (SE)

**Inflow (11452600) vs. Total Outflow (11452901) - sum of 11452800 and 11452900**

WY 2010		230%	35%	209%	nd
WY 2011		32%	23%	32%	28%
WY 2012		24%	18%	23%	30%
WY 2013		nd	36%	nd	21%
WY 2014		nd	nd	nd	nd
WY 2010-2014 sum		nd	28%	nd	nd

sum
5-yr

16%	41%	nd	nd
10%	13%	nd	nd
9%	9%	nd	nd
20%	25%	nd	nd
nd	nd	nd	nd
13%	22%	nd	nd
13%	14%	nd	nd

**Inflow (11452600) vs. Combined Outflow (11452901) - weighted average of 11452800 and 11452900**

WY 2010		16%	20%	17%	15%
WY 2011		15%	22%	15%	15%
WY 2012		20%	18%	19%	16%
WY 2013		23%	27%	23%	22%
WY 2014		nd	nd	nd	nd
WY 2010-2014 sum		16%	22%	16%	15%

sum
5-yr

10%	43%	nd	nd
17%	20%	nd	nd
25%	21%	nd	nd
18%	28%	nd	nd
nd	nd	nd	nd
16%	26%	nd	nd
16%	18%	nd	nd

of TE for whole water RHg(II) were not computed because only pRHg(II) was analyzed; fRHg(II) and nfRHg(II) were not determined.

### **3.6 Within-Basin Processes: Habitat, Sediment, Biota, and Water-Quality**

#### **3.6.1 Habitat Mapping**

The USGS categorized the Basin Habitat at two levels of detail, Level 1 based upon land use categories and Level 2 based upon sub-habitat categories. The USGS calculated the habitat mapped acreage of the Basin as 3,252 acres (1,316 ha) and identified the dominant land use type as agriculture (47.3%; Corn, Pumpkin, or Tomato) followed by floodplain (39.1%), of which 18.3% is classified as mixed woody and 17.1% is classified as non-woody, 2.8% is classified as mowed, and 1.0% is classified as tule. Riparian habitats represented only 3.7% of total land use, as they were concentrated only along naturally developed stream channels. Open Water represented 2.7% of the land use (2.2% as stream channel, and 0.5% as irrigation canal Level 2 sub-habitats). Roads (and associated infrastructure such as slope aprons) represented 7.2% of the land use, and include Level 2 sub-habitats of levee roads (3.5%, both drivable portion and apron) and interior roads (3.7%).

#### **3.6.2 Sediment**

The USGS performed statistical analysis of sediment data examining the spatial and temporal trends for the various Hg species and the geochemical factors most closely associated with individual Hg species. These model results are presented graphically and described in detail in the USGS SIR (USGS, 2015). A summary of the statistical model results for THg, MeHg and RHg(II) is presented below.

##### **3.6.2.1 Sediment Total Mercury**

For the complete April 2010–May 2013 data set (n = 251, including replicate samples), concentrations of THg in bed sediment (0-2 cm depth) ranged from 64 to 3,795 ng/g (dry weight), with a mean ( $\pm$  std. dev.) of  $404 \pm 317$  ng/g dry wt., a median value of 335 ng/g and an interquartile range of 275 to 440 ng/g (Table 12 in USGS, 2015). The USGS reported that this distribution overlaps with that for pTHg-g in the suspended sediment from water samples which had median values of 236 ng/g in inflows and 273 ng/g in the flow-weighted average combined outflow (Table 6 in USGS, 2015).

The USGS reported that the THg concentrations were significantly greater for Open Water sites (Cache Creek main channel) than for Floodplain sites, whereas Agricultural and Riparian sites had THg concentrations that were not significantly different from either of the other two Level 1 habitats. Normalizing sediment THg concentrations to sediment organic matter content (as measured by %LOI) provided a contrasting trend to that of the sediment THg concentration alone; [THg/LOI] was significantly higher in the Agricultural and Open Water sites compared to Floodplain and Riparian sites. The relationships involving [THg/LOI] are perhaps best explained by variations in organic matter (as represented by LOI) more than variations in THg. Statistical analysis comparing the Level 2 sub-habitats

mixed woody and mixed non-woody floodplain resulted in no significant differences for either THg or [THg/%LOI]. Similarly, when the definitions were broadened so that woody habitats included both mixed-woody riparian and mixed-woody floodplain sites and non-woody habitats included mowed and tule floodplain in addition to mixed non-woody floodplain sites, there were no differences between woody and non-woody floodplain with regard to either THg or [THg/%LOI].

### 3.6.2.2 Sediment Methylmercury

The Basin surface sediment MeHg concentrations ranged from 0.38 to 23.7 ng/g dry wt. (ppb) with a mean ( $\pm$  std. dev.) of  $4.13 \pm 3.82$  ng/g dry wt. and a median of 2.87 ng/g dry wt. (n=251). Normalized to THg, %MeHg values ranged from 0.06% to 7.01%, with a mean ( $\pm$  std. dev.) of  $1.26 \pm 1.204\%$  and a median of 0.83% (n=251). A zone of comparatively low MeHg concentration is situated in the southwest corner of the Basin where the creek channel changes flow direction from south to southeast. A zone of comparatively higher MeHg concentrations is situated in the southeast corner of the Basin. During 2013, sediment MeHg concentrations were somewhat lower in May, compared to February/March, in the northwest corner of the Basin. The sediment MeHg concentrations were significantly greater for Floodplain and Riparian sites, compared to Agricultural and Open Water sites, as was the case for %MeHg. The spatial trend of sediment MeHg concentration showed a strong increase from west to east. With MeHg concentration normalized to sediment organic content (MeHg/%LOI), the differences among habitat types were not as pronounced. However, a significant positive increase from west to east was observed for [MeHg/%LOI] akin to what was found for sediment MeHg concentration alone. The USGS reported that sediment MeHg concentration normalized to sediment THg concentration (%MeHg), had results comparable to MeHg concentration alone, and the spatial and temporal trends were in all manner similar. The statistical analysis comparing levels of mixed woody to mixed non-woody floodplain identified statistical differences between these two sub-habitat groupings for the sediment MeHg (ln transformed) data, but not for [MeHg/%LOI] or for %MeHg data. However, a post-hoc student's t test, comparing the two habitats showed no statistical difference between mixed woody floodplain (back-transformed mean $\pm$ std.error,  $6.61 \pm 0.92$  ng/g dry wt.) and mixed non-woody floodplain (back-transformed mean $\pm$ std.error,  $4.21 \pm 0.69$  ng/g dry wt.) and when the definitions of woody and non-woody habitats were broadened as described above for THg, neither MeHg, [MeHg/%LOI] nor %MeHg had significant differences for these two sub-habitat groupings.

### 3.6.2.3 Sediment Reactive Mercury

The USGS reported that the Basin surface sediment RHg(II) concentrations ranged from 0.13 to 11.2 ng/g dry wt., with a mean ( $\pm$  std. dev.) of  $3.61 \pm 2.65$  ng/g dry wt. and a median of 3.80 ng/g dry wt. (n=251). Normalized to THg, %RHg(II) values ranged from 0.01% to 3.45%, with a mean ( $\pm$  std. dev.) of  $1.08 \pm 0.86\%$  and a median of 0.97% (n=251). These data show a general concentration increase along the Cache Creek flow path, from the northwest corner to the south east corner of the Basin. During 2013, sediment RHg(II) concentrations were generally higher in May, compared to February/March. A Tukey pair-wise comparison ranking for sediment RHg(II) data indicated that Agricultural and Riparian sites had

the highest concentrations, whereas Open Water sites had the lowest. For [RHg(II)/%LOI] the spatial pattern was Agricultural > Riparian > Floodplain > Open Water. For RHg(II) normalized to THg [%RHg(II)], Agricultural, Riparian and Floodplain sites all had equally high values, compared to Open Water sites, which were significantly lower. The USGS reported that the sediment RHg(II) concentration decreased with latitude from south to north, decreased with longitude from west to east, and increased over time during dry periods. The same spatial/temporal trends were seen for the [RHg(II)/%LOI] data and the %RHg(II) data.

The USGS reported that data for sediment RHg(II) data (ln transformed) sediment %LOI, % dry wt., % silt-clay, Fe(II)<sub>AE</sub>, Fe(III)a and Fe(III)c all exhibited a positive trend with sediment RHg(II) concentration, with the exception of Fe(II)<sub>AE</sub>, which exhibited a negative trend. This is consistent with RHg(II) and Fe(III) species representing oxidizing conditions. The statistical analysis comparing levels of mixed woody to mixed non-woody floodplain identified no statistical differences between these two sub-habitat groupings for the sediment RHg(II), [RHg(II)/%LOI] or for %RHg(II). When the definition of woody and non-woody habitats was broadened, all three RHg(II) metrics were significantly higher in the case of woody sites, compared to non-woody sites.

#### 3.6.2.4 Ancillary Sediment Parameters

The USGS also assessed potential drivers that influence the spatial and temporal distribution of Hg species within the Basin. The suite of sediment non-mercury parameters included %LOI, % dry weight, TRS, % silt-clay, Fe(II)<sub>AE</sub>, Fe(III)a, Fe(III)c, Fe<sub>T</sub> and %Fe(II)<sub>AE</sub>/Fe<sub>T</sub>. For these non-mercury parameters, spatial trends and differences among land use categories were identified, the details of which are summarized below.

- The following parameters increased from west to east: Fe(II)<sub>AE</sub>, Fe(III)c, Fe<sub>T</sub>, % silt-clay;
- The following parameter decreased from west to east: % dry weight;
- The following parameters increased from south to north: Fe(II)<sub>AE</sub>, Fe<sub>T</sub>, %Fe(II)<sub>AE</sub>/Fe<sub>T</sub>;
- The following parameter decreased from south to north: % dry weight;
- The following parameters increased temporally during wet-dry cycles: % dry weight, Fe(III)c; and
- The following parameters decreased temporally during wet-dry cycles: %LOI, % silt-clay, Fe(II)<sub>AE</sub>, %Fe(II)<sub>AE</sub>/Fe<sub>T</sub>.

#### 3.6.2.5 Sequential Extractions for Mercury Speciation

The USGS ran statistical analyses of sequential extraction data on mercury speciation, the details of which are described in their SIR Report (USGS, 2015). This analysis showed that the two most chemically labile mercury fractions (F1, deionized water and F2, pH 2 with acetic acid and hydrochloric

acid) have very low sequentially extracted mercury ( $Hg_{SE}$ ) concentrations ( $< 1$  ng/g dry wt.), across all sites sampled. In contrast, the KOH extractable fraction (F3), which is associated with organic-bound Hg and the most recalcitrant fraction (F5), which is associated with cinnabar ( $HgS$ ), have the highest  $Hg_{SE}$  concentrations (117 and 130 ng/g dry wt., respectively), across all sites sampled. Similarly, the analysis showed that F1 and F2 were the smallest percentages ( $< 0.5\%$ ) of the total mercury pool (sum of all fractions =  $THg_{SE}$ ), and the F3 and F5 fractions were the largest percentages of  $THg_{SE}$  ( $\%Hg_{SE}$  40% and 45%, respectively), across all sites sampled. Differences among habitat types existed only for the F3 fraction, and for all other fractions there was no significant difference in the  $\%Hg_{SE}$  among habitat types. In the case of F3 specifically, the  $\%Hg_{SE}$  was significantly larger for the Floodplain category than for the Agricultural category; whereas the Open Water and Riparian categories were not significantly different from either Floodplain or Agricultural, or from each other.

### 3.6.3 Biological Sampling

Presented in the following sections are summaries of the biological sampling and analytical results performed by the USGS in association with the Basin mercury control studies. The biological sampling activities included the collection and analyses of caged and wild fish tissue, bird eggs, and surface water; the details of which are presented in the USGS SIR Report (USGS, 2015).

#### 3.6.3.1 Mercury in Caged Mosquitofish

Of the 1,200 female mosquitofish introduced into 40 cages (30 fish/cage) in the Basin (fig. 7), 120 fish were lost in four vandalized cages. Of the 1,080 female mosquitofish introduced into the 36 remaining cages (30 fish/cage), 985 (mean = 27 fish/cage; range: 21-30) were successfully retrieved after 31 days, of which the USGS randomly selected up to 15 fish per cage for THg determination. The average THg concentration (geometric mean  $\pm$  standard deviation) of all caged fish at the time of retrieval was  $0.29 \pm 0.19$  micrograms per gram ( $\mu g/g$ ) dw ( $n = 531$ ; range: 0.06-1.56  $\mu g/g$  dw). The average baseline THg concentration (geometric mean  $\pm$  standard deviation) in reference mosquitofish at the time of introduction was  $0.01 \pm 0.01$   $\mu g/g$  dw ( $n = 15$  reference fish; range 0.003 – 0.021  $\mu g/g$  dw). Thus, the geometric mean THg concentration in caged fish increased by a factor of nearly 30 over the 31-day exposure period.

Among the caged mosquitofish retrieved from cages along Cache Creek (16 of the 36 cages,  $n = 235$  fish), THg concentrations increased with creek distance into the Basin, varied with fish mass at introduction, and varied in the change in fish mass over the 31-day exposure period between fish retrieval and introduction. THg concentrations in caged fish increased with creek distance over the approximately 5.7 mile (9.2 km) stretch of Cache Creek, from 0.12  $\mu g/g$  dw 210 yards (200 m) downstream from the bridge at County Road 102, to 0.34  $\mu g/g$  dw at the low-flow outlet of the Basin. On the average, each 0.5 g increase in fish mass from the time of introduction to retrieval resulted in an increase in THg concentrations of  $0.13 \pm 0.03$   $\mu g/g$  dw. The fish with lower mass at the time of introduction accumulated more THg because they grew more during the 31-day exposure period. Thus, on average, the fish with

larger mass at introduction had lower THg concentration at the end of the exposure period than the fish that started with smaller mass.

The USGS further assessed the effect of habitat type on caged fish THg concentrations using mosquitofish retrieved from all 36 cages placed throughout the Basin. This assessment revealed that caged fish THg concentrations at the time of retrieval varied with the habitat type where the cage was placed, fish mass at the time of introduction, and the change in fish mass over the 31-day exposure period. Least squares means caged fish THg concentrations were greatest in mixed non-woody floodplain habitat ( $0.55 \pm 0.10 \mu\text{g/g dw}$ ) and mixed woody floodplain habitat ( $0.44 \pm 0.10 \mu\text{g/g dw}$ ), followed by irrigation canals ( $0.27 \pm 0.05 \mu\text{g/g dw}$ ), tule wetland habitat ( $0.23 \pm 0.05 \mu\text{g/g dw}$ ), creek habitat past the low-flow outlet of the Basin ( $0.23 \pm 0.10 \mu\text{g/g dw}$ ), and creek habitat within the Basin ( $0.23 \pm 0.02 \mu\text{g/g dw}$ ).

### 3.6.3.2 Mercury in Wild Mosquitofish

The USGS collected 104 wild mosquitofish from 13 sampling locations, of which 9 of the sampling locations were in Cache Creek within the Basin. THg concentrations (geometric mean  $\pm$  standard deviation) in the sampled wild mosquitofish were  $0.74 \pm 0.29 \mu\text{g/g dw}$  ( $n = 104$ ; range: 0.19-1.90  $\mu\text{g/g dw}$ ). In comparison, caged mosquitofish ( $0.29 \mu\text{g/g dw}$ ) reached up to 39% of the THg concentrations in wild mosquitofish after being exposed for just 31 days.

Among only wild mosquitofish collected from Cache Creek within the Basin ( $n = 70$ ), THg concentrations increased with creek distance into the Basin, but did not vary with fish standard length. Model-predicted estimates revealed that wild fish THg concentrations increased over the approximately 5.3 mile (8.6 km) stretch of Cache Creek; ranging from 0.43  $\mu\text{g/g dw}$  875 yards (800 m) downstream from the bridge at County Road 102, to 0.77  $\mu\text{g/g dw}$  at the low-flow outlet of the Basin.

The USGS found that, among the wild mosquitofish collected throughout the study area ( $n = 104$ ), THg concentrations varied significantly by wetland habitat type, but did not vary with fish length. Least squares mean wild fish THg concentrations were greatest in mixed non-woody floodplain habitat ( $1.15 \pm 0.10 \mu\text{g/g dw}$ ), followed by mixed woody floodplain ( $0.87 \pm 0.08 \mu\text{g/g dw}$ ) and creek habitat beyond the low-flow outlet of the Basin ( $0.68 \pm 0.17 \mu\text{g/g dw}$ ). THg concentrations in wild mosquitofish were lowest in creek habitat within the Basin ( $0.64 \pm 0.03 \mu\text{g/g dw}$ ), which did not differ statistically from creek habitat past the low-flow outlet of the Basin.

### 3.6.3.3 Mercury in Bird Eggs

During 2012 and 2013, the USGS collected 316 bird eggs from four species (house wren; tree swallow; Bewick's wren, and ash-throated flycatcher) nesting in 186 of the 286 nest boxes installed within the Basin (fig. 8). The USGS reported nest box occupancy (including boxes where eggs were not collected) at 46% in 2012 and 78% in 2013. The USGS also collected six marsh wren eggs and five mourning dove eggs from natural nests, for a total of 327 bird eggs. Only one egg per nest was collected.

The USGS first assessed the effects of species, year, and a species×year interaction on bird egg THg concentrations using all bird eggs collected in 2012 and 2013. Least squares mean egg THg concentrations were greater in 2012 than in 2013 and varied by species. There was no evidence of a species×year interaction. THg concentrations were highest in tree swallows and ash-throated flycatchers, followed by marsh wrens, house wrens, and Bewick's wrens, the three species of which did not differ statistically from one another, and finally mourning doves.

Next, the USGS assessed how THg concentrations varied among bird eggs collected along the length of Cache Creek within the Basin. House wrens were the only species to nest at riparian habitat locations along the entire length of the creek within the Basin. This analysis showed that the THg concentrations in house wren eggs increased with creek distance in 2012, but not in 2013. Model-predicted estimates revealed that house wren egg THg concentrations in 2012 increased over the approximately 4.4 mile (7 km) stretch of nest boxes along Cache Creek within the Basin; from approximately 0.13 µg/g fresh-wet-weight (fww) at the first nest box placed 1.2 miles (1900 m) downstream from the Road 102 bridge, to approximately 0.19 µg/g fww at the last nest box placed approximately 5.5 miles (8800 m) downstream from the bridge.

The USGS also assessed the effect of habitat type within radii of 115 ft (35 m) and 328 ft (100 m) from the nest boxes on egg THg concentrations using house wren and tree swallow eggs collected from all nest boxes in 2012 and 2013. Among house wrens, individual regressions of egg THg concentration and the percentage of each habitat type indicated that egg THg concentrations increased with the proportion of the nest box area comprised of interior roads and the proportion of the nest box area comprised of mixed non-woody floodplain habitat at radii of 115 ft (35 m) and 328 ft (100 m), respectively. Among tree swallows, the USGS found no relationship between egg THg concentration and the percentage of any individual habitat type at either radius.

#### 3.6.4 Water-Quality Sampling Paired with Fish Cages

The USGS collected water-quality samples at 28 fish-cage stations during March-April 2013 to provide a “snapshot” of conditions within the Basin. Water-quality data are provided in Appendix 2 (Tables A2-1 through A2-6) of the USGS SIR Report. These data show that surface water concentrations of THg and MeHg differed between habitats within the Basin for each Hg species analyzed for this assessment. For the purpose of this assessment, the N-S segment of Cache Creek (adjacent to the western levee, fig. 7) is considered separately from the W-E segment of the creek in the southern part of the Basin.

Concentrations of fTHg were highest in the non-woody floodplain and lowest in both creek channel segments, which did not differ from each other statistically, whereas pTHg was higher (10 to 20 ng/L) for all habitats except for the N-S segment of the creek channel and the wetland habitat. Similar to fTHg, fMeHg was highest in the non-woody floodplain; however, only the N-S segment of the main creek channel was significantly lower than the other habitats including the W-E segment of the channel. In contrast to pTHg, pMeHg was highest in the floodplain habitats and lowest in the N-S segment of the main creek channel and the wetlands. The gravimetric concentrations on the suspended particles also

differed between habitats for pTHg-g and pMeHg-g, but the trends were different. The MeHg/THg ratio in the dissolved fraction (%fMeHg) was generally higher in the floodplain (woody and non-woody) habitats and the W-E segment of the channel than in the other habitats, but the differences were not statistically significant.

In summary, there were systematic variations among habitats for nearly all of the THg and MeHg parameters measured. The Floodplain: mixed non-woody, Floodplain: mixed woody and Open Water: canal habitats were consistently in the highest tier of concentration of fTHg, pTHg, fMeHg, pMeHg, pMeHg-g, and pMeHg-g. The Floodplain: tule wetland category was in the top tier for all of the above parameters except for pTHg-g, and the Open Water: creek, W-E segment was in the top tier for all parameters except fTHg. In contrast, the Open Water: creek, N-S segment was in the bottom tier for all THg and MeHg parameters. (For pMeHg-g, all habitats were in the same tier because of relatively large variations within habitats).

The USGS reported that the DOC concentration and optical character differed between habitats within the Basin. Concentrations of DOC were highest in the non-woody floodplain and lowest in the main channel of the creek. The relative aromaticity of the dissolved organic matter (DOM), measured as  $SUVA_{254}$  (Weishaar et al., 2003), was greatest in the woody floodplain and lowest in the N-S segment of the creek's main channel. Absorption slopes also differed within the Basin, being generally higher in the wetland and non-woody floodplain and generally lower in the creek channel habitats. Absorption slopes reflect the relative contribution of terrestrial and microbial DOM, but they are also affected by photodegradation (Fleck et al., 2014). Fluorescence, normalized to DOC concentration to reflect concentration-independent compositional differences, differed between habitats, although the differences were variable across an Excitation-Emission Matrix (EEM) landscape. Indicators of humic DOM (peaks A and C, fluorescent dissolved organic matter (FDOM), and humic index (HIX)) and soil-derived fulvic DOM (peak D) were generally low in the N-S segment of the creek channel and generally high in the W-E segment and the irrigation canal habitat (USGS, 2015, Figures 53-54). The fluorescent indicators of algal and/or microbial activity (peaks B and T) were higher in the N-S segment than the rest of the habitats. Indicators of photodegradation (peaks Z and N) showed more photo-depletion of the DOM in the N-S segment of the creek channel (Fleck et al., 2014).

The USGS performed a qualitative look at the optical characterization of DOM which indicated distinct differences between habitats. This was evidenced by absorbance scans showing differences in shape and concentration between the creek channel segments and the other basin habitats across the measurable spectral ranges of the samples. Within the creek channel the segments differed, with the N-S segment having higher absorbance in the deep ultraviolet (< 240 nanometers (nm)) range, and the W-E segment having higher absorbance at longer wavelengths (>240 nm). Because the concentration of DOC was lower in the channel than in other habitats, the absorbance values at longer wavelengths in the visible range (> 400 nm) were below the reporting limit of the measurement. In contrast, many of the samples from the other basin habitats had much higher absorbance in the mid-ultraviolet (240 to 340 nm) range.

Although some of the difference was due to concentration effect on absorbance, the DOC normalized to SUVA<sub>254</sub> values indicate that there were compositional differences as well.

Concentrations of MeHg in the surface waters of Cache Creek varied markedly within the Basin during the March-April 2013 sampling period. Dissolved (<0.3 μm) fMeHg concentrations were greater in the W-E channel segment, but did not change significantly over the total distance along the channel. However, there was an interaction between channel segment and distance where fMeHg concentrations decreased by as much as 0.05 ng/L per mile (0.03 ng/L per km) from N to S (cage 1 to 40, fig. 7) at which point they increased by up to 300 % (cage 40 to 27) and then increased by as much as 0.03 ng/L per mile (0.02 ng/L per km) from W to E (cage 27 to 15). Similar to the dissolved phase, pMeHg (ng/L) was higher in the W-E channel segment than the N-S segment, and there was an interaction between channel segment and distance. However, the trends with distance within each segment were different, as pMeHg increased across the total distance from the Inflow at Road 102 but that was driven primarily by the difference between segments, as pMeHg concentrations decreased by approximately 0.2 ng/L per mile (0.1 ng/L per km) along the N-S channel segment, increased by up to 300% from cage 40 to 27, and then did not change with distance in the W-E channel segment. The concentration of MeHg on the suspended particles (pMeHg-g) did not differ significantly by distance or between channel segments, although the difference between segments was nearly significant.

Concentrations of THg did not change with distance for either the dissolved or particulate phases; fTHg did not change with distance or channel segment. Volumetric pTHg also did not change with distance or channel segment. There was no interaction between channel segment and distance for either form of THg. The amount of THg associated with suspended particles did not differ by channel segment or distance along the channel, although there was nearly a significant interaction between the two, where pTHg-g appeared to increase from N to S and then stay consistent from W to E.

The MeHg/THg ratio in the dissolved fraction (%fMeHg) was higher in the W-E segment than the N-S segment of the creek channel, but did not change significantly with distance along the channel. The MeHg/THg ratio for particulates (%pMeHg) did not differ significantly between segments, but had a nearly significant decrease with distance along the channel.

The USGS reported that the DOM character and DOC concentration both varied with creek distance. For DOC concentration, there was an interaction between distance along the creek channel and segment (N-S versus W-E) within the Basin. DOC decreased in the N-S segment and then increased in the W-E segment of the creek channel. The interaction between distance and segment led to no significant change in DOC over the total creek distance expanding from Road 102 to the low-flow outlet.

Optical data indicated changes in DOM character with creek distance; however, the low number of samples collected restricted the power of the model. The aromaticity, measured as SUVA<sub>254</sub>, increased by only 15 to 20% along total distance along the channel within the Basin and was nearly statistically significant. Absorption slopes appeared to not change over distance but the model lacked sufficient

power to determine the significance. Among the standard, diagnostic fluorescence indicators, only peak B and HIX changed significantly over distance along the channel. Peak B decreased whereas HIX increased with distance. Most fluorescence peaks differed primarily between channel segments (habitat) and not with distance within the segments; or along the total distance, so the fluorescence data generally reflected a difference between segments, as presented above.

The USGS reported other water-quality parameters that varied with creek distance. Water temperature, like DOM, differed between segments but not along channel distance. The temperature of the W-E segment of the creek channel was nearly twice (80% higher, in °C) than that of the N-S segment. Concentration of TSS, chlorophyll-a, and pheophytin-a all decreased with creek distance. The ratio particulate organic carbon (POC)/TSS also decreased with distance. POC itself decreased with distance, but was not quite statistically significant; total particulate nitrogen (TPN)/POC did not change significantly with creek distance. Dissolved salts, measured as chloride and specific conductance, increased with distance, particularly along the W-E segment, probably reflecting an evaporative trend.

### 3.6.5 Water-Fish Relationships

The USGS reported that fish THg concentrations were closely related to fMeHg surface-water concentrations for co-located samples; a linear least-squares regression indicates that 80% of the variability in fish THg can be explained by fMeHg concentration. In comparison, pMeHg concentration only accounted for 40% of the variability in fish THg alone. By comparison, fTHg explained only 48% of the variability in fish THg. However, the data appear to indicate two separate relationships within the dataset. One group of sites, which included all of the creek channel sites and wetlands as well as three floodplain sites (Group 1, USGS, 2015, figure 55A) were generally lower in fish THg but increased more dramatically as fMeHg increased. The other group (Group 2) was generally higher in fish THg but the fish THg increased to a lesser degree as fMeHg increased. The two groups were not habitat-driven and no biogeochemical measurement discriminated between them. Fish feeding behavior may provide the best explanation for the separation between the groups. If the floodplain sites are considered separately, the fish with higher THg (Group 2) occurred exclusively where chlorophyll-a and pheophytin-a concentration were low in the water column and fish THg decreased with increasing chlorophyll-a and pheophytin-a (USGS, 2015, figure 55A). These differences may be related to different fish diet in the creek channel and wetland sites versus the floodplains. An alternate explanation is the dual role that DOM may play on THg and MeHg bioavailability. Fish THg also exhibits a dual relationship with DOC where the Group 2 sites have elevated fish THg relative to DOC compared with Group 1 sites (USGS, 2015, figure 55C). However, at the Group 1 sites, the relative contribution of peak N (algal-derived DOM; Coble, 1998) to the DOC concentration is strongly positively related to fish THg, whereas in the floodplains there is a negative relationship (USGS, 2015, figure 55D) which may explain the difference between fish THg concentrations in Groups 1 and 2.

The mechanism behind this physical explanation is difficult to pinpoint but may be one of four identified possibilities: 1) the relative contribution of peak N may simply reflect algal productivity that may lead to

biodilution in the floodplain sites but is the primary vector of bioaccumulation in the creek habitat, 2) lower relative contribution of peak N may simply reflect a larger contribution of DOC from a non-algal source that is more readily bioaccumulated in the floodplain habitats, 3) a lower relative contribution of peak N may reflect greater relative photodegradation which could either lead to greater photodemethylation leading to the opposite effect seen here or may lead to more degradation of the type of DOM that binds THg and MeHg resulting in more THg and MeHg bioavailability, or 4) the contribution of peak N to DOM could also be indicative of a different algal/planktonic source in the floodplain habitats that the fish do not like, such as *Microcystis*.

### **3.7 Subsurface Conditions**

The USGS utilized the deep soil core data to estimate historical sedimentation rates in the Basin and to assess the vertical distribution of THg and MeHg in the subsurface sediments. The details of this work are presented in the USGS SIR Report (USGS, 2015) and summarized below.

#### **3.7.1 Historical Sedimentation Rates**

Detailed sub-sampling of cores and analysis of Cs-137 for the purpose of dating was accomplished at drill sites 9 through 15 (Fig. 9). Raw data for Cs-137 analyses and information on methods, quality assurance, and quality control are available in a USGS Data Series Report (Arias et al., in review). Values of Cs-137 activity were determined on subsampled 1.2 in (3-cm) vertical intervals. For each of the seven vertical profiles where Cs-137 was determined, the depth of maximum Cs-137 was chosen, representing heaviest fallout from atmospheric testing of atomic weapons in 1963 (Ritchie and McHenry, 1990).

An example of a profile for which the maximum Cs-137 fallout is indicated is shown on Figure 12 below.

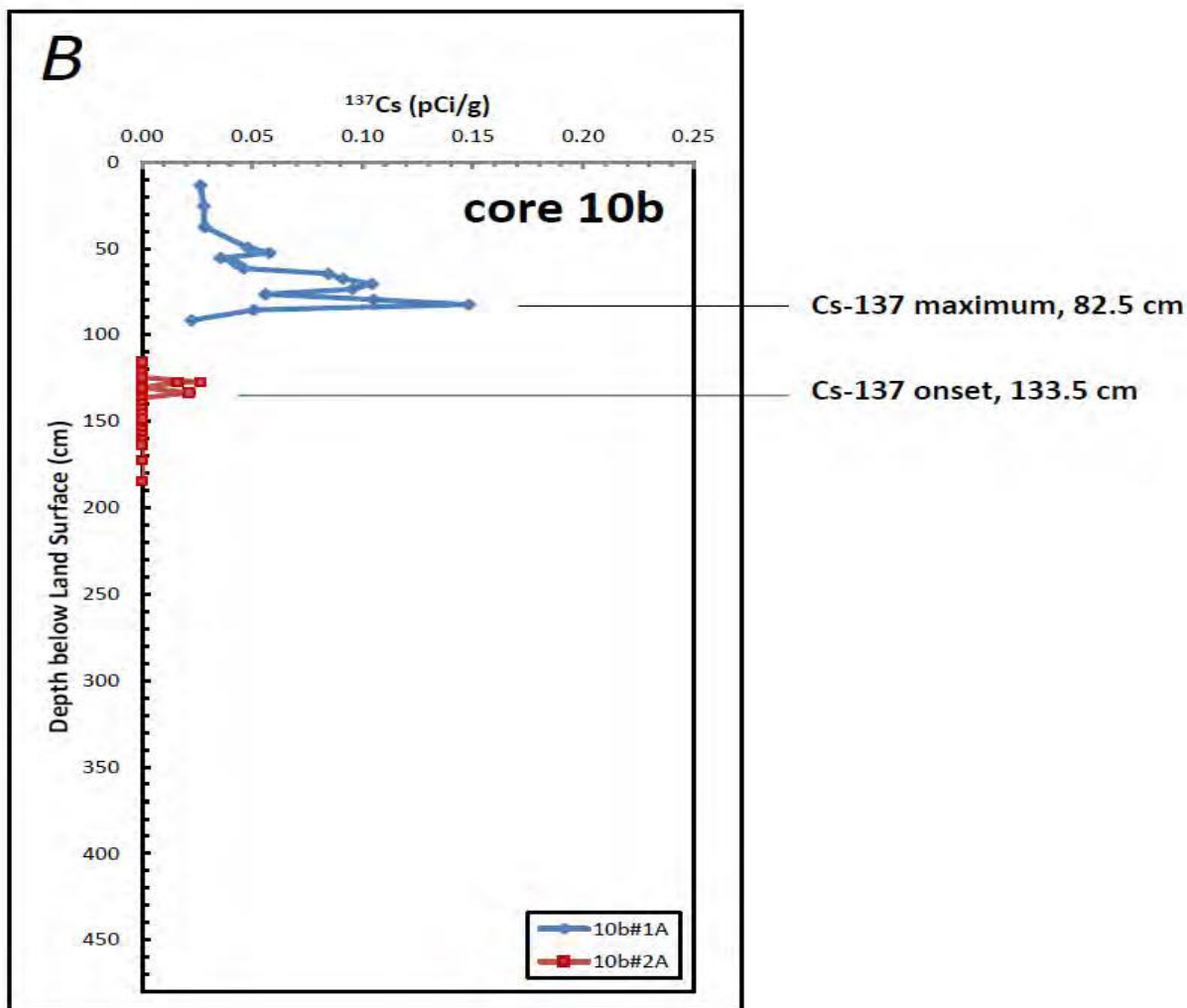


**Figure 12. Profile for Soil Core 10b**

The above profile is for drill site 10. Similar profiles for all seven sites where Cs-137 was analyzed are given in Appendix 6 (Fig. A6-1) of the USGS SIR Report (USGS, 2015). Based on the depth selected for the 1963 horizon for each of the seven profiles, the USGS calculated corresponding average sediment deposition rates. The USGS provided two different sets of average values; excluding site 9 from both sets of averages because the site was not part of the Basin until 1993, when the western levee was moved approximately one-half mile (805 m) to the west. The two sets of averages are: 1) sites 10 through 15, and 2) sites 10, 11, 12, 13, and 15. The latter set excludes site 14, which is located in the northeastern corner of the Basin, and includes five sites in an E-W traverse near the southern boundary of the Basin (fig. 9). For each of the two sets of sites, the apparent sediment deposition rate is compiled for the period 1963 to year of coring (2011 or 2012). The average sedimentation rate ( $\pm$  standard deviation) for sites 10,

11, 12, 13, and 15 for 1963 to the date of coring was  $0.89 \pm 0.22$  inches per year (in/yr) ( $2.27 \pm 0.55$  centimeters per year (cm/yr)).

Using the average deposition rate the USGS projected downward to predict the depth of the 1937 horizon (origin of the CCSB) as shown below on Figure 13.

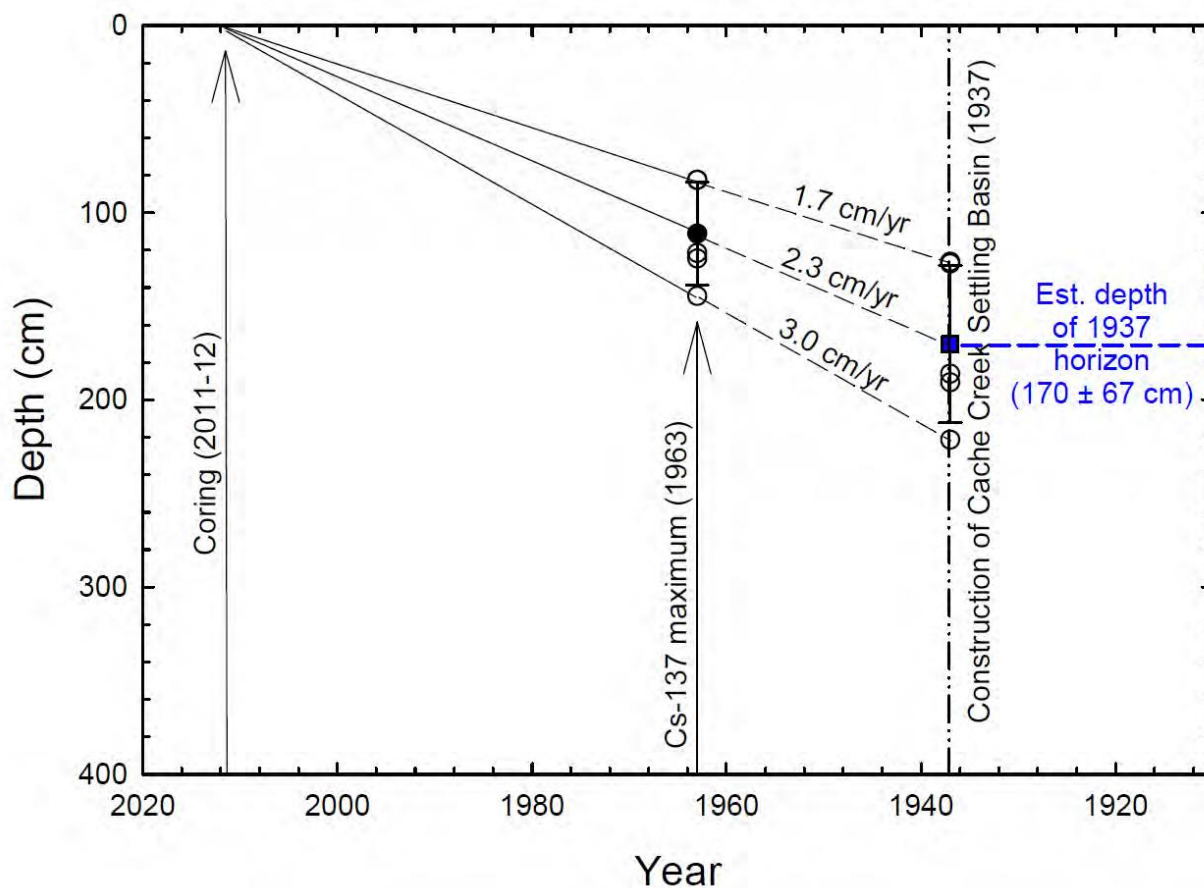


**Figure 13. Plot of Projected Depth of 1937 Basin Horizon**

Using the average deposition rate from 1963 to the year of drilling (0.9 in/yr or 2.27 cm/yr), and applying the standard deviation to predict uncertainty, this depth is estimated to be  $5.6 \pm 1.4$  ft ( $1.70 \pm 0.42$  m) below land surface. The range of deposition rates at sites 10, 11, 12, 13, and 15 is 0.66 in/yr to 1.16 in/yr (1.68 cm/yr to 2.95 cm/yr). The range in estimated depth of the 1937 horizon for individual sites are 4.1 ft (1.26 m) at site 11 to 7.3 ft (2.21 m) at site 12. Based on these calculations, it is estimated that, in general, the top 6 to 7 ft (approximately 2 m) in the Basin represents post-1937 material, and material deeper than about 8 ft (2.5 m) below land surface probably represents material deposited prior to initial Basin construction in 1937.

### 3.7.2 Vertical Profiles of Total Mercury and Methylmercury

Vertical profiles of THg for the 15 coring sites based on 7.9-in (20-cm) composite samples are shown on Figure 14 below.

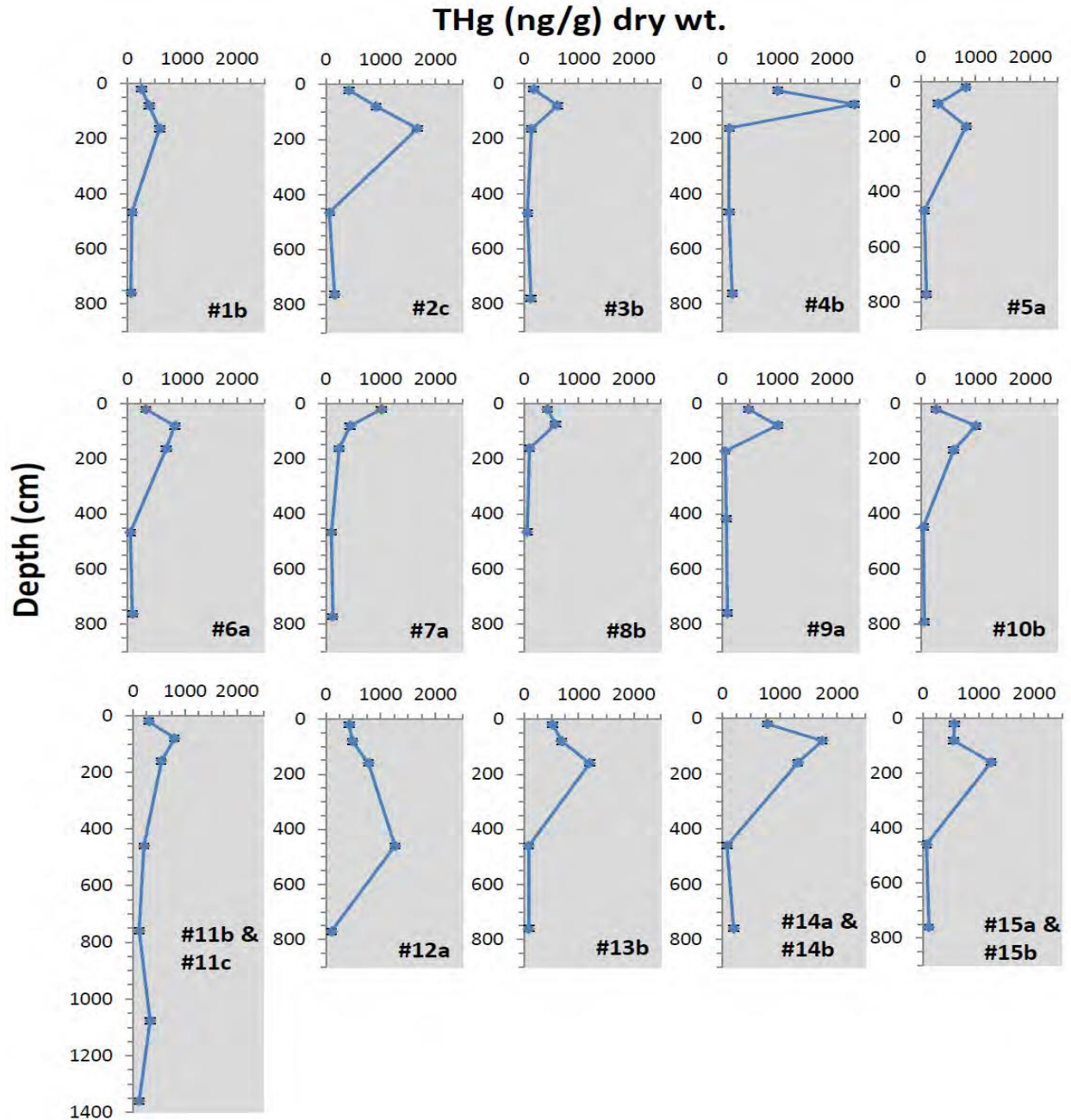


**Figure 14. Vertical Profiles of THg in Soil Cores**

As illustrated in Figure 14, the greatest measured values of THg in 7.9-in (20-cm) composite core samples are typically found at one of the top three depths intervals, 3.9–11.8 in (10-30 cm), 27.6–35.4 in (70-90

cm), or 59–66.9 in (150-170 cm). Based on the Cs-137 results, all of these depths likely represent material deposited in the Basin after its construction in 1937. Concentrations of THg in the deeper intervals, 177-185 in (450-470 cm) and 295-303 in (750-770 cm) were uniformly low, with the exception of the 177-185 in (450-470 cm) depth sample at site 12, which had THg greater than 1,000 ng/g (ppb). Site 12 also gave anomalous results for Cs-137, with some traces of detectable material at depths as great as 145.7 in (370 cm.).

Vertical profiles of MeHg at the 15 coring locations are shown on Figure 15. Similar to THg, the highest measured values are in the top three intervals sampled, at depths less than 66.9 in (170 cm) below land surface, with the exception of site 12. It is likely that excavation or other disturbance in the area of site 12 caused post-1937 material to occur at the observed depths with elevated THg and MeHg concentrations.

The USGS made a comparison of THg in the shallow surface sediment (0-2 cm) with the deeper cored intervals. The USGS reported that for THg, the 0-2 cm data are significantly lower than the data from 27.6–35.4 in (70-90 cm), and are not significantly different than the data from the 3.9-11.8 in (10-30 cm) and 59-66.9 in (150-170 cm) depth intervals. The samples collected from shallower than 78.7 in (200 cm) are significantly higher in THg than the samples from 177.2-185 in (450-470 cm) and 295-303 in (750-770 cm) depth, which are interpreted to be pre-1937 (and possibly pre-Gold Rush).

A similar analysis comparing 0-2 cm data to the deep cores was done for MeHg. The shallow surface material (0-2 cm) had the highest MeHg. The top three cored intervals 3.9-11.8 in (10-30 cm), 27.6-35.4 in (70-90 cm), and 59-66.9 in (150-170 cm) were significantly lower in MeHg than the 0-2 cm layer, and were significantly higher in MeHg than the underlying intervals.

As a check on variability and consistency, the USGS compared analyses of THg in 1.2 in (3-cm) intervals used for Cs-137 dating to the 7.9 in (20-cm) composite samples (SIR Report, Appendix 6, Fig. A6-2). In each case, the 1.2 in (3-cm) and 7.9 in (20-cm) THg data track one another quite closely overall, but there are several outliers in the 1.2 in (3-cm) data, indicative of a “nugget effect” likely from individual grains of cinnabar (HgS) and/or metacinnabar (m-HgS) contributing to the THg results.

### MeHg (ng/g) dry wt.

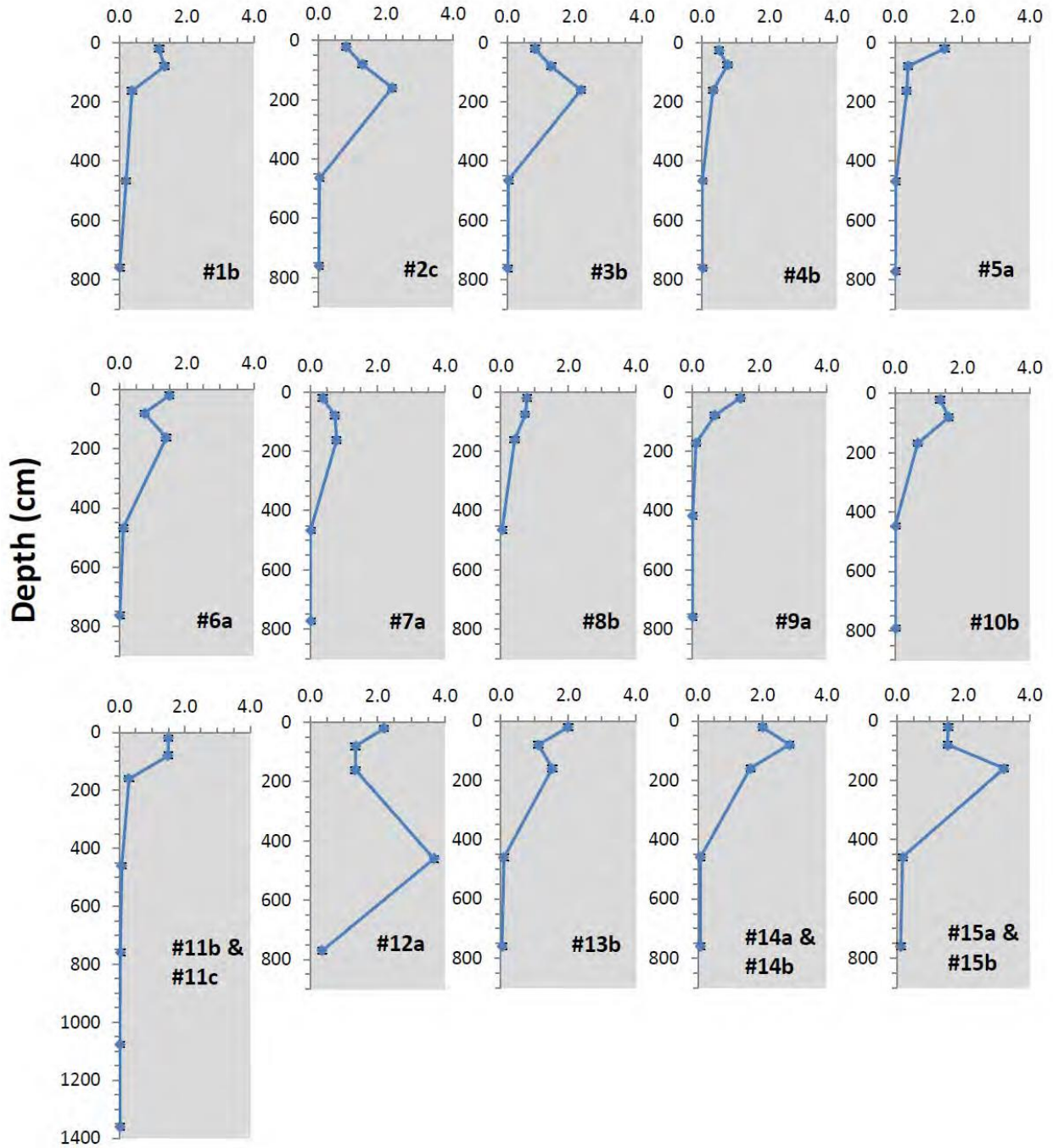


**Figure 15. Vertical Profiles of MeHg in Soil Cores**

### 3.8 Grain-Size Distribution

The USGS provided grain-size distribution data for each of the 7.9 in (20-cm) composite samples collected from the drill cores (Arias et. al., in review) and reported that the grain-size distribution data are consistent with the interpretation that the shallower intervals (less than 78.7 in, 200 cm depth) were deposited in the Basin after 1937. Grain size distribution plots for each of the coring sites are included in Appendix 6, Fig. A6-7 of the USGS SIR Report and plots showing grain-size distribution data for the 7.9 in (20-cm) composite samples as a function of depth for all sites are included as Figures 62A-E in the USGS SIR Report (USGS, 2015). In these plots, one can see that sandy material (modes of at least 100 micrometers (um)) in percentages greater than 5% are present only in the material from depths of 59-66.9 in (150-170 cm) or shallower. The deeper intervals 177.2-185 and 295.3-303.1 in (450-470 and 750-770 cm) consist primarily of silt with low percentages (less than 5%) of very fine sand at some locations. A summary plot showing the percentages of sand, silt, and clay at each of the 5 depths for composite (7.9-in, 20-cm) samples is shown below in Figure 16. Although there is some sand in the deeper intervals, 14.8–15.4 ft (450–470 cm) and 24.6–25.3 ft (750-770 cm), sand is more abundant in the three shallowest intervals, 0.3–1.0 ft (10–30 cm), 2.3–3.0 ft (70–90 cm), and 4.9–5.6 ft (150–170 cm), consistent with the function of the Basin in trapping sand beginning in 1937.

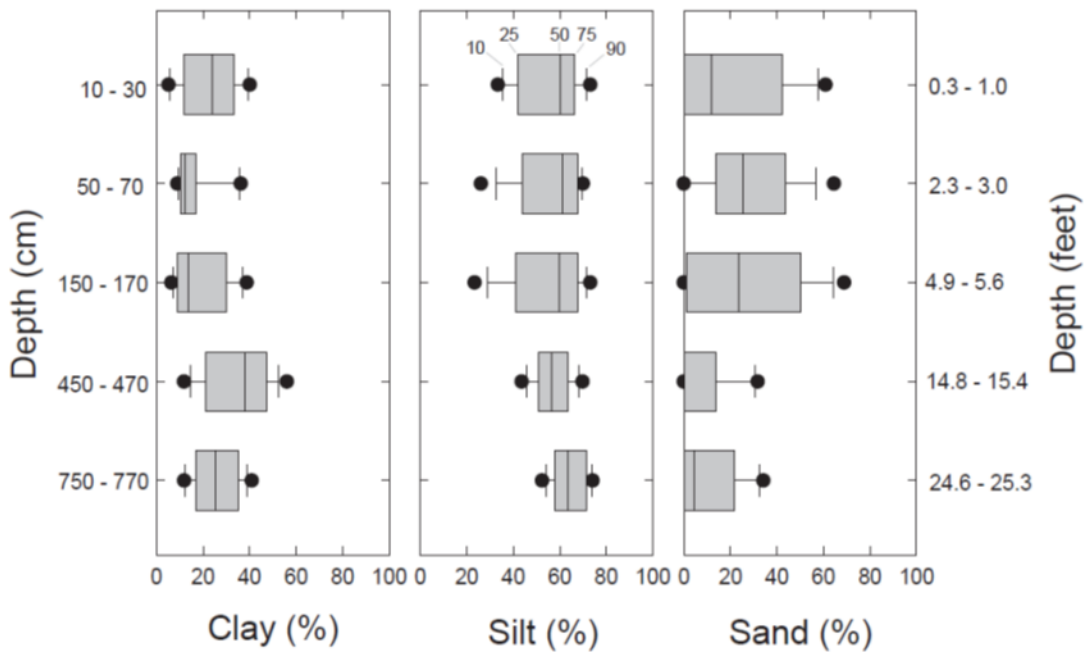


**Figure 16. Summary Plot of Sand, Silt, and Clay Percentages for 20-cm Composite Samples.**

### 3.9 Discussion of USGS Findings

The USGS SIR Report (USGS, 2015) provides a discussion of their findings summarized by various media sampled and analyzed; surface water, sediment, and biota. The USGS findings are summarized below.

#### 3.9.1 Surface Water

The USGS compared the TE and load calculations presented above for THg and MeHg to available historical data for the Basin and the requisite TMDLs. In establishing the TMDLs for the Basin, the CVRWQCB evaluated available data for loads of THg, MeHg, and suspended sediment entering and exiting the Basin for two efforts: (1) the Cache Creek, Bear Creek, and Harley Gulch TMDL for mercury (Cooke et al., 2004 aka “Staff Report”, approved as a Basin Plan Amendment in 2006); and (2) the Sacramento-San Joaquin Delta TMDL for mercury and methylmercury (Wood et al., 2010a, approved as a Basin Plan Amendment in 2011). The USGS compared the CVRWQCB’s published load estimates and Basin TE for various time periods between Water Years 1984 and 2003 with the results from this study as well as the estimates of TE of THg and suspended sediment made by CDM (2004a).

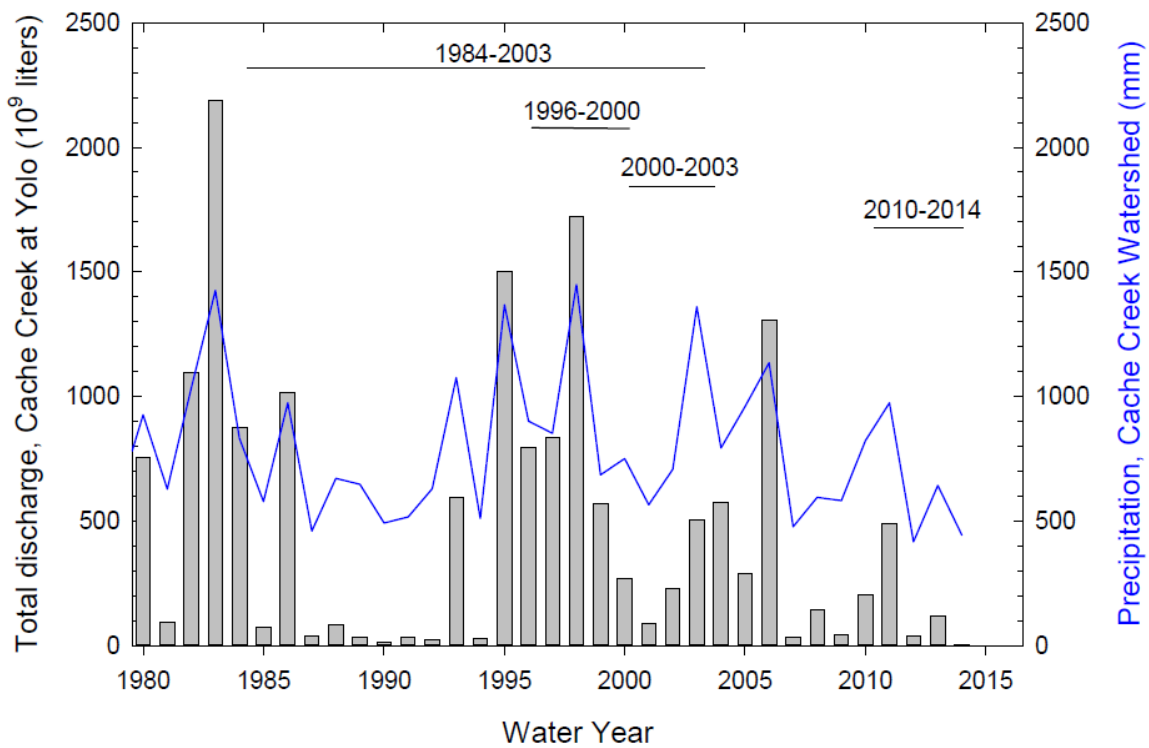
Prior to Water Year 2009, the only quantitative flow information available for the Basin was the stream gage at Cache Creek at Yolo, located about 5 mi (8 km) upstream of the inflow to the Basin at Road 102. The gaging station at Yolo is still used by USGS for Basin inflows (with a 2-hour lag time during high-flow conditions). However, DWR in being pro-active to the Basin Plan Amendments, starting in WY 2009 contracted with the USGS to directly measure the outflows from the Basin at two gaging stations (fig. 2): the low-flow outlet (11452900) and the south abutment of the weir/spillway (11452800). Starting in WY2013, water-quality and suspended sediment samples have also been taken by USGS at the north abutment of the spillway/weir (384115121402501, Fig. 2). The CVRWQCB estimates of loads and TE for the period 1984–2003 assumed that the flow into the Basin was equal to the flow out either on a daily or instantaneous basis. The hydrographs for Water Years 2010–13 (figs. A-D) indicate that there are sometime significant differences between inflows and outflows, which are attributed to travel time and basin filling. On days following relatively large storm events, the Basin may approach steady-state flow conditions, in which the flow in is approximately equal to the flow out on a given day; however, there are many other days with transient conditions. Thus, the assumption that the flow out of the Basin was equal to the flow into the Basin represents an additional degree of uncertainty that has not been quantified, in the pre-2009 calculations of loads out of the Basin and the corresponding TE.

##### 3.9.1.1 Total Mercury Loads

For Water Years 1996–2000 the CVRWQCB estimated that the average annual THg load into the Basin was 369 kg/yr and the load out was 226 kg/yr (Cooke et al., 2004). This period was considered to be unusually wet, so a 20-year average was calculated for Water Years 1984–2003, a period with approximately equal numbers of wet and dry years (Cooke et al., 2004) using flow data for that period combined with concentration data from 1996–2000. Based on this approach, the CVRWQCB estimated

the annual THg load into the Basin during 1984–2003 at 224 kg/yr with a corresponding load out of the Basin of 125 kg/yr. In comparison, the THg loads calculated in this study for Water Years 2010–14 were considerably lower than the CVRWQCB estimates, averaging 32 kg/yr for the inflow and 13 kg/yr for the combined outflow (Table 3.1).

An important factor contributing to lower observed loads during WYs 2010–14 compared with WYs 1996–2000 and WYs 1984–2003 is the below-average rainfall and streamflow during WYs 2010–14 as can be seen below in Figure 17; time-series plots of streamflow data from the gaging station Cache Creek at Yolo (USGS gage 11452500), which represents flow into the Basin. Compared to the long-term average streamflow (WYs 1904–2014), 1984–2003 was very close (ratio of 1.01 to long-term average), whereas 1996–2000 was well above average (ratio of 1.81). The periods 2000–03 and 2010–14 were both below the long-term (1904–2014) average, with ratios of 0.59 and 0.37, respectively (data from <http://waterdata.usgs.gov>).



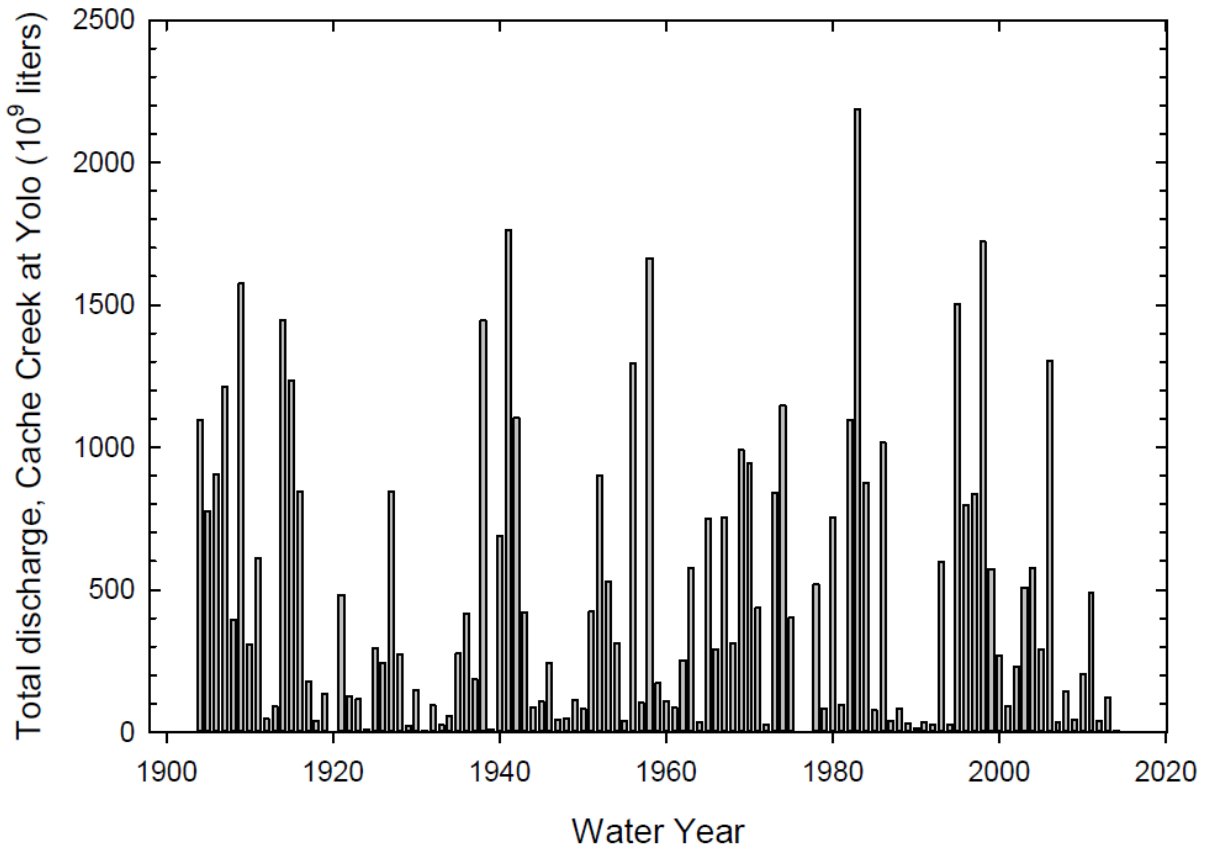


**Figure 17. Time-series Plots of Streamflow Data for Yolo Gage**

Another possible factor contributing to lower THg loads exiting the Basin is the variation in gravimetric concentration of THg on suspended particulates (pTHg-g). Estimates of mean pTHg-g during WYs 1996–2000 were 500 ng/g (equal to ppb) for both inflow and outflows based on the ratio THg/TSS and the ratio of THg loads to sediment loads (Cooke et al., 2004; Wood et al., 2010a). The data from Foe and Croyle (1998) for WY's 1997–1998 indicate that p-THg-g (calculated as the ratio of volumetric THg/TSS concentrations) had a mean of 370 ng/g at high flow (n=11) and a mean of 450 ng/g at low flow (n=5) (USGS, 2015, Table 22). Mean values of pTHg-g during WYs 2010–14 from this study were 255 ng/g for inflows, and 284 ng/g for combined outflows, a little more than half of the 500 ng/g value estimated by the CVRWQCB. These differences may be related to remediation activities at mercury mine sources in the upper Cache Creek watershed, such as the Abbott mine and Turkey Run mine in Harley Gulch where a large calcine pile was stabilized during 2006–07 (J. Cooke, personal communication, 2015). While this apparent decrease in p-THg-g is expected to continue as additional upstream mercury sources

are remediated, future monitoring will be needed to determine whether this apparent decrease will be sustained in wetter years.

Calculations of TE using historical data indicate average THg trapping within the Basin of 39% to 51% (USGS, 2015, Table 21). For this study, the USGS calculated the average value of TE for THg at 59%. This value was computed for wwTHg, which includes loads based on nonfiltered samples as well as the sum of fTHg and pTHg loads. To enable averaging of the multiple load estimation methods used in this study, the USGS added the loads of fTHg to the various estimated loads of pTHg (Table 3.1) so that wwTHg loads from this study could be compared with results from the previous studies. The overall wwTHg TE value of 59% from this study is just less than the average historical calculated value of 60.6% TE for pTHg.

### 3.9.1.2 Methylmercury Loads

For Water Years 1996–2000 the CVRWQCB estimated that the average annual MeHg load into the Basin was 72.5 g/yr and the load out was 86.6 g/yr (Cooke et al., 2004), indicating some production of MeHg within the Basin. The 20-year average MeHg load out of the Basin for Water Years 1984–2003, calculated using concentration data from 1996–2000, was 270 g/yr (Cooke et al., 2004); no estimate was given for MeHg loads into the Basin during this period. Wood et al., (2010a) estimated an average MeHg load of 137 g/yr out of the Basin during WYs 2000–03. In contrast to THg, the MeHg loads into the Basin calculated in this study for Water Years 2010–14 were considerably higher than the CVRWQCB estimates; averaging 408 g/yr for the inflow and 183 g/yr for the combined outflow (Table 3.3), which is in a similar range to the CVRWQCB estimates despite the different flow conditions.

The much lower flows during WYs 2010–14 compared with WYs 1996–2000 and WYs 1984–2003 apparently did not have as much effect on MeHg loads as on THg loads. Data on the gravimetric concentration of MeHg on suspended particulates (pMeHg-g) are not available for the previous studies. Comparison with data from the previous studies indicate higher average wwMeHg concentrations during this study by a factor of approximately 2 in inflows (0.19 ng/L in previous studies versus 0.39 ng/L in the present study) and a factor of about 1.2 to 1.4 in outflows (0.41 ng/L and 0.5 ng/L in previous studies versus 0.61 ng/L in the present study).

TE calculations using historical data indicate variable MeHg trapping within the Basin depending on flow conditions. During individual storm events, positive values of TE were observed, up to 27% (Cooke et al., 2004), whereas during low-flow conditions, a net increase in MeHg concentration was observed, corresponding to negative values of TE. During the present study, the average value of TE for MeHg was 55% computed for wwMeHg, which includes loads based on nonfiltered samples as well as the sum of fMeHg and pMeHg. To average the multiple load estimation methods used by the USGS in this study, they added the loads of fMeHg to the various estimated loads of pMeHg (Table 3.3). The overall wwMeHg TE value of 55% from this study is slightly less than the average value of 57.3% TE for pMeHg. Also, the results of the present study regarding an increase in fMeHg loads from inflow to

outflow are consistent with the previous work indicating an increase in wwMeHg at low flows, when one would expect a higher proportion of fMeHg and less pMeHg at lower flow velocity.

### 3.9.1.3 Comparison of THg and MeHg Loads to Regulatory Allocations

The CVRWQCB issued load allocations for THg and MeHg in water exiting the Basin as part of the TMDL process (Cooke et al., 2004, Wood et al., 2010b), as summarized in the USGS SIR (USGS, 2015, Table 23). The THg load allocation is a reduction of 50%; based on the “existing” load of 118 kg/yr, the target THg load would be 59 kg/yr. During the period of this study, WYs 2010–14, the average THg load exiting the basin was 13 kg/yr, substantially below the “existing” load cited by Wood et al. (2010a). The MeHg load allocation in the Basin Plan is a reduction to 21.5% of “existing” loads, with a cap of 30 g/yr; the “existing” MeHg load for Basin outflow in the Delta TMDL Staff Report was 137 g/yr (Wood et al., 2010b). Due to the below-average flow conditions during WYs 2010–14, the average MeHg load exiting the Basin during this study was 183 g/yr, somewhat higher than the “existing” load in the Delta TMDL staff report.

### 3.9.1.4 Within-Basin Water Quality

Spatial trends in MeHg in water, especially the systematic changes with distance along the creek channel as it flows through the Basin, are indicative of conditions that lead to elevated MeHg in the eastern part of the Basin compared to the western part. The USGS interprets that integrated results of the DOM concentration and character measurements suggest that the wetland and non-woody floodplain habitats produce more DOM of a more labile nature than the other habitats. In the N-S segment of the creek channel, relatively low DOC concentrations coupled with the low  $SUVA_{254}$  values and high absorption slopes suggest a less degraded (photo or microbial) DOM. Fluorescence data suggest that the N-S segment of the creek channel had enhanced microbial DOM production and photo-degradation. The non-woody floodplain also had some indication of photo-degradation of DOM but less microbial production. The W-E segment of the channel and the canal habitats (and non-woody floodplain to a lesser degree) had higher contribution of soil-derived DOM. Based on the Fluorescence Index and peak N, more microbial- and algal/plankton- derived DOM in the W-E segment of the creek channel is suggested than for the N-S segment (McKnight et al., 2001; Coble, 1998). These differences in DOM character among habitats are interpreted by USGS as being important with regard to MeHg formation and bioaccumulation within the Basin.

## 3.9.2 Sediment

USGS’s detailed statistical analysis of the sediment geochemical data on mercury species and other constituents for samples collected within the Basin during 2010–13 revealed a number of important and overarching trends to consider when assessing various management options for the Basin. Discussions of how the findings to date may have implications for specific management actions are presented in Sections 4.0 and 6.0. The following sections present a summary of USGS’s evaluation of the results documented

above as a step toward formulating a more comprehensive conceptual model based on what the sediment mercury data reveal about biogeochemical processes affecting mercury cycling in the Basin.

### 3.9.2.1 Land Use and Organic Content are Key Drivers of Mercury Speciation

One of the most important conclusions associated with the sediment results is that land use within the Basin exerts a dominant control on sediment geochemistry, particularly with regard to organic matter, and this subsequently exerts a primary control on mercury cycling (including methylation and bioaccumulation) within the Basin. Although some significant differences in THg concentration were observed among the Level 1 land use categories (for example, Agriculture > Floodplain), these habitat differences were modest compared to those found for the more environmentally relevant and biogeochemically active sub-sets of the THg pool, namely MeHg and RHg(II). Reinforcing this conclusion is the observation that THg concentration normalized to organic matter (that is, [THg/%LOI]) showed stronger spatial trends among the land use categories than did THg concentration alone, which was largely driven by the strong differences in sediment organic content among land categories (that is, %LOI for Floodplain and Riparian > Open Water and Agricultural).

Another interesting aspect of the effect of habitat type was the significantly higher concentration of RHg(II) (as well as [RHg(II)/LOI] and %RHg(II)) observed in woody vs non-woody habitats. Although this did not result in higher MeHg concentrations in woody habitats, it does likely reflect the increased leaf area and litter fall associated with trees (relative to other vegetation) and the process by which leaves can act as effective collectors of atmospheric inorganic Hg(II) associated with dry deposition (Grigal, 2002; Driscoll et al., 2007).

One aspect of the data results that did not show significant differences among habitat types was for the fraction-specific mercury concentrations ( $Hg_{SE}$ ) associated with the sequential extractions. Thus, while there were very notable differences in the  $Hg_{SE}$  concentrations among the five fractions, with very low concentrations of the two most labile fractions (F1 and F2) and higher concentrations for some of the chemically more resistant fractions (especially F3 and F5), the overall distribution among fractions did not significantly change as a function of habitat. This relationship indicates that there is a very small, but likely a very important, pool of labile sediment mercury in all of the primary habitat types. Further, most of the sediment THg within the Basin exists either as organic or particulate bound (F3) or as HgS (cinnabar or meta-cinnabar, F5), because one would not expect much mercury-gold (HgAu) amalgam based on the relatively small number of historical gold mines in the Cache Creek watershed compared with historical mercury mines (Domagalski et al., 2003a, b, 2004). In contrast to the absolute  $Hg_{SE}$  concentrations, the % $Hg_{SE}$  data (each fraction normalized to the sum of all five fractions) did show one fraction-specific example where there existed a significant difference among habitat types, as % $Hg_{SE}$  for F3 was larger for Floodplain (51% of  $THg_{SE}$ ) than for Agricultural (30% of  $THg_{SE}$ ). This trend was very likely caused by the much higher organic content of the Floodplain areas compared to Agricultural areas.

### 3.9.2.2 Hydrology is a Key Factor Affecting Reactive Mercury Trends

USGS's examination of the spatial and temporal trends for non-Hg sediment parameters sheds additional light on some overall physical and geochemical dynamics that are occurring within the Basin. Considering the seasonal hydrology of the Basin in a 'typical' year, there is a period of initial flood-up (early winter through spring), followed by a period of draining of most of the water outside of the Cache Creek main channel, and then a prolonged period of drying of exposed soils from late spring through the following late fall or early winter. In addition, during the draining period, the Basin largely drains from west to east, a function of the slightly lower elevation on the eastern side (UCD, 2012). This implies that overall, the eastern side of the settling basin remains wetter for longer during the period of rising seasonal temperatures (late spring into early summer). This temporal and spatial pattern of flooding, draining, and drying has many implications for sediment chemistry, which are evident in the statistical analysis conducted on the non-Hg sediment parameters. For example, sediment % dry weight was found to decrease from west to east (that is, % wet weight increased from west to east) and increased over the course of the water year. As sediment dries out, it becomes more oxidized, which can cause chemically reduced species (for example,  $\text{Fe(II)}_{\text{AE}}$ ) to become re-oxidized. Based on results of USGS's statistical analysis (Model A) results,  $\text{Fe(II)}_{\text{AE}}$  increased from west to east and decreased over time (as did  $\% \text{Fe(II)}_{\text{AE}}/\text{Fe}_T$ ), trends consistent with the temporal and spatial pattern of sediment wetting/drying and associated with Fe(II) re-oxidation. In contrast, sediment  $\text{RHg(II)}$  concentrations decreased from west to east and increased over time, which is consistent with previous reports of  $\text{RHg(II)}$  being negatively correlated with chemically reducing (and typically wetter) sediment conditions (Marvin-DiPasquale et al., 2009, 2014). For the current data set, all of the  $\text{RHg(II)}$  metrics; ( $\text{RHg(II)}$  concentration itself,  $[\text{RHg(II)}/\% \text{LOI}]$ , and  $\% \text{RHg(II)}$ ) were negatively correlated with both  $\text{Fe(II)}_{\text{AE}}$  concentration and with  $\% \text{Fe(II)}/\text{Fe}_T$ , to various degrees. Among the strongest of these correlations was sediment  $\text{RHg(II)}$  concentration (Log10 transformed) versus  $\% \text{Fe(II)}/\text{Fe}_T$ . The  $\% \text{Fe(II)}/\text{Fe}_T$  metric gives a measure of how much of the total iron pool is in the reduced (ferrous) form, and is thus one surrogate for sediment redox status. It is evident that locations with both high concentrations of  $\text{RHg(II)}$  and low  $\% \text{Fe(II)}/\text{Fe}_T$  tend to be Agricultural, but also include a sub-set of the Riparian and Floodplain sites, whereas locations having low  $\text{RHg(II)}$  concentrations and high  $\% \text{Fe(II)}/\text{Fe}_T$  are dominated by Open Water and Floodplain sites. Thus, of the four primary land use categories, Floodplain appears to exhibit the widest range of redox conditions, as measured by  $\% \text{Fe(II)}/\text{Fe}_T$ .

Another important physical characteristic of the Basin is the increase in finer grained sediment (% silt-clay) from west to east, demonstrating that during flooding, the coarser particles settle out on the western side of the Basin. Because of the large surface-area-to-volume ratio of small particles, it is common in many environments to observe increasing THg concentration with decreasing grain size (for example, Hunerlach et al., 2004; Alpers et al., 2006). However, that was not found to be the case for the current data set. The lack of a significant grain size effect on THg might reflect particulate HgS and meta-cinnabar (m-HgS) of various size classes, originating in the Hg mining areas of the upper Cache Creek watershed, confounding the typical Hg relationship with grain size. In contrast,  $\text{RHg(II)}$  was found to

increase with decreasing grain size (increasing %silt-clay). Although RHg(II) actually decreased from west to east (as discussed above), as the %silt-clay fraction increased, so the spatial trend for RHg(II) was clearly independent of the effect of grain-size on RHg(II) concentration, driven primarily by wetting/drying cycles tied to Basin hydrology.

### 3.9.2.3 Methylmercury as the Focus

Because it is MeHg, and not THg, that poses the most concern with respect to ecosystem health, and to human health through sport fish consumption, the focus of USGS's spatial trend analyses was on MeHg and the factors that lead to its formation, including RHg(II), a likely precursor to MeHg. Notably, sediment MeHg concentrations were most elevated in Floodplain and Riparian habitats compared to Agricultural and Open Water habitats, paralleling the trend on sediment organic content. This relationship is not surprising because organic matter fuels microbial processes, including microbial Hg(II)-methylation, and has long been recognized as an important control on MeHg production (Furutani and Rudd, 1980; Lambertsson and Nilsson, 2006). More significant is the west to east increase in sediment MeHg concentration, a trend that was not observed for either THg concentration nor for sediment organic content (as %LOI), although the trend for the latter was positive (increasing from west to east) but not statistically significant. While it is yet unclear what specifically drives this west-to-east increase in sediment MeHg concentration, there was a coincident decrease in sediment RHg(II) concentration from west to east, which may imply the depletion of RHg(II) in the west to east direction at the expense of MeHg production. A similar opposing trend between sediment MeHg and RHg(II) concentrations was seen temporally, as MeHg decreased while RHg(II) increased with cumulative degree-day. These opposing trends are somewhat akin to those recently reported for rice growing areas of the Yolo Bypass Wildlife Area, where the rate constant for Hg(II)-methylation ( $k_{\text{meth}}$ ) was negatively correlated with sediment RHg(II) concentration (Marvin-DiPasquale et al., 2014)

### 3.9.2.4 Controls on Methylmercury Production

Although MeHg production rates were not measured explicitly during the study period covered in this report, the %MeHg metric has often been used as a surrogate for 'methylation efficiency' (Korthals and Winfrey, 1987; Gilmour et al., 1998; Krabbenhoft et al., 1999; Benoit et al., 2003; Sunderland et al., 2006; Drott et al., 2008; Scudder et al., 2009) and can thus provide clues as to where and when MeHg production might be greatest. Because statistical analysis of %MeHg correlations with other parameters paralleled those for MeHg concentration, the observations that MeHg concentration and %MeHg were highest in Floodplain and Riparian habitats, increased from west to east, and were highest earlier in the water year when conditions were wetter, implies that the same was likely true for net MeHg production overall.

It is generally understood that MeHg production is a function of two overarching factors: a) the activity and distribution of microbes that are involved in the Hg(II)-methylation process (largely iron- and sulfate-reducing bacteria), and b) the availability of Hg(II) to those communities of microbes (Ullrich et al.,

2001; Marvin-DiPasquale and Agee, 2003; Marvin-DiPasquale et al., 2014). The studies reported here have directly measured surrogate for the latter in the form of RHg(II), but do not have a direct measure of the former. However, by examining sediment parameters known to influence microbial processes generally (such as temperature and organic matter), and parameters known to be impacted by microbial iron reduction (such as Fe speciation) and microbial sulfate reduction (for example, TRS, and  $p_w[\text{SO}_4^{2-}]$ ), inferences can be drawn as to which (of the two) microbial processes may be playing the dominant role in MeHg production within the Basin, and when it is most active.

The results from statistical analysis (sediment Model A, table 13 in USGS, 2015) showed that both MeHg concentration and %MeHg are negatively correlated with the temporal metric, cumulative degree-day. Thus it can be inferred that, for the Basin as a whole, net MeHg production is highest during the period of flooding (typically in winter or early spring) and decreases after the Basin is largely drained and the various non-creek areas begin to dry out (typically late spring thru fall). The results from other data analysis (sediment Models B–E, table 14 in USGS, 2015) also confirm that both MeHg concentration and %MeHg are positively correlated with sediment organic content. This relationship is consistent with the concept that organic matter is a key driver for all heterotrophic microbial processes, including MeHg production. It is then not surprising that the two land-use types with the highest organic content (Floodplain and Riparian) also had the highest MeHg concentration and %MeHg.

As has been noted in other studies (for example, Scudder et al., 2009, a national survey), THg concentration is a poor predictor of MeHg production and MeHg concentration. The same is true for the Basin, as sediment THg concentration was poorly correlated with sediment MeHg concentration and only weakly correlated with %MeHg. However, when sediment THg concentration was normalized to sediment organic matter concentration (that is,  $[\text{THg}/\text{LOI}]$ ), a stronger negative correlation was found with %MeHg. This correlation was also stronger than the one between %MeHg and %LOI and between %MeHg and RHg(II). Thus, the strong effect of sediment organic content on MeHg production, particularly as it relates to THg concentration relative to organic content, was quite evident. One way to think about this is that, although THg (largely composed of inorganic Hg(II) of which a small fraction is reactive, RHg(II)) is a necessary component for MeHg production, it is really the sediment organic content that fuels the microbial processes, and the smaller the ratio between THg concentration and sediment organic content, the larger the effect on net MeHg production. In this light, the  $[\text{THg}/\text{LOI}]$  metric appears to be a better predictor of MeHg production than sediment THg, RHg(II), or %LOI. The strong negative correlation between %MeHg and  $[\text{THg}/\text{LOI}]$  is shown below on Figure 18 (fig 65 in USGS, 2015).

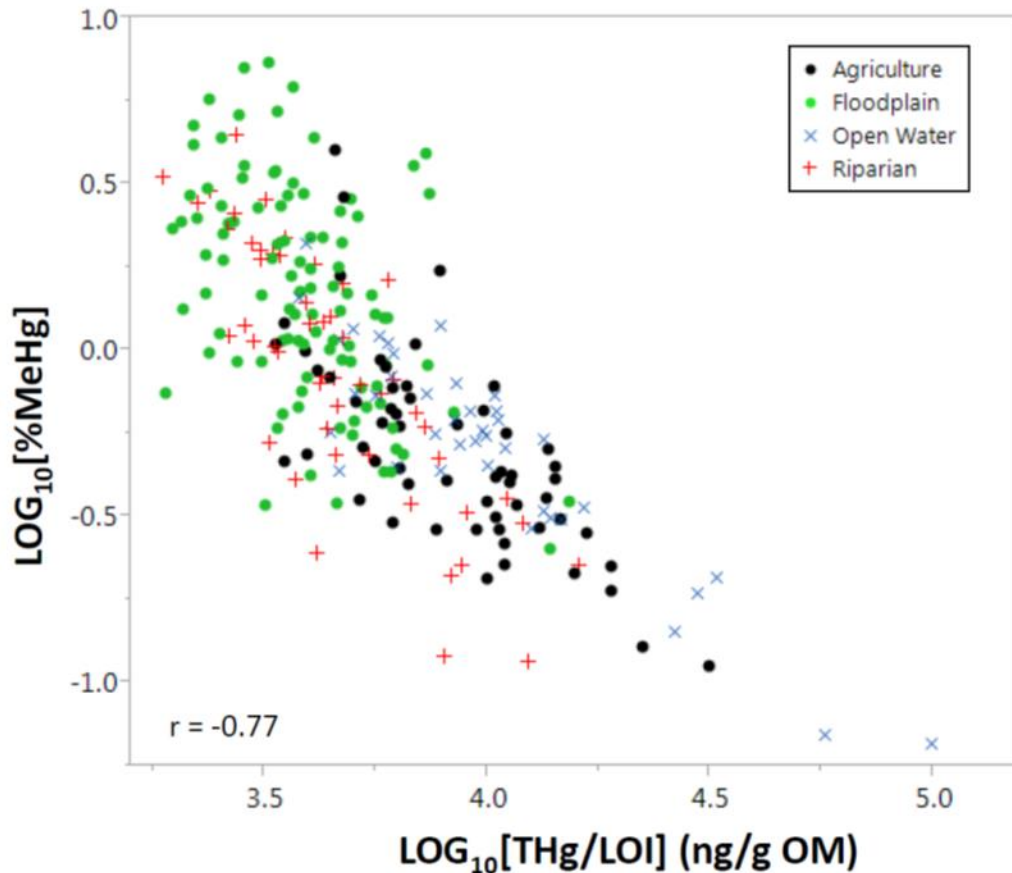


**Figure 18. Plot of %MeHg versus THg/LOI**

Of the two dominant microbial processes that are most commonly associated with MeHg production, iron reduction and sulfate reduction, data from this study suggest that iron reduction is likely more important in terms of MeHg production within the Basin. This conclusion is based upon the following results: a) both  $\text{Fe(II)}_{\text{AE}}$  and  $\text{Fe(III)}_{\text{c}}$  were identified as significantly correlated with both sediment MeHg concentration and %MeHg (Models B-E, table 14 USGS, 2015), whereas sediment TRS concentration (associated with microbial sulfate reduction) was not; and b) both MeHg and %MeHg increased with  $\text{Fe(II)}_{\text{AE}}$ , the end product of microbial  $\text{Fe(III)}$ -reduction. Although  $\text{Fe(III)}_{\text{c}}$  (well crystalline ferric iron) also showed a positive correlation with both MeHg and %MeHg, as opposed to a negative correlation that might be expected from dominant iron reduction, this likely reflects the positive influence of available  $\text{Fe(III)}$  on the MeHg production process overall, as  $\text{Fe(III)}_{\text{c}}$  is the dominant form of both  $\text{Fe(III)}$  and  $\text{Fe}_T$  in Basin sediment. There was no correlation between either MeHg or %MeHg and  $\text{Fe(III)}_{\text{a}}$  (amorphous or poorly crystalline ferric iron).

It must be noted that substrate concentrations (in this case, forms of iron and sulfur) are not necessarily reflective of microbial rates, and the two should not be conflated. Specifically, a low  $\text{Fe(II)}_{\text{AE}}$

concentration (or low %Fe(II)<sub>AE</sub>/Fe<sub>T</sub> value) may imply a large degree of Fe(II) re-oxidation, rapid Fe(II)/(III) cycling and very high rates of microbial Fe(III)-reduction (Windham-Myers et al., 2009). This is particularly true for sediment prone to oxidation by wetting followed by drying, such as the Floodplain and Riparian habits. Although both Floodplain and Open Water sites actually had equally high Fe(II)<sub>AE</sub> concentrations, the former is more prone to Fe(II)-re-oxidation caused by drying compared to the latter, and thus one might expect more rapid Fe(II)/(III) cycling for Floodplain sites than for Open Water sites, leading to higher %MeHg, as was found to be the case.

### 3.9.3 Biota

Geometric mean mercury concentrations in bird eggs were up to 32% higher in house wrens and up to 33% higher in tree swallows during 2012 than during 2013. During 2012, the Basin had a much larger area that was flooded during the spring, and for a longer period of time, than during 2013. Fluctuating water levels can enhance the methylation and release of Hg from sediments (Ullrich et al., 2001). Consequently, periods of drought, such as those observed in 2013 and especially in 2014, can alter the MeHg dynamics in wetlands that contribute substantially to mercury methylation and ultimately bioaccumulation.

#### 3.9.3.1 Mercury Increased with Creek Distance into the Settling Basin

In addition to the differences in THg concentrations in wildlife among years, the USGS also reported that THg concentrations in birds and fish differed by habitat type and creek distance within the Basin. For both caged and wild mosquitofish, THg concentrations increased with creek distance into the Basin. THg concentrations in caged fish increased by up to 183% over the approximately 5.7 mile (9.2 km) reach of Cache Creek, from 0.12 µg/g dw 656 ft (200 m) downstream from the bridge at County Road 102, to 0.34 µg/g dw at the low-flow outlet of the Basin. Similarly, mean THg concentrations in wild fish increased by up to 79% over the approximately 5.3 mile (8.6 km) stretch of Cache Creek, from 0.43 µg/g dw 2,624 ft (800 m) downstream from the bridge at County Road 102, to 0.77 µg/g dw at the low-flow outlet. THg concentrations in house wren eggs increased with creek distance in 2012, when the Basin was wetter; but not in 2013, when the Basin was mostly dry during the breeding season. In 2012, THg concentrations in house wren eggs increased by up to 46% over the approximately 4.3 mile (7 km) stretch of nest boxes along Cache Creek from approximately 0.13 µg/g fww at the first nest box placed 6,232 ft (1900 m) downstream from the bridge, to approximately 0.19 µg/g fww at the last nest box placed 5.5 miles (8800 m) downstream from the bridge. A similar increase in THg and MeHg concentrations in water with creek distance was also reported by the USGS during the March-April 2013 fish-cage experiment.

#### 3.9.3.2 Mercury was Highest in Floodplain Habitats

Mercury concentrations in biota differed by wetland habitat type, especially in fish. Fish THg concentrations were highest in mixed non-woody floodplain habitat, followed by mixed woody floodplain habitat, irrigation canals, tule wetland habitat, and creek habitat. Additionally, THg concentrations in house wren eggs increased with the amount of mixed non-woody floodplain habitat located within 328

feet (100 m) of the nest box. These results suggest that floodplain habitats, which experience a higher frequency of wetting and drying than other habitats in the Basin, have the highest potential for THg bioaccumulation in fish and wildlife. In general, intermittent, shallow, and initial flooding of wetlands can enhance the methylation and release of THg from sediments (Ullrich et al., 2001). Other studies also have found that shallow and intermittent flooding of wetlands tends to result in higher THg and MeHg concentrations in fish (Bodaly and Fudge, 1999; Snodgrass et al., 2000; Ackerman and Eagles-Smith, 2010). Because the Basin receives a variable amount of water flow from year to year, it is expected that MeHg concentrations will be highest in fish and wildlife during years with the most flooding for short periods of time during the spring breeding season.

### 3.9.3.3 Mercury Exposure Risk to Fish

Mercury concentrations in caged fish increased by up to 2,800% over the 31-day exposure period within the various Basin habitats. Despite this rapid increase in THg, the caged fish still only reached up to 39% of the THg concentrations observed in wild mosquitofish which had been exposed to this local inorganic THg and MeHg throughout their entire lives. Overall, 39% of caged mosquitofish exceeded a proposed dietary benchmark for behavioral impairment in piscivorous birds ( $0.10 \mu\text{g/g ww}$ ) (Depew et al., 2012) and 16% exceeded a proposed dietary benchmark for reproductive impairment in piscivorous birds ( $0.18 \mu\text{g/g ww}$ ) (Depew et al., 2012) during the 31-day exposure period. In comparison, 96% and 63% of wild mosquitofish exceeded these toxicity benchmarks, respectively.

### 3.9.3.4 Mercury Exposure Risk to Birds

There are few known toxicity benchmarks for songbirds, but songbirds are thought to be more sensitive to mercury than other bird species, such as mallards, where more toxicity benchmarks have been established (Heinz et al., 2009). Overall, 71% of house wrens exceeded  $0.10 \mu\text{g/g fww MeHg}$ , which is a level suggested where closely-related Carolina wrens may experience a 10% reduction in nest success (Jackson et al., 2011). Also, 49% of tree swallows exceeded  $0.32 \mu\text{g/g fww MeHg}$ , which is a calculated LC50 (lethal concentration causing 50% mortality) where 50% of eggs injected with MeHg failed to hatch (Heinz et al., 2009).

## **4 Long-term Environmental Benefits and Costs of Sustaining TrapPING Efficiency**

The November 10, 2011, TMDL for the Basin requires submittal of a report describing the long-term environmental benefits and costs of sustaining the Basin's mercury trapping abilities indefinitely. While a mercury control measure implemented for the Basin will provide the benefit of decreased mercury loads entering the Yolo Bypass, the control measure(s) could also result in local or regional adverse impacts to humans, wildlife and the environment. This section evaluates the potential benefits and associated potential adverse impacts related to maintaining the Basin in its current capacity as well as several possible basin management options for improving the Basins mercury TE, including: sediment excavation; raising the weir; notching the training levee; enlarging the Basin, grading the Basin, changing land use practices; and others.

For an assessment of this magnitude it is essential to understand the surficial processes within the Basin that contribute to or minimize methylation within the Basin because MeHg is of the greatest concern to the ecosystem as this form of Hg is readily taken up by fish and birds. To improve the understanding of mercury methylation and MeHg bioaccumulation processes within the Basin the USGS assessed the spatial variability of THg and MeHg in sediment, biota, and surface water among each dominant habitat type within the Basin as presented in the USGS SIR (USGS, 2015) and summarized previously in Section 3.6.3.

The USGS with the assistance of DWR environmental scientist defined the dominant habitat types within the Basin and the USGS performed statistical analyses to assess the THg and MeHg concentrations within each habitat type and whether spatial and/or temporal trends occur across the Basin. The following sections summarize the various temporal and spatial trends identified from the USGS analytical results; a summary of proposed basin management concepts (further described in Section 6.0) and the potential environmental impacts linked to those proposed management actions. An evaluation of costs associated with various proposed management actions is included with the evaluation of remedial alternatives presented in Section 6.4.

### **4.1 Summary of in-Basin Sample Analytical Results and Trends**

- The sediment studies showed that land use and organic matter influences mercury cycling more than THg concentration alone. The floodplain and riparian land use types had the greatest MeHg concentrations (Figure 25A, USGS, 2015) a trend parallel that of sediment organic content (Figure 33A, USGS, 2015).
- The fish and bird egg collection studies also echoed the higher THg concentrations in the floodplain habitat. For both the fish and bird egg collection studies, the highest THg concentration came from the mixed non-woody floodplain habitat (Figure 38 and Table A5-5, USGS, 2015).
- The THg concentrations increased with creek distance into the Basin as exhibited in the sampled water and in the caged fish, wild fish, (Figures 35 and 36, USGS, 2015) and the 2012 bird egg collection

studies, which is based on the collection of 40 house wren eggs. The 2013 bird egg collection studies showed very little effect of creek distance on egg THg concentration, which is based on the collection of 216 house wren eggs.

- With regards to spatial trends, MeHg concentration increased from west to east within the Basin, with the greatest concentration in the floodplain habitats (Figure 26A, USGS, 2015). The Basin drains from west to east, implying that the east side of the Basin is wetter for a longer period of time. MeHg production was also highest in the early part of the water year and decreased with time (Figure 26B, USGS, 2015).
- Iron reduction [ $\text{Fe(II)}_{\text{AE}}$ ] has been found to be correlated to the MeHg production within the Basin.  $\text{Fe(II)}_{\text{AE}}$  is more prone to re-oxidation caused by wetting and drying, which would tend to occur more frequently in floodplain habitats, leading to higher methylation of mercury (Figure 25C, USGS, 2015).
- Mercury concentrations were higher in house wren and tree swallow eggs in 2012 than during 2013. In 2012, only 40 house wren eggs and 7 tree swallow eggs were sampled, whereas, in 2013, 216 house wren eggs and 40 tree swallow eggs were sampled (Table 19, USGS, 2015). The Basin had a much larger area that was flooded during the spring for a longer period of time during 2012, than during 2013. Methylation and release of mercury from sediments may be enhanced by fluctuating water levels as in 2012, but the disparity in the data collected for 2012 compared to 2013 may unduly influence this potential trend.
- During the 31-day exposure for the caged mosquito in the Basin, 39% of the caged mosquitofish exceeded the proposed fish-eating bird dietary benchmark for behavioral impairment ( $0.10 \mu\text{g/g ww}$ ) and 16% exceeded the proposed dietary benchmark for reproductive impairment ( $0.18 \mu\text{g/g ww}$ ) for piscivorous birds.
- Seventy-one percent of the house wren eggs collected in the Basin exceeded a THg concentration of  $0.10 \mu\text{g/g fww}$ , a suggested level where closely-related Carolina wrens may experience a 10% reduction in nest success. Forty-nine percent of the tree swallow eggs collected from the Basin exceeded  $0.32 \mu\text{g/g fww}$ , which is calculated as the lethal concentration causing 50% mortality.

#### **4.2 Summary of Possible Management Actions to Increase Trapping Efficiency**

In DWRs December 9, 2013, response to the November 10, 2011, CVRWQCB TMDL directive letter for the Basin, DWR agreed to evaluate several possible basin management options for improving the Basins mercury TE, including: no action (baseline conditions); sediment excavation; raising the weir; notching the training levee; enlarging the Basin, grading the Basin, changing land use practices; and others. In the SIR the USGS assessed the potential suspended sediment and mercury TE and mercury methylation impacts associated with these identified possible basin management options (Table 25, USGS, 2015). A summary of this evaluation follows along with an interpretation of likely environmental impacts to the

Basin associated with each of the possible management actions. Projected capital outlay and annual operation and maintenance costs for each option are presented in Section 6.0.

**No Action:** No changes are implemented at the Basin. The current TE of the Basin is approximately half of the sediment and THg transported by Cache Creek. If No Action is taken for the Basin, the sediment and THg TE will decrease with time as more sediment fills the Basin, allowing more sediment and pTHg to exit the Basin and enter the Delta through the Yolo Bypass. The MeHg TE will not change. With regards to bioaccumulation within the Basin, no changes are anticipated for fish and birds from what is currently observed. The current observed spatial trend of increasing MeHg concentrations from west to east and temporal trends of higher MeHg concentrations during the flooding period are anticipated to remain unchanged. No changes are anticipated for MeHg production during flooding. Based on the historical reported aggradation rates, the remaining basin life (trap > 30%) is estimated at approximately 15-years. DWR's Sacramento Maintenance Yard has reported that their historical annual operation and maintenance costs for the Basin are approximately \$200,000 to \$1,300,000. Thus, the anticipated cost to maintain the Basin as is for its estimated remaining lifespan would be in the neighborhood of \$3 to \$20 million without a single basin improvement. Potential costs for the evaluated control alternatives are further discussed in Section 6.4.

**Sediment Excavation:** Trapping efficiency of sediment and pTHg will increase initially with the removal of sediment, but will decrease with time as sediment fills the Basin. USGS researchers estimate that by 2012, 4.1 to 5.6 feet (1.26 to 1.70 m) of sediment was deposited since the Basin was created in 1937. The USGS is uncertain as to how sediment excavation would affect the MeHg TE and also uncertain about how the effects of this management action will influence bioaccumulation of mercury within the Basin for fish and birds, as these processes are dependent on other factors besides sediment THg concentrations. However, if flow dynamics and habitat within the Basin remain largely unchanged from the current condition, MeHg production, and fish and bird bioaccumulation would likely remain unchanged from the conditions observed in this study. The observed spatial trend of increasing MeHg concentrations from west to east and temporal trends of higher MeHg concentrations during the flooding period are anticipated to remain unchanged, assuming that sediment removal does not change the flow of water and draining pattern within the Basin.

**Raising the Outlet Weir:** The vertical storage capacity of the Basin would be increased by raising the outlet weir 6 ft (1.8 m) which would increase sediment and pTHg TE. Raising the outlet weir would allow a greater extension of time to reach the current sediment TE. Based on the sediment deposition estimate of 4.1 to 5.6 ft (1.26 to 1.70 m) in a 75-year period, it is anticipated that 0.66 to 0.9 inches (1.7-2.3 cm) of sediment would be deposited each year. The observed spatial trend of increasing MeHg concentrations from west to east and temporal trends of higher MeHg concentrations during the flooding period are anticipated to remain unchanged, assuming that sediment removal does not change the flow of water and draining pattern within the Basin. The length of time the Basin remains inundated with flood water will increase. Therefore, the USGS suggest with a medium level of certainty that the overall

MeHg production will increase as a result of the extended inundation. Though uncertain about how the effects of this management action will influence bioaccumulation of mercury within the Basin for fish and birds, should MeHg production increase, there is potential for bioaccumulation within the Basin for fish and birds to likely increase.

**Notching the Training Levee:** The main effect that this management action will promote is the deposition of coarser grained sediment along the western edge of the Basin. There is uncertainty regarding the deposition of the finer grained particulates as these processes are dependent on flow velocities and water residence time within the Basin. Since sediment grain size was not a significant factor in explaining the spatial distribution of MeHg (USGS, 2015), the USGS assumes with a moderate to low degree of certainty that the observed spatial trend of increasing MeHg concentrations from west to east would most likely remain the same. The USGS is uncertain as to the effect on MeHg TE and also uncertain about the effects this management action will have on the bioaccumulation of mercury within the Basin for fish and birds, as it may be dependent on other factors. The length of time the Basin remains inundated with flood water is assumed to remain the same so the overall MeHg production will remain unchanged and therefore, bioaccumulation in fish and birds would also likely remain unchanged.

**Enlarging the Basin:** Sediment TE and pTHg TE will increase initially with enlargement of the Basin, but will decrease with time as sediment fills the Basin. Land use is considered the dominant factor in the spatial concentration of all forms of mercury in the Basin. With regards to MeHg in sediment, the concentration is shown to be the greatest in the floodplain and riparian sites. Should the non-agricultural floodplain habitat increase, MeHg production would also increase. Though a specific location within the Basin may have lower amounts of MeHg in this scenario, the production of MeHg is spread out over a larger area, possibly producing more MeHg overall. The USGS (USGS, 2015) is uncertain as to the MeHg TE and also uncertain about how the effects of this management action will influence bioaccumulation of mercury within the Basin for fish and birds. Though the USGS is uncertain about how the effects of enlarging the Basin will influence bioaccumulation of mercury, should MeHg production increase with the increase of non-agricultural floodplain habitat, there is likely potential for bioaccumulation for fish and birds to increase. Assuming the flow of water and draining pattern within the Basin remain the same, the spatial trend of increasing MeHg concentrations from west to east would most likely remain the same. The temporal trend of overall MeHg production will remain unchanged as the flooding period is assumed to remain unchanged.

**Grading the Basin:** More area within the Basin will be utilized for flood water inundation, which will initially increase sediment TE and pTHg TE by increasing the area within the Basin for sediment deposition to occur. Grading the Basin to promote inundation in the northern portion would decrease the current agricultural land use and increase the non-agricultural floodplain habitat. The MeHg sediment concentration is greatest in the non-agricultural floodplain areas, thus there is an expectation that MeHg production would increase. The USGS (USGS, 2015) is uncertain as to the effects of this management action on MeHg TE and also uncertain about how the effects this management action will

influence bioaccumulation of mercury within the Basin for fish and birds. Although uncertain about how the effects of grading the Basin will influence bioaccumulation of mercury, should MeHg production increase with the increase of non-agricultural floodplain habitat, there is likely potential for bioaccumulation for fish and birds to increase. The current temporal trend of overall MeHg production will remain unchanged as the flooding period will remain unchanged, but grading the Basin would likely impact water flow and floodwater inundation time, potentially impacting the current spatial trend of increasing MeHg concentrations from west to east.

**Modify Land Use Practices:** Land use is one of the main factors that affect the concentration of MeHg within the Basin. The USGS (USGS, 2015) reports that the Basin is currently comprised of 47.3 percent agriculture and 39.1 percent non-agricultural floodplain habitats; with the non-agricultural floodplain habitat having the highest concentration of MeHg in sediment. Trapping efficiency of sediment pTHg is anticipated to increase slightly by increasing non-agricultural floodplain habitat. Should the non-agricultural floodplain habitat increase, sediment MeHg concentration is also anticipated to increase. Organic matter is a key driver for heterotrophic microbial processes, including MeHg production. As non-agricultural floodplain habitat has greater amount of organic debris compared to that of the agricultural habitat, more MeHg will be produced should non-agricultural floodplain habitat increase. Bioaccumulation within the Basin for fish and birds would likely increase with greater MeHg concentration if the non-agricultural floodplain habitat is increased. Assuming that modifying land use practices do not alter the flow or floodwater inundation time, the increasing trend of MeHg concentration from west to east and the current observed temporal trend is likely to persist. Should agricultural habitat increase, the current spatial and temporal trend should remain unchanged, but the MeHg concentration should likely decrease. The TE of sediment, THg, and MeHg would decrease slightly. With the decrease of MeHg due to greater agricultural land use, the in-basin mercury accumulation in fish and eggs would also likely decrease slightly.

**Others:** Other potential land-use/basin modifications that may affect the TE and MeHg production and bioaccumulation within the Basin could include lengthening the primary channel to increase open water habitat; adding or using existing gates to increase or decrease water holding times; utilizing passive coagulants to increase settling of fine particles; and/or use of aeration or other oxygenating features to improve aerobic conditions within the Basin. cursory evaluation of these alternatives as with those discussed above shows both potential advantages and disadvantages to TE and in-basin MeHg production associated with these options.

If the primary channel is lengthened by creating a meandering pattern the sediment and pTHg TE is anticipated to increase slightly due to increased travel time. However, the MeHg TE is anticipated to also increase slightly due to longer periods of inundation. It is unknown how lengthening the channel will affect water flow within the Basin, therefore the spatial trend of MeHg across the Basin is unknown. It is also unknown how the sediment MeHg concentration and bioaccumulation in fish and eggs will be

affected by lengthening the primary channel. No changes are anticipated to the current observed temporal trend of higher MeHg concentrations during the flooding period.

If existing or new gates were used to slow the release of water from the Basin, the TE of sediment and pTHg is anticipated to moderately increase due to the longer water holding time, allowing for the sediment to settle out. It is unknown how this management action would affect MeHg TE. In-basin MeHg production is anticipated to increase slightly, which would potentially cause a slight increase in the bioaccumulation in fish and eggs within the Basin. The observed spatial trend of increasing MeHg concentrations from west to east and temporal trends of higher MeHg concentrations during the flooding period are anticipated to remain unchanged, assuming that the flow of water and draining pattern within the Basin does not change.

Utilization of polymers to bind to sediment particles and allow the particles to settle out could create an increase in the TE of sediment and pTHg and a moderate increase in TE for MeHg. With regards to in-basin MeHg production, it is unknown how utilizing this management action will affect the sediment MeHg concentration or the current west to east spatial increase in MeHg across the Basin. The current temporal trends of higher MeHg concentrations during the flooding period are anticipated to remain unchanged. The in-basin mercury accumulation in fish and eggs is anticipated to increase slightly with the potential increased TE of MeHg. Polymers can be expensive and full-scale implementation of this alternative would likely never be economically feasible. However, small-scale pilot-test cells within the Basin might be an effective interim measure for reducing MeHg levels exiting the Basin while a full-scale alternative is being developed.

Aeration to actively oxygenate still waters settling in the Basin would have no effect on the TE of the Basin, but could minimize the production of MeHg within the Basin by regulating surface water from reducing conditions favorable for mercury methylation. Given the large surface area of the Basin, implementation of this alternative may not be economically feasible.

### **4.3 Environmental Implications**

The ultimate goal of the TMDL is to reduce the mercury load into the Delta. Generally, floodplain habitats are effective in trapping sediment. As the sediment is settling out in the floodplain habitats within the Basin, the studies show that there is increased MeHg production due to the breakdown of organic matter within the non-agricultural floodplains which fuels methylation of mercury within the sediment. The floodplain habitats also tend to have a longer period of floodwater inundation which also increases MeHg production. Management activities which increase the acreage of non-agricultural floodplains within the Basin will likely increase in-basin mercury accumulation, which will likely also increase the mercury bioaccumulation in the biota.

In Summary, increasing sediment and pTHg TE within the Basin would decrease the mercury load that would potentially go into the Delta, but the trade-off is having localized effects of greater MeHg production and bioaccumulation within the Basin.

## **5 CACHE CREEK WATERSHED STUDY (UCD, USGS)**

The Cache Creek Watershed (Figure 19) drains approximately 1,150 square miles (2,978.5 square km) to the Basin. Containing abandoned mercury and gold mines and natural sources such as geothermal springs and mercury-enriched soils, the Watershed is a significant contributor of mercury to the Sacramento-San Joaquin Delta. Understanding sources and distribution of mercury in Cache Creek and developing possible control strategies to reduce exports out of the watershed are necessary to effectively control sediment loading rates into and out of the Basin.

The overall objective of this study was to evaluate the Cache Creek Watershed's flow, sediment and mercury conditions from its tributaries for historical and future conditions by coupling the Watershed Environmental Hydrology Modeling (WEHY) and Global Climate Change Modeling (GCM) approaches. In an attempt to obtain flow, sediment, and mercury data to serve as the upper boundary condition for the Basin TE Study, DWR contracted with UCDJ AHL to develop a numerical model of the Cache Creek Watershed. The purpose of this effort was to generate a detailed hydrograph with the associated sediment and mercury mass loading rates for the entire watershed. In addition, there was an attempt to identify sub-basins within the watershed that produce high mass loading rates that contain elevated mercury concentrations.

### **5.1 Methodology**

UCDJ AHL coupled GCM with the WEHY model to generate realistic computations for water, sediment, and mercury balances in the Cache Creek Watershed for historical and future climate conditions. WEHY is a physically based watershed hydrology and sediment/nutrient/heavy metal transport model based upon spatially-averaged hydrologic conservation equations and transport equations to account for the effect of spatial heterogeneity in land surface and subsurface conditions on the hydrology and environmental processes. Modeling efforts were used to develop a range of predictions of sediment loads entering the Basin for the entire anticipated flow regime, up to a 200-year event.

By developing a detailed geographical information system (GIS) for variables such as the vegetation, land use/land cover conditions, soils, topography and geology of the watershed, parameter values were objectively estimated by computer algorithms relating values to land surface and subsurface conditions rather than simply fitting the model. The model was then run over an ensemble of 13 possible realizations of the future hydro-climate conditions over the Cache Creek Watershed, in an attempt to generate a range of TE for the Basin as a result.

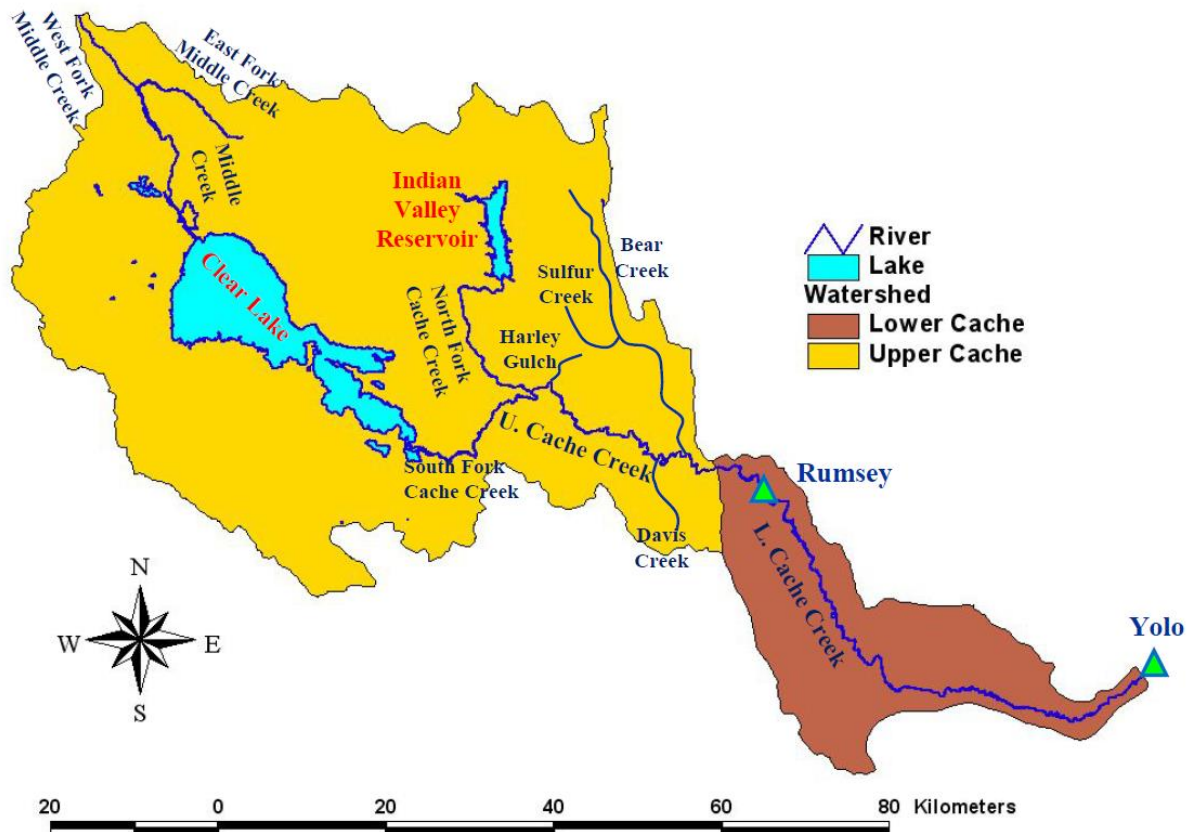


**Figure 19. Outline of Cache Creek Watershed**

## 5.2 Results and Discussion

For model calibration simulated flows were compared against the observed flow data collected at Rumsey and Yolo stations for the years 1950-2011. These comparisons yielded very satisfactory results with the correlation coefficient of 0.87 even when considering that the unknown operating criteria of the existing reservoirs within the watershed had to be determined by modeling a range of flow scenarios. However, due to the lack of concurrent flow, sediment and mercury data collected from within the watershed, the sediment, and mercury conditions are quite uncertain. A consequence of the lack of concurrent flow with sediment data is that the sediment rating curve necessary for the estimation of sediment inflows into the Basin has substantial uncertainty for flows above 13,000 cfs. One way to fill the gap in the sediment rating curve is to develop a comprehensive field sampling program for collecting concurrent flow, sediment, and mercury data. However, the costs to initiate and manage this comprehensive of a field program are prohibitive. In lieu of these data, DWR will continue collecting concurrent flow-sediment-mercury field data that cover a range of flow conditions at the Rumsey station through June 2016. These data can then be utilized to calibrate and validate the environmental module of the WEHY model for the Cache Creek Watershed.

## **6 CACHE CREEK FEASIBILITY STUDIES**

Federal and state agencies as well as the local community are engaged in several independent feasibility studies that potentially impact the current operation and maintenance activities and thus, the functionality of the Basin. These studies include USACE and their evaluation of the lower leveed section of Cache Creek; the CVFPB in their evaluation of the Basin and other proposed improvements to the Yolo Bypass as part of the BWFS for the Sacramento River Basin; and the City of Woodland in their recently awarded UFRR grant. Each of these studies involves consideration of alternatives that could impact the Basin, as summarized in the following sections.

### **6.1 Lower Cache Creek Feasibility Study (USACE)**

USACE began work on the LCCFS in 2013 and reached the Alternatives (identification) Milestone in May 2014. The objective of the LCCFS is to provide improvements to the level of flood protection for the City of Woodland and neighboring properties. Of the alternatives under study by USACE, one alternative routes excess flood flows overland around the southwest corner of the Basin and another involves constructing a flood barrier north of the City combined with a weir and/or gates through the Basin west levee, allowing excess floodwaters to enter the Basin. Other USACE alternatives include: (1) routing excess flood flows north of Cache Creek through a new weir and overland bypass system into the Colusa Basin Drain, and (2) improving and/or setting back the existing levee systems on the right bank of Lower Cache Creek upstream of the Basin and expanding the Basin's north boundary to extend due east. The latter alternatives identified by USACE will require acquisition of flowage easements over a significant acreage of agricultural lands.

USACE coordinates Project Delivery Team (PDT) meetings regularly to review the progress of the study and the various alternatives being considered. In January 2015, DWR voiced concern over the potential disturbance of mercury-laden soil in the Basin alignment and any proposed changes made to the geometry that may result in a reduction of the sediment and mercury TE.

### **6.2 Cache Creek Settling Basin Feasibility Study (CVFPB)**

The 2012 Central Valley Flood Protection Plan (CVFPP) recommended a State Systemwide Investment Approach (SSIA) for flood risk management in the Central Valley and includes implementation of the BWFS for the Sacramento River Basin. The BWFS integrated with the Central Valley Conservation Strategy (CS), National Marine Fisheries Service (NMFS) Biological Opinions (BiOps) for Long-Term Operations of the Central Valley Project (CVP) and State Water Project (SWP), and Regional Flood Management Planning (RFMP) efforts are designed to provide an integrated solution to flood management in the Sacramento Valley.

The Sacramento BWFS outlines a multitude of planning processes and outreach efforts conducted in earlier phases of the process to improve flood management in the Central Valley. The BWFS represents a

feasibility level of analysis where system solutions have been refined to a sufficient level of detail that close integration with other projects and programs is possible.

Because of its strategic location and features, the Yolo Bypass is currently the focus of several major interagency planning efforts aimed at improving flood conveyance, fisheries and wildlife habitats, water supply and water quality, agricultural land preservation, and economic development. As such, DWR prepared a Yolo Bypass feasibility assessment in the context of the CVFPP and BWFS framework, with the intent of formulating and expediting implementation of high-priority actions in the Yolo Bypass, which will achieve the goals and objectives of the CVFPP. This analysis is to be included as part of the Sacramento River BWFS, scheduled for completion in 2016 and was informed by major infrastructure assessments carried out during the CVFPP planning process, including urban and non-urban levee integrity assessments, assessments of flood control structures as documented in the Flood Control System Status Report (DWR, 2011), development of the Conservation Framework and Strategy, and many other available sources.

The key features that comprise the Yolo Bypass system include Fremont Weir at the northern end of the bypass; Knights Landing Ridge Cut; the Basin; Willow Slough Bypass Channel northeast of Davis; Sacramento Weir north of West Sacramento; Putah Creek southeast of Davis; the Sacramento River Deep Water Ship Channel; Cache Slough and Lindsey Slough levees near Rio Vista; and the east and west bypass levees that connect these features. The west levee of the bypass is absent south of Putah Creek for a stretch of about seven miles (11.3 km) due to high ground. These features were constructed incrementally over time.

In a letter, dated March 22, 2013, the CVFPB requested USACE, Sacramento District, to perform a reconnaissance study for the Basin to address flood control and recent mercury-related environmental concerns. Issues mentioned as likely to be considered included: (1) the possibility of adjacent area flooding as the Basin fills in; (2) requirements for accreditation of the Basin levees to urban standards; (3) improving the Basin sediment TE; and (4) managing THg and MeHg loads to the Yolo Bypass.

The CVFPB also addressed a proposal dated December 2, 2014, to USACE headquarters (CECW-CE) in a response to a notice in the Federal Register. The proposal is for a general reevaluation report (GRR) to determine the extent of necessary improvements to the Basin. The intent is to investigate the historical and projected performance of the Basin and identify feasible alternatives for extending its life. The proposal identifies CVFPB and DWR as the two non-Federal sponsors identified at the present time.

Both documents identify the current limited design life of the Basin and the need to evaluate alternatives for longer term sediment trapping capabilities as well as the added concern of reducing mercury releases to the Yolo Bypass. While USACE has not formally responded to either of the communications, the 2014 proposal has been included in the Annual Report of the USACE issued in February 2015. Further, the BWFS being prepared by DWR and the CVFPB includes a technical memorandum for the Basin that summarizes an independent feasibility study of alternatives for improvements to the Basin that may

satisfy the four issues identified above. The BWFS Draft technical memorandum forms the basis for the Basin control alternatives discussed and assessed in Section 6.4.

### **6.3 City of Woodland UFRR Grant**

The Woodland Integrated Flood Risk Reduction Basin Project (Proposed Project) has been proposed by the City of Woodland as an extension of the LCCFS being advanced by USACE and the CVFPP adopted by the CVFPB in June 2012. The City pursued funding from DWR through its UFRR program to advance design and construction of the Proposed Project. DWR has awarded the City a \$5 million grant to further develop and assess the Proposed Project and the scope of work to be performed under that grant is in development.

The Proposed Project is an extension of the plan recommended in an earlier 2003 LCCFS, and similar to the plan expected to be recommended in the current USACE study. There are three primary differences between the USACE recommended plan from the 2003 LCCFS and the Proposed Project:

1. The Proposed Project includes a bypass channel to convey flood waters from Cache Creek around the south side of the Basin and discharging them into the Yolo Bypass. This modification prevents entrapment of flood waters by the west levee of Basin; a significant public concern that led to the termination of the 2003 study. The Proposed Project also includes consideration of nonstructural actions for those properties that will remain in the floodplain north of the City.

2. The City is evaluating the ability to integrate the Westside Railroad Relocation Project to both increase the value and type of benefits that are achieved, to identify other potential funding partners, and to assist with enabling future flood system improvement projects that will increase the flood management system flexibility, robustness, and resiliency.

3. Included in the City's concept proposal scope is a feasibility study identifying the range of options that would extend the functional life of the Basin and reduce mercury outflow. This study would be coordinated with both the BWFS team and DWR Maintenance office to identify a recommended plan that would inform the State in identification of a State Preferred Action.

### **6.4 CCSB Control Alternatives to Decrease Mercury Loads from the Basin**

As discussed above, DWR and CVFPB are considering solutions that are consistent with the CVFPP while staying cognizant of USACE flood protection evaluations. While DWR, CVFPB, and USACE are not responsible for the high concentrations of Hg or MeHg in Cache Creek as mercury is naturally occurring in the watershed as well as from past mining operations in the upstream portions of the Cache Creek, the agencies along with local interests must work together to find solutions for sediment and mercury management in the Basin. These management solutions must be developed through engagement of USACE and the CVRWQCB as the project and alternative assessments are evaluated.

In this light DWR and the CVFPB prepared the technical memorandum as part of the BWFS to specifically evaluate an array of options for improvements to the Basin. The memorandum is intended to serve as a starting point to open discussion with USACE, CVRWQCB, and local agencies and forms the basis of the discussions in the following sections. The alternatives discussed in the following sections present an array of options for improving sediment and THg TE in the Basin and the possible implications for the reduction of MeHg loads to the Yolo Bypass. Maintaining adequate containment of these components is deemed important for long-term ecological health in the Delta as well as maintaining the hydraulic efficiency in the Yolo Bypass.

#### 6.4.1 Alternatives Constraints

DWR and CVFPB are focused on improving operations and extending the functional life of the Basin. Specifically, the objective is to develop an alternative that will extend the functional life of the Basin by at least 50 years (to year 2068) while also being responsive to the CVRWQCB directives of reducing THg and MeHg loads as described in the Basin Plan (TMDL process). These objectives must be met within the appropriate cost constraints imposed on any public works project. The selected alternative must also meet the primary objective without unduly impacting the concerns of local agencies, such as improving flood protection in the Lower Cache Creek watershed and for the City of Woodland.

#### 6.4.2 Descriptions of Alternatives

An evaluation of management actions for maintaining or extending the functional life of the Basin is provided in this section, including statements of operational assumptions, benefits, drawbacks, implementation and O&M costs, and ability to meet performance measures.

The five alternatives include:

1. Baseline (existing) conditions
2. Raise existing outlet weir with phased notching of training levee, as proposed by USACE
3. Sediment stockpile within existing footprint of the Basin
4. Sediment stockpile within existing Basin footprint and settling basin expansion
5. Basin expansion for sediment stockpile, larger settling basin, and additional weir

#### 6.4.3 Common Elements Among the Alternatives

Although not a specific element of any of the alternatives, the possibility of limiting land uses within the Basin to reduce Hg and MeHg loads exiting the Basin is a possibility with implementation of any of the alternatives. Based on our studies, modifying land uses is likely to have the most profound effect on MeHg concentrations due to the impacts land uses have on MeHg production (USGS, 2015). MeHg concentrations are significantly higher in non-agricultural floodplain and riparian areas of the Basin as compared to other areas. Any land use shifts that change frequently wetted, floodplain and riparian areas

to open water or agricultural use are likely to reduce MeHg concentrations. Additionally, vegetation management that reduces organic debris (including mowing and removal of organic material from floodplain and riparian areas) is also likely to reduce MeHg concentrations. The alternatives are summarized in Table 6-1 and discussed in the following sections.

**Table 6.1. Summary Comparison of Alternatives**

CCSB Alternatives	CCSB Expansion (acres)	Stockpile Footprint (acres) Storage Capacity (acre-foot)	Estimated Increase in Trapping Efficiency of Sediment and Particulate THg	Projected Functional Life of CCSB (years <sup>1</sup> )	Meets 50-year Life Extension Objective	Meets Hg Reduction Objective Meets MeHg Reduction Objective (Low, Med, High)	Estimated Initial Capital Costs (\$ millions)	Estimated Annual Operating Costs (\$ millions)
1 Baseline (Existing)	0	0	0	10-15	No	No No	0	0.2 to 1.3
2 6-ft weir raise training levee degrade (USACE)	0	0	10%	25	No	No Low	12 to 16	0.2 to 1.3
3 Sediment stockpile in NW corner of CCSB	0	300 17,000	5%	50	Yes	Yes Moderate	16 to 21	3 to 4
4 Sediment stockpile in CCSB and settling area expansion	300	300 17,000	10%	55	Yes	Yes Low	31 to 40	3 to 4
5 Expand CCSB for sediment stockpile and 465-acre settling area, and add weir	600	300 17,000	15%	60 <sup>+</sup>	Yes	Yes Moderate	54 to 71	3 to 4

6.4.4 No Action

The “Baseline Condition” alternative would leave the Basin “as-is” and would make no major modifications to related infrastructure or current O&M. The risks associated with this alternative include excess sediment in the Yolo Bypass and potentially elevated levels of THg and MeHg that could increase over time. There would be no initial capital costs for this option, and annual operating costs would continue to be \$0.2 to \$1.3 million per year. The sediment TE of the Basin would continue to diminish as would the long-term operational sustainability.

Based on the historical estimated aggradation rate of 340 acre-ft/yr, the remaining useful life (maintain TE > 30%) of the Basin may be only 10 to 15 years, however based on the accumulation rate calculated in this study (270 acre-ft/yr), the estimated remaining useful life of the Basin could be as much as 20 percent greater than the 10–15 year estimate. Better estimates of operational life will be available after an elevation survey of the Basin is completed in November 2015. Given the projected limited remaining life of the Basin, baseline conditions fall short of meeting the performance objective of extending the Basin

operations by 50 years and therefore, the No Action Alternative is removed from further evaluation. However, this alternative provides a reference to relate the costs and benefits of other alternatives. The following list summarizes assumptions, benefits, drawbacks, and anticipated costs for the No Action Alternative:

**Assumptions – No Action Alternative**

- Cache Creek flows would be routed consistent with historic operations (limited to 30,000 cfs through the Basin).
- City of Woodland’s flood protection alternatives would not impact the Basin’s baseline configuration and operations.

**Benefits – No Action Alternative**

- No initial costs.
- No additional permits required.
- Remaining sediment-trapping life estimated at 10 to 15 years.

**Drawbacks – No Action Alternative<sup>1</sup>**

- Up to 500,000 cubic yards of sediment will be released to the Yolo Bypass and Delta every year, as TE decreases. This assumes that sediment supply from upstream watershed areas is not reduced.
- Does not meet 50-year sediment-trapping performance measure.
- MeHg concentrations, spatial and temporal distribution, and bioaccumulation in the Basin will remain unchanged from current levels. This assumes that mercury loads from upstream sources is not reduced.
- Does not meet CVRWQCB regulatory requirements, in support of the Hg and MeHg reduction performance measures.

**Anticipated Costs – No Action Alternative**

- Implementation cost: \$0.
- Annual O&M cost: \$0.2 to \$1.3 million.

**6.4.5 Modify the Basin per O&M Manual Requirements**

USACE’s alternative for improving the Basin involves raising the Basin’s weir by 6 ft (1.8 m) (from El. 35 to 41 feet [NAVD 88]), by 2017-2018, or when the sediment removal efficiency is reduced to 30% or lower, whichever occurs first. In addition, the USACE plan calls for 400-ft (122 m) sections of the interior east training levee be notched at 1,100-ft (335 m) intervals every 5 years, starting 25 years after construction (2017-2018) until year 45 (2037-2038). The purpose of the incremental training levee notching is to direct flows to different parts of the Basin, thereby using the full Basin area and more evenly distributing sediments throughout the Basin. Additionally, this alternative established in

connection with the 1987 General Design Memorandum (GDM) and the last improvements performed by USACE in 1992-1993 is further detailed in the Draft Cache Creek Settling Basin O&M Manual – Sac Levee Unit No. 522 (USACE, 2007).

Raising the Basin's weir could result in a raise of the Cache Creek hydraulic profile between the Basin and County Road 102, located approximately ½ mile (805 m) upstream and west of the Basin. A raise in the hydraulic profile in the leveed reach of Lower Cache Creek is currently deemed unacceptable by the City of Woodland, which is in the process of developing a 200-year level of urban flood protection. Raising the hydraulic profile in Lower Cache Creek could further limit the conveyance of flood flows in the leveed reach of Lower Cache Creek. The noted reach has very limited capacity of conveying the equivalent of a 10-year flow (approximately 30,000 cfs) with 3 ft (0.9 m) of freeboard.

The limited 25-year additional design life achieved by this alternative does not meet the 50-year performance objective for the Basin. In addition, the alternative is not considered responsive to the TMDL directives mandated by the CVRWQCB because it would have little or no direct effect on reducing MeHg loads out of the Basin. Therefore, this alternative is not evaluated further in this Report. The following list summarizes assumptions, benefits, drawbacks, and anticipated costs for this alternative:

#### **Assumptions – Weir Raise and Notched Training Levee Alternative**

- Cache Creek flows would continue to be routed consistent with historic operations (Capacity limited to 30,000 cfs through the Basin).
- The Basin levee raises constructed in 1992-1993 east of County Road 102 will be sufficient to handle any backwater raise due to the proposed Basin outlet weir raise.
- City of Woodland's Preferred Plan would not impact the Basin operations.

#### **Benefits – Weir Raise and Notched Training Levee Alternative**

- Based on USACE designs, the functional life of the Basin under this alternative is possibly greater than 25 years (but less than 50 years).
- This plan has been modeled and adopted by USACE.
- Estimated to increase sediment and pTHg TE by 10%

#### **Drawbacks – Weir Raise and Notched Training Levee Alternative**

- Requires specific capital outlay without a plan to meet the needs of a 50-year sediment-trapping performance measure.
- Training levee notches may increase sediment and THg TE, but are unlikely to affect net MeHg production or export.
- Raising the outlet weir and notching the training levee is not likely to reduce MeHg concentrations or loads (due in part to a longer period of inundation) or change the spatial distribution of MeHg within the Basin.

- Not likely to meet CVRWQCB TMDL requirements of increasing sediment and THg TE and reducing MeHg concentration or loads relative to existing baseline conditions.

#### **Anticipated Costs – Weir Raise and Notched Levee Alternative**

- Implementation cost: \$12 to \$16 million.
- Annual O&M cost: \$0.2 to \$1.3 million.

#### **6.4.6 Sediment Stockpile – Modifying Land Use Practices**

This alternative includes the establishment of a sizeable sediment stockpile in the topographically elevated northwestern portion of the Basin. This portion of the Basin has not historically experienced inundation during high flow events. Thus, the use of settling basin acreage in the northwestern portion to stockpile sediment would not reduce the sediment TE of the Basin. It is estimated that moving accumulated sediment into the stockpile of about 17,000 acre-feet (or about 27 million cubic yards) could extend the useful life of the Basin by approximately 50 years (17,000 acre-feet/340 acre-feet per year) or greater.

This alternative requires limited initial and O&M costs while potentially achieving the desired 50-year extended operational life of the Basin. However, the proposed stockpile area would likely no longer be available for cultivation. By removing accumulated sediment and lowering the surface elevation in the active sediment settling basin area, trapping velocities are expected to decrease and basin retention time would increase, thus improving long-term TE. However, additional hydraulic and sediment transport modeling of the Basin coupled with appropriate monitoring, is necessary to provide verification of the improved TE associated with this approach. Regular excavation and grading operations within the Basin could limit anaerobic and anoxic conditions conducive to mercury methylation.

This option would likely require vegetation removal and the presence of earthmoving equipment in the low-flow areas between May 1 and November 1. The vegetation removal would likely reduce the organic content of the soils, resulting in lower potential to produce MeHg (as documented in the Yolo Bypass by Windham-Meyers et al., 2009). As much of the Basin is farmed, earthmoving operations could be scheduled around cultivation activities. The estimated fill volume used in evaluation for this alternative is based on a 300-acre footprint, with a 2:1 length to width ratio. At a 50-year design height, the stockpile would be 70 to 80 feet high, with three horizontal to one vertical (3H:1V) side slopes and a 10H:1V slope on one end for easier equipment access. The stockpile would be topographically prominent relative to the surrounding area.

This alternative could work in conjunction with City of Woodland’s proposed off-haul sediment management program to potentially relocate some of the accumulated sediments to the Yolo County landfill or other uses, as can be permitted, to further extend the useful life of the Basin and reduce the volume of sediment to be stockpiled. Assumptions, benefits, drawbacks, and anticipated costs for the Stockpile Alternative are summarized below:

### **Assumptions – Stockpile Alternative**

- Appropriate modeling is needed to confirm approach.
- Suitable procedures will be used for managing, handling and moving high-moisture sediments to a stockpile.
- Applicable permits will be obtained.
- City of Woodland’s Preferred Plan would not impact the Basin operations.

### **Benefits – Stockpile Alternative**

- Meets the 50-year sediment-trapping requirement performance measure.
- Estimated to increase sediment and pTHg TE by 5 percent.
- Is expected to reduce MeHg levels within and exiting the Basin by de-vegetating floodplain or riparian areas and limiting anaerobic conditions.

### **Drawbacks – Stockpile Alternative**

- Does not address loss of settling basin capacity due to City of Woodland’s potential encroachment of the Basin’s southwest corner.
- Grading of sediments may reduce MeHg production but the spatial and temporal distribution would likely remain unchanged without other basin modifications.
- Does not specifically increase sediment TE nor decrease MeHg production.
- Does not fully address long-term sediment-trapping.
- Requires best maintenance practices for stockpile management in perpetuity.

### **Anticipated Costs – Stockpile Alternative**

- Implementation cost: \$16 to \$21 million.
- Annual O&M cost: \$3 to \$4 million.

#### **6.4.7 Enlarge Basin**

This alternative includes the proposed stockpile within the northwest corner of the Basin as detailed above and two possible expansion scenarios: a small, topographically low, 300-acre (121 ha) settling basin expansion in the northeastern portion of the Basin; and a larger expansion totaling 600 acres (242 ha). The smaller expansion would require construction of new levees and removal of existing levees. The total area of the expansion would be 300 acres (121 ha); 95 percent of that area would be used for increased trapping capacity and 5 percent would be needed for construction of a new north levee.

The small expansion alternative would obtain the same benefits as noted for the Stockpile Alternative, and could potentially improve the effective sediment TE by 15% or greater above current levels (requires

confirmation using hydraulic and sediment transport models for the Basin). This enlargement of the sediment trapping area could also potentially extend the life of the Basin by 55 years or more.

This alternative can also work in conjunction with City of Woodland's proposed off-haul sediment management program to potentially relocate some of the accumulated sediments to the Yolo County landfill or other uses, as can be permitted, to further extend the useful life of the Basin and the volume of stockpiled material. A summary of assumptions, benefits, drawbacks, and anticipated costs for the small expansion alternative is presented below.

#### **Assumptions – Small Enlargement Alternative**

- Appropriate modeling is needed to confirm improved TE of this approach.
- Suitable procedures will be used for managing, handling and moving high-moisture sediments to a stockpile.
- Applicable permits will be obtained.
- This alternative could include a simultaneous degrade of limited portions of existing non-urban levee and construction of the new non-urban levee on the northeast corner of the Basin.
- Removal of a portion of the southwest corner of the Basin as part of the USACE Lower Cache Creek modifications could take place after the expansion is completed in the northeast corner of the Basin.
- City of Woodland's Preferred Plan would not change the design flow into the Basin.

#### **Benefits – Small Enlargement Alternative**

- Estimated to increase the sediment and pTHg TE by 15%.
- Could increase the sediment-trapping life to 50+ years.
- Is expected to reduce MeHg levels within and exiting the Basin by de-vegetating floodplain or riparian areas thus limiting anaerobic conditions within the original Basin; however, additional MeHg production is possible within the expanded area depending on how vegetation is managed.
- Addresses loss of settling basin capacity due to City of Woodland's potential removal of a portion of the Basin's southwest corner.

#### **Drawbacks – Small Expansion Alternative**

- Enlarged area of the Basin is not likely to facilitate a reduction in MeHg production or affect MeHg spatial or temporal distribution without other basin alterations.
- The existing topographically low area, with no outlet, in the northeast corner of the Basin may result in ponding and wetlands development, potentially increasing the MeHg production in this portion of the Basin depending on how vegetation is managed.
- Requires best maintenance practices for stockpile management in perpetuity.

### **Anticipated Costs – Small Expansion Alternative**

- Implementation cost: \$31 to \$40 million.
- Annual O&M cost: \$3 to \$4 million

The large expansion alternative includes an expansion in the northeast corner of the Basin to accommodate a 300-acre (121 ha) stockpile included in the previous two alternatives combined with an additional 300 acres (121 ha) of sediment trapping area and an additional weir in the topographically low area (relative to the land surrounding the Basin). The additional acreage could increase the Basin's effective sediment and pTHg TE by as much as 20%, based on the relative increase in effective trapping area. Hydraulic and sediment transport modeling will be needed to provide further verification of the improved trapping efficiencies associated with this alternative. This combined approach of an enlarged trapping area and stockpile could extend the life of the Basin by more than 55 years.

The total area proposed for the large expansion alternative is 600 acres (242 ha). The area allocation would be about 50% for sediment storage and 50% sediment trapping, with 15 acres (6 ha) set aside for non-urban levee construction. The expanded settling area would likely require the construction of a new weir and low-flow outlet on the northeast side of the Basin to prevent ponding, minimize MeHg production and further improve the TE. The new weir would be about 1,700 ft (518 m) long and the crest elevation would be the same as the existing weir at El. 35 feet (NAVD 88). The proposed large expansion alternative is shown on Figure 20.

This alternative can also work in conjunction with City of Woodland proposed off-haul sediment management program to potentially relocate some of the accumulated sediments to the Yolo County landfill or other uses, as can be permitted, to further extend the useful life of the Basin. Assumptions, benefits, drawbacks, and anticipated costs for the large expansion alternative follow:

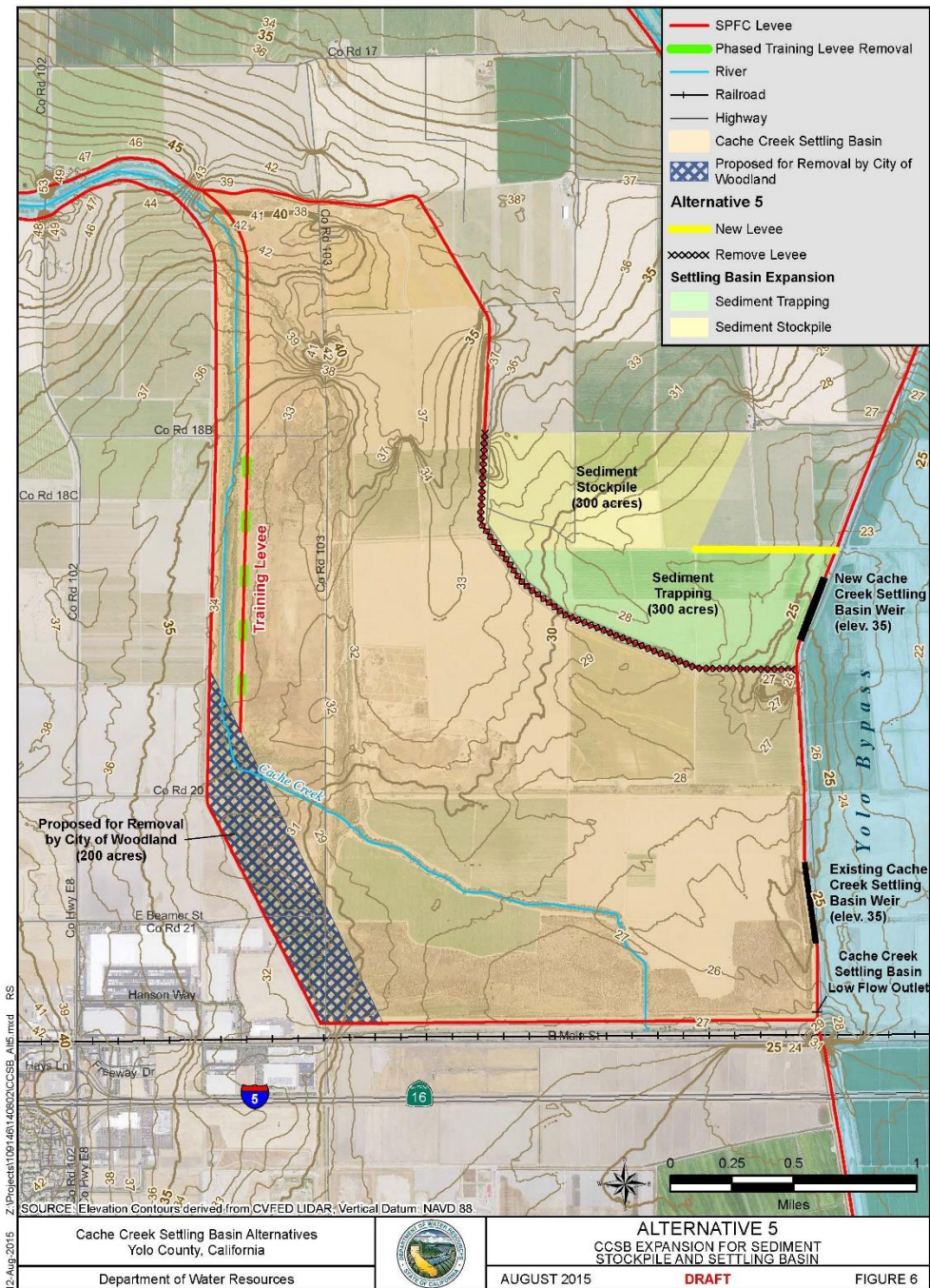


**Figure 20. Proposed Large Basin Expansion Alternative**

**Assumptions – Large Expansion Alternative**

- Appropriate modeling is required to confirm benefits of this approach.
- An outflow weir and low flow culvert through the Yolo Bypass levee in the northeast expansion area would be part of Basin modifications to increase settling efficiency.

- Suitable procedures will be used for managing, handling and moving high-moisture sediments to a stockpile.
- Applicable permits will be obtained.
- This alternative could include a simultaneous degrade of the existing non-urban levee and construction of a new non-urban levee on the northeast corner of the Basin.
- Construction of the sediment stockpile in the northeast expansion area could interfere with construction of a new non-urban levee in the area of the stockpile.

#### **Benefits – Large Expansion Alternative**

- Estimated to increase the sediment and pTHg TE by 20% due to additional acreage.
- Increases sediment-trapping life beyond the 50 year performance measure requirement.
- Is expected to reduce MeHg levels within and exiting the Basin by de-vegetating floodplain or riparian areas thus limiting anaerobic conditions within the Basin.
- Addresses the loss of settling basin capacity due to the City of Woodland’s potential removal of a portion of the Basin’s southwest corner.
- Addresses the need for temporary increased basin flow capacity due to the City of Woodland’s or USACE’s potential option of constructing a weir and/or gate in the west levee of the Basin.
- With suitable management of flows, the weir in the northeast corner could be used to increase residence time, thus increasing sediment TE and total flows through the Basin.

#### **Drawbacks – Large Expansion Alternative**

- Not likely to significantly reduce MeHg production.
- Could increase MeHg production in the expanded area depending on how vegetation is managed.
- Requires best maintenance practices for stockpile management in perpetuity.

#### **Anticipated Costs – Large Expansion Alternative**

- Range for implementation: \$54 to \$71 million.
- Annual O&M cost: \$3 to \$4 million.

#### **6.4.8 Others**

Activities that will likely be needed in conjunction with a Basin modification approach to reduce the mercury methylation process may include periodic re-grading of the Basin or focused sediment removal; modification of land use practices that would improve basin draining and minimize the formation of wetted floodplains with high organic content; focused aeration or chemical oxidation; and/or use of chemical amendments to fixate bond, or flocculate mercury-containing sediments. Other potential land-use/Basin modifications that may affect the TE of pTHg and net production of MeHg within the Basin

could include lengthening the primary channel to increase open-water habitat or adding or using existing gates to increase or decrease water holding times. As discussed in section 4.0, much like the above evaluated alternatives, there are both potential advantages and disadvantages to TE and in-basin MeHg production and bioaccumulation associated with these options.

## **6.5 Comparison of Alternatives**

Comparisons of the BWFS identified Basin alternatives with respect to dimensions of their expansion elements, expanded fee title or easement requirements, and extended functional life for sediment entrapment and storage are presented on Table 6.2 at the end of this section. Also presented on Table 6.2 is a summary of the estimated costs associated with the quantities as well as costs for ongoing sediment management operations. A final comparison of the Basin alternatives summarizing compliance with sediment management and TMDL objectives and addressing each alternative's constraints/limitations and the opportunities/benefits is provided on Table 6.3.

The No Action and Weir Raise with Notched Training Levee Alternatives do not meet the performance objective for improving sediment TE and extending the functional life of the Basin, nor are they responsive to the TMDL directives mandated by the CVRWQCB and performance objectives relating to the reduction of Hg and MeHg exiting the Basin. Accordingly, these alternatives were removed from further consideration.

Comparison of the remaining three alternatives indicates that Sediment Stockpile Alternative requires the lowest initial capital cost while achieving the desired 50-year extended operational life of the Basin and has no apparent impact on the surrounding agricultural areas; however, the proposed stockpile area is currently farmed and this acreage would be taken out of production. This alternative provides limited long-term operational flexibility because operating space limitations could be exacerbated with the further reduction of usable space by the City of Woodland's proposed removal of 200 or more acres (81 ha) from the southwest corner of the Basin. Thus, this alternative may not be considered a suitable and adaptable solution for sustaining the future functional life of the Basin. In addition, this alternative would have little to no effect for meeting the TMDL objectives.

The Small Expansion Alternative adds a sediment-trapping component that could possibly accommodate the City of Woodland's proposed removal of 200 or more acres (81 ha) from the southwest corner of the Basin. However, a limitation may be the topographically low area with no outlet in the northeast corner of the Basin that could result in ponding and wetlands development potentially increasing MeHg production in this portion of the Basin. In addition, this alternative does not address possible installation of a weir and/or gates in the Basin's west levee to route overland flows into the Basin. Based on these drawbacks, the Small Expansion Alternative would require modifications to become a suitable solution for sustaining the future functional life of the Basin.

The Large Expansion Alternative (fig. 20) appears to address the proposed removal of usable space in the Basin by the City of Woodland, as well as other important concerns including sediment stockpile storage

and a topographically low area that could drain into the Yolo Bypass. With a second, more distant weir, the Basin could be managed to provide more residence time for flows in the Basin allowing for additional sedimentation time and potentially greater TE. This second weir would also be available if additional overland flows are routed into the Basin via a weir and/or gates in the west levee, as is being considered by USACE. Although, there is a larger initial cost, this alternative appears to offer a longer-term solution because of greater operational flexibility in terms of sediment TE and sediment stockpiling. The larger, topographically low sediment-settling area, combined with the second weir could allow for more efficient settling basin management. By trapping more sediment, this alternative would reduce transport of pTHg out of the Basin and is expected to reduce MeHg levels by modifying land use to remove vegetation and reduce the organic content of the soil and sediment and minimize habitats conducive to MeHg formation, consistent with TMDL directives and the performance measures regarding THg and MeHg load reduction.

As part of any preferred alternative, DWR would evaluate an enhanced O&M plan that includes sediment excavation/grading and vegetation management that could serve to minimize the conditions that promote increased MeHg production.

Table 6.2. CCSB Alternatives: Dimensions, Quantities, and Extended Life Expectancy

CCSB Alternative	Existing Levee and Weir Modifications (feet)				New Weir and Levees (feet)		Required CCSB Expansion (acres)				Stockpile Storage Capacity (acre-feet)	Extended Life Expectancy (years)
	Strengthen /Raise Urban Levees	Improve Non-Urban Levees	Raise Weir	Levee Removal	New Levee	New Weir	Right-of-way for Levees	Area for Sediment Stockpile	Area for Sediment Settling	Total Area Required		
<i>Alternative 1: Baseline Condition</i>	0	0	-	-	-	-	-	-	-	0	-	10-15
<i>Alternative 2: Weir Raised and Training Levee Removal (USACE)</i>	0	0	1,700	2,000-	-	-	-	-	-	-	-	25
<i>Alternative 3: Sediment Stockpile in CCSB</i>	0	0	-	-	-	-	0	0	0	0	17,000	50
<i>Alternative 4: Sediment Stockpile in CCSB and Settling Basin Expansion</i>	0	0	-	7,250	7,240	-	30	0	300	330	17,000	55
<i>Alternative 5: CCSB Expansion for Sediment Stockpile and Settling Basin</i>	0	0	-	7,250	2,970	1,740	15	300	470	780	17,000	60+

1. Assume right-of-way easements required where levee raises cannot be extended into CCSB. New levees require right-of-way easements.
2. Calculations are preliminary rough estimates.
3. Extended life expectancy assumes 340 acre-feet of sediment per year deposited in the CCSB.
4. Stockpile storage capacities based on a 300-acre footprint, 2:1 L:W ratio, and 70 to 80 feet high, with 3H:1V side slopes on three sides and 10H:1V on the access slope.
5. Extended life expectancy is based on discussion of existing design life, estimated basin area/volume increases, stockpile volumes and USACE design average sediment trapping rate of 340 acre-feet/year.

**Table 6.3. Comparison of CCSB Alternatives**

<b>CCSB Alternative</b>	<b>Meets Sediment Management Objective of 50 Years</b>	<b>Responsive to CVRWQCB Objectives<sup>1</sup></b>	<b>Constraints / Limitations</b>	<b>Opportunities / Benefits</b>
<i>Alternative 1: Baseline Condition</i>	NO (5-10 years)	NO	Limited functional life.	Does not require modifications to the facility.
<i>Alternative 2: Weir Raised and Training Levee Removal (USACE defined)</i>	NO (25 years)	No plan in place (25-year limit)	Requires significant structural modifications. Does not address current/future environmental concerns.	Included in original USACE design memorandum (1987) and Draft O&M Manual (2007).
<i>Alternative 3: Sediment Stockpile with in CCSB</i>	Yes (50 years)	Yes	Seasonal limitation for stockpiling. <sup>2</sup>	Extends functional life of facility. Increased trapping efficiency. Consistent with TMDL directives.
<i>Alternative 4: Sediment Stockpile within CCSB and Settling Basin Expansion</i>	Yes (55 years)	Possibly with modifications.	Requires property acquisition. Seasonal limitation for stockpiling. <sup>2</sup>	Extends functional life of facility. Increased trapping efficiency. Consistent with TMDL directives.
<i>Alternative 5: CCSB Expansion for Sediment Stockpile and Settling Basin</i>	Yes (60+ years)	Yes	Requires property acquisition. Seasonal limitation for stockpiling. <sup>2</sup>	Extends functional life of facility. Increased trapping efficiency. Consistent with TMDL directives.

1. This metric refers to the responsiveness of the alternative to the Central Valley Regional Water Quality Control Board (CVRWQCB) in terms of management of total mercury and methylmercury relative to the TMDL directives for the CCSB and into other related bodies of water (Yolo Bypass and the Delta).

2. This option would require initial vegetation removal in the active sediment settling basin area and earthmoving equipment seasonally limited between May 1 and November 1

## **7 LONG-TERM FUNDING SOURCES**

DWR has utilized Proposition 1E Bond funds to initiate the mercury control studies summarized herein. This funding is sufficient to continue the control studies through June 2016, and will likely be unavailable for future studies or corrective actions for the Basin. DWR utilizes general funds to support the maintenance yard in performing their mandated routine O&M activities as well as periodic extraordinary maintenance activities. DWRs general fund budget has decreased in recent years and the maintenance yard fully utilizes their annual budgets such that there is little to no surplus to be utilized for non-routine activities.

DWR has no source of long-term funding to support further studies or implementation of corrective measures for the CCSB. Any future modifications to the Basin will require a tremendous capital outlay by the State and other local, state, and federal sponsors. State and federal legislative authorization will be necessary to fund the improvement and the project must be supported with mutual aid agreements from other benefitting communities and agencies including USACE, the CVFPB, Yolo County and the City of Woodland.

## 8 CONCLUSIONS AND RECOMMENDATIONS

The overall Basin suspended sediment TE calculated by the USGS from the studies summarized herein range from 29% (WY 2012, USGS LOADEST model) to 77% (WY 2010, USGS GLCAS model); with a five year annual average of 70% for WY's 2010-2014 (Table 3.5). The UCD modeled suspended sediment TE calibrated up to 15,900 cfs is conservatively predicted at 49%. This calculated range of annual suspended sediment TE is generally consistent with historical estimates. Total mercury species TE's ranged from 6% (WY 2012, pTHg, from USGS LOADEST model for suspended sediment) to 74% (WY 2011, pRHg(II), from USGS LOADEST model for suspended sediment) with a nonfiltered sample five-year annual average of 59% (Table 3.5); as with sediment, the mercury species TE results were generally consistent with, although slightly greater than results of historical studies. Filtered MeHg (fMeHg) (USGS LOADEST model) was the only constituent to demonstrate an increase in load leaving the Basin (Table 3.7). The five-year annual average fMeHg increase was calculated at 20% when summing the two outfall loads and at 34% when using the flow-weighted average of the two outfall loads.

Using the same five year data set (WY 2010-2014) as for the TE calculations (Tables 3.5 to 3.8) and based solely on nonfiltered sample results, the USGS calculated annual sediment loads into the Basin ranging from 0 kg/yr (WY 2014) to  $470 \times 10^6$  kg/yr (WY 2011) with a five-year average annual suspended sediment load of  $145 \times 10^6$  kg/yr (Table 3.1). The USGS reported the annual THg load into the Basin ranging from 0 kg (WY 2014) to 119 kg (WY 2011); with a five-year annual average of 32 kg/yr. The calculated average annual THg load leaving the Basin into the Yolo Bypass for this same data set ranged from 0 kg to 64 kg; with an annual five year average of 13 kg when using the sum of the total flows. When using the combined flow-weighted average, the THg load out of the Basin for this same five year data set ranged from 0 to 162 kg (WY 2011); with a five-year annual average of 14 kg (Table 3.3). It should be noted that both THg outflow quantification scenarios yield annual averages approximately a full order of magnitude less than the 118 kg/yr estimated by the CVRWQCB in their 2010 Staff Report (CVRWQCB, 2010) and less than a quarter of the 59 kg/yr load (50% THg load reduction) mandated by the TMDL. The lower THg loads during this study period (WY's 2010-2014) compared with the periods of previous studies (1996-2003) can be attributed primarily differences in how flows out of the Basin were calculated as well as below-average rainfall and discharge during Water Years 2010-14, however a decrease in the THg concentration of suspended particles may also have contributed to THg load reduction.

The same five-year data set yielded annual MeHg loads exiting the Basin ranging from 0 grams (WY 2014) to 697grams (WY 2011), with a five-year annual average of 183 grams (Table 3.3); although the same order of magnitude, this MeHg load is greater than the 137 g/yr estimated by the CVRWQCB in their Staff Report (CVRWQCB, 2010). The higher MeHg loads during WY's 2010-14 compared with previously studied periods (WY's 2000-2003) are likely due to the dryer conditions during 2010-14 as well as the accumulation of denser vegetation in the non-agricultural floodplain and riparian zones of the Basin for this time frame. These findings are consistent with a conceptual model in which MeHg

production and loads are decoupled to some degree from THg transport. This finding further supports that the CVRWQCB mandated annual MeHg load reduction of 78.5 percent, corresponding to a maximum 30 g/yr exiting the Basin will be unachievable without significant reductions in MeHg loads from upstream sources and in-Basin land-use modifications that reduce the non-agricultural floodplain and riparian acreage.

Using Cs-137 dating, the USGS calculated an average annual aggradation rate of approximately 0.9 inches (2.3 cm) per year for the years 1963 to 2012. This annual volume equates to approximately 270 acre-ft/yr; similar to, but less than the 340 acre-ft/year loads estimated by USACE when designing the 1993 Basin expansion.

Temporal and spatial analyses of the data collected for these studies show that there is no significant correlation between THg and MeHg concentration or grain sizes within the Basin sediments. Elevated MeHg concentration was most closely correlated with habitat, specifically non-agricultural floodplains and riparian zones, and other wetland habitats with elevated organic carbon.

When compared to the relative toxicity benchmarks for fish, the Basin appears to have relatively high THg and MeHg concentrations in fish and wildlife. Mercury concentrations in birds and fish also differed by habitat type as well as creek distance within the Basin. Fish THg concentrations were highest in mixed non-woody floodplain habitat, followed by mixed woody floodplain habitat, irrigation canals, tule wetland habitat, and creek habitat. THg concentrations in house wren eggs increased with the amount of mixed non-woody floodplain habitat located within 328 feet (100 m) of the nest box. These results show that the Basin floodplain and riparian habitats, which have denser vegetation and more organic carbon than agricultural and open-water habitats, have the highest potential for THg bioaccumulation in fish and wildlife. Because the Basin receives a variable amount of water flow from year to year, it is expected that MeHg concentrations will be highest in fish and wildlife during years with the most flooding for short periods of time during the spring breeding season. For both caged and wild mosquitofish, THg concentrations increased with creek distance into the Basin. Although from a substantially smaller data set, the USGS infers that THg concentrations in house wren eggs increased with creek distance in 2012, when the Basin was wetter; but not in 2013, when the Basin was mostly dry during the breeding season. THg and MeHg concentrations in surface water also increased with creek distance during Spring 2013

The initial evaluation of potential remedial alternatives for the Basin revealed a projected remaining basin life of 10 – 15 years based on current bathymetric conditions and estimates of pre-existing suspended sediment loads. Based on the aggradation rate estimate in our studies, the projected remaining basin life could be up to 20 % greater than this 10-15 year estimate (340 acre-ft/yr versus 270 acre-ft./yr). Implementation of the USACE Draft O&M Manual requirements (weir raise, training levee notching) is projected to extend the Basin lifespan for an additional 25 years and also improve TE up to 10%. However, neither the current condition nor the Draft O&M Improvement condition is expected to decrease MeHg production within the Basin as neither of these approaches include land-use alterations that would substantially change the volume of land used for wetted floodplain and riparian habitats. Each

of the other proposed basin modifications include enlargement and/or land-use modifications to decrease the volume of wetted floodplain and riparian habitats. While it is apparent that any of these other potential basin modifications will provide lifespan expansion of up to 60 years and improvements in overall TE, the effect on MeHg production within the Basin remains largely uncertain. Based on the data collected to date, it is clear that Basin enlargements alone or basin-capacity improvements through periodic sediment removal will be insufficient to decrease the MeHg loads exiting the Basin. Changes to the Basins current water stilling and movement practices as well as the elimination of vegetated floodplain habitats will be required to alter the current mercury methylation processes occurring within the Basin. Further hydraulic and sediment transport modeling is necessary to evaluate possible flood inundation areas as well as the TE and mercury load affects that may result from implementation of the evaluated potential remedial alternatives. DWR currently has no funding or contracts to continue flow modeling and mercury monitoring efforts beyond June 2016.

DWR is committed to completing their contract with USGS which will continue to collect flow measurements and sediment and water-quality samples consistent with the methodologies described herein through June 2016. There is an approximate 2-year lag between when the USGS collects their data and when it has been through peer-review and approved for release for public use. While these data are collected and reviewed DWR will continue to have UCD and the USGS update their TE models as the data become available. A more statistically supported model output will provide less uncertainty to the Basin's TE and load estimates and help support informed decision making regarding appropriate modifications for the Basin. Following completion of the USGS and UCD studies, DWR will prepare a plan for improvements to the Basin to decrease mercury loads from the Basin as required by the RWQCB Basin Plan Amendment. However, DWR has no current funding mechanisms to solely implement any basin improvements or continue the control studies beyond our current contractual commitments.

The selected Basin improvement plan must consider an alteration that can provide substantial flood risk reduction and water-quality improvements while also meeting the multiple concerns of the diverse regulatory and community interests as well as being fiscally responsible such that it can be funded. This is a challenge not likely to be easily met without aggressive pursuit of the elimination of THg and MeHg sources in the upstream watershed including possible installation of structures to entrain mercury-laden-sediment within the watershed.

## 9 REFERENCES

- Ackerman, J.T., and Eagles-Smith, C.A. (2010). Agricultural wetlands as potential hotspots for mercury bioaccumulation: experimental evidence using caged fish: *Environmental Science and Technology*, v. 44, p. 1451–1457.
- Alpers, C.N., Hunerlach, M.P., Marvin-DiPasquale, M.C., Antweiler, R.C., Lasorsa, B.K., De Wild, J.F., and Snyder, N.P. (2006). Geochemical data for mercury, methylmercury, and other constituents in sediments from Englebright Lake, California, 2002: U.S. Geological Survey Data Series 151, 95 p. <http://pubs.usgs.gov/ds/2006/151/>
- Arcement, G.J. Jr. and Schneider, V.R. (1989). Guide for Selecting Manning's Roughness Coefficients for Natural Channel and Flood Plains. U.S. Geological Survey. WSP 2339. <http://www.fhwa.dot.gov/bridge/wsp2339.pdf>
- Arias, M.R., Alpers, C.N., Marvin-DiPasquale, M., Fuller, C.C., Agee, J.L., Morita, A.Y., and Salas, A. (201X, in review). Sediment mercury, iron, sulfur, grain-size, and loss-on-ignition analyses from 2011 and 2012 coring campaigns, Cache Creek Settling Basin, Yolo County, California. U.S. Geological Survey Data Series XXX.
- Benoit, J.M., Gilmour, C.C., Heyes, A., Mason, R.P., and Miller, C.L. (2003). Geochemical and biological controls over methylmercury production and degradation in aquatic ecosystems, in Cai, Y., and Braids, O.C., eds., *Biogeochemistry of Environmentally Important Trace Elements*: Washington, DC, American Chemical Society, p. 262–297.
- Bodaly, R., and Fudge, R. (1999). Uptake of mercury by fish in an experimental boreal reservoir: *Archives of Environmental Contamination and Toxicology*, v. 109, p. 103–109.
- Brazelton, W. (2010). Rating Curve for Cache Creek Settling Basin Weir. EMAIL to Kara Carr. April 21, 2010.
- Camenen, B. (2007). Simple and general formula for the settling velocity of particles. *Journal of Hydraulic Engineering*, 133 (2), 229–233.
- Carr, K. (2006). Swimming Behavior Response of Adult White Sturgeon, *Acipenser Transmontanus*, to Velocity, Turbulence Intensity and Turbulent Kinetic Energy in a Vertical Slot Passageway (Master's Thesis). University of California, Davis.
- CDM (2004a). Final Technical Memorandum: Cache Creek Settling Mercury Study, Phase 1 - Existing Conditions. April, 2004.
- CDM (2004b). Technical Memorandum: Cache Creek Settling Mercury Study, Phase 2 - Sediment Transport Modeling. July, 2004.

CDM (2007). Technical Memorandum: Cache Creek Settling Mercury Study, Phase 3 - Alternatives Evaluation. August, 2007.

Cheng, N. S. (1997). Simplified settling velocity formula for sediment particle. *Journal of Hydraulic Engineering*, 123 (2), 149–152.

Coble, P.G., Del Castillo, C.E., and Avril, B. (1998). Distribution and optical properties of CDOM in the Arabian Sea during the 1995 Southwest Monsoon: *Deep-Sea Research II*, v. 45, p. 2195–2223.

Cooke, J., Foe, C., Stanish, S., and Morris, P. (2004). Cache Creek, Bear Creek, and Harley Gulch TMDL for Mercury. Staff Report, Central Valley Regional Water Quality Control Board, November, 2004.  
[http://www.waterboards.ca.gov/rwqcb5/water\\_issues/tmdl/central\\_valley\\_projects/cache\\_sulphur\\_creek/index.shtml](http://www.waterboards.ca.gov/rwqcb5/water_issues/tmdl/central_valley_projects/cache_sulphur_creek/index.shtml)

Cooke, J., and Morris, P. (2005). Amendments to The Water Quality Control Plan for the Sacramento River and San Joaquin River Basins for the Control of Mercury in Cache Creek, Bear Creek, and Harley Gulch: Central Valley Regional Water Quality Control Board, Final Staff Report. Sacramento. October, 2005. Available at:  
[http://www.waterboards.ca.gov/centralvalley/water\\_issues/tmdl/central\\_valley\\_projects/cache\\_sulphur\\_creek/index.shtml](http://www.waterboards.ca.gov/centralvalley/water_issues/tmdl/central_valley_projects/cache_sulphur_creek/index.shtml)

Depew, D.C., Basu, N., Burgess, N.M., Campbell, L.M., Evers, D.C., Grasman, K.A., and Scheuhammer, A.M. (2012). Derivation of screening benchmarks for dietary methylmercury exposure for the common loon (*Gavia immer*): rationale for use in ecological risk assessment: *Environmental Toxicology and Chemistry*, v. 31, p. 2399–2407.

De Vriend, D.J., (1999). Flow measurements in a Curved Rectangular Channel, Laboratory of Fluid Mechanics, Department of Civil Engineering, Delft University of Technology, Internal report no. 9-79.

Domagalski, J.L., Alpers, C.N., Slotton, D.G., Suchanek, T.H., Ayers, S.M. (2003a). Mercury and methylmercury concentrations and loads in the Cache Creek Watershed, California, January 2000 through May 2001, U.S. Geological Survey Water-Resources Investigations Report 03-3047, 105 p.  
<http://loer.tamug.tamu.edu/calfed/Report/Final/USGSCacheloadings.pdf>

Domagalski, J.L., Slotton, D.G., Alpers, C.N., Suchanek, T.H., Churchill, R., Bloom, N., Ayers, S.M., and Clinkenbeard, J. (2003b). Summary and Synthesis of Mercury Studies in the Cache Creek Watershed, California, 2000-2001. U.S. Geological Survey Water-Resources Investigations Report 03-4355, 30 p.  
<http://water.usgs.gov/pubs/wri/wri034335/>

Domagalski, J.L., Alpers, C.N., Slotton, D.G., Suchanek, T.H., Ayers, S.M. (2004). Mercury and methylmercury concentrations and loads in the Cache Creek Watershed, California. *Science of the Total Environment*. v. 327, p. 215–237. <http://loer.tamug.tamu.edu/calfed/Report/Publications/Cachestoen.pdf>

Driscoll, C.T., Han, Y.-J., Chen, C.Y., Evers, D.C., Lambert, K.F., Holsen, T.M., Kamman, N.C., and Munson, R.K. (2007). Mercury contamination in forest and freshwater ecosystems in the northeastern United States: *BioScience*, v. 57, no. 1, p. 17.

Drott, A., Lambertsson, L., Bjorn, E., and Skyllberg, U. (2008). Do potential methylation rates reflect accumulated methylmercury in contaminated sediments?: *Environmental Science and Technology*, v. 42, p. 153–158.

DWR, (2011). Central Valley Flood Management Planning Program, Flood Control System Status Report, Draft, July 2011

Engelund, F. and Hansen, E. (1967). A monograph on Sediment Transport in Alluvial Streams. Teknisk Vorlag, Copenhagen, Denmark.

Fleck, J.A., G. Gill, B.A. Bergamaschi, T.E.C. Kraus, B.D. Downing, and C.N. Alpers. (2014). Concurrent photolytic degradation of aqueous methylmercury and dissolved organic matter. *Science of the Total Environment*. <http://dx.doi.org/10.1016/j.scitotenv.2013.03.107>

Froehlich, D.C. (1989). HW031.D—Finite Element Surface-Water Modeling System: Two-dimensional flow in a horizontal plane—user’s manual: Federal Highway Administration Report FHWA-RD–88–177. 285 p.

Furutani, A., and Rudd, J.W.M. (1980) Measurement of mercury methylation in lake water and sediment samples: *Applied Environmental Microbiology*, v. 40(4), p. 770–776.

Garbrecht, J., Kuhnle, R. and Alonson, C. (1995). A Sediment Transport Capacity Formulation for Application to Large Channel Networks. *Journal of Soil and Water Conservation* 50(5), 527–529.

Gilmour, C.C., Riedel, G.S., Ederington, M.C., Bell, J.T., Benoit, J.M., Gill, G.A., and Stordal, M.C. (1998). Methylmercury concentrations and production rates across a trophic gradient in the northern Everglades: *Biogeochemistry*, v. 40, no. 2-3, p. 327–345.

Grigal, D.F. (2002). Mercury sequestration in forests and peatlands: A Review: *Journal of Environmental Quality*, v. 32, p. 393-405.

Guo, J. (2002). Logarithmic matching and its applications in computational hydraulics and sediment transport. *J. Hydraul. Res.*, 40(5), 555–565.

Heinz, G.H., Hoffman, D.J., Klimstra, J.D., Stebbins, K.R., Kondrad, S.L., and Erwin, C.A. (2009). Species differences in the sensitivity of avian embryos to methylmercury: *Archives of Environmental Contamination and Toxicology*, v. 56, p. 129–138.

Huang, Sui Liang (2007). Effects of using different sediment transport formulae and methods of computing Manning's roughness coefficient on numerical modeling of sediment transport. *Journal of Hydraulic Research*, 45:3, 347-356

Hunerlach, M.P., Alpers, C.N., Marvin-DiPasquale, M., Taylor, H.E., and De Wild, J.F. (2004). Geochemistry of mercury and other trace elements in fluvial tailings upstream of Daguerre Point Dam, Yuba River, California, August 2001: U.S. Geological Survey Scientific Investigations Report 2004-5165, 66 p. <http://pubs.usgs.gov/sir/2004/5165/>

Jackson, A.K., Evers, D.C., Etterson, M.A., Condon, A.M., Folsom, S.B., Detweiler, J., Schmerfeld, J., and Cristol, D.A. (2011). Mercury exposure affects the reproductive success of a free-living terrestrial songbird, the Carolina Wren (*Thryothorus ludovicianus*): *The Auk*, v. 128, p. 759-769.

Jia, Y., and Sam S.Y. Wang, (2001a). CCHE2D: Two-dimensional Hydrodynamic and Sediment Transport Model for Unsteady Open Channel Flows Over Loose Bed. Technical Rep. No. NCCHETR-2001-1, National Center for Computational Hydroscience and Engineering, The University of Mississippi. <<http://www.ncche.olemiss.edu/sites/default/files/files/docs/cche2d/techmanual.pdf>>

Jia, Y., and Sam S.Y. Wang, 2001b. CCHE2D Verification and Validation Tests Documentation Technical Rep. No. NCCHETR- (2001-2). National Center for Computational Hydroscience and Engineering, The University of Mississippi. <<http://www.ncche.olemiss.edu/sites/default/files/files/docs/cche2d/validation.pdf>>

Julien, P. Y. (2002). *River Mechanics*. Cambridge University Press.

Kantoush, S.A., De Cesare, G., Boillat, J.-L., Schleiss, A.J. (2008). Flow field investigation in a rectangular shallow reservoir using UVP, LSPIV and numerical modeling. *Journal of Flow Measurement and Instrumentation* 19 (3-4), 139-144.

Koltun, G.F., Eberle, Michael, Gray, J.R., and Glysson, G.D. (2006). User's manual for the Graphical Constituent Loading Analysis System (GCLAS): U.S. Geological Survey Techniques and Methods, book 4, chap. C1, 51 p.

Korthals, E.T., and Winfrey, M.R. (1987). Seasonal and spatial variations in mercury methylation and demethylation in an oligotrophic lake: *Applied Environmental Microbiology*, v. 53, p. 2397-2404.

Krabbenhoft, D.P., Wiener, J.G., Brumbaugh, W.G., Olson, M.L., DeWild, J.F., and Sabin, T.J. (1999). A national pilot study of mercury contamination of aquatic ecosystems along multiple gradients. U. S. Geological Survey, Toxic Substance Hydrology Program Water-Resources Investigation Report 99-4018B, 147-160 p. On-line: <http://pubs.er.usgs.gov/usgspubs/wri/wri994018B>

Lambertsson, L., and Nilsson, M. (2006) Organic material: The primary control on mercury methylation and ambient methyl mercury concentrations in estuarine sediments: *Environmental Science and Technology*, v. 40(6), p. 1822–1829.

Laursen, E. M. (1958). The Total Sediment Load of Streams. *Journal of the Hydraulics Division*, 84(1), 1-36.

Lustig, L.K. and Busch R.D. (1967). Sediment Transport in Cache Creek Drainage Basin in the Coast Ranges West of Sacramento, California. Geological Survey professional paper, 562-A.

Marvin-DiPasquale, M., and Agee, J.L. (2003). Microbial mercury cycling in sediments of the San Francisco Bay-Delta: *Estuaries*, v. 26(6), p. 1517–1528.

Marvin-DiPasquale, M., Alpers, C.N., and Fleck, J.A. (2009). Mercury, methylmercury, and other constituents in sediment and water from seasonal and permanent wetlands in the Cache Creek Settling Basin and Yolo Bypass, Yolo County, California, 2005–06: U.S. Geological Survey Open File Report 2009-1182, 69 p., On-Line: <http://pubs.usgs.gov/of/2009/1182/>

Marvin-DiPasquale, M., Windham-Myers, L., Agee, J.L., Kakouros, E., Kieu, L.H., Fleck, J., Alpers, C.N., and Stricker, C. (2014). Methylmercury production in sediment from agricultural and non-agricultural wetlands in the Yolo Bypass, California: *Science of the Total Environment*, v. 484, p. 288–299.

McKnight, D.M., Boyer, E.W., Westerhoff, P.K., Doran, P.T., Kulbe, T., and Andersen, D.T. (2001) Spectrofluorometric characterization of dissolved organic matter for indication of precursor organic material and aromaticity. *Limnology and Oceanography*, v. 46, p. 38–48.

McLaughlin R.J., Jr. (1959). The settling properties of suspensions. *Journal of Hydraulics Division, Proceedings of the American Society of Civil Engineers* 85(HY12): 9–41.

Meyer-Peter, E., & Müller, R. (1948). Formulas for Bed-load Transport. Report on Second Meeting of IAHR, Stockholm, Sweden, 39-64.

Mohanty, K. P., Dash, S. S., and Khatua, K. K. (2012). Flow investigations in a wide meandering compound channel. *International Journal of Hydraulic Engineering*, 1(6), 83-94.

Negm, A. M., Abdulaziz, T., Nassar, M., & Fathy, I. (2010). Predication of life time span of High Aswan Dam Reservoir using CCHE2D simulation model. In *Proceeding 14th International Water Technology Conference* (pp. 611-626).

Newton, C.T., 1951. An experimental investigation of bed degradation in an open channel. *Transactions of the Boston Society of Civil Engineers*, (pp. 28-60).

- Proffit, G.T. and A.J. Sutherland, (1983). Transport of Non-uniform Sediment. *Journal of Hydraulic Research* 21(1), 33–43.
- Rajaratnam, N. and Ahmadai, R. 1981, Hydraulics of channels with flood-plains. *Journal of Hydraulic Research, IAHR*, Vol. 19, No. 1, (pp. 43-60).
- Ritchie, J.C., and McHenry, J.R. (1990). Application of radioactive fallout cesium-137 for measuring soil erosion and sediment accumulation rates and patterns: A review. *Journal of Environmental Quality* v. 9, p. 215–233.
- Scudder, B.C., Chasar, L.C., Wentz, D.A., Bauch, N.J., Brigham, M.E., Moran, P.W., and Krabbenhoft, D.P. (2009). Mercury in fish, bed sediment, and water from streams across the United States, 1998-2005: U.S. Geological Survey Scientific Investigations Report 2009-5109, 74 p.  
<http://pubs.usgs.gov/sir/2009/5109/>
- Snodgrass, J.W., Jagoe, C.H., Bryan, Jr., A.L., Brant, H.A., and Burger, J. (2000). Effects of trophic status and wetland morphology, hydroperiod, and water chemistry on mercury concentrations in fish: *Canadian Journal of Fisheries and Aquatic Sciences*, v. 57, p. 171–180.
- Soni, J. P. (1981). Laboratory study of aggradation in alluvial channels. *Journal of Hydrology*, 49(1), 87-106.
- Sunderland, E.M., Gobas, F.A.P.C., Branfireun, B.A., and Heyes, A. (2006). Environmental controls on the speciation and distribution of mercury in coastal sediments: *Marine Chemistry*, v. 102, p. 111– 123.
- UCD (2012). Final Report for Cache Creek Settling Basin / Yolo Bypass Project, January 1, 2009 – July 31, 2012. UC Davis J. A. Hydraulics Laboratory. July 31, 2012.
- UCD (2014). Cache Creek Settling Basin Trap Efficiency Study Progress Report, April 15, 2013 – April 30, 2014. UC Davis J. A. Hydraulics Laboratory. May 1, 2014, updated September 25, 2015.
- UCD (2015). Cache Creek Settling Basin Trap Efficiency Study Progress Report, May 1, 2014 – June 15, 2015. UC Davis J. A. Hydraulics Laboratory. June 15, 2015, revised September 23, 2015.
- UCD (2015a). Final Report - Study of the Water, Sediment and Mercury Inflows to Cache Creek Settling Basin based on Cache Creek Watershed Hydrology and Future Climate Conditions. UC Davis J. A. Hydraulics Laboratory. December 20, 2014; revised September 25, 2015.
- Ullrich, S.M., Tanton, T.W., and Abdrashitova, S.A. (2001). Mercury in the aquatic environment: a review of factors affecting methylation: *Critical Reviews in Environmental Science and Technology*, v. 31, no. 3, p. 241–293.

USACE (1961). Supplement to Standard Operation and maintenance manual, Sacramento Flood Control Project, Unit 126, Cache Creek Levees and Settling basin, Yolo Bypass to High Ground, November, 1961.

USACE (1987). Final General Design Memorandum No. 1, Cache Creek, California, Cache Creek Settling Basin. U.S. Army Corps of Engineers, Sacramento District. p. 3-20. January.

USACE, (1997). Sediment Deposition in the Cache Creek Training Channel. Memorandum for Chief, Western Region Section. Sacramento, California. March.

USACE (2007). Cache Creek Basin, California: Cache Creek Settling Basin Enlargement: “Draft” Operations and Maintenance Manual. US Army Corps of Engineers Sacramento District. March, 2007.

USGS, (2013). Progress Report for the Period May 2011 through June 2013, Cache Creek Settling Basin Mercury Studies. Alpers et. al. August 8, 2013.

USGS, (2014). Progress Report for the Period July 2013 through June 2014, Cache Creek Settling Basin Mercury Studies. Alpers et. al. July 31, 2014.

USGS, (2015). Draft - Mercury Studies in the Cache Creek Settling Basin, Yolo County, California: Preliminary Results, 2010 -14. November 16, 2015.

USGS: Water Data for USA. Sites 11452600, 11452800, 11452900, 11452901, 11452905.  
<<http://nwis.waterdata.usgs.gov/nwis>>

Van Rijn, L. C. (1986). Manual sediment transport measurements. Delft, The Netherlands: Delft Hydraulics Laboratory Wang Sam S.Y., and Hu, K.K., 1992. Improved methodology for formulating finite-element hydrodynamic models. In T,J, Chung, (ed) Finite Element in Fluids, Volume 8, Hemisphere Publication Cooperation, pp 457-478.

Wang Sam S.Y., and Hu, K.K. (1992). “Improved methodology for formulating finite-element hydrodynamic models”, In T,J, Chung, (ed) Finite Element in Fluids, Volume 8, Hemisphere Publication Cooperation, pp 457-478.

Weishaar, J.L., Aiken, G.R., Bergamaschi, B.A., Fram, M.S., Fujii, R., and Mopper, K. (2003). Evaluation of specific ultraviolet absorbance as an indicator of the chemical composition and reactivity of dissolved organic carbon: Environmental Science and Technology, v. 37, p. 4702–4708.

Wood, M.L., Foe, C., Cooke, J., and Louie, S.J. (2010a), Sacramento – San Joaquin Delta Estuary TMDL for Methylmercury. Staff Report. Draft Report for Public Review. Regional Water Quality Control Board – Central Valley Region. February 2010, 233 p.  
[http://www.swrcb.ca.gov/rwqcb5/water\\_issues/tmdl/central\\_valley\\_projects/delta\\_hg/april\\_2010\\_hg\\_tmdl\\_hearing/index.shtml](http://www.swrcb.ca.gov/rwqcb5/water_issues/tmdl/central_valley_projects/delta_hg/april_2010_hg_tmdl_hearing/index.shtml)

Windham-Myers, L., Marvin-DiPasquale, M., Krabbenhoft, D.P., Agee, J.L., Cox, M.H., Heredia-Middleton, P., Coates, C., and Kakouros, E. (2009). Experimental removal of wetland Wu Weiming, and Sam S.Y. Wang (1999). Movable Bed Roughness in Alluvial Rivers. *Journal of Hydraulic Engineering*. ASCE, Vol. 125, No.12, pp.1309-1312.

Wu, Weiming, Sam S.Y. Wang, Y. F. Jia, (2000). Non-Uniform Sediment Transport in Alluvial Rivers. *Journal of Hydraulic Research*, 38(6).

Wu, W., 2001. CCHE2D: Sediment Transport Model (Version 2.1) Technical Rep. No. NCCHETR-2001-3, National Center for Computational Hydroscience and Engineering, The University of Mississippi.

Xu, Y., Wang, S.S.Y., Jia, Y. (2001). “Application of a Depth-Integrated Two-Dimensional Numerical Model to the Lauffen Reservoir on the Neckar River”. Accepted, 27th International Conference of IAHR, Beijing, China, Sept. 2001 Yang, C. T. (1973). Incipient Motion and Sediment Transport. *Journal of the Hydraulics Division*, 99(10), 1679-1704.

Zhang, R. J. (1989). *Sediment Dynamics in Rivers*. Beijing: Water Resources Press. (in Chinese).



**Cache Creek Settling Basin / Yolo Bypass Project  
Contract No. 4600010003**

**Cache Creek Settling Basin Trap Efficiency Study  
Progress Report  
April 15, 2013 – April 30, 2014**

Prepared for

**California Department of Water Resources**

Prepared By

Kara Carr  
Ali Ercan  
Tongbi Tu  
Hossein Bandeh  
M. Levent Kavvas (Principal Investigator)

**UC Davis J. A. Hydraulics Laboratory**

Department of Civil and Environmental Engineering  
University of California, Davis  
One Shields Avenue  
Davis, CA 95616

**May 1, 2014  
Revised September 23, 2015**

Table of Contents	
List of Figures .....	2
List of Tables .....	5
Acknowledgements.....	6
1 Introduction.....	6
1.1 Background.....	7
1.2 Objective.....	8
2 Flow Sampling by UCDJAHL.....	9
3 Two-dimensional Flow and Sediment Transport Model.....	9
3.1 CCHE2D.....	10
3.2 Third-party Calibration and Validation.....	10
3.2.1 NCCHE Calibration and Validation.....	11
3.2.2 Non-Principal Calibration and Validation.....	17
4 CCHE2D Flow Simulations.....	22
4.1.1 Calibration by 18-22 March 2011 event at Road 102.....	29
4.1.2 Validation by 18-22 March 2011 flow event inside CCSB.....	32
4.1.3 Validation by 23-27 March 2011 flow event at Road 102 and inside CCSB .....	47
5 References .....	67
Appendix.....	69

## LIST OF FIGURES

Figure 3.1. Flume dimension and recirculation pattern of Xie (1994) experiments (from Jia and Wang, 2001b) .....	11
Figure 3.2 Comparisons of the simulated (line) and measured (circles) flow field in the channel of sudden expansion, a: $Q=0.01815\text{m}^3/\text{s}$ , b: $Q=0.03854\text{m}^3/\text{s}$ (Jia and Wang, 2001b) .....	12
Figure 3.3 Mesh system of the 180-degree U-shaped channel (Jia and Wang, 2001b).....	13
Figure 3.4 Simulated and measured velocities of the 180-degree U-shaped channel (Jia and Wang, 2001b) .....	13
Figure 3.5 Definition sketch of the compound channel components (Jia and Wang, 2001b) .....	14
Figure 3.6 Comparison of measured and simulated velocity in a compound channel (Jia and Wang, 2001b) .....	14
Figure 3.7 Comparison of measured and simulated bed elevations, bed aggradation experiment (Jia and Wang, 2001b) .....	15
Figure 3.8 Comparison of experimental and simulated results, bed degradation experiment (Jia and Wang, 2001b) .....	16
Figure 3.9. Suspended sediment verification results, River Nechar, Germany: a. sediment concentration contour plot; b. comparison of measured and computed sediment concentrations (Jia and Wang, 2001b).....	17
Figure 3.10 Flow field from (a) UVP (b) LSPIV (c) CCHE2D and (d) comparison of velocity magnitude vectors obtained from all three methods .....	18
Figure 3.11 Experimental set-up for meandering compound channel Mohanty et al. (2012).....	19
Figure 3.12 Normalized depth averaged velocity diagrams for each of the five runs (a) Run 1 (b) Run 2 (c) Run 3 (d) Run 4 (e) Run 5 (Mohanty et al., 2012) ..	19
Figure 3.13 Shear velocity diagrams for each of the five runs (a) Run 1 (b) Run 2 (c) Run 3 (d) Run 4 (e) Run 5, (Mohanty et al., 2012).....	20
Figure 3.14 Huang (2000) Channel degradation comparison, utilizing each bed roughness method for (a) Wu et al. (2000) bed-load formula, (b) Wu et al. (2000) bed-material load formula, (c) Modified Ackers–White bed-material formula, (d) Modified Engelund–Hansen bed-material load formula and (e) SEDTRA module .....	21
Figure 3.15 Calibration results for cross section bed level in 2003 (a) section 13 and (b) section 16 (Negm et al., 2010).....	22
Figure 3.16 Verification results for cross section bed level in 2007 (a) section 13 and (b) section 16 (Negm et al., 2010).....	22
Figure 3.17 Predicted bed elevation for sections 13 and 16 plotted against corresponding measured bed elevation (Negm et al., 2010) .....	22
Figure 4.1 Mesh from Cache Creek at Yolo to Road 102 .....	24
Figure 4.2 Simulation Mesh for CCSB .....	25
Figure 4.3 Elevation contour of simulated extent from Cache Creek at Yolo to Rd 102.....	26
Figure 4.4 Elevation contour of simulated extent, Rd 102 through CCSB including approximate locations of result comparison points .....	27

Figure 4.5 Rating curve for the USGS site 11452800, CCSB overflow weir. ....28

Figure 4.6 Rating curve for USGS site 11452900, CCSB low flow culvert. ....28

Figure 4.7 (a) Results of CCHE2D water surface elevation at Rd 102 for various bed roughness and measured water surface elevation at Rd 102, and (b) percent error of simulated water surface elevations for various bed roughness methods31

Figure 4.8 (a) Results of CCHE2D water surface elevation at Rd 102 for various grain size distributions, (b) percent error of simulated water surface elevations at Rd 102 for various grain size distributions .....32

Figure 4.9 Comparison plots of 18-22 March 2011 simulation, (a) Inflow discharge at Cache Creek at Yolo with time steps for results display, (b) Calibrated water surface elevation at Rd 102 for entire simulation duration, (c) Water Surface Elevation validation at Site C for entire simulation duration, (d) Water Surface Elevation validation at Overflow Weir for entire simulation duration .....34

Figure 4.10 Water depth results at selected times on rising limb of storm hydrograph, 1 and 2 (peak flow) of 18-22 March 2011 event; Cache Creek at Yolo to Rd 102 .....35

Figure 4.11 Water depth results at selected times on falling limb of hydrograph, 3 and 4 of 18-22 March 2011 event; Cache Creek at Yolo to Rd 102.....36

Figure 4.12 Velocity magnitude results at selected times on rising limb of hydrograph, 1 and 2 (peak flow) of 18-22 March 2011 event; Cache Creek at Yolo to Rd 102 .....37

Figure 4.13 Velocity magnitude results at selected times on falling limb of hydrograph, 3 and 4 of 18-22 March 2011 event; Cache Creek at Yolo to Rd 102 .....38

Figure 4.14 CCSB water depth results, March 2011, at selected times on rising limb of hydrograph, 1 and 2 (peak flow) of 18-22 March 2011 event. ....39

Figure 4.15 CCSB water depth results, March 2011, at selected times on falling limb of hydrograph, 3 and 4 of 18-22 March 2011 event.....40

Figure 4.16 CCSB velocity magnitude results, March 2011, at selected times on rising limb of hydrograph, 1 and 2 (peak flow) of 18-22 March 2011 event.....41

Figure 4.17 CCSB velocity magnitude results, March 2011, at selected times on falling limb of hydrograph, 3 and 4 of 18-22 March 2011 event .....42

Figure 4.18 CCSB velocity magnitude result with scaled directional vectors, at selected time 1 of 18-22 March 2011 event .....43

Figure 4.19 CCSB velocity magnitude result with scaled directional vectors, at selected time 2 of 18-22 March 2011 event .....44

Figure 4.20 CCSB velocity magnitude result with scaled directional vectors, at selected time 3 of 18-22 March 2011 event .....45

Figure 4.21 CCSB velocity magnitude result with scaled directional vectors, at selected time 4 of 18-22 March 2011 event .....46

Figure 4.22 Comparison plots of 23-27 March 2011 validation simulation, (a) Inflow discharge at Cache Creek at Yolo with time steps for results display, (b) Water surface elevation validation at Rd 102 for entire simulation duration, (c) Water Surface Elevation validation at Site C for entire simulation duration, (d)

Water Surface Elevation validation at Overflow Weir for entire simulation duration .....	48
Figure 4.23 Water depth validation simulation results, Yolo to Rd 102, at selected times 1 and 2 of 23-27 March 2011 event.....	49
Figure 4.24 Water depth validation simulation results, Yolo to Rd 102, at selected times 3 (peak flow) and 4 of 23-27 March 2011 event .....	50
Figure 4.25 Water depth validation simulation results, Yolo to Rd 102, at selected time 5 of 23-27 March 2011 event .....	51
Figure 4.26 Water depth validation results, CCSB, at selected times 1 and 2 of 23-27 March 2011 event .....	52
Figure 4.27 Water depth validation results, CCSB, at selected times 3 (peak flow) and 4 of 23-27 March 2011 event .....	53
Figure 4.28 Water depth validation results, CCSB, at selected time 5 of 23-27 March 2011 event .....	54
Figure 4.29 Velocity magnitude validation results, Yolo to Rd 102, at selected times 1 and 2 of 23-27 March 2011 event.....	55
Figure 4.30 Velocity magnitude validation results, Yolo to Rd 102, at selected times 3 (peak flow) and 4 of 23-27 March 2011 event .....	56
Figure 4.31 Velocity magnitude validation results, Yolo to Rd 102, at selected time 5 of 23-27 March 2011 event. ....	57
Figure 4.32 Velocity magnitude validation simulation results, CCSB, at selected times 1 and 2 of 23-27 March 2011 event.....	58
Figure 4.33 Velocity magnitude validation simulation results, CCSB, at selected times 3 (peak flow) and 4 of 23-27 March 2011 event .....	59
Figure 4.34 Velocity magnitude validation simulation results, CCSB, at selected time 5 of 23-27 March 2011 event .....	60
Figure 4.35 CCSB validation velocity magnitude result with scaled directional vectors, at selected time 1 of 23-27 March 2011 event.....	62
Figure 4.36 CCSB validation velocity magnitude result with scaled directional vectors, at selected time 2 of 23-27 March 2011 event.....	63
Figure 4.37 CCSB validation velocity magnitude result with scaled directional vectors, at selected time 3 (peak flow) of 23-27 March 2011 event .....	64
Figure 4.38 CCSB validation velocity magnitude result with scaled directional vectors, at selected time 4 of 23-27 March 2011 event.....	65
Figure 4.39 CCSB validation velocity magnitude result with scaled directional vectors, at selected time 5 of 23-27 March 2011 event.....	66
Figure A.0.1 Dr. Ercan and Dr. Carr on the Sacramento River, ADCP Trial Run December 13, 2013 .....	69
Figure A.0.2 Tracker Guide V-14 Boat purchased for sediment and velocity measurements within the CCSB .....	69
Figure A.0.3 ADCP transmitter and float.....	70

## LIST OF TABLES

Table 3.1 Flow conditions for the sudden expansion channel experiments conducted by Xie (1994) and simulated by Jia and Wang, (2001b).....	11
Table 3.2 Flow conditions for the 180-degree U-shaped channel, (from Jia and Wang, 2001b). .....	12
Table 3.3 Parameters of the compound channel experiment (Jia and Wang, 2001b).....	14
Table 3.4 Sediment and initial flow conditions, bed aggradation experiment performed by Soni (1981) (from Jia and Wang, 2001b). .....	15
Table 3.5 Sediment and initial flow conditions, bed degradation experiment performed by Newton (1951) (from Jia and Wang, 2001b). .....	16
Table 3.6 Hydraulic parameters for the experimental runs, meandering compound channel (Mohanty et al., 2006).....	19
Table 4.1 Grain size distributions applied with Wu and Wang (1999) roughness simulations. ....	29
Table 4.2 Normalized root mean square error for simulated water surface elevations at Rd 102 for each bed roughness method.....	32
Table 4.3 NRMSE and Nash Coefficient for calibration and validation simulations. ....	33

## ACKNOWLEDGEMENTS

We thank the personnel at U.S Geological Survey Sacramento Field Office for sharing sediment and flow data at Cache Creek Settling Basin.

This research was funded through a contract with the Department of Water Resources (Contract No. 4600010003). We thank Mr. Frederick Gius for his insight and support, and Mr. John Nosacka, who coordinated the efforts and resources between Department of Water Resources and UC Davis J. Amorocho Hydraulics Laboratory during the study,

## 1 INTRODUCTION

This report describes the Cache Creek Settling Basin (CCSB) / Yolo Bypass Project progress during April 15th, 2013 through April 14th, 2014. Objectives for this year of the study included:

Objective 1. A field measurement sampling program was to be conducted throughout the wet season to enable sampling of 2-D velocity and discharge along transects north of the low flow channel within the settling basin. Samples were to be taken at regular intervals during storm events and while sufficient water remains in the basin to facilitate sampling. These measurements were to be incorporated in 2-D flow and sediment transport models evaluation as they become available. This objective was not met as sufficient discharge did not occur in Year 1. There was no storm event during the study period which provided sufficient inundation of the CCSB. All supplies necessary for sampling were secured.

Objective 2. Field measurements as supplied by USGS were to be catalogued and incorporated into the 2-D flow and sediment transport models for updated calibration and validation as they become available. This objective was met, as all available data was catalogued and stored in our data bank. Additionally, field measurements were utilized in calibration and validation of the 2-dimensional flow and sediment transport model. Calibration and validation was possible for flows up to 15900 cubic feet per second (cfs), the largest discharge record supplied by USGS.

Year 1 Objective 3. 2-D flow and sediment transport model results were to be analyzed utilizing all the available flow and sediment data, and further data gaps noted. This objective was partially met. Hydrodynamic modeling has been validated for flows with an exceedance probability of 41-percent or more. Simulations of larger magnitude flows are not validated, and additional sampling of flow and sediment is required to increase confidence in the model's performance and applicability at larger discharge magnitudes. As previously identified, additional samples of coincident flow and sediment, taken periodically over the duration of a storm event, are required. Such samples were not

available in this year of the study due to lack of storm events within the study period. Further sediment grain size distribution and sediment concentration at the inlet and outlet of the CCSB are also necessary for validation of the sediment transport model.

### **1.1 Background**

Cache Creek Settling Basin, located two miles east of the City of Woodland, California, was originally built in 1938. The primary function of the CCSB is to remove a significant portion of the sediment load from Cache Creek to avoid its deposition in the Yolo Bypass, thereby preserving the capacity of the bypass for conveying flood flows. The Yolo Bypass serves to protect Sacramento and surrounding areas from flooding with a design flow of 216,000 cfs. Cache Creek delivers large amounts of sediment to the Settling Basin every year, and is the main source of mercury to the San Francisco Bay-Delta. In addition to preserving the flood flow capacity of the Yolo Bypass; entrapment of sediment in the Basin is instrumental in diminishing the mercury load to the San Francisco Bay-Delta, making the Basin fundamental in preserving water quality. The sediment entering the CCSB is a legacy of the California Gold Rush and mercury mining in California's Coastal range. A number of abandoned, un-reclaimed and partially reclaimed mercury mines are situated in the Cache Creek watershed. Furthermore, aggregate mining of Cache Creek has increased channel incision and sediment loading in the creek (Thayer, 2009).

The CCSB has been modified many times since 1938 in order to redistribute sediment settling patterns and increase sediment storage capacity. From 1991 to 1993, the Basin was radically altered. Surrounding levees were raised 12 feet, the training channel was relocated, and a new outlet weir was built 5 feet higher than the previous weir, representing the current conditions. At the time of alteration it was believed the Basin would retain 340 acre-feet of sediment per year, at a 55% trap efficiency, and that an additional 50 years of sediment storage was being provided. This postulated trap efficiency is based on an action plan outlined in the USACE 2007 Cache Creek Settling Basin Operations and Maintenance Manual, in which the outlet weir is to be raised an additional 6-feet at year 25 (2018) of the project, or when the trap-efficiency becomes 30%. Also beginning in year 25 of the project, 400-foot sections of the interior training levee will be removed every five years, starting with a section 1100 feet upstream from the current terminus of the training channel. Each subsequent 400-foot section will be removed 1100 feet upstream from the section that is removed previously.

In order to determine whether the trap-efficiency and sedimentation rate in the Basin are meeting design requirements set forth by USACE, the personnel at UC Davis J. Amorocho Hydraulics Laboratory (UCDJ AHL) began evaluating the settling basin trap efficiency through application of the National Center for Computational Hydroscience and Engineering's CCHE2D model of two-dimensional depth averaged flow and sediment transport. The evaluation was

conducted with respect to the current Settling Basin design as defined by 2006 and 2008 surveys of the Basin, utilizing field measurements of suspended sediment and flow into, within, and out of the Cache Creek Settling Basin as provided by USGS, as well as by the physical sedimentation modeling performed at the UCDJ AHL in 2009.

## **1.2 Objective**

The major objectives of this study are:

- i. to perform field measurements by UCDJ AHL staff of 2-D velocities and flow within the Settling Basin to be incorporated in calibration and validation of 2-D flow and sediment transport models. Because of the 2-D nature of flow in the basin and the desire to capture the 2-D spread of sediment within the basin, it is critical to capture internal transects, as well as inflow and outflow sections. Additionally, field measurements performed by UCDJ AHL staff will provide a dense sampling of flow and velocity during storm events, capturing multiple samples as a storm hydrograph passes through the Basin.
- ii. to incorporate flow and suspended sediment measurements provided by USGS in order to calibrate and validate the 2-D flow and sediment transport models. Currently available flow and sediment measurements are insufficient to support the simulations' claim of loading as they do not provide means of calculating loads into the basin, moving through the basin and exiting the basin. It is essential for calibration and validation of the models that these sediment measurements be concurrent with velocity/flow measurements. Additional data will ultimately result in a more reliable estimate of the settling basin trap efficiency with respect to current and future settling basin design.

Furthermore, UCDJ AHL will provide DWR with a method of reevaluating sedimentation for any further augmentation proposals. Estimates of trap efficiency will be produced for a range of possible future climate conditions. The mean trap efficiency as well as the 95% confidence bands will be provided.

## **2 FLOW SAMPLING BY UCDJ AHL**

In order to calibrate and validate the 2-dimensional flow and sediment conditions within the CCSB, a flow measurement campaign has been initiated by the UCDJ AHL. Dr. Ali Ercan and Dr. Kara Carr attended the formal USGS training course, "Streamflow Measurement using ADCP's in November 2013. A StreamPro ADCP with all necessary components and software, boat and boating equipment, trailer, and suitable laptop were purchased throughout the final quarter of 2013. Trial measurements utilizing the equipment necessary in the CCSB sampling campaign were conducted in December 2013. See Attachment A for pictures.

When flow is present in the CCSB, north of the low flow channel, flow velocity will be sampled. Sampling transect locations will be determined by flow and inundation conditions. The StreamPro ADCP will be used for measurement of flow velocity. A GPS mounted on the ADCP unit will allow for recognition of sampling locations and application of collected data to calibration and validation of the two-dimensional flow and sediment discharge model.

Due to the lack of weather, flow and sediment measurements in the CCSB have not been collected by UCDJ AHL at the time of this report.

## **3 TWO-DIMENSIONAL FLOW AND SEDIMENT TRANSPORT MODEL**

Two-dimensional modeling was selected for representation of the CCSB, as vertical velocities and accelerations are believed to be small when compared with the significant 2-D horizontal velocities and accelerations. Selection of a suitable two-dimensional flow and sediment transport model was completed after identifying factors that are crucial to the success of the trap efficiency estimation.

These factors include:

1. accurate representation of the Basin's training channel which has changed significantly since its construction due to deposition of sediment;
2. routing of flow and sediment from the output of the Cache Creek watershed study (Cache Creek at Yolo) to the inlet of the CCSB at Road 102;
3. calibration and validation of the two-dimensional model with well-timed and well-placed measurements of flow and sediment properties;
4. long term simulations that encompass the full range of flows historically observed in the Basin as well as future predictions which incorporate climatic uncertainty;
5. simulations of flow which represent the transience of both sediment loads and flows entering the CCSB.

### **3.1 CCHE2D**

Developed at the National Center for Computation Hydroscience and Engineering at the University of Mississippi (NCCHE), CCHE2D is a two-dimensional depth averaged unsteady flow and sediment transport model. CCHE2D simulates the movement of water, and both cohesive and non-cohesive sediment. Flow modeling is based on depth-averaged Navier-Stokes equations, while sediment transport is modeled as total load by solving the depth-averaged convection-diffusion equation of the suspended sediment load, and the continuity equation of bed load. The system of equations is discretized using the Efficient Element Method, a finite element method described by Wang and Hu (1992). Detailed description of the solution method can be found in the CCHE2D Technical Manual (Jia and Wang, 2001a). The model provides user options in the sediment transport description. Five sediment transport formulas are available; Wu et al. (2000) bed-load formula, Wu et al. (2000) bed-material load formula, Modified Ackers–White bed-material formula (Proffitt and Sutherland, 1983), Modified Engelund–Hansen bed-material load formula (Engelund and Hansen, 1967) and SEDTRA module (Garbrecht et al., 1995) for bed-material load. There are three methods for estimating Manning’s roughness coefficient; users defined value, movable bed roughness formula of Wu and Wang (1999) and that of Van Rijn (1996). The formulas can be applied to steady or unsteady flow boundary conditions. The developers at NCCHE state that the model is developed for application to the study of unsteady, turbulent, free surface open channel flow and sediment transport problems in channels with highly irregular topography (Jia and Wang, 2001b). CCHE2D is well suited to application to the CCSB for a number of reasons:

1. the model strictly enforces mass conservation, a property that leads to more reliable and accurate results.
2. the model is capable of representing transience in the flow and sediment boundary conditions for multiple inlets and outlets
3. wetting and drying of the simulated domain is represented
4. the model can simulate mixed flow, representing both subcritical and supercritical flow in a channel reach.
5. secondary flow in bends affects direction of bed shear and mean flow; the sediment module includes the curvature effects for enhanced representation of sediment transport in bends.
6. bed roughness is updated within the model as simulations progress, to account for the effect of sediment grain size and bed form on bed roughness.

### **3.2 Third-party Calibration and Validation**

Calibration and validation simulations performed by numerous authors reinforce the applicability of the CCHE2D model to the CCSB.

### 3.2.1 NCCHE Calibration and Validation

Model developers at NCCHE present a series of verification tests for flow and sediment transport in the technical report, *CCHE2D Verification and Validation Tests Documentation* (Jia and Wang, 2001b). The following examples, all referenced from the technical report, are based on cases of analytical solution, physical model data, and natural open channel flow.

Flow in a channel with sudden expansion was simulated with CCHE2D. Simulation results were compared to velocity measurements taken during physical experiments performed by Xie (1994). Experiments were conducted for two different flow magnitudes, in a concrete flume whose dimension and flow recirculation pattern are shown in Figure 3.1. Table 3.1 contains the physical and flow parameters for each of the two test cases. Velocity measurements were taken for each flow magnitude at 11 cross sections in the experimental flume. As is seen in Figure 3.2, measured and simulated velocities correspond well, and CCHE2D performs well simulating this complicated 2-dimensional flow field. At the end of the training channel, there is a sudden expansion to the Settling Basin, which makes this problem relevant to modeling of 2-dimensional flow in CCSB.

Table 3.1 Flow conditions for the sudden expansion channel experiments conducted by Xie (1994) and simulated by Jia and Wang, (2001b).

Discharge (m <sup>3</sup> /s)	Width (m)	Depth (m)	Step Height (m)	Slope	Approach Main Velocity (m/s)	Approach Froude Number	Recirculation Length (m)
0.01815	1.2	0.101	0.6	1/1000	0.30	0.30	4.60
0.03584	1.2	0.105	0.6	1/1000	0.60	0.60	4.60

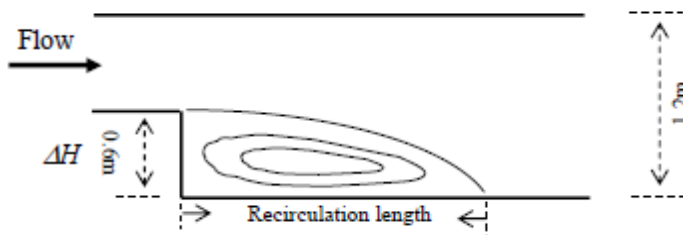


Figure 3.1. Flume dimension and recirculation pattern of Xie (1994) experiments (from Jia and Wang, 2001b)

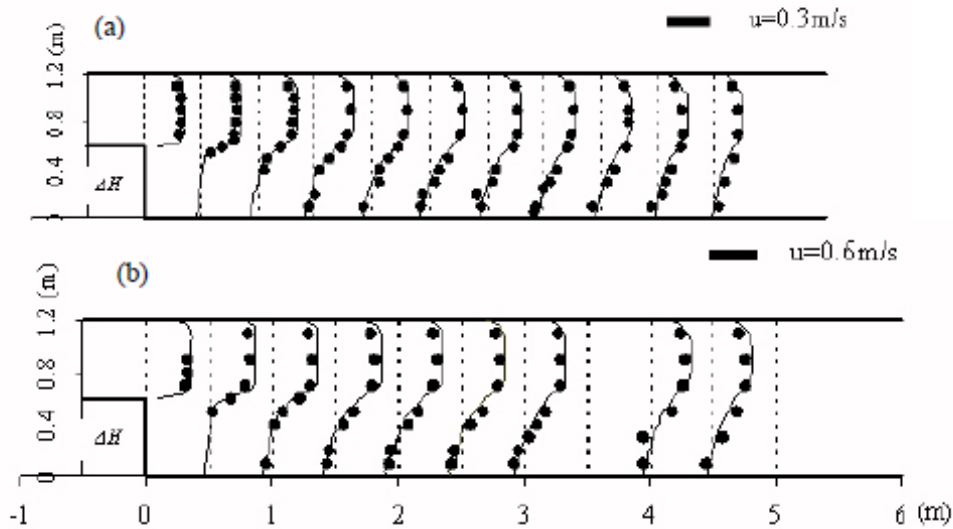


Figure 3.2 Comparisons of the simulated (line) and measured (circles) flow field in the channel of sudden expansion, a:  $Q=0.01815\text{m}^3/\text{s}$ , b:  $Q=0.03854\text{m}^3/\text{s}$  (Jia and Wang, 2001b)

Flow in a 180-degree U-shaped channel, representative of severe meander was also presented in the manual. The developers simulated physical experiments originally conducted by De Vriend (1979). Again, comparisons of detailed horizontal velocities were made at many cross sections along the simulated channel length. Flow and physical parameters are tabulated in Table 3.2, while the simulation mesh, and velocity comparisons are shown in Figure 3.3 and 3.4 respectively. Once more, the 2-dimensional flow field is well simulated as experimental and simulated water velocities match closely.

Table 3.2 Flow conditions for the 180-degree U-shaped channel, (from Jia and Wang, 2001b).

Discharge ( $\text{m}^3/\text{s}$ )	Width (m)	Depth (m)	Slope	Mean Velocity (m/s)	Reynolds Number	Froude Number
0.180	1.7	0.1953	0	0.542	1513	0.392

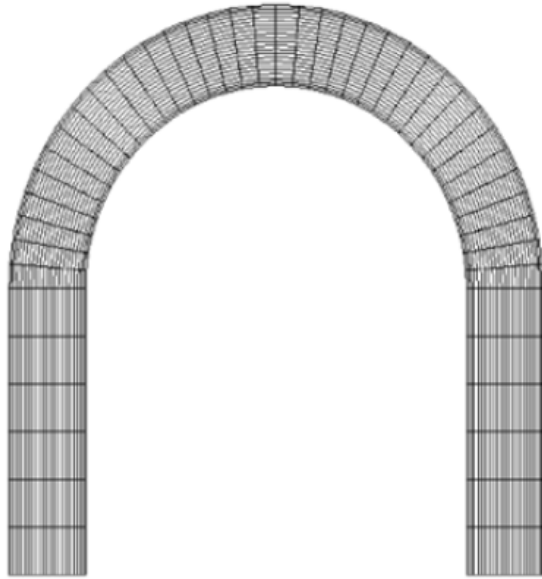


Figure 3.3 Mesh system of the 180-degree U-shaped channel (Jia and Wang, 2001b)

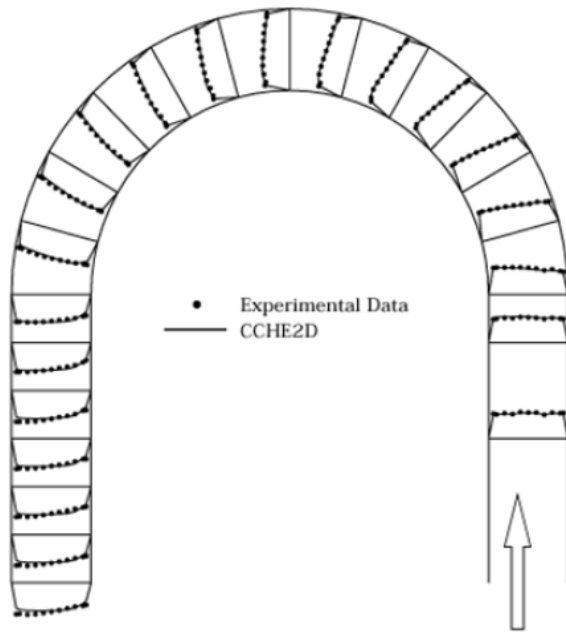


Figure 3.4 Simulated and measured velocities of the 180-degree U-shaped channel (Jia and Wang, 2001b)

The final verification of CCHE2D's flow modeling capability is highly applicable to the CCSB, as it compares flow field simulations of a compound channel to velocity measurements in an experimental flume. In this experimental case, there is a main flow channel with a flood plain on one side of the channel only. A definition sketch is shown in Figure 3.5. Experimental parameters of the physical experiment conducted by Rajaratnam and Ahmadi (1981) are shown in Table 3.3. Flow comparisons of the experimental measurements to three different

simulation results, which varied the eddy viscosity coefficient and boundary slip coefficient are presented in Figure 3.6. The results improve with adjustment of the boundary slip coefficient, and provide verification that the model performs well in representing flow fields in compound channels.

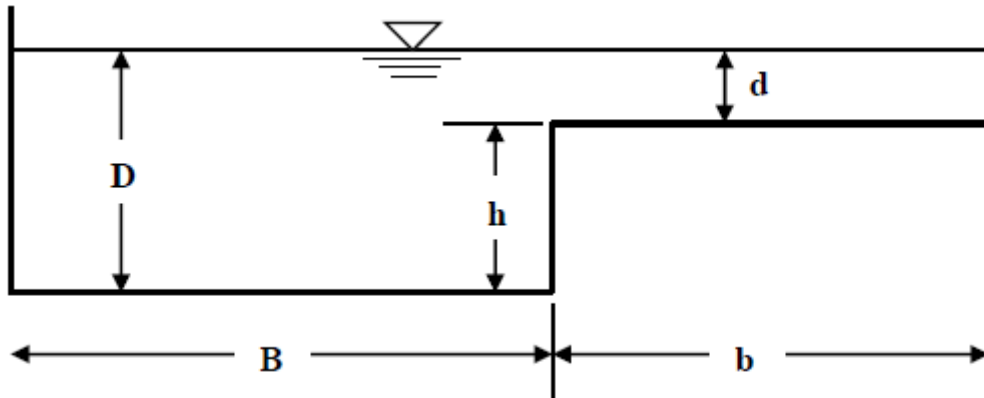


Figure 3.5 Definition sketch of the compound channel components (Jia and Wang, 2001b)

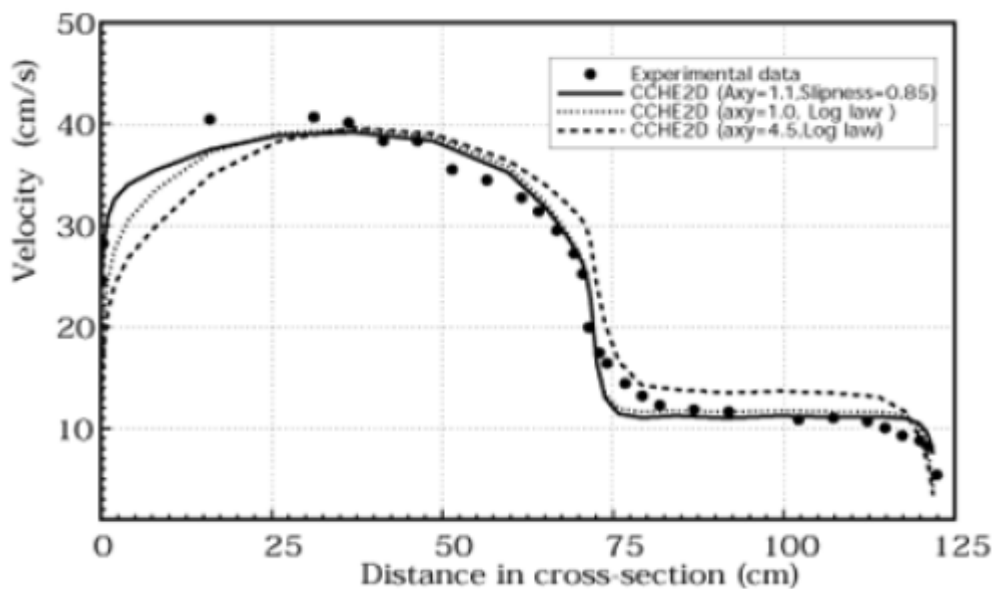


Figure 3.6 Comparison of measured and simulated velocity in a compound channel (Jia and Wang, 2001b)

Table 3.3 Parameters of the compound channel experiment (Jia and Wang, 2001b).

D (cm)	d (cm)	h (cm)	B (cm)	b (cm)	Discharge (m <sup>3</sup> /s)
11.28	1.52	9.75	71.1	50.8	0.027

Sediment transport verification was presented in the manual for cases of bed aggradation and degradation by comparing simulation results to flume experiment results, and suspended sediment transport in a meandering river was simulated and compared to field measurements in the River Nechar, in Germany.

A flume experiment of channel aggradation conducted by Soni (1981) was simulated based on the flow and sediment conditions given in Table 3.4. Results of the simulation and experiment are presented in Figure 3.7, in which bed elevation is presented at thirty-minute intervals through the experiment. The trend of bed elevation increasing with time is clear and the agreement between simulated and experimental values is clear.

Table 3.4 Sediment and initial flow conditions, bed aggradation experiment performed by Soni (1981) (from Jia and Wang, 2001b).

Unit Discharge (m <sup>2</sup> /s)	Mean velocity (m/s)	d <sub>50</sub> (m)	Bed Roughness (m)	Depth (m)	Bed Slope	Froude Number
0.0355	0.493	0.0003	0.022	0.072	0.00427	0.34

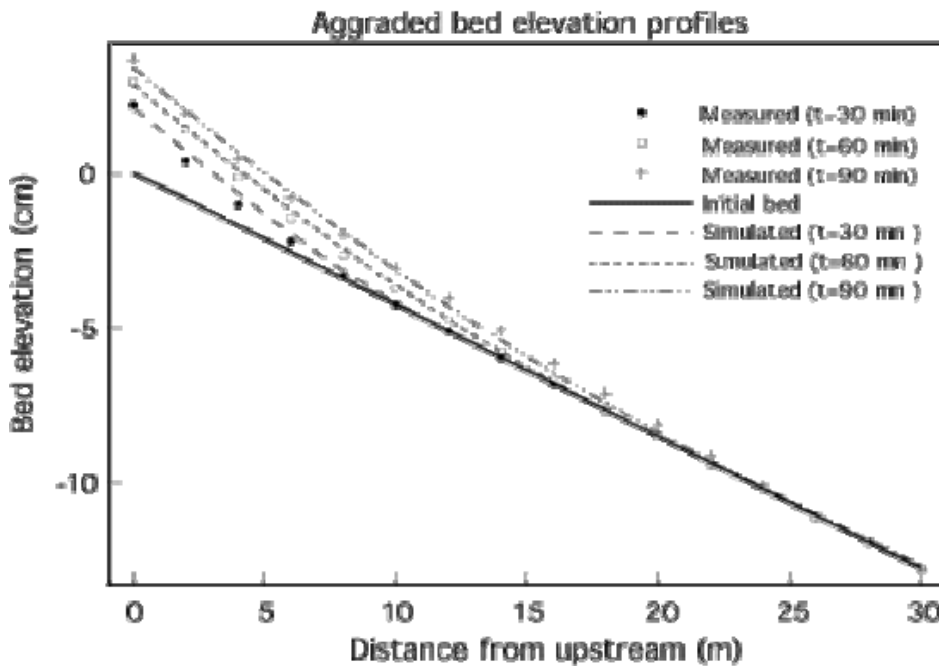


Figure 3.7 Comparison of measured and simulated bed elevations, bed aggradation experiment (Jia and Wang, 2001b)

A flume experiment of bed degradation conducted by Newton (1951) was simulated, based on the conditions given in Table 3.5. The simulations for bed degradation were conducted using the Van Rijn bed roughness model, one of the two bed roughness models applicable in the CCHE2D model. Additionally, the non-equilibrium sediment transport relationship selected for application in this case is the Bell-Sutherland relation. These selections are described in more detail in Jia and Wang (2001a). The bed degradation results for the experiment and simulation are compared in Figure 3.8. Experimental bed elevation was measured every hour through a 24-hour experiment, and simulated results are plotted to compare to reported experiment results at  $t = 1, 2, 3, 4, 5$  and 24 hours.

Table 3.5 Sediment and initial flow conditions, bed degradation experiment performed by Newton (1951) (from Jia and Wang, 2001b).

Unit Discharge (m <sup>3</sup> /s)	Mean Velocity (m/s)	d <sub>50</sub> (m)	Bed Roughness (m)	Bed Slope	Froude Number
0.0185	0.45	0.00069	0.041	0.00416	0.50

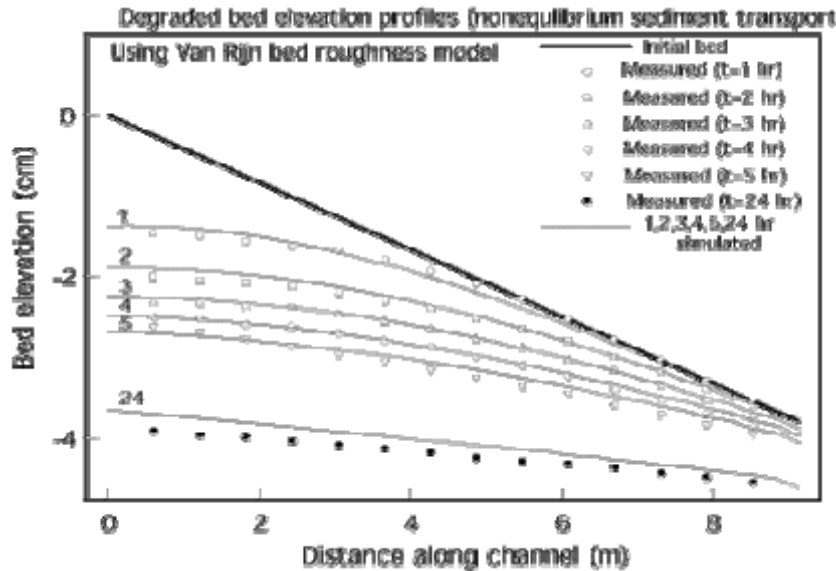


Figure 3.8 Comparison of experimental and simulated results, bed degradation experiment (Jia and Wang, 2001b)

The River Nechar, in Germany is a natural river channel with a complicated geometry consisting of sharp bends and wider flood plains. Suspended sediment concentration was measured by Xu et al. (2001) along several cross sections of the natural river, and compared to CCHE2D unsteady flow and sediment simulations of the river system performed by the model developers. Figure 3.9(a) provides a contour plot of suspended sediment concentration for the simulated system. The solid blue areas represent the flood plains, and the cross sections used for comparison are marked in the figure. Comparisons of the suspended sediment concentrations are shown in Figure 3.9(b). Correspondence of measured and computed sediment concentration is similar in each cross section, regardless of distance from the inlet boundary, and along each cross section regardless of the distance from the bank. CCHE2D predicts the suspended sediment concentration well in both the lateral and longitudinal directions.

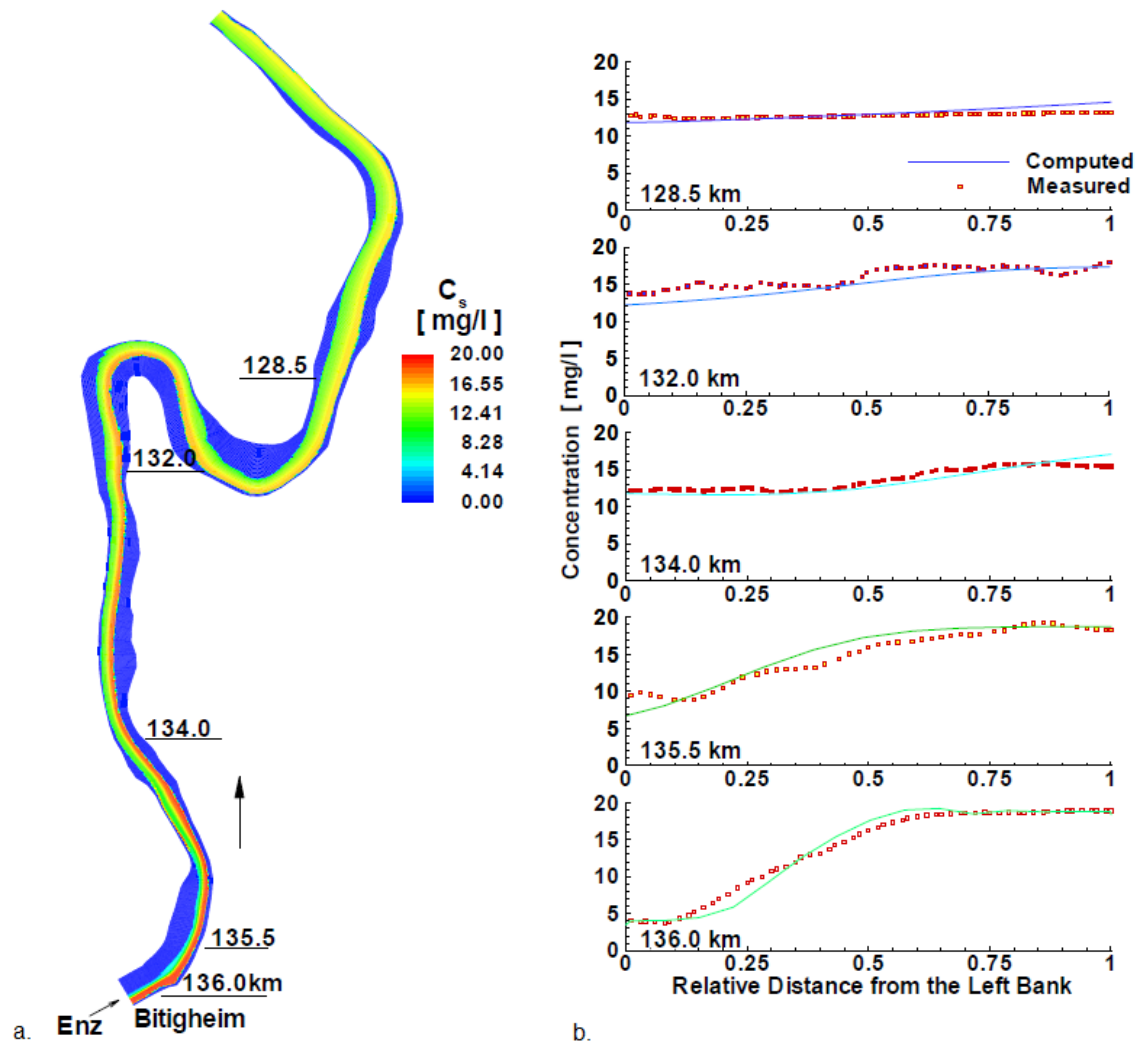


Figure 3.9. Suspended sediment verification results, River Nechar, Germany: a. sediment concentration contour plot; b. comparison of measured and computed sediment concentrations (Jia and Wang, 2001b)

### 3.2.2 Non-Principal Calibration and Validation

A number of investigations have been performed by parties unaffiliated with the development of CCHE2D to verify use of CCHE2D as a 2-dimensional flow and sediment transport model. A select group is presented here as their findings support the application of CCHE2D to the CCSB.

Kantoush et al. (2008) studied the influence of reservoir geometry on flow pattern and sedimentation, focusing on shallow rectangular reservoirs. The authors aimed to compare the abilities of ultrasonic doppler velocity profilers (UVP), large-scale particle image velocimetry (LSPIV), and numerical simulation by CCHE2D to create a 2-dimensional flow field representation. They conducted lab experiments in which detailed velocity measurements were taken to map the flow field in a shallow reservoir model. Although the study involved

sedimentation patterns, the authors did not present results comparing sediment transport in the model with simulations using CCHE2D. The experiments involved low flow velocities and reservoir geometry that created recirculation and eddies in the reservoir interior, as is expected in portions of the CCSB. Comparison of velocity maps produced from UVP, LSPIV, and CCHE2D are presented in Figure 3.10. CCHE2D can represent the recirculating flow pattern measured and created in the experimental reservoir.

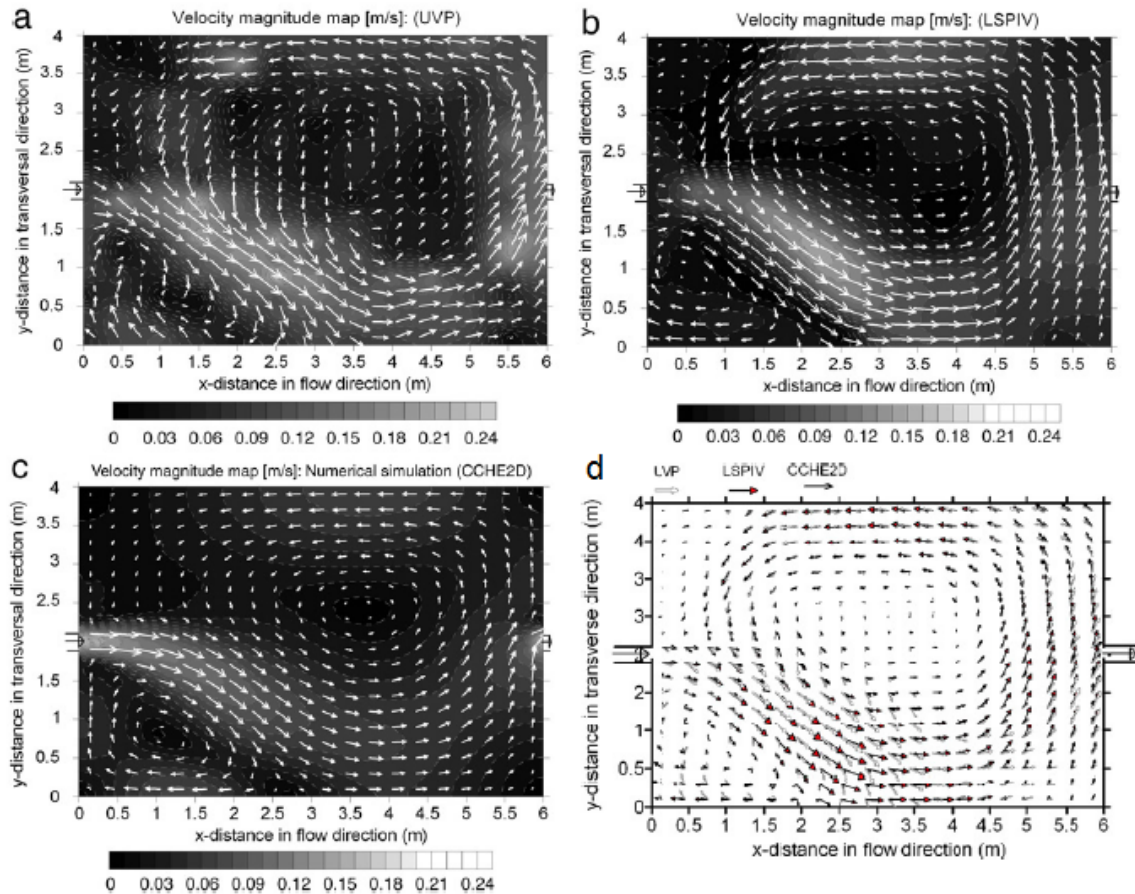


Figure 3.10 Flow field from (a) UVP (b) LSPIV (c) CCHE2D and (d) comparison of velocity magnitude vectors obtained from all three methods

Mohanty et al. (2012) conducted a study to investigate flow in a wide meandering compound channel. Physical experiments were conducted using a sinusoidal river with trapezoidal main channel and wide flood plains on either bank (Figure 3.11). Five experimental runs were conducted with different discharge magnitudes and overbank depths as tabulated in Table 3.6. Experimental values of velocity and boundary shear distribution for each run were then compared to CCHE2D simulation results, and Conveyance estimation System model results for each of the five experiments. Simulated results of normalized velocity are shown in Figure 3.12. CCHE2D measurements agree so well with the experimental measurements, the two are difficult to distinguish in the figure. Comparisons of shear stress are displayed in Figure 3.13, and again the match

between CCHE2D results and measured values is quite good. The authors conclude that CCHE2D is a "viable research tool in the field of river engineering".

Table 3.6 Hydraulic parameters for the experimental runs, meandering compound channel (Mohanty et al., 2006).

Sl. no. of Runs	*Discharge Q in lit/s	Overbank depth H in cm	Relative depth $\beta(H-h/H)$	Froude no.(Fr)	Reynolds no.(R)
1	17.074	8.06	0.19354839	0.2199681	19681.77
2	27.617	8.55	0.23976608	0.28274994	27641
3	47.245	9.5	0.31578947	0.33944679	38865.04
4	70.338	10.2	0.3627451	0.40923323	52128.25
5	93.667	11	0.40909091	0.4432553	63233.17

\*--Discharges as per measured from contour diagram

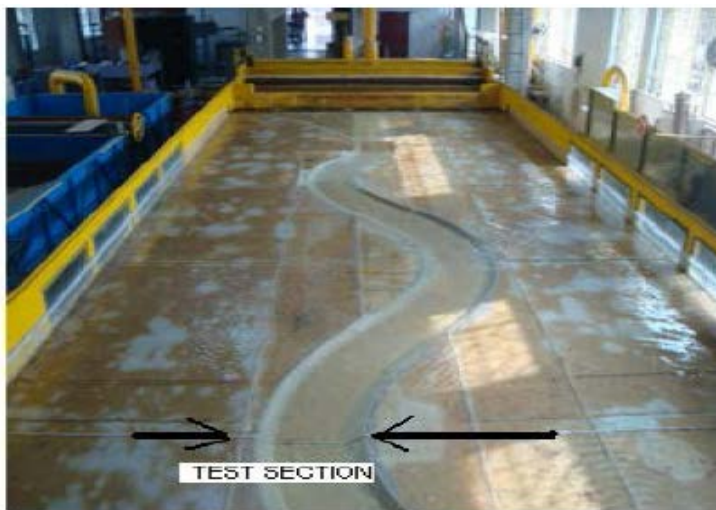


Figure 3.11 Experimental set-up for meandering compound channel Mohanty et al. (2012)

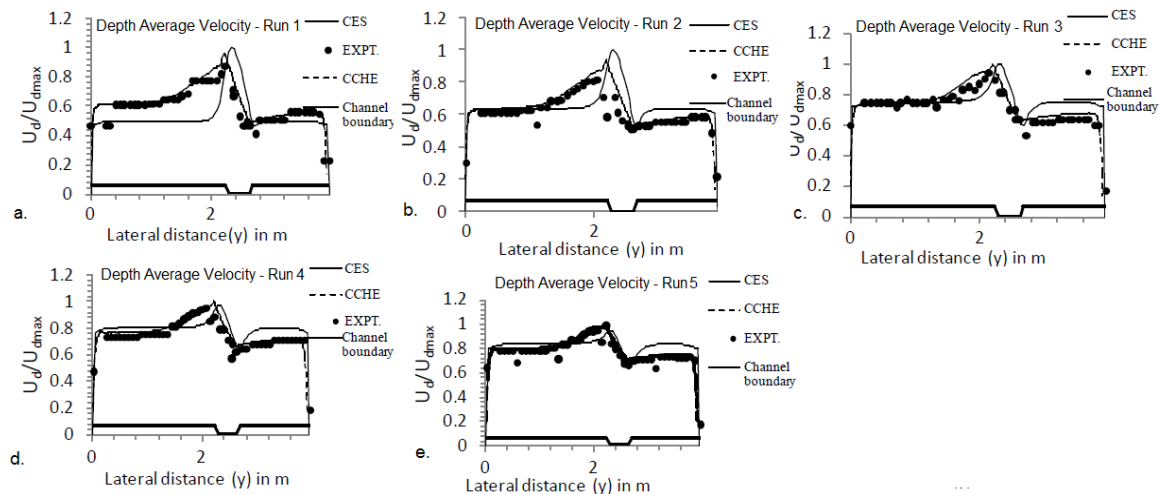


Figure 3.12 Normalized depth averaged velocity diagrams for each of the five runs (a) Run 1 (b) Run 2 (c) Run 3 (d) Run 4 (e) Run 5 (Mohanty et al., 2012)

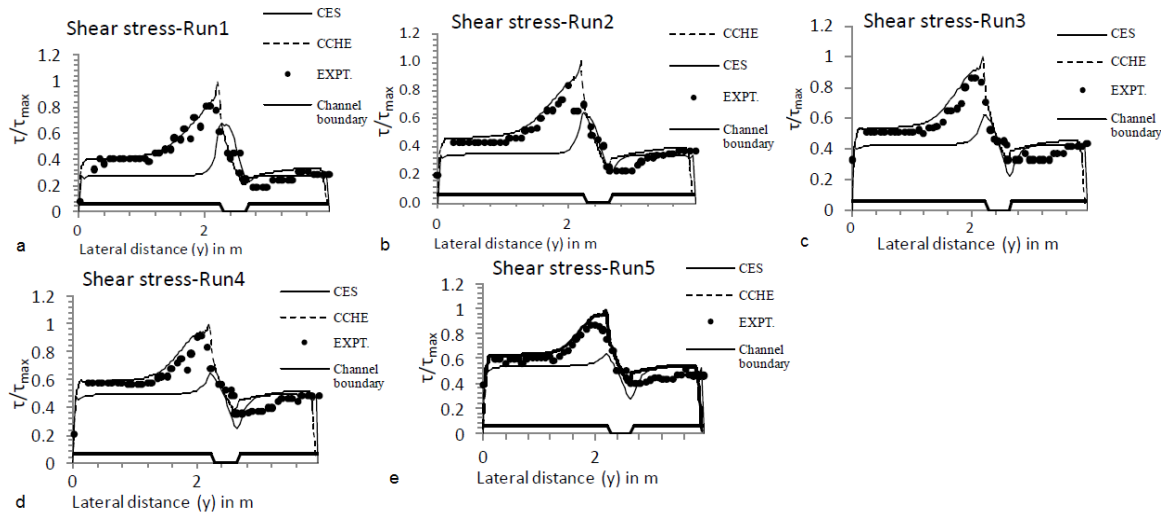


Figure 3.13 Shear velocity diagrams for each of the five runs (a) Run 1 (b) Run 2 (c) Run 3 (d) Run 4 (e) Run 5, (Mohanty et al., 2012)

Investigations into the capability of CCHE2D to represent sediment transport, erosion and deposition have been undertaken as well. Huang (2007) is an example of the complexities of sediment transport modeling. The author investigated the effects of the five different sediment transport formulae; Wu et al. (2000) bed-load formula, Wu et al. (2000) bed-material load formula, Modified Ackers–White bed-material formula, Modified Engelund–Hansen bed-material load formula and SEDTRA module for bed-material load, and the three methods for estimating Manning’s roughness coefficient: users defined value, movable bed roughness formula of Wu and Wang (1999) and that of Van Rijn (1996), which are available in CCHE2D for both steady and unsteady flow boundary conditions. As the results for unsteady flow conditions are relevant to the work presented herein, they alone are presented. Figure 3.14 contains plots comparing experimentally measured bed degradation data to the simulation results for the 15 possible combinations. The author concludes that not only is a moveable bed roughness formula needed in sediment transport modeling, but that testing of the transport formulae is significantly needed in order to find the best formula for each application.

Negm et al. (2010) utilized CCHE2D to study the scouring and silting processes in the Sudanese portion of the High Aswan Dam Reservoir in an effort to determine the reservoir's life span. Their CCHE2D representation of the reservoir was calibrated and verified with field data, and applied to predict cross sections along the reservoir for 2010, 2020, 2030 and 2040. Calibration results for bed level prediction of two cross sections are displayed in Figure 3.15. Verification results for bed level prediction of two cross sections are displayed in Figure 3.16. The verification results are a good fit to measured bed elevation, as can be seen in Figure 3.17. The plot shows a 1:1 correspondence line, with model data plotted versus measured data in which a perfect fit would lay directly on the 1:1 line. Divergence in measured and modeled results is small enough for

the authors to conclude that CCHE2D can be used as a long-term predictor of bed elevation change, and ultimately reservoir life time span.

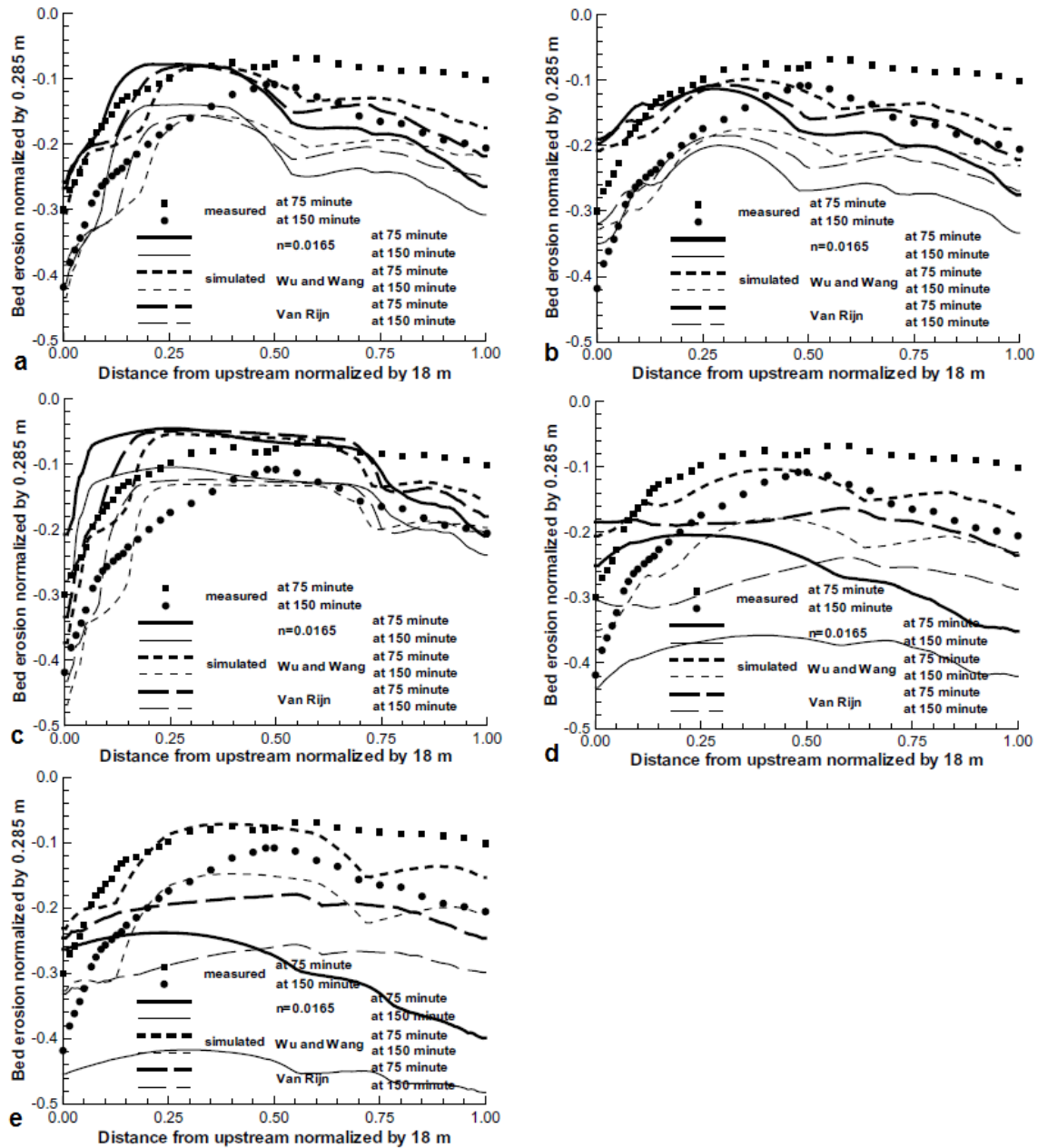


Figure 3.14 Huang (2000) Channel degradation comparison, utilizing each bed roughness method for (a) Wu et al. (2000) bed-load formula, (b) Wu et al. (2000) bed-material load formula, (c) Modified Ackers–White bed-material formula, (d) Modified Engelund–Hansen bed-material load formula and (e) SEDTRA module

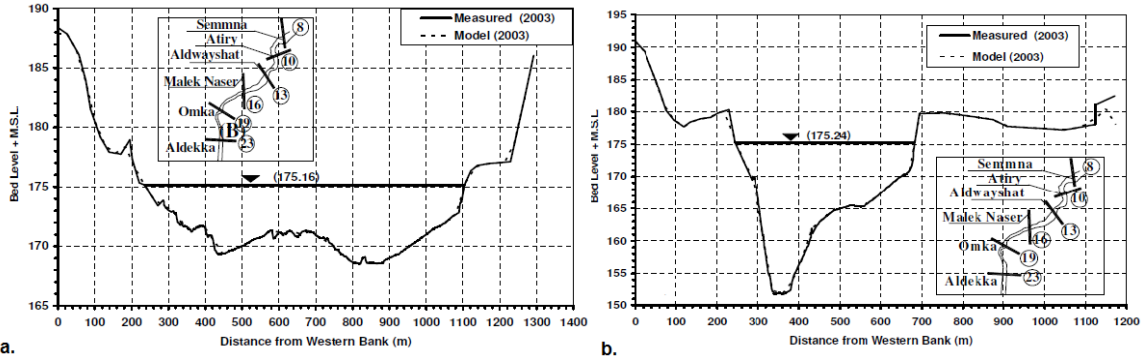


Figure 3.15 Calibration results for cross section bed level in 2003 (a) section 13 and (b) section 16 (Negm et al., 2010)

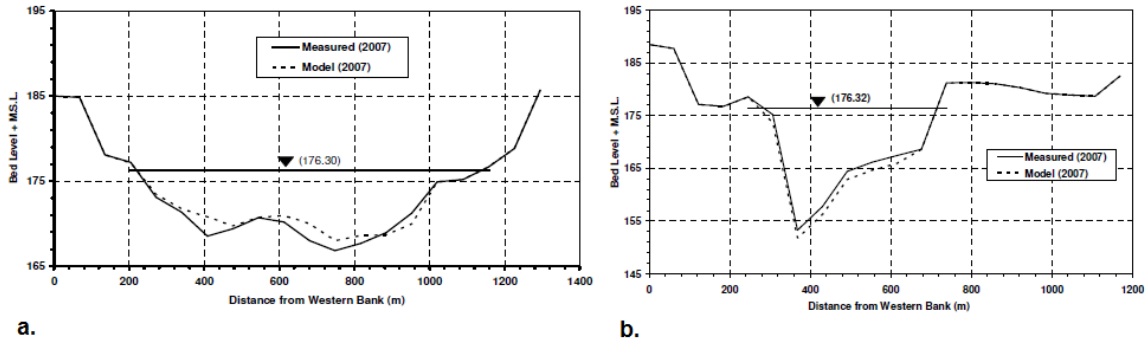


Figure 3.16 Verification results for cross section bed level in 2007 (a) section 13 and (b) section 16 (Negm et al., 2010)

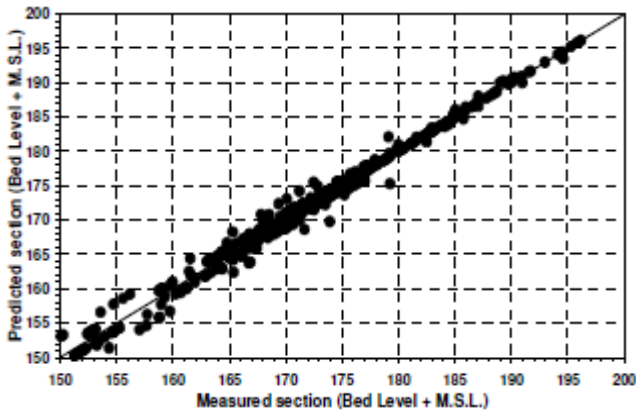


Figure 3.17 Predicted bed elevation for sections 13 and 16 plotted against corresponding measured bed elevation (Negm et al., 2010)

#### 4 CCHE2D FLOW SIMULATIONS

Numerical simulations of the river and basin from Cache Creek at Yolo to the outlets of the CCSB were initiated, calibrated and validated for observed flows up to 15,000 cfs. Mesh generation is the initial step in simulating flow and sediment transport, and is an integral and time consuming component of successful numerical simulation. In order to adequately describe the topography, and accurately represent the hydrodynamics of the CCSB a dense mesh was created, which optimized accuracy without sacrificing computational time required for each simulation. It is not realistic to use Road 102 as the upstream boundary condition for the CCSB simulations as there is limited flow data.

Therefore, the simulation area of the CCHE Settling Basin model was extended to include Cache Creek at Yolo where there exists a long-standing 15-minute flow record. Moreover, a considerable number of sediment measurements with concurrent flow measurements are also available at Cache Creek at Yolo. The simulation mesh of the extent from Cache Creek at Yolo to Rd 102 is shown in Figure 4.1. The simulation mesh for the CCSB is shown in Figure 4.2. The computational domain is composed of about 15,400 computational nodes from Cache Creek at Yolo to Road 102 and about 60,013 computational nodes from Road 102 to overflow weir. The total number of nodes is more than 75,000 for the entire computational domain. The complex bathymetry and the flow dynamics in the training channel and in the Settling Basin make it necessary to have such dense computational nodes. The mesh is sufficiently dense that visualization of the full extent is difficult, and a magnified region is shown in each figure. Corresponding elevation contours for the extent from Yolo to Rd 102, and the CCSB are shown in Figures 4.3 and 4.4 respectively. Figure 4.4 also contains approximate locations of the measurement stations used for calibration and validation of simulation results.

The simulations utilized inflow boundary data taken from instantaneous flow data at the Cache Creek at Yolo gauge (source: <http://nwis.waterdata.usgs.gov>, USGS 11452500) from March 18, 2011 through March 22, 2011. The simulations also utilized rating table boundary conditions at the overflow weir, as provided by USGS (Brazelton, W. 2010 "Rating Curve for Cache Creek Settling Basin Weir") and at the outlet culvert box of the low flow channel (source: <http://nwis.waterdata.usgs.gov>, USGS 11452900). The rating curve for the overflow weir is shown in Figure 4.5, and the rating curve for the low flow culvert is shown in Figure 4.6.

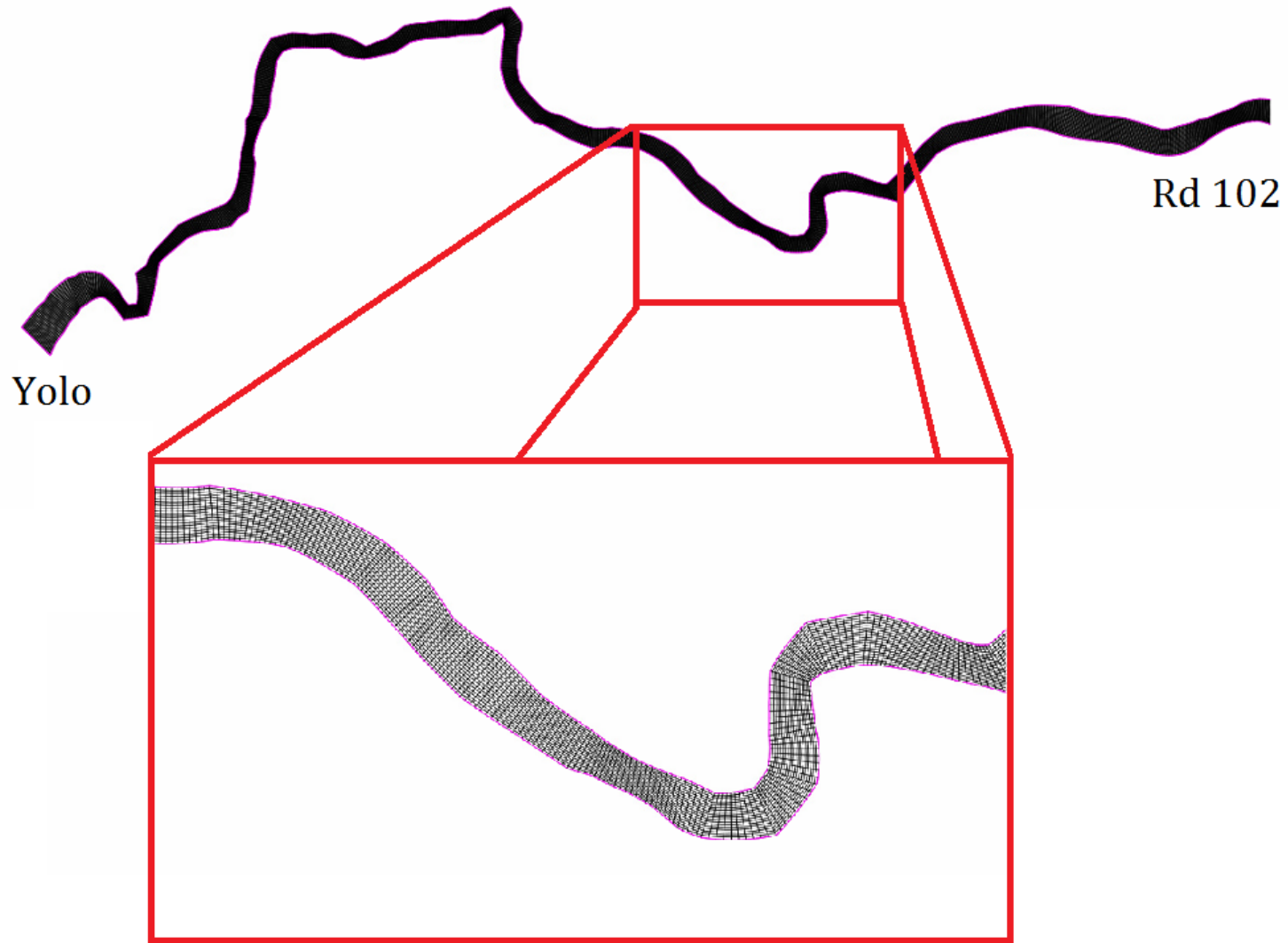


Figure 4.1 Mesh from Cache Creek at Yolo to Road 102

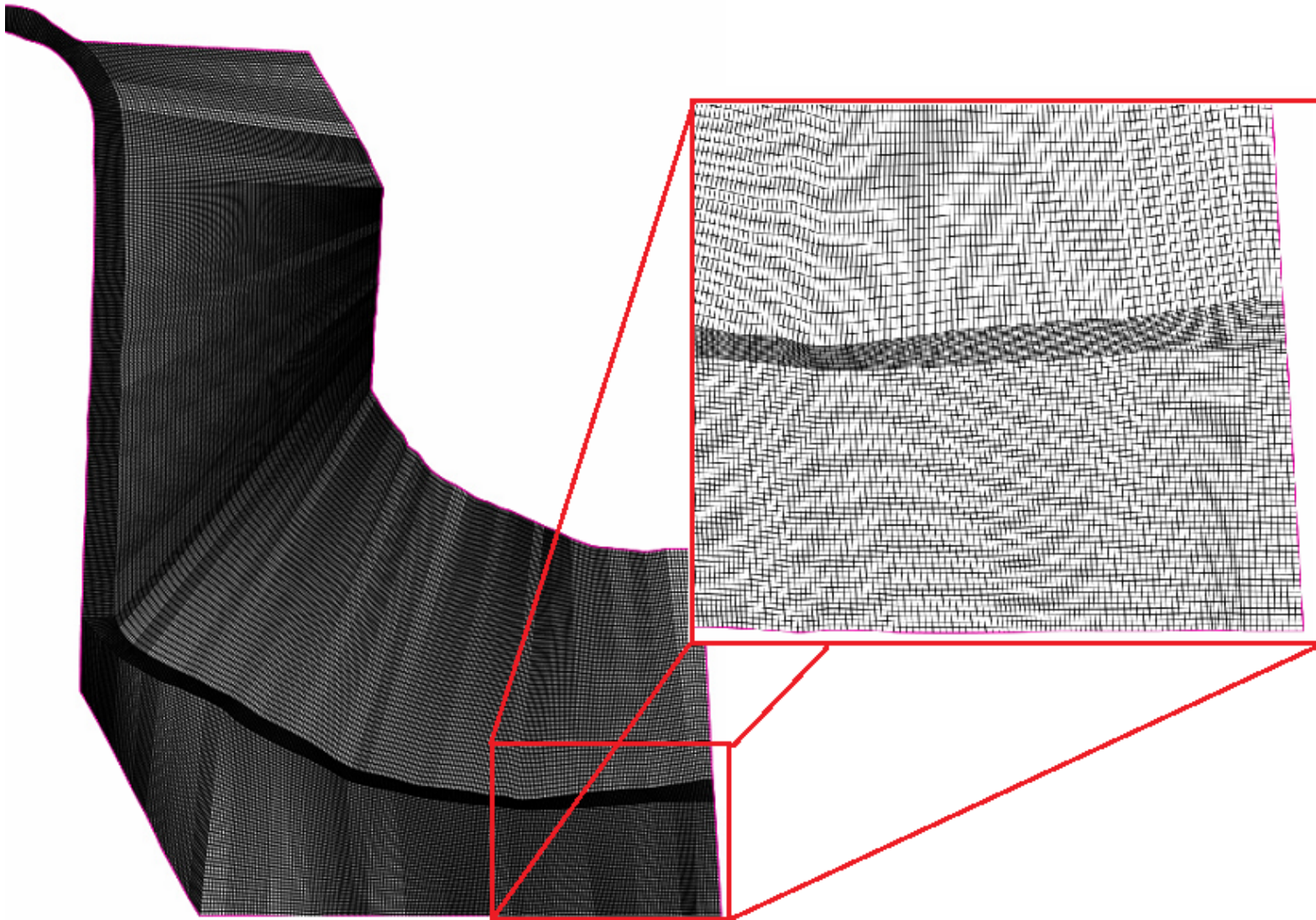


Figure 4.2 Simulation Mesh for CCSB



Figure 4.3 Elevation contour of simulated extent from Cache Creek at Yolo to Rd 102

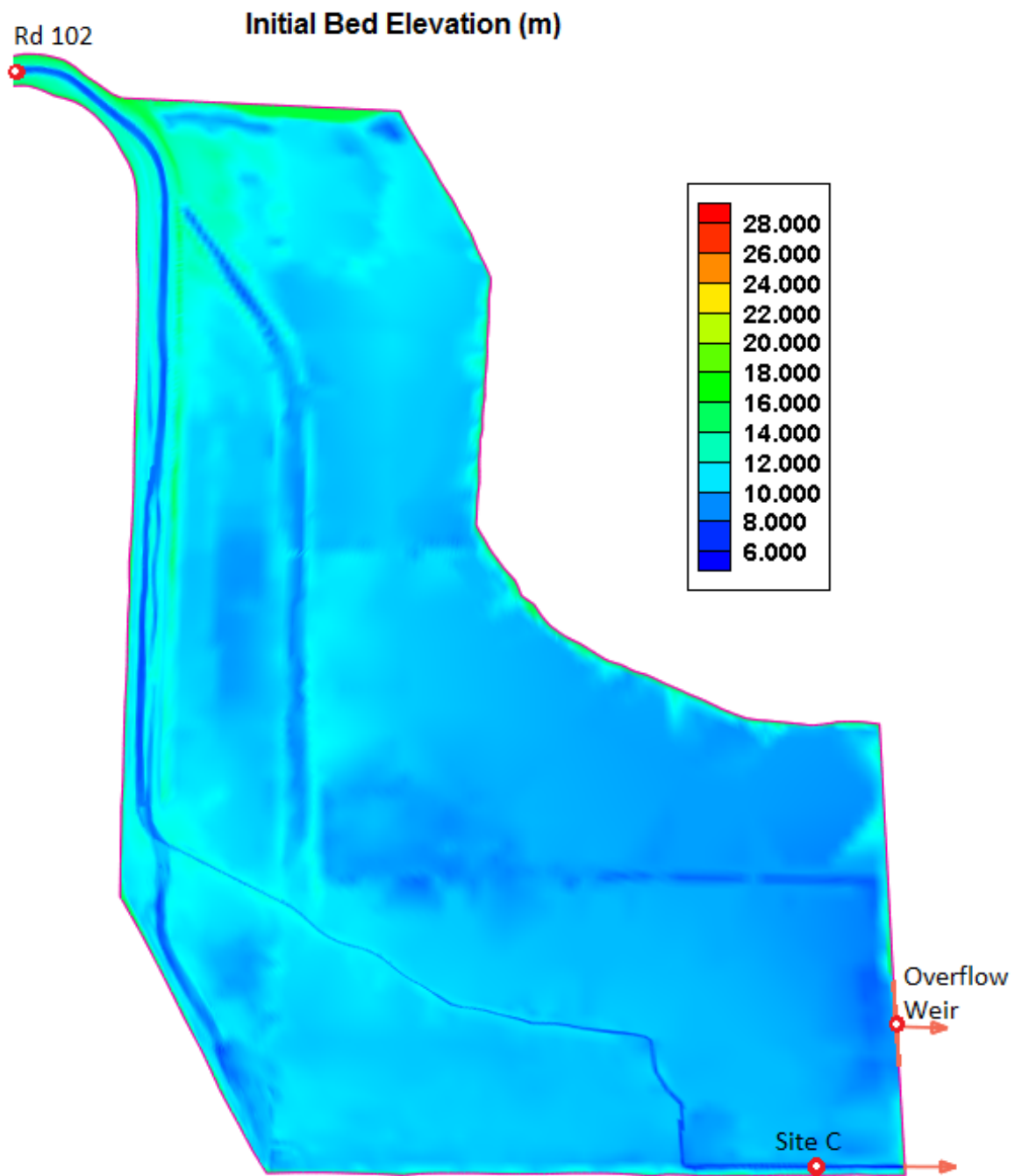


Figure 4.4 Elevation contour of simulated extent, Rd 102 through CCSB including approximate locations of result comparison points

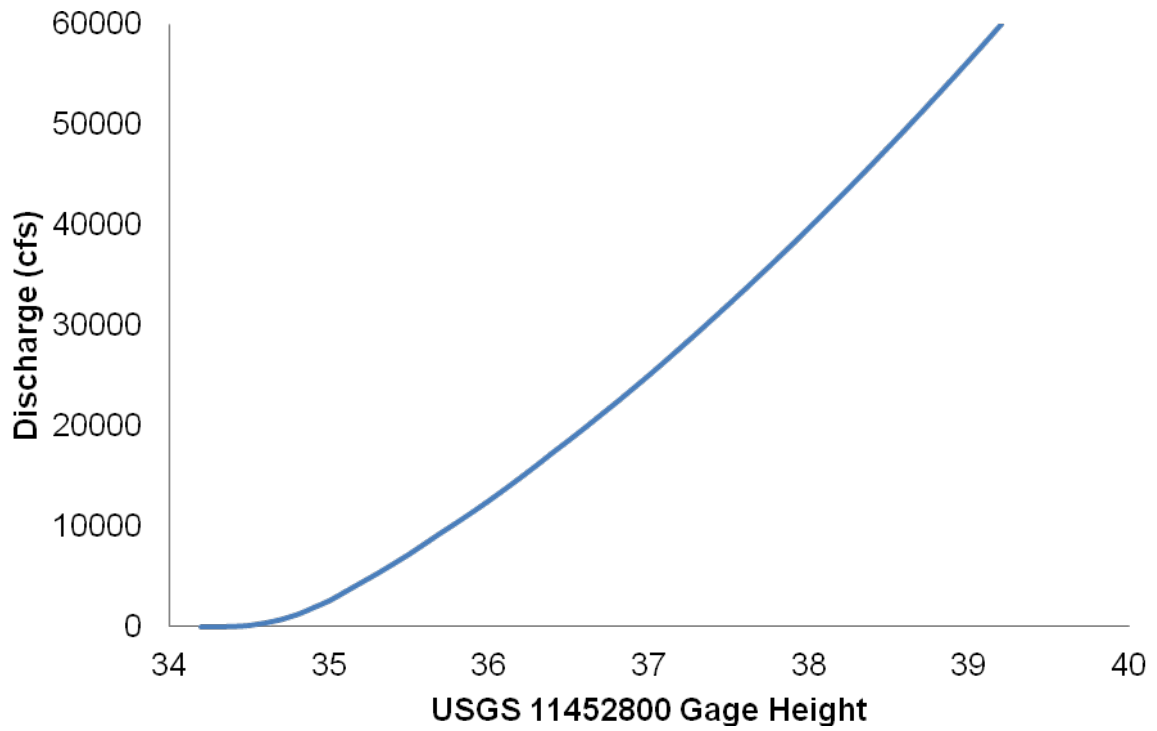


Figure 4.5 Rating curve for the USGS site 11452800, CCSB overflow weir.

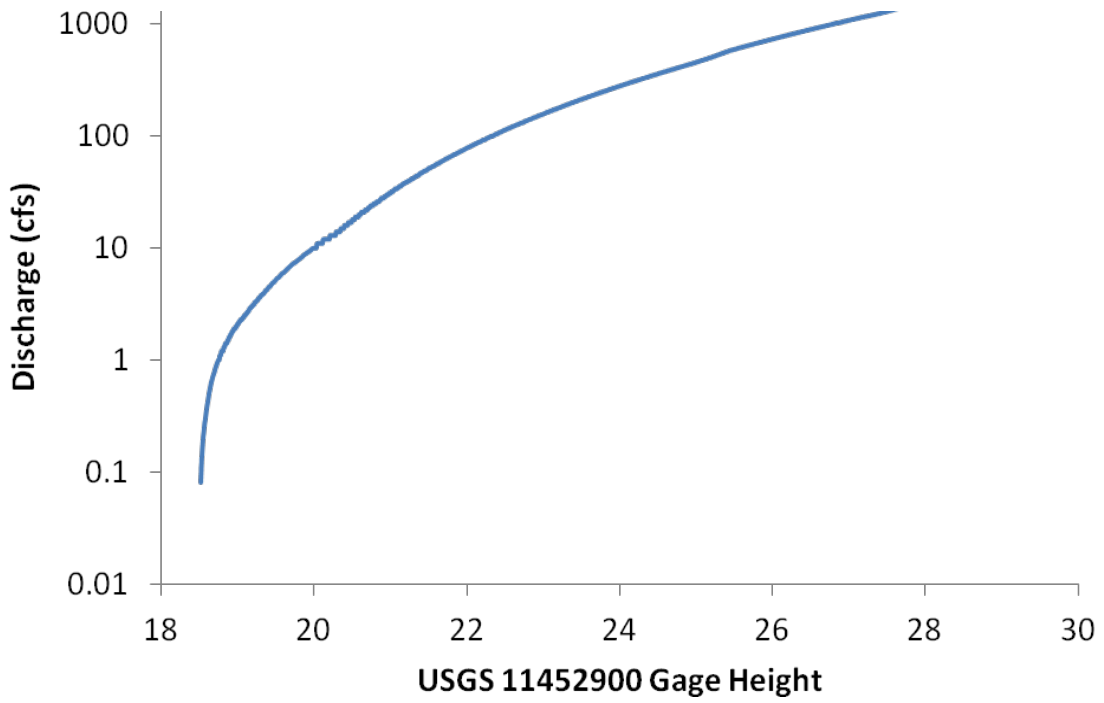


Figure 4.6 Rating curve for USGS site 11452900, CCSB low flow culvert.

#### 4.1.1 Calibration by 18-22 March 2011 event at Road 102

Correct specification of parameters such as; time step, turbulence model, wall slipiness, bed roughness and bed sediment grain size are essential to accurate representation of field conditions. CCHE2D requires that bed grain size distribution be defined by specifying the D16, D50 and D90 sediment sizes. As noted previously, the model also allows either user specified bed roughness, or to select one of two bed roughness formulae (Wu and Wang, 1999 and van Rijn 1986) which calculate roughness as a function of the grain size distribution.

Sensitivity analyses were performed to determine what bed roughness method and sediment grain size distribution should be applied when simulating the CCSB. Simulations were run for each of the two bed roughness formulae, and different specified values of bed roughness. Results of the simulations at Rd 102 were compared to measured water surface elevation values provided by USGS (B. Brazelton, personal communication, November 4, 2011). Water surface elevation results at Rd 102 for various bed roughness methods are presented in Figure 4.7, along with the USGS data. Figure 4.7 also contains a plot of the percent error for each bed roughness method. The Wu and Wang (1999) solution of bed roughness has been selected for application to the CCSB as it provides the highest level of agreement between the simulated and measured water data. Using a constant roughness value for all flow conditions is not realistic for the Settling Basin's dynamic flow conditions. Moreover, bed elevation is changing due to deposition and erosion in the Settling Basin. The roughness formula of Wu and Wang (1999) considers flow and bed elevation change and utilizes a more realistic roughness value considering the Froude number at each grid node.

Once identified as the most suitable bed roughness method, the Wu and Wang (1999) formula was tested with three different grain size specifications, to identify sensitivity to grain size and to calibrate model roughness. The three different distributions of grain size, denoted A, B and C, are presented in Table 4.1. Simulation results of water surface elevation at Rd 102 corresponding to these parameters are plotted in Figure 4.8, along with the measured data. The percent error for simulation results for each of the grain size distributions is also plotted in Figure 4.8, and it can be observed that distribution B performs the best.

Table 4.1 Grain size distributions applied with Wu and Wang (1999) roughness simulations.

	Grain Size Distribution		
	A	B	C
D16 (mm)	0.127	0.254	1.270
D50 (mm)	0.286	0.572	2.861
D90 (mm)	2.293	4.585	22.926

The normalized root mean square errors for the best performance trials of each bed roughness method are tabulated in Table 4.2. The normalized root mean

square error  $\left( \text{NRMSE} = \sqrt{\frac{\sum_{i=1}^n (x_{1,i} - x_{2,i})^2}{n (x_{1,\max} - x_{1,\min})^2}} \right)$ , where  $x_1$  are the measured values,  $x_2$

are the modeled values, and  $n$  is the number of time steps evaluated, is used to aid in comparison of each case. Its value indicates the level of agreement between the measured and modeled values. The lower the NRMSE, the less variance there exists in the difference of the model and measured values over all time steps.

The CCHE model utilizing Wu and Wang (1999) bed roughness method with grain size distribution B in Table 4.1 is selected as the best solution through the calibration process, and is validated for 18-22 March 2011 flow event by observed water elevations at site C and overflow weir. Moreover, the entire CCHE model of CCSB is validated for 23-27 March 2011 flow event by the observed water elevations at three locations: Road 102, site C and overflow weir.

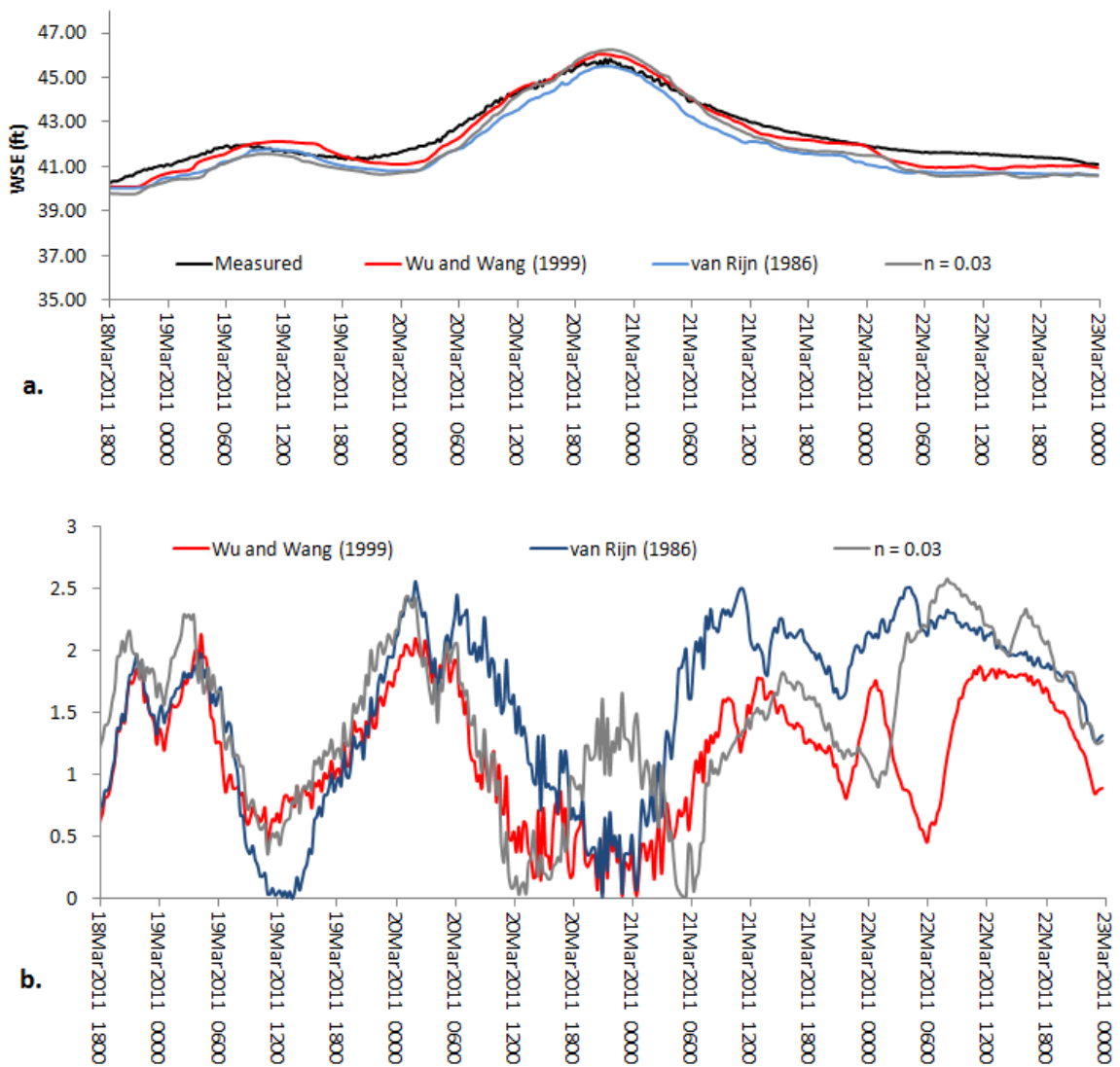


Figure 4.7 (a) Results of CCHE2D water surface elevation at Rd 102 for various bed roughness and measured water surface elevation at Rd 102, and (b) percent error of simulated water surface elevations for various bed roughness methods

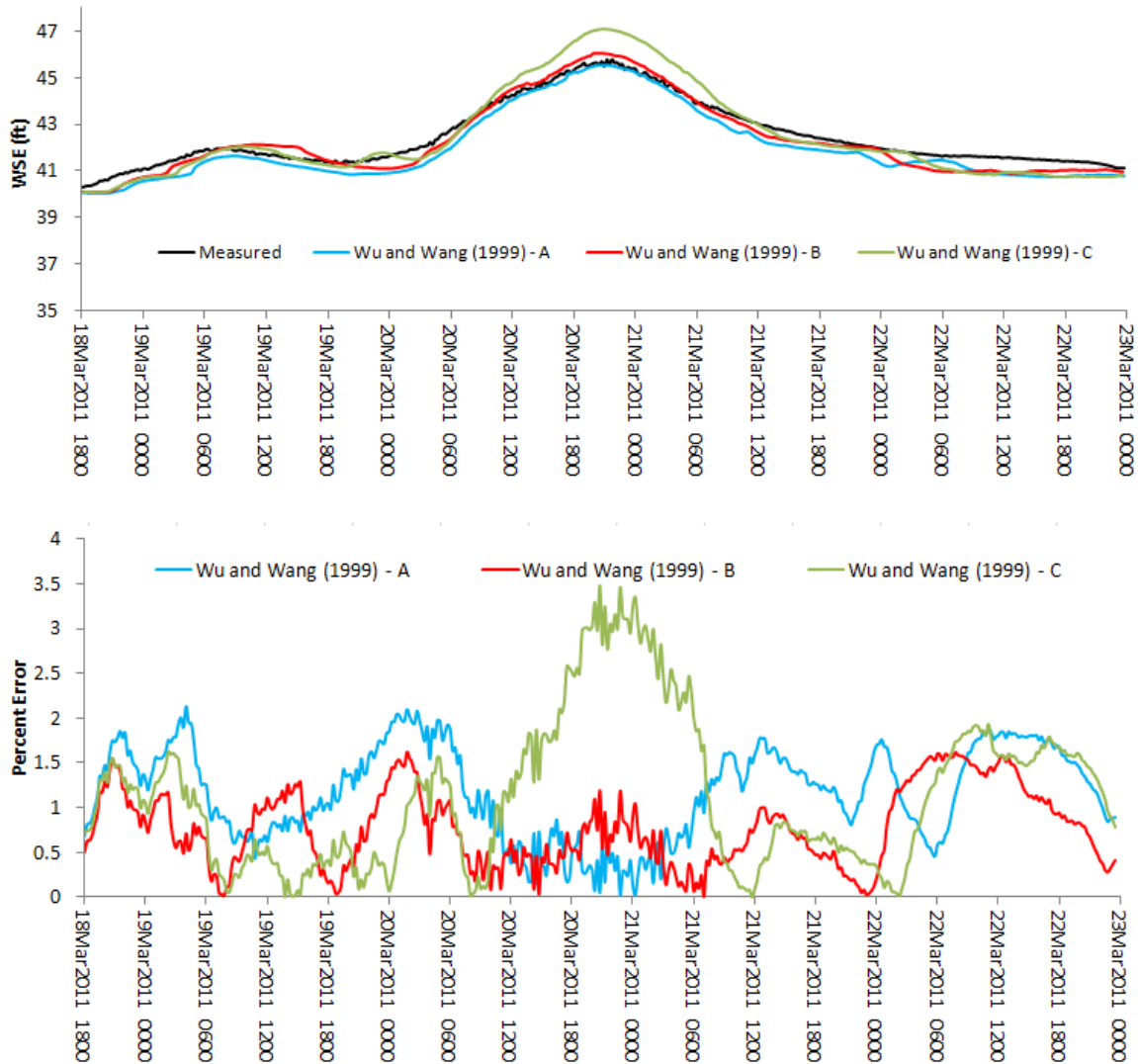


Figure 4.8 (a) Results of CCHE2D water surface elevation at Rd 102 for various grain size distributions, (b) percent error of simulated water surface elevations at Rd 102 for various grain size distributions

Table 4.2 Normalized root mean square error for simulated water surface elevations at Rd 102 for each bed roughness method

	Wu and Wang (1999)	van Rijn (1986)	n = 0.03
NRMSE	0.07	0.13	0.12

#### 4.1.2 Validation by 18-22 March 2011 flow event inside CCSB

After calibration of the roughness formula by observed water elevations at Road 102 for 18-22 March 2011 event, simulated water elevations at the overflow weir and at site C are validated by the observed counterparts.

For 18-22 March 2011 event validation inside CCSB, inlet boundary flow data was taken from instantaneous flow data at the Cache Creek at Yolo gauge (source: <http://nwis.waterdata.usgs.gov>, USGS 11452500) which provides 15-minute flow data. The validation simulation ran from March 18, 2011 16:45 through March 22, 2011 20:45 and had a maximum discharge of 15900 cfs (exceedance probability 41.4-percent). Simulation results are plotted in Figure 4.9 along with water surface elevation data provided by USGS (B. Brazelton, personal communication, November, 4, 2011) at Road 102, Site C in the interior of the CCSB, and at the overflow weir. The inflow boundary flow hydrograph is also provided in Figure 4.9. There is good agreement between the water surface elevation simulated by CCHE2D and the measured data provided by USGS for each of the validation points: Rd 102, site C, and the overflow weir. The locations of these validation points are referenced in Figure 4.4. The performance of the numerical model can be represented by the NRMSE, as described in the previous section, as well as by the Nash-Sutcliffe Model Efficiency coefficient (Nash Coefficient). The Nash Coefficient is a means of assessing the predictive power of hydrological models and is defined as  $E = 1 - \frac{\sum_{t=1}^T (Q_o^t - Q_m^t)^2}{\sum_{t=1}^T (Q_o^t - \bar{Q}_o)^2}$ , where  $Q_o$  are the observed field values, and  $Q_m$  are the simulated model values. An efficiency of 1 ( $E = 1$ ) corresponds to a perfect match between model values and the observed values. The NRMSE and Nash Coefficient for both validation cases, and the validation simulation are presented in Table 4.3.

Table 4.3 NRMSE and Nash Coefficient for calibration and validation simulations

Event	18-22 March 2011			23-27 March 2011		
Peak Flow at Cache Creek at Yolo	15,900 cfs			14,300 cfs		
Mode	Calibration	Validation		Validation		
Location	Rd 102	Site C	Weir	Rd 102	Site C	Weir
NRMSE	0.07	0.11	0.09	0.12	0.07	0.08
Nash Coefficient	0.93	0.83	0.90	0.69	0.90	0.87

The inflow hydrograph shown in Figure 4.9 also indicates four specific time steps for which water depth and velocity contour plots are provided in later figures. Water depth and velocity magnitude results from the calibration simulation for the extent of Cache Creek between Yolo and Rd 102 at time steps 1 through 4 are presented in Figures 4.10-4.13. Note that the units displayed are metric corresponding to the computational format of CCHE2D. Water depth and velocity magnitude results from the validation simulation for the CCSB are presented in Figures 4.14-4.17. Water depth contours indicate inundation area of the basin, and are shown for select time references, as indicated in Figure 4.9. Velocity magnitudes are displayed in Figures 4.16 and 4.17 for those select time references. Velocity magnitude and vectors indicating direction of flow for the southern portion of the settling basin, including the terminus of the training

channel, low flow channel, and overflow weir are provided in Figures 4.18 through 4.21 for the four time steps indicated. Velocity vectors are scaled relative to each other. However, magnitudes must be read from the contour provided.

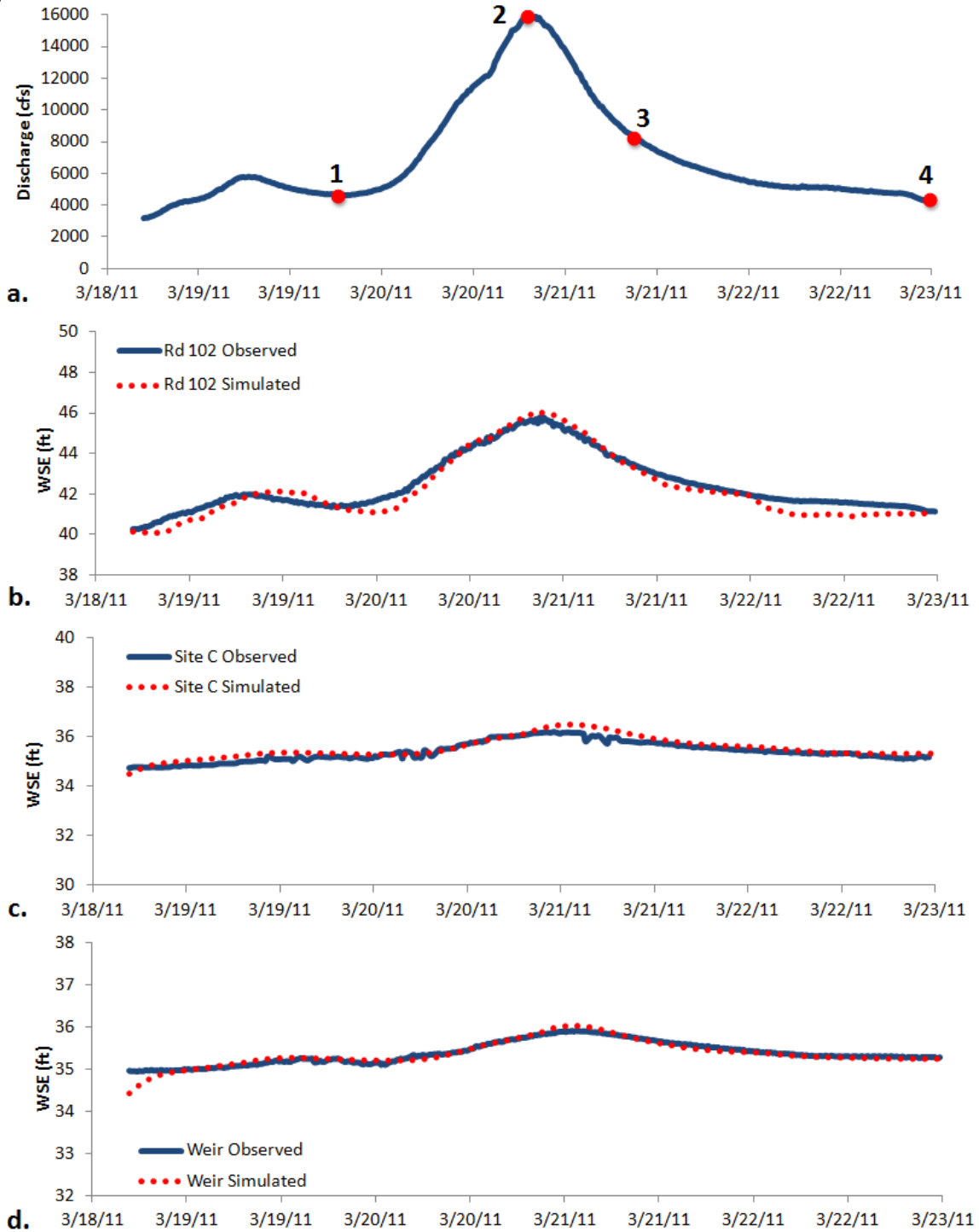


Figure 4.9 Comparison plots of 18-22 March 2011 simulation, (a) Inflow discharge at Cache Creek at Yolo with time steps for results display, (b) Calibrated water surface elevation at Rd 102 for entire simulation duration, (c) Water Surface Elevation validation at Site C for entire simulation duration, (d) Water Surface Elevation validation at Overflow Weir for entire simulation duration

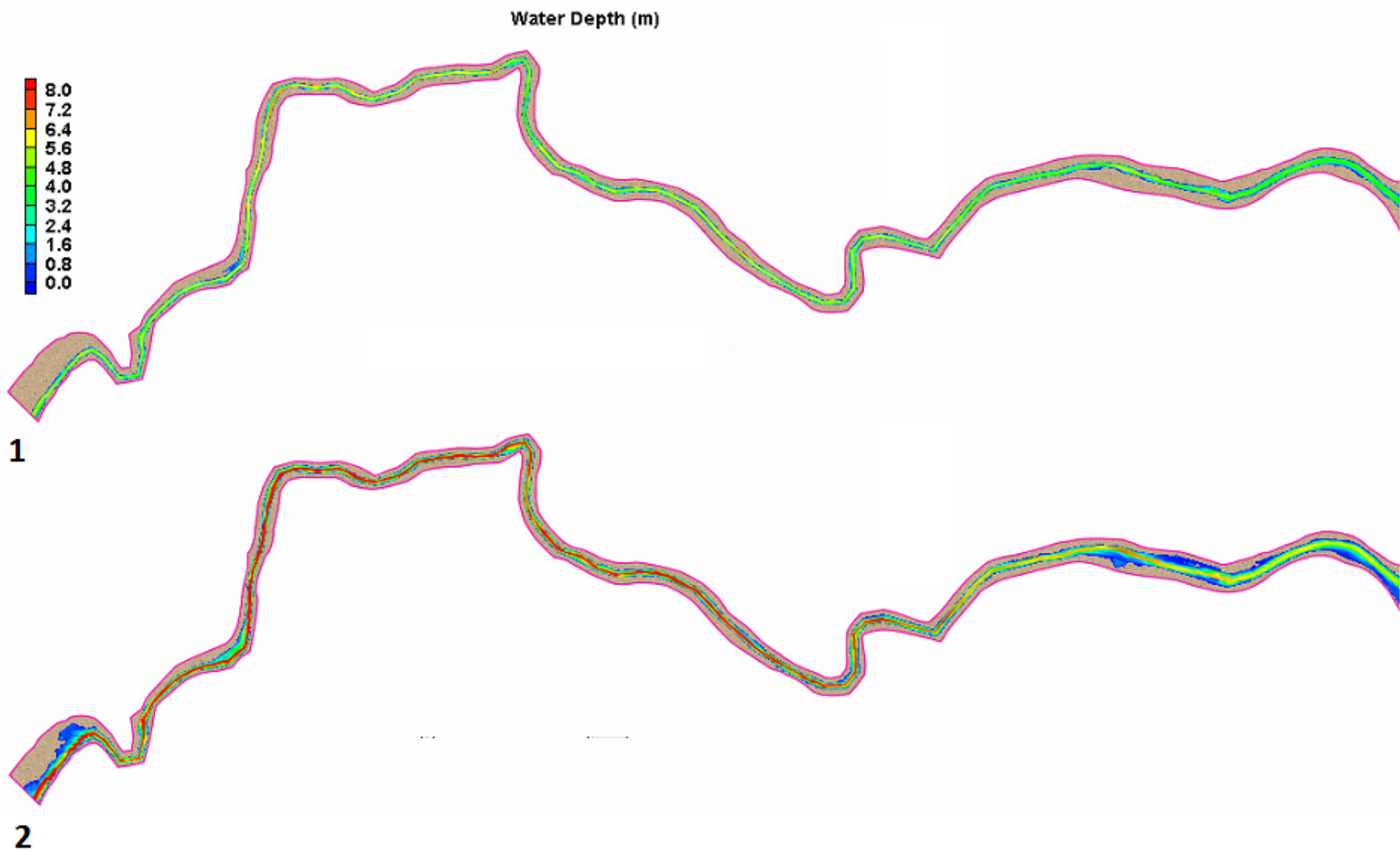


Figure 4.10 Water depth results at selected times on rising limb of storm hydrograph, 1 and 2 (peak flow) of 18-22 March 2011 event; Cache Creek at Yolo to Rd 102

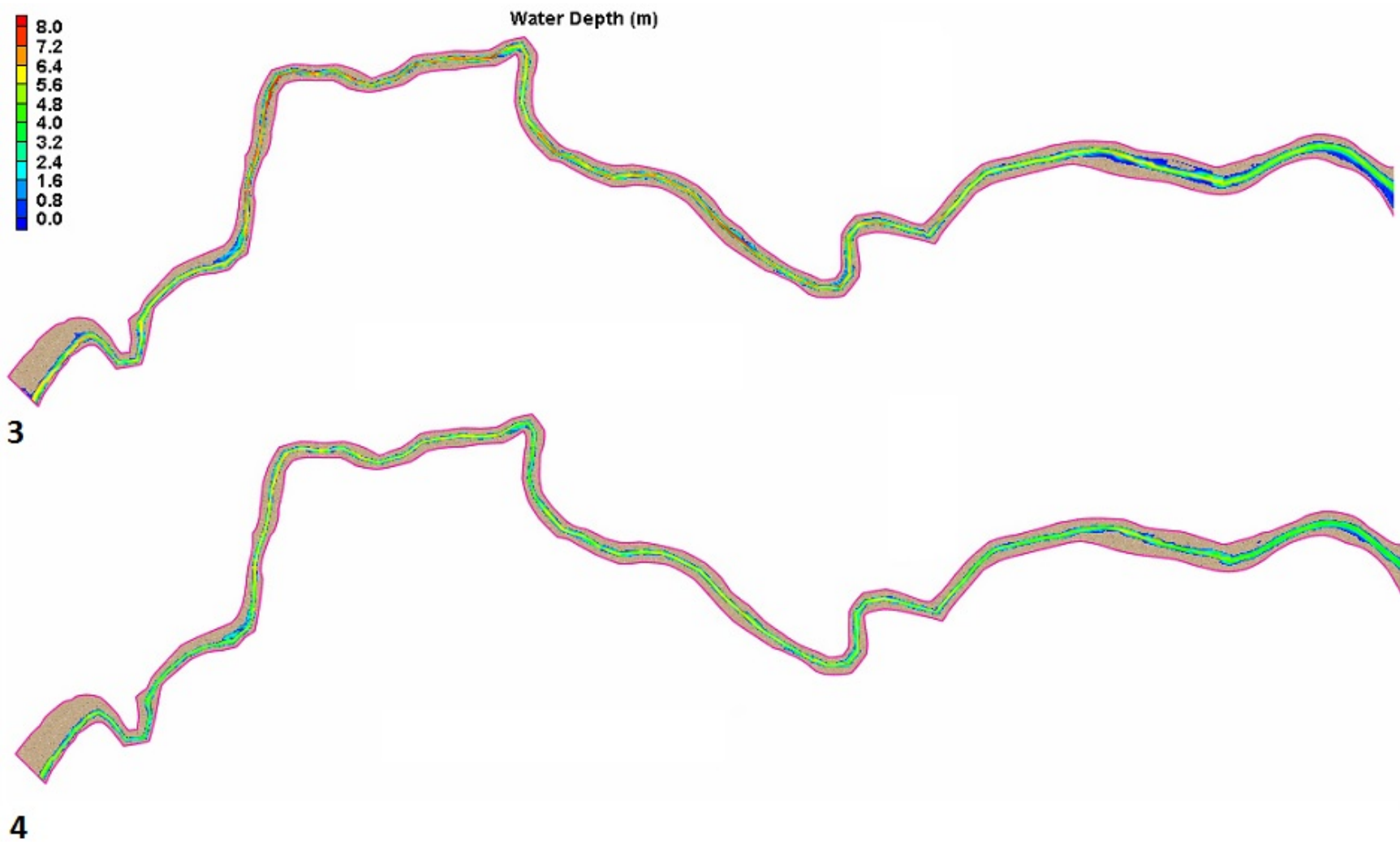


Figure 4.11 Water depth results at selected times on falling limb of hydrograph, 3 and 4 of 18-22 March 2011 event; Cache Creek at Yolo to Rd 102

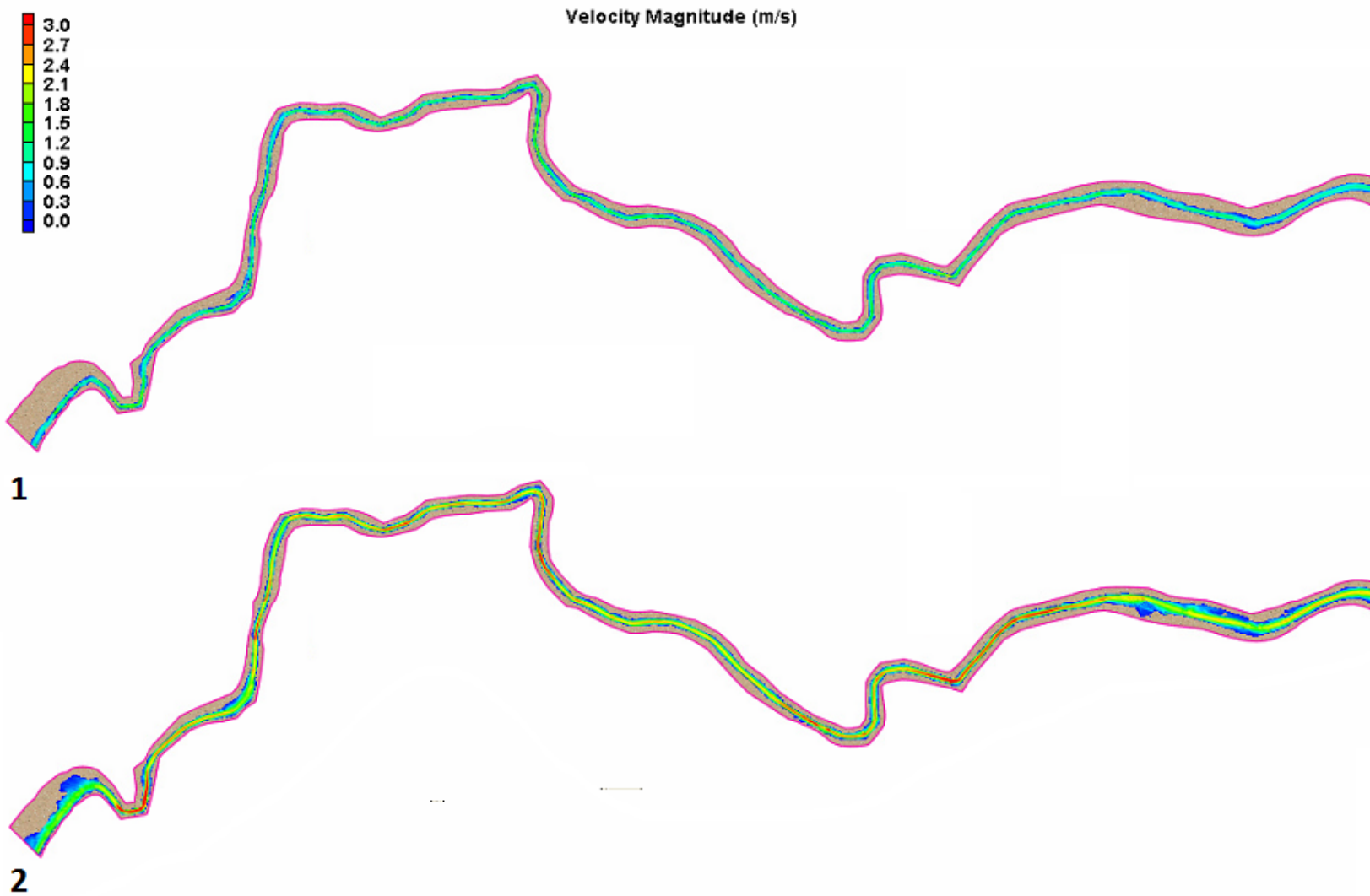


Figure 4.12 Velocity magnitude results at selected times on rising limb of hydrograph, 1 and 2 (peak flow) of 18-22 March 2011 event; Cache Creek at Yolo to Rd 102

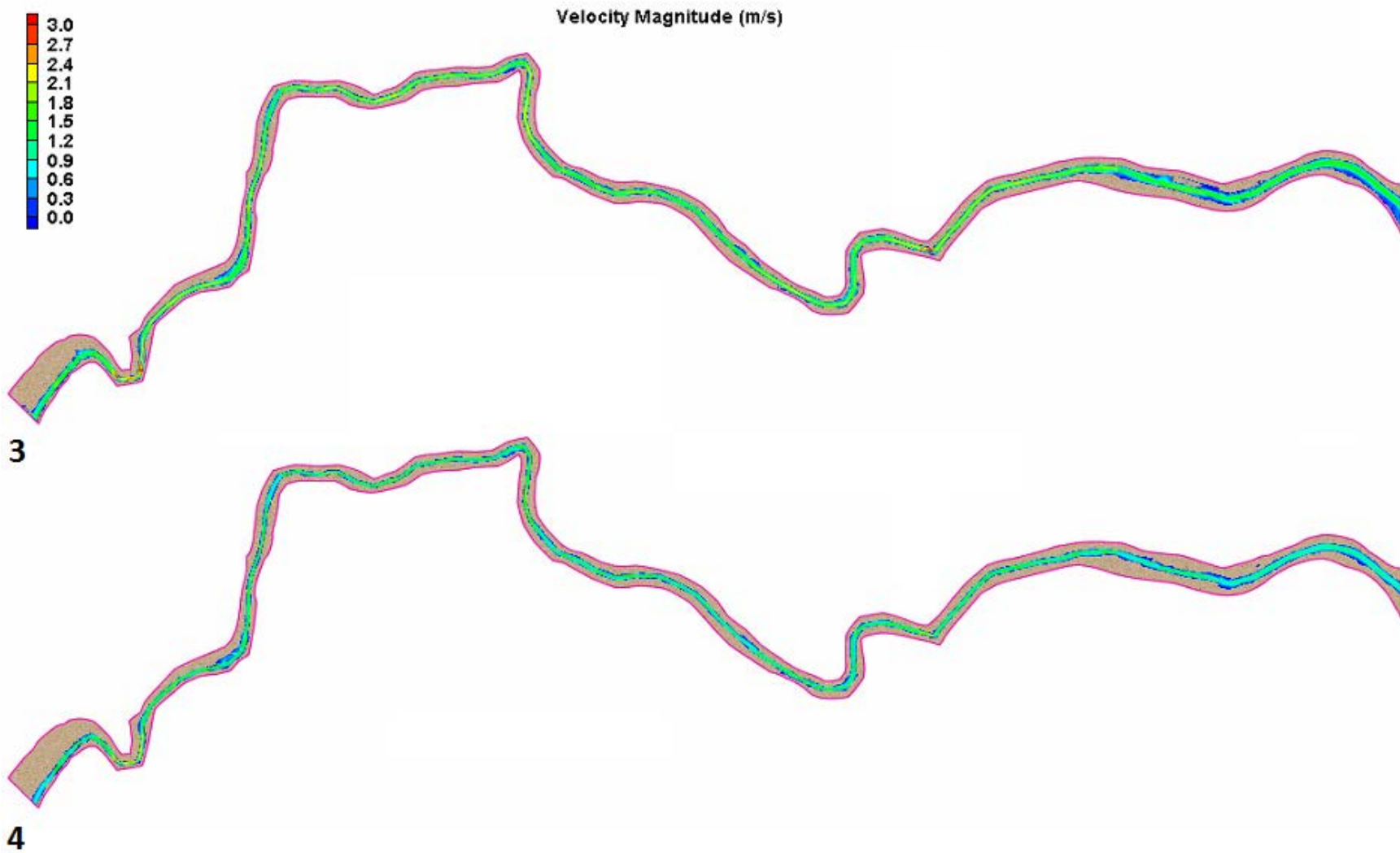


Figure 4.13 Velocity magnitude results at selected times on falling limb of hydrograph, 3 and 4 of 18-22 March 2011 event; Cache Creek at Yolo to Rd 102

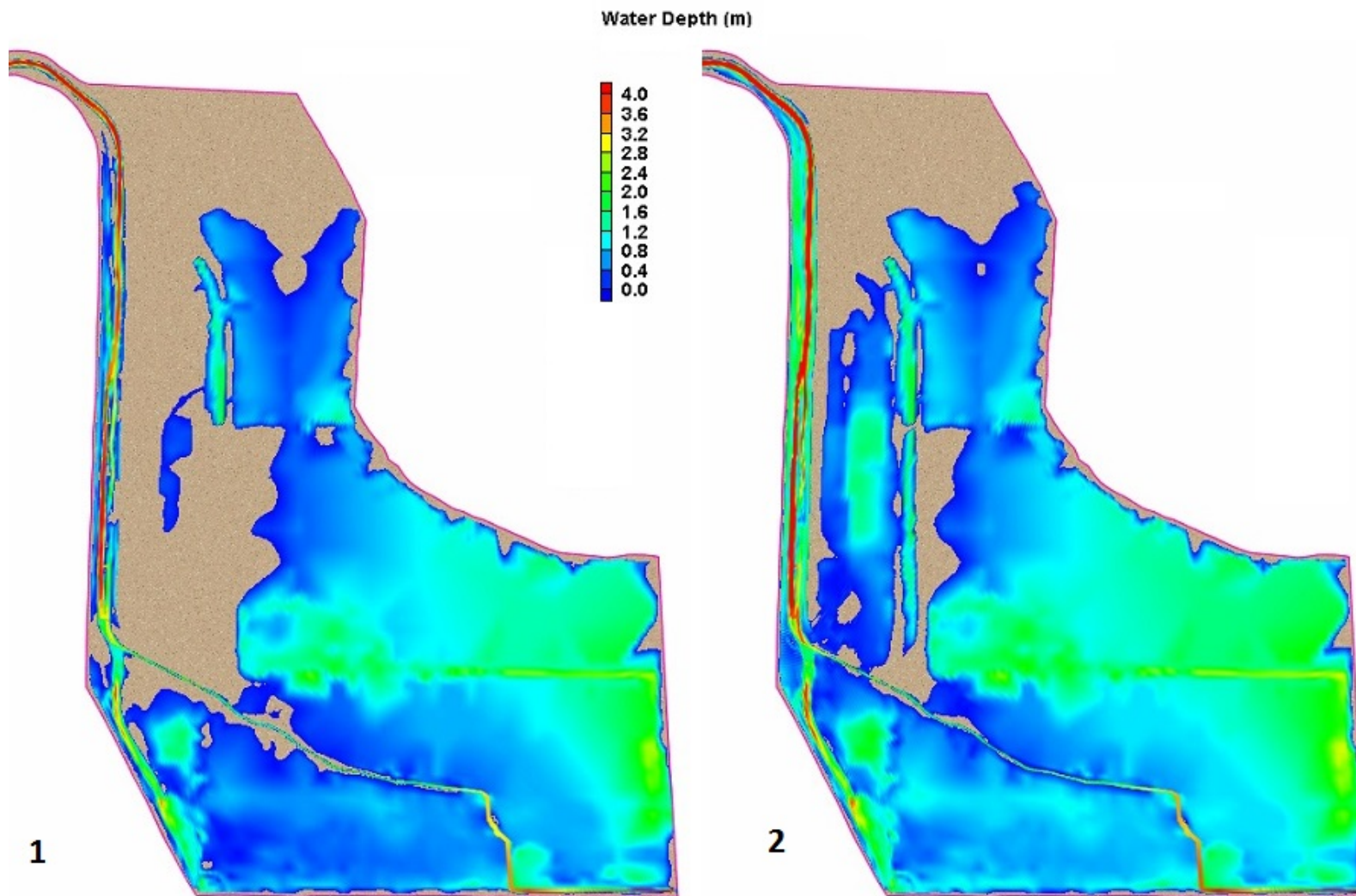


Figure 4.14 CCSB water depth results, March 2011, at selected times on rising limb of hydrograph, 1 and 2 (peak flow) of 18-22 March 2011 event.

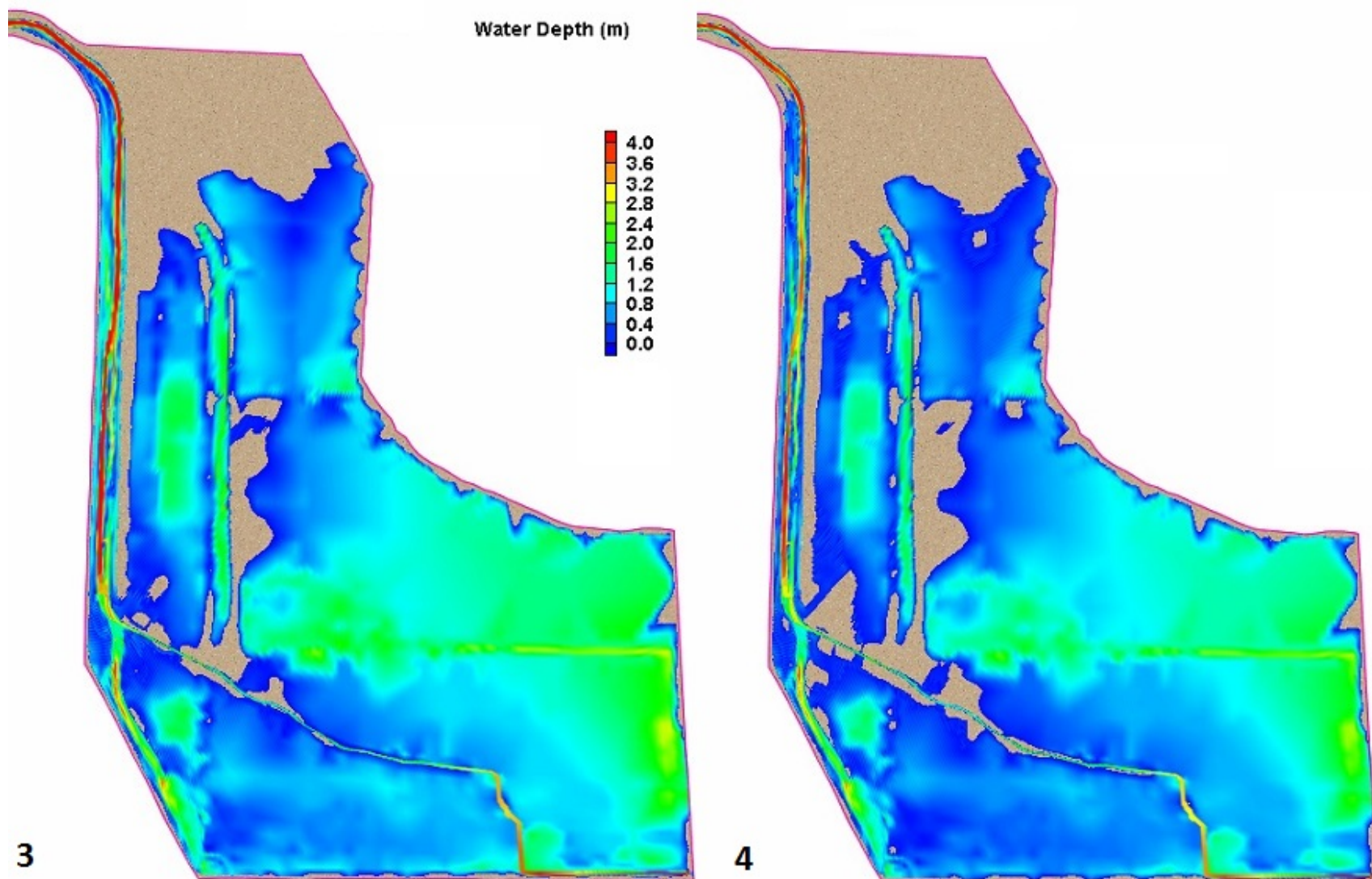


Figure 4.15 CCSB water depth results, March 2011, at selected times on falling limb of hydrograph, 3 and 4 of 18-22 March 2011 event

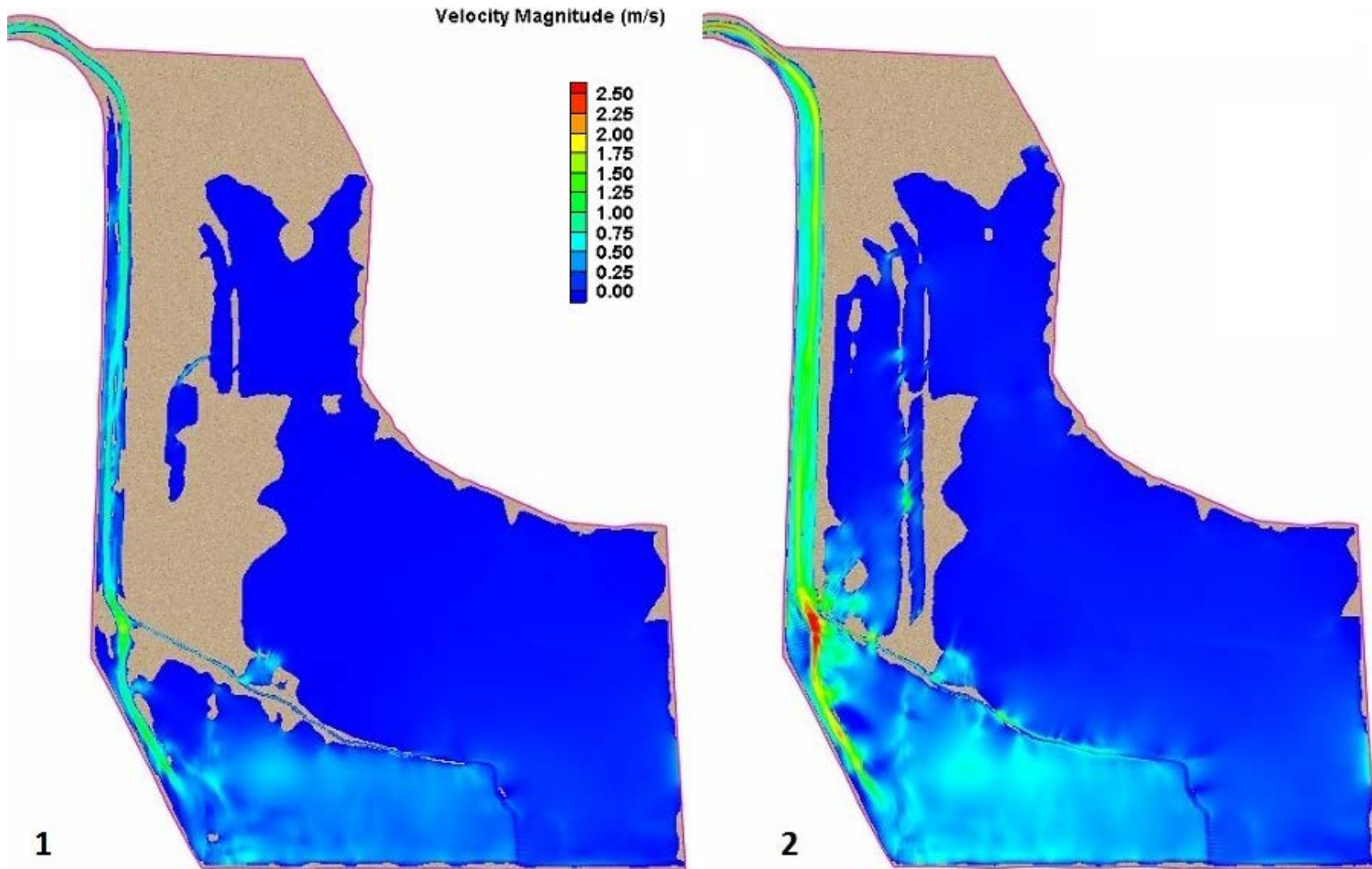


Figure 4.16 CCSB velocity magnitude results, March 2011, at selected times on rising limb of hydrograph, 1 and 2 (peak flow) of 18-22 March 2011 event



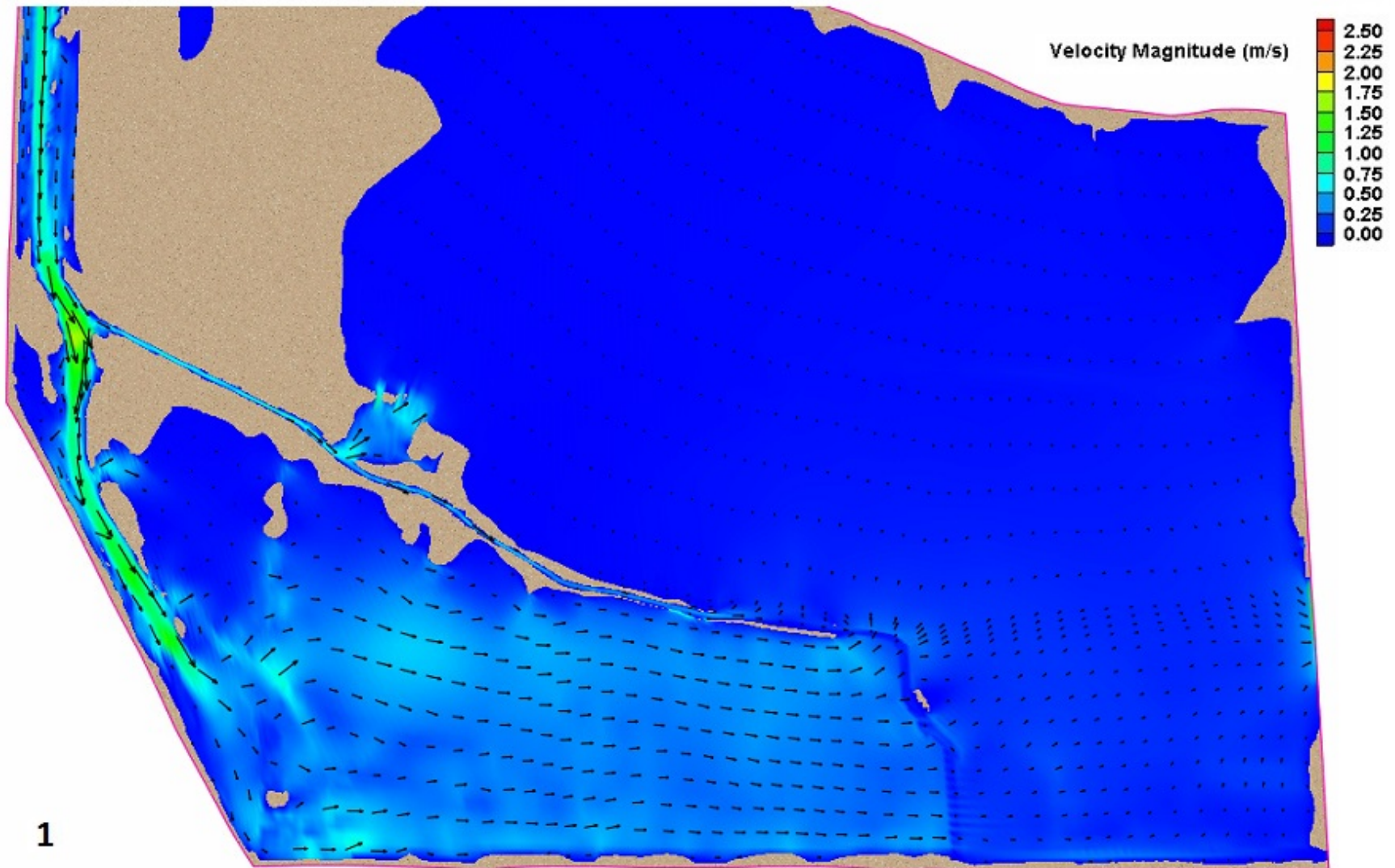


Figure 4.18 CCSB velocity magnitude result with scaled directional vectors, at selected time 1 of 18-22 March 2011 event

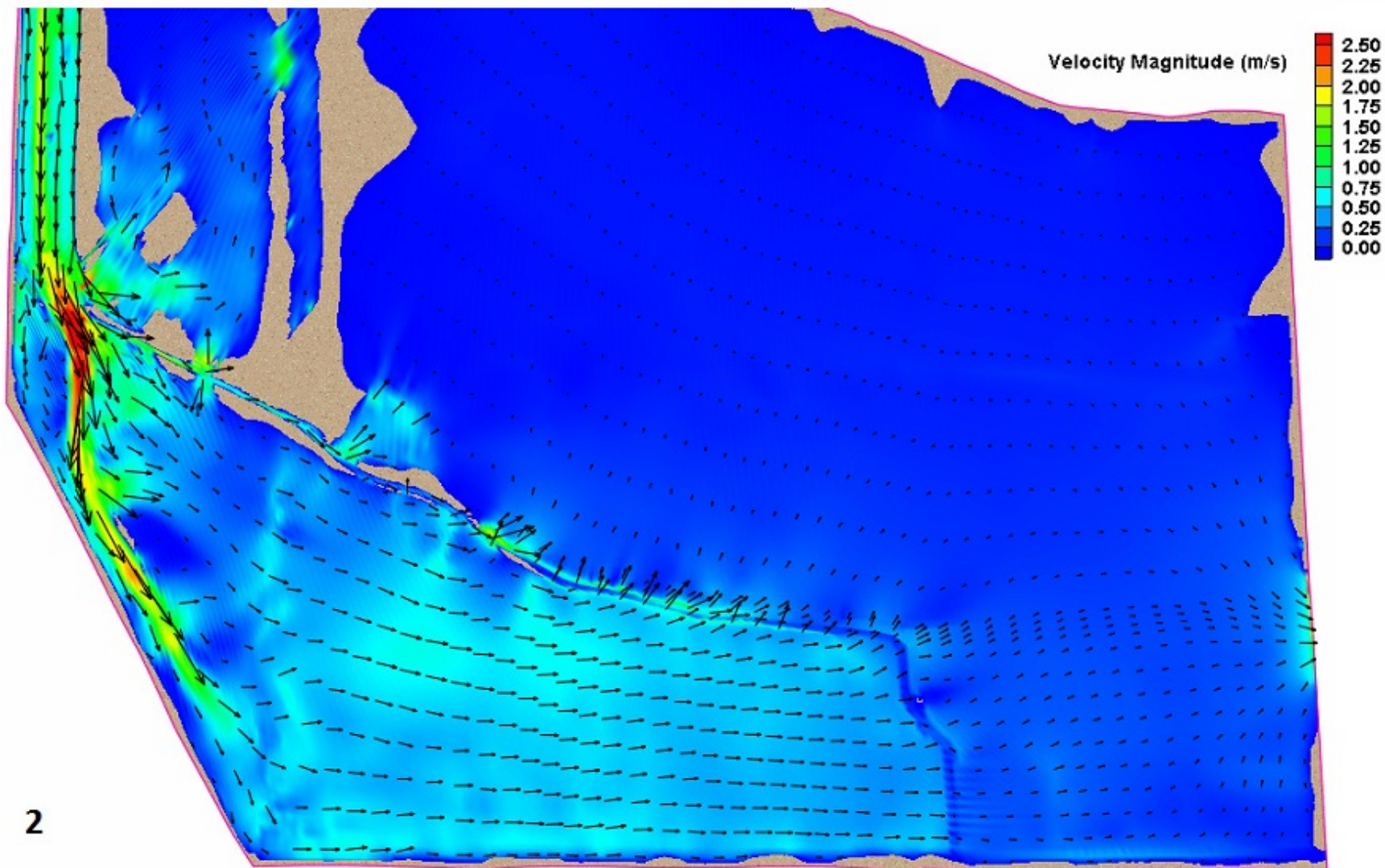


Figure 4.19 CCSB velocity magnitude result with scaled directional vectors, at selected time 2 of 18-22 March 2011 event

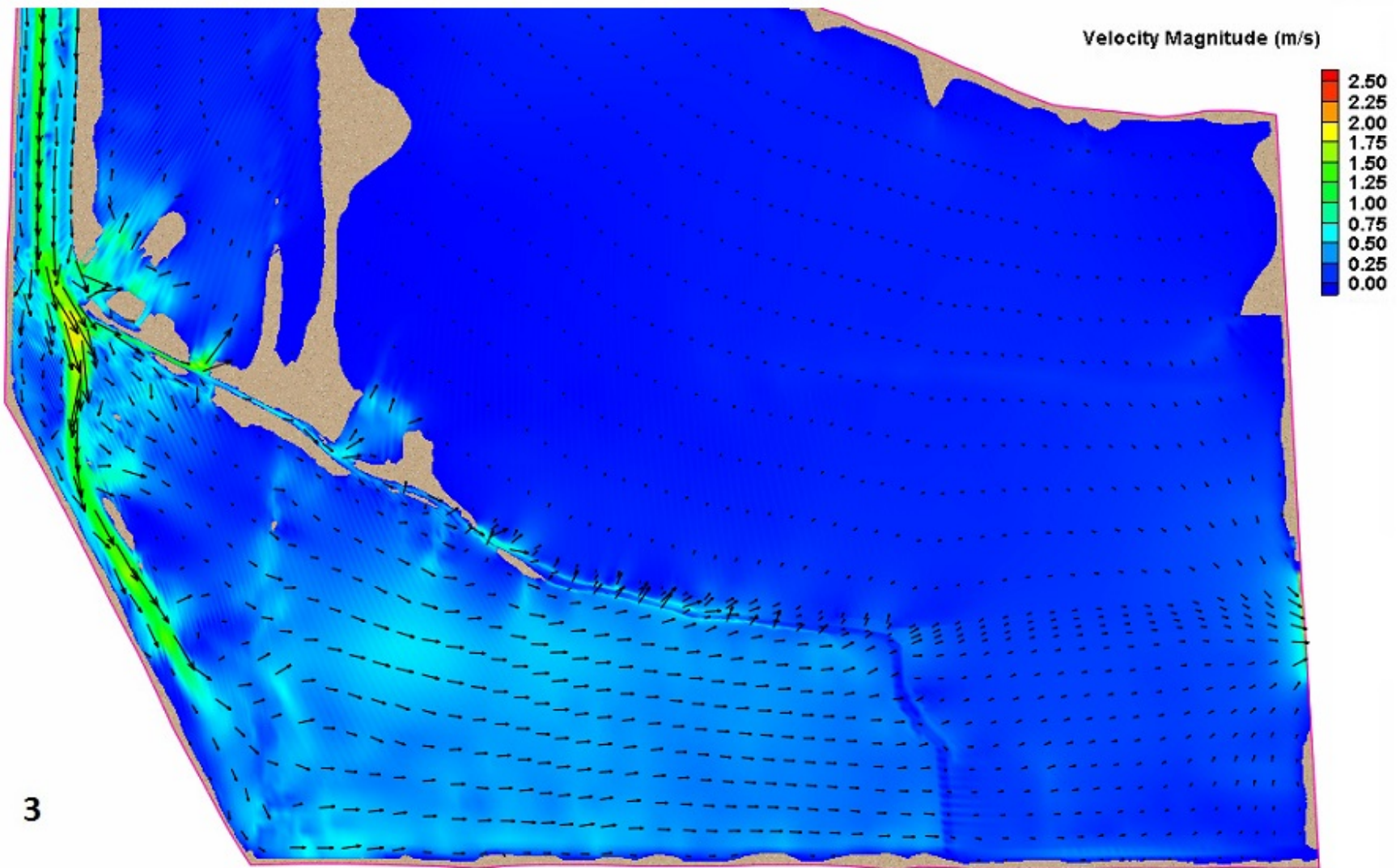
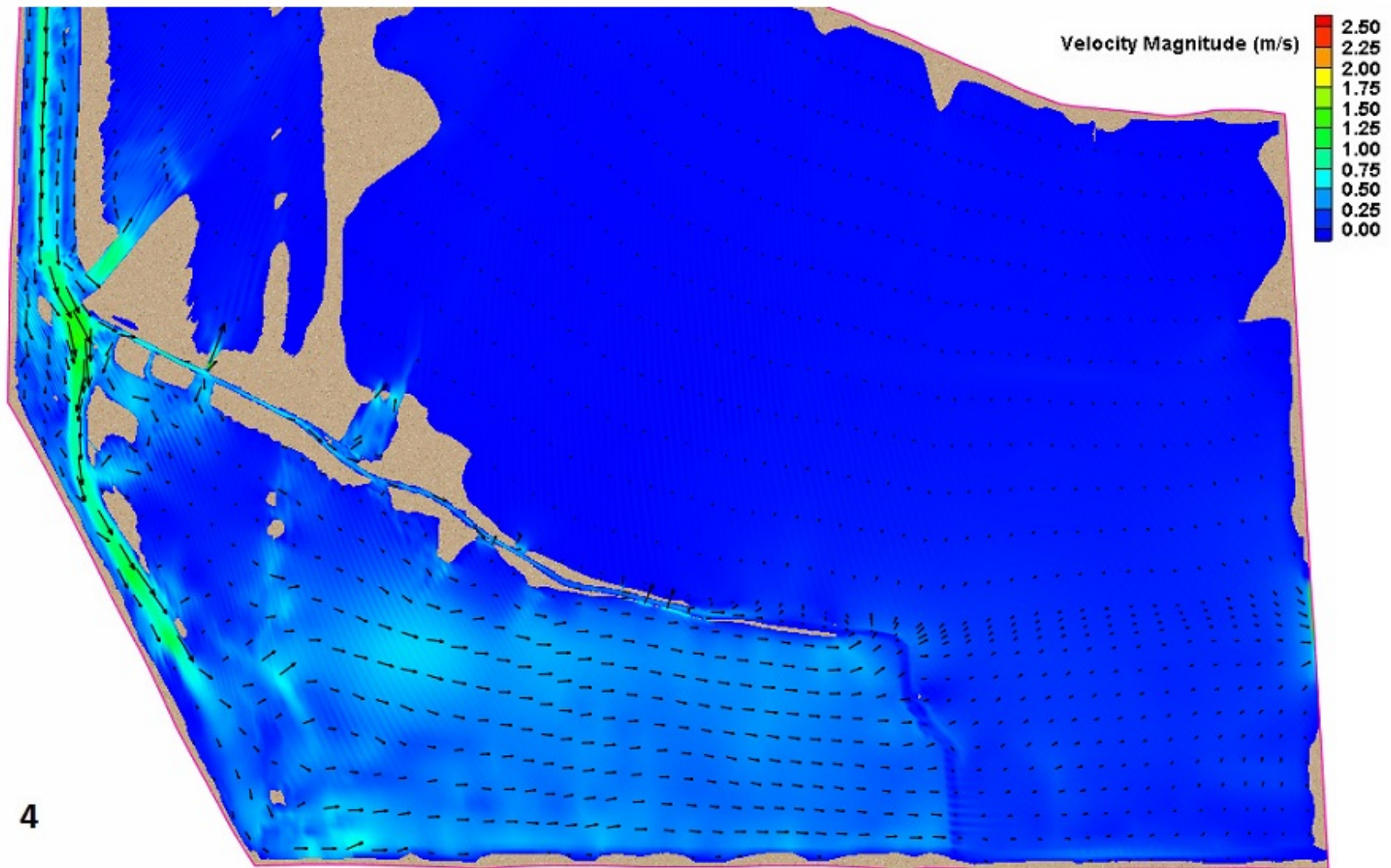


Figure 4.20 CCSB velocity magnitude result with scaled directional vectors, at selected time 3 of 18-22 March 2011 event



4

Figure 4.21 CCSB velocity magnitude result with scaled directional vectors, at selected time 4 of 18-22 March 2011 event

### **4.1.3 Validation by 23-27 March 2011 flow event at Road 102 and inside CCSB**

A validation simulation was conducted for the full extent of the simulation mesh shown in Figures 3.20 and 3.21 and for an inflow boundary condition for flow set as discharge at Yolo from March 23, 2011 04:15 through March 27, 2011 23:45, with a peak flow discharge of 14,300 cfs, a flow with an exceedance probability of 50-percent. The inflow hydrograph presented in Figure 4.22, is a storm hydrograph with multiple peaks, the largest of which occurs near the mid-point of the nearly 5-day hydrograph duration (labeled time selection 3). The simulation results are plotted, along with water surface elevation data collected during the storm event at Rd 102, Site C and the Overflow Weir in Figure 4.22. There is good agreement between modeled and measured water surface elevation data, illustrating that the model is capable of simulating transient flows, and can handle wetting and drying of the CCSB as inundation area directly relates to water surface elevation. Table 4.3 contains the NRMSE and Nash Coefficient results for the validation simulation. At site C and the overflow weir the NRMSE is less 0.05 or less, and the Nash Coefficient is greater than 0.87, demonstrating that the model is predicting inundation and water surface elevation very well. Water surface elevations at the weir are in good agreement throughout the simulation, suggesting that discharge is also well represented through the duration. Water surface elevation contours for select times in the storm hydrograph are shown in Figure 4.23 through 4.25 for the extent from Yolo to Rd 102, and in Figure 4.26 through 4.28 for the CCSB from Rd 102 to the outlets. Velocity contours at select time steps, for the extent from Yolo to Rd 102, are shown in Figures 4.29 through 4.31. The velocity contours for the CCSB are shown in Figures 4.32 through 4.34. Figures 4.35 through 4.39 contain velocity contours and velocity vectors for the southern portion of the CCSB, focusing on the terminus of the training levee, the low flow channel and the overflow weir. Velocity vectors are scaled relative to each other. However, the magnitudes must be read from the contours.

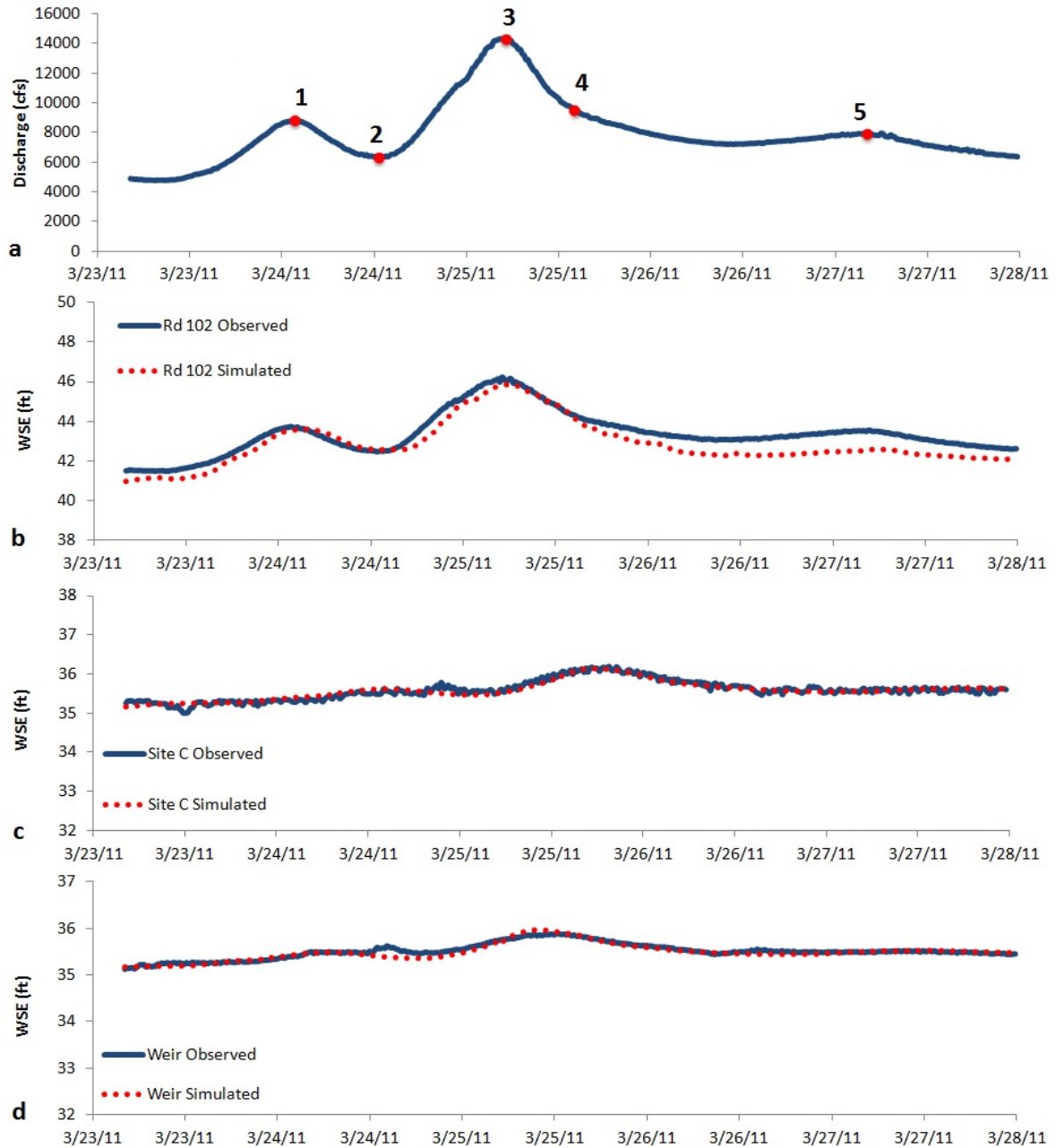


Figure 4.22 Comparison plots of 23-27 March 2011 validation simulation, (a) Inflow discharge at Cache Creek at Yolo with time steps for results display, (b) Water surface elevation validation at Rd 102 for entire simulation duration, (c) Water Surface Elevation validation at Site C for entire simulation duration, (d) Water Surface Elevation validation at Overflow Weir for entire simulation duration



Figure 4.23 Water depth validation simulation results, Yolo to Rd 102, at selected times 1 and 2 of 23-27 March 2011 event

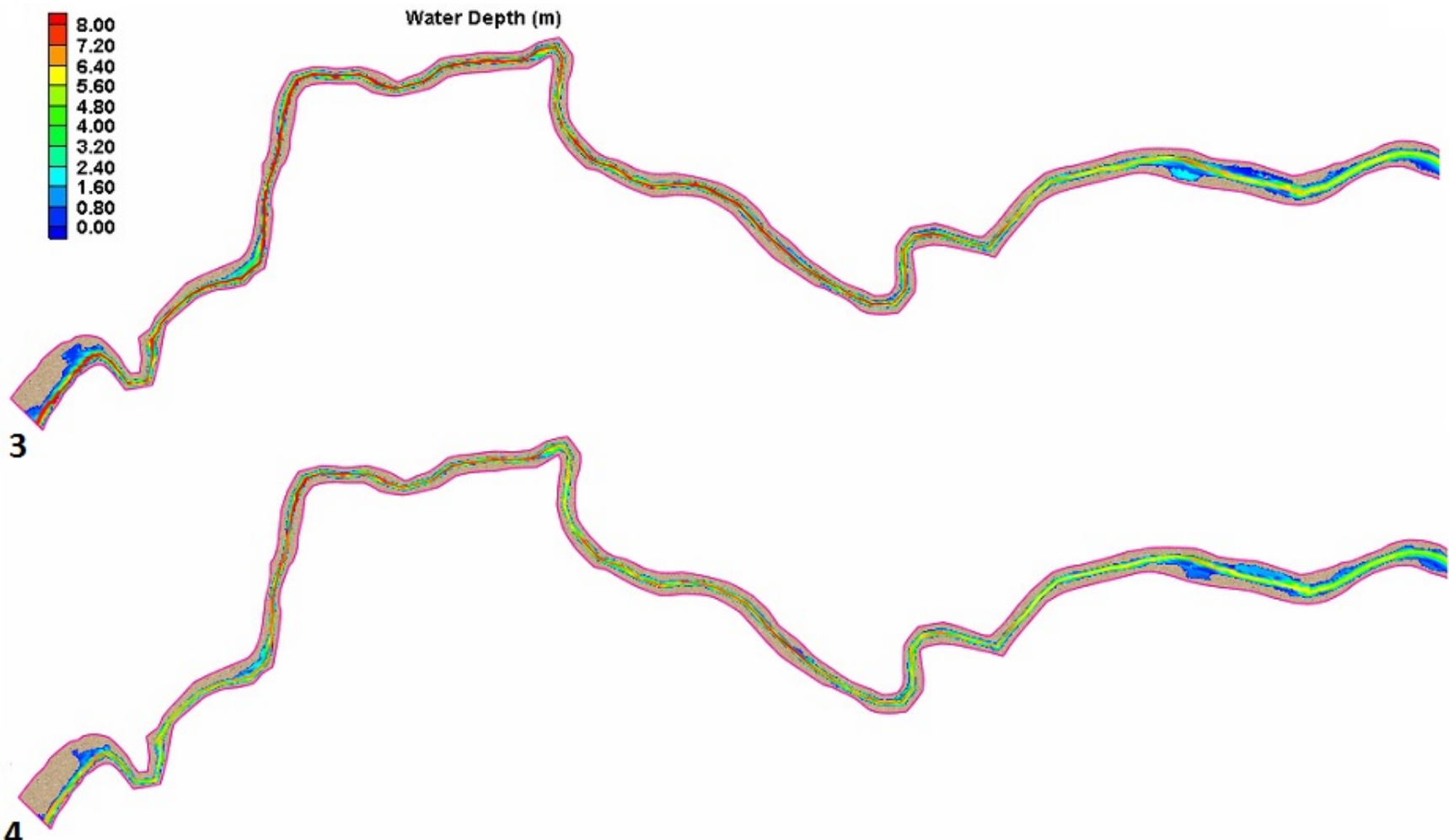
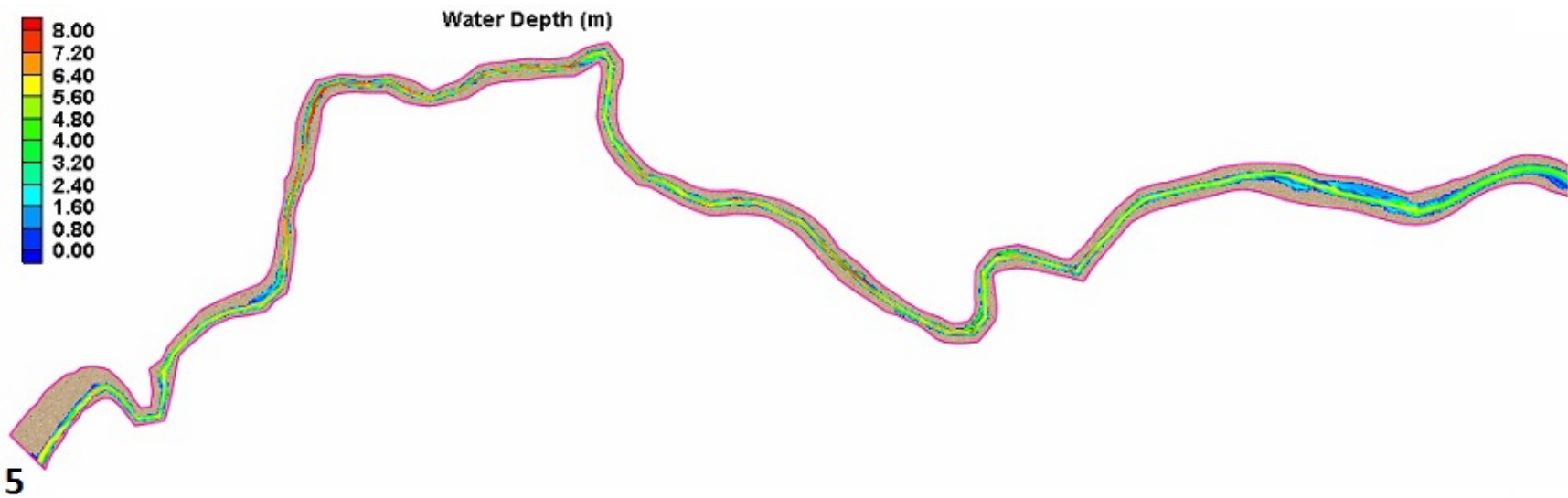


Figure 4.24 Water depth validation simulation results, Yolo to Rd 102, at selected times 3 (peak flow) and 4 of 23-27 March 2011 event



5

Figure 4.25 Water depth validation simulation results, Yolo to Rd 102, at selected time 5 of 23-27 March 2011 event

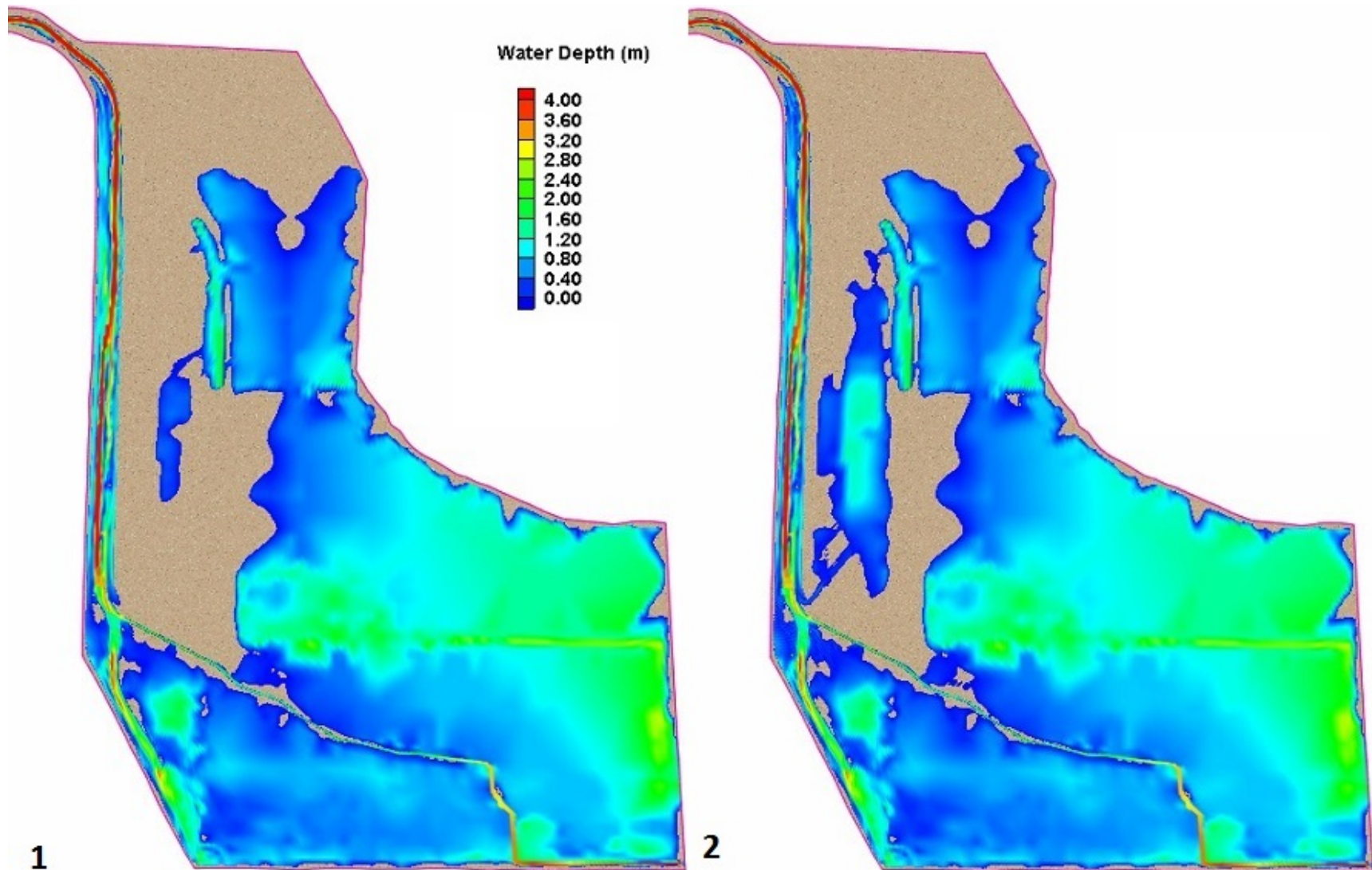


Figure 4.26 Water depth validation results, CCSB, at selected times 1 and 2 of 23-27 March 2011 event

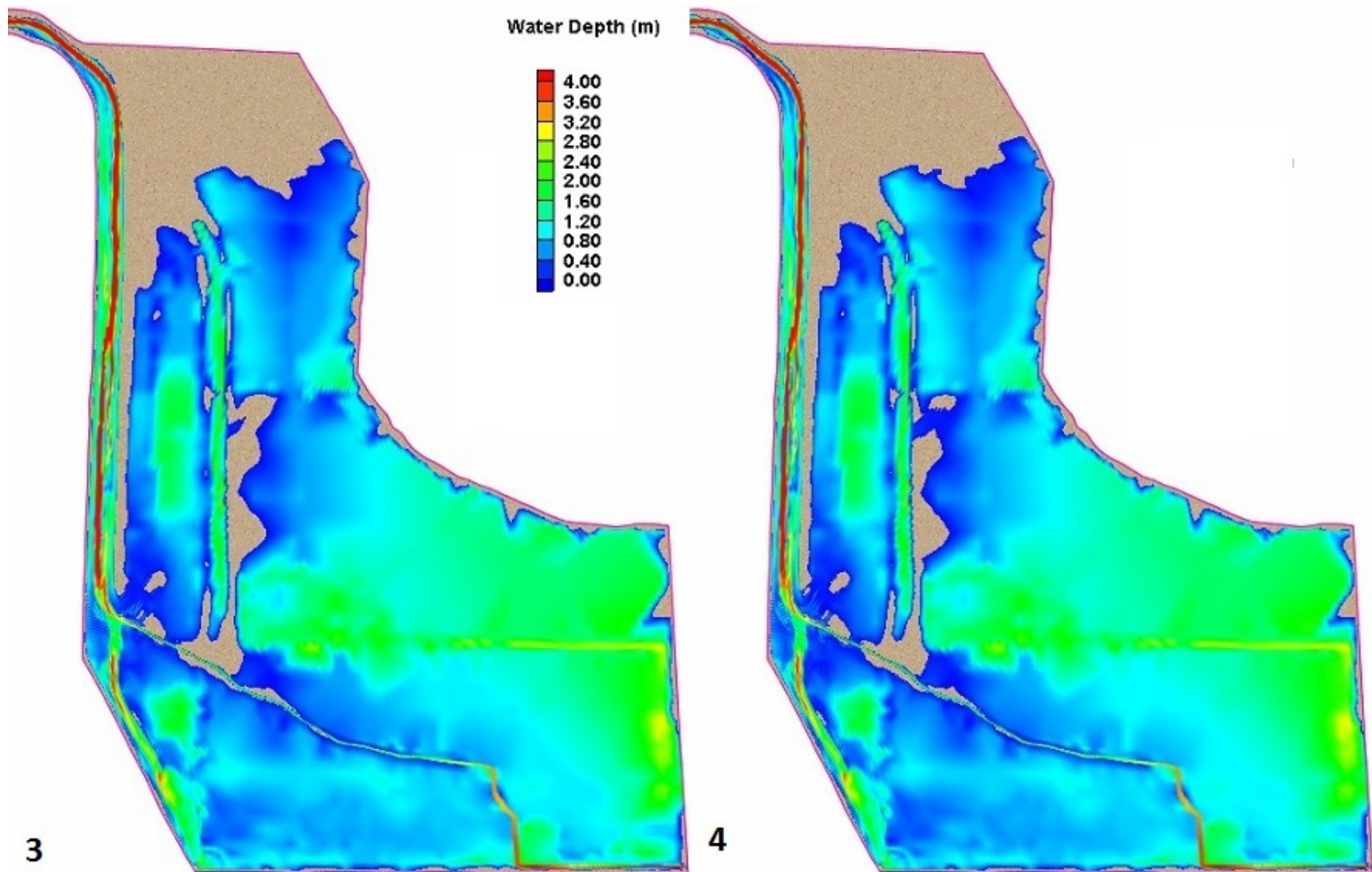
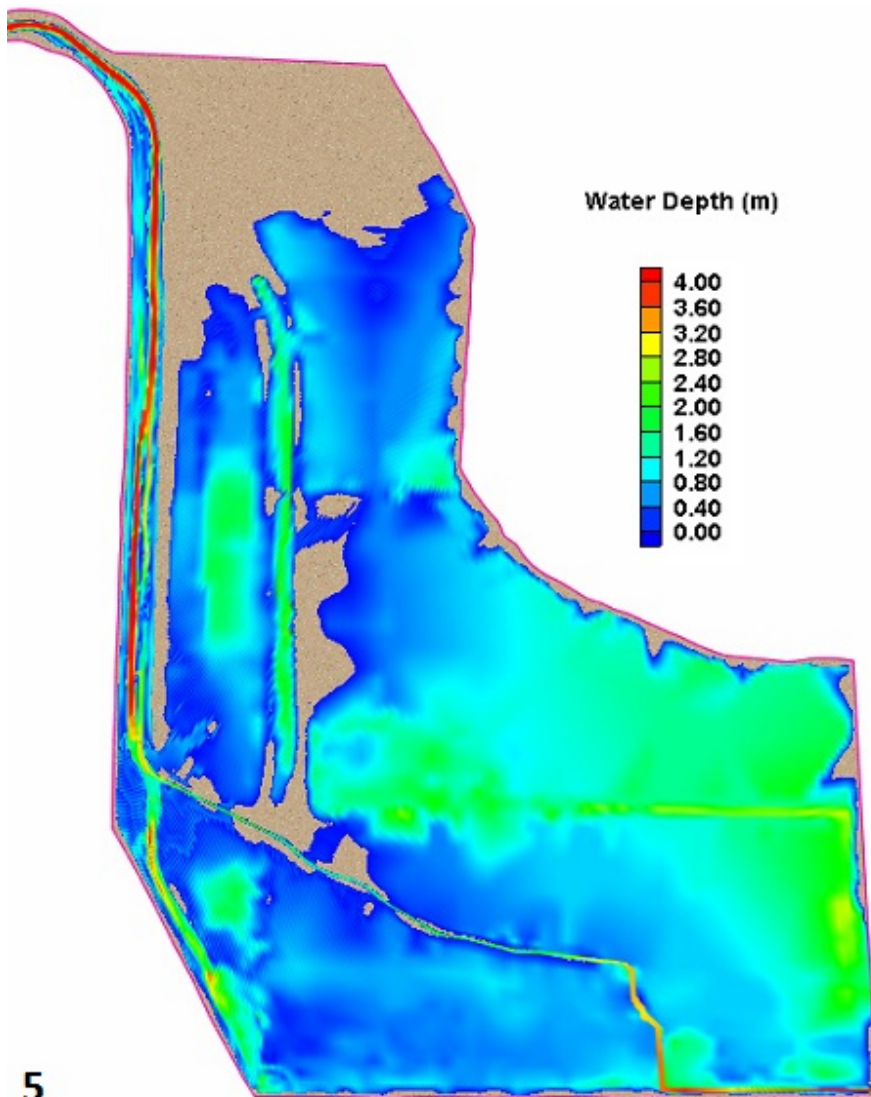


Figure 4.27 Water depth validation results, CCSB, at selected times 3 (peak flow) and 4 of 23-27 March 2011 event



5

Figure 4.28 Water depth validation results, CCSB, at selected time 5 of 23-27 March 2011 event



Figure 4.29 Velocity magnitude validation results, Yolo to Rd 102, at selected times 1 and 2 of 23-27 March 2011 event

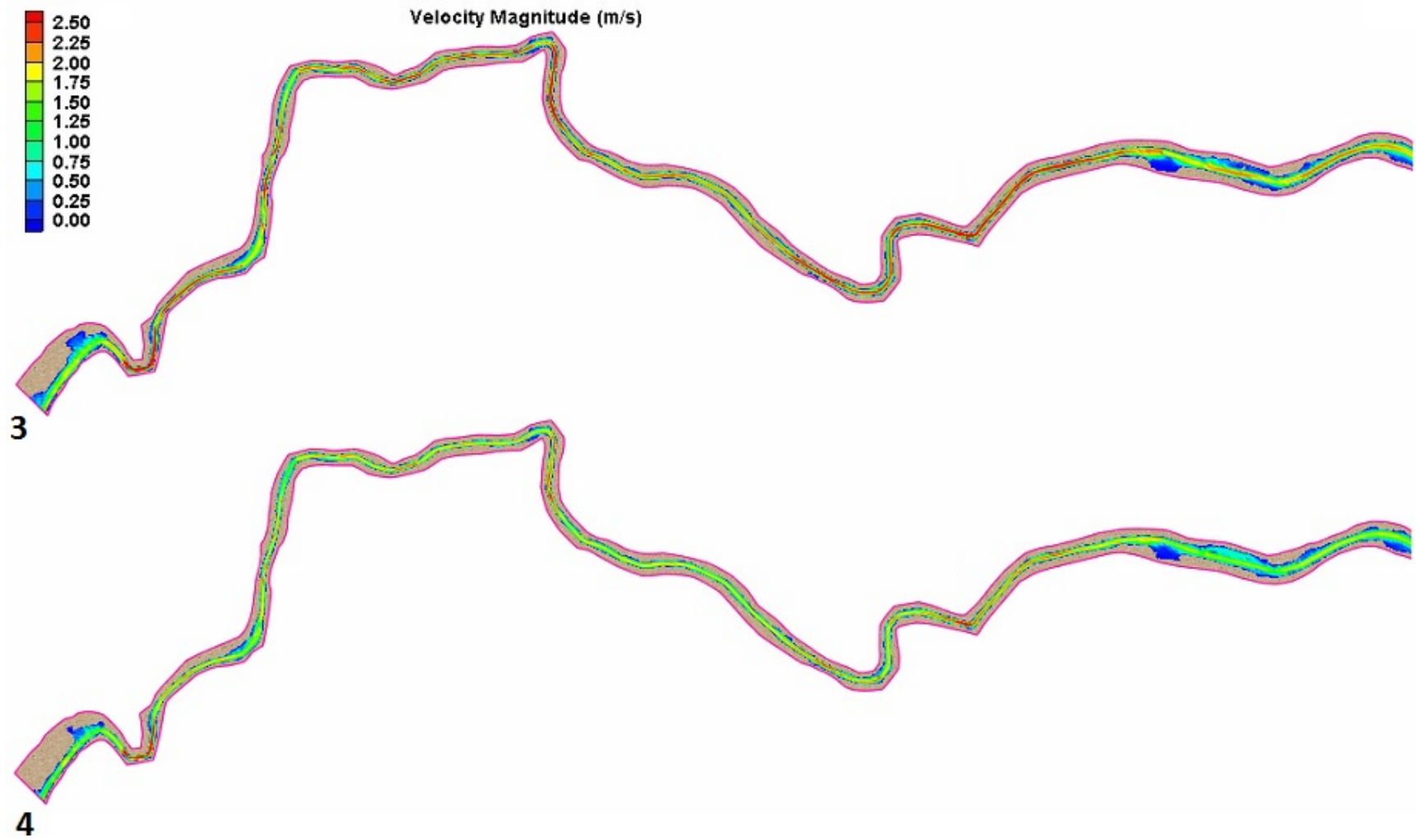
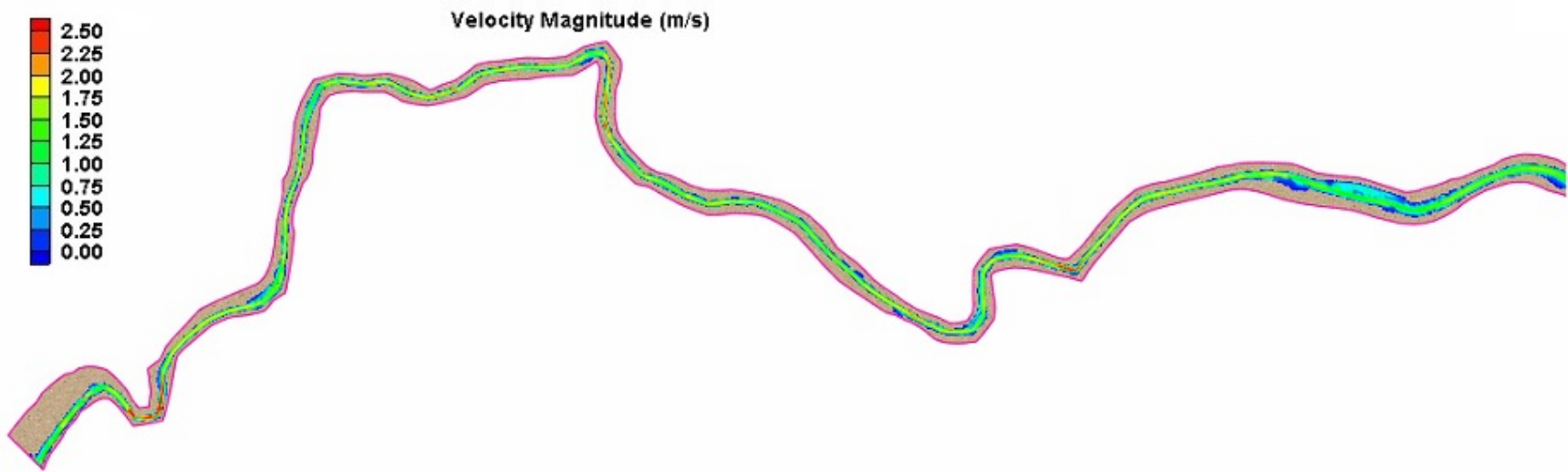


Figure 4.30 Velocity magnitude validation results, Yolo to Rd 102, at selected times 3 (peak flow) and 4 of 23-27 March 2011 event



5

Figure 4.31 Velocity magnitude validation results, Yolo to Rd 102, at selected time 5 of 23-27 March 2011 event.

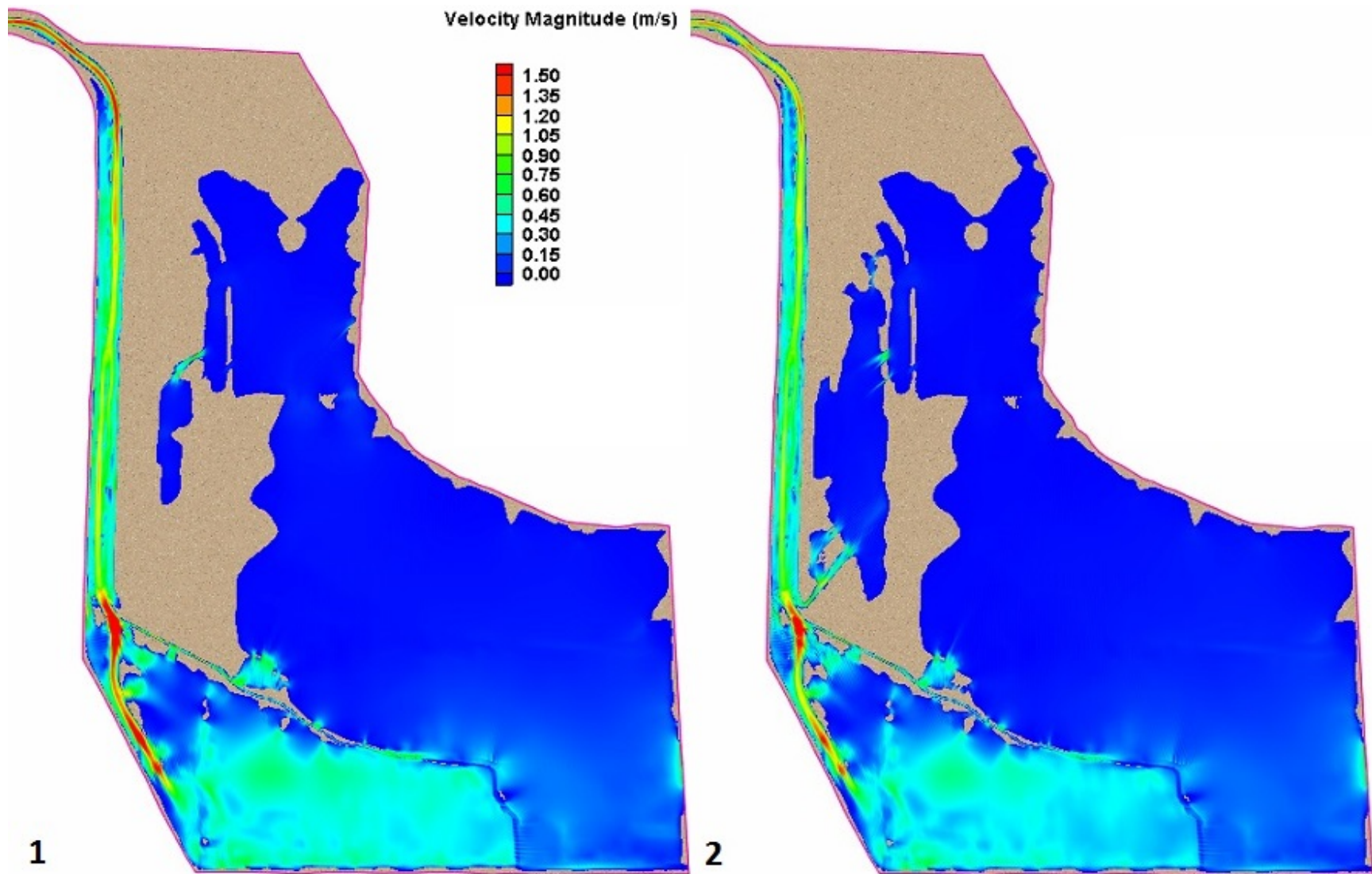


Figure 4.32 Velocity magnitude validation simulation results, CCSB, at selected times 1 and 2 of 23-27 March 2011 event

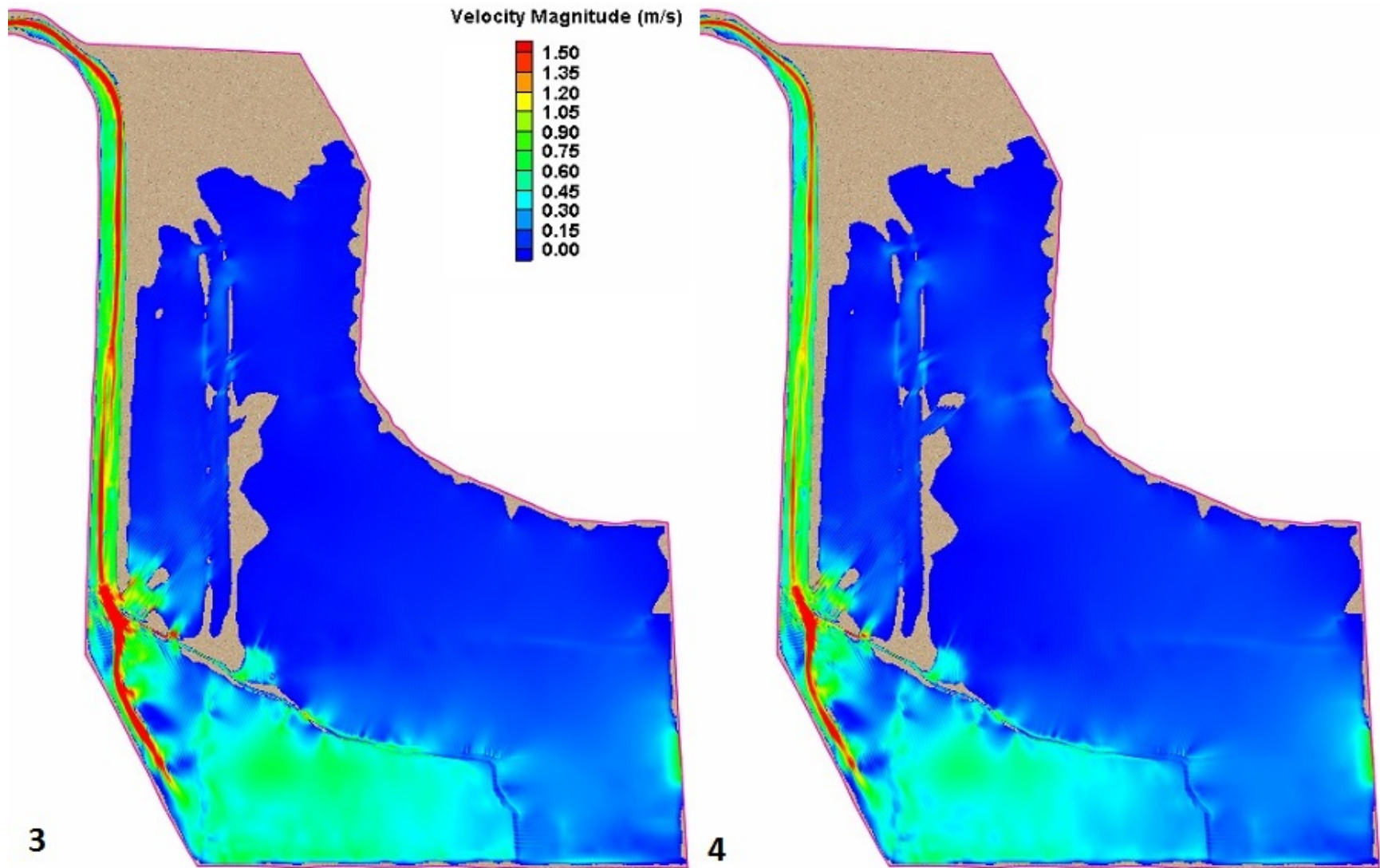


Figure 4.33 Velocity magnitude validation simulation results, CCSB, at selected times 3 (peak flow) and 4 of 23-27 March 2011 event

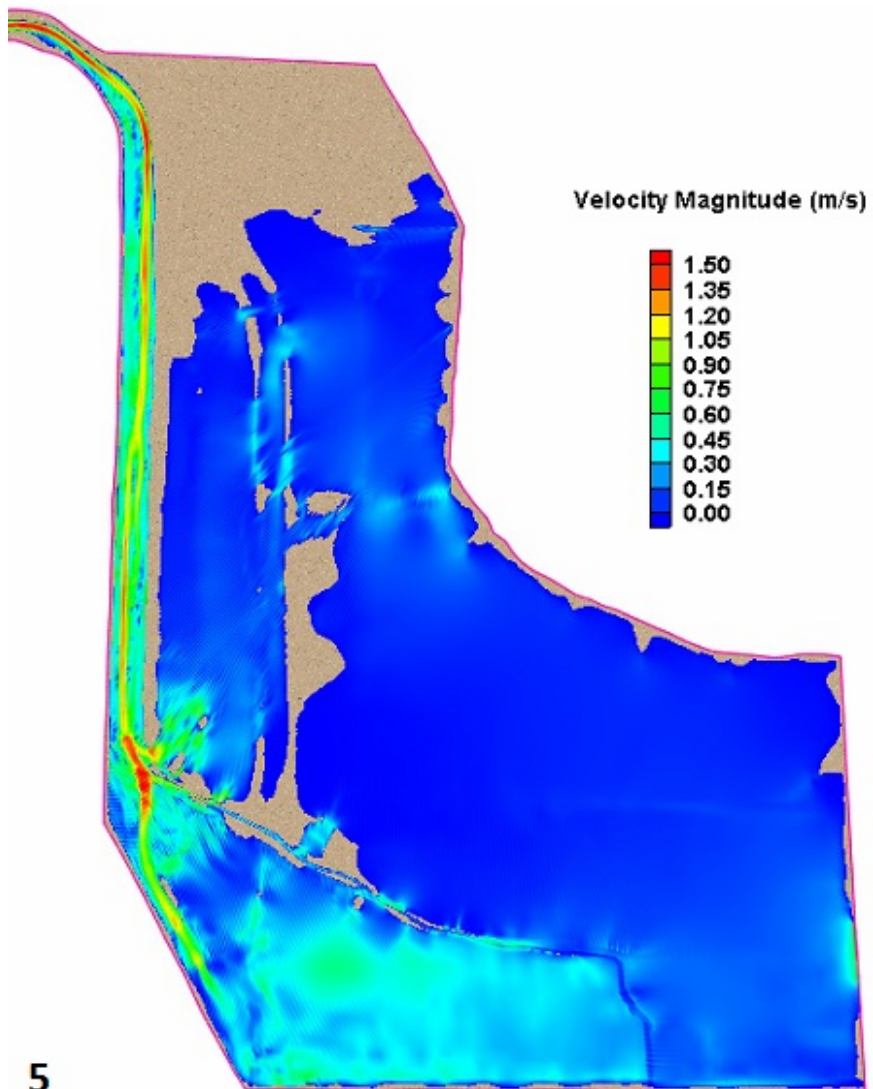


Figure 4.34 Velocity magnitude validation simulation results, CCSB, at selected time 5 of 23-27 March 2011 event

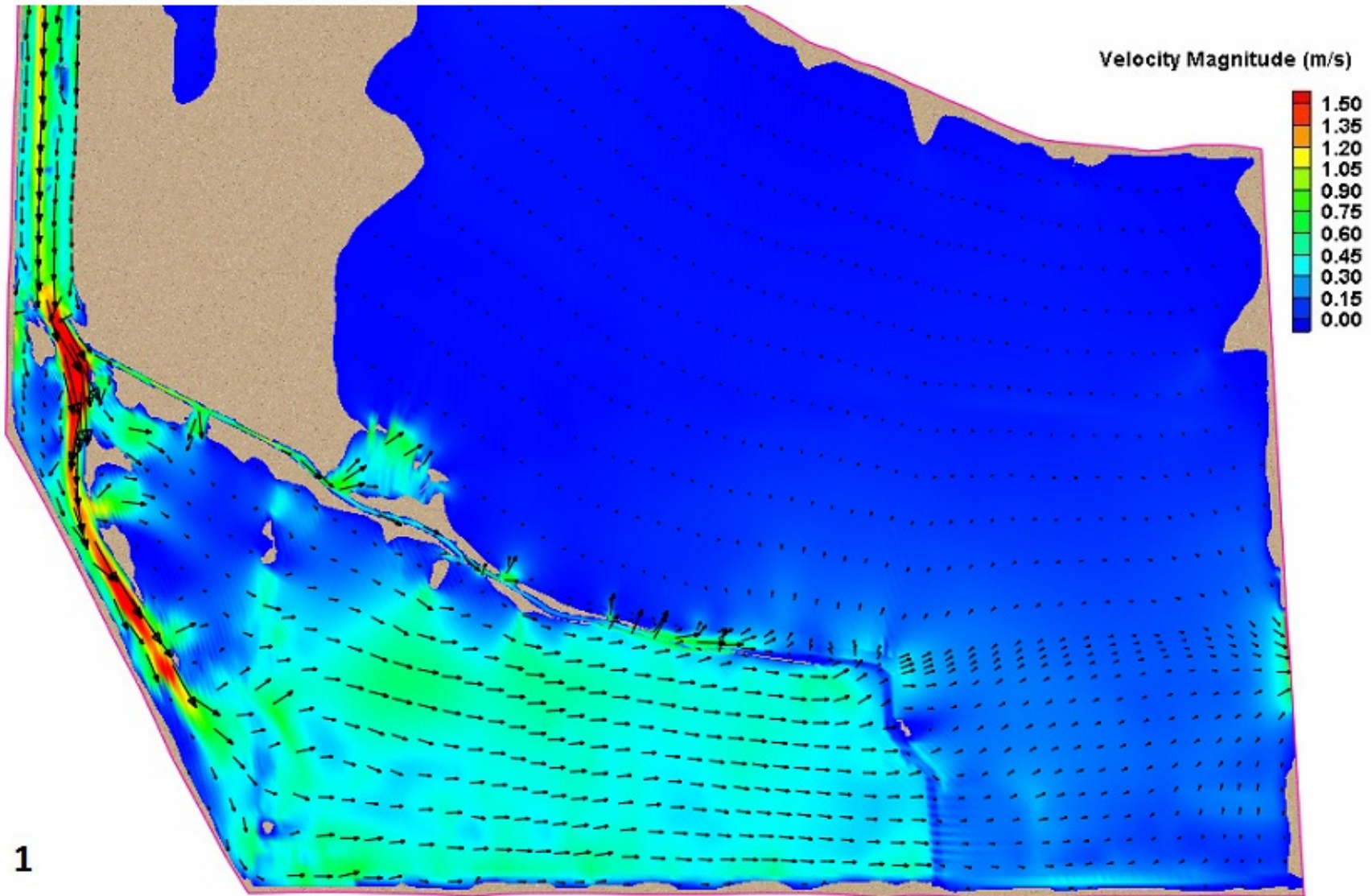


Figure 4.35 CCSB validation velocity magnitude result with scaled directional vectors, at selected time 1 of 23-27 March 2011 event

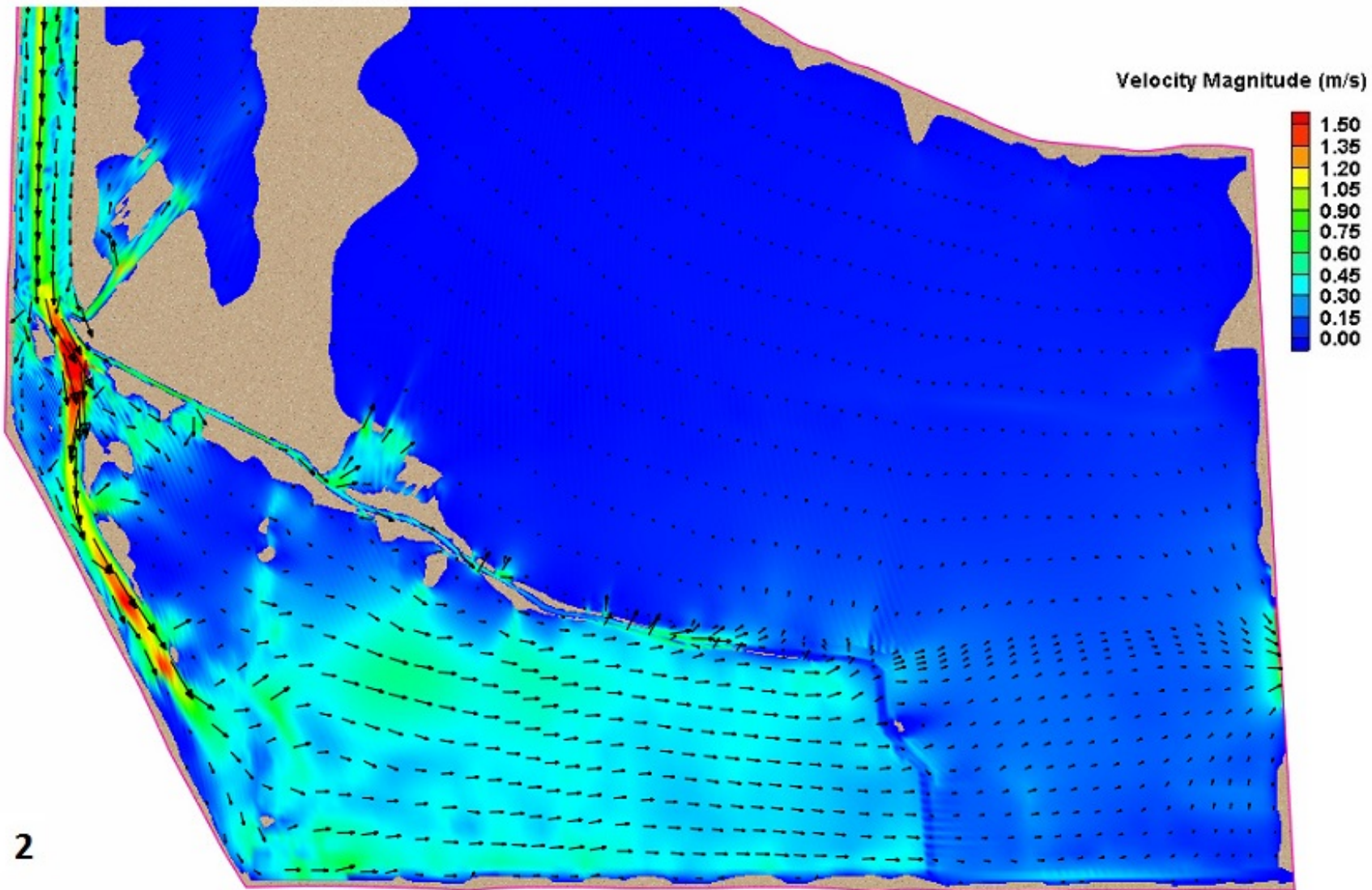


Figure 4.36 CCSB validation velocity magnitude result with scaled directional vectors, at selected time 2 of 23-27 March 2011 event

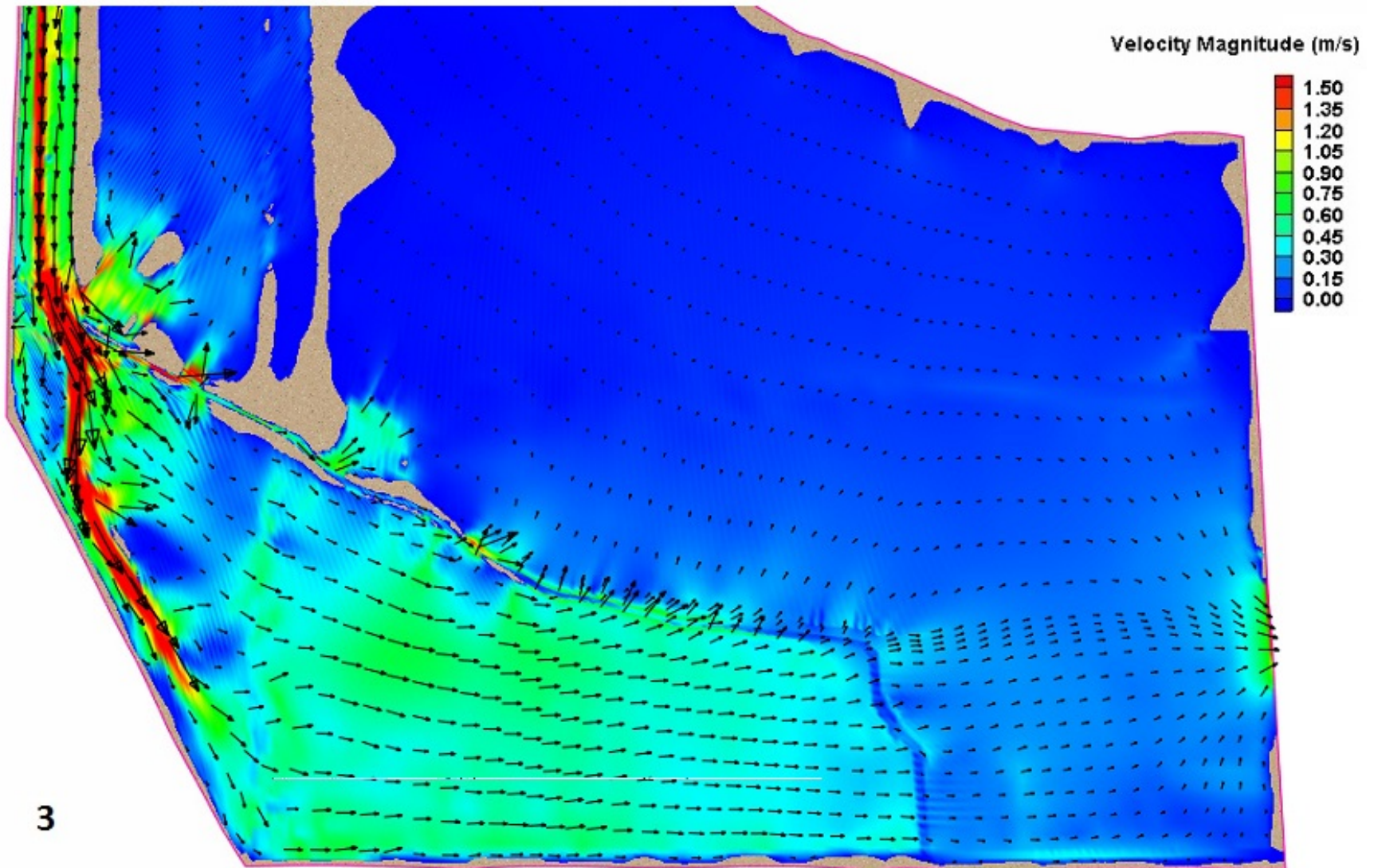
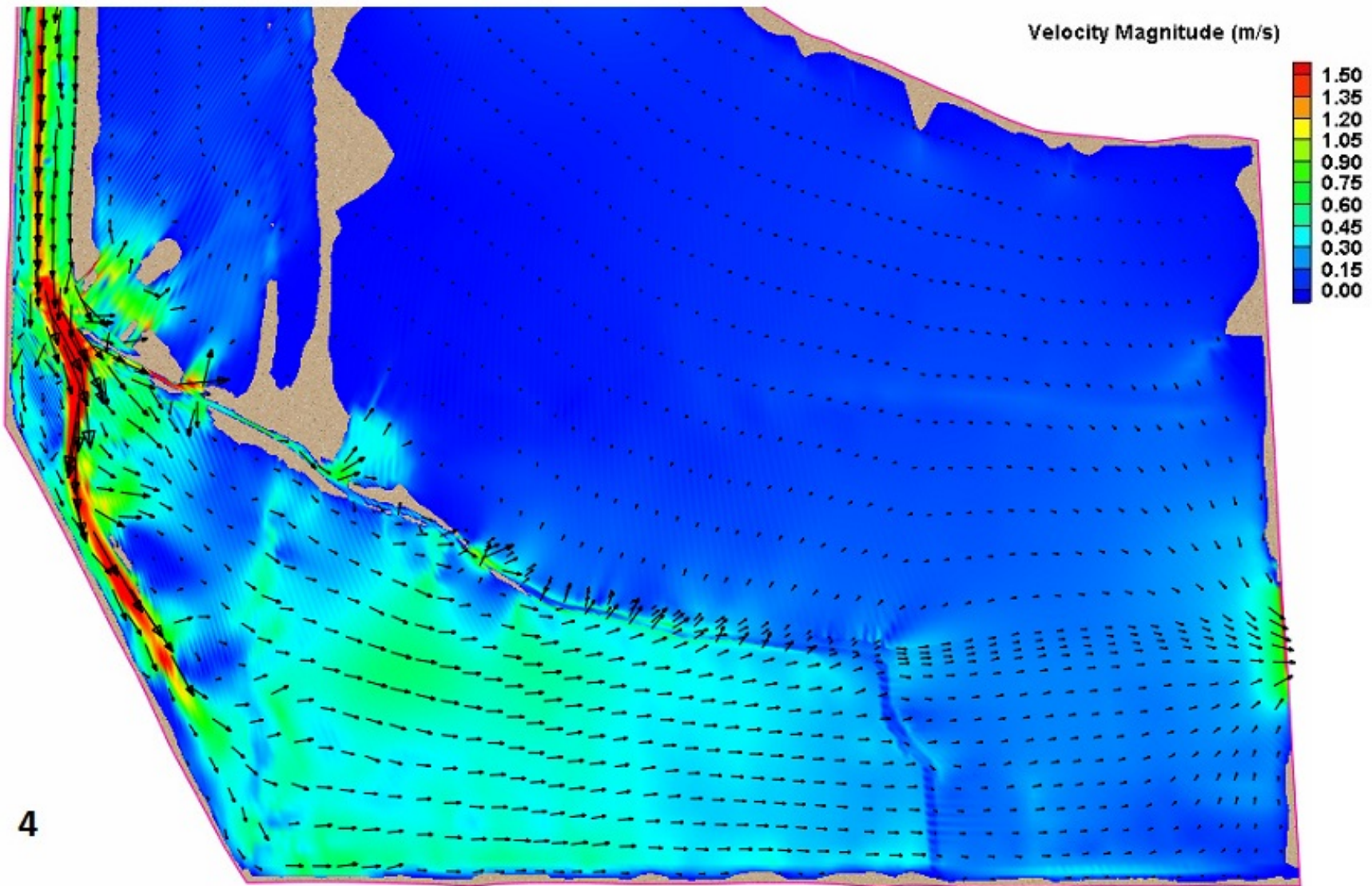


Figure 4.37 CCSB validation velocity magnitude result with scaled directional vectors, at selected time 3 (peak flow) of 23-27 March 2011 event



4

Figure 4.38 CCSB validation velocity magnitude result with scaled directional vectors, at selected time 4 of 23-27 March 2011 event

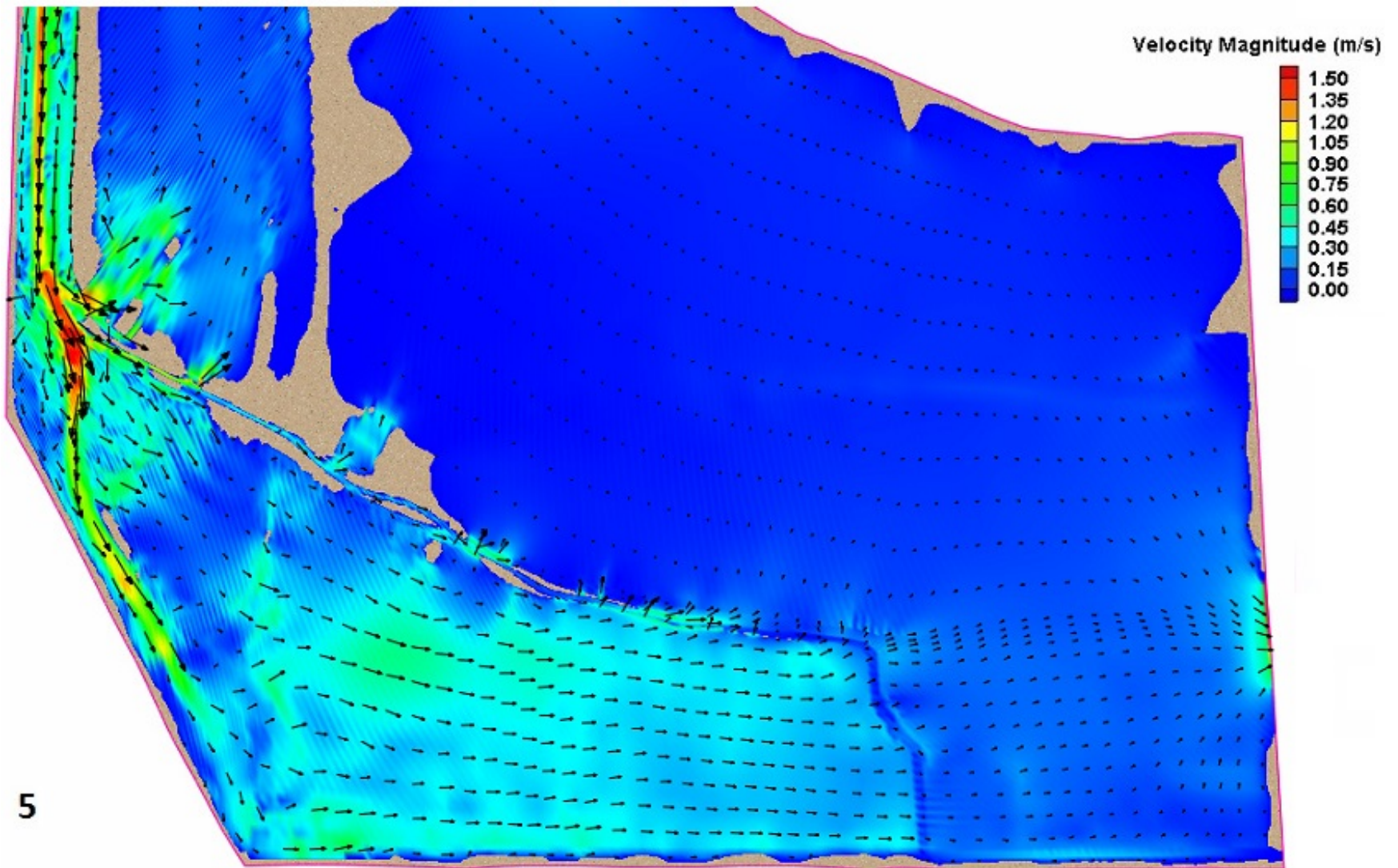


Figure 4.39 CCSB validation velocity magnitude result with scaled directional vectors, at selected time 5 of 23-27 March 2011 event

## 5 REFERENCES

- Brazelton, W. (2010). "Rating Curve for Cache Creek Settling Basin Weir" EMAIL to Kara Carr. April 21, 2010.
- De Vriend, D.J., (1999) Flow measurements in a Curved Rectangular Channel, Laboratory of Fluid Mechanics, Department of Civil Engineering, Delft University of Technology, Internal report no. 9-79.
- Engelund, F. and Hansen, E. (1967). "A monograph on Sediment Transport in Alluvial Streams". Teknisk Forlag, Copenhagen, Denmark.
- Garbrecht, J., Kuhnle, R. and Alonson, C. (1995). "A Sediment Transport Capacity Formulation for Application to Large Channel Networks". Journal of Soil and Water Conservation 50(5), 527–529.
- Huang, Sui Liang (2007): "Effects of using different sediment transport formulae and methods of computing Manning's roughness coefficient on numerical modeling of sediment transport." Journal of Hydraulic Research, 45:3, 347-356
- Jia, Y., and Sam S.Y. Wang, 2001a. *CCHE2D: Two-dimensional Hydrodynamic and Sediment Transport Model for Unsteady Open Channel Flows Over Loose Bed*. Technical Rep. No. NCCHETR- 2001-1, National Center for Computational Hydroscience and Engineering, The University of Mississippi.  
<<http://www.ncche.olemiss.edu/sites/default/files/files/docs/cche2d/techmanual.pdf>>
- Jia, Y., and Sam S.Y. Wang, 2001b. *CCHE2D Verification and Validation Tests Documentation* Technical Rep. No. NCCHETR- 2001-2, National Center for Computational Hydroscience and Engineering, The University of Mississippi.  
<<http://www.ncche.olemiss.edu/sites/default/files/files/docs/cche2d/validation.pdf>>
- Kantoush, S.A., De Cesare, G., Boillat, J.-L., Schleiss, A.J., 2008. "Flow field investigation in a rectangular shallow reservoir using UVP, LSPIV and numerical modeling." Journal of Flow Measurement and Instrumentation 19 (3-4), 139-144.
- Mohanty, K. P., Dash, S. S., and Khatua, K. K. (2012). "Flow investigations in a wide meandering compound channel." International Journal of Hydraulic Engineering, 1(6), 83-94.
- Negm, A. M., Abdulaziz, T., Nassar, M., & Fathy, I. (2010). "Predication of life time span of High Aswan Dam Reservoir using CCHE2D simulation

- model." In Proceeding 14th International Water Technology Conference (pp. 611-626).
- Newton, C.T., 1951, "An experimental investigation of bed degradation in an open channel", Transactions of the Boston Society of Civil Engineers, (pp. 28-60).
- Proffit, G.T. and A.J. Sutherland, (1983). "Transport of Non-uniform Sediment". Journal of Hydraulic Research 21(1), 33-43.
- Rajaratnam, N. and Ahmadai, R. 1981, "Hydraulics of channels with flood-plains", Journal of Hydraulic Research, IAHR, Vol. 19, No. 1, (pp. 43-60).
- Rijn, L. C. van (1986). Manual sediment transport measurements. Delft, The Netherlands: Delft Hydraulics Laboratory
- Soni, J. P. (1981). Laboratory study of aggradation in alluvial channels. *Journal of Hydrology*, 49(1), 87-106.
- Thayer, R. (2009) "Cache Creek Nature Preserve." Putah and Cache: A Thinking Mammals Guide to the Watershed. University of California, Davis. June 8, 2009.  
<[http://bioregion.ucdavis.edu/book/13\\_Lower\\_Cache\\_Creek/13\\_03\\_circ\\_c\\_cnp.html](http://bioregion.ucdavis.edu/book/13_Lower_Cache_Creek/13_03_circ_c_cnp.html)>
- Wang Sam S.Y., and Hu, K.K., 1992 "Improved methodology for formulating finite-element hydrodynamic models", In T,J, Chung, (ed) Finite Element in Fluids, Volume 8, Hemisphere Publication Cooperation, pp 457-478.
- Wu Weiming, and Sam S.Y. Wang (1999). "Movable Bed Roughness in Alluvial Rivers." Journal of Hydraulic Engineering, ASCE, Vol. 125, No.12, pp.1309-1312.
- Wu, Weiming, Sam S.Y. Wang, Y. F. Jia, (2000). "Non-Uniform Sediment Transport in Alluvial Rivers". Journal of Hydraulic Research, 38(6).

## APPENDIX



Figure A.0.1 Dr. Ercan and Dr. Carr on the Sacramento River, ADCP Trial Run December 13, 2013



Figure A.0.2 Tracker Guide V-14 Boat purchased for sediment and velocity measurements within the CCSB



Figure A.0.3 ADCP transmitter and float

**Cache Creek Settling Basin / Yolo Bypass Project  
Contract No. 4600010003**

**Cache Creek Settling Basin Trap Efficiency Study  
Progress Report  
May 1, 2014 – June 15, 2015**

Prepared for

**California Department of Water Resources**

Prepared By

Kara Carr  
Ali Ercan  
Tongbi Tu  
Hossein Bandeh  
M. Levent Kavvas (Principal Investigator)

**UC Davis J. A. Hydraulics Laboratory**

Department of Civil and Environmental Engineering  
University of California, Davis  
One Shields Avenue  
Davis, CA 95616

**June 15, 2015  
Revised September 23, 2015**

## TABLE OF CONTENTS

Table of Contents .....	2
List of Figures.....	3
List of Tables.....	5
1. Introduction .....	6
1.1. Background.....	7
1.2. Objective .....	8
2. Flow Sampling by UCDJ AHL .....	8
2.1. Flow Inundation Observations.....	12
3. CCSB Flow and Sediment Transport Simulations.....	14
3.1. Sediment Inflow Boundary Condition .....	15
3.2. Trap Efficiency of Current Bathymetry .....	18
3.3. Modification Scenarios .....	19
3.3.1. Alternative A .....	19
3.3.2. Alternative B .....	20
3.3.3. Alternative C .....	20
3.3.4. Alternative D .....	20
4. Future Work .....	32
5. References.....	33

## LIST OF FIGURES

Figure 2.1 ADCP velocity measurement transects taken December 18, 2014. Labeled with measurement start and end time. Relative location within CCSB shown in upper left. ....	9
Figure 2.2 ADCP velocity transect contours a) transect 1 b) transect 2 c) transect 3. ...	10
Figure 2.3 ADCP velocity transect contours a) transect 4 b) transect 5 c) transect 6. ...	11
Figure 2.4 ADCP velocity transect contours a) transect 7 b) transect 8. ....	12
Figure 2.5 Simulated water depth contour (left) representing simulated inundation and corresponding location of photographs showing view to the east (top right) and south (bottom right) from the northern levee. ....	13
Figure 2.6 Simulated water depth contour (left) representing simulated inundation and corresponding location of photographs showing view to the south (top right) and southeast (bottom right) from the northern levee. ....	13
Figure 2.7 Simulated water depth contour (left) representing simulated inundation and corresponding location of photographs showing view to the south (top right) and northwest (bottom right) from the northern levee. ....	14
Figure 3.1 Upstream flow boundary condition for all modeled sediment transport scenarios. ....	15
Figure 3.2 1986 USACE suspended sediment load regression, and 1997 USACE total sediment load regression. ....	17
Figure 3.3 Upstream sediment boundary condition for all modeled sediment transport scenarios. ....	18
Figure 3.4 Bed elevation contour map, Alternative A, current bathymetry. ....	22
Figure 3.5 Bed elevation contour map, Alternative B, weir raised 6 feet. ....	22
Figure 3.6 Bed elevation contour map, Alternative C, 400 foot section removed from end of training channel. ....	23
Figure 3.7 Bed elevation contour map, Alternative D, weir raised 6 feet, and 400 foot section removed from end of training channel. ....	23
Figure 3.8 Bedload transport rate for time steps 1-5, Alternative A. Minimum transport rate (blue) is 0.0 kg/s, maximum transport rate (red) is 0.80 kg/s. ....	24
Figure 3.9 Suspended sediment concentration for time steps 1-5, Alternative A. Minimum concentration (blue) is 0.0 kg/m <sup>3</sup> , maximum concentration (red) is 0.50 kg/m <sup>3</sup> . ....	25
Figure 3.10 Bedload transport rate for time steps 1-5, Alternative B. Minimum transport rate (blue) is 0.0 kg/s, maximum transport rate (red) is 0.80 kg/s. ....	26
Figure 3.11 Suspended sediment concentration for time steps 1-5, Alternative B. Minimum concentration (blue) is 0.0 kg/m <sup>3</sup> , maximum concentration (red) is 0.50 kg/m <sup>3</sup> . ....	27
Figure 3.12 Bedload transport rate for time steps 1-5, Alternative C. Minimum transport rate (blue) is 0.0 kg/s, maximum transport rate (red) is 0.80 kg/s. ....	28
Figure 3.13 Suspended sediment concentration for time steps 1-5, Alternative C. Minimum concentration (blue) is 0.0 kg/m <sup>3</sup> , maximum concentration (red) is 0.50 kg/m <sup>3</sup> . ....	29
Figure 3.14 Bedload transport rate for time steps 1-5, Alternative C. Minimum transport rate (blue) is 0.0 kg/s, maximum transport rate (red) is 0.80 kg/s. ....	30

Figure 3.15 Suspended sediment concentration for time steps 1-5, Alternative D.  
Minimum concentration (blue) is 0.0 kg/m<sup>3</sup>, maximum concentration (red) is 0.50 kg/m<sup>3</sup>.  
..... 31

## LIST OF TABLES

Table 2.1	Transect names, timing, and SNR.....	9
Table 3.1	NRMSE and Nash Coefficient for calibration and validation simulations.....	15
Table 3.2	Lustig and Busch (1967) Total sediment-discharge data from Cache Creek at the Yolo Sediment stations.....	16
Table 3.3	1997 USACE memorandum total sediment load rating curve data. ....	17
Table 3.4	Sediment trap efficiency under the current bathymetric condition for three scenarios of CCHE2D parameter definition.....	19
Table 3.5	Trap efficiency percentage of bathymetric modification scenarios. ....	21

## ACKNOWLEDGMENTS

We thank the personnel at the U.S Geological Survey's (USGS) Sacramento Field Office and the Sacramento Water Science Center for the sharing of sediment and flow data, as well as valuable input on sampling procedures and CCSB conditions.

This research was funded through a contract with the Department of Water Resources (Contract No. 4600010003). We thank Mr. Frederick Gius and Kevin Brown for their insights and support, and Mr. John Nosacka, who coordinated the efforts and resources between Department of Water Resources (DWR) and UC Davis J. Amorocho Hydraulics Laboratory, and aided in the implementation of Acoustic Doppler Current Profiler (ADCP) measurements during the study.

## 1. INTRODUCTION

This report describes the Cache Creek Settling Basin (CCSB) / Yolo Bypass Project progress during May 1, 2014, through June 15th, 2015. Objectives for this year of the study included:

Year II Objective 1. Field measurement sampling program was to be continued in Year II in the wet season to enable sampling of 2-dimensional velocity and discharge along transects as needed and decided by Objective 3 of Year I.

Samples were taken for a single discharge event, representing the first effort of field sampling in the CCSB. Due to the drought conditions in California, this event was one of the rare opportunities to take samples from the CCSB during the second year of the project. The velocity transects will be incorporated as validation data for the CCHE2D simulation of the corresponding flow event.

Year II Objective 2. Similar to Objective 2 of Year I, field measurements provided by USGS were to be catalogued and incorporated into the 2-D flow and sediment transport models for updated calibration and validation.

Available data were catalogued and stored in our data bank. Of particular importance is the December 11-12, 2014, storm event, which had a maximum measured discharge of 17,800 cubic feet per second (cfs) (provisional data via (<http://nwis.waterdata.usgs.gov/> site 11452500). The USGS has not yet provided the associated water surface elevation, discharge, and sediment data for the Road 102 site 11452600 (Cache C Inflow to Settling Basin Nr Yolo Ca), or Site C within the CCSB (384041121402601). Provisional gage height, discharge and sediment concentration data are available for the Cache Creek at Yolo gauge (11452500). Provisional gage height, discharge and turbidity data are available for the overflow weir (11452800).

Year II Objective 3. 2-D flow and sediment transport models results were to be analyzed utilizing all the available flow and sediment data, and further data gaps would be noted.

The objective was met. Samples of coincident flow and sediment, taken periodically over the duration of a storm event are required to aid in calibration and

validation of the sediment transport model. Further sediment grain size distribution and sediment concentration at the inlet and outlet of the CCSB are also necessary to support the sediment transport model. Preliminary trap efficiency values are estimated based on the available sediment rating curve at Cache Creek at Yolo and under the default sediment transport model settings, which will be calibrated and validated when the CCSB survey, as planned in the summer of 2015, is available. The detailed survey of the basin is required for calibration of the sediment transport model parameters.

### **1.1. Background**

CCSB, located two miles east of the City of Woodland, California, was originally built by the United States Army Corp of Engineers (USACE) in 1938. The primary function of the CCSB is to remove a significant portion of the sediment load from Cache Creek to avoid its deposition in the Yolo Bypass, thereby preserving the capacity of the bypass for conveying flood flows. The Yolo Bypass serves to protect Sacramento and surrounding areas from flooding with a design flow of 216,000 cfs. Cache Creek delivers sediment to the Settling Basin during each wet year, and per the Central Valley Regional Water Quality Control Board (CVRWQCB) is a source of mercury to the San Francisco Bay-Delta. In addition to preserving the flood flow capacity of the Yolo Bypass; entrapment of sediment in the Basin is instrumental in diminishing the mercury load to the San Francisco Bay-Delta, making the Basin fundamental in preserving water quality. The sediment entering the CCSB is a legacy of the California Gold Rush and mercury mining of the naturally occurring “economically recoverable deposits of mercury” in California's Coastal range (Domagalski et al. 2004). A number of abandoned, un-reclaimed and partially reclaimed mercury mines are situated in the Cache Creek watershed. Furthermore, aggregate mining of Cache Creek has increased channel incision and sediment loading in the creek (Thayer, 2009).

The CCSB has been modified by USACE many times since 1938 to redistribute sediment settling patterns and increase sediment storage capacity. From 1991 to 1993, the Basin was radically altered. Surrounding levees were raised 12 feet, the training channel was relocated, and a new outlet weir was built 5 feet higher than the previous weir, representing the current conditions. At the time of alteration USACE believed the Basin would retain 340 acre-feet of sediment per year, at a 55% trap efficiency, and that an additional 50 years of sediment storage was being provided. This postulated trap efficiency is based on an action plan outlined in the USACE 2007 Cache Creek Settling Basin DRAFT Operations and Maintenance Manual, in which the outlet weir is to be raised 6-feet at year 25 (2018) of the project, or when the trap-efficiency becomes 30%. Also beginning in year 25 of the project, 400-foot sections of the interior training levee will be removed every five years, starting with a section 1100 feet upstream from the current terminus of the training channel. Each subsequent 400-foot section will be removed 1100 feet upstream from the section that is removed previously.

To assess whether the trap-efficiency and sedimentation rate in the Basin are meeting design requirements set forth by USACE, the personnel at UC Davis J. Amorocho Hydraulics Laboratory (UCDJHL) began evaluating the settling basin trap efficiency through application of the National Center for Computational Hydroscience and

Engineering's CCHE2D model of two-dimensional depth averaged flow and sediment transport. The evaluation was conducted with respect to the current Settling Basin design as defined by 2006 and 2008 surveys of the Basin, utilizing field measurements of suspended sediment and flow into, within, and out of the CCSB as provided by USGS, as well as by the physical sedimentation modeling performed at the UCDJ AHL in 2009.

### **1.2. Objective**

The major objectives of this study are:

i. to perform field measurements by UCDJ AHL staff of 2-D velocities and flow within the Settling Basin to be incorporated in calibration and validation of 2-D flow and sediment transport models. Because of the 2-D nature of flow in the basin and the desire to capture the 2-D spread of sediment within the basin, it is critical to capture internal transects, as well as inflow and outflow sections. Additionally, field measurements performed by UCDJ AHL staff will provide a dense sampling of flow and velocity during storm events, capturing multiple samples as a storm hydrograph passes through the Basin.

ii. to incorporate flow and suspended sediment measurements provided by USGS to calibrate and validate the 2-D flow and sediment transport models. Available flow and sediment measurements are insufficient to support the simulations' claim of loading due to the lack of concurrent (flow and sediment) data into and out of the basin. It is essential for calibration and validation of the models that these sediment measurements be concurrent with velocity/flow measurements. Additional data will ultimately result in a more reliable estimate of the settling basin trap efficiency with respect to current and future settling basin design. Additional concurrent data will also serve to characterize the sediment rating curve for flows over 12,000 cfs, a region that is currently under-defined.

Furthermore, UCDJ AHL will provide DWR with a method of reevaluating sedimentation for any further augmentation proposals. Estimates of trap efficiency will be produced for a range of possible future climate conditions. The mean trap efficiency as well as the 95% confidence bands will be provided.

## **2. FLOW SAMPLING BY UCDJ AHL**

To increase accuracy of velocity representations in the 2-dimensional flow and sediment model of the CCSB, a flow measurement campaign was initiated by the UCDJ AHL. Due to lack of storm events during this study period, only one visit was made to measure velocity in the CCSB. Dr. Ali Ercan, Dr. Kara Carr, and Mr. John Nosacka, visited the basin on Dec 18, 2014, to collect transects of ADCP flow velocity measurements. The eight transect locations, identified by their time stamps in Figure 2.1, were chosen based on accessibility and flow conditions. Location mapping was made possible by a Global Positioning System (GPS) mounted on the ADCP unit. Simulations of the corresponding flow event are ongoing, with preliminary inundation comparisons

presented in the next section. Velocity measurements may be utilized in subsequent modeling efforts, if necessary. .

For ease of reference, the ADCP measurement transects are named in order of their measurement, as shown in Table 2.1. Included in Table 2.1 is the signal to noise ratio (SNR) for the measured velocities. SNR, given as the mean of the measured values divided by their standard deviation, signifies whether the measured values are significantly different from zero. While the SNR values are all greater than one, they are fairly low as a result of small water velocities relative to boat velocities. The velocity contour plots of the 8 transects are depicted in Figures 2.2-2.4.

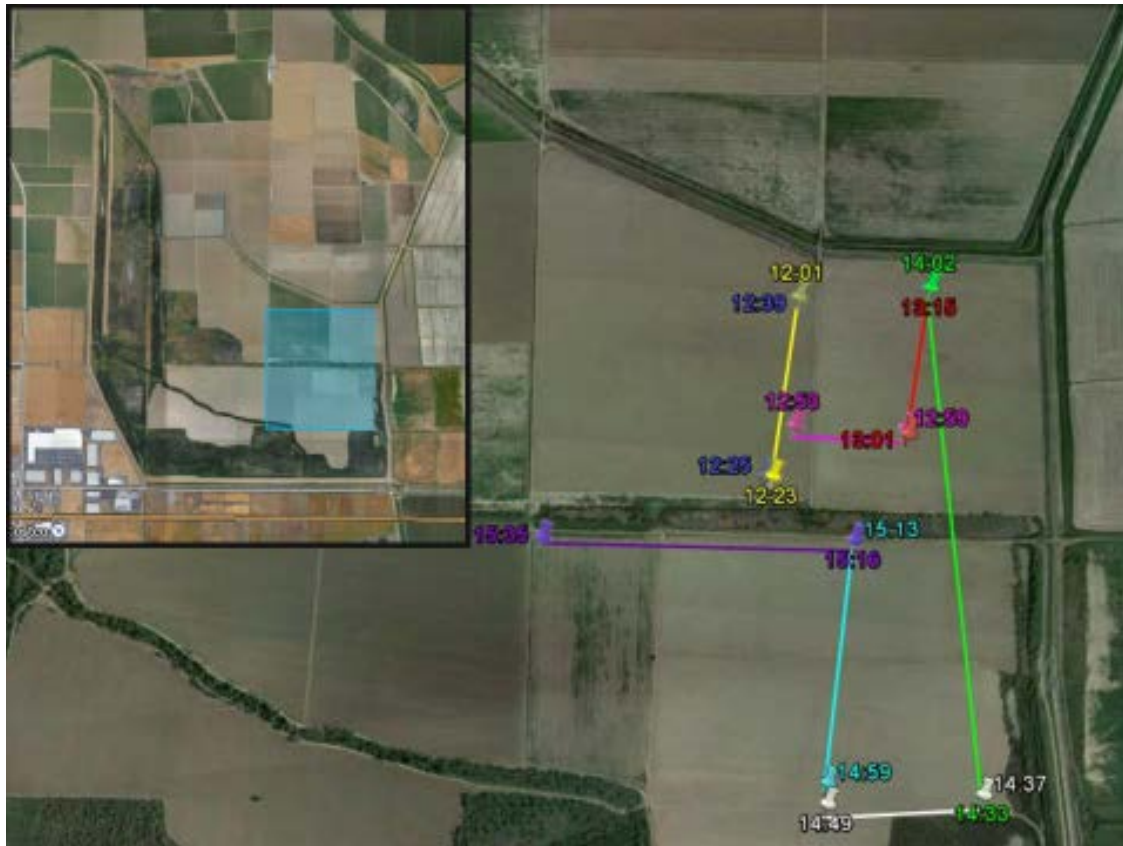


Figure 2.1 ADCP velocity measurement transects taken December 18, 2014. Labeled with measurement start and end time. Relative location within CCSB shown in upper left.

Table 2.1 Transect names, timing, and SNR

Transect Name	Start Time	End Time	SNR
1	12:01	12:23	1.84
2	12:25	12:39	1.58
3	12:53	12:59	1.76
4	13:01	13:15	1.88
5	14:02	14:33	1.65
6	14:37	14:49	1.81
7	14:59	15:13	1.85
8	15:16	15:35	1.70

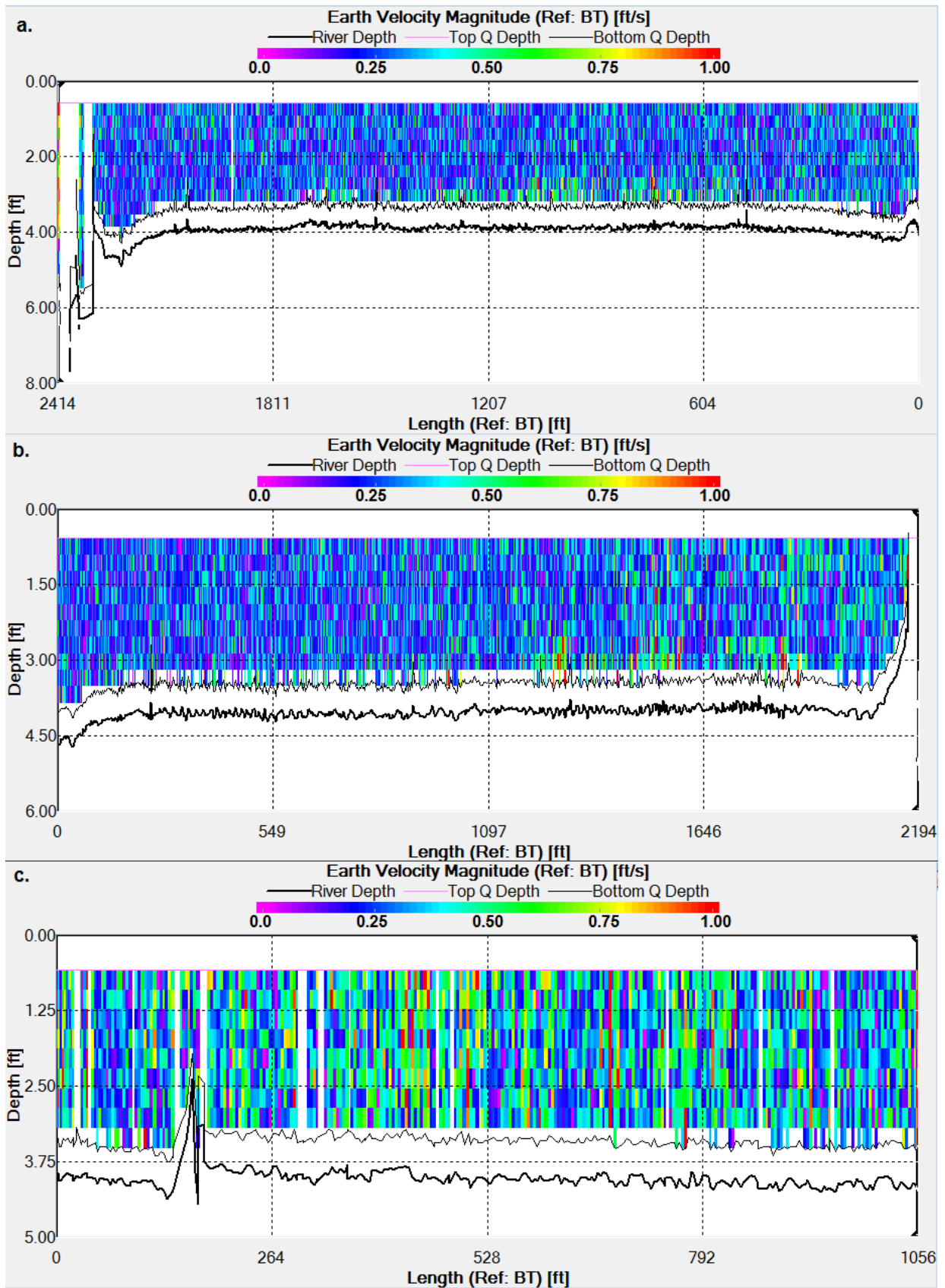


Figure 2.2 ADCP velocity transect contours a) transect 1 b) transect 2 c) transect 3.

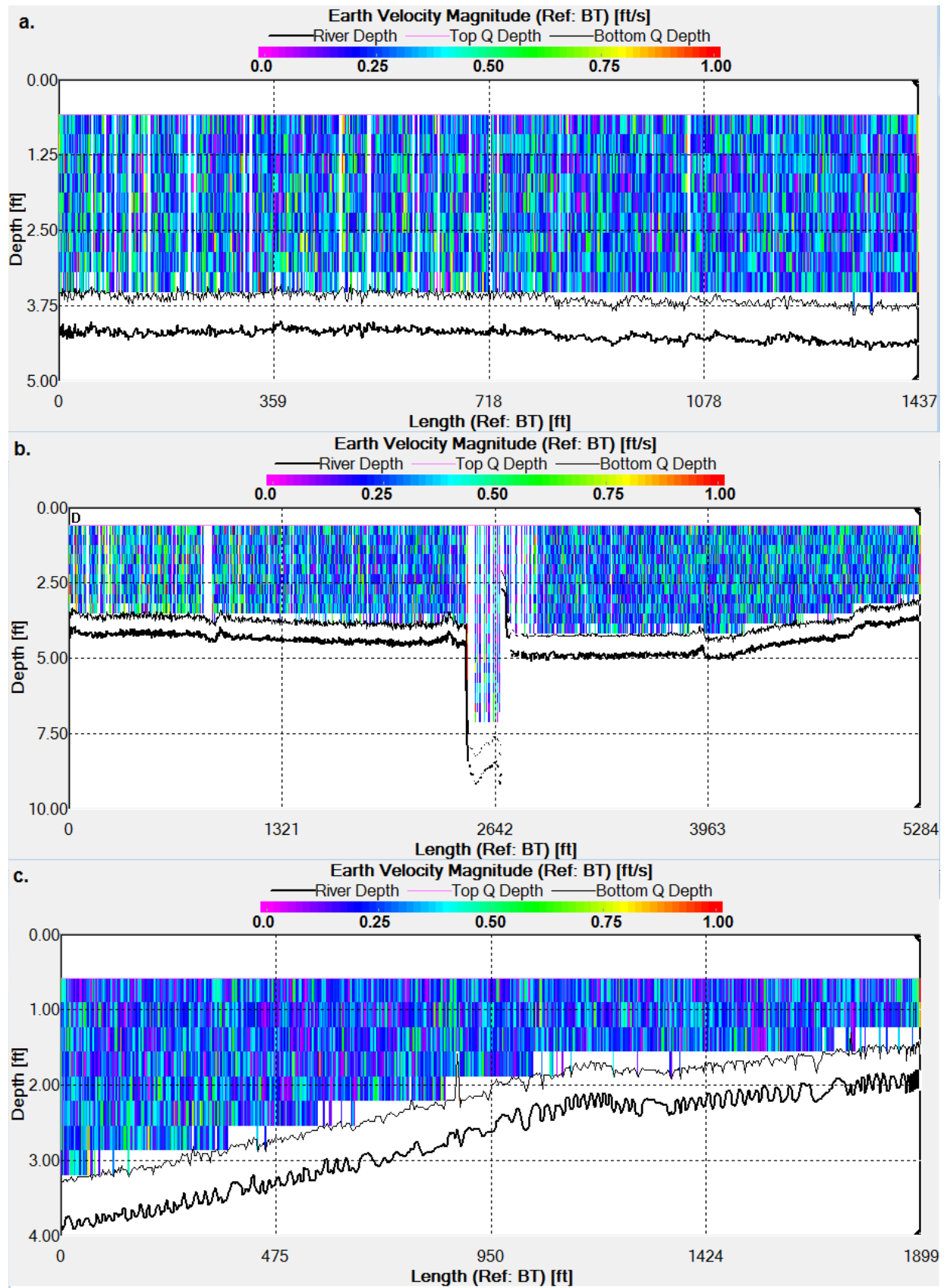


Figure 2.3 ADCP velocity transect contours a) transect 4 b) transect 5 c) transect 6.

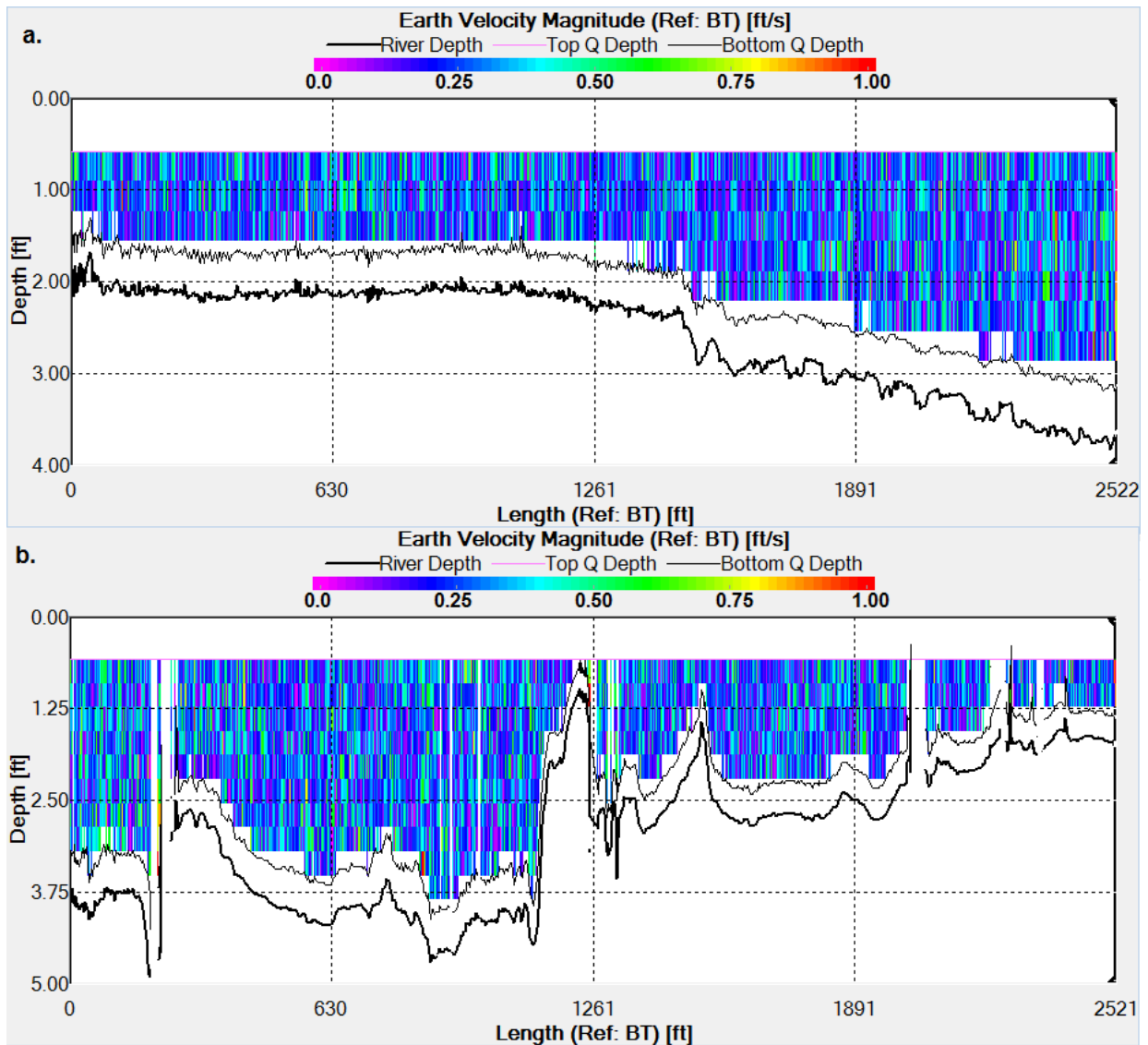


Figure 2.4 ADCP velocity transect contours a) transect 7 b) transect 8.

## 2.1. Flow Inundation Observations

Flow inundation observations were made during the December 18, 2014 site visit. A number of pictures were taken at three recorded geolocations to compare field inundation conditions in the northern section of the basin with simulated results. Water depth results from the numerical simulation which indicate inundation extent are displayed on Figures 2.5 – 2.7. Also in the figures are photographs from indicated areas, showing actual inundation of the northernmost section of the basin. Under visual inspection, simulation and field conditions corresponded well.

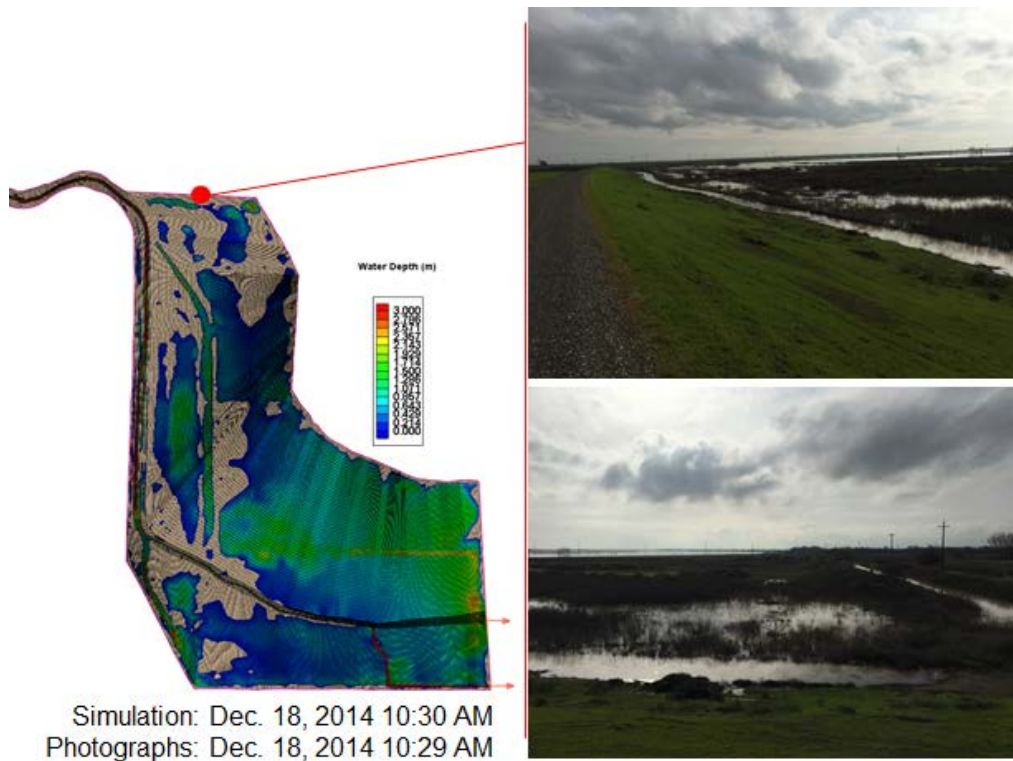


Figure 2.5 Simulated water depth contour (left) representing simulated inundation and corresponding location of photographs showing view to the east (top right) and south (bottom right) from the northern levee.

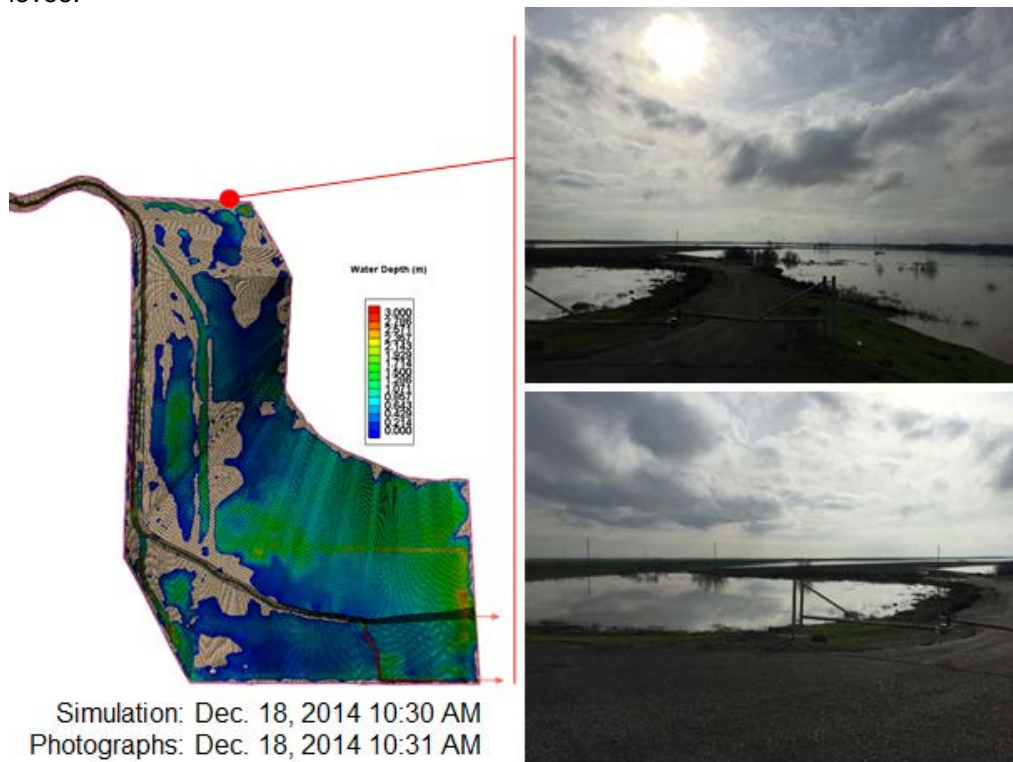


Figure 2.6 Simulated water depth contour (left) representing simulated inundation and corresponding location of photographs showing view to the south (top right) and southeast (bottom right) from the northern levee.

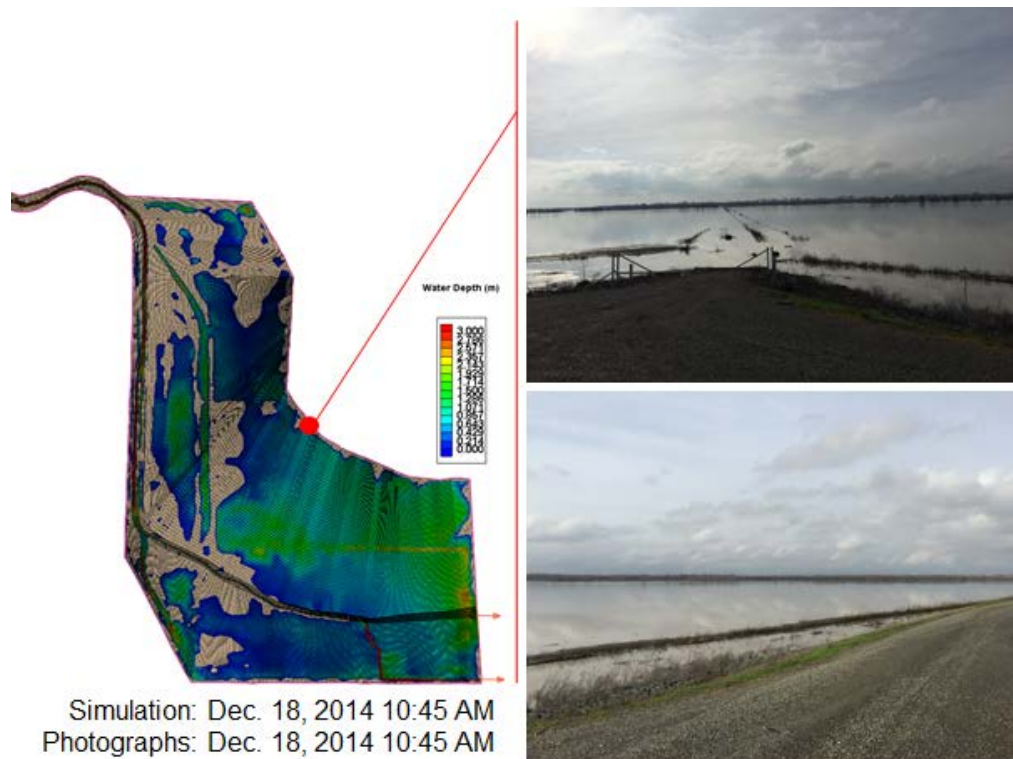


Figure 2.7 Simulated water depth contour (left) representing simulated inundation and corresponding location of photographs showing view to the south (top right) and northwest (bottom right) from the northern levee.

### 3. CCSB FLOW AND SEDIMENT TRANSPORT SIMULATIONS

The validated flow model, used in the numerical simulations presented herein, is described in detail in the CCSB Trap Efficiency Study Progress Report dated May 1, 2014 (Carr et al. 2014). Each numerical simulation presented herein was performed using the CCHE2D model, developed at the National Center for Computational Hydroscience and Engineering at the University of Mississippi. CCHE2D is a two-dimensional depth averaged unsteady flow and sediment transport model that simulates the movement of water, and both cohesive and non-cohesive sediment. Performance of the calibrated and validated model, with respect to flow, can be inferred from the normalized root mean square error, and Nash-Sutcliffe Model Efficiency coefficient (Nash Coefficient) contained in Table 3.1. Note that the calibration of the model was performed utilizing water surface elevations at the Rd 102 gauge only (USGS gauge 11452600), allowing for validation of model performance through comparison of water surface elevation results at two other gauging stations in the basin, Site C (USGS site 384041121402601) and the Overflow Weir (USGS gauge 11452800). The hydrodynamic model performed very well, with good correspondence in water depths distributed both spatially and temporally.

Sediment transport simulations were performed utilizing upstream flow boundary data taken from instantaneous flow data at the Cache Creek at Yolo gauge (source: <http://nwis.waterdata.usgs.gov>, USGS 11452500) from March 18, 2011, through March

22, 2011. These data correspond to the flow validation simulation that has the highest flow magnitude fully simulated by the model at the time of this report. The simulated hydrograph is displayed in Figure 3.1. The simulations are not calibrated with respect to sediment transport, and therefore results presented herein are preliminary, and subject to change following sediment transport calibration and validation. Calibration will be performed upon receipt of the 2014/2015 survey data.

Table 3.1 NRMSE and Nash Coefficient for calibration and validation simulations.

Event	18-22 March 2011			23-27 March 2011		
Peak Flow at Cache Creek at Yolo	15,900 cfs			14,300 cfs		
Mode	Calibration	Validation		Validation		
Location	Rd 102	Site C	Weir	Rd 102	Site C	Weir
NRMSE	0.07	0.11	0.09	0.12	0.07	0.08
Nash Coefficient	0.93	0.83	0.90	0.69	0.90	0.87

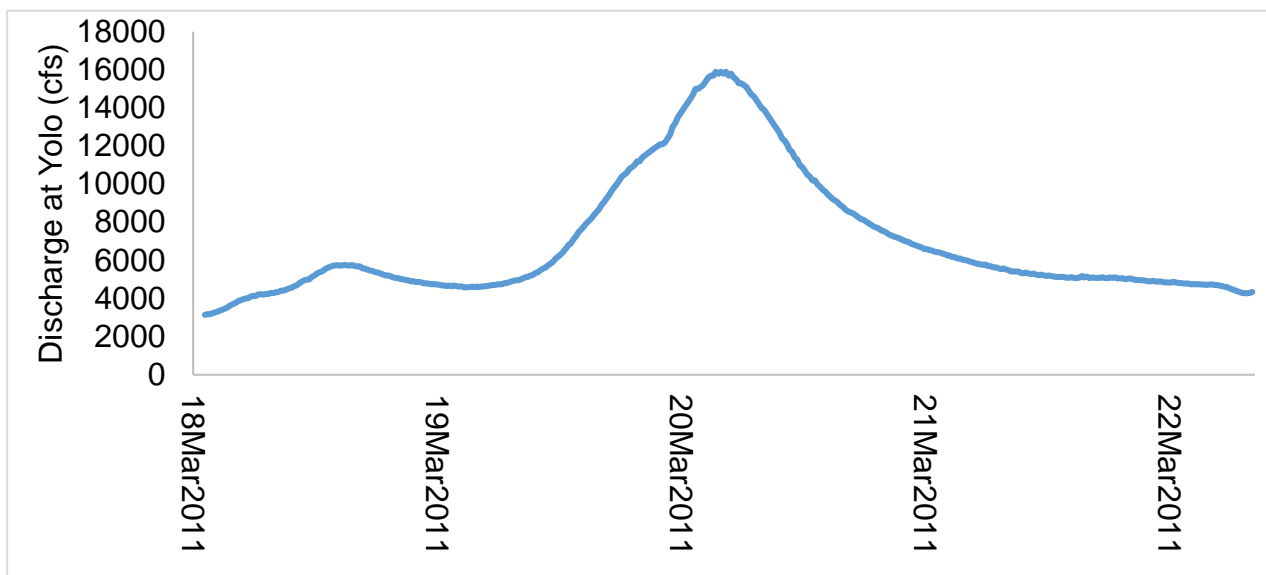


Figure 3.1 Upstream flow boundary condition for all modeled sediment transport scenarios.

### 3.1. Sediment Inflow Boundary Condition

Sediment loading conditions for the simulations were assigned using the total sediment load rating curve developed by USACE and described in the 1997 HEC-6 Analysis Technical Memorandum (USACE 1997). The memorandum states that the rating curve is a regression line based on a set of instantaneous suspended sediment samples collected by the USGS between 1943 and 1971 at the Cache Creek at Yolo station. Because the USACE curve provides a single sediment load per discharge magnitude, without reference to time of occurrence (rising or falling limb), some uncertainties are introduced. Typically sediment loads are higher on the rising limb of a hydrograph than

for sediment loads for an equivalent discharge on the falling limb. The averaging effect of disregarding the time-signature for data used in the curve introduces error, especially in simulations of Cache Creek where duration of the storm event is short, and the flow changes rapidly. Long term simulations, are less sensitive to this averaging effect.

More importantly, the 1997 USACE memorandum mentions dependence on the regression line defined in the 1986 USACE Cache Creek Settling Basin: Final General Design Memorandum. The data from which this regression was created are not included in the referenced work. Historical data on the USGS website contain only 121 sediment samples for the date ranges specified in the reference. Of those, 108 are for flows less than 10,000 cfs, 10 are for flows between 10,000 – 15,000 cfs, and only 3 are available for flows over 15,000 cfs. Therefore, there is inherent uncertainty in the rating curve regression for flows larger than 10,000 cfs. Additionally, the 1986 USACE regression represents suspended load only. However, the 1997 USACE memorandum expands the regression to include bedload, following the method outlined in Lustig and Busch (1967). Lustig and Busch (1967) determined the percentage of total load attributed to bedload, and related it to suspended load, using 7 instantaneous measurements of total and suspended load as shown in Table 3.2. The data, collected from 1959-1964, are limited to flow magnitudes under 13,000 cfs. The 1997 USACE memorandum applies the relation of bedload to suspended load to create a total load rating curve regression, the points defining the regression, as given in the memorandum, are listed in Table 3.3. Figure 3.2 includes the sediment rating curve regressions for the 1986 and 1997 USACE memorandums. The resulting sediment load hydrograph for the numerical simulations is provided in Figure 3.3.

Table 3.2 Lustig and Busch (1967) Total sediment-discharge data from Cache Creek at the Yolo Sediment stations.

Date	Instantaneous Water Discharge (cfs)	Mean Velocity (ft/sec)	Suspended Sediment Load (tons/day)	Bedload (tons/day)	Total Sediment Load (tons/day) <sup>1</sup>
15-Jan-1959	276	1.96	118	58	176
16-Feb-1959	12800	6.18	272700	6900	279600
17-Feb-1959	6000	5.07	65100	2130	67230
18-Mar-1959	109	1.65	4	18	22
3-Feb-1960	748	2.64	1293	257	1550
9-Feb-1960	7540	5.31	62700	5310	68010
28-Jan-1964	396	2.54	96	24	120

<sup>1</sup>. Total sediment load is related to instantaneous water discharge through application of the “modified Einstein method”. The method relates hydraulic geometry of the cross section, concentration of suspended sediment, and particle size distribution of suspended and bed material.

Table 3.3 1997 USACE memorandum total sediment load rating curve data.

Discharge (cfs)	Suspended Load (tons/day)	Bedload (tons/day)	Total Load (tons/day)
50	7	8	15
100	22	19	41
500	320	80	400
1000	1010	180	1190
5000	14450	920	15370
10000	45450	1890	47340
20000	143000	3700	146700
30000	279600	5700	285300
60000	879940	13400	893340

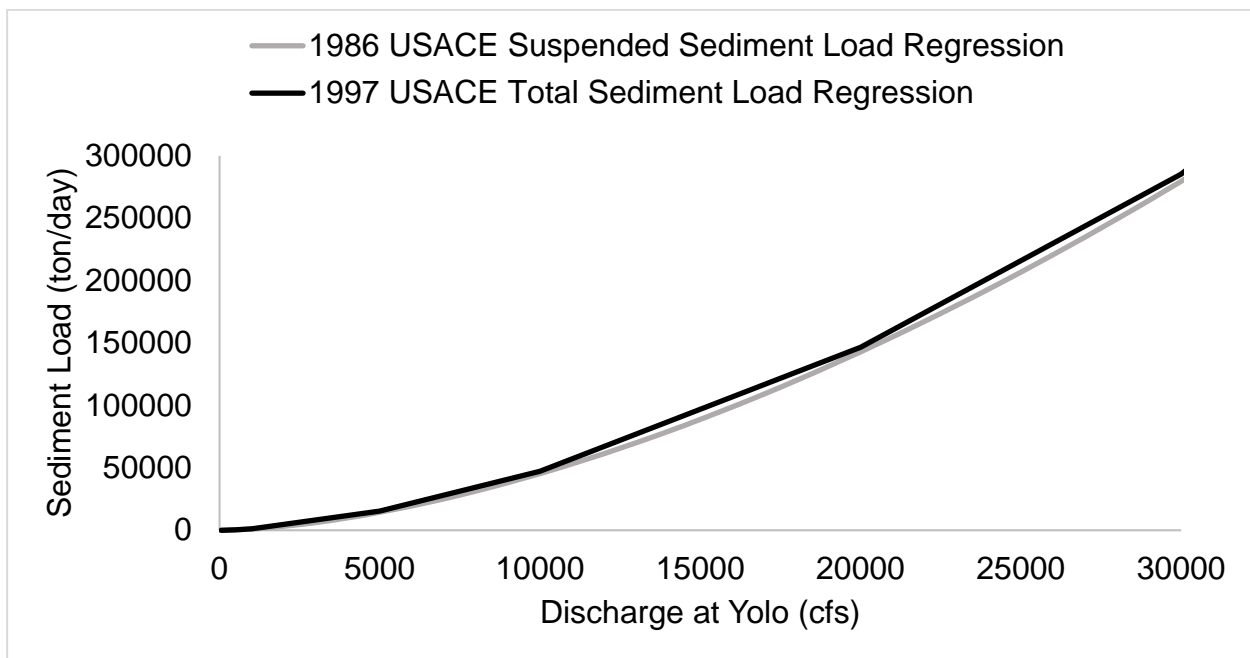


Figure 3.2 1986 USACE suspended sediment load regression, and 1997 USACE total sediment load regression.

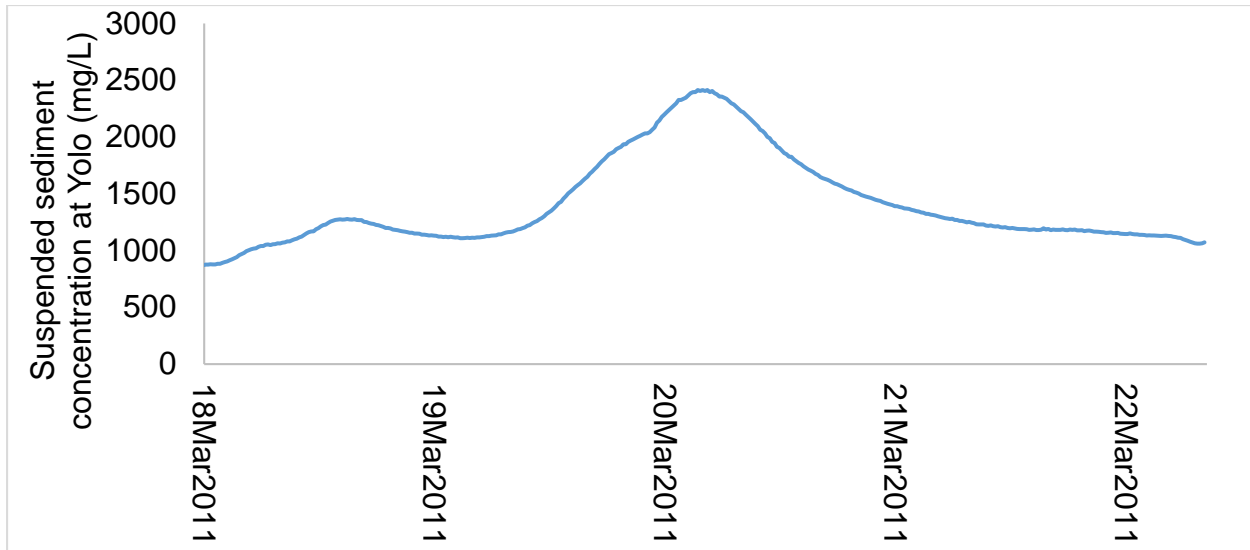


Figure 3.3 Upstream sediment boundary condition for all modeled sediment transport scenarios.

### **3.2. Trap Efficiency of Current Bathymetry**

Utilizing the CCHE2D model under the upstream boundary conditions described in Sections 3 and 3.1, simulations were run for the “current” bathymetric conditions of Cache Creek from Cache Creek at Yolo through the CCSB for 18-22 March 2011 period. The current condition is defined by surveys taken in 2006 and 2008.

A sensitivity analysis was run on the uncalibrated model to assess the reaction of CCHE2D to sediment transport parameters. The trap efficiency was calculated under three different scenarios. Scenario A uses the default sediment transport parameters of CCHE2D. The model defaults the suspended transport capacity coefficient to 1.0, and the sediment transport capacity equation to that described by the Wu, Wang, Jia method (Wu, 2001). Scenario B sets the sediment transport capacity coefficient to 0.9, and as Scenario A, uses the Wu, Wang, Jia method. Scenario B therefore has a suspended sediment transport capacity that is 90% of that for Scenario A. Scenario C was run with the suspended transport capacity coefficient set to 1.0, and the SEDTRA sediment transport capacity module was assigned. The SEDTRA module (Garbrecht et al. 1995) uses three transport relations for different size classes. The Laursen (1958) formula is used for size classes 0.010 mm to 0.25 mm, the Yang (1973) formula for size classes from 0.25 mm to 2.0 mm, and the Meyer-Peter and Mueller’s (1948) formula for size classes from 2.0 mm to 50.0 mm. For each simulation, the sediment bed grain size, and roughness solution method were set as outlined in the description of flow calibration in the CCSB Trap Efficiency Study Progress Report dated May 1, 2014. Trap efficiencies for the three different simulated scenarios of sediment transport under the current condition are provided in Table 3.4.

The trap efficiencies were calculated by determining the difference in the sediment inflow volume entering the CCSB at Rd 102 and that exiting the basin, over the entire simulation duration. When the suspended transport capacity coefficient was altered

from the default of 1.0 to 0.9, the trap efficiency changed, increasing by 15.6%. When the SEDTRA sediment transport equation was utilized instead of the default equation, the trap efficiency increased by 18.8%. The sensitivity analysis of the selection of the suspended transport capacity coefficient or the sediment transport equation demonstrate the significance of the calibration and validation of the sediment transport modeling. The uncertainty and variability of the sediment trap efficiency estimates can be limited by calibration and validation of the sediment transport module of the CCHE2D model.

Table 3.4 Sediment trap efficiency under the current bathymetric condition for three scenarios of CCHE2D parameter definition.

Scenario	Suspended Transport Capacity Coefficient	Sediment Transport Equation	Sediment Trap Efficiency
A	1.0	Wu, Wang, Jia method	47.0%
B	0.9	Wu, Wang, Jia method	62.6%
C	1.0	SEDTRA	65.8%

### **3.3. Modification Scenarios**

Simulations were run for the current condition, and three additional bathymetric conditions within the basin. The current bathymetry, as defined by 2006 and 2008 surveys of the CCSB, is denoted Alternative A. Alternative B raises the weir 6 feet, from its current elevation of 32.5 feet, to 38.5 feet, but does not otherwise change the bathymetry of the basin. Alternative C removes a 400 foot section from the terminus of the training levee, but does not otherwise change the bathymetry of the basin. Alternative D is the combination of Alternatives B and C, such that the weir is raised 6 feet, and the 400 foot section of training levee is removed. Each alteration scenario was run with the default parameters of the model: suspended transport capacity coefficient of 1.0, sediment transport capacity equation of Wu, Wang, Jia method (Wu, 2001) such that they may be compared relative to each other. Bed elevation contour maps are shown in Figures 3.4 through 3.7 for Alternatives A, B, C, and D respectively. The resulting trap efficiency for each of the simulated alternatives is tabulated in Table 3.5.

#### **3.3.1. Alternative A**

As previously noted, the simulated trap efficiency of the CCSB, for Alternative A, was most conservatively found to be 47%. Shown in Figures 3.8 and 3.9, respectively, are the bedload transport rate, and suspended sediment concentration contour plots of the simulation results. Each figure contains the 5 time steps identified on the hydrograph to show the evolution of these parameters with time and flow magnitude. It should be noted that the volume of sediment in the water as flow recedes below the weir elevation should be largely deposited in the basin.

### **3.3.2. Alternative B**

Simulated trap efficiency of Alternative B, in which the overflow weir is raised 6 feet is 72.8%. The relative increase in trap efficiency, for this event, compared to the current condition is nearly 26%. Shown in Figures 3.10 and 3.11 are the bedload transport rate, and suspended sediment concentration contour plots of the simulation results for the 5 identified time steps on the hydrograph. Compared to the bed load of Alternative A, Figure 3.10 displays a clear band of higher bed load transport across the southern portion of the basin. According to Figure 3.11, the suspended sediment concentration is low in the northern portion of the basin for the duration of the flow event. The simulation suggests that relative to the current bathymetry, raising the weir will enhance sediment trap efficiency, but less sediment will be transported to the northern portion of the basin.

### **3.3.3. Alternative C**

Simulated trap efficiency of Alternative C, in which 400 feet of training levee is removed from the downstream end is 48.6%. The 1.6% increase from the current condition suggests that removal of just this initial section of training levee will not significantly alter sediment dynamics and sediment retention. The bedload transport rate, and suspended sediment concentration contour plots of the simulation results are shown on Figures 3.13 and 3.13. Both the bedload and suspended sediment concentration are altered when compared to the current condition. The slight increase in bedload transport rate in the northern portion of the basin is more obvious than that in the southern portion, however there is a slight increase in bedload transport over the entire simulation domain. The same pattern of increase is seen in Figure 3.13 for suspended sediment concentration.

### **3.3.4. Alternative D**

Simulated trap efficiency of Alternative D, in which 400 feet of training levee are removed from the downstream end and the weir is raised 6 feet, is 75.3%. Again the alteration of the weir elevation has a significant effect on sediment retention. The bedload transport rate, and suspended sediment concentration contour plots of the simulation results are illustrated in Figures 3.1.4 and 3.1.5. Comparison of Alternative D and Alternative B (raised weir alone) shows that there is a 2.5% increase in sediment retention when the terminus of the training levee is removed in addition to the weir being raised. Comparing Alternative D to the current condition shows a 28.3% increase in trap efficiency. As with Alternative B, there is a clear band of bed load transport across the southern portion of the basin, whereas the suspended sediment concentration is more uniformly distributed.

Table 3.5 Trap efficiency percentage of bathymetric modification scenarios, under default parameters of the model: suspended transport capacity coefficient of 1.0, sediment transport capacity equation of Wu, Wang, Jia method (Wu, 2001).

Trap Efficiency Percentage			
Alternative A <sup>1</sup>	Alternative B <sup>2</sup>	Alternative C <sup>3</sup>	Alternative D <sup>4</sup>
47.0% <sup>5</sup>	72.8%	48.6%	75.3%

<sup>1</sup>The current bathymetry, as defined by 2006 and 2008 surveys of the CCSB, is denoted Alternative A.

<sup>2</sup>Alternative B raises the weir 6 feet, from its current elevation of 32.5 feet, to 38.5 feet, but does not otherwise change the bathymetry of the basin.

<sup>3</sup>Alternative C removes a 400 foot section from the terminus of the training levee, but does not otherwise change the bathymetry of the basin.

<sup>4</sup>Alternative D is the combination of Alternatives B and C, such that the weir is raised 6 feet, and the 400 foot section of training levee is removed.

<sup>5</sup>When the sediment model parameters are changed, the trap efficiency of Alternative A ranges from 47 to 65.8%. Please see Table 3.4.

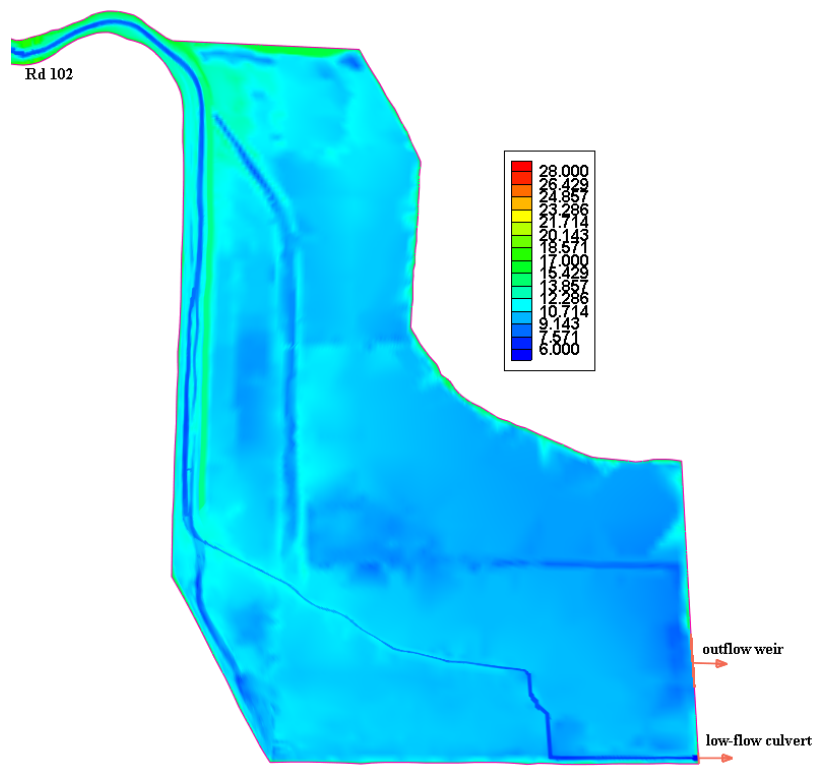


Figure 3.4 Bed elevation contour map, Alternative A, current bathymetry.

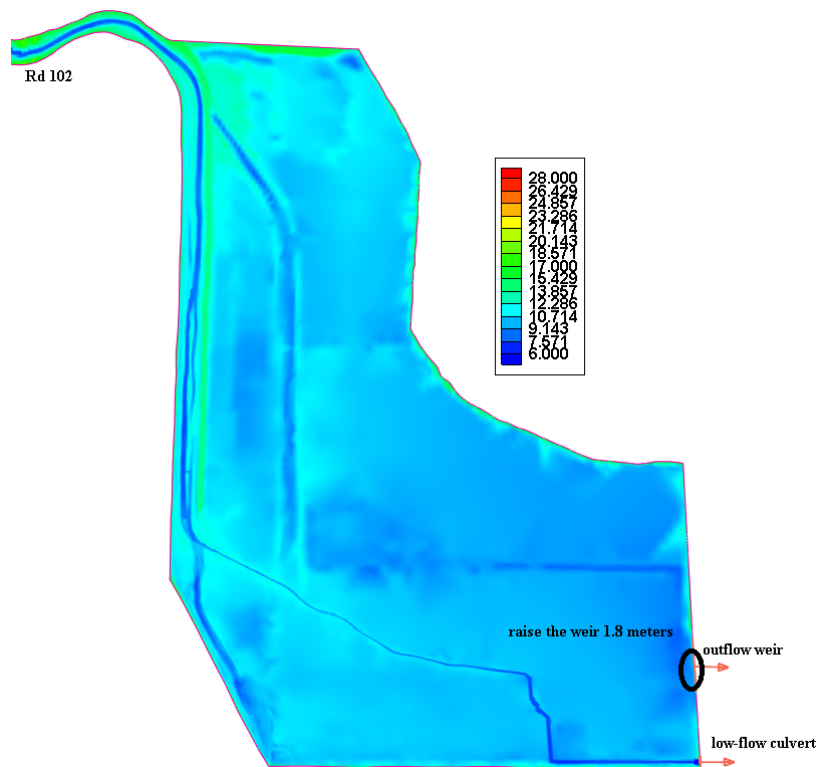


Figure 3.5 Bed elevation contour map, Alternative B, weir raised 6 feet.

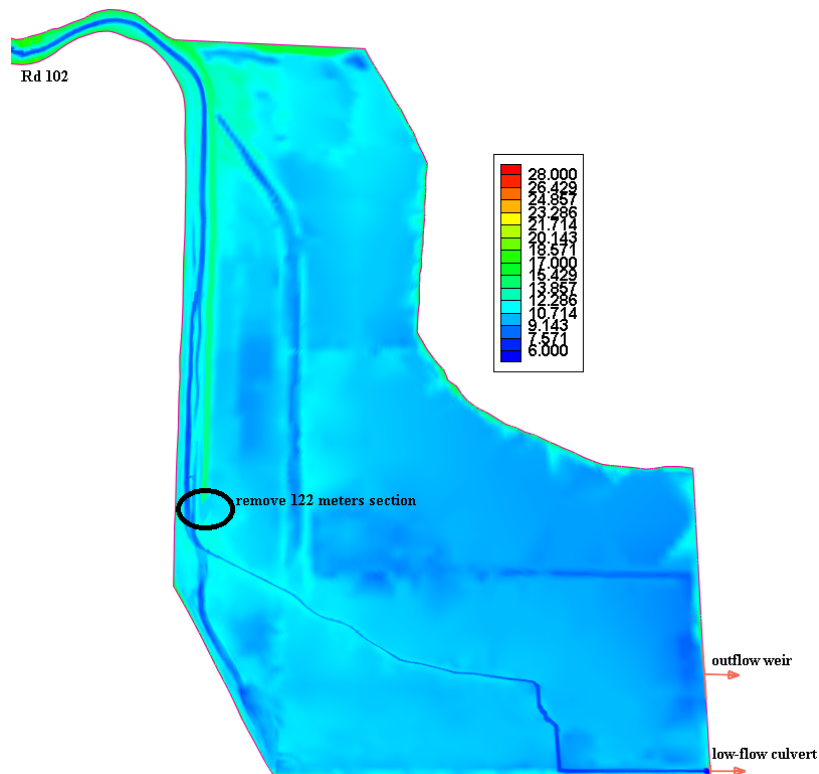


Figure 3.6 Bed elevation contour map, Alternative C, 400 foot section removed from end of training channel.

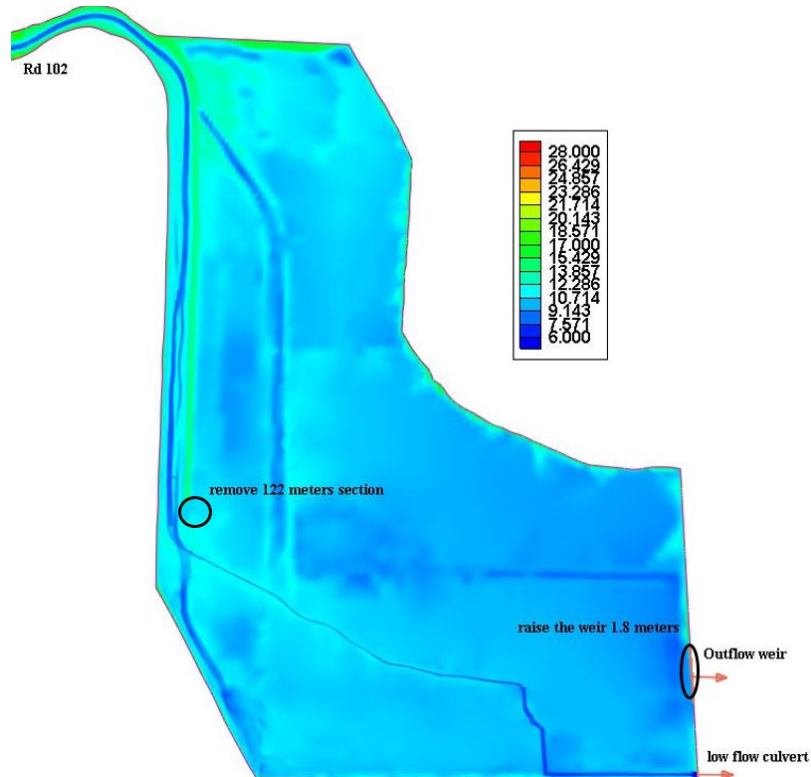


Figure 3.7 Bed elevation contour map, Alternative D, weir raised 6 feet, and 400 foot section removed from end of training channel.

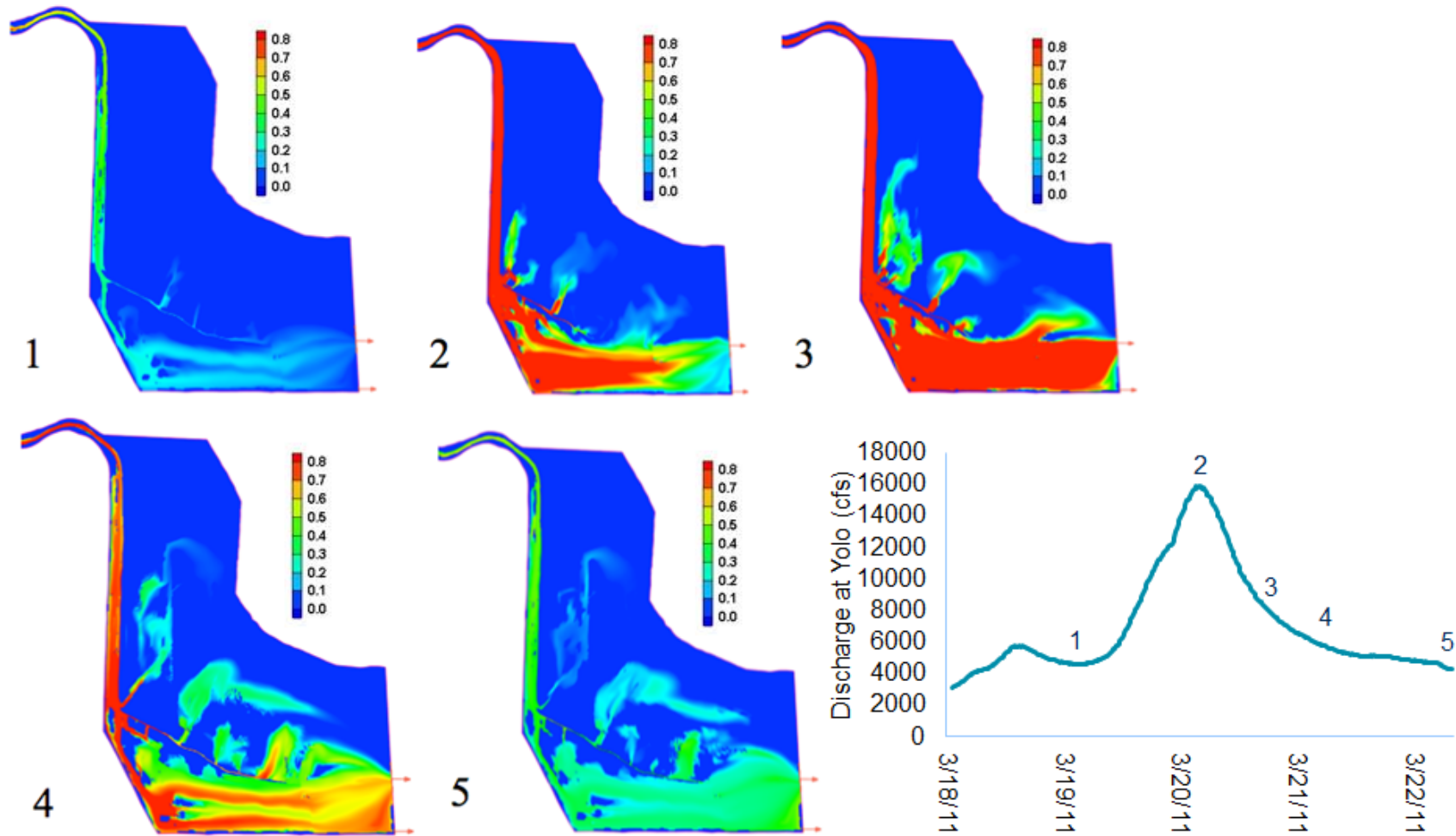


Figure 3.8 Bedload transport rate for time steps 1-5, Alternative A. Minimum transport rate (blue) is 0.0 kg/s, maximum transport rate (red) is 0.80 kg/s.

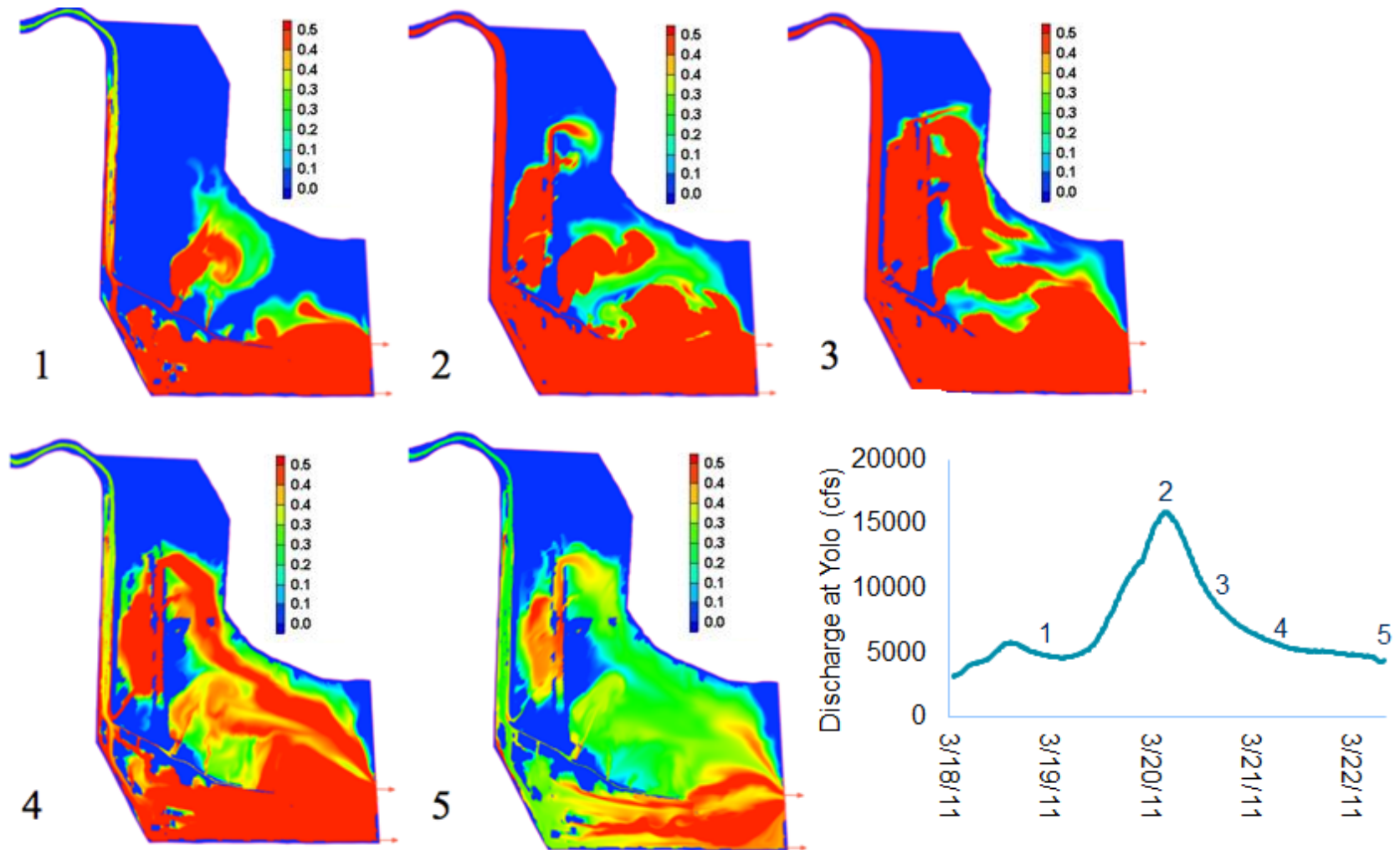


Figure 3.9 Suspended sediment concentration for time steps 1-5, Alternative A. Minimum concentration (blue) is 0.0 kg/m<sup>3</sup>, maximum concentration (red) is 0.50 kg/m<sup>3</sup>.

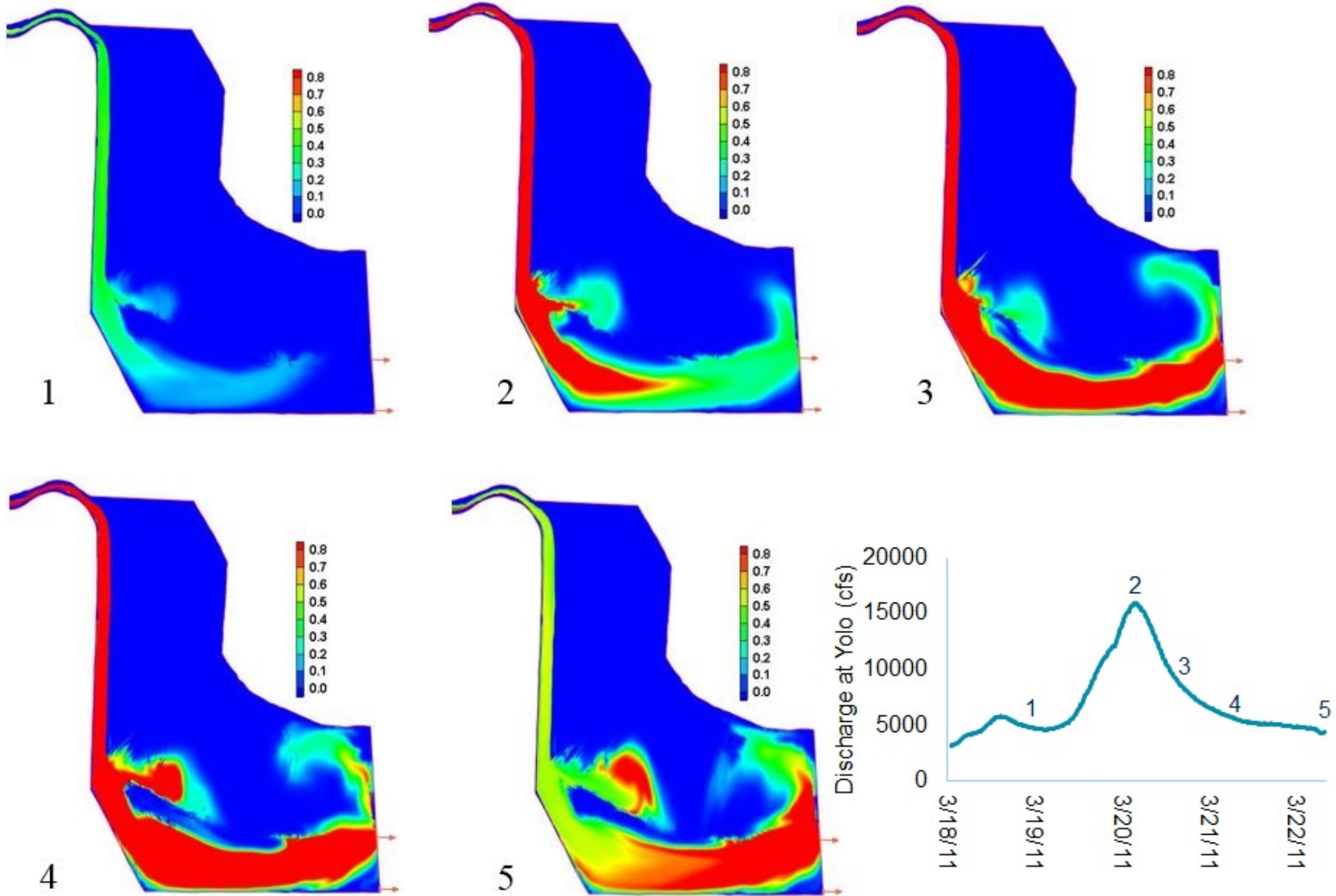


Figure 3.10 Bedload transport rate for time steps 1-5, Alternative B. Minimum transport rate (blue) is 0.0 kg/s, maximum transport rate (red) is 0.80 kg/s.

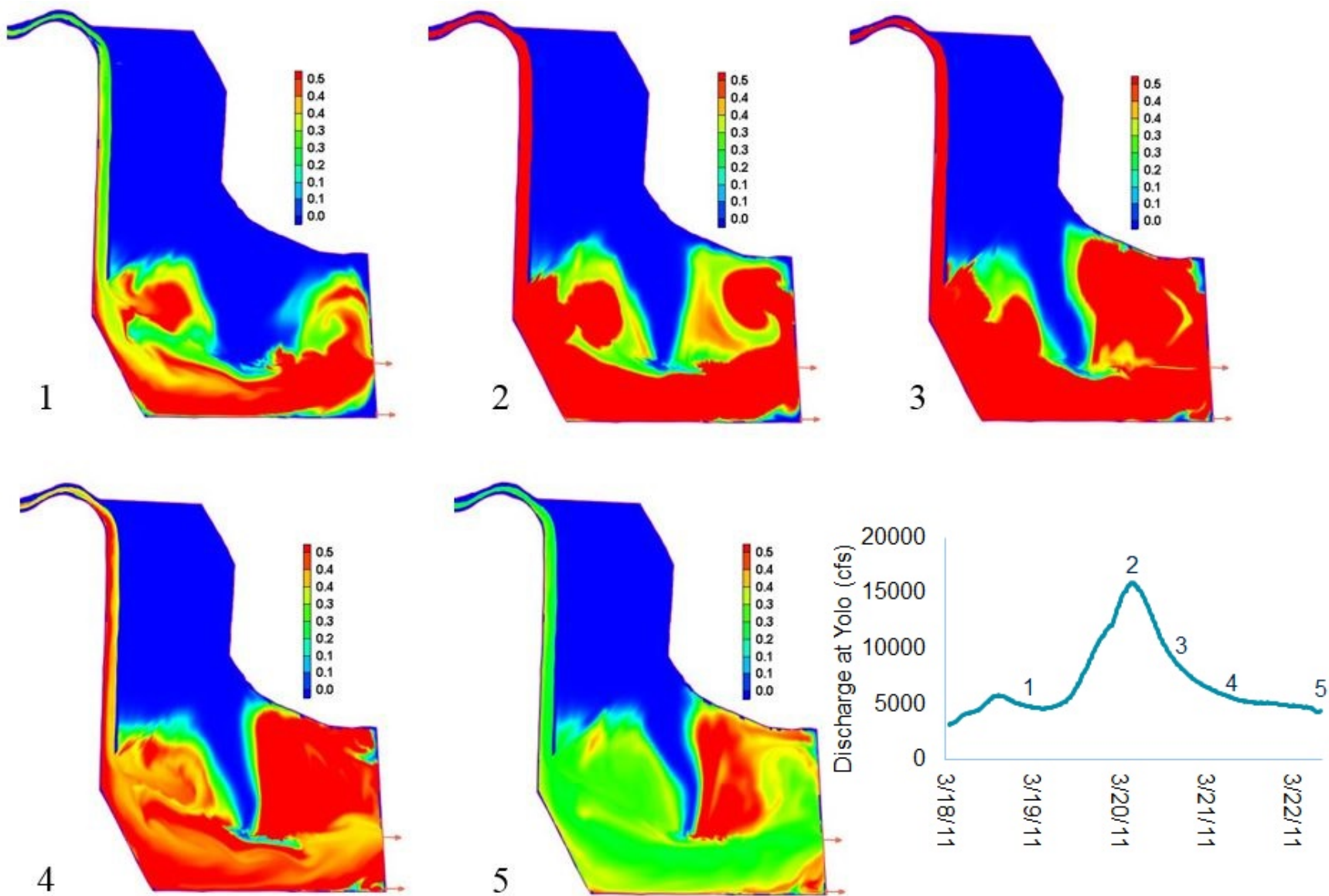


Figure 3.11 Suspended sediment concentration for time steps 1-5, Alternative B. Minimum concentration (blue) is 0.0 kg/m<sup>3</sup>, maximum concentration (red) is 0.50 kg/m<sup>3</sup>.

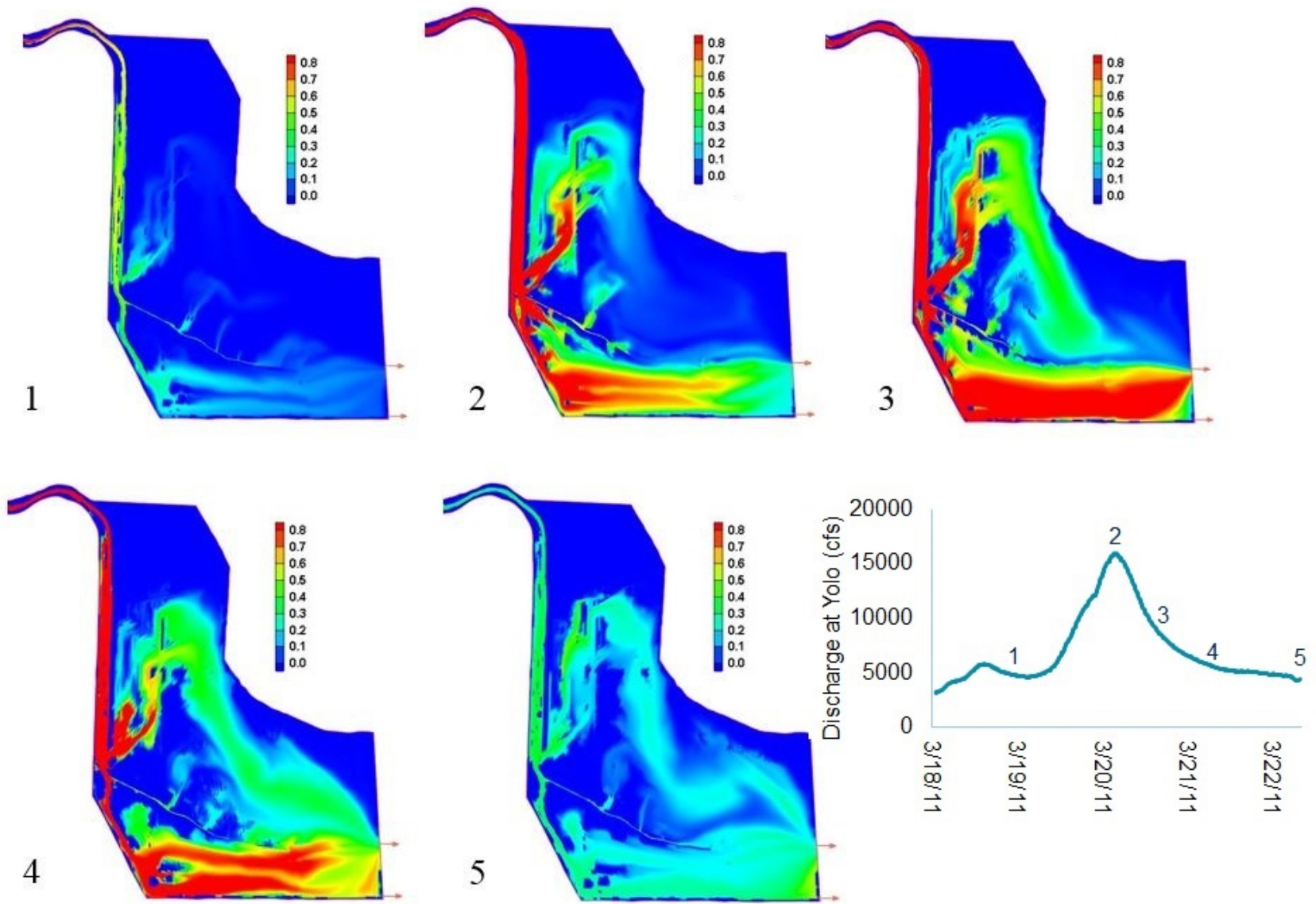


Figure 3.12 Bedload transport rate for time steps 1-5, Alternative C. Minimum transport rate (blue) is 0.0 kg/s, maximum transport rate (red) is 0.80 kg/s.

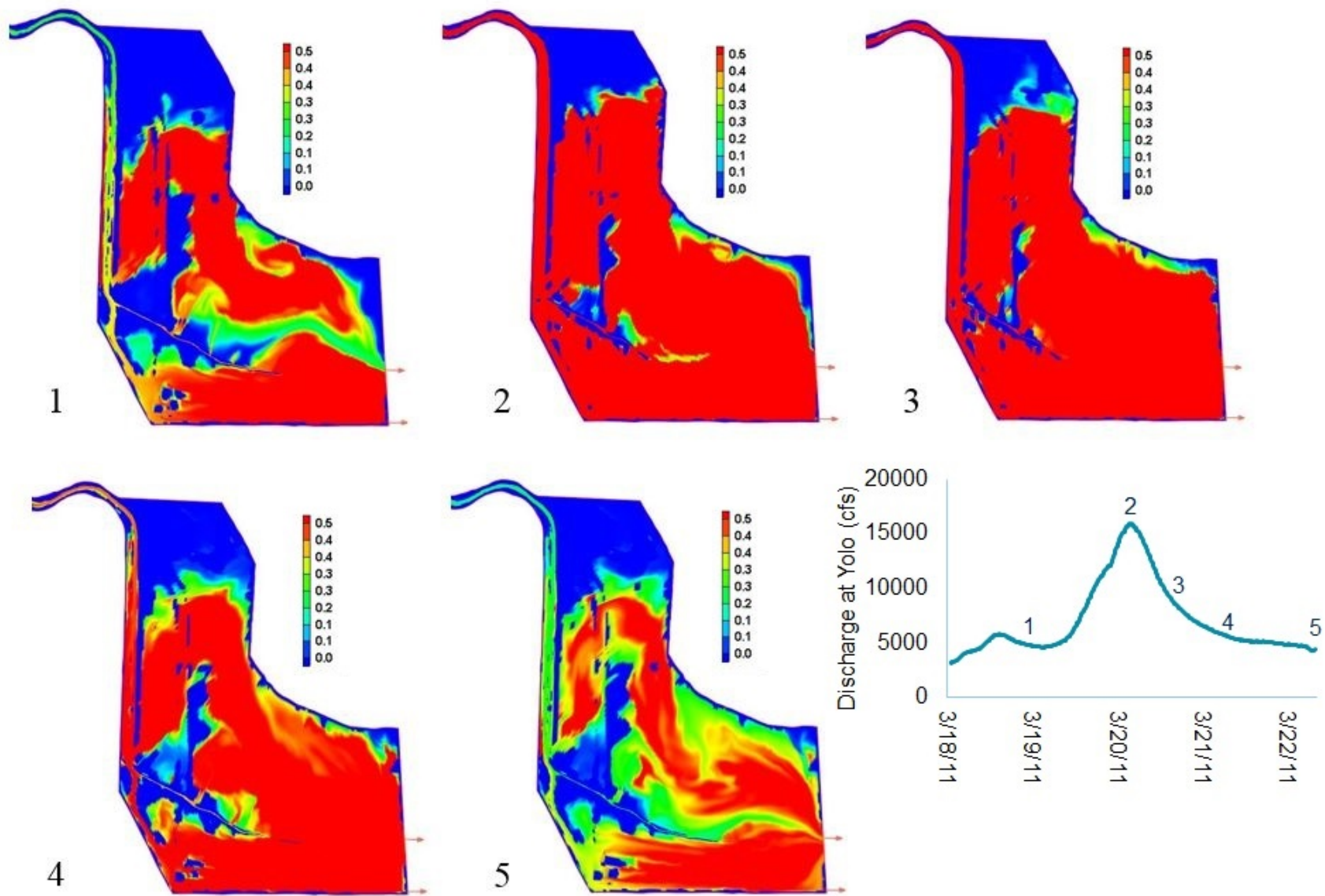


Figure 3.13 Suspended sediment concentration for time steps 1-5, Alternative C. Minimum concentration (blue) is 0.0 kg/m<sup>3</sup>, maximum concentration (red) is 0.50 kg/m<sup>3</sup>.

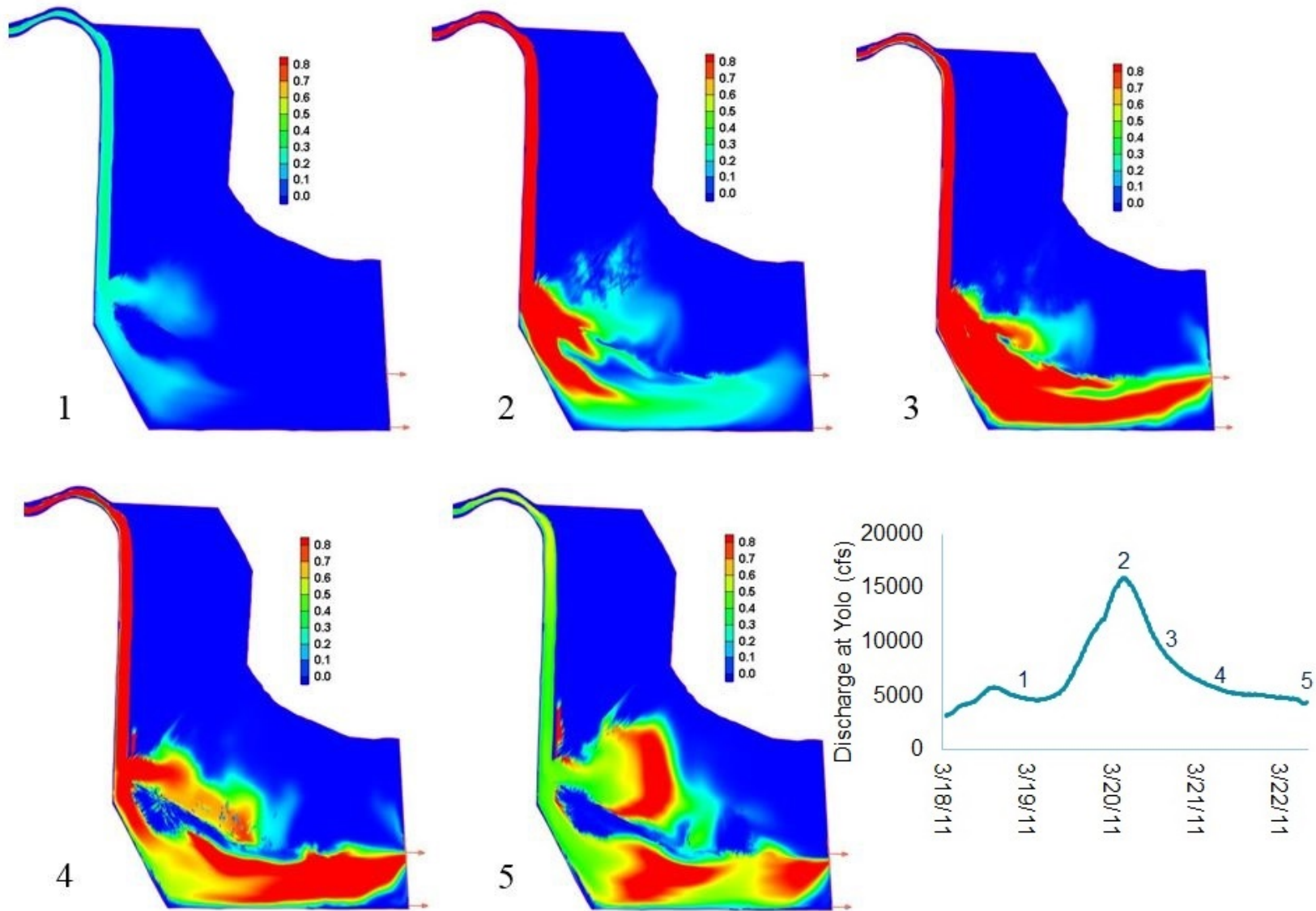


Figure 3.14 Bedload transport rate for time steps 1-5, Alternative C. Minimum transport rate (blue) is 0.0 kg/s, maximum transport rate (red) is 0.80 kg/s.

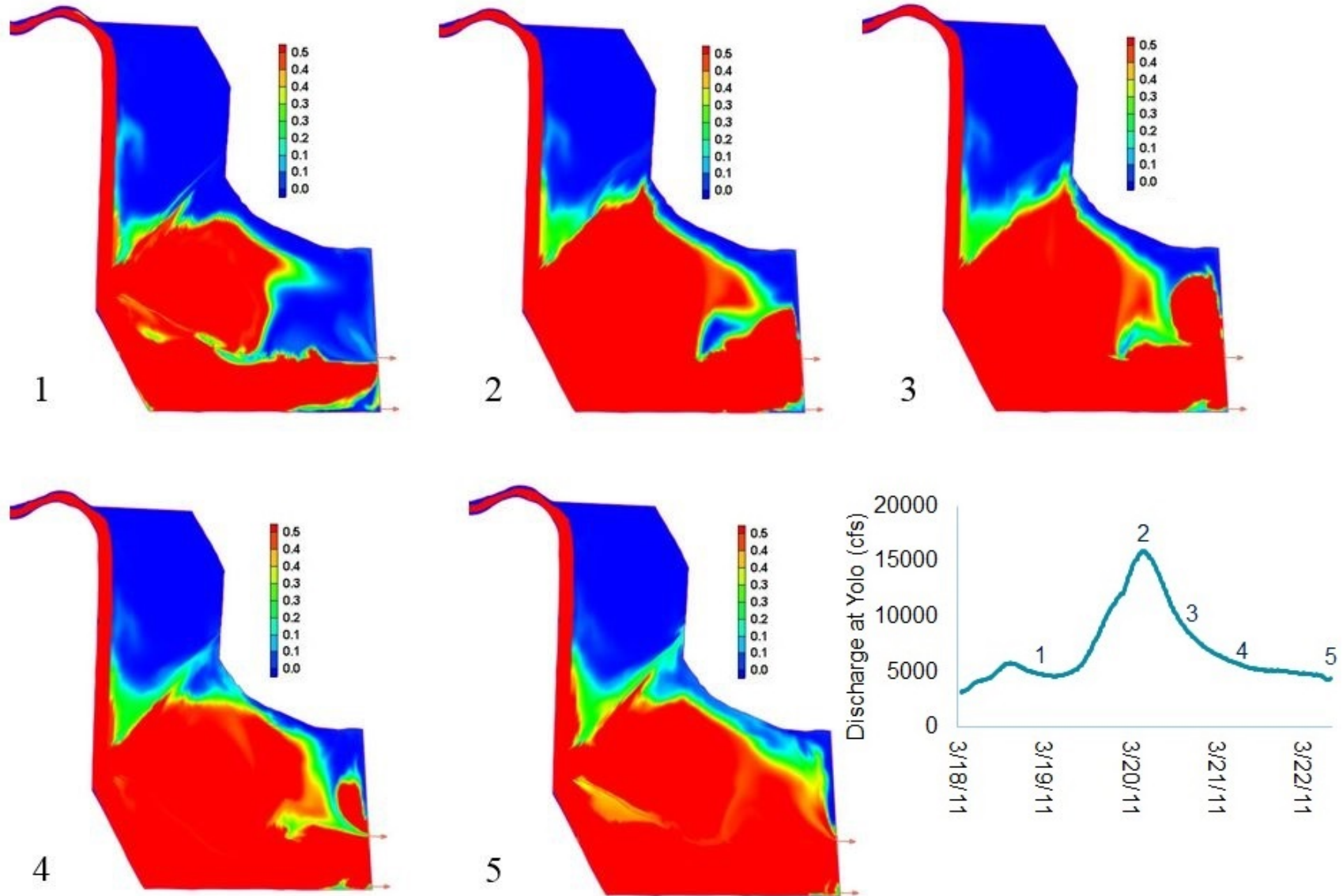


Figure 3.15 Suspended sediment concentration for time steps 1-5, Alternative D. Minimum concentration (blue) is 0.0 kg/m<sup>3</sup>, maximum concentration (red) is 0.50 kg/m<sup>3</sup>.

#### **4. CONCLUDING REMARKS AND FUTURE WORK**

Trap efficiency estimates were provided for the current bathymetry of the CCSB using three parameter setting scenarios of the CCHE2D model. Under the three scenarios, trap efficiency ranged from 47 to 65.8%. A more realistic trap efficiency value will be provided following calibration of the sediment transport model. Calibration is reliant on survey data and volume differential from the 2006/2008 and 2014/2015 surveys of the CCSB.

Trap efficiency estimates were also supplied for three modification scenarios with bathymetric configurations that differed from the current condition. Each configuration was simulated using the default parameters of the sediment transport model to allow comparison of modification scenario performance. Reliability of such modification scenario trap efficiency estimates will be improved by calibration of the sediment transport model.

Flow sampling will continue in the subsequent year of the CCSB Trap Efficiency Study, with the goal of measuring velocities under conditions not seen in the study thus far. Such measurements will provide further verification of flow dynamics in the CCSB.

Data provided by the USGS Sacramento field office, and the California Water Science Center will be incorporated into the modeling to aid in calibration and validation of sediment transport in the CCHE2D model. Particularly, measurements of coincident suspended sediment concentration and discharge at Yolo, Rd 102, and the overflow weir will be used to increase model accuracy. Sediment cores obtained by the USGS from the CCSB may provide valuable information on the historical sediment deposition rates in the Settling Basin. Sediment cores may be especially helpful if they can provide information on the sediment deposition rates after 1993, when major bathymetric changes were made to the training channel of the CCSB. The information on the sediment deposition rates by the sediment cores will be analyzed and utilized in the calibration/validation process of the sediment model if possible.

Following completion of the planned 2015 basin survey, flow and sediment transport will be simulated for the period between the two most recent surveys. The numerical model will be calibrated to match the trap efficiency based on the depositional difference between the two survey sets, as calculated and reported by DWR. The surveys will allow calculation of depositional volume from 2006 to 2015.

Reconstructed flows produced by the Cache Creek Watershed Hydrology Study (UCDJAHL, 2014) will be simulated with the calibrated model, utilizing the sediment rating curve described in 1997 HEC-6 Analysis Technical Memorandum. The Cache Creek Watershed study provides an extensive period of hourly flow, from October 1950 through September 2010 at Cache Creek at Yolo, the upstream boundary of our CCHE2D simulation. Trap efficiency of the CCSB, under the current bathymetric conditions, can then be computed utilizing the reconstructed hourly historical flows and

the corresponding sediment conditions, obtained from the available sediment rating curve.

## 5. REFERENCES

- Carr, K, Ercan, A., Tu, T., Bandeh, H., Kavvas, M. L. (2014). Cache Creek Settling Basin/Yolo Bypass Project, Annual Report I. Submitted to CA DWR, Contract No. 4600010003, May 1, 2014.
- Domagalski, J.L., Slotton, D. G., Alpers, C. N., Suchanek, T. H., Churchill, R., Bloom, N., Ayers, S. M., & Clinkenbeard, J. (2004). Summary and Synthesis of Mercury Studies in the Cache Creek Watershed, California, 2000-01. US Department of the Interior, US Geological Survey.
- Garbrecht, J., Kuhnle, R., & Alonso, C. (1995). A Sediment Transport Capacity Formulation for Application to Large Channel Networks. *Journal of Soil and Water Conservation*, 50(5), 527-529.
- Laursen, E. M. (1958). The Total Sediment Load of Streams. *Journal of the Hydraulics Division*, 84(1), 1-36.
- Lustig, L. K., and R.D. Busch, (1967). Sediment transport in Cache Creek drainage basin in the Coast Ranges West of Sacramento, California: US Geol. Survey Prof. Paper, 562.
- Meyer-Peter, E., & Müller, R. (1948). Formulas for Bed-load Transport. *Report on Second Meeting of IAHR*, Stockholm, Sweden, 39-64.
- Thayer, R. (2009) "Cache Creek Nature Preserve." Putah and Cache: A Thinking Mammals Guide to the Watershed. University of California, Davis. June 8, 2009. [http://bioregion.ucdavis.edu/book/13\\_Lower\\_Cache\\_Creek/13\\_03\\_circ\\_ccnp.htm](http://bioregion.ucdavis.edu/book/13_Lower_Cache_Creek/13_03_circ_ccnp.htm)
- University of California, Davis., J. Amorocho Hydraulics Laboratory (2014). Study of the Water, Sediment and Mercury Inflows to Cache Creek Settling Basin based on Cache Creek Watershed Hydrology and Future Climate Conditions, Draft Final Report. Submitted to CA DWR, Contract No. 4600009009, December 30, 2014.
- U.S. Army Corps of Engineers. 1987. Final General Design Memorandum No. 1, Cache Creek, California, Cache Creek Settling Basin. U.S. Army Corps of Engineers, Sacramento District. January.
- U.S. Army Corps of Engineers, Sacramento District. 1997. Sediment Deposition in the Cache Creek Training Channel. Memorandum for Chief, Western Region Section. Sacramento, California. March.

Wu, W., 2001. *CCHE2D: Sediment Transport Model (Version 2.1)* Technical Rep. No. NCCHETR- 2001-3, National Center for Computational Hydroscience and Engineering, The University of Mississippi.

Yang, C. T. (1973). Incipient Motion and Sediment Transport. *Journal of the Hydraulics Division*, 99(10), 1679-1704.

**Final Report for the project**

**Agreement No.: 4600009009**

**Study of the Water, Sediment and Mercury Inflows to  
Cache Creek Settling Basin based on Cache Creek  
Watershed Hydrology  
and  
Future Climate Conditions**

**By**

**University of California, Davis  
J. Amorocho Hydraulics Laboratory**

Originally submitted on 12/30/2014, revised on 9/25/2015

## Table of Contents

1. Introduction.....	7
1.1. Purpose of the Project .....	7
1.2. Scope of Work .....	8
2. Background.....	10
2.1. Cache Creek Watershed.....	10
3. Methodology.....	12
3.1. Regional Hydro-Climate Modeling .....	14
3.2. Hydrology and Environmental Modeling .....	15
4. Sediment and Mercury Data Compilation and Data Gap Analysis .....	16
4.1. Soil Erosion in Cache Creek Watershed.....	16
4.2. Sensitivity Analysis for trap efficiency at CCSB .....	19
4.2.1 Results and Discussion .....	20
4.3. Data Availability and Recommendations for Data Collection .....	27
4.3.1 Data Availability.....	27
4.3.2 Recommendations for Data Collection.....	37
5. Reconstruction of Historical and Projection of Future Climate Conditions.....	38
5.1. Setting up the MM5 modeling domains over Cache Creek watershed.....	39
5.2. Regional Climate Model validation based on NCAR/NCEP reanalysis data-based climate variables .....	41
5.3. Model validation of GCM-based climate variables.....	46
5.4. Reconstruction of historical climate data.....	49
5.5. Projection of Future Climate Conditions .....	58
5.5.2 Projection of air temperature and solar radiation under future climate conditions.....	62
6. Reconstruction of Historical and Projection of Future Hydrologic Conditions .....	64
6.1. Implementation of WEHY Model .....	64
6.1.1 Delineation of stream reaches and model computational units .....	64
6.1.2 Estimation of WEHY model parameters .....	66
6.1.3 Estimation of historical climate conditions for each model computational unit (MCU) in WEHY model .....	70
6.2. Calibration and Validation of WEHY Model for Streamflow Simulations.....	74
6.3. Reconstruction of historical flow conditions .....	79
6.4. Future Flow Simulation and Flood Frequency Analysis .....	81
7. Discussion, Conclusions and Recommendations.....	87
7.1 Recommendations for future actions.....	91

8. References.....	93
--------------------	----

### List of Figures

Figure 1- Cache Creek Watershed .....	12
Figure 2- A schematic description of the modeling approach for the historical conditions .....	13
Figure 3- A schematic description of the modeling approach for future conditions .....	14
Figure 4- A schematic description of the Universal Soil Loss Equation calculation .....	17
Figure 5- Estimated parameters for USLE over the Cache Creek watershed.....	18
Figure 6- The soil erosion map of Cache Creek Watershed using USLE .....	18
Figure 7- Daily Average Discharge (cfs) at Cache Creek at Yolo between 1904-2008 water years .....	21
Figure 8- Daily Average Discharge (cfs) at Cache Creek at Yolo during 1980-1989 water years .....	22
Figure 9- The sediment rating curve at Cache Creek at Yolo that is used in this study .....	22
Figure 10- Available streamflow gauges for this study .....	27
Figure 11- Historical field/lab sampling data from USGS .....	28
Figure 12- Historical field/lab suspended sediment and mercury data from Cooke et al. (2004) .....	29
Figure 13- Available historical field/lab sediment and mercury data from Cooke et al. (2004) and USGS .....	30
Figure 14- Overview of sampling locations for Cache Creek Canyon (Foe and Bosworth, 2008) .....	31
Figure 15- Sampling locations from Cache Creek, North Fork downstream toward Bear Creek (Foe and Bosworth, 2008).....	32
Figure 16- Sampling locations from Cache Creek, North Fork downstream toward Bear Creek, continued (Foe and Bosworth, 2008).....	33
Figure 17- Sampling locations from Cache Creek, North Fork downstream toward Bear Creek, continued (Foe and Bosworth, 2008).....	34
Figure 18- Sampling locations at Bear Creek (Bosworth and Morris, 2009) .....	35
Figure 19- Sampling locations at the tributaries of Bear Creek (Bosworth and Morris, 2009)....	36
Figure 20- Overview of desired sampling locations (11 locations).....	38
Figure 21- Depiction of four nested domains used for the MM5 simulation for the Cache Creek watershed .....	41
Figure 22- Example comparison of mean monthly precipitation for December, January and February between PRISM data and MM5 simulation results during 1950 to 2007 .....	42
Figure 23- Graphical comparison of mean monthly precipitation between PRISM data and MM5 simulation results over Cache Creek watershed during 1950 to 2007 .....	43
Figure 24- Graphical comparison of monthly precipitation between PRISM data and MM5 simulations during 1950 to 2007.....	43
Figure 25- Comparisons of simulated (MM5-NCEP) and observed (CDEC) monthly mean temperature from 2000 through 2011 at KNO station. No bias-correction was applied. ....	45
Figure 26- Comparisons of simulated (MM5-NCEP) and observed (CDEC) monthly mean solar radiation from 2000 through 2011 at KNO station. No bias-correction was applied. ....	45
Figure 27- Comparisons of MM5-simulated monthly precipitation versus PRISM monthly precipitation from water year 1901 to water year 1999 for Cache Creek watershed .....	47

Figure 28- Quartile-quartile plot of Cache Creek watershed average monthly precipitation between MM5-simulated (based on GCM historical simulations) and PRISM precipitation during water year 1951 to water year 1999. Red color indicates the comparisons for CCSM3-based precipitation and blue color indicates the comparisons for ECHAM5-based precipitation. ....	48
Figure 29- Comparisons of 10-year moving Cache Creek watershed average annual precipitation between PRISM observations and MM5-simulated precipitation during water year 1901 to water year 1999.....	49
Figure 30- Chi-square goodness-of-fit test results of Cache Creek watershed average monthly precipitation between PRISM and MM5-simulated precipitation during water year 1951 to water year 1999.....	49
Figure 31- Sample spatial plots of NCAR/NCEP reanalysis data-based MM5 simulation results for the mean monthly precipitation (February, April, June, August, October and December) during 1950 – 2011 over Cache Creek watershed. ....	51
Figure 32- Sample spatial plots of NCAR/NCEP reanalysis data-based MM5 simulation results for 61-year average monthly mean air temperature (February, April, June, August, October and December) during 1950 – 2011 over Cache Creek watershed. ....	52
Figure 33- Sample spatial plots of NCAR/NCEP reanalysis data-based MM5 simulation results for 61-year average monthly mean shortwave solar radiation (February, April, June, August, October and December) during 1950 – 2011 over Cache Creek watershed.....	53
Figure 34- Sample plots of historical basin-average monthly precipitation, monthly mean air temperature, wind speed, shortwave solar radiation and longwave solar radiation that were reconstructed by MM5 regional climate model during 1950 – 2011 over Cache Creek watershed by downscaling the NCAR/NCEP reanalysis data (continued in the next page) .....	54
Figure 35- Sample plots of historical basin-average monthly precipitation, monthly mean air temperature, wind speed, shortwave solar radiation and longwave solar radiation that were reconstructed by MM5 regional climate model during 1950 – 2000 over Cache Creek watershed by downscaling the GCM (CCSM3 and ECHAM5) historical control simulations (continued next page).....	56
Figure 35- Sample plots of historical basin-average monthly precipitation, monthly mean air temperature, wind speed, shortwave solar radiation and longwave solar radiation that were reconstructed by MM5 regional climate model during 1950 – 2000 over Cache Creek watershed by downscaling the GCM (CCSM3 and ECHAM5) historical control simulations.....	57
Figure 36- Comparison of historical GCM control run-based MM5 simulation versus the future GCM (ECHAM5 and CCSM3)-based MM5 projection of ensemble average annual precipitation (ensemble average of 13-projection realizations) for Cache Creek watershed.....	59
Figure 37- Comparison of the future mean monthly precipitation (ensemble average of 13-projection realizations) at early 21 <sup>st</sup> century, at mid-21 <sup>st</sup> century and at the end of the 21 <sup>st</sup> century against the historical mean monthly precipitation during wy1990-wy1999 over Cache Creek watershed .....	60
Figure 38- Comparison of Cache Creek watershed-average annual 72-hour maximum precipitation between the historical period (wy1901 – wy1999) and the projection period (wy2001 – wy2099) .....	61
Figure 39- Comparison of historical and MM5-downscaled GCM (ECHAM5 and CCSM3) projections of annual mean air temperature (ensemble average of 13-projection realizations) for Cache Creek Watershed.....	62

Figure 40- Comparison of historical and MM5-downscaled GCM (ECHAM5 and CCSM3) projections of annual mean solar radiation (ensemble average of 13-projection realizations) for Cache Creek watershed.....	63
Figure 41- Delineated 43 stream reaches in the WEHY model for the Cache Creek watershed .	65
Figure 42- Delineated 86 model computational units (MCUs) in the WEHY model for the Cache Creek watershed.....	65
Figure 43- Leaf Area Index (LAI) obtained from MODIS satellite data for the Cache Creek watershed .....	67
Figure 44- Sample of distributed land surface parameters based on the CalSIL data and reference information for the Cache Creek watershed .....	68
Figure 45- Sample of distributed soil hydraulic parameters based on the SSURGO data and reference information for the Cache Creek watershed .....	69
Figure 46- Sample plots of NCAR/NCEP reanalysis data-based 61-year average monthly precipitation, monthly mean air temperature, wind speed and shortwave solar radiation at each model computational unit (MCU) for January and July during 1950 – 2011 over Cache Creek watershed. ....	71
Figure 47- Sample plots of CCSM3 GCM-based 61-year average monthly precipitation, monthly mean air temperature, wind speed and shortwave solar radiation at each model computational unit (MCU) for January and July during 1950 – 2000 over Cache Creek watershed.....	72
Figure 48- Sample plots of ECHAM5 GCM-based 61-year average monthly precipitation, monthly mean air temperature, wind speed and shortwave solar radiation at each model computational unit (MCU) for January and July during 1950 – 2000 over Cache Creek watershed. ....	73
Figure 49- Location of observation stations for model calibration and validation.....	75
Figure 50- Calibration results for hourly flow discharge at Rumsey CDEC station and Yolo USGS station during 10/1997-9/1999.....	76
Figure 51- Validation results for monthly flow discharge at Rumsey CDEC station during 1993 – 2010 (cms) .....	77
Figure 52- Validation results for monthly flow discharge at Yolo USGS station during 1993 – 2010 (cms) .....	77
Figure 53- Validation results of monthly flow discharge at Rumsey CDEC station during 1993 – 1999 using the operation rules for Clear Lake and Indian Valley reservoirs (cms) .....	78
Figure 54- Validation results of monthly flow discharge at Yolo CDEC station during 1993 – 1999 using the operation rules for Clear Lake and Indian Valley reservoirs (cms) .....	79
Figure 55- Reconstructed monthly mean discharge based on the NCAR/NCEP reanalysis data from October, 1950 to September, 2010 at Rumsey CDEC station .....	80
Figure 56- Reconstructed monthly mean discharge based on the NCAR/NCEP reanalysis data from October, 1950 to September, 2010 at Yolo USGS station.....	80
Figure 57- Projected Hourly Flow Hydrographs at Yolo gauging station based on SRES Scenarios .....	81
Figure 58-Annual maximum model-simulated streamflows during 21 <sup>st</sup> century at Yolo gauging station.....	83
Figure 59- Histograms of annual maximum flows separated into 45-year increments (2010-2054, and 2055-2099) for all flow projections during 21 <sup>st</sup> century at Yolo station.....	84

Figure 60- Relative frequency histogram of annual maximum flows separated into 45-year increments (2010-2054, and 2055-2099) for all flow projections during 21 <sup>st</sup> century at Yolo gauging station .....	85
Figure 61-Evolution of the annual maximum flow as function of return period throughout the 21 <sup>st</sup> century for all flow projections at Yolo gauging station .....	85

### **List of Tables**

Table 1- Discharge (cfs) versus total sediment load (tons per day) at Cache Creek at Yolo .....	23
Table 2- Sensitivity analyses for sediment balance and trap efficiency in CCSB using a 50-year simulation.....	24
Table 3- Sensitivity analyses for sediment balance and trap efficiency in the training channel using a 50-year simulation.....	25
Table 4- Sensitivity analyses for sediment balance and trap efficiency in CCSB using 100-year simulation.....	26
Table 5- Statistical test results for the comparison of MM5-simulated (NCEP) versus PRISM precipitation during 1950 – 1999 for the Cache Creek watershed.....	44
Table 6. Summary statistics for model-projected annual maximum flows during the two time periods of the 21 <sup>st</sup> century at Yolo gauging station .....	83
Table 7. Annual maximum flow discharge (cms) as function of return period during the two selected time periods in 21 <sup>st</sup> century .....	85

## **1. Introduction**

### **1.1. Purpose of the Project**

Cache Creek Settling Basin (CCSB), located two miles east of Woodland, California, was constructed to preserve the floodway capacity of Yolo Bypass by entrapping sediment. Cache Creek is the main source of mercury entering San Francisco Bay-Delta. Entrapping sediment also entraps mercury, so the settling basin also helps preserve aquatic life of San Francisco Bay-Delta. The major objectives of this study are as follows:

- i.** To perform flow, suspended sediment, and mercury data compilation and gap analysis for Cache Creek watershed. An initial study showed that mercury data in the watershed is scarce and a grab sampling program is needed. The UC Davis group will coordinate with DWR and USGS to establish additional grab sampling programs in the watershed.
  
- ii.** To develop detailed flow, sediment and mercury conditions for Cache Creek and its tributaries for historical and future conditions by coupling the Watershed Environmental Hydrology Modeling and Climate Change Modeling approaches. The purpose is to provide concurrent flow, sediment and mercury information in the Cache Creek watershed in order to provide better sediment and mercury loading estimates. Reconstruction of realistic and comprehensive historical and future climate and flow conditions will eliminate the need to install and maintain new flow stations and rain gages within the basin.
  
- iii.** To use the simulated flow, sediment and mercury conditions in the Cache Creek watershed to investigate opportunities for trapping part of the mercury at upstream locations of the Cache Creek watershed, thereby reducing the mass loading rate of sediment into the Basin.

iv. To extend and support the ongoing Cache Creek Settling Basin / Yolo Bypass Project with Contract No. 4600008165. In addition to modeling flow, sediment transport and sediment trap efficiency in CCSB, mercury transport and mercury trap efficiency are planned to be modeled. Once calibrated and validated, Cache Creek Watershed Environmental Hydrology Modeling will lead to better prediction of sediment and mercury inlet boundary conditions for CCSB. Sediment and mercury trap efficiency under different climate change projections is planned to be investigated. Climate change projections may be more severe than the current conditions leading to more adverse loading conditions for CCSB. With growing public concern and with the passage of Global Warming Solutions Act of 2006 (Assembly Bill 32), there is increasing pressure to address global warming within the context of National Environmental Policy Act (NEPA) and California Environmental Quality Act (CEQA).

## **1.2. Scope of Work**

The major objectives of the proposed project, stated above, are to be realized by means of the following project milestones:

Milestone 1: Perform the flow, suspended sediment, and mercury data compilation and data gap analyses for Cache Creek Watershed. An initial study showed that mercury data in the watershed is scarce and a grab sampling program is needed. UC Davis group will collaborate with DWR and USGS to finalize details of an additional grab sampling program in the watershed.

Milestone 2: Downscale dynamically an ensemble of GCM (Global Climate Model) simulations of the historical and future climatic conditions that are at coarse resolution over California (grid resolution ~200-300km) to a grid resolution of 3 km over Cache Creek Watershed by means of the atmospheric model component of a Regional Hydro-climate model (RegHCM) (Chen et al. 1996; Kavvas et al. 2000, 2007; Yoshitani et al. 2001) in order to simulate the historical and projected atmospheric and hydrologic conditions under the historical observed emission conditions and under future greenhouse gas emissions scenarios SRES A1B, SRES A1FI, SRES A2, and SRES B1 from the Special Report on Emissions Scenarios (SRES) (Nakicenovic et al. 2000) from the worst-case scenario SRES A1FI to the best-case scenario SRES B1.

Milestone 3 : Initiate the coupling of the regional-scale atmospheric model component with Watershed Environmental Hydrology Model (WEHY) (Kavvas et al. 2004). Required parameter maps for the WEHY model will be prepared using GIS with the existing soil, land cover and elevation databases. Boundary conditions of WEHY model will be prepared based on the simulation results of the regional-scale atmospheric model component.

Milestone 4 : Apply the WEHY model's hydrologic module to Cache Creek Watershed for the historical period in order to calibrate and validate the hydrologic module by the historical flow data.

Milestone 5 : Run the WEHY model using boundary conditions developed from future climate conditions.

Milestone 6: Estimate the flood frequencies for Cache Creek Watershed based on 13 different future hydro-climate simulation conditions, obtained by RegHCM for the Cache Creek watershed under 13 future climate projections from GCMs with various GHG Emissions Scenarios.

Milestone 7: After obtaining the field sampling data on concurrent flow, sediment and mercury, calibrate and validate the environmental module of WEHY model to implement the model to Cache Creek watershed.

Milestone 8: After its calibration and validation by concurrent flow, sediment and mercury field sampling data over Cache Creek watershed, run the WEHY-Environmental module to reconstruct the historical and project the future concurrent flow, sediment and mercury conditions over the watershed. The calibrated and validated WEHY model for Cache Creek watershed will be run under projected future climate conditions (based on 13 different future hydro-climate projections, obtained from downscaling 13 future climate projections of GCMs under the previously-mentioned 4 different SRES scenarios by means of the regional hydro-climate model of Cache Creek watershed) to provide the concurrent flow, sediment and mercury

inflow conditions to the Cache Creek Settling Basin (CCSB). By means of the estimated flow, sediment and mercury inflow conditions for CCSB, both for the historical period as well as the future period during 21<sup>st</sup> century, the already calibrated and validated hydrodynamic model of the CCSB can then be run to predict reliably the trap efficiencies at CCSB.

Milestone 9: Use the results of historical and future concurrent flow, sediment and mercury conditions at Cache Creek watershed, estimated by WEHY model, to investigate opportunities for trapping part of the mercury at upstream locations within Cache Creek watershed. From the WEHY model-estimated historical and future concurrent flow, sediment and mercury conditions at the Cache Creek watershed, the data gaps in sediment rating curve will be completed.

## **2. Background**

### **2.1. Cache Creek Watershed**

The Cache Creek watershed drains approximately 3,000-km<sup>2</sup> to the CCSB, which discharges to the Yolo Bypass before flowing into the Sacramento River. Containing abandoned mines and natural sources such as geothermal springs and mercury-enriched soils, the Cache Creek watershed is a significant contributor of mercury to the Sacramento-San Joaquin Delta. This mercury pollution causes adverse health effects for both humans and wildlife in the Cache Creek watershed, and downstream in the Sacramento River, Sacramento-San Joaquin Delta, and the San Francisco Bay. Therefore, understanding sources and distribution of mercury in Cache Creek and developing control strategies to reduce exports is necessary.

Cache Creek Watershed is composed of upper (approximately 2,500 km<sup>2</sup>) and lower (approximately 500 km<sup>2</sup>) Cache Creek basins (see Figure 1). Upper Cache Creek has two major tributaries: the North Fork of Cache Creek and Bear Creek. Reservoirs at Indian Valley and Clear Lake control and regulate water flowing into lower Cache Creek. The lower Cache Creek basin flows into the CCSB. A weir is located at the outlet of the settling basin to help entrap sediment.

A number of inactive mines lie in the watershed, draining into Cache Creek. Runoff from historic mercury mines in the Rathburn-Petray group discharge primarily to Bear Creek. Harley Gulch drains a 14 km<sup>2</sup> subwatershed in the upper Cache Creek basin. The inactive Turkey Run and Abbott mercury mines drain to Harley Gulch. Davis Creek drains also into the upper Cache Creek basin. Davis Creek subwatershed includes the Reed, Harrison and Manhattan mercury mines. Sulphur Creek flows from its headwaters to Bear Creek. Inactive mines along the creek include the Elgin, Clyde, Empire, Manzanita, West End, Central, Cherry Hill, and Wide Awake mines. Sources of mercury in Cache Creek watershed include discharge from numerous inactive mines, erosion of stream beds and banks containing mercury, natural and anthropogenic erosion of soils with naturally occurring mercury, natural and altered geothermal springs, and atmospheric deposition (Central Valley Regional Water Quality Control Board, 2005 and 2008). Occurrence of methyl-mercury in Cache Creek largely parallels the sources of total mercury. Upper Cache Creek watershed is the major source of methyl-mercury. Clean sediment entering the streambed in the lower Cache Creek watershed dilutes sediment mercury concentrations. Mercury loads from the major and mine-related tributaries (North Fork Cache Creek, Clear Lake outflow, Bear Creek, Harley Gulch, and Davis Creek) contribute 12-15 percent of the mercury loads measured in Cache Creek at Rumsey. The majority of the inorganic mercury loads are from unknown source areas, which include smaller, unmeasured tributaries and mercury in the creek bed and banks (Central Valley Regional Water Quality Control Board, 2004 and 2005).

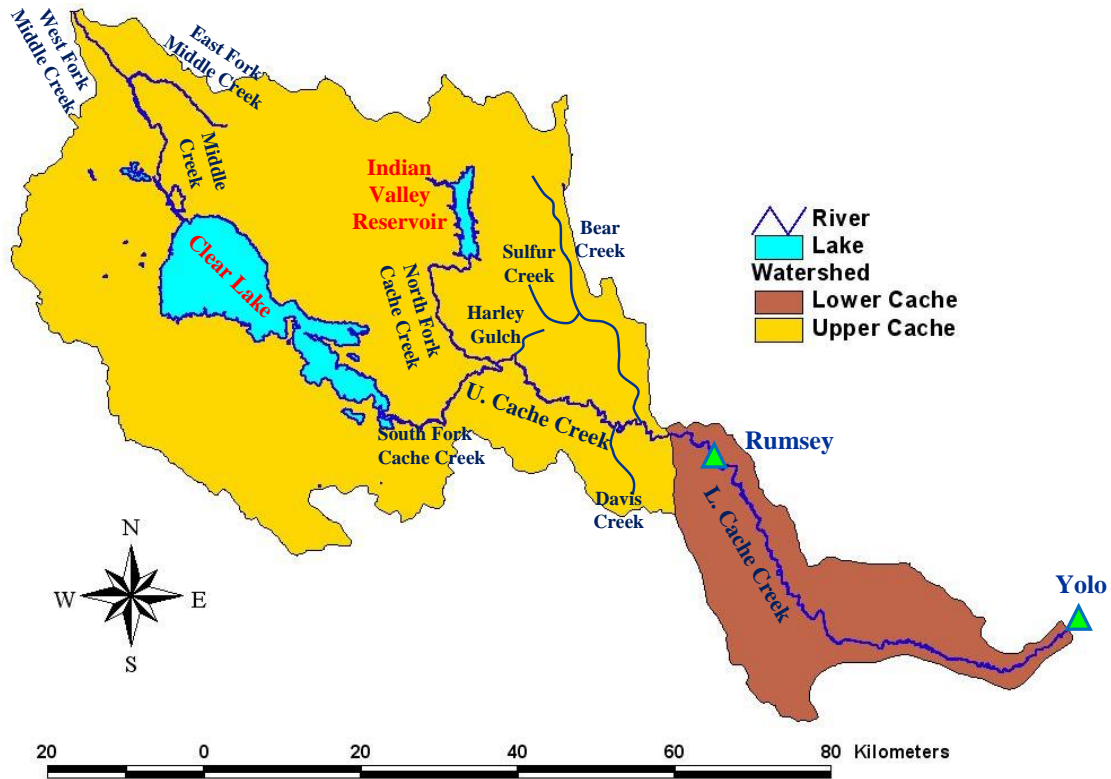
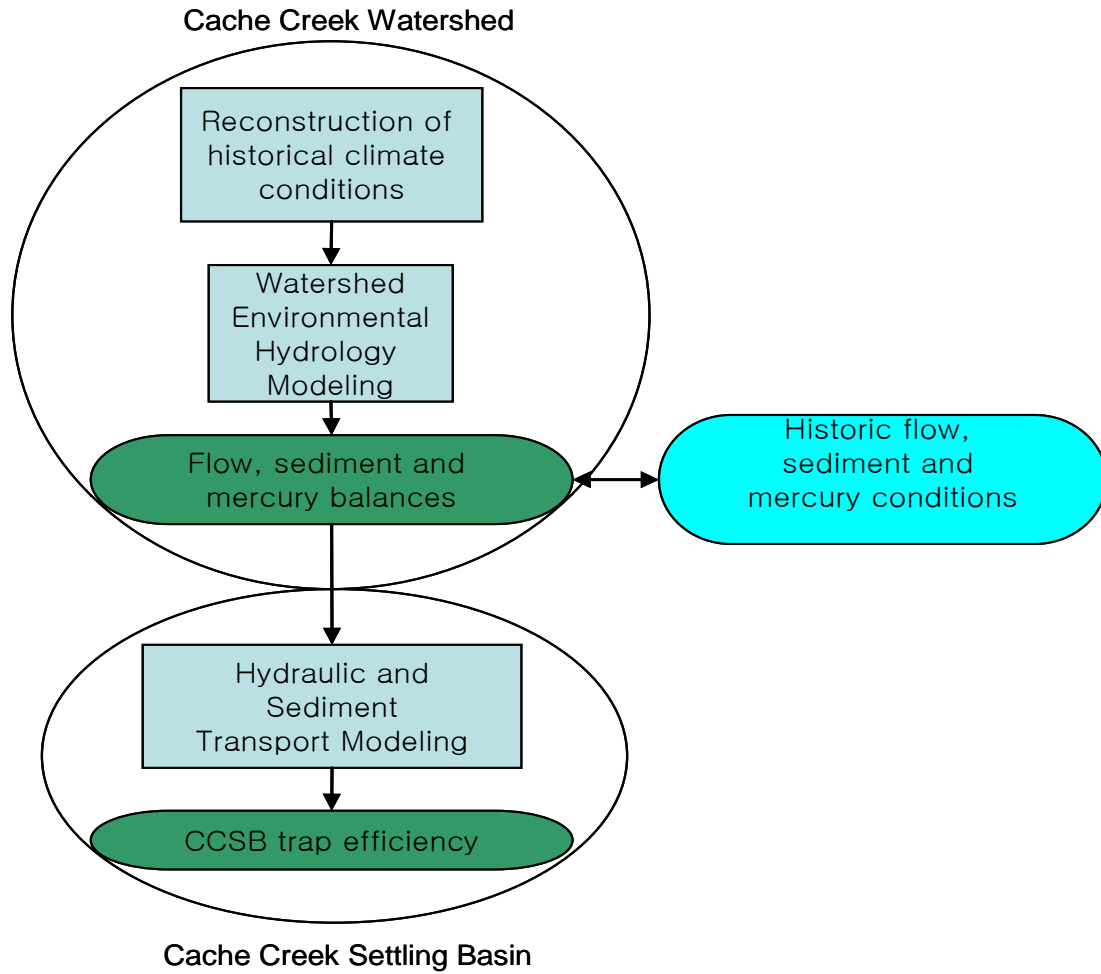


Figure 1- Cache Creek Watershed

### 3. Methodology

Climate change and Watershed Environmental Hydrology Modeling approaches facilitate realistic and comprehensive computation of water, sediment and mercury balances in the Cache Creek Watershed for historical and future climate conditions. The models are to be calibrated and validated by means of comparisons of the model-simulated historical flows, sediment and mercury conditions in the watershed against corresponding historical observations. By means of an ensemble of 13 possible realizations of the future hydro-climate conditions over Cache Creek Watershed, simulated by the models, an ensemble prediction of trap efficiency of CCSB can then be performed by hydraulic and sediment / mercury transport modeling using boundary conditions that can be built from the model-simulated water, sediment and mercury outflows from the Cache Creek Watershed into the CCSB. Schematics of modeling approaches for historical and future climate conditions are depicted in Figures 2 and 3, respectively.



**Figure 2- A schematic description of the modeling approach for the historical conditions**

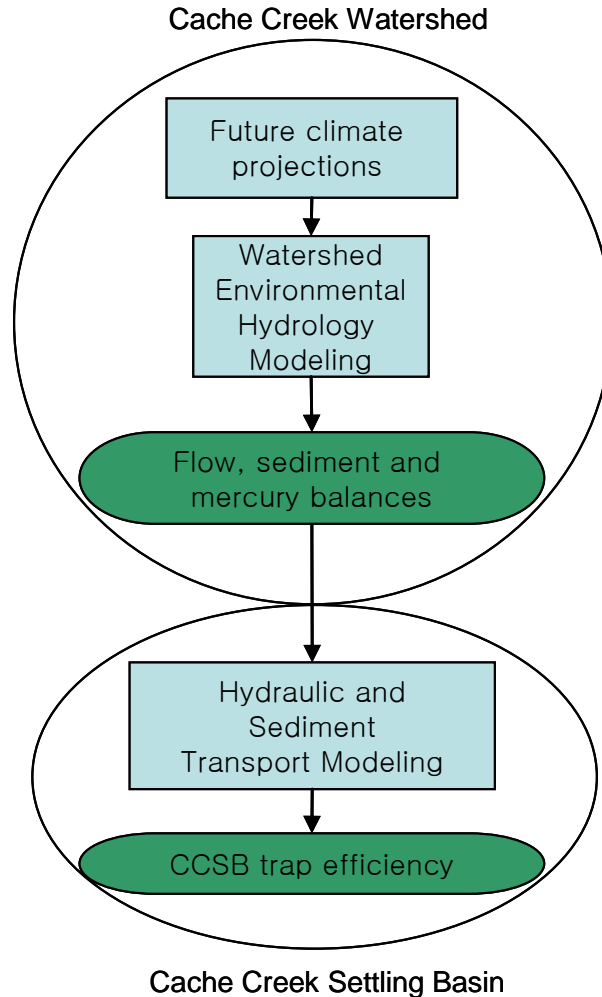


**Figure 3- A schematic description of the modeling approach for future conditions**

### **3.1. Regional Hydro-Climate Modeling**

The dynamical downscaling of the GCM climate simulations may be performed by means of a Regional Hydro-climate model (RegHCM) to a grid resolution of 3km over the Cache Creek Watershed. The RegHCM consists of two major model components: a mesoscale (regional scale) atmospheric model component, and a regional land surface hydrology model component (Chen et. al. 1996; Kavvas et. al. 1998; Kavvas et al. 2000, 2007). The atmospheric model component of the RegHCM is MM5 (the Fifth Generation Mesoscale Model) from NCAR (US National Center for Atmospheric Research). The regional land surface hydrology model is based on upscaled hydrologic conservation equations (Chen et. al. 1993; Chen et. al., 1994a,b; Kavvas et

al. 1998). It has been applied to hydro-meteorological phenomena over a wide range of scales at various locations around the world, ranging from continental-scale cyclone development to local valley flows (Chen et. al. 2008; Ohara et. al. 2008; Shaaban et. al. 2008).

The Penn State/NCAR Mesoscale Model (PSU/NCAR) originated from The Pennsylvania State University in the early 70's. The Fifth-Generation NCAR / Penn State Mesoscale Model (MM5) (Grell et al. 1995) is the latest in a series of models developed from a mesoscale (regional scale) model originally documented by Anthes and Warner (1978). The PSU/NCAR mesoscale model is a limited-area, hydrostatic or nonhydrostatic, terrain-following sigma-coordinate model designed to simulate or predict regional-scale atmospheric circulation over any limited area on Earth. It is continuously being improved by contributions from users at several universities and government laboratories. The most recent version of The Penn State/NCAR Mesoscale Model is the Fifth-Generation Penn State/NCAR Mesoscale Model (MM5).

### **3.2. Hydrology and Environmental Modeling**

The Watershed Environmental Hydrology model (WEHY) is an award-winning watershed hydrology model (ASCE 2006 Best paper award) recently developed (Kavvas et al, 2004, Chen et al, 2004a,b; Kavvas et al. 2006) after about a decade of research effort. WEHY is a physically based watershed hydrology and sediment/nutrient/heavy metal transport model based upon areally-averaged hydrologic conservation equations and transport equations in order to account for the effect of spatial heterogeneity in land surface and subsurface conditions on the hydrologic flow and environmental processes.

By developing a detailed geographical information system (GIS) for the vegetation, land use/land cover conditions, soils, topography and geology of the watershed being modeled, model parameters are objectively estimated by computer algorithms relating parameter values to land surface and subsurface conditions, rather than simply fitting the model. As such, it is applicable to the modeling of hydrologic processes at any geographical location, even in ungauged or data-poor basins.

In its land surface hydrology component, WEHY model describes interception, bare soil evaporation, direct evaporation from ponded water over the plant leaves, soil water flow, and plant transpiration. The boundary layer component of MM5 provides information on the velocity, temperature, and relative humidity profiles in the atmosphere above the land surface. Evapotranspiration from land surfaces to the atmosphere is computed by means of the boundary layer velocity and relative humidity information on one hand, and from the soil water flow process and plant physiology that dictate the soil moisture availability, on the other. Soil water flow is computed as a component of the WEHY model. The model can describe both the Hortonian (infiltration excess) runoff mechanism as well as the variable-source-area runoff mechanism (Dunne, 1978). As such, it is applicable both to vegetated watersheds as well as to arid/semiarid watersheds.

WEHY subdivides a watershed first into model computational units (MCU) that are delineated from the digital elevation map of the watershed by means of a geographic information system (GIS) analysis (Chen et al. 2004a). These MCUs are either individual hillslopes or first-order-subwatersheds within a watershed. Their identification and delineation are described in Chen et al.(2004a). WEHY computes the surface and subsurface hillslope hydrologic processes that take place at these MCUs, in parallel and simultaneously.

In its environmental module (Kavvas et al. 2006), the WEHY model simulates sediment, nutrient and heavy metal transport through a watershed by means of physically-based transport equations. In the WEHY model erosion, deposition and transport processes of sediment take place in various domains, starting from hillslope interrill areas, moving to rills, and then to streams

## **4. Sediment and Mercury Data Compilation and Data Gap Analysis**

### **4.1. Soil Erosion in Cache Creek Watershed**

Erosion is the detachment of soil particles caused by water or glacial ice. Eroded sediment is both a physical and chemical pollutant. Chemically, eroded sediment degrades water quality and transports nutrients such as phosphorus, nitrogen, and heavy metals such as mercury.

The potential source areas of sediment and mercury in Cache Creek Watershed can be approximately identified through the Universal Soil Loss Equation (USLE). Identifying source areas will help in the development of boundary conditions of sediment and mercury transportation in Cache Creek Watershed. A schematic description of the Universal Soil Loss Equation calculation methodology is depicted in Figure 4. Using USLE, the average annual soil loss can be calculated by

$$A = R \cdot K \cdot LS \cdot C \cdot P$$

where  $A$  is average annual soil loss (ton/acre/year),  $R$  is rainfall factor (ft-ton-in. / acre-h-year),  $K$  is erodibility factor (ton/acre/R),  $LS$  is length slope factor,  $C$  is soil cover factor, and  $P$  is conservation practice factor.

Figure 5 shows the estimated parameters of USLE. The soil erosion map of Cache Creek Watershed is plotted using USLE in Figure 6. Mercury point sources are located at high erosion areas in the upper Cache Creek Watershed. In lower Cache Creek Watershed, there is a high erosion area but no mercury point source. Therefore, sediment entering from lower Cache Creek watershed acts to dilute the sediment mercury concentrations. The soil erosion map will help the development of boundary conditions for sediment and mercury transport in Cache Creek Watershed.

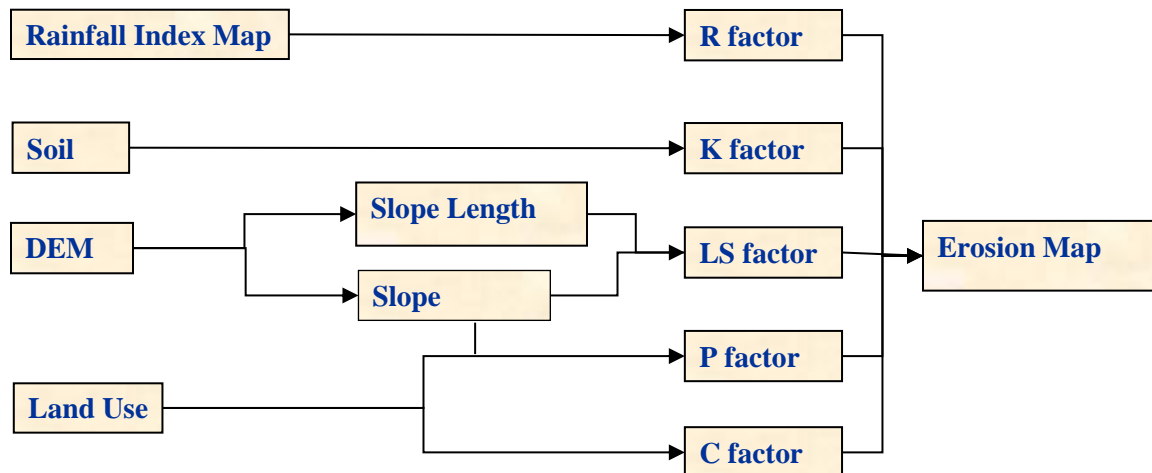


**Figure 4-** A schematic description of the Universal Soil Loss Equation calculation

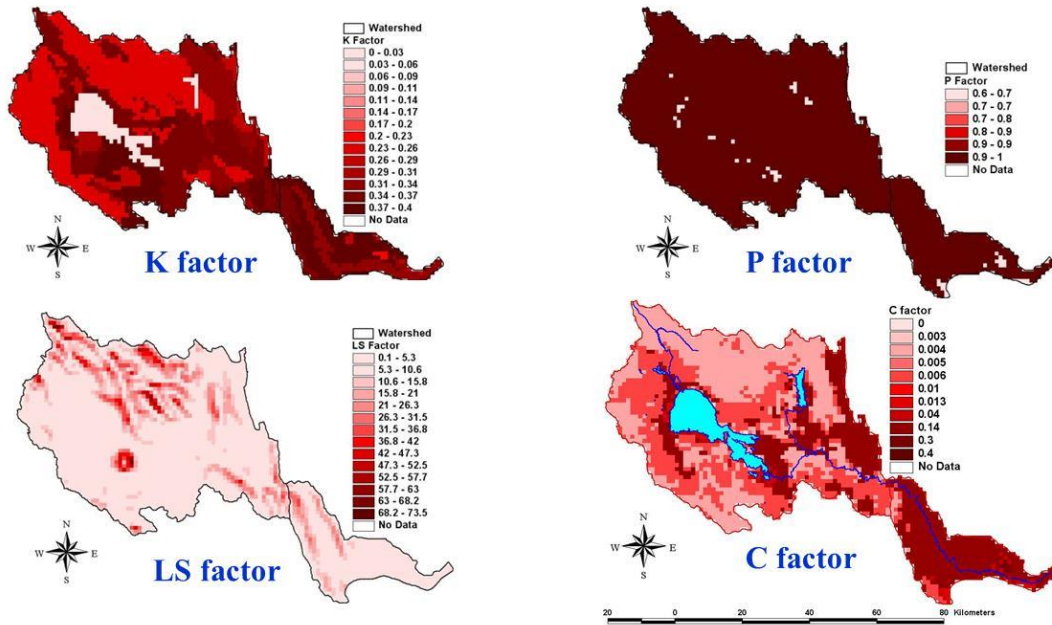


Figure 5- Estimated parameters for USLE over the Cache Creek watershed

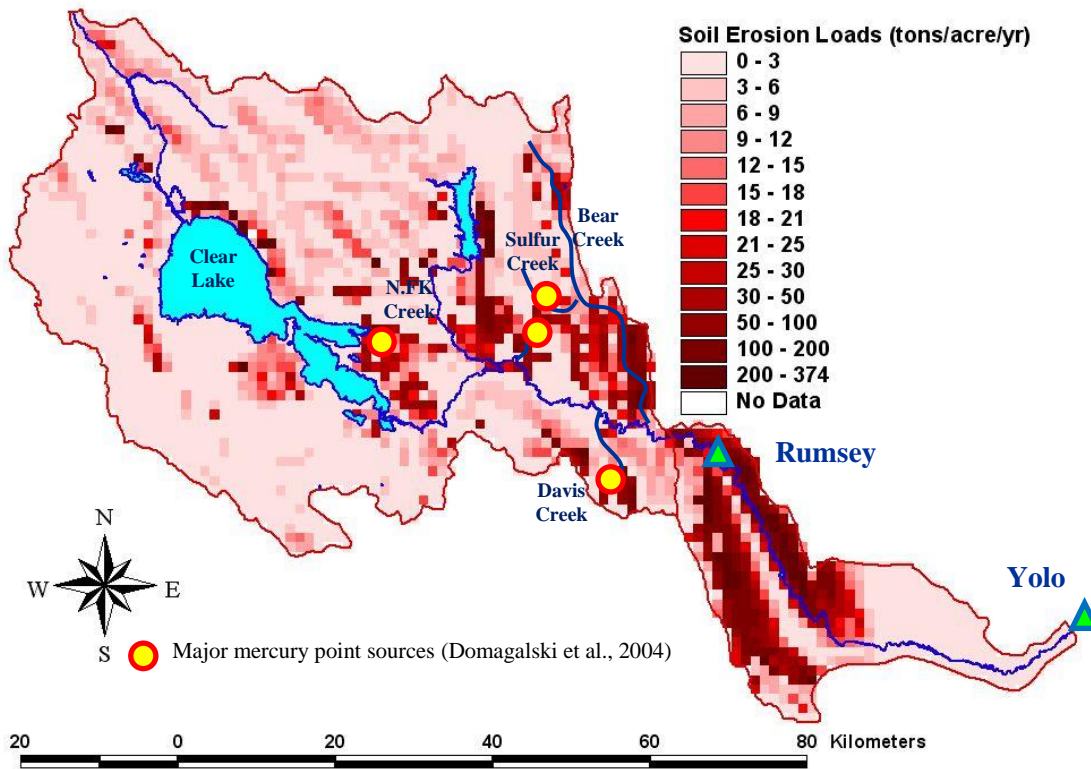


Figure 6- The soil erosion map of Cache Creek Watershed using USLE

## **4.2. Sensitivity Analysis for trap efficiency at CCSB**

Recently, a CCSB Mercury Study assessed potential modifications of CCSB to increase sediment and mercury deposition while improving the quality of Cache Creek outflows (CDM, 2004a, 2004b, 2007).

Conclusions about sediment and mercury trap efficiency of CCSB in CDM (2007) study were based on HEC-6 model (CDM, 2004b) that was developed by US Army Corps of Engineers in 1997. The Corps model only covers the training channel portion of CCSB. CDM (2004b) extended the Corps model from the outlet of the training channel to greater CCSB area based on a 2D hydraulic model that was developed by the Corps (documented in 1987 General Design Memorandum). Model input was based on the 1983 survey data. Using HEC-6 model described in CDM (2004b).

We present the influence of the sediment rating curve and inlet flow conditions on CCSB sediment trap efficiency. Our analyses showed that trap efficiency is very much dependent on the sediment rating curve and inlet flow conditions. Therefore, a rigorous approach should be used to determine the sediment rating curve and inlet flow conditions.

### **a) Inflow Boundary Conditions**

The Corps constructed a computational hydrograph for simulating the entire 50-year project life using USGS daily flows at the Yolo stream gage from 1980-1989. This 10-year period was repeated five times to generate the 50-year simulation period (CDM, 2004b). Daily Average Discharge (cfs) at Cache Creek at Yolo during water years 1904-2008 and 1980-1989 are depicted in Figures 7 and 8, respectively. Repeating the relatively short 10-year historical flow record for analysis purposes may not be representative of the real life conditions. The 30,000 cfs discharge, which is the design capacity of upstream Cache Creek levee system, has approximately a 10-year return period. Hence, this 30,000 cfs discharge is added every 10-years in our sensitivity analysis.

### **b) Sediment Rating Curve**

“The Corps developed the inflowing sediment load estimate as described in the 1997 HEC-6 analysis (Corps 1997). The sediment inflow is input into the model as a relationship between streamflow discharge rate versus total sediment load (in tons/day), which includes both bedload and suspended load. This relationship was based primarily on a sediment-discharge curve documented in the General Design Memorandum (Corps 1987), which was ultimately derived from long-term instantaneous samples collected by the USGS between 1943 and 1971.” (CDM, 2004b).

Instantaneous suspended sediment load data are available from 10/14/1957 to 09/30/1986 for Cache Creek at Yolo. (source: <http://nwis.waterdata.usgs.gov>, USGS 11452500). This dataset is depicted in Figure 9. Bed load was measured to be 7.3% of suspended sediment load at Cache Creek at Yolo for the water years 1960-1963 in Lustig and Busch (1967). Total sediment load at Cache Creek at Yolo was measured and a regression line was given in Lustig and Busch (1967). However, the regression equation does not represent flows larger than 13000 cfs. In our sensitivity analysis, three rating curves are used and they are tabulated in Table 1 below. The actions to fill the data gaps in the sediment rating curve can be completed by generating simultaneously the sediment loads and the corresponding flows larger than 13000 cfs. Such concurrent sediment and flow data can be obtained by gauge observations or simulations of WEHY-Hydrologic and Environmental module. The observation method cannot be accomplished easily since the flows larger than 13000 rarely happen. In the meantime, simulation method using WEHY model is able to generate numerous concurrent sediment and flows larger than 13000 cfs. However, WEHY model can only provide those concurrent data by simulations after calibration and validation processes by means of observations. In this project, the calibration and validation processes for WEHY-Environmental module could not be accomplished due to insufficient concurrent flow, sediment and mercury data. Without calibration and validation, the environmental module cannot generate reliable sediment and mercury data that can then be used to produce the sediment rating curve. Therefore, collection of field sediment and mercury data is crucial for accomplishing the objectives of this project.

#### **4.2.1 Results and Discussion**

The sediment balance and trap efficiency in CCSB and in the training channel, obtained from a 50 year simulation, are tabulated in Tables 2 and 3, respectively. Using the assumptions described in CDM (2004b), the average trap efficiency in CCSB is 51%, 30%, 60% and 60% during the periods 2008-2043, 2008-2018, 2018-2028, and 2028-2043, respectively. Using the new assumptions for flow and sediment rating curves (“new estimate”), the average trap efficiency in CCSB is obtained as 43%, 11%, 60% and 57% during the periods 2008-2043, 2008-2018, 2018-2028, and 2028-2043, respectively. More conservative results were obtained using the sediment rating curve given in Lustig and Busch (1967). According to Table 3, the trap efficiency of the training channel is considerably lower when compared to that of the settling basin. The sediment trap efficiency in CCSB, obtained by means of a 100 year simulation, is tabulated in Table 4. This table shows that the life span of CCSB is very much dependent on the inflow conditions and the sediment rating curve used.

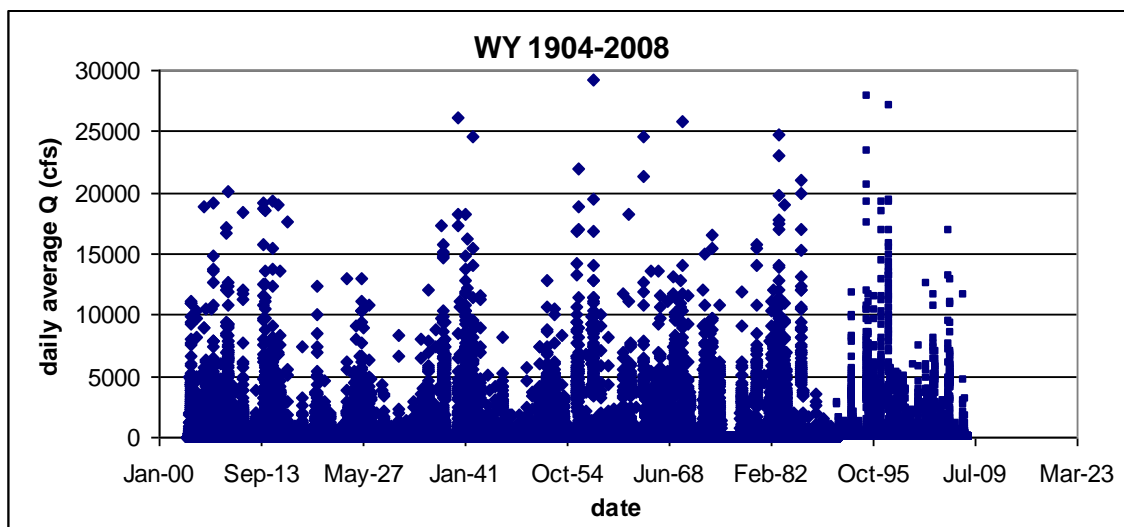


**Figure 7- Daily Average Discharge (cfs) at Cache Creek at Yolo between 1904-2008 water years**

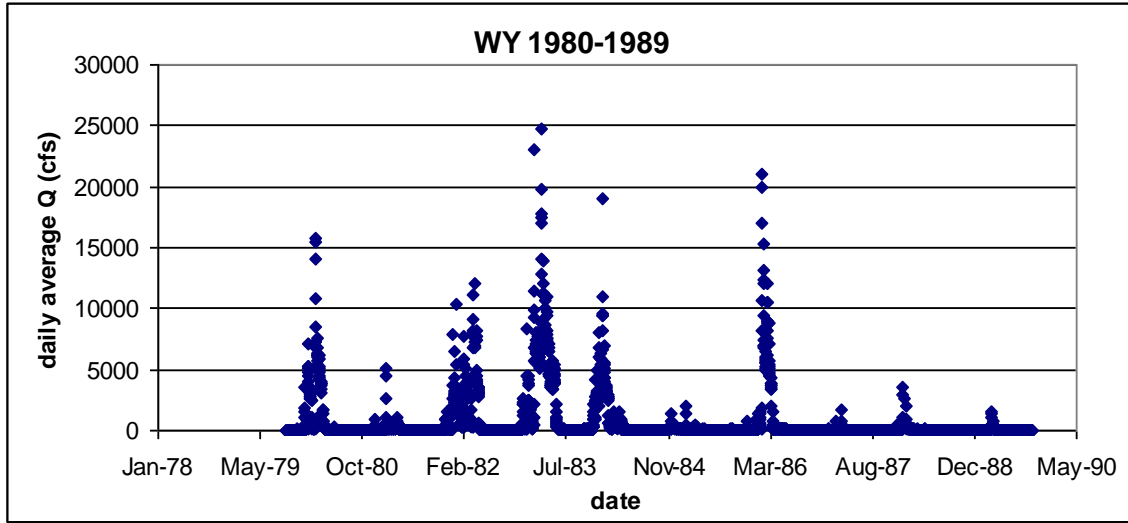


Figure 8- Daily Average Discharge (cfs) at Cache Creek at Yolo during 1980-1989 water years

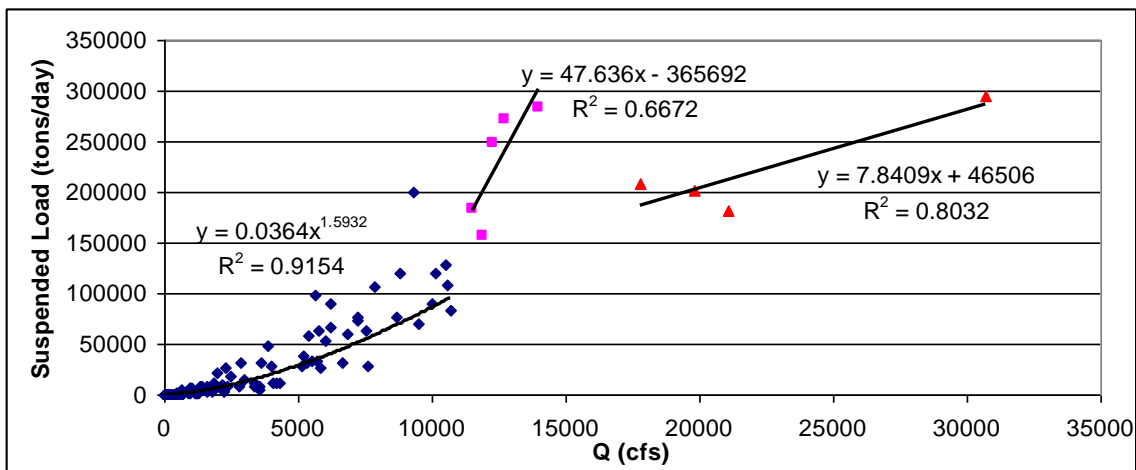


Figure 9- The sediment rating curve at Cache Creek at Yolo that is used in this study

**Table 1- Discharge (cfs) versus total sediment load (tons per day) at Cache Creek at Yolo**

Q (cfs)	CDM (2004b) <sup>1</sup>	New estimation <sup>2</sup>	Lustig and Busch (1967) <sup>3</sup>
50	15	20	4
100	41	60	17
500	400	780	420
1,000	1,188	2,352	1,658
5,000	15,350	30,555	40,190
10,000	47,340	92,189	158,660
20,000	146,700	218,256	626,329
30,000	285,300	302,423	1,398,424
<sup>1</sup> Corps developed the inflowing sediment load estimate as described in Corps 1997. CDM (2004b) used the same rating curve.			
<sup>2</sup> Developed for sensitivity analysis using instantaneous suspended sediment load data from 10/14/1957 to 09/30/1986. Bed load is assumed to be 7.3% of suspended sediment load (Lustig and Busch, 1967).			
<sup>3</sup> $Q_s = 0.00189Q_w^{1.981}$ where $Q_s$ is total sediment discharge in tons per day and $Q_w$ is water discharge in cfs.			

**Table 2- Sensitivity analyses for sediment balance and trap efficiency in CCSB using a 50-year simulation**

	CDM (2004b) <sup>1</sup>		New Estimate <sup>2</sup>		Lustig and Busch (1967) <sup>3</sup>	
	1993-2043 <sup>4</sup>	1983-2043 <sup>5</sup>	1993-2043 <sup>4</sup>	1983-2043 <sup>5</sup>	1993-2043 <sup>4</sup>	1983-2043 <sup>5</sup>
<b>Years 2008-2043</b>						
Sediment outflow (ac-ft)	11074	12040	23976	24322	43801	46343
Sediment inflow (ac-ft)	22390	22537	42341	42515	70216	71078
Trapped (ac-ft)	11316	10497	18365	18193	26416	24735
Ave. Trap eff.	0.51	0.47	0.43	0.43	0.38	0.35
Ave. trapped per year (ac-ft)	323	300	525	520	755	707
<b>Years 2008-2018<sup>6</sup></b>						
Sediment outflow (ac-ft)	4943	5895	11841	12120	20052	20219
Sediment inflow (ac-ft)	7097	7135	13306	13377	21706	22111
Trapped (ac-ft)	2154	1240	1465	1257	1654	1892
Ave. Trap eff.	0.3	0.17	0.11	0.09	0.08	0.09
Ave. trapped per year (ac-ft)	215	124	147	126	165	189
<b>Years 2018-2028</b>						
Sediment outflow (ac-ft)	2735	2743	5276	5239	8729	8907
Sediment inflow (ac-ft)	6823	6878	13161	13223	21905	22174
Trapped (ac-ft)	4088	4135	7885	7984	13176	13267
Ave. Trap eff.	0.6	0.6	0.6	0.6	0.6	0.6
Ave. trapped per year (ac-ft)	409	414	788	798	1318	1327
<b>Years 2028-2043</b>						
Sediment outflow (ac-ft)	3395	3402	6859	6962	15020	17216
Sediment inflow (ac-ft)	8469	8524	15873	15915	26605	26792
Trapped (ac-ft)	5074	5122	9014	8953	11585	9576
Ave. Trap eff.	0.6	0.6	0.57	0.56	0.44	0.36
Ave. trapped per year (ac-ft)	338	341	601	597	772	638

<sup>1</sup> HEC-6 simulation in 2004 TM

<sup>2</sup> Same assumptions as HEC-6 model described in CDM (2004b) except 30000 cfs flow is added every 10 years and new sediment rating curve is used (see Table 1).

<sup>3</sup> Same assumptions as HEC-6 model described in CDM (2004b) except 30000 cfs flow is added every 10 years and the sediment rating curve of Lustig and Busch (1967) is used (see Table 1).

<sup>4</sup> 1993-2043 is the HEC-6 simulation period in 2004 TM

<sup>5</sup> Instead of 1993, HEC-6 model started at 1983 since the cross-section of the settling basin was constructed using 1983 survey data.

<sup>6</sup> In the year 2018 the weir at the outlet of the settling basin is assumed to be raised 6 ft.

**Table 3- Sensitivity analyses for sediment balance and trap efficiency in the training channel using a 50-year simulation.**

	CDM (2004b) <sup>1</sup>		New Estimate <sup>2</sup>		Lustig and Busch (1967) <sup>3</sup>	
	1993-2043 <sup>4</sup>	1983-2043 <sup>5</sup>	1993-2043 <sup>4</sup>	1983-2043 <sup>5</sup>	1993-2043 <sup>4</sup>	1983-2043 <sup>5</sup>
<b>Years 2008-2043</b>						
Sediment outflow (ac-ft)	22390	22537	42341	42515	70216	71078
Sediment inflow (ac-ft)	23713	23713	44434	44434	74830	74830
Trapped (ac-ft)	1324	1176	2093	1919	4613	3752
Ave. Trap eff.	0.06	0.05	0.05	0.04	0.06	0.05
Ave. trapped per year (ac-ft)	38	34	60	55	132	107
<b>Years 2008-2018<sup>6</sup></b>						
Sediment outflow (ac-ft)	7097	7135	13306	13377	21706	22111
Sediment inflow (ac-ft)	7403	7403	13921	13921	23273	23273
Trapped (ac-ft)	305	268	615	544	1567	1162
Ave. Trap eff.	0.04	0.04	0.04	0.04	0.07	0.05
Ave. trapped per year (ac-ft)	31	27	61	54	157	116
<b>Years 2018-2028</b>						
Sediment outflow (ac-ft)	6823	6878	13161	13223	21905	22174
Sediment inflow (ac-ft)	7398	7398	13911	13911	23266	23266
Trapped (ac-ft)	575	520	750	689	1361	1092
Ave. Trap eff.	0.08	0.07	0.05	0.05	0.06	0.05
Ave. trapped per year (ac-ft)	57	52	75	69	136	109
<b>Years 2028-2043</b>						
Sediment outflow (ac-ft)	8469	8524	15873	15915	26605	26792
Sediment inflow (ac-ft)	8912	8912	16602	16602	28291	28291
Trapped (ac-ft)	443	389	728	687	1686	1499
Ave. Trap eff.	0.05	0.04	0.04	0.04	0.06	0.05
Ave. trapped per year (ac-ft)	30	26	49	46	112	100

<sup>1</sup> HEC-6 simulation in 2004 TM

<sup>2</sup> Same assumptions as HEC-6 model described in CDM (2004b) except 30000 cfs flow is added every 10 years and a new sediment rating curve is used (see Table 1).

<sup>3</sup> Same assumptions as HEC-6 model described in CDM (2004b) except 30000 cfs flow is added every 10 years and the sediment rating curve of Lustig and Busch (1967) is used (see Table 1).

<sup>4</sup> 1993-2043 is the HEC-6 simulation period in 2004 TM

<sup>5</sup> Instead of 1993, HEC-6 model started at 1983 since the cross-section of the settling basin was constructed using the 1983 survey data.

<sup>6</sup> In the year 2018 the weir at the outlet of the settling basin is assumed to be raised 6 ft.

**Table 4- Sensitivity analyses for sediment balance and trap efficiency in CCSB using 100-year simulation.**

	CDM (2004b) <sup>1</sup>	New Estimate <sup>2</sup>	
	1993-2093 <sup>3</sup>	1993-2093 <sup>3</sup>	1983-2093 <sup>4</sup>
<b>Years 2008 - 2043</b>			
Ave. Trap eff.	0.51	0.43	0.43
Ave. trapped per year (ac-ft)	323.3	522.5	519.9
Sediment inflow (ac-ft)	22390	42221	42514
<b>Years 2008 and 2093</b>			
Ave. Trap eff.	0.51	0.31	0.29
Ave. trapped per year (ac-ft)	351.3	395.1	376.9
Sediment inflow (ac-ft)	57990	109461	109609
<b>Years 2008 - 2018<sup>5</sup></b>			
Ave. Trap eff.	0.30	0.11	0.09
Ave. trapped per year (ac-ft)	215.4	146.5	125.5
Sediment inflow (ac-ft)	7097	13306	13361
<b>Years 2018 - 2028</b>			
Ave. Trap eff.	0.60	0.60	0.60
Ave. trapped per year (ac-ft)	408.8	788.5	798.0
Sediment inflow (ac-ft)	6823	13161	13236
<b>Years 2028 - 2038</b>			
Ave. Trap eff.	0.60	0.57	0.57
Ave. trapped per year (ac-ft)	420.0	760.2	756.3
Sediment inflow (ac-ft)	7010	13283	13320
<b>Years 2038 - 2048</b>			
Ave. Trap eff.	0.59	0.51	0.48
Ave. trapped per year (ac-ft)	422.7	676.6	648.1
Sediment inflow (ac-ft)	7171	13347	13379
<b>Years 2048 - 2058</b>			
Ave. Trap eff.	0.57	0.35	0.30
Ave. trapped per year (ac-ft)	405.3	474.3	407.2
Sediment inflow (ac-ft)	7097	13395	13364
<b>Years 2058 - 2068</b>			
Ave. Trap eff.	0.55	0.16	0.13
Ave. trapped per year (ac-ft)	389.5	211.0	173.5
Sediment inflow (ac-ft)	7105	13422	13441

<sup>1</sup> HEC-6 model described in CDM (2004b)

<sup>2</sup> Same assumptions as HEC-6 model described in CDM (2004b) except 30000 cfs flow is added every 10 year and new sediment rating curve is used (see Table 1).

<sup>3</sup> 50 year simulation (1993-2043) period used in CDM (2004b) is extended to 100 year by using the same flow data twice.

<sup>4</sup> Instead of 1993, HEC-6 model started at 1983 since cross-section of the settling basin was constructed using 1983 survey data.

<sup>5</sup> In year 2018, weir at the outlet of the settling basin is assumed to be raised 6 ft.

### 4.3. Data Availability and Recommendations for Data Collection

#### 4.3.1 Data Availability

Observation data are crucial for model calibration and validation for both watershed hydrology and environmental modeling. The information on available data for this study has been surveyed through various data sources such as CDEC, USGS web-based inventories and reports related to the Cache Creek watershed.

#### a) Streamflow Data

Figure 10 shows the available streamflow gauges from USGS, CDEC, and Yolo Flood Control and Water Conservation District. The purple-color tables indicate the flow gauges with real-time flow data and the yellow-color tables indicate the flow gauges with daily flow data. As shown in Figure 10, most real-time (or hourly) data are available only since late 1990s and are not sufficient for model calibration and validation.

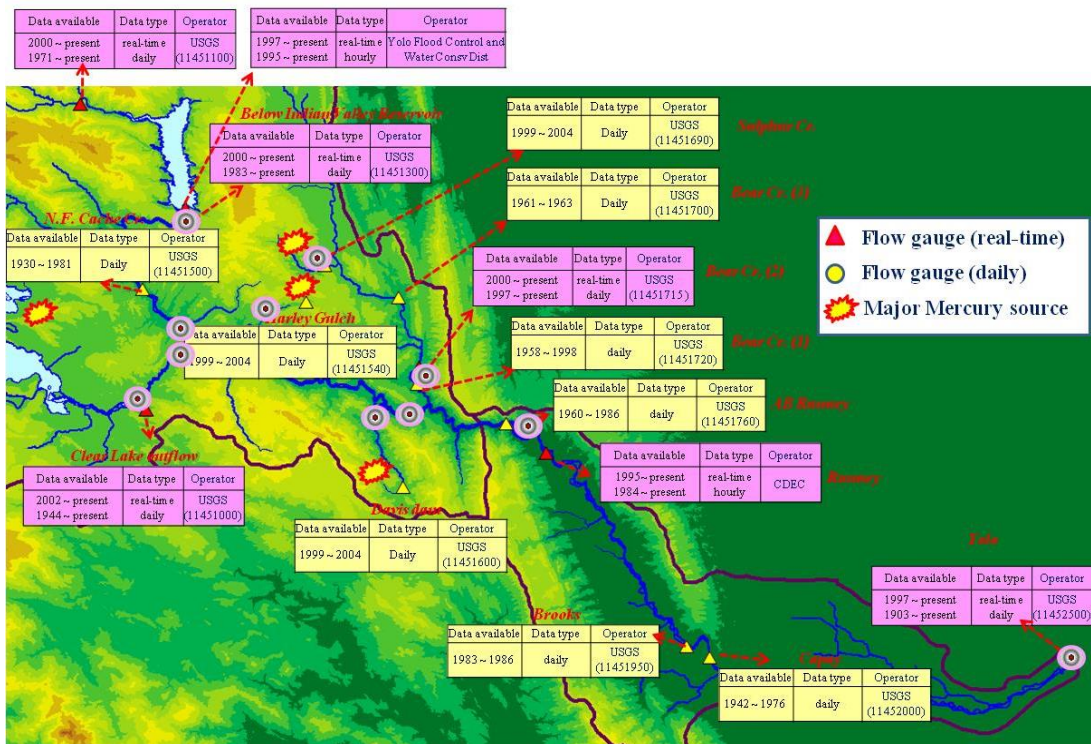


Figure 10- Available streamflow gauges for this study

## b) In-water Mercury/Sediment Data

Figure 11 shows the availability of historical field/lab sampling data from USGS web-based inventory. The data from USGS were sampled instantaneously for both (mercury or/and sediment) solute and flow. However, most total suspended sediment and mercury data have been obtained from occasional samples.

Figure 12 shows the available data from Cooke et al. (2004) who collected the data through several projects. Although the collected data include the solutes (TSS, THg, MeHg, and flow), it is not clear whether the flow and solutes were sampled simultaneously. It should be noted that the simultaneous solute/flow data are crucial to estimate the water quality loads such as sediment and mercury. The data availability of mercury and sediment in water from USGS and Cooke et al. (2004) studies is shown in Figure 13. Instantaneous grab sampling data concurrent with flow data are required for model calibration and validation.

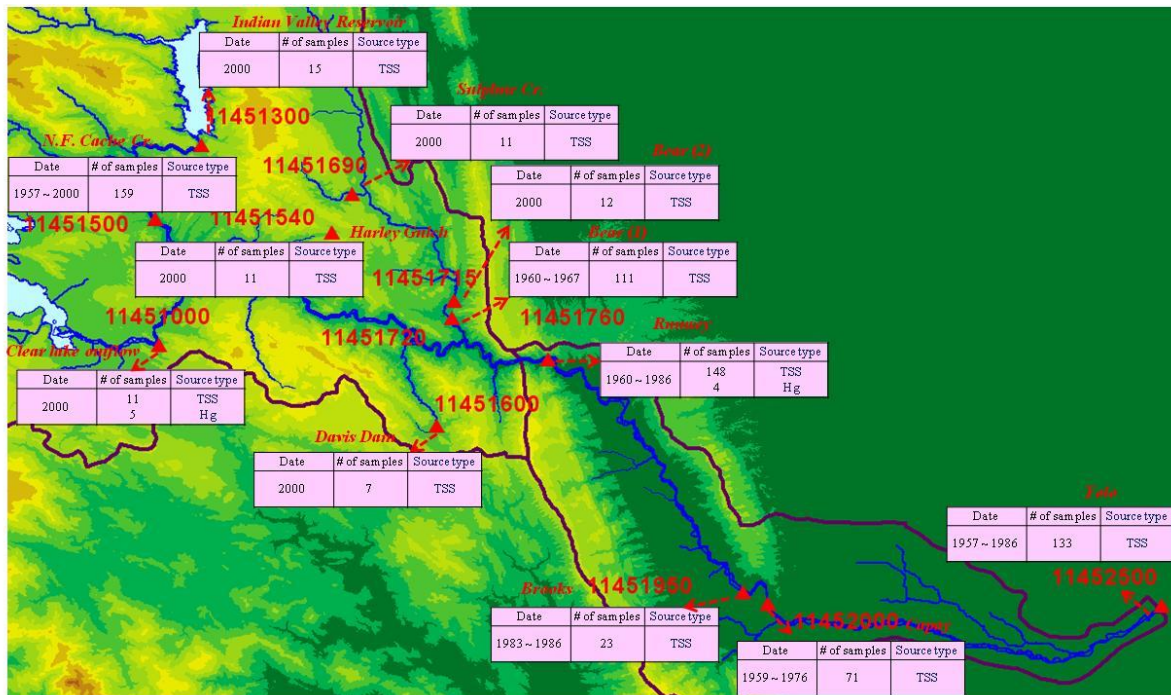
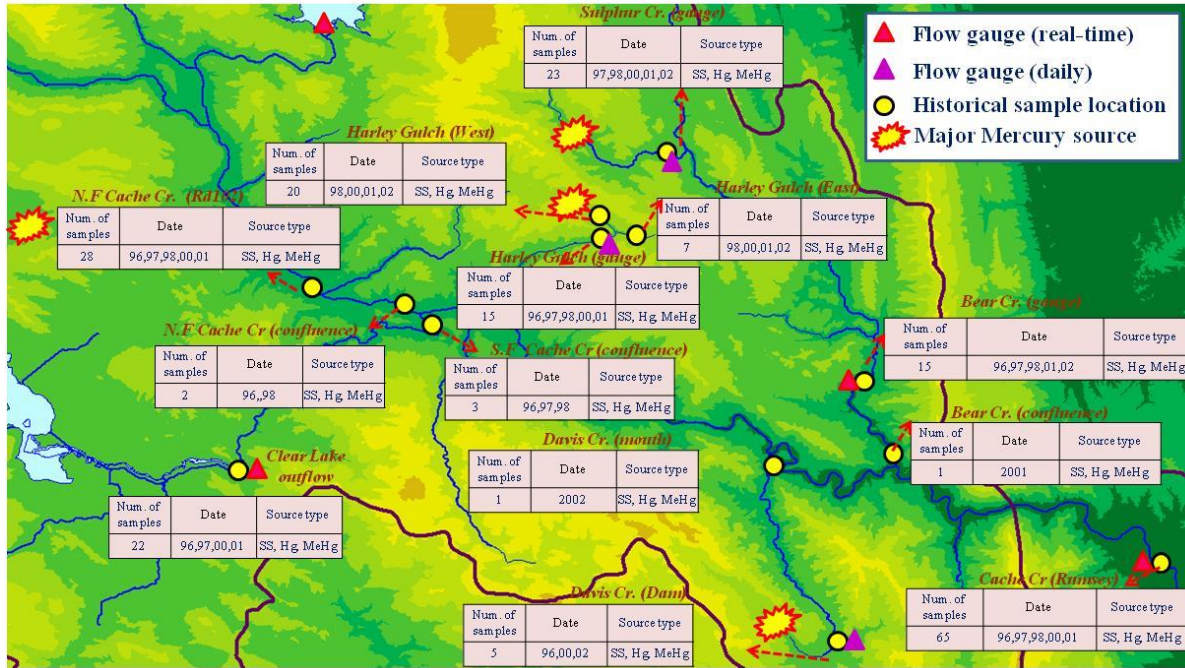


Figure 11- Historical field/lab sampling data from USGS



**Figure 12- Historical field/lab suspended sediment and mercury data from Cooke et al. (2004)**

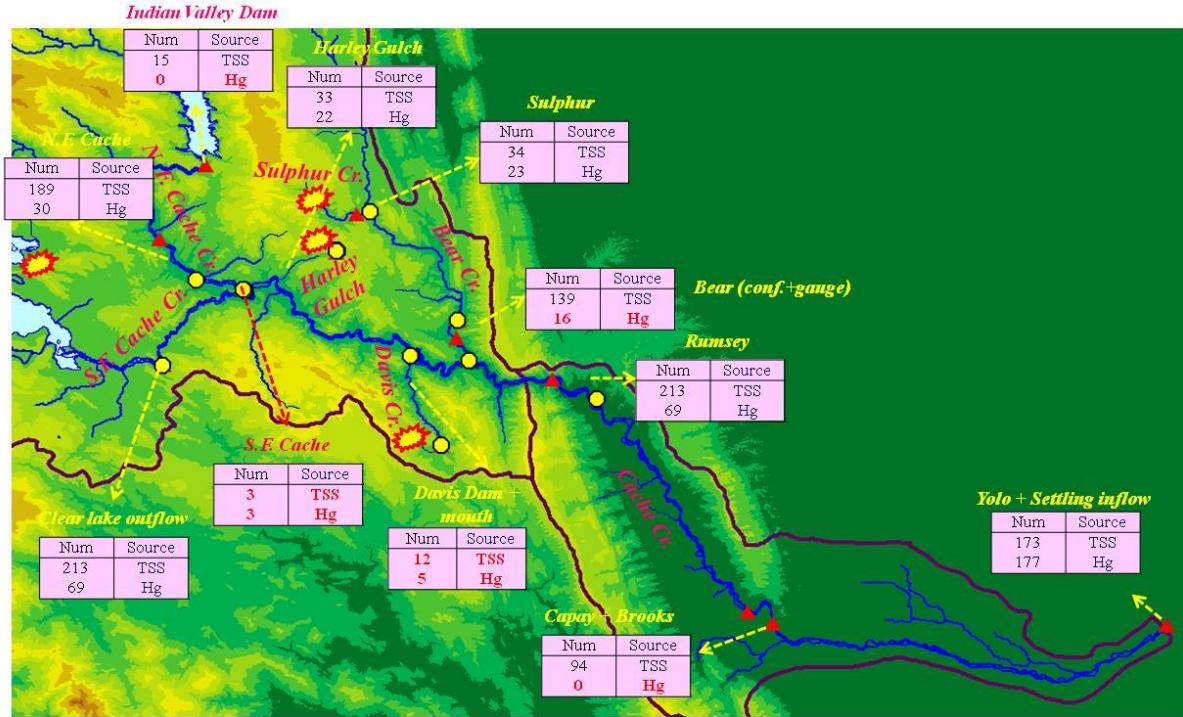
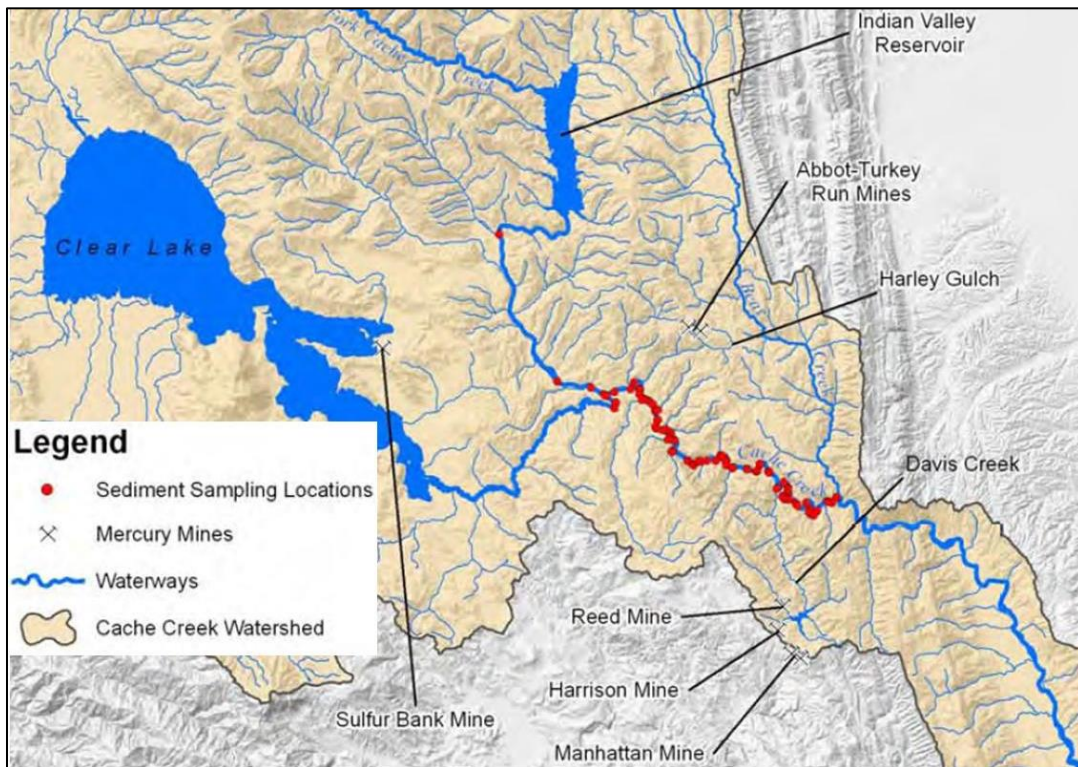


Figure 13- Available historical field/lab sediment and mercury data from Cooke et al. (2004) and USGS

### c) Mercury/ Sediment Data in Soils

The mercury in the stream may be in suspension or may be deposited, and this phenomenon can be accounted for in model simulations. Some valuable mercury and sediment data in soils has been reported (Foe and Bosworth, 2008; Bosworth and Morris, 2009). The mercury in sediment samples was collected in the depositional areas, streambeds, and banks (Bosworth and Morris, 2009 for Bear Creek and its tributaries; Foe and Bosworth, 2008 for Cache Creek Canyon) as showed in Figures 14 through 19. The sampling locations cover the major mercury source areas from the Clear lake outflow to upstream of Rumsey. However, there is no data between Rumsey and Yolo. In fact, the mercury concentration decreases from Rumsey toward Yolo. Capay dam is located between Rumsey and Yolo, and it may play an important role in mercury and suspended sediment trapping and transport. Hence, additional mercury data within the stream are required for realistic model simulations. One necessary sampling location would be between Rumsey and Capay dam, and another location would be between Capay dam and Yolo.



**Figure 14- Overview of sampling locations for Cache Creek Canyon (Foe and Bosworth, 2008)**

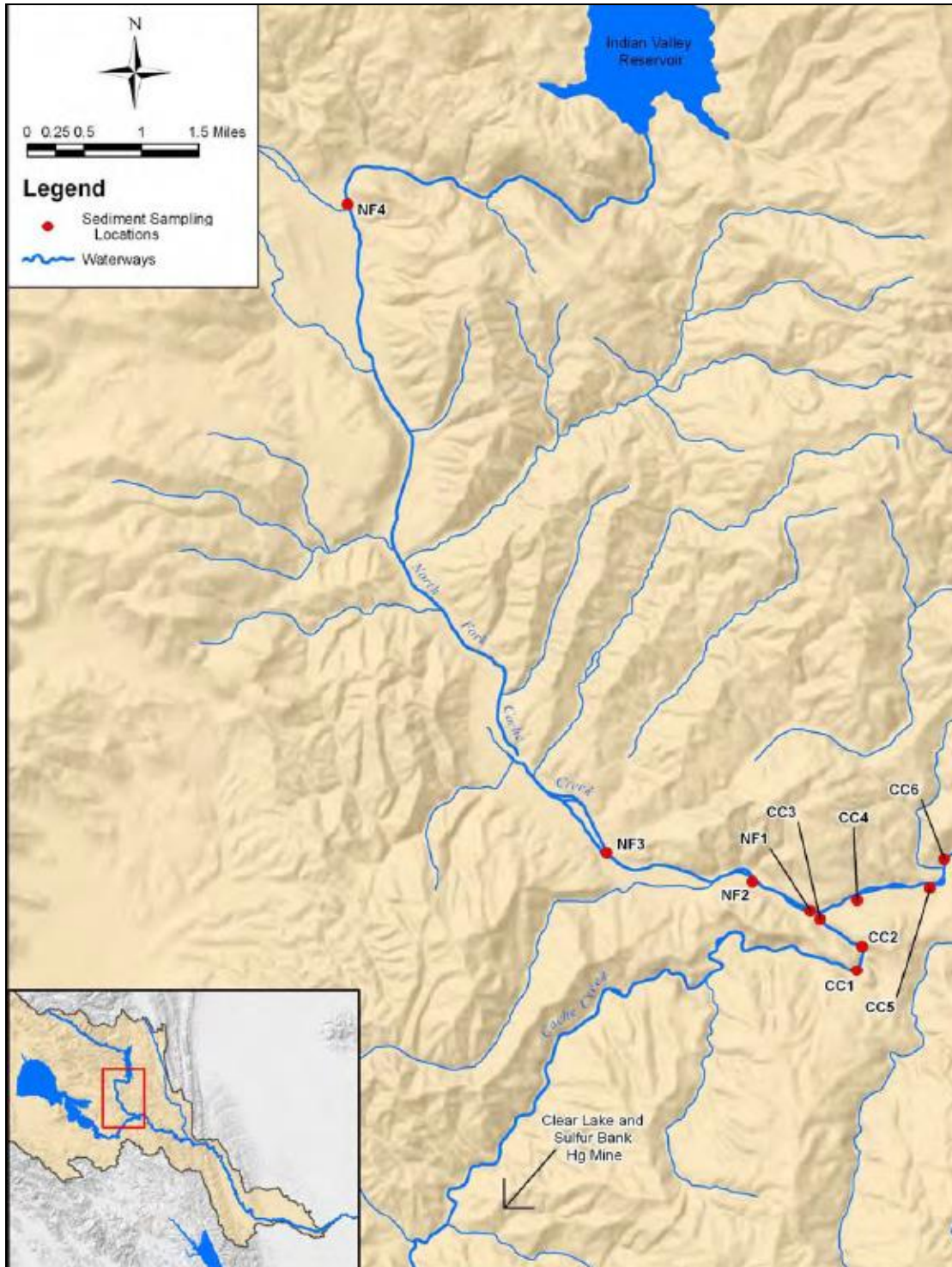


**Figure 15- Sampling locations from Cache Creek, North Fork downstream toward Bear Creek (Foe and Bosworth, 2008)**

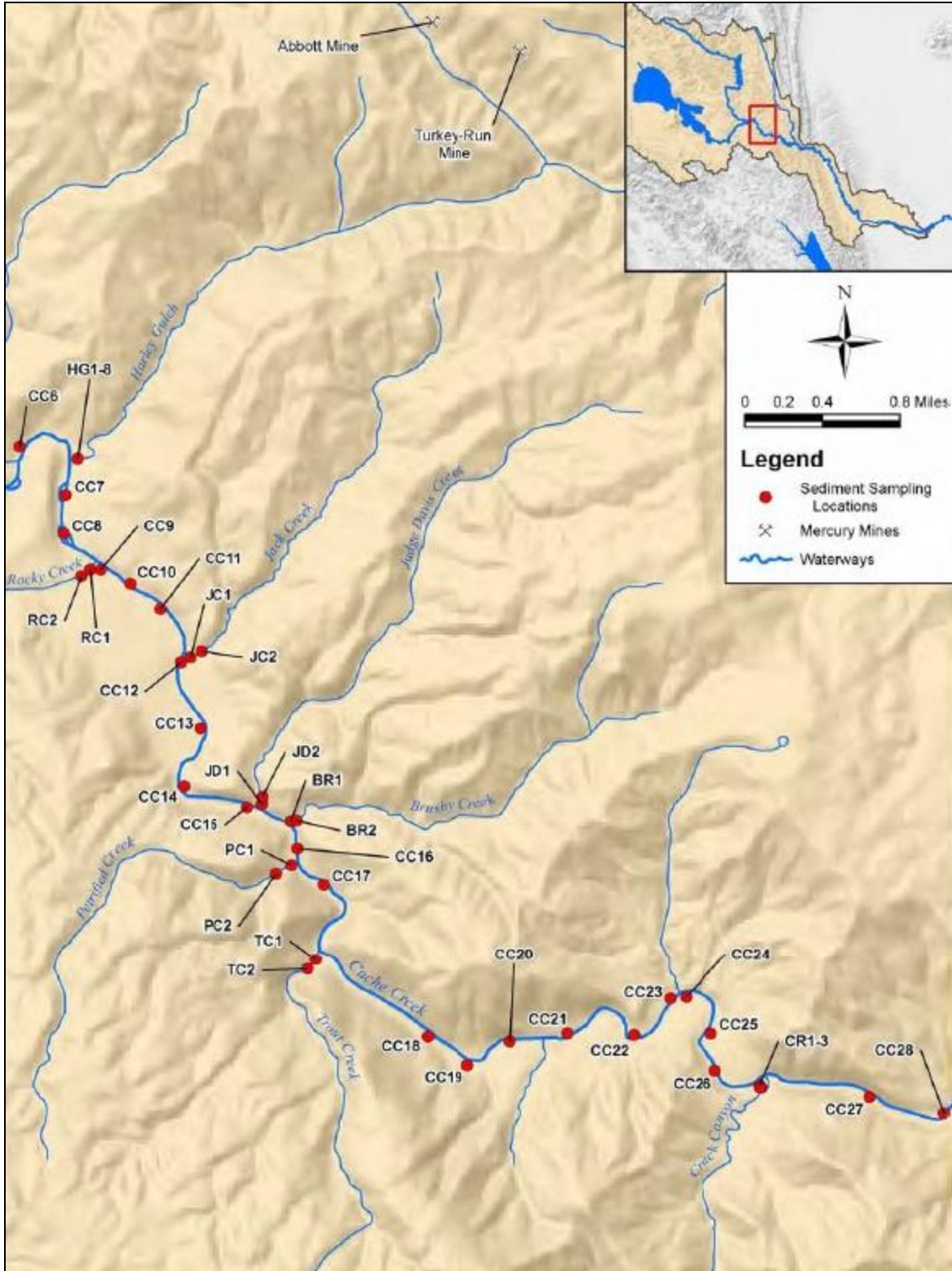


**Figure 16- Sampling locations from Cache Creek, North Fork downstream toward Bear Creek, continued (Foe and Bosworth, 2008)**

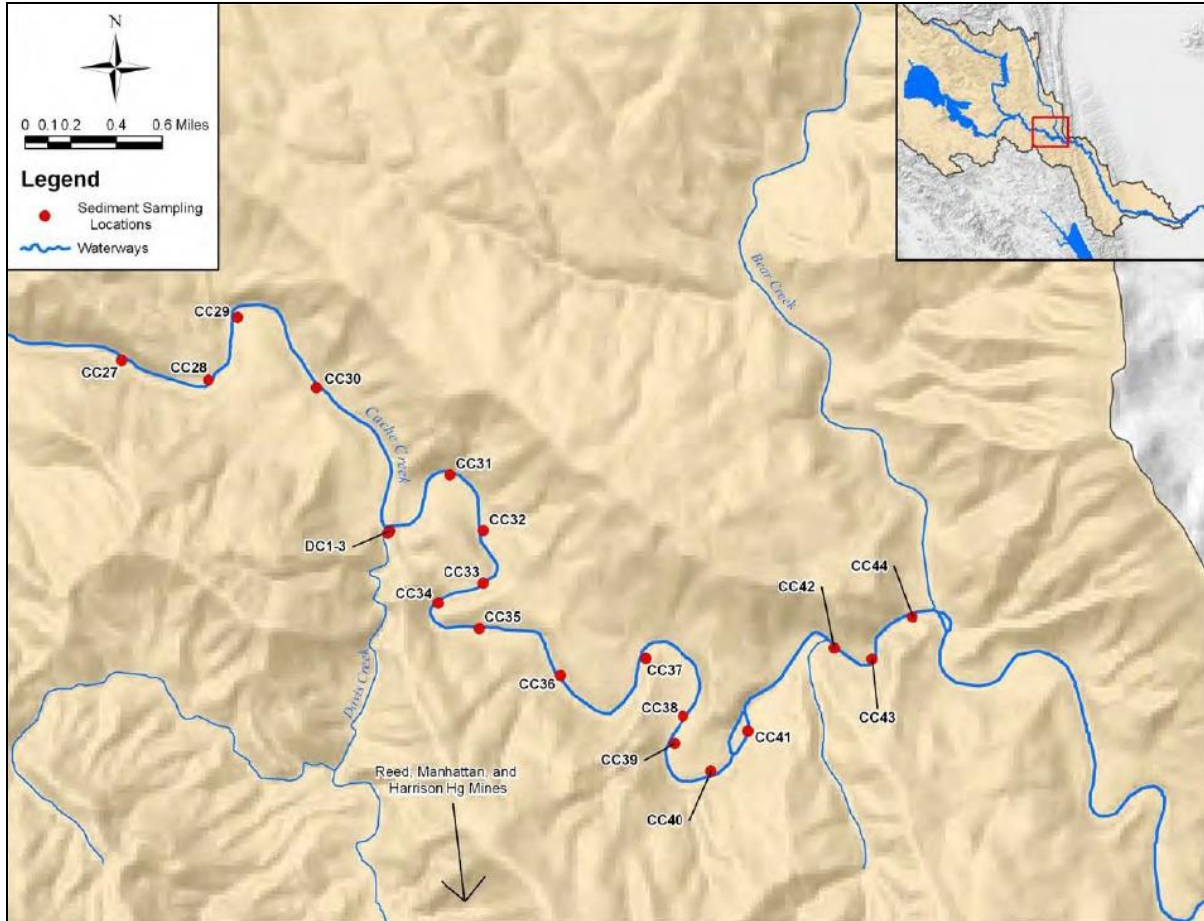


**Figure 17- Sampling locations from Cache Creek, North Fork downstream toward Bear Creek, continued (Foe and Bosworth, 2008)**

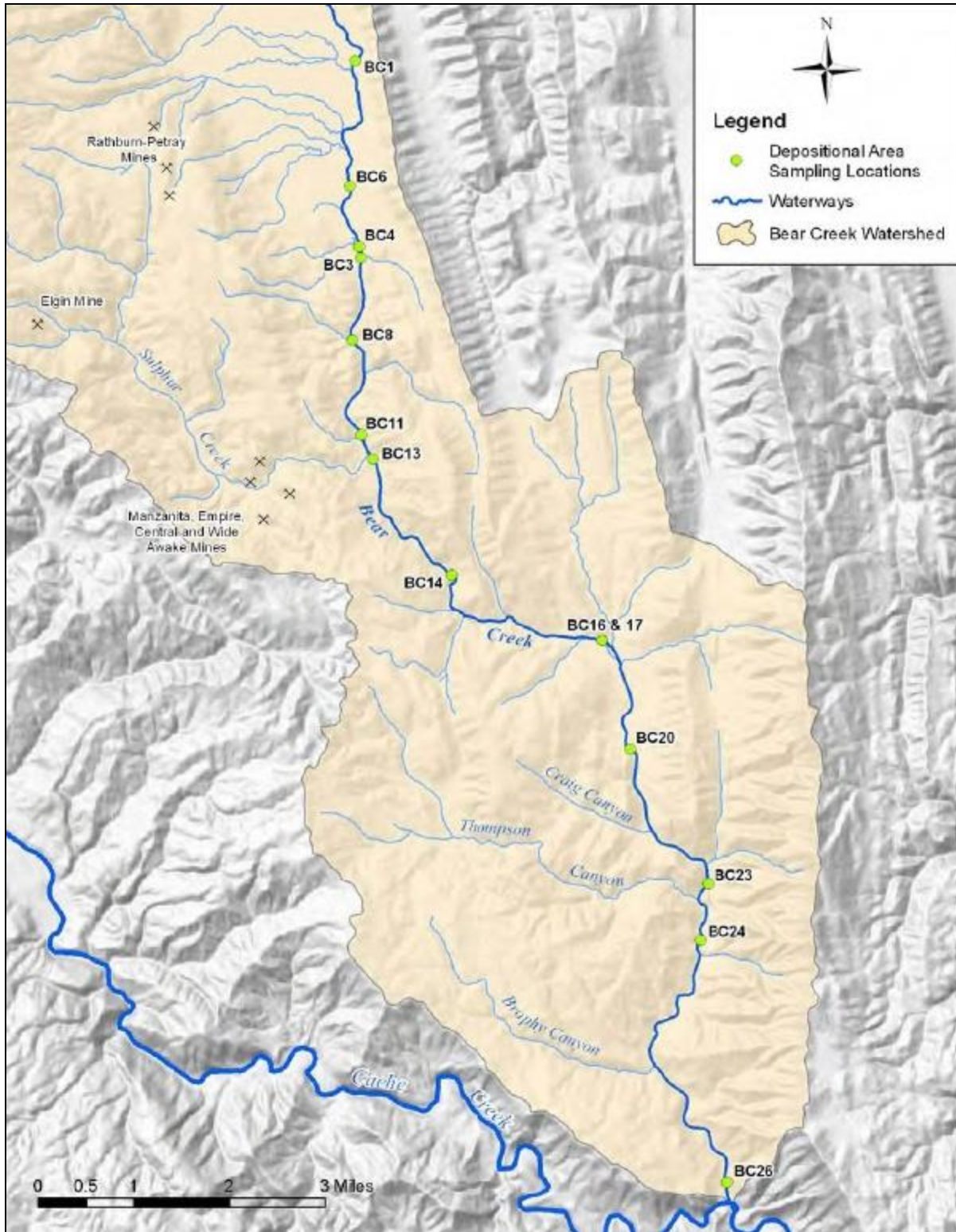


Figure 18- Sampling locations at Bear Creek (Bosworth and Morris, 2009)

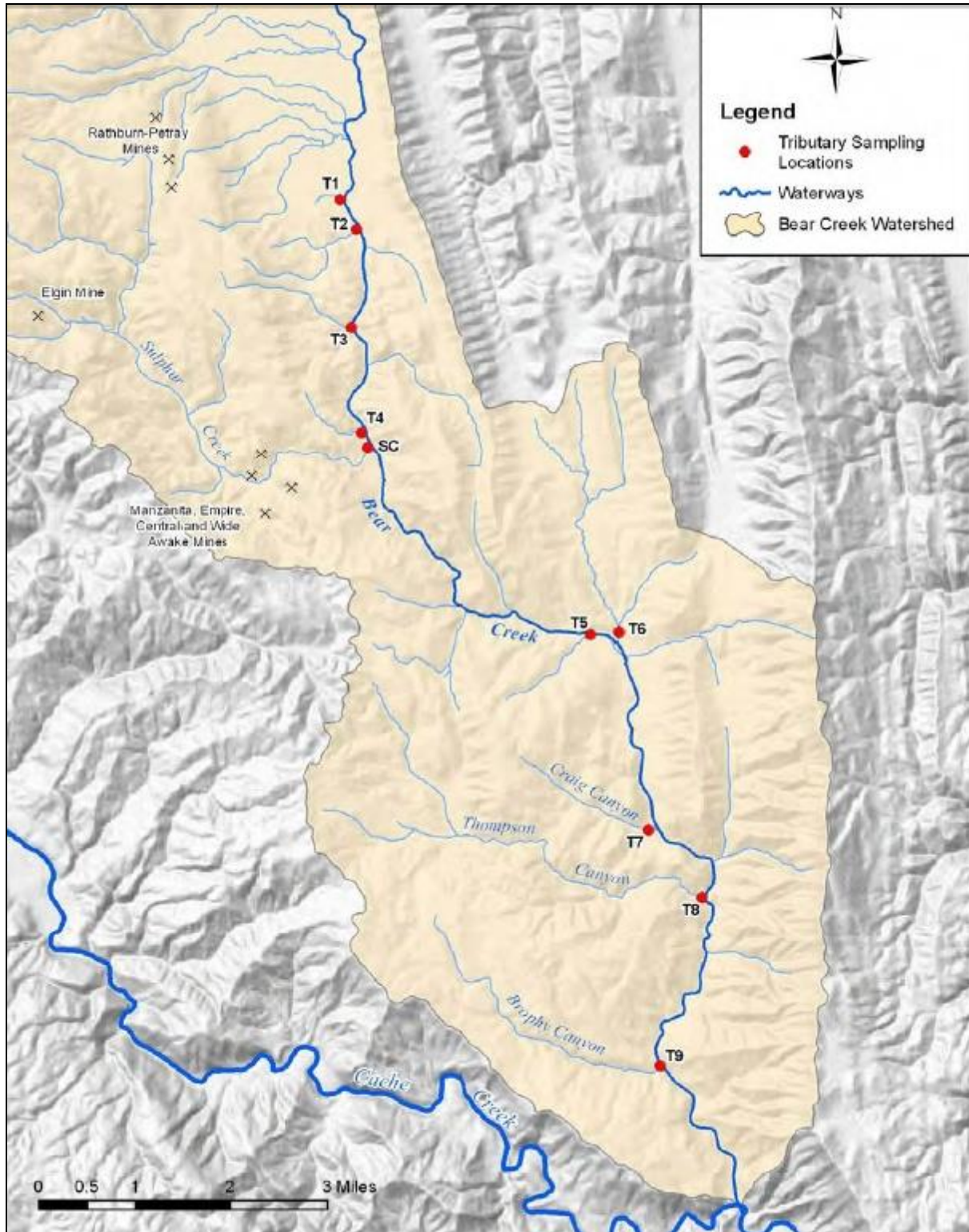


Figure 19- Sampling locations at the tributaries of Bear Creek (Bosworth and Morris, 2009)

### 4.3.2 Recommendations for Data Collection

As stated above, the data collected in various previous projects at Cache Creek watershed are insufficient for utilization in the calibration and validation of WEHY environmental hydrology model fundamentally due to lack of concurrent flow-sediment-mercury observations. There is an urgent need for a field-monitoring program at several locations, distributed over the watershed.

The desired sampling locations are shown in Figure 20 below. However, the substantial cost of realizing the desired sampling program is recognized. As such, if it is not possible to perform the monitoring at the 11 desired locations due to cost constraints, it is still absolutely essential to carry out a sampling program for sediment and mercury, simultaneously with the flow observations, at least at the Rumsey station. Accordingly, the following sampling data which should be collected simultaneously with streamflow data, are recommended as essential for the calibration and validation of an environmental hydrology model, such the WEHY model, in order to produce reliable and scientifically defensible simulations of flow, sediment and mercury at the Yolo station in order to be able to reconstruct the portion of the sediment rating curve corresponding to flows above 13000 cfs:

- **Instantaneous grab sampling data (suspended sediment, and mercury)**
  - At Rumsey station
- **Data on Mercury within the streambed (soil) at**
  - At Rumsey station

which should be collected **concurrently with flow measurements.**

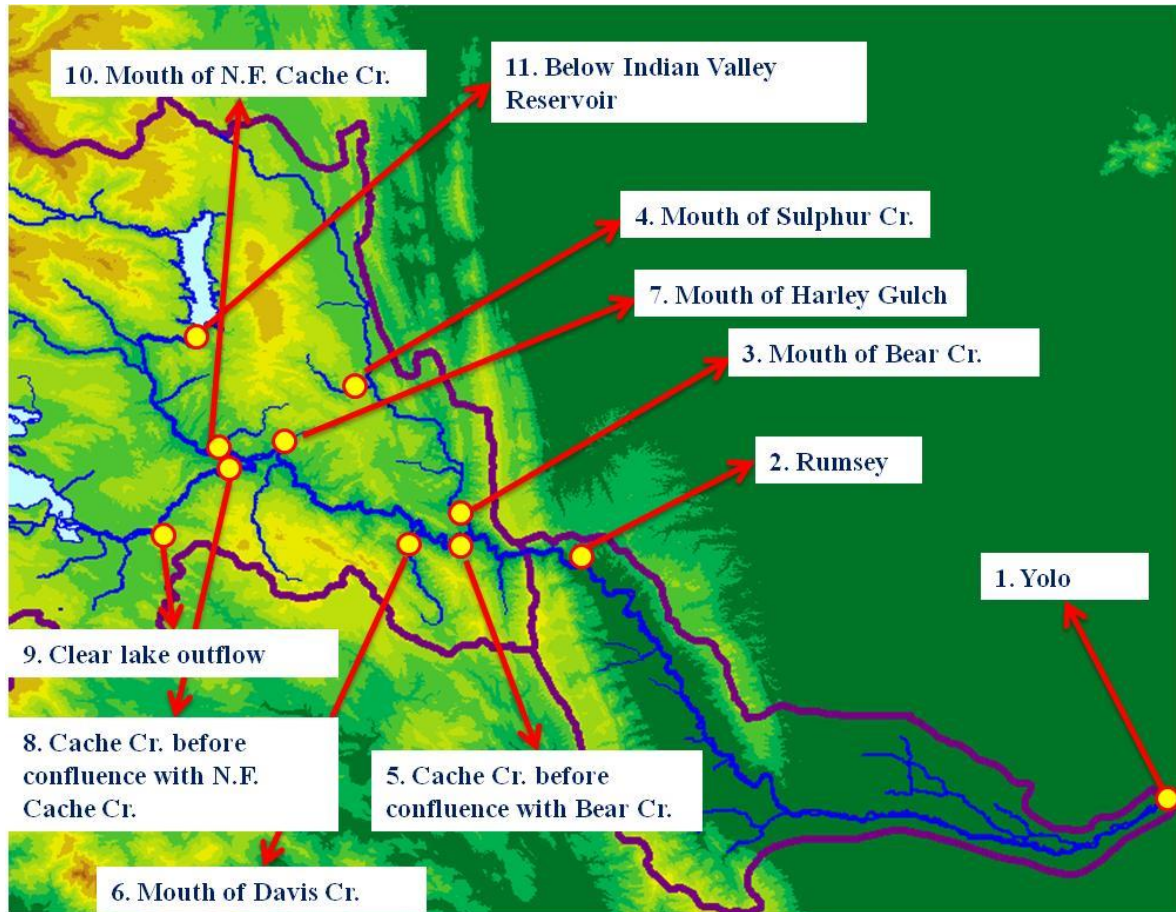


**Figure 20- Overview of desired sampling locations (11 locations)**

## **5. Reconstruction of Historical and Projection of Future Climate Conditions**

Since the hydrologic module of the WEHY model was successfully calibrated and validated for the Cache Creek watershed, it was possible to reconstruct the historical flows and to project the outflows from the watershed during the 21<sup>st</sup> century under various emission scenarios, two global climate models and various initial conditions. In the following the details of this work are given.

## 5.1. Setting up the MM5 modeling domains over Cache Creek watershed

Spatially distributed atmospheric data at fine time intervals are required to simulate streamflow using the WEHY model. However, atmospheric data at hourly time intervals for sufficiently long periods are scarce within the Cache Creek watershed. Hence, the historical atmospheric data were reconstructed during the simulation periods at hourly intervals and at 3km grid resolution over the whole Cache Creek watershed.

The methodology for generating a reconstructed atmospheric variable at the scale of the Cache Creek watershed begins with obtaining the NCAR/NCEP global reanalysis data from NCAR via anonymous file transfer protocol (ftp). The NCAR/NCEP reanalysis data comprise a global set of atmospheric data on a regular grid with a horizontal spatial scale of approximately 210×210 km for latitudes near the Cache Creek watershed. Reanalysis data are derived from the analysis of various data sources including land surface, ship, rawinsonde, pibal, aircraft, and satellite. These data are assimilated into a global circulation model to create an atmospheric database that is uniform in space and time and is consistent with the observed values (Kalnay et al. 1996). The reanalysis data products used for this project are atmospheric data (pressure, winds, relative and specific humidity, temperature, and potential temperature) at 6-h intervals over the Cache Creek watershed and surrounding land and ocean.

These data are used as initial and boundary conditions for the mesoscale (regional-scale) climate model MM5. The fifth-generation NCAR/Penn State University mesoscale model (MM5) is the latest in a series of regional-scale atmospheric models developed from a mesoscale model documented in Grell et al. (1994). The PSU/NCAR mesoscale model is a limited-area, hydrostatic or nonhydrostatic, terrain-following sigma-coordinate model designed to simulate or predict mesoscale and regional-scale atmospheric circulation over any limited area on earth. Hydrostatic simulations assume the hydrostatic approximation for vertical motion in the atmosphere that is suitable for large-scale (greater than 20 km grid scale) simulations. In its nonhydrostatic mode, the MM5 model simulates the full vertical momentum equation and, as such, can describe satisfactorily the air motions over steep mountainous terrain at small grid scales (such as a few kilometers) suitable for atmospheric inputs into a watershed model. MM5

contains a wide range of physical process routines to model advection, diffusion, radiation, boundary layer processes, surface layer processes, moisture dynamics, and cumulus convection. The MM5 has flexible grid sizes and multiple nesting capabilities. These nesting capabilities can be run in both two-way and one-way nesting modes and allow MM5 to be coupled with either atmospheric data (such as NCAR/NCEP historical reanalysis data) or other models (such as General Circulation Model simulation data) that are at larger grid resolution. Therefore, MM5 is capable of atmospheric process simulations on any grid scale, limited only by the data resolution, data quality, and computational resources available.

When coupled with large-resolution historical atmospheric data, such as NCEP/NCAR reanalysis data, MM5 can reconstruct these atmospheric data (precipitation, temperature, radiation, relative humidity, wind, etc.) at significantly finer spatial resolutions. This higher resolution data are more suitable for watershed hydrologic modeling studies. In this project, four one-way nested grids were set up within the model to create a downscaling process from the 210×210 km scale reanalysis data to the 3×3 km scale over the Cache Creek watershed.

Figure 21 shows the spatial extent of the four grid domains. Each nested grid has a spatial resolution of 1/3 of the parent grid and focuses more on the project area of the Cache Creek watershed. The 1/3 ratio is recommended in the user documentation for MM5 (Grell et al. 1994). The first domain has a spatial grid resolution of 81 km, the second 27 km, the third 9 km, and the fourth 3 km. This series of nested domains allows the large-scale archived atmospheric data to be economically downscaled to the region of interest at the desired resolution. Data for seven variables were extracted: precipitation, atmospheric temperature, relative humidity, wind speed, incoming solar radiation, downward longwave radiation, and latent heat flux. In addition to these variables, dew point temperature was computed from the simulation results and stored.

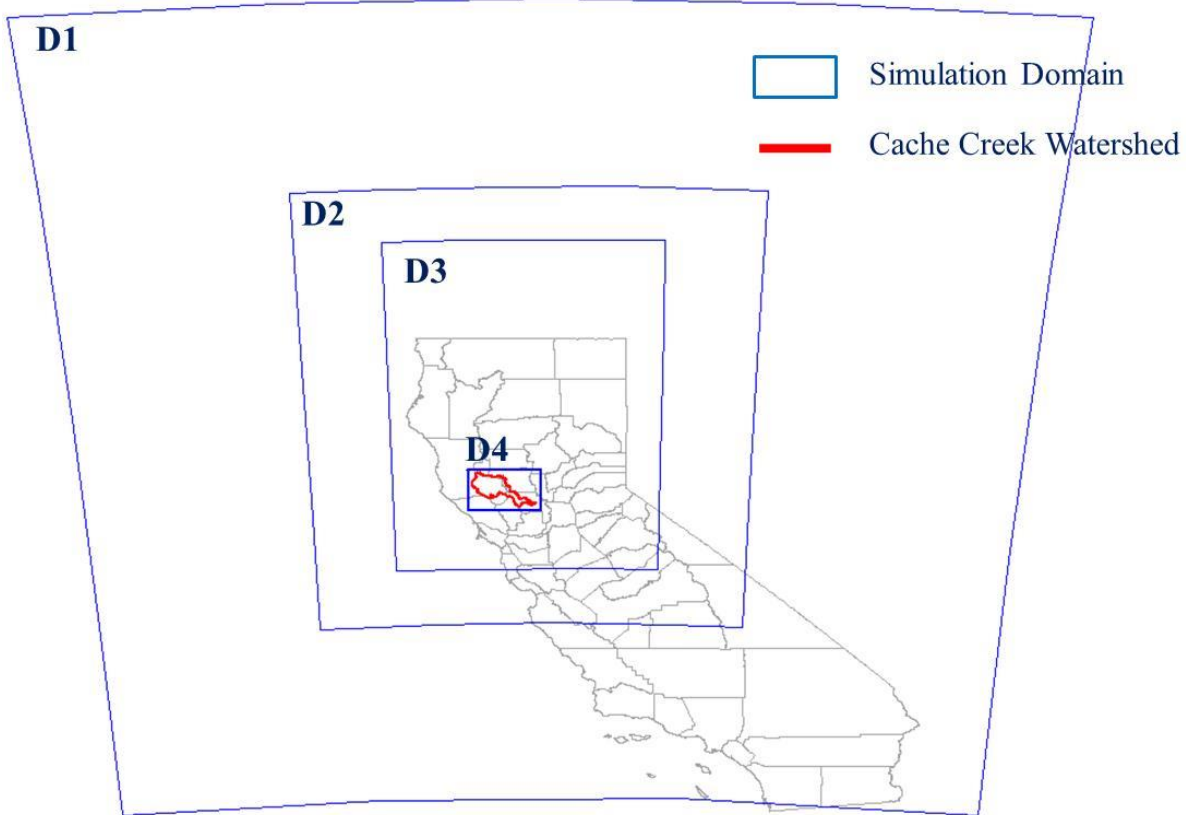


**Figure 21- Depiction of four nested domains used for the MM5 simulation for the Cache Creek watershed**

## **5.2. Regional Climate Model validation based on NCAR/NCEP reanalysis data-based climate variables**

Figure 22 shows the sample comparisons between MM5-simulated historical precipitation fields and PRISM data for the mean monthly precipitation of December, January, and February from 1950 to 2007 over Cache Creek watershed. NCAR/NCEP global reanalysis data that were used for the initial and boundary conditions of the regional climate model MM5 for the above-mentioned period, have coarse grid resolution of approximately 210km by 210 km. These coarse resolution data were then downscaled by MM5 regional atmospheric model to 3 km by 3 km grids over Cache Creek watershed.

In general, the spatial distributions of mean monthly precipitation for December, January, and February, reconstructed by MM5 by downscaling the NCAR/NCEP reanalysis data, match reasonably well with the PRISM monthly data. Figure 23 shows the graphical comparison of

mean monthly precipitation from 1950 to 2007. The MM5 simulation results match the PRISM monthly data almost perfectly.

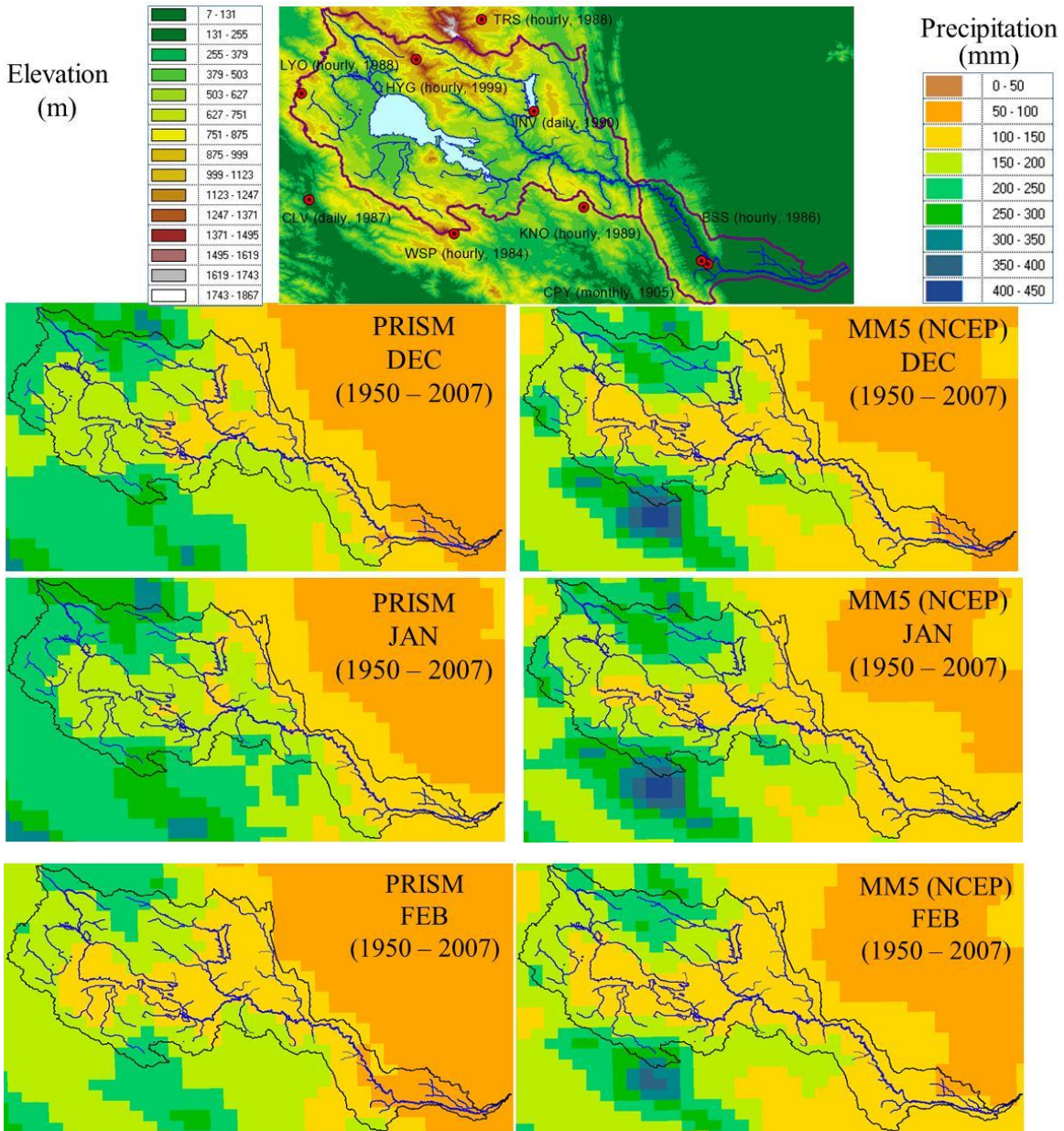


**Figure 22- Example comparison of mean monthly precipitation for December, January and February between PRISM data and MM5 simulation results during 1950 to 2007**

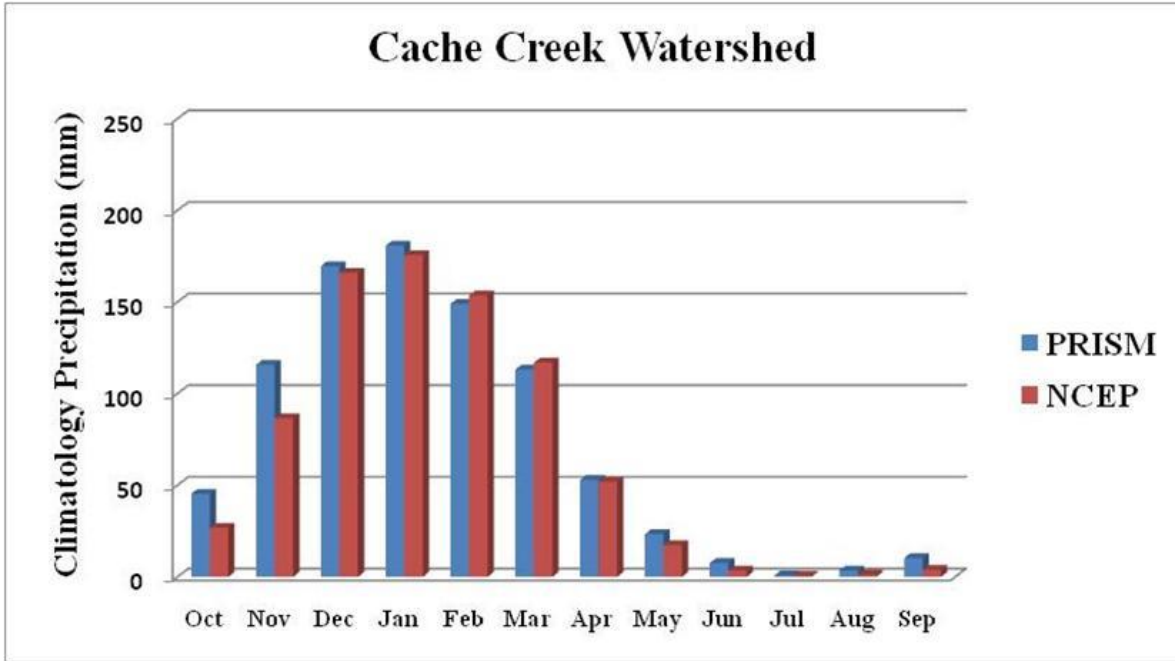


Figure 23- Graphical comparison of mean monthly precipitation between PRISM data and MM5 simulation results over Cache Creek watershed during 1950 to 2007

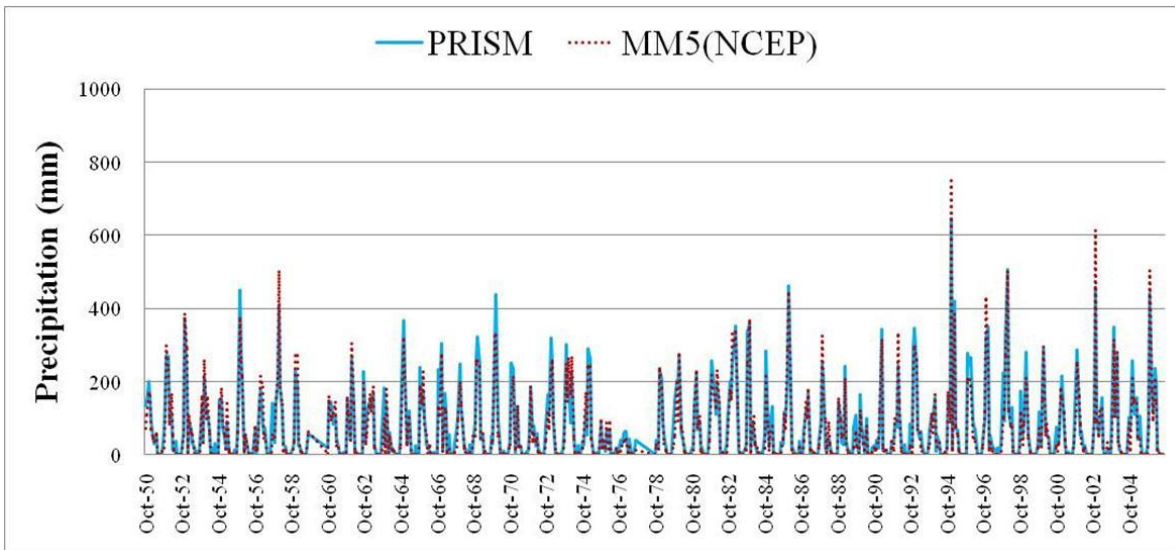


Figure 24- Graphical comparison of monthly precipitation between PRISM data and MM5 simulations during 1950 to 2007

**Table 5- Statistical test results for the comparison of MM5-simulated (NCEP) versus PRISM precipitation during 1950 – 1999 for the Cache Creek watershed**

Statistical value	PRISM	MM5(NCEP)
<i>Mean</i> (mm)	72.71	66.98
<i>STDEV</i> (mm)	97.82	98.10
<i>RMSE</i> (mm)		28.84
Nash-Sutcliffe efficiency ( $E_{NS}$ )		0.91
Correlation coefficient ( $R$ )		0.96
Chi-square critical ( $\alpha=0.05$ )		18.31
Chi-square calculated		7.29

Figure 24 compares graphically the monthly basin-averaged precipitation from 1950 to 2007 from the MM5 simulation results (by downscaling the NCAR/NCEP reanalysis data) and the PRISM data. MM5 simulation results match the PRISM data quite well, as can be seen in Fig 24. In order to test the performance of MM5-simulation more comprehensively, the MM5-simulated versus corresponding PRISM values were evaluated by mean, standard deviation (*STDEV*), correlation coefficient ( $R$ ), root mean square error, Nash-Sutcliffe efficiency ( $E_{NS}$ ), and Chi-square goodness-of-fit test from 1950 to 2007 (see Table 5). The mean and standard deviation (*STDEV*) are similar to PRISM values. The correlation coefficient ( $R$ ) is 0.96 and Nash-Sutcliffe efficiency ( $E_{NS}$ ) value is 0.91. Furthermore, the MM5 simulation results passed the Chi-square goodness-of-fit test. It should be noted that no bias-correction was necessary for MM5-simulated precipitation values.

Only one station, KNO of CDEC, had observations of air temperature and solar radiation to use for validation of MM5 simulations. Figure 25 and Figure 26 show the comparisons of the MM5-simulated (based on NCEP/NCAR reanalysis data) and ground-observed monthly mean values for air temperature (Figure 25) and solar radiation (Figure 26) during 2000 – 2011 at KNO CDEC station. As shown in these figures, the MM5-simulated monthly mean air temperature and solar radiation values matched the ground-observed KNO CDEC station values perfectly. As such, the comparison results and statistical tests indicate the reliability and capability of MM5

historical climate simulations by downscaling the coarse-resolution atmospheric observations from NCEP/NCAR reanalysis data.

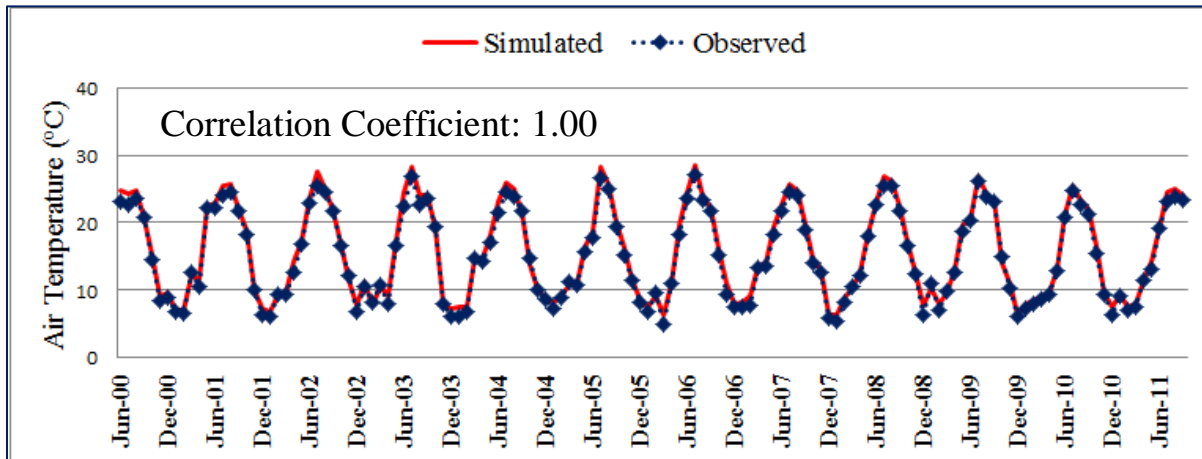


**Figure 25-** Comparisons of simulated (MM5-NCEP) and observed (CDEC) monthly mean temperature from 2000 through 2011 at KNO station. No bias-correction was applied.

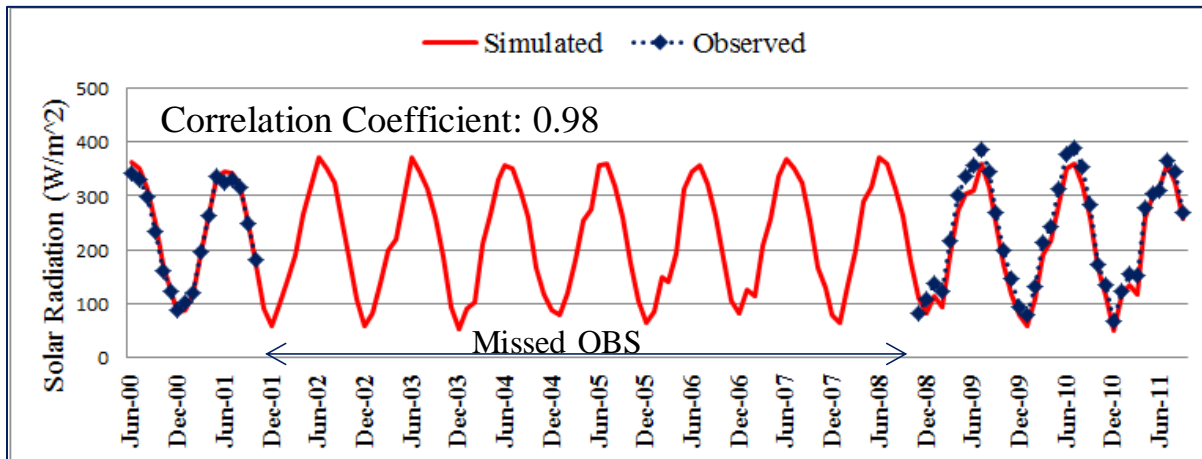


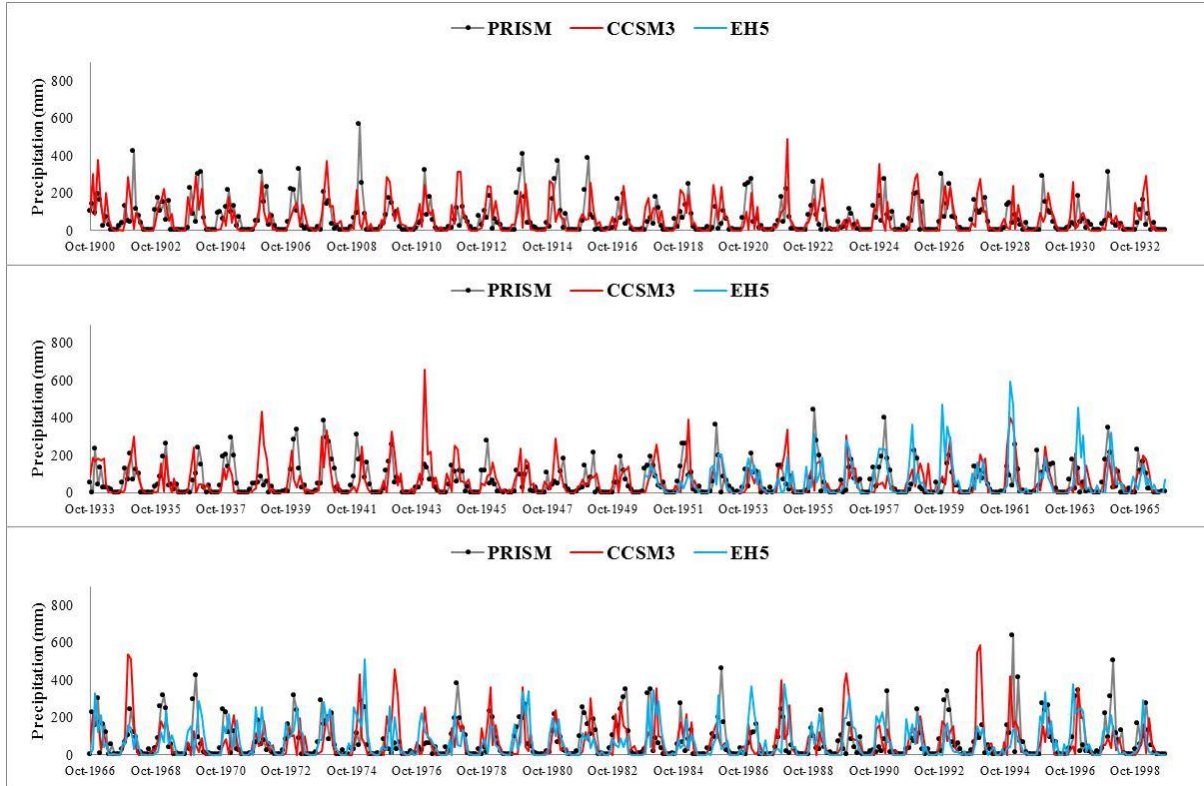
**Figure 26-** Comparisons of simulated (MM5-NCEP) and observed (CDEC) monthly mean solar radiation from 2000 through 2011 at KNO station. No bias-correction was applied.

### **5.3. Model validation of GCM-based climate variables**

In order to be able to perform comparisons between the historical climate conditions and the 21<sup>st</sup> century future climate conditions that are projected based on downscaling two global climate model (ECHAM5-GCM and the CCSM3-GCM) projections, it is necessary also to simulate the historical climate conditions based on the historical climate simulations of the two GCMs in order to achieve consistency among the comparisons.

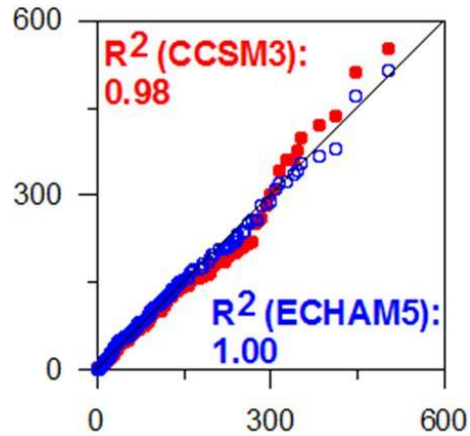
As such, GCM-based MM5 historical climate simulations for the late twentieth century (ECHAM5: 1950-1999, CCSM3: 1900-1999) were also performed over Cache Creek watershed. It is noted that the ECHAM5-GCM and the CCSM3-GCM based precipitation simulations by MM5 include biases and require correcting. For this project, the bias correction was conducted based on the monthly climatology of precipitation from the PRISM data. The determined bias was then incorporated into ECHAM5-GCM-based and CCSM3-GCM-based future precipitation projections by MM5 over Cache Creek watershed.

Figure 27 compares graphically the MM5-simulated precipitation (by downscaling CCSM3 and ECHAM5 GCM outputs) and PRISM precipitation with respect to monthly basin-averaged precipitation from 1900 to 1999 for CCSM3 and from 1950 to 1999 for ECHAM5 over Cache Creek watershed. In this Figure 27, the MM5 simulation results match the PRISM monthly data reasonably well.



**Figure 27- Comparisons of MM5-simulated monthly precipitation versus PRISM monthly precipitation from water year 1901 to water year 1999 for Cache Creek watershed**

Unlike NCAR/NCEP reanalysis data based MM5 simulations, GCM-based MM5 simulation results may not be suitable for comparison to the time-series of observed precipitation because the GCM simulations focus on the climatology of the specified period rather than the prediction of actual precipitation during the period. Thus, it is more important whether the distribution of the GCM-based MM5 simulation results is comparable to the corresponding distribution of observations. The quartile-quartile plot is a good method to see whether the distribution of simulated values deviate from the distribution of observed values. Figure 28 shows the comparison of quartile-quartile plot for the Cache Creek watershed average monthly precipitation between MM5-simulated (based on GCM historical simulations) and PRISM precipitation during water year 1951 to water year 1999. As shown in Figure 28, MM5-simulated precipitation values from both CCSM3 and ECHAM5 GCMs are distributed very well against PRISM precipitation values.



**Figure 28- Quartile-quartile plot of Cache Creek watershed average monthly precipitation between MM5-simulated (based on GCM historical simulations) and PRISM precipitation during water year 1951 to water year 1999. Red color indicates the comparisons for CCSM3-based precipitation and blue color indicates the comparisons for ECHAM5-based precipitation.**

Long-term precipitation trends were also investigated based on the 10-year moving average of annual precipitation between GCMs-based MM5 simulations and PRISM values during water year 1901 to water year 1999 (see Figure 29). In general, the MM5-simulated precipitation trends are similar to the corresponding precipitation trends from PRISM.

The Chi-square goodness-of-fit test comparing the GCMs-based MM5 simulations versus the corresponding PRISM values during water years 1951 to 1999, was also passed (see Figure 30). As such, these comparison results and statistical tests indicate the reliability and capability of MM5 reconstruction of the historical climate conditions by downscaling historical climate simulations from a GCM's historical control run.

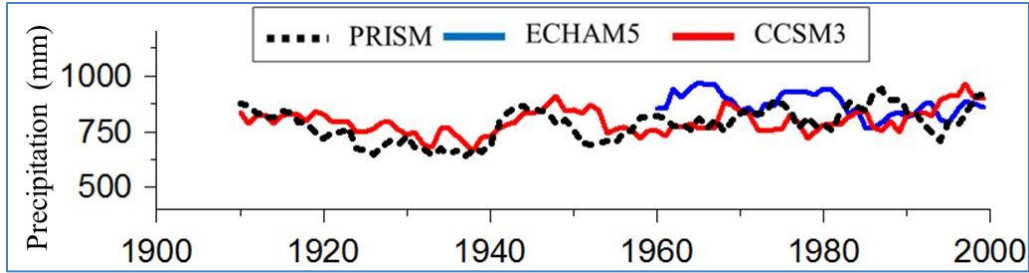


**Figure 29- Comparisons of 10-year moving Cache Creek watershed average annual precipitation between PRISM observations and MM5-simulated precipitation during water year 1901 to water year 1999**

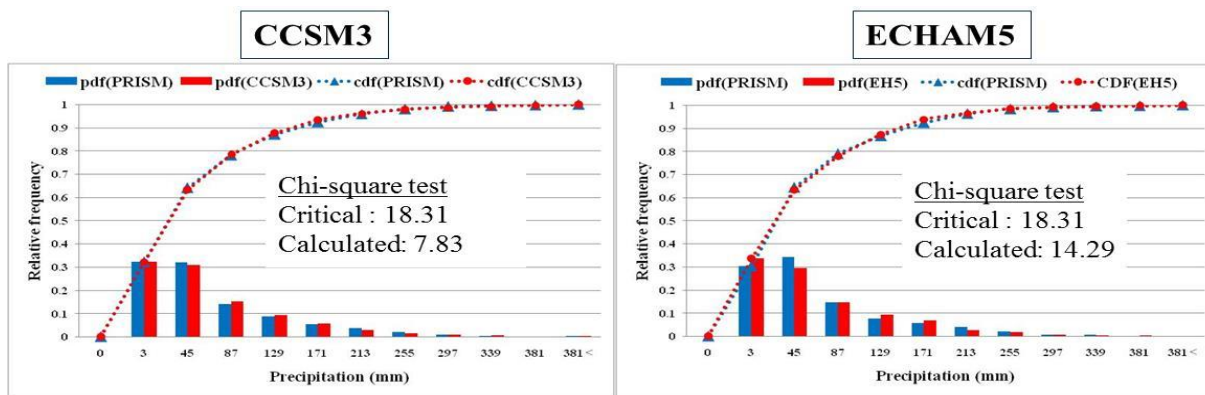


**Figure 30- Chi-square goodness-of-fit test results of Cache Creek watershed average monthly precipitation between PRISM and MM5-simulated precipitation during water year 1951 to water year 1999**

#### 5.4. Reconstruction of historical climate data

It is possible to develop a full historical flow record at Cache Creek watershed outlet (taken as Yolo station) by reconstructing the missing historical flow data by the calibrated and validated WEHY watershed model, provided that the corresponding historical climate data are also reconstructed by a regional climate model, such as MM5, over the watershed. Based on such a full flow record at the Yolo station, it is then possible to simulate the historical sediment inflow conditions to Cache Creek Settling Basin once a comprehensive sediment rating curve is developed. In the following, the details on the reconstruction of the historical climate conditions during 1951-2011 water years period over Cache Creek watershed will be given. In a later section, the reconstruction of the corresponding historical flow conditions will be discussed.

Reconstruction of historical climate data based on the NCAR/NCEP reanalysis data from water year 1951 through water year 2011 and on the two GCM outputs (CCSM3 and ECHAM5) from water year 1951 through water year 1999 was completed to build the necessary atmospheric boundary conditions for WEHY model's flow simulations over the watershed.

Figure 31 through Figure 33 show sample spatial plots of NCAR/NCEP reanalysis data-based MM5 simulation results for 61-year average monthly precipitation, monthly mean air temperature and monthly mean shortwave solar radiation fields during 1950 – 2011 over Cache Creek watershed. It can be seen clearly from Figure 31 that MM5-simulated precipitation fields show banded precipitation structures around the mountain ridges due to the orographic effects over Cache Creek watershed. Meanwhile the spatial fields of MM5-simulated air temperature show dependence on elevation since the high elevations around mountain ridges have relatively low temperatures while the low elevations have relatively high temperatures (see Figure 32). Atmospheric data such as precipitation, short and long wave radiation, wind speed, relative humidity and air temperature are crucial information for the WEHY watershed model. However, it is difficult to obtain such spatially distributed hydro-atmospheric data in sparsely-gauged watersheds like Cache Creek at fine resolutions in time and space. By means of MM5-downscaled climate data for a historical period of 61 years and for the 21<sup>st</sup> century future period it was possible to construct the necessary atmospheric data for the WEHY watershed model's flow simulations.

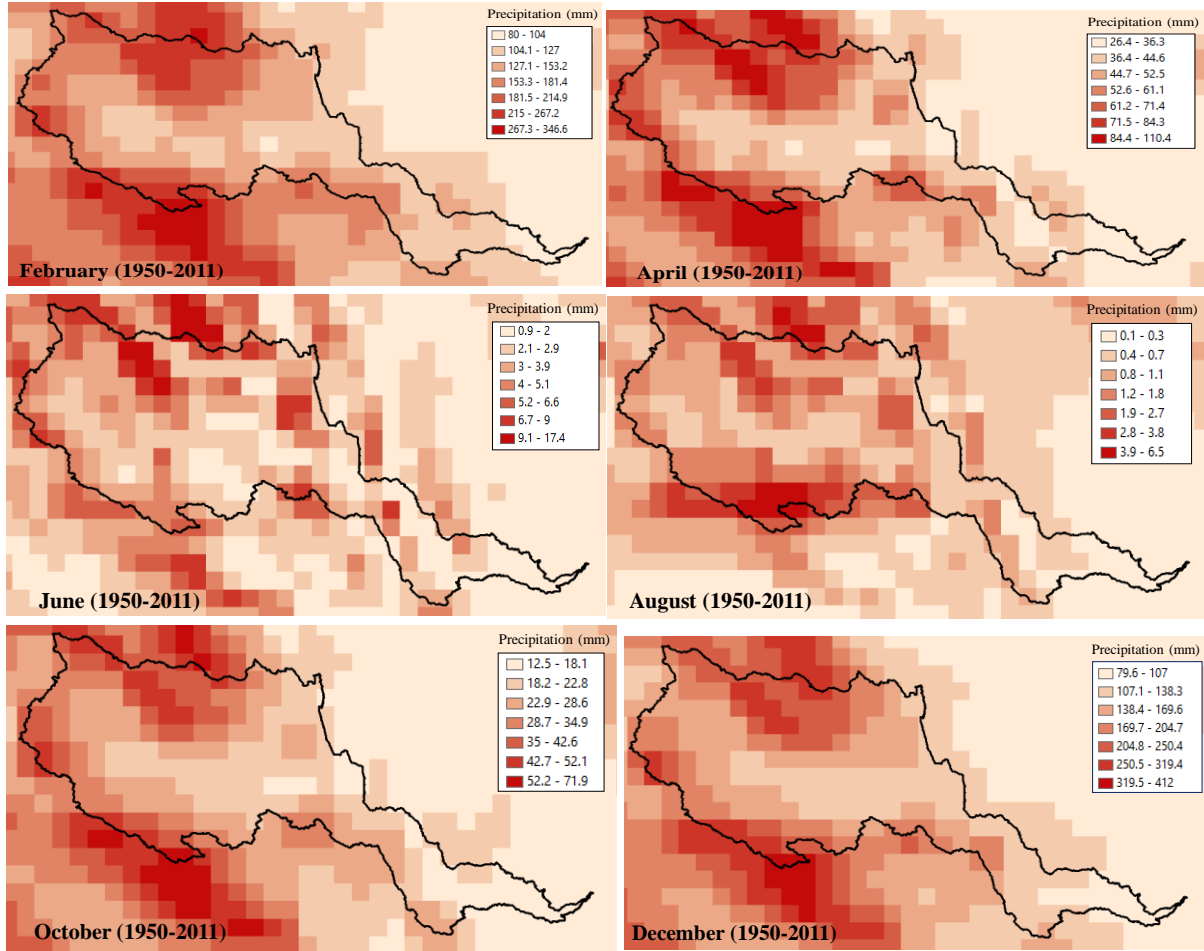


**Figure 31- Sample spatial plots of NCAR/NCEP reanalysis data-based MM5 simulation results for the mean monthly precipitation (February, April, June, August, October and December) during 1950 – 2011 over Cache Creek watershed.**

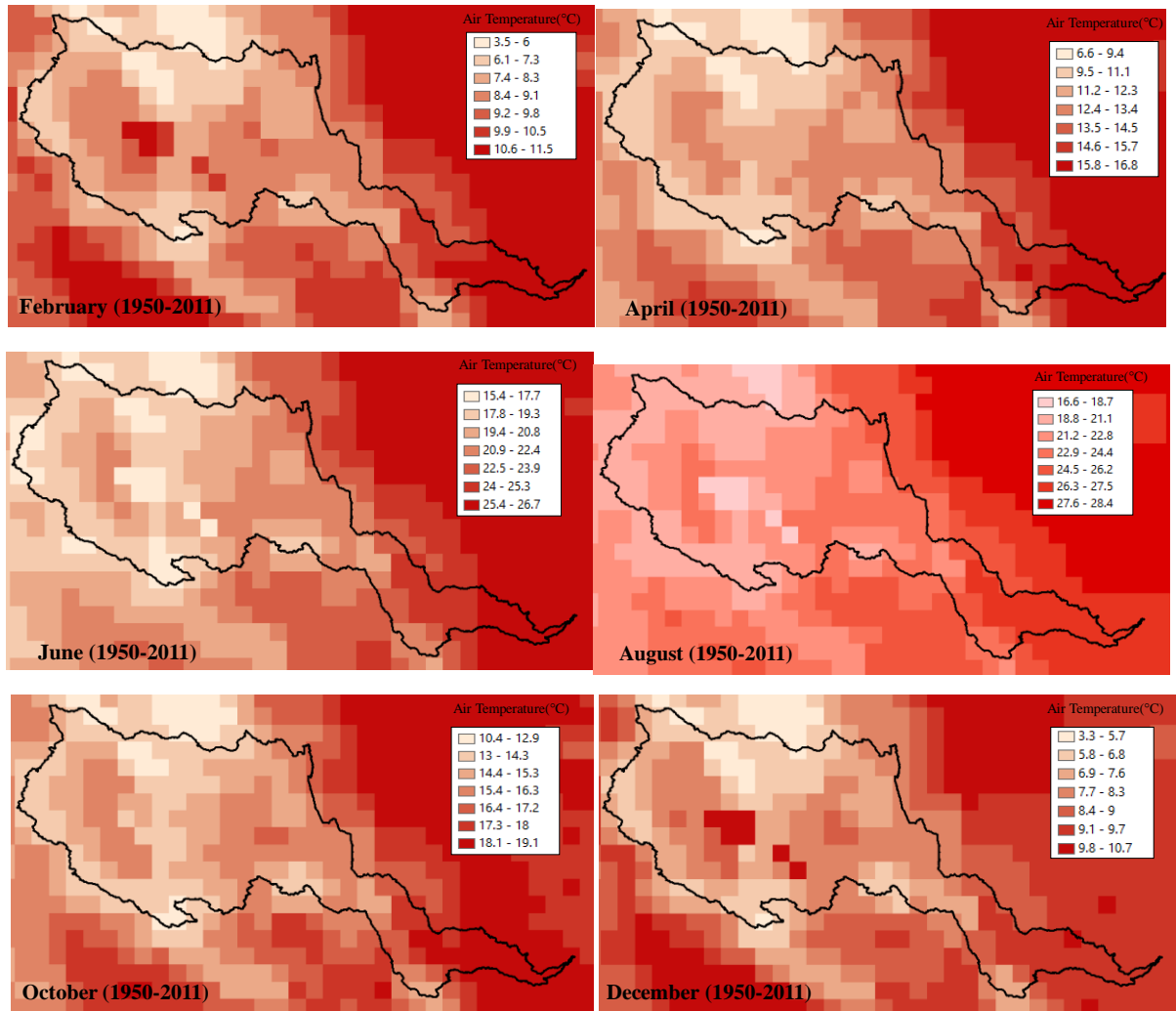


**Figure 32- Sample spatial plots of NCAR/NCEP reanalysis data-based MM5 simulation results for 61-year average monthly mean air temperature (February, April, June, August, October and December) during 1950 – 2011 over Cache Creek watershed.**

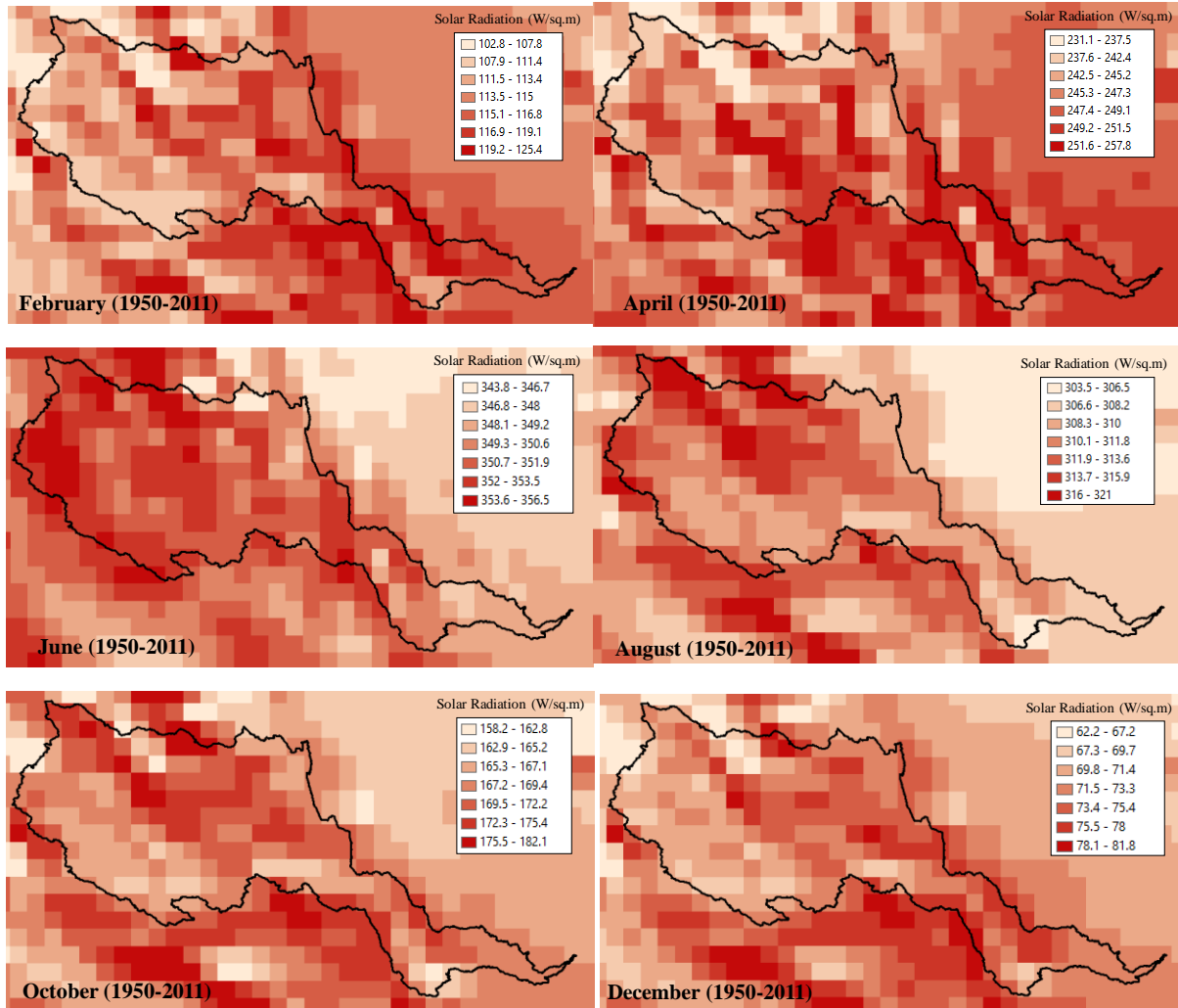


**Figure 33- Sample spatial plots of NCAR/NCEP reanalysis data-based MM5 simulation results for 61-year average monthly mean shortwave solar radiation (February, April, June, August, October and December) during 1950 – 2011 over Cache Creek watershed.**

Figure 34 and Figure 35 show the sample plots of basin-average monthly precipitation, monthly mean air temperature, wind speed, shortwave solar radiation and longwave solar radiation over the Cache Creek watershed that were reconstructed by MM5 simulations using NCAR/NCEP reanalysis historical data and from the GCM (CCSM3 and ECHAM5)-based historical climate simulation data. The historical climate data were then used as input data for the WEHY model flow simulations.

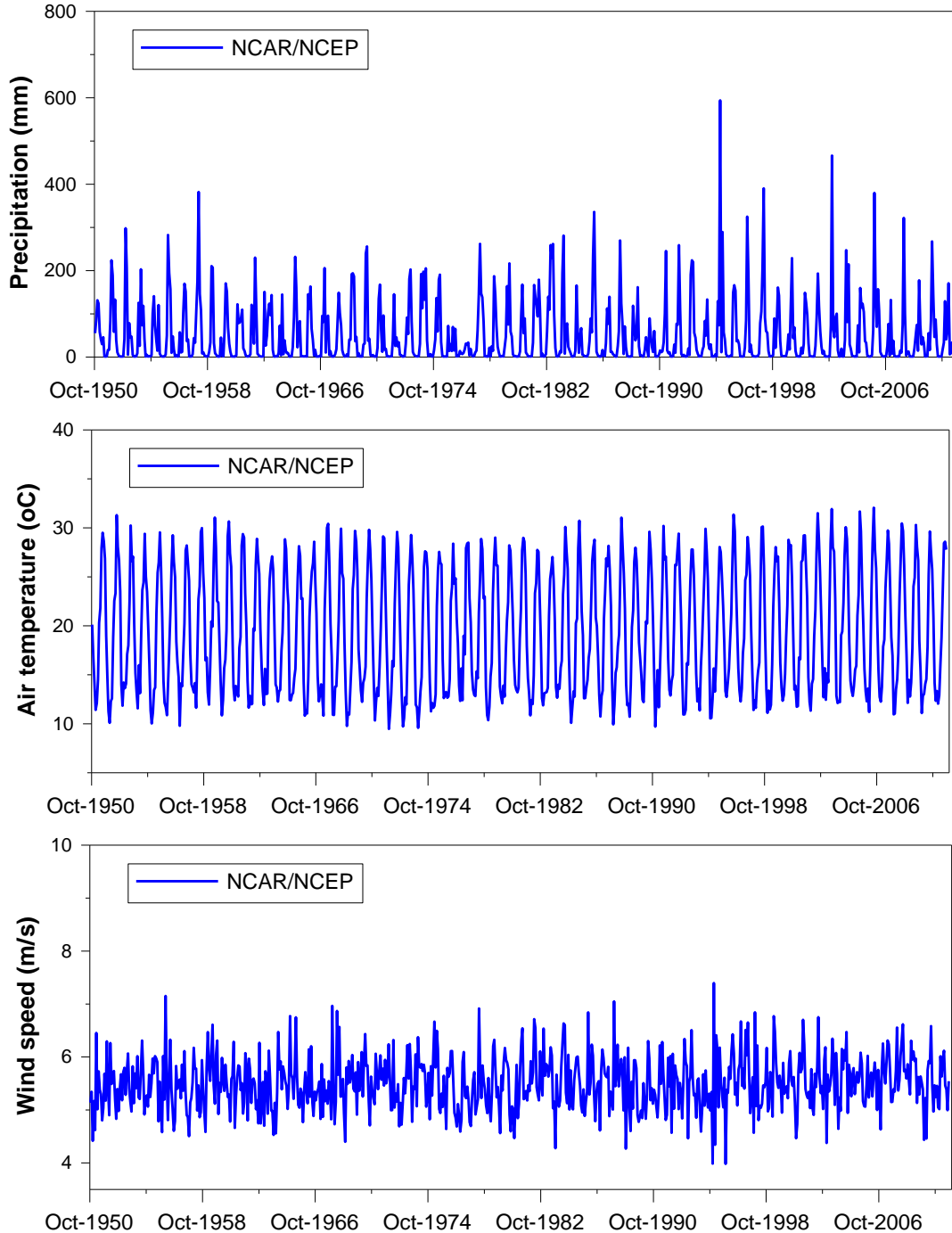


**Figure 34- Sample plots of historical basin-average monthly precipitation, monthly mean air temperature, wind speed, shortwave solar radiation and longwave solar radiation that were reconstructed by MM5 regional climate model during 1950 – 2011 over Cache Creek watershed by downscaling the NCAR/NCEP reanalysis data (continued in the next page)**

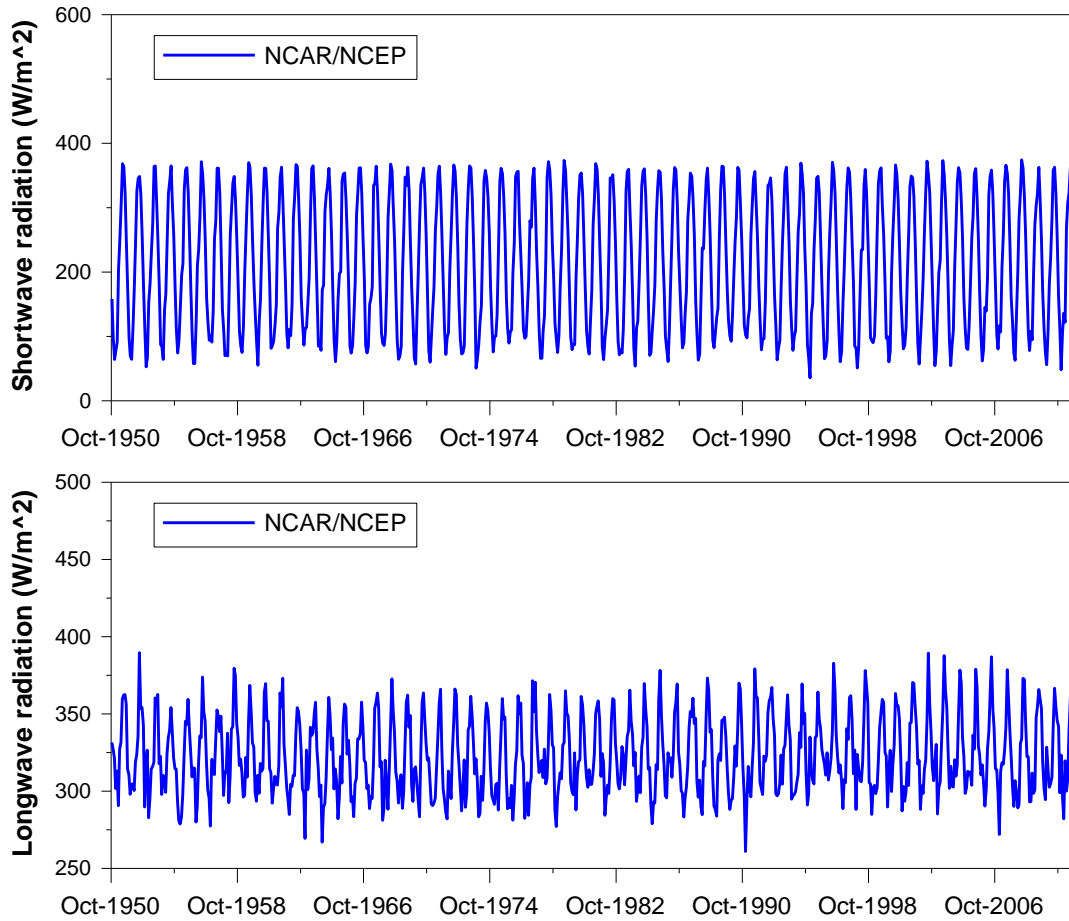


**Figure 34- Sample plots of historical basin-average monthly precipitation, monthly mean air temperature, wind speed, shortwave solar radiation and longwave solar radiation that were reconstructed by MM5 regional climate model during 1950 – 2011 over Cache Creek watershed by downscaling the NCAR/NCEP reanalysis data**

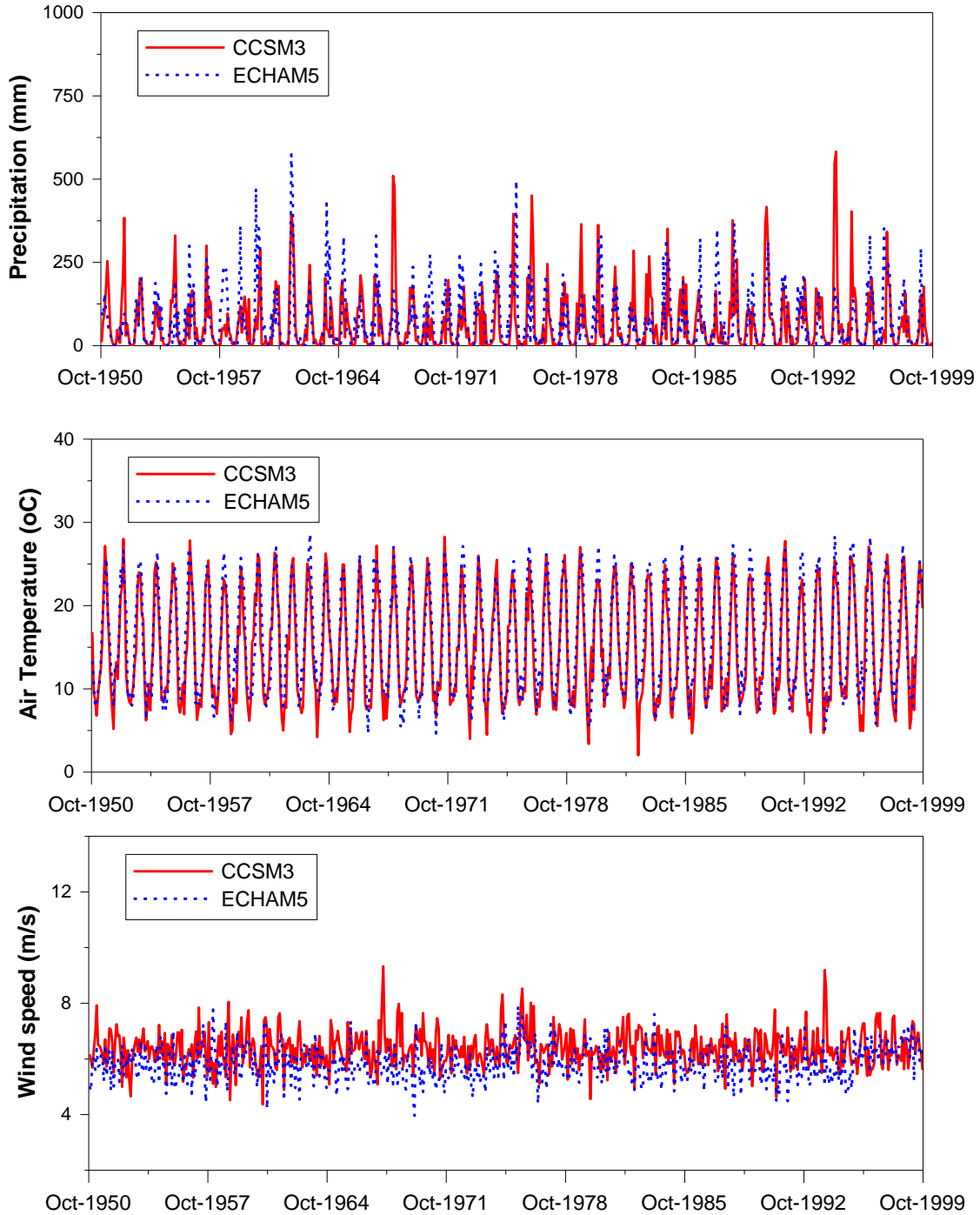


**Figure 35- Sample plots of historical basin-average monthly precipitation, monthly mean air temperature, wind speed, shortwave solar radiation and longwave solar radiation that were reconstructed by MM5 regional climate model during 1950 – 2000 over Cache Creek watershed by downscaling the GCM (CCSM3 and ECHAM5) historical control simulations (continued next page)**

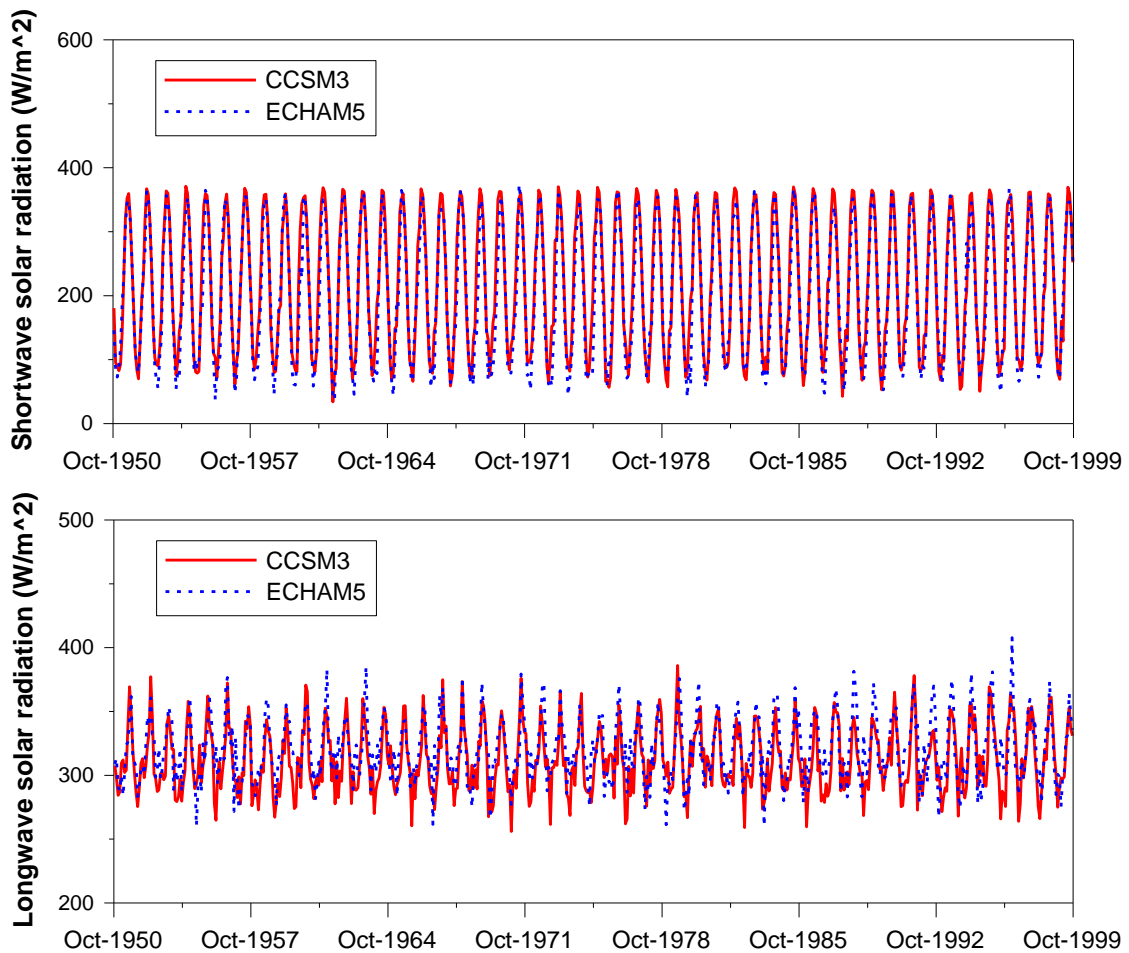


**Figure 35- Sample plots of historical basin-average monthly precipitation, monthly mean air temperature, wind speed, shortwave solar radiation and longwave solar radiation that were reconstructed by MM5 regional climate model during 1950 – 2000 over Cache Creek watershed by downscaling the GCM (CCSM3 and ECHAM5) historical control simulations**

## **5.5. Projection of Future Climate Conditions**

In order to quantify the flow conditions at Cache Creek watershed under the future hydro-climate conditions by means of WEHY model simulations, it is necessary to first project the future climate conditions by the regional climate model MM5. Then these future climate conditions provide the necessary climate input data for the WEHY model's simulations of the future hydrologic conditions over the Cache Creek watershed that provide the inlet boundary conditions for the CCSB hydraulic model.

MM5 regional climate model's projections of the 21<sup>st</sup> century future climate conditions over Cache Creek watershed were based on 9 climate projections from ECHAM5 GCM (A1B1, A1B2, A1B3, A2-1, A2-2, A2-3, B1-1, B1-2, and B1-3 scenarios) and 4 climate projections from CCSM3 GCM (A1B, B1, A2, and A1FI scenarios). In this report, three climate variables (precipitation, air temperature and solar radiation) are presented as sample future climate variables constructed by MM5 regional climate model over Cache Creek watershed.

### **5.5.1 Projection of precipitation under future climate change conditions**

It is difficult to select a specific GCM and a specific emissions scenario for the projection of the future climate because the future climate conditions are unknown and evolving in time and space. One plausible approach for future climate projections is to consider an ensemble of projections and then use the ensemble average of all individual projection realizations (13 realizations in this project) with a confidence band.

In this study, the future projection of precipitation under a changing climate is based on the ensemble of projections by the regional atmospheric model MM5, based on 9-projection realizations from ECAHM5 GCM (under A1B1, A1B2, A1B3, A2-1, A2-2, A2-3, B1-1, B1-2, and B1-3 scenarios), and on 4-projection realizations from CCSM3 GCM (under A1B, B1, A2, and A1FI scenarios). Figure 36 compares the GCM control run-based MM5 historical precipitation simulation against the GCM projections-based future MM5-projected ensemble average annual Cache Creek watershed-average precipitation with 95 % confidence interval. As

shown in Figure 36, a trend in annual precipitation over Cache Creek watershed cannot be claimed, based on Mann-Kendall test (at 95% confidence level).

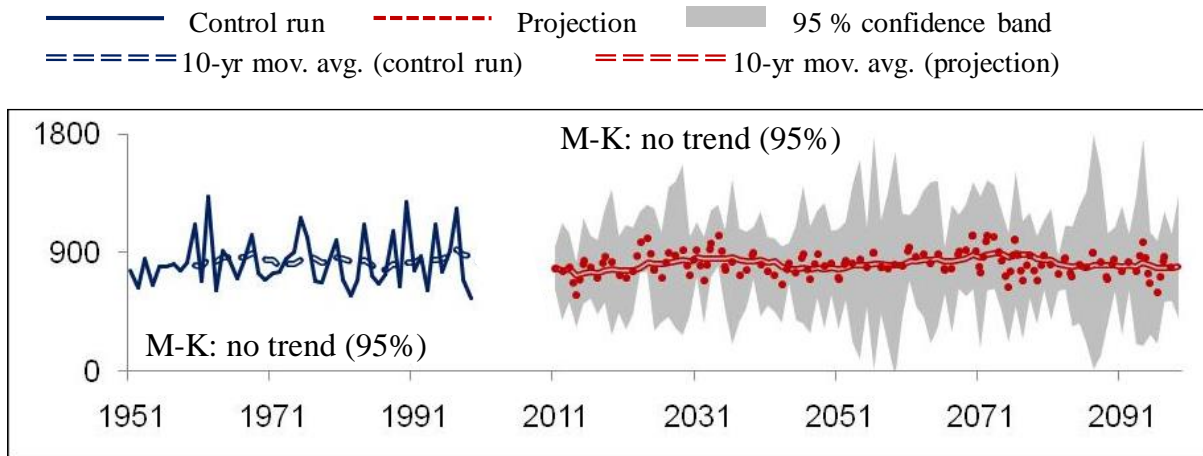


**Figure 36- Comparison of historical GCM control run-based MM5 simulation versus the future GCM (ECHAM5 and CCSM3)-based MM5 projection of ensemble average annual precipitation (ensemble average of 13-projection realizations) for Cache Creek watershed**

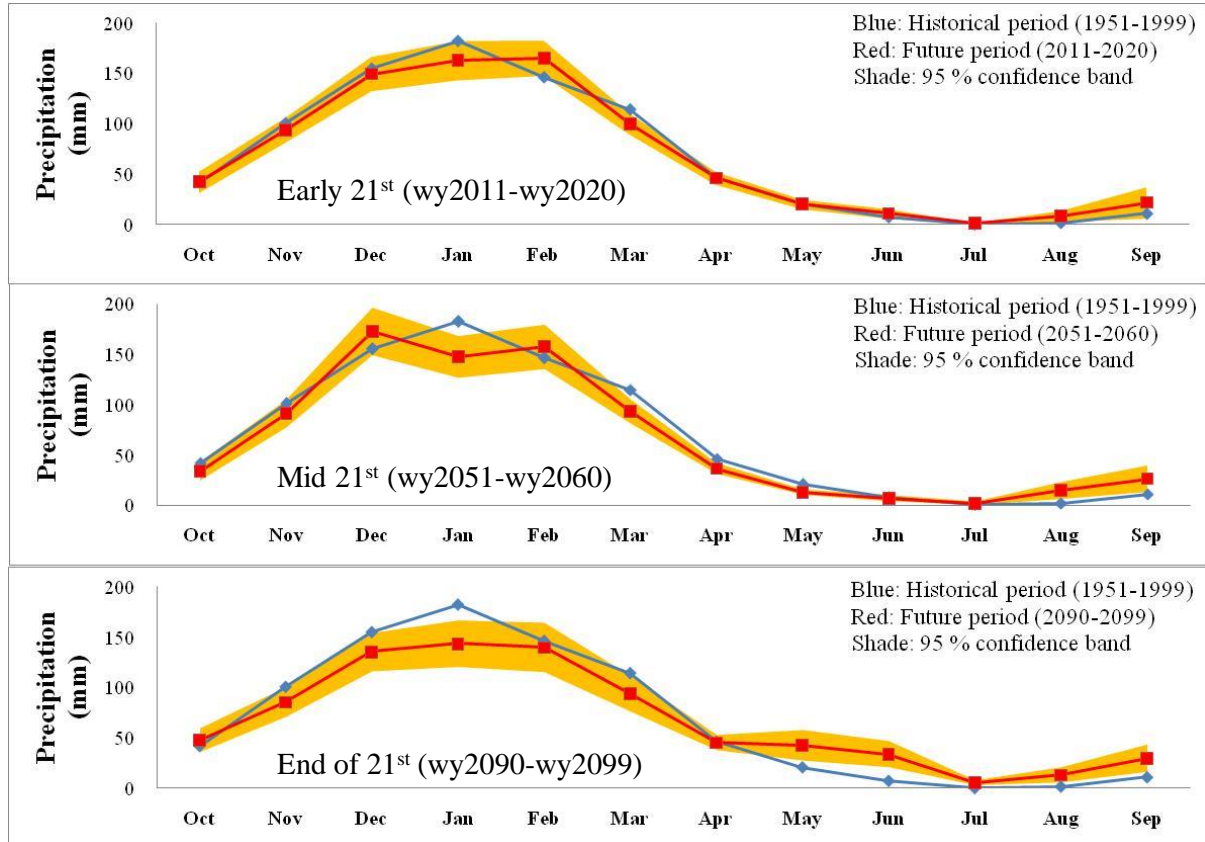


**Figure 37- Comparison of the future mean monthly precipitation (ensemble average of 13-projection realizations) at early 21<sup>st</sup> century, at mid-21<sup>st</sup> century and at the end of the 21<sup>st</sup> century against the historical mean monthly precipitation during wy1990-wy1999 over Cache Creek watershed**

Figure 37 shows the GCM-based future projections by MM5 simulations for mean monthly precipitation during each 10-year period at the early-, mid- and end of the 21<sup>st</sup> century together with their respective confidence bands (95 %), compared against the historical mean monthly precipitation for Cache Creek watershed. If the historical mean monthly precipitation at each month is within the confidence band of the GCM-based future projections by MM5, the projected future mean monthly precipitation is not significantly different than the historical mean monthly precipitation. Meanwhile, if the historical mean monthly precipitation at any month is outside the confidence band of the corresponding GCM emission scenario-based future projection for that month, the future mean monthly precipitation for that month is significantly different than the historical mean monthly precipitation for the specified month. From Figure 37 it may be inferred that the projected mean monthly precipitation is significantly less during

January at the mid-21<sup>st</sup> century (wy2051-wy2060) and at the end of the 21<sup>st</sup> century (wy2090-wy2099) when compared against the corresponding historical mean monthly precipitation (wy1990-wy1999) over Cache Creek watershed. Meanwhile the projected mean monthly precipitation is significantly increased during the dry season (May, June, August and September) at the end of the 21<sup>st</sup> century (wy2090-wy2099) when compared against the corresponding historical mean monthly precipitation (wy1990-wy1999) over Cache Creek watershed.

Additionally, the Cache Creek watershed -average annual 72-hour maximum precipitation values are compared between the historical period (wy1901 – wy1999) and the projection period (wy2001 – wy2099) in Figure 38. The projected annual 72-hour maximum precipitation values, based on the MM5 downscaled CCSM3 GCM's projections for A1B, A2, B1 and A1FI scenarios, have in general heavier tails than the historical annual 72-hour maximum precipitation values. Furthermore, CCSM3 GCM's A1FI scenario-based MM5 projection of annual 72-hour maximum precipitation values also have a heavier relative frequency histogram tail than the historical annual 72-hour maximum precipitation values.

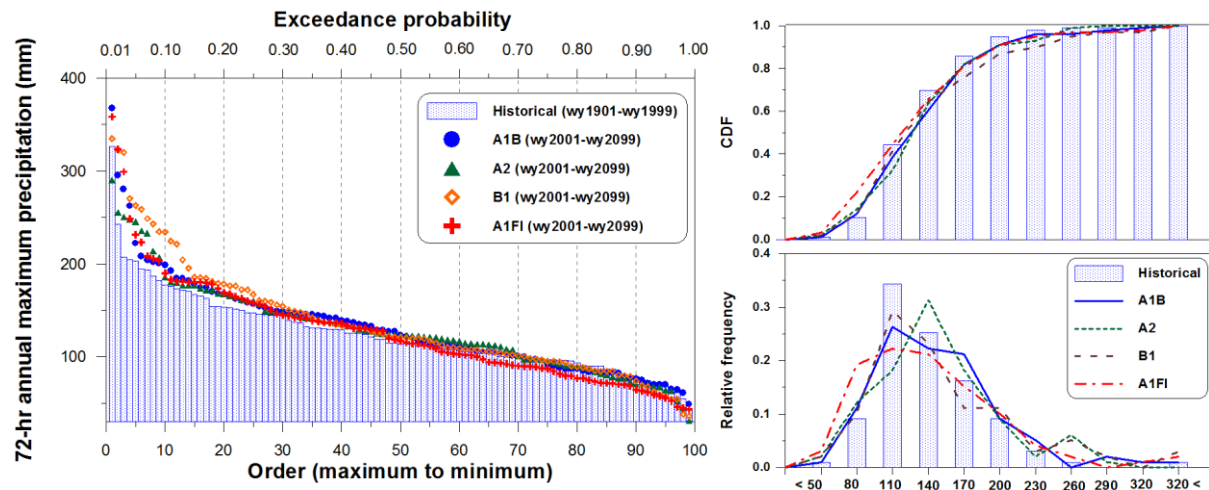


**Figure 38- Comparison of Cache Creek watershed-average annual 72-hour maximum precipitation between the historical period (wy1901 – wy1999) and the projection period (wy2001 – wy2099)**

### 5.5.2 Projection of air temperature and solar radiation under future climate conditions

Air temperature and solar radiation for the future 21<sup>st</sup> century climate was also projected based on the downscaling of ECHAM5 GCM projections (for A1B1, A1B2, A1B3, A2-1, A2-2, A2-3, B1-1, B1-2, and B1-3 emission scenarios) and on the downscaling of CCSM3 GCM projections (for A1B, B1, A2, and A1FI emission scenarios) of the 21<sup>st</sup> century climate.

Unlike precipitation, the annual mean air temperature, which is shown in Figure 39, has a clear warming trend toward the end of the 21<sup>st</sup> century when compared against the historical period. The change in annual mean air temperature is about 3.0 °C at the end of the 21<sup>st</sup> century over Cache Creek watershed. Meanwhile, no significant trend was found in the annual mean solar radiation toward the end of the 21<sup>st</sup> century, as shown in Figure 40.

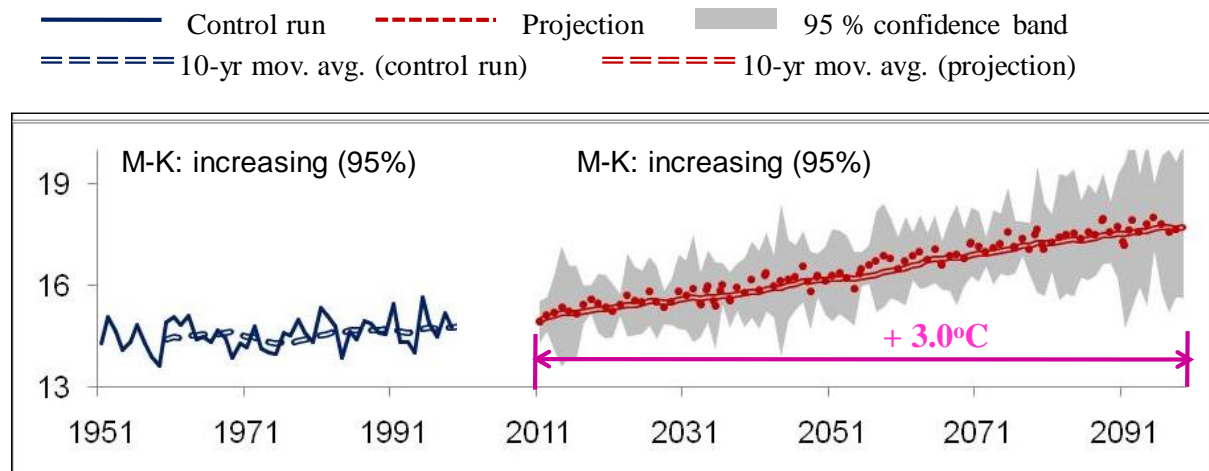


**Figure 39- Comparison of historical and MM5-downscaled GCM (ECHAM5 and CCSM3) projections of annual mean air temperature (ensemble average of 13-projection realizations) for Cache Creek Watershed**

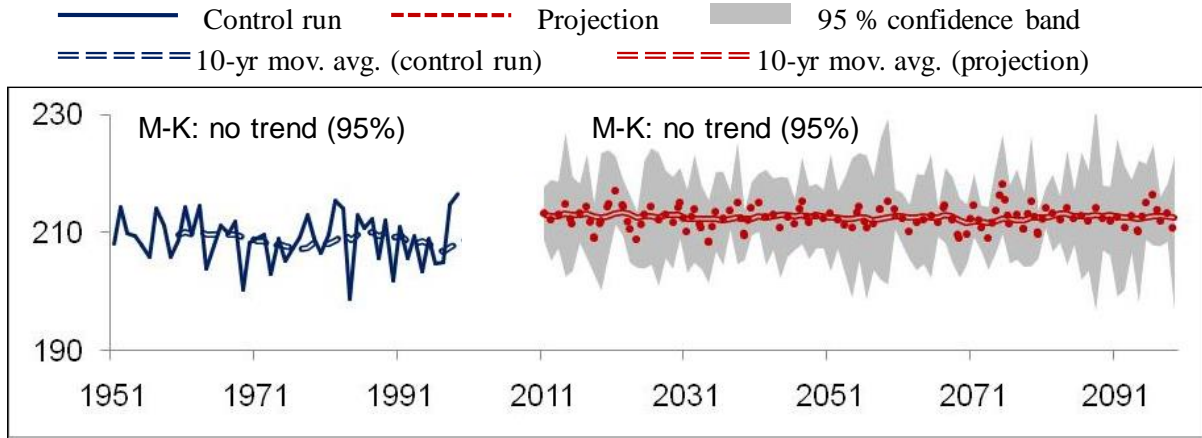


**Figure 40- Comparison of historical and MM5-downscaled GCM (ECHAM5 and CCSM3) projections of annual mean solar radiation (ensemble average of 13-projection realizations) for Cache Creek watershed**

## **6. Reconstruction of Historical and Projection of Future Hydrologic Conditions**

### **6.1. Implementation of WEHY Model**

#### **6.1.1 Delineation of stream reaches and model computational units**

The Watershed Environment Hydrology (WEHY) model (Chen et al, 2004a,b; Kavvas et al, 2004; Kavvas et al, 2006), utilizes the upscaled hydrologic conservation equations to account for the effect of heterogeneity within natural watersheds such as the Cache Creek watershed. First, the watershed is subdivided into model computational units (MCUs). These MCUs are either individual hillslopes or first-order-subwatersheds, and account for the surface and subsurface hillslope hydrologic processes.

The Cache Creek watershed was delineated into 43 stream reaches (see Figure 41) and 86 hillslopes (MCUs) (see Figure 42) by means of geographic information system (GIS) analysis of 30-m resolution U.S. Geological Survey Digital Elevation Model. In Figure 42, besides the 86 hillslopes (MCUs), 43 subbasins are shown, within each of which two hillslopes (MCUs) are separated by a channel reach. The overland flow and subsurface stormflow from two neighboring hillslopes carry flows uniformly into a channel reach. These flows are computed for each hillslope MCU. The 43 stream reaches form the channel network. Once the hillslope flow is generated for MCUs, hourly hillslope flows are fed to the channel network as lateral input, and routed further to the basin outlet.

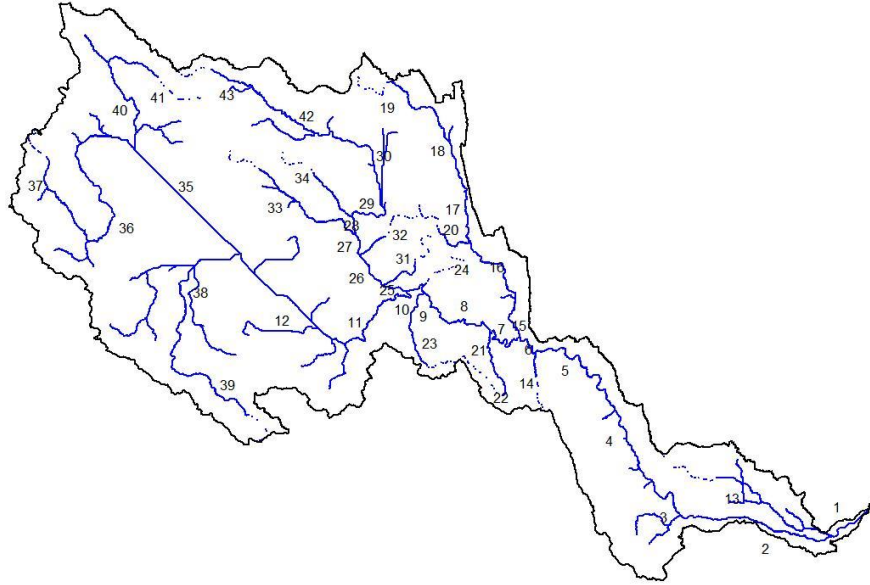


**Figure 41- Delineated 43 stream reaches in the WEHY model for the Cache Creek watershed**

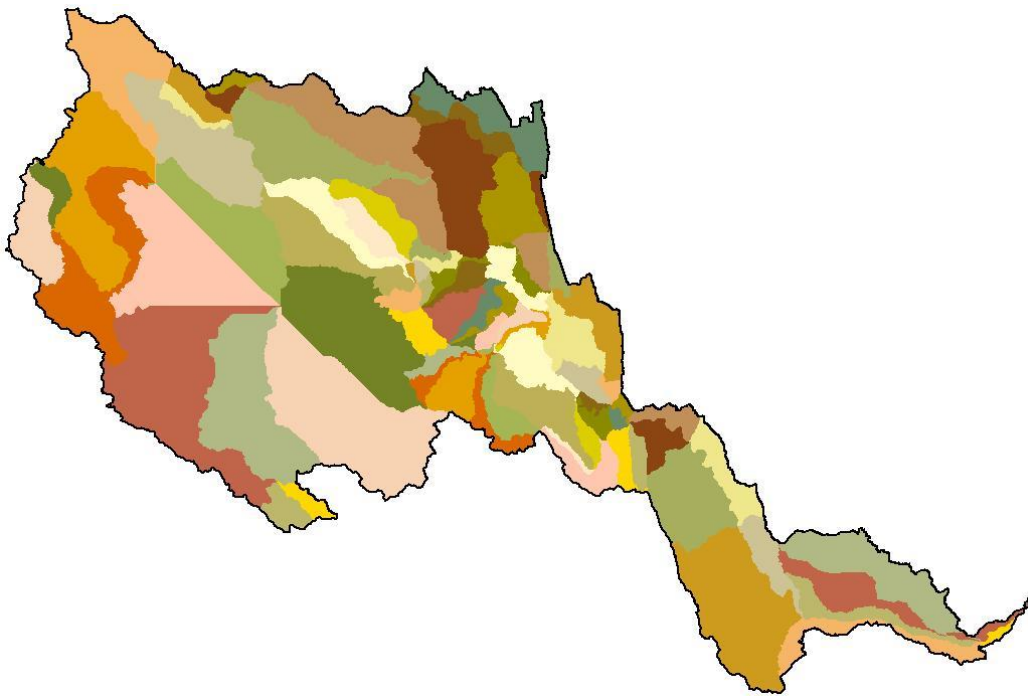


**Figure 42- Delineated 86 model computational units (MCUs) in the WEHY model for the Cache Creek watershed**

### 6.1.2 Estimation of WEHY model parameters

WEHY model is a physically based hydrologic model requiring physical parameters including geomorphologic parameters, soil hydraulic parameters, and land surface parameters. Geomorphologic parameters for the delineated stream reaches and MCUs in the WEHY model for the Cache Creek watershed were estimated from the prepared GIS database. These geomorphologic parameters such as surface slope, aspect, flow direction, and elevation, define the flow domains and the configurations of rills and interrill areas for MCUs of the WEHY model for the Cache Creek watershed.

The WEHY model also requires the land surface parameters (leaf area index, roughness height, albedo, emissivity and vegetation root depth) and soil hydraulic parameters (saturated hydraulic conductivity, soil depth, soil porosity and bubbling pressure) with a time and spatial variability in order to account for the heterogeneity within the watershed.

Land surface parameters were estimated using the multi-source land cover data from California Wildlife Habitat Relationships (CWHR) and reference information from Asner et al. (2003), Scurlock et al. (2001) and Canadell et al. (1996). Monthly mean Leaf Area Index values were obtained from MODIS satellite driven data (1 km spatial resolution). Soil parameters were estimated using the Soil Survey Geographic (SSURGO) Database (Natural Resources Conservation Service, NRCS) and reference information from Gale and Grigal (1987), Canadell et al. (1996), McCuen et al. (1981) and Yoshitani et al. (2002).

These parameters were acquired and stored in the Cache Creek watershed GIS database. In Figure 43 the estimated leaf area index, as function of the month of the year is shown. Figure 44 shows the land surface parameters, while Figure 45 shows the soil hydraulic parameters obtained from this database.

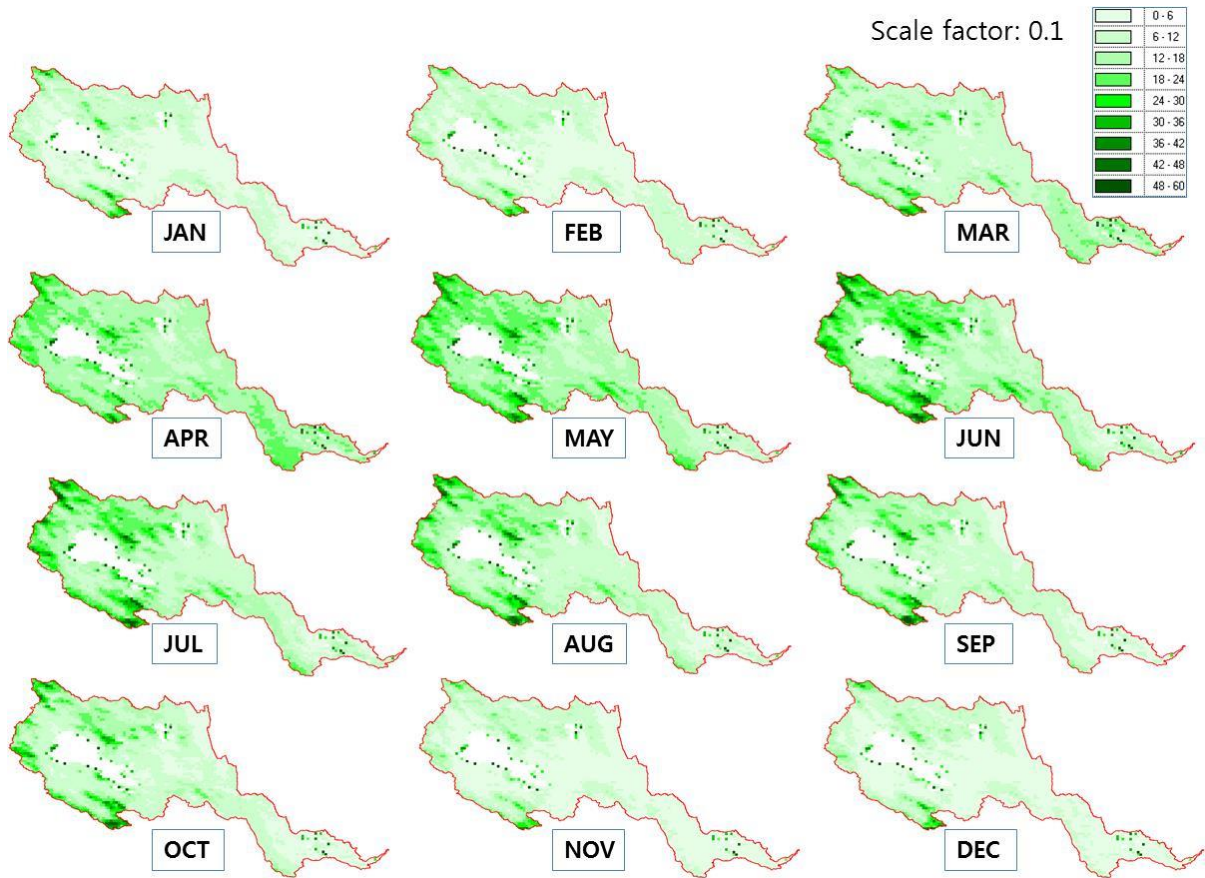


**Figure 43- Leaf Area Index (LAI) obtained from MODIS satellite data for the Cache Creek watershed**

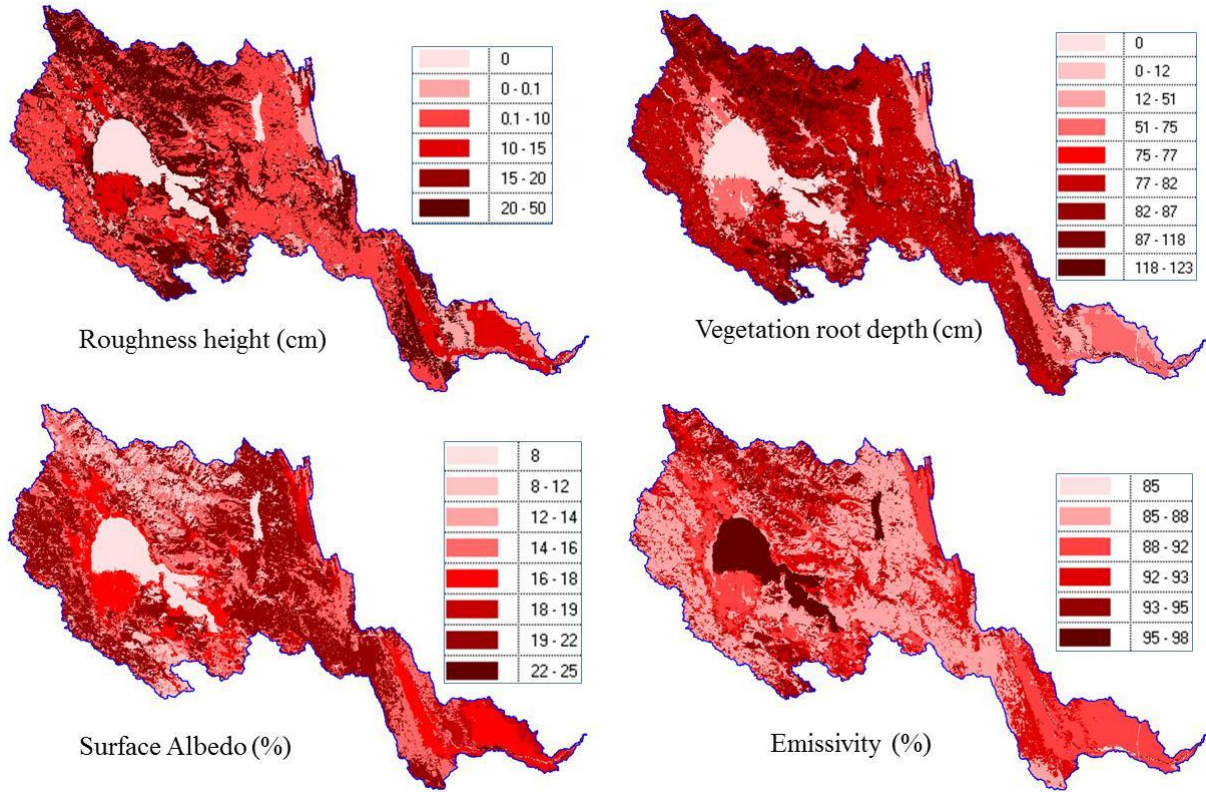


**Figure 44- Sample of distributed land surface parameters based on the CalSIL data and reference information for the Cache Creek watershed**

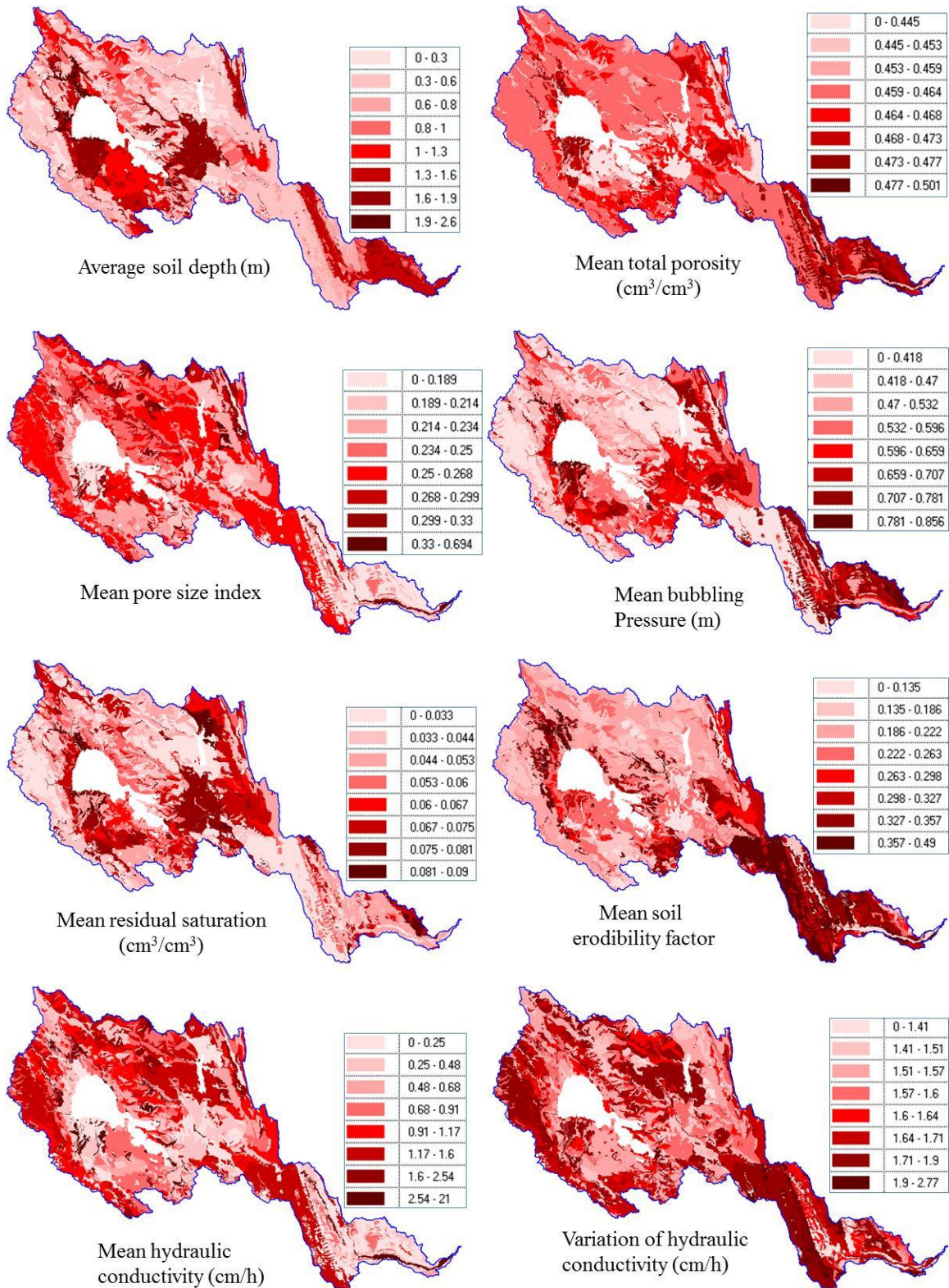


**Figure 45- Sample of distributed soil hydraulic parameters based on the SSURGO data and reference information for the Cache Creek watershed**

### **6.1.3 Estimation of historical climate conditions for each model computational unit (MCU) in WEHY model**

The reconstructed historical climate conditions at each MM5 simulation grid point cannot be connected directly to WEHY model because an MCU's geometry does not coincide with the shape of the rectangular MM5's grids. In order to account for the effect of topography on the hydrologic processes, it is necessary to quantify the atmospheric inputs such as precipitation, air temperature, solar radiation and wind speed at each of the MCUs within the modeled watershed.

Figure 46 shows sample plots of 61-year average monthly precipitation, monthly mean air temperature, wind speed and shortwave solar radiation from the NCAR/NCEP reanalysis data for each MCU for January and July during 1950 – 2011. Figure 47 and Figure 48 show the sample plots of GCMs (CCSM3 and ECHAM5)-based averaged monthly precipitation, monthly mean air temperature, wind speed and shortwave solar radiation at each model computational unit (MCU) for January and July during 1950 – 2000 over Cache Creek watershed. The reconstructed historical climate conditions at each model computational unit are used directly as input atmospheric data set for the WEHY model.

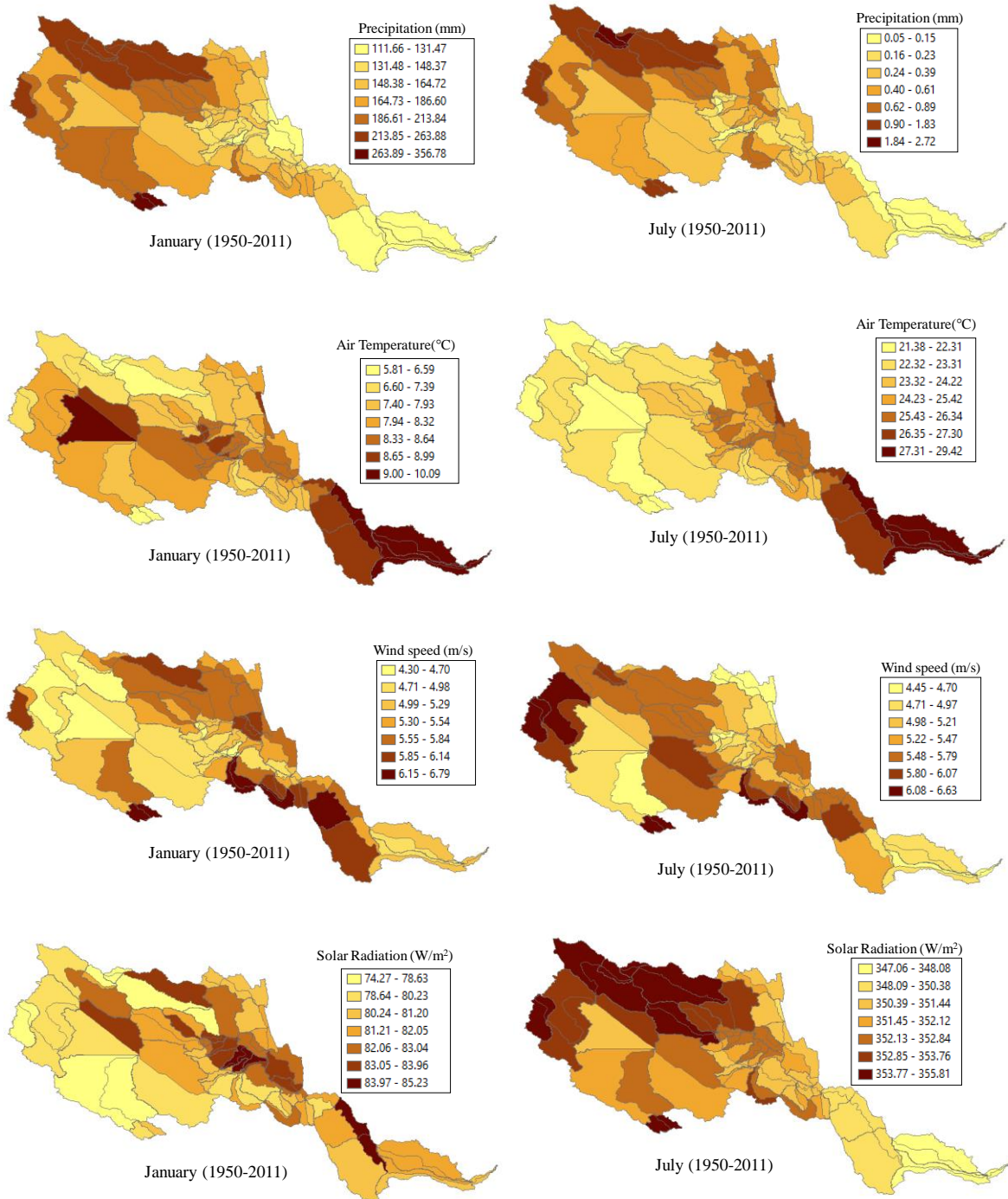


**Figure 46- Sample plots of NCAR/NCEP reanalysis data-based 61-year average monthly precipitation, monthly mean air temperature, wind speed and shortwave solar radiation at each model computational unit (MCU) for January and July during 1950 – 2011 over Cache Creek watershed.**

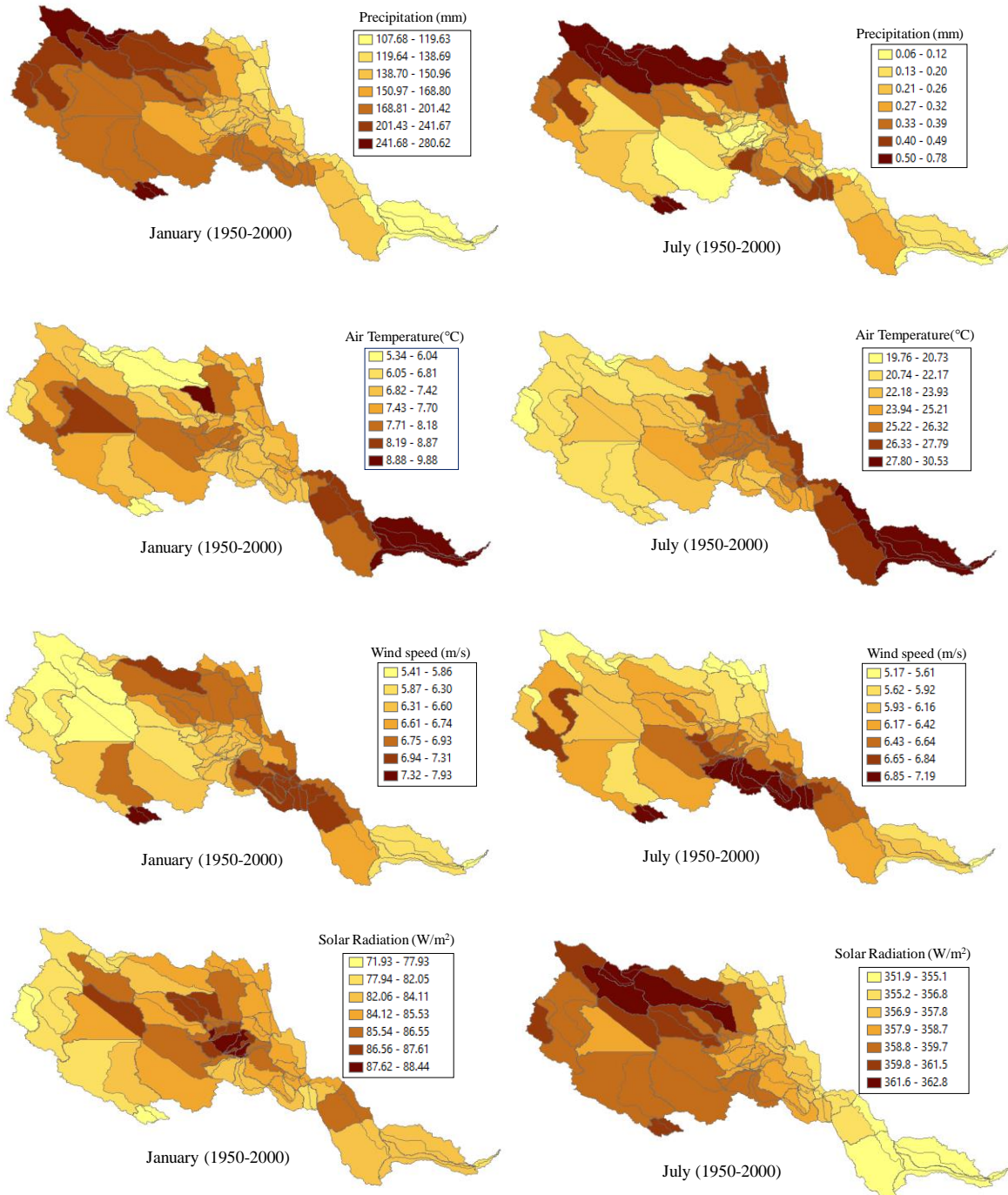


**Figure 47- Sample plots of CCSM3 GCM-based 61-year average monthly precipitation, monthly mean air temperature, wind speed and shortwave solar radiation at each model computational unit (MCU) for January and July during 1950 – 2000 over Cache Creek watershed.**

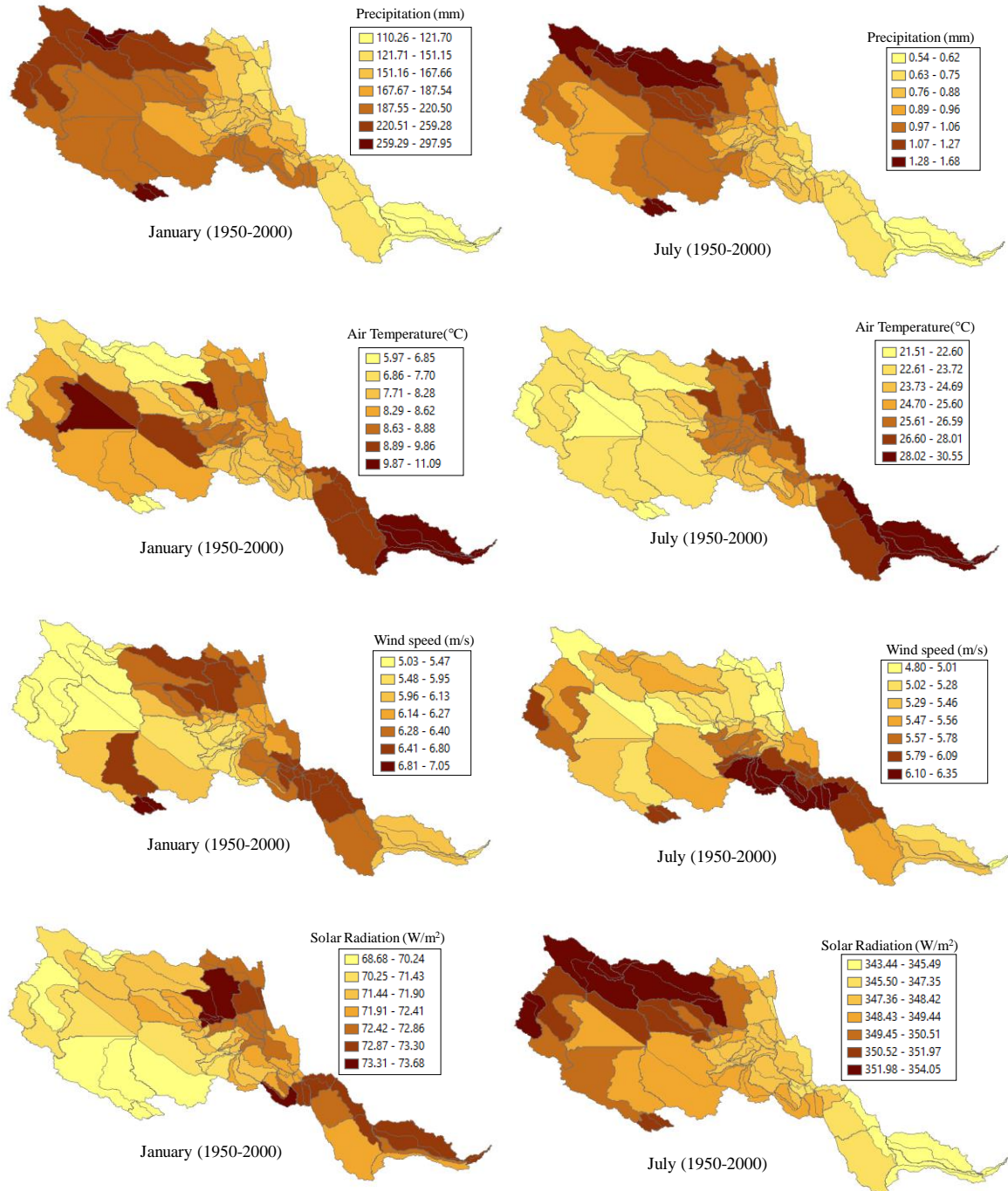


**Figure 48- Sample plots of ECHAM5 GCM-based 61-year average monthly precipitation, monthly mean air temperature, wind speed and shortwave solar radiation at each model computational unit (MCU) for January and July during 1950 – 2000 over Cache Creek watershed.**

## **6.2. Calibration and Validation of WEHY Model for Streamflow Simulations**

Using the estimated WEHY model parameters and the implemented climate conditions for each model computational unit, the hydrology component of the Watershed Environmental Hydrology (WEHY) model performed hydrologic simulations for the Cache Creek watershed. Two flow observation stations (Yolo USGS and Rumsey CDEC stations in Figure 49) were used for model calibration (2 years: wy1998 – wy1999) and validation (18 years: wy1993 – wy2010). For model calibration purposes, the NCAR/NCEP reanalysis data-based MM5 historical climate simulation results were used as the input atmospheric data for WEHY model. As can be seen in Figure 49, the two reservoirs (Clear Lake and Indian Valley reservoir) located upstream of Cache Creek watershed, play an important role for both flood control and water conservation. The Capay diversion dam, located downstream of Cache Creek, is also important, diverting irrigation water through two canals (West Adams canal and Winters canal). The operation rules for these hydraulic structures are crucial to simulate the historical flow conditions by WEHY model. The operation rules for Clear Lake were obtained from the documentation of the Solano and Gopcevic Decrees (Superior Court of the State of California, 1978) and from public documents of Lake County, and were incorporated into WEHY model. However, the information on the operation rules for Capay diversion dam and Indian Valley reservoir is very limited. As such, the operation rules for Capay diversion dam and for Indian Valley reservoir were developed for the WEHY model based on the comparison of model simulations with historical observations and on the limited available information.

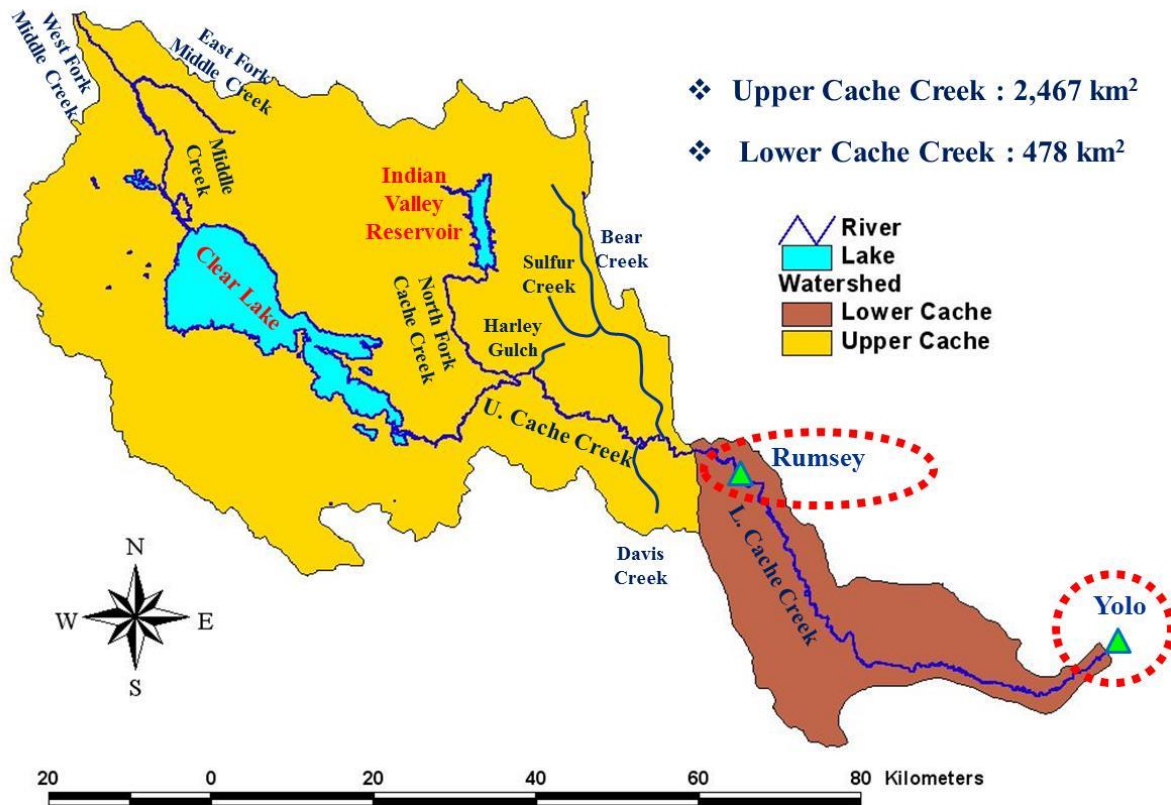
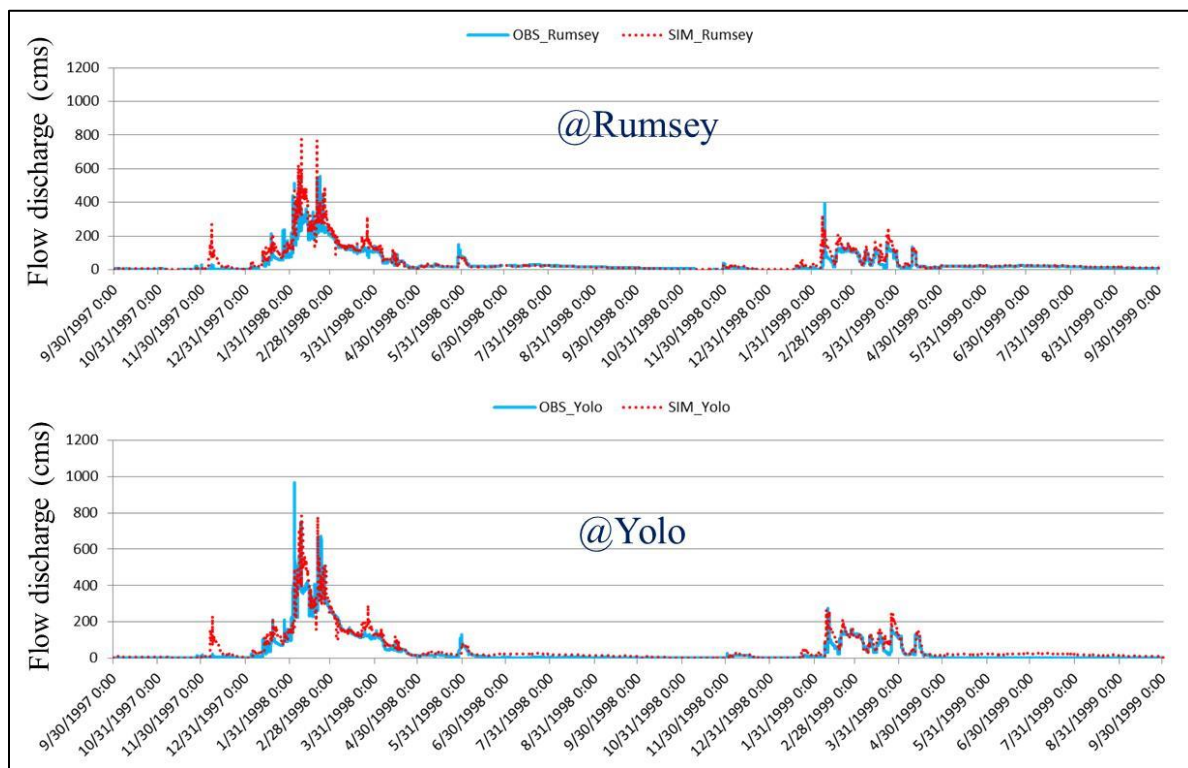


**Figure 49- Location of observation stations for model calibration and validation**

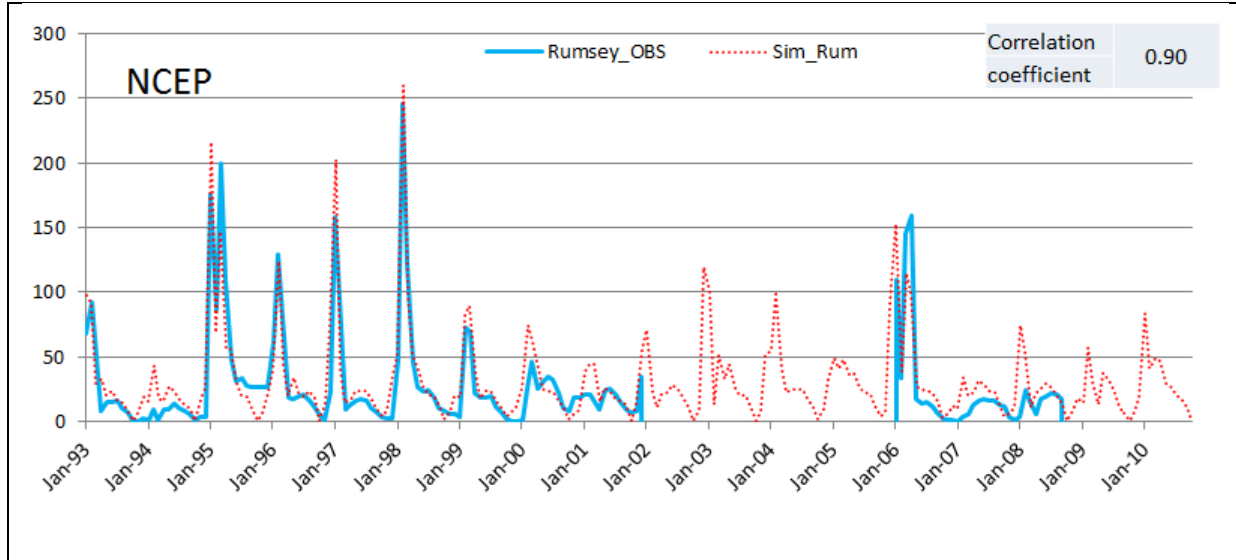
Using the estimated model parameters and the implemented climate conditions for each model computational unit, the WEHY model simulated the hydrologic conditions in the Cache Creek watershed. As stated earlier, the information on the operation rules for Clear Lake, Indian Valley Reservoir and Capay diversion dam is very limited. Hence, the observed outflow from two dams (Clear Lake and Indian Valley Reservoir) were first used in order to test the WEHY model performance instead of using the simulated outflow from the two dams.

Figure 50 shows the model calibration results (October 1997 -September 1999: 2 years) at Yolo USGS station and Rumsey CDEC station. This figure compares graphically the observed and simulated hourly discharge values at the two flow gauging stations. As can be seen in Figure 50, the model-simulated hydrographs match the corresponding observations at both Rumsey CDEC station and Yolo USGS station. The rising and the recession segments of the simulated hydrographs are very similar to the corresponding observations. The timing and magnitude of peak discharges are also very similar in comparisons both at Rumsey and Yolo stations.

Using the same parameter sets, determined through the calibration process, a validation run was performed for years between 1993 and 2010 for the Cache Creek watershed. Figures 51 and 52 show the validation results of monthly (1993 – 2010: 18 years) flow discharge at Rumsey CDEC station and Yolo USGS station. The NCAR/NCEP reanalysis - MM5 simulation-based WEHY streamflow simulations match almost perfectly the corresponding observations. However, it is important to note that in these model simulations the observed outflows from Clear Lake and Indian Valley Reservoir were used.



**Figure 50- Calibration results for hourly flow discharge at Rumsey CDEC station and Yolo USGS station during 10/1997-9/1999**



**Figure 51- Validation results for monthly flow discharge at Rumsey CDEC station during 1993 – 2010 (cms)**

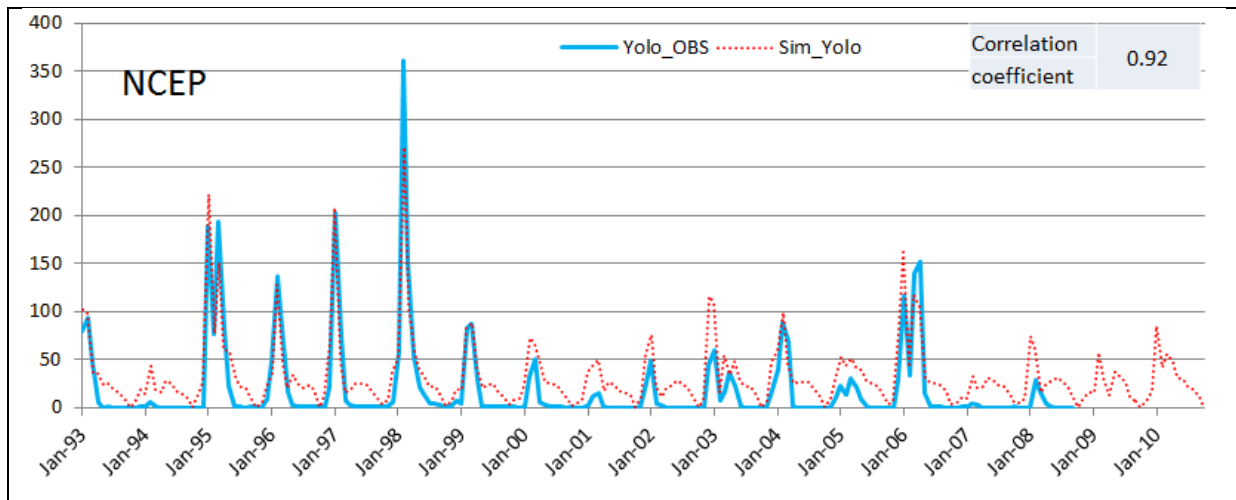


**Figure 52- Validation results for monthly flow discharge at Yolo USGS station during 1993 – 2010 (cms)**

Although the flow simulation results by WEHY model were calibrated and validated satisfactorily, the operation rules for the existing reservoirs should be incorporated into the model in order to reconstruct the historical flows and to project the future flows for the Cache Creek watershed reliably. The operation rules for Clear Lake and Indian Valley Reservoir were incorporated to WEHY model based on the given information and historical records and on some

preliminary model simulations. Additionally, the operation rule for Capay diversion dam was derived based on the historical records.

Figures 53 and 54 show the comparison results at Rumsey flow station and at Yolo flow station between observed flows and the corresponding model-simulated flows after applying the operation rules for Clear Lake, Indian Valley Reservoir and Capay diversion dam into the model simulations. As shown in these figures, simulated flow after application of operation rules is similar to the WEHY simulation results with observed outflows from Clear Lake and from Indian Valley Reservoir. In other words, inclusion of operation rules into the WEHY model enabled the model to reproduce the historical flow behavior quite well at Rumsey and Yolo flow gauging stations. Consequently, the same operation rules for these reservoirs were used in WEHY model's simulations of the future flows within the Cache Creek watershed.

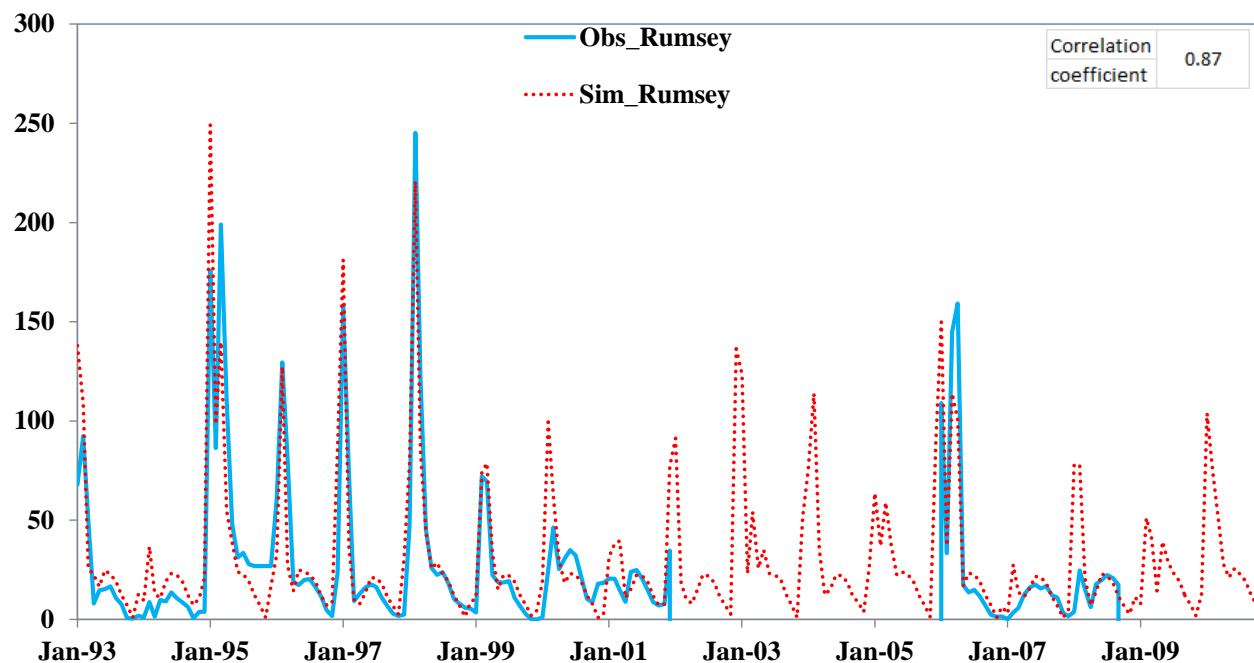


**Figure 53- Validation results of monthly flow discharge at Rumsey CDEC station during 1993 – 1999 using the operation rules for Clear Lake and Indian Valley reservoirs (cms)**

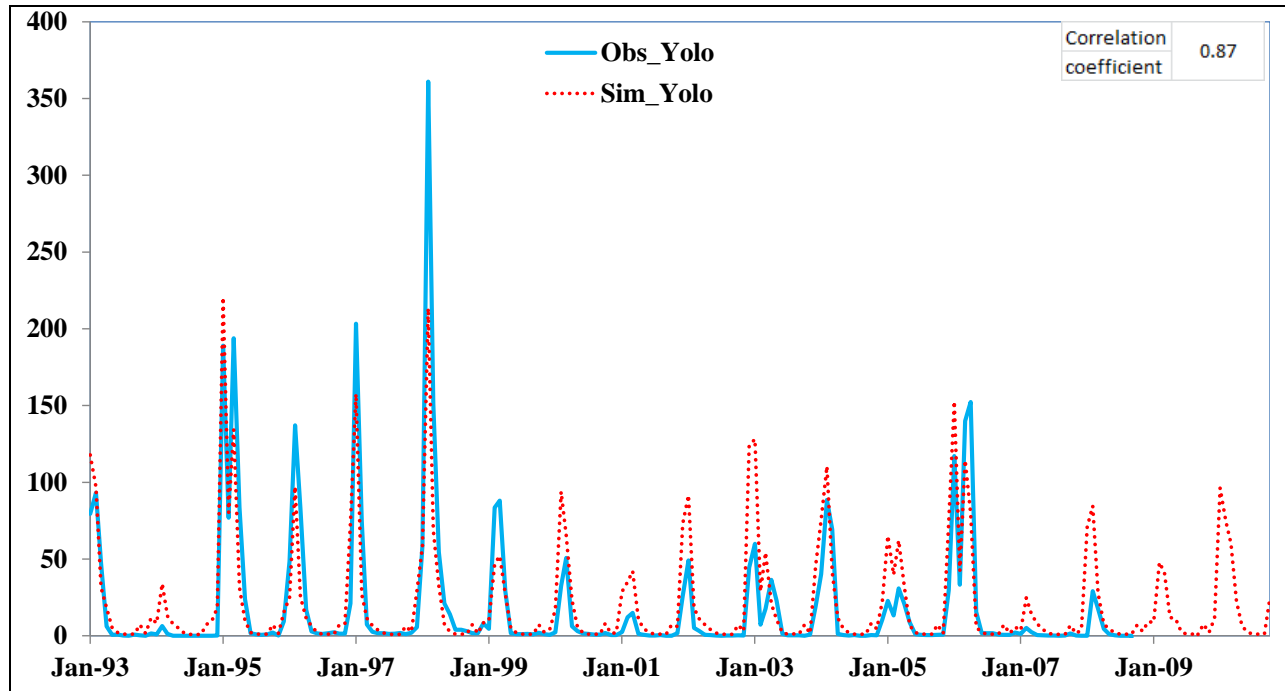


**Figure 54- Validation results of monthly flow discharge at Yolo CDEC station during 1993 – 1999 using the operation rules for Clear Lake and Indian Valley reservoirs (cms)**

### **6.3. Reconstruction of historical flow conditions**

The historical flow conditions from October, 1950 to September, 2010 were reconstructed based on the NCAR/NCEP reanalysis data and the calibrated and validated WEHY model. The operation rules for Clear Lake, Indian Valley Reservoir and Capay diversion dam were incorporated in this reconstruction. Figures 55 and 56 show the reconstructed monthly mean flow discharge at Rumsey CDEC station and Yolo USGS station, respectively, from October 1950 to September 2010.

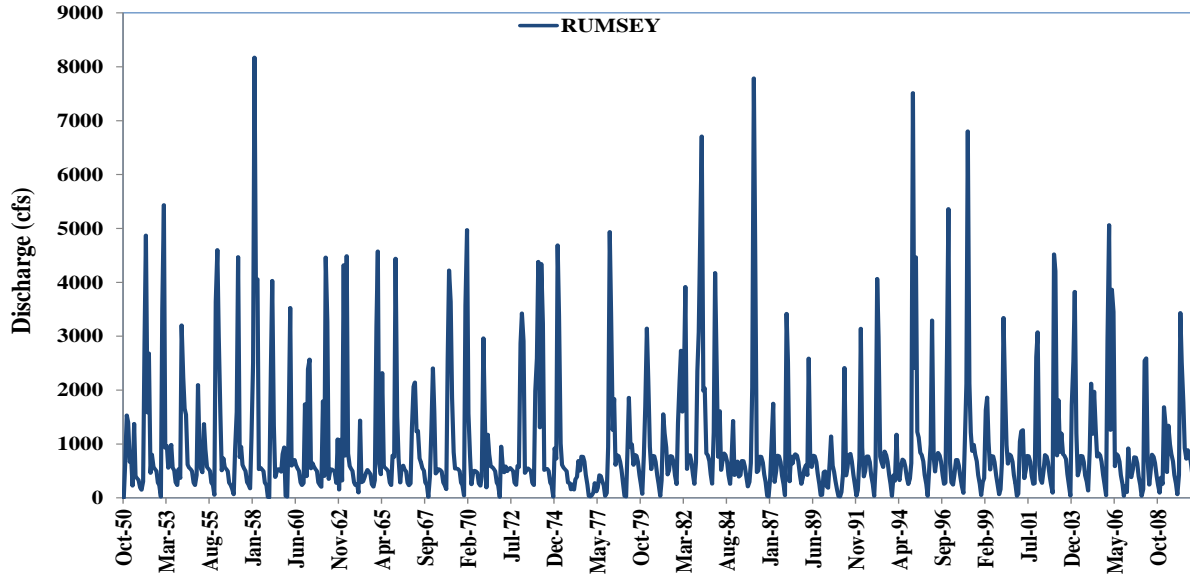


**Figure 55- Reconstructed monthly mean discharge based on the NCAR/NCEP reanalysis data from October, 1950 to September, 2010 at Rumsey CDEC station**

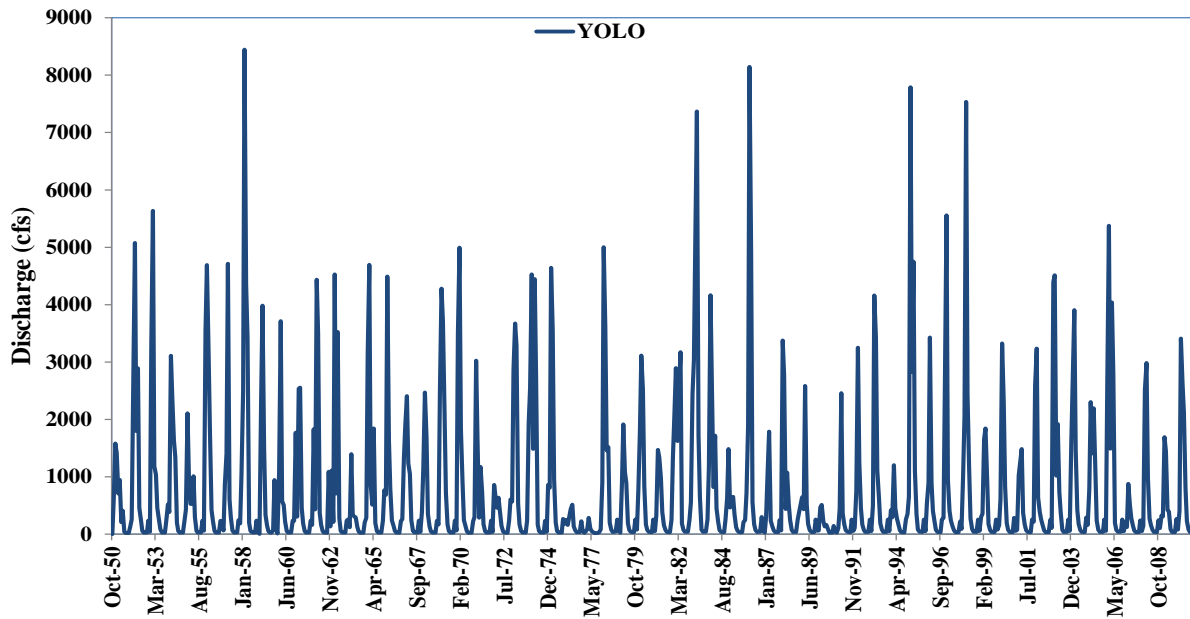


**Figure 56- Reconstructed monthly mean discharge based on the NCAR/NCEP reanalysis data from October, 1950 to September, 2010 at Yolo USGS station**

## 6.4. Future Flow Simulation and Flood Frequency Analysis

The calibrated and validated WEHY model hydrologic module projected the future flows throughout the 21<sup>st</sup> century by using as its input the projected future climate conditions that were previously described.

WEHY simulations produced thirteen individual hourly flow time series for water years 2010 through 2099, which are shown in Figure 57. These hydrographs were computed at the Yolo USGS station before Cache Creek enters the Yolo settling basin. Streamflows are presented in cubic meters per second ( $\text{m}^3/\text{s}$ ) and will be referred to as cms. These results form an ensemble of possible future flows under a broad range of climate change scenarios.

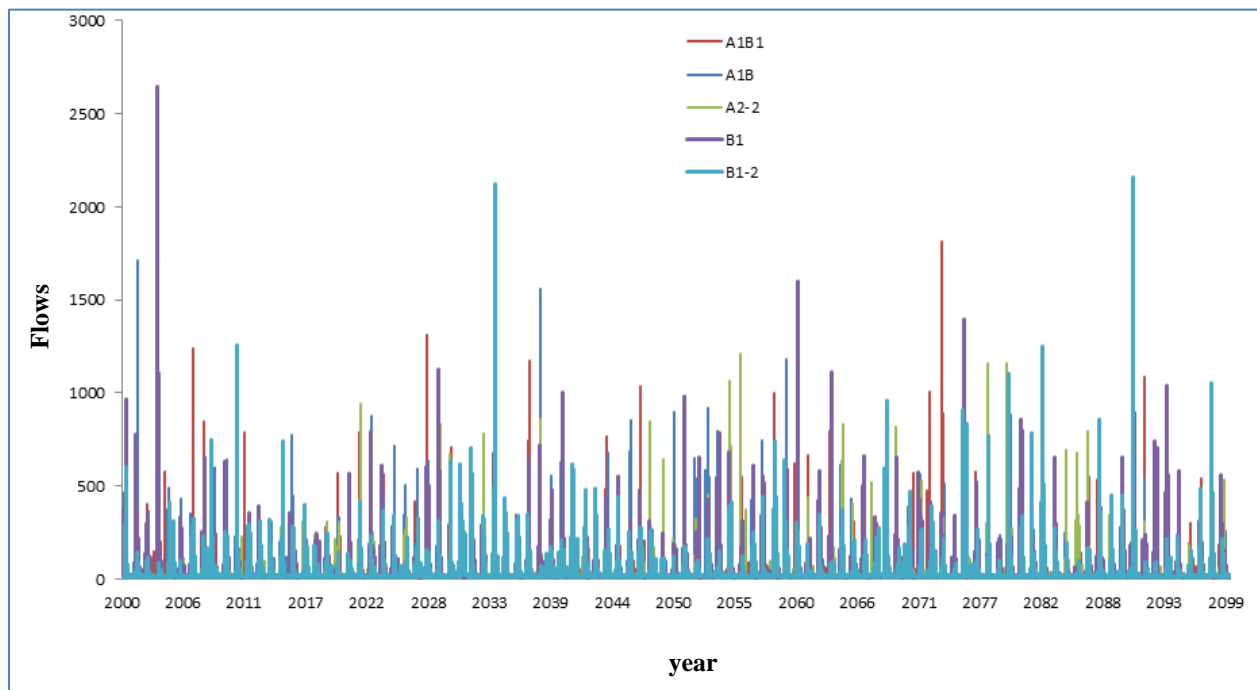


**Figure 57- Projected Hourly Flow Hydrographs at Yolo gauging station based on SRES Scenarios**

System trends throughout time may not be discernable from the time series data. Transforming data into the frequency domain may elucidate behaviors of interest. Given the inescapable uncertainty in studying future events, system behaviors are more meaningful to examine than specific events. Probability of future events of interest has traditionally been estimated through frequency analysis- the fitting of a probability distribution to a series of observations. Such

analysis allows for predictions beyond the range of observed data and provides summary statistics. While useful and routinely employed, this method is not without its limitations. The fitted distribution is reflective of historical observations, and the short streamflow records that are available may be insufficient to describe the system. Fitting a distribution also assumes that the underlying distribution is not changing in time, and that the system is stationary with past events representing future events. Climate change challenges this assumption of stationarity.

Performing frequency analysis of future simulated streamflows using the modeling chain described above addresses the above limitations of data scarcity and the assumption of stationarity. Comparing analyses of the first-half and second-half of the 21<sup>st</sup> century, enables the study of how the flood regime may be changing in time. Frequency analysis is performed on annual maximum flow. This dataset is shown in Figure 58. Summary statistics for the projected annual maximum flows during the 21<sup>st</sup> century at Yolo gauging station are given in Table 6 below. These series of annual maxima (for all realizations) were then divided into two time windows of 45 years: 2010-2054, and 2055-2099. These annual maxima are assumed to be independent but with different identical distributions within 2010-2054 and 2055-2099 time windows of the 21<sup>st</sup> century. Under this assumption of local stationary within each of these 45-year time windows, from the simulated annual maximum flows of Figure 58, one distinct frequency histogram for each of the two time windows within 21<sup>st</sup> century were estimated. The computed histograms which show the number of annual maximum flow occurrences as function of flow discharge, are shown in Figure 59 for the two time windows during 21<sup>st</sup> century. Histograms are useful for visualizing the distribution of flow magnitudes, predicted number of occurrences and relative occurrence likelihood. Meanwhile, the probabilistic behavior of the projected annual maximum flows during the 21<sup>st</sup> century at Yolo gauging station is shown in Figure 60 by means of their relative frequency histograms as they evolve by climate change during the two consecutive time windows of the 21<sup>st</sup> century. Since the annual maximum flood return period is a fundamental decision variable in the planning and management of hydraulic structures, the annual maximum flows as function of return period were also computed from the projected flows during the 21<sup>st</sup> century at Yolo gauging station. As shown in Figure 61, the annual maximum flow as a function of return period varies not only with the return period but

also as a function of the time window within 21<sup>st</sup> century, reflecting the effect of changing climate on the extreme flows at Cache Creek watershed.

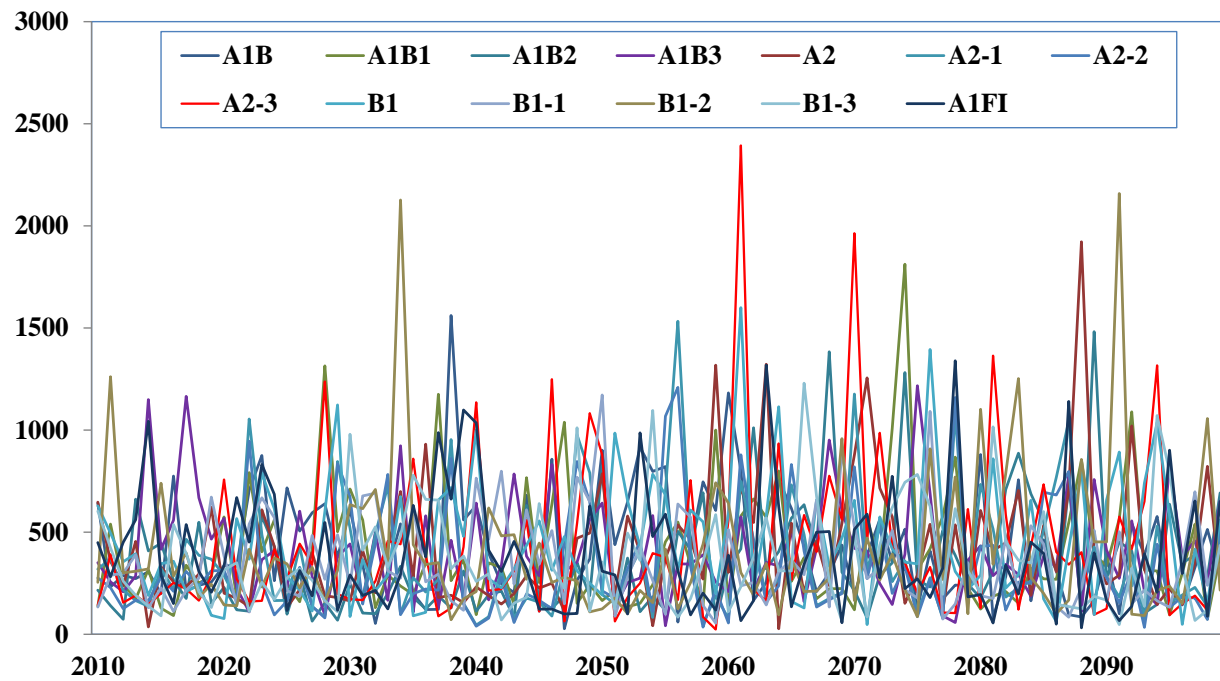


**Figure 58-Annual maximum model-simulated streamflows during 21<sup>st</sup> century at Yolo gauging station**

**Table 6. Summary statistics for model-projected annual maximum flows during the two time periods of the 21<sup>st</sup> century at Yolo gauging station**

Time Period	Mean (cms)	Maximum (cms)	Variance	Skewness
2010-2054	377.51	2126.3	79766.11	1.87
2055-2099	435.16	2394	113908.5	1.80

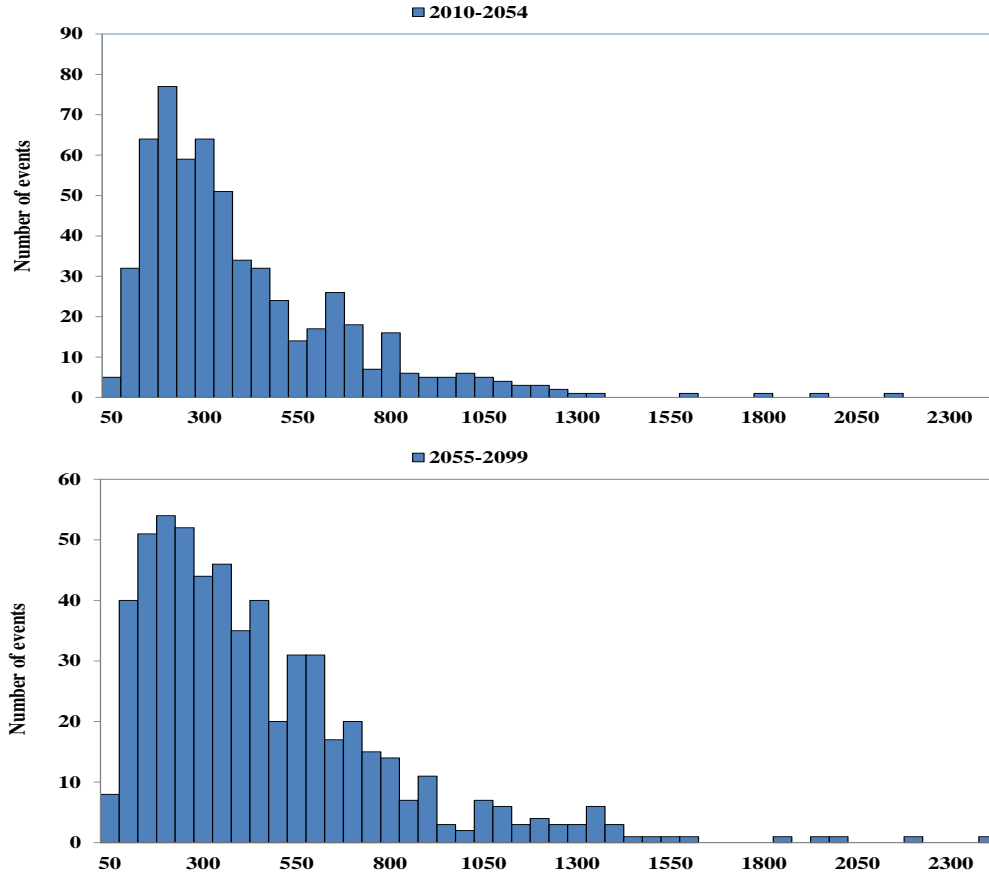
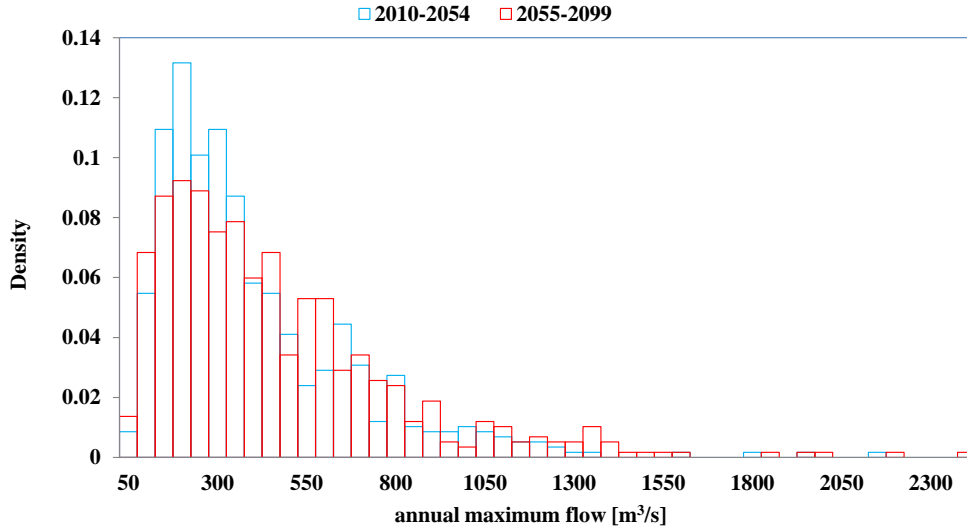
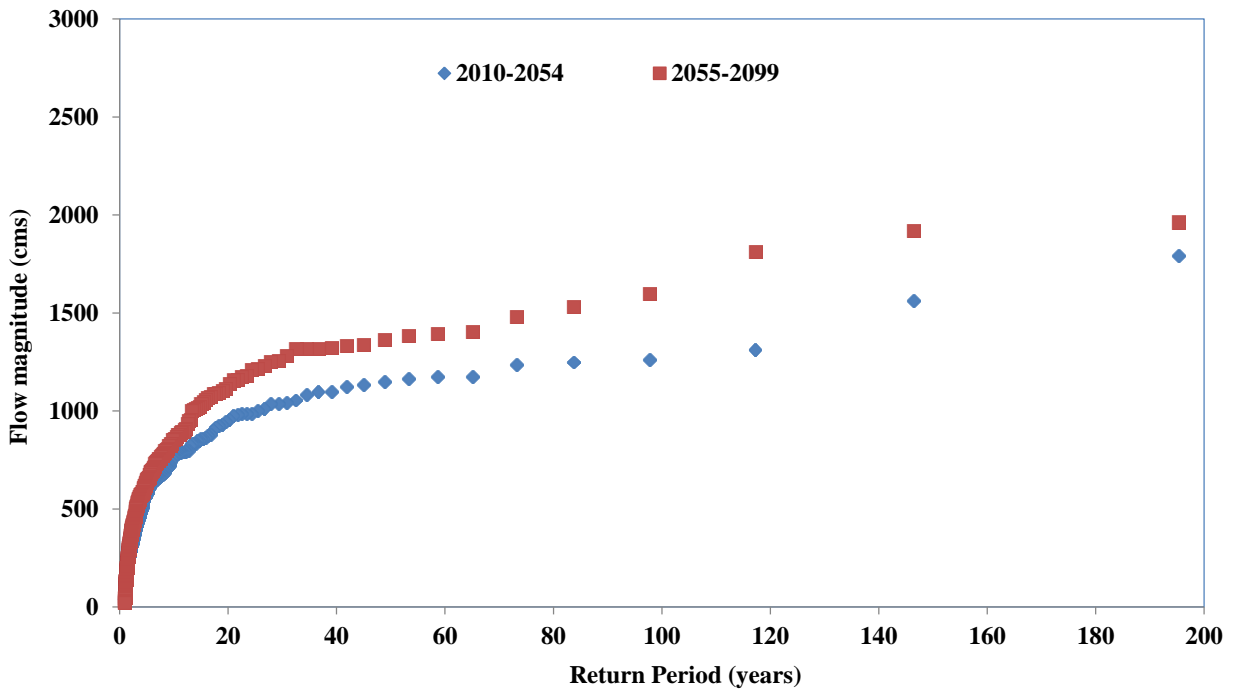


Figure 59- Histograms of annual maximum flows separated into 45-year increments (2010-2054, and 2055-2099) for all flow projections during 21<sup>st</sup> century at Yolo station



**Figure 60- Relative frequency histogram of annual maximum flows separated into 45-year increments (2010-2054, and 2055-2099) for all flow projections during 21<sup>st</sup> century at Yolo gauging station**



**Figure 61-Evolution of the annual maximum flow as function of return period throughout the 21<sup>st</sup> century for all flow projections at Yolo gauging station**

Figures 60 and 61 show the evolution of the flood regime as the magnitudes of simulated extreme events grow throughout the 21<sup>st</sup> century. This evolution is noticeable for flood events exceeding the channel capacity of 850 cms (~30,000 cfs). The most extreme event during 2010 through 2054 is 2,126.3 cms (75,089cfs), increasing to 2,394 cfs (84,543 cfs) during 2055 through 2099.

**Table 7. Annual maximum flow discharge (cms) as function of return period during the two selected time periods in 21<sup>st</sup> century**

<b>Return Period</b>	<b>2010-2054</b>	<b>2055-2099</b>
200 years	1797.5 cms	1973.3 cms
100 years	1267.5 cms	1625.1 cms

Return period flows were linearly interpolated from calculated exceedance probabilities. No extrapolation of relative frequencies (a fundamental step of standard frequency analysis) was necessary in this study, given the extensive dataset of model-simulated flows. Return periods were calculated using the Weibull plotting position. Referring to Table 7, comparing 2010-2054 and 2055-2099, the 100-year flood discharge magnitude grows 28% and the 200-year flood discharge magnitude grows 9.7 %.

While the methodology used in this study is computationally intensive, this new physically-based framework for computing the flood frequencies does not rely on the assumption of stationarity. These results support the discussion on the intensification of the water cycle under climate change and the hypothesis of floods growing in magnitude (Huntington 2006, Hirabayashi et al. 2008, Milly et al. 2008). Evolution of the return period flood flows and other descriptive statistics suggests that traditional flood frequency analysis and the assumption of stationarity may no longer be the best way to study and describe the future extreme flow events.

The simulated annual maximum flows underscores the importance of concurrent flow and sediment observations to augment the sediment-rating curve as the calculated 100-year floods for the two selected time periods during the 21<sup>st</sup> century all exceed 13,000 cfs when the curve becomes sparsely populated. These simulated flows and flood frequency analysis provide input data for the simulations of hydraulics in the Cache Creek Settling basin and would be useful in future water quality studies of the Cache Creek Watershed.

## **7. Discussion, Conclusions and Recommendations**

Due to lack of concurrent flow, sediment and mercury data within the Cache Creek watershed, the sediment and mercury conditions within the Cache Creek watershed are quite uncertain. As a consequence of such lack of concurrent flow and sediment data, the sediment rating curve that is necessary for the estimation of sediment inflows into the Cache Creek Settling Basin (CCSB) has substantial uncertainty for flows above 13,000 cfs. One way to fill the gap in the sediment rating curve and to gain a better understanding of sediment and mercury conditions within the Cache Creek watershed is to develop a comprehensive field sampling program for collecting concurrent flow, sediment and mercury data at various locations within the watershed, as proposed in Figure 20 of this report. However, such a field sampling program is cost prohibitive. A financially feasible field program can focus on one or two key flow gauging station locations, such as Rumsey station and/or Yolo station, within the watershed in order to collect the necessary concurrent flow, sediment and mercury data. However, one may have to wait for a long time for the occurrences of flows that exceed 13,000cfs in order to develop a sufficiently large sample of concurrent flow and sediment discharges in order to be able to fill the gap in the sediment rating curve for flows above 13,000cfs. An alternative approach to filling the gap in the sediment rating curve is to combine computer modeling of flow-sediment-mercury with a field sampling program where the field collected concurrent flow-sediment-mercury data, at least at one gauging station, such as Rumsey, can then be utilized for the calibration and validation of a watershed environmental hydrology model, such as the WEHY model. Once calibrated and validated by the field data, the WEHY model can then be utilized to reconstruct the historical concurrent flow and sediment conditions at the Cache Creek watershed that can then be used to fill the gap in the sediment rating curve for inflows to the CCSB for flows exceeding 13,000cfs. Hence, the main objective of this project was to develop detailed flow, sediment and mercury conditions for Cache Creek and its tributaries for historical and future conditions by coupling the Watershed Environmental Hydrology (WEHY) model with a regional climate model (MM5 in this project) in order to simulate concurrent flow, sediment and mercury information in the Cache Creek watershed both for the historical period as well as for the 21<sup>st</sup> century. Then such information could be used to fill the gap in the sediment rating curve, and to provide better estimates of sediment and mercury loads to CCSB. Reconstruction of realistic and comprehensive historical and future climate, flow, sediment and mercury conditions would

eliminate the need to install and maintain many flow-sediment-mercury stations and rain gages within the Cache Creek watershed. The simulated flow, sediment and mercury conditions in the Cache Creek watershed could then be used also to investigate opportunities for trapping part of the mercury at upstream locations of the Cache Creek watershed, thereby reducing the mass loading rate of sediment into the Basin.

Once the sediment rating curve is constructed for the full range of flow conditions by means of the WEHY model-estimated concurrent flow-sediment-mercury outflows from the Cache Creek watershed, it could then be utilized to predict the concurrent flow and sediment inflows reliably into CCSB as the upper boundary condition of the CCSB hydrodynamic model. By means of such a reliable inflow boundary condition, the hydrodynamic model of CCSB could then estimate reliably the trap efficiencies for the CCSB during the 21<sup>st</sup> century under various engineering action scenarios.

Within the above framework, DWR and USGS have initiated a field sampling program, focusing on collecting concurrent flow-sediment-mercury data at the Rumsey station. However, the performance period of this project coincided with a severe drought period in California, and no significant flows were recorded at the Rumsey station during the project period. Under these circumstances the UC Davis J AHL, the contractor for this project, was still able to implement a regional climate model, MM5, over Cache Creek watershed at 3km spatial grid resolution, and was able to reconstruct the historical climate conditions during 1950-2010 at hourly intervals over the whole watershed. This exercise was accomplished by means of dynamically downscaling the coarse-grid-resolution NCAR/NCEP reanalysis historical climate data at about 280km grid resolution to 3km grid resolution over the Cache Creek watershed by means of the MM5 regional climate model. This modeling approach was validated by comparison of historical precipitation, reconstructed by NCAR/NCEP reanalysis data-based MM5 simulations, against PRISM data over the watershed, and by comparing the MM5-simulated historical air temperature and solar radiation against observations at a field station by means of various statistical measures.

Once the historical climate conditions were reconstructed for the 1950-2010 period by the NCAR/NCEP reanalysis data-based MM5 simulations, these climate information were input into the hydrologic module of WEHY model in order to calibrate and validate it with historical flow data in Cache Creek watershed. Since the hydrologic module of WEHY model is fully-physically-based, almost all of its parameters are estimated objectively from the existing land databases. However, few parameters of WEHY model, such as stream widths and roughness coefficients, still need to be estimated by calibration based on available flow data. Also, the operation rules of the main reservoirs in the watershed (Clear Lake, Indian Valley Reservoir and Capay Dam) had to be derived from existing documents and from model simulations. Accordingly, two years of flow data at Rumsey and Yolo stations were used for model calibration. Once the WEHY model hydrologic module was calibrated, it was then run with the reconstructed climate inputs for a separate 8-year period over Cache Creek watershed in order to simulate the flows in space at various locations along the main Cache Creek and along its tributaries at hourly intervals during this period. Then these simulated flows were compared against their observed counterparts at Rumsey and Yolo stations for their validation. These comparisons yielded very satisfactory model performance results with the correlation coefficient of 0.87 even when the unknown operation policies of the existing reservoirs within the watershed had to be determined by the project team. Once the WEHY model's hydrologic module was validated in this way, the calibrated model was then run for the October 1950- September 2010 period with the reconstructed climate data over the watershed as its input, to reconstruct the flows at hourly increments along the Cache Creek main river branch and along its tributaries to obtain the comprehensive information on the flow conditions within the watershed during October 1950- September 2010.

In order to reconstruct the historical sediment and mercury conditions at Cache Creek watershed during October 1950-September 2010 at hourly increments, it was then necessary to calibrate and validate the environmental module of WEHY model (Kavvas et al. 2006) by the concurrent flow-sediment-mercury field sampling data. However, during the project performance period, due to extremely dry conditions at the watershed no such data could be collected. As such, it was not possible to calibrate and validate the environmental module of WEHY model, and, hence, it was not possible to simulate neither the historical nor the future sediment and mercury loads

within Cache Creek watershed or from the watershed to the CCSB. Consequently, due to lack of field data on concurrent flow-sediment-mercury during the project performance period it was not possible to fill the gap in the sediment rating curve for flows above 13,000cfs although there are quite a few WEHY model-simulated flows at Yolo station during 21<sup>st</sup> century that exceed 13,000cfs, as may be seen from Figure 57. Consequently, the Milestones 7 and 9 of the project could not be accomplished while only the flow part of Milestone 8 could be accomplished.

Under these circumstances, as explained in Section 4.1., the project team resorted to utilizing the Universal Soil Loss Equation (USLE) in order to approximately identify the potential source areas of sediment and mercury in Cache Creek watershed. A map that identifies these potential source areas, in terms of annual soil erosion loads, was developed and is given in Figure 6.

With the calibrated and validated WEHY model hydrologic module for Cache Creek watershed it was also possible to project the future flow conditions over the watershed, based on the dynamically-downscaled ensemble of 13 climate projections from two GCMs (German ECHAM5 and NCAR's CCSM3) by the regional climate model MM5 under a wide spectrum of future greenhouse gas emission scenarios (A1B, A2, B1 and A1FI). However, before embarking onto this exercise, this projection approach was validated by first dynamically-downscaling the historical control run climate simulations of ECHAM5 and CCSM3 GCMs at 3km grid resolution over the Cache Creek watershed, and comparing these simulations against corresponding PRISM data. From these comparisons the model bias due to uncertainty in the GCM control simulations was identified and corrected. Afterwards, the bias-corrected historical precipitation simulations of the model were compared against the corresponding PRISM data with favorable statistical test results, thus validating this modeling approach. Then the validated modeling approach was applied to the downscaling of the ensemble of 13 future climate projections from ECHAM5 and CCSM3 GCMs for the 21<sup>st</sup> century at 3km grid resolution and hourly time intervals over the Cache Creek watershed. The identified model bias during historical comparisons was then incorporated to the downscaled future climate projections in order to account for this model bias. Then these bias-corrected future climate conditions during the 21<sup>st</sup> century were input to WEHY model's hydrologic module in order to simulate the detailed flow conditions over Cache Creek watershed at hourly intervals along the main Cache

Creek branch and its tributaries throughout the 21<sup>st</sup> century. Then based on the 1170 years of flow data from the ensemble of 13 projections during 2010 through 2099, shown in Figure 57, it was then possible to perform a comprehensive flood frequency analysis of the outflows from Cache Creek watershed at Yolo gauging station, and estimate the 100-year and 200-year return period annual maximum flood peak discharges at the Yolo station without resorting to any extrapolation of the frequency curve (such extrapolation is a standard step in the classical frequency analysis). The results of this frequency analysis are summarized in Table 7 and Figures 59, 60 and 61. As may be seen from these figures and Table 7, which are in cubic meters per second (cms) flow discharge units, the flood frequencies evolve during two periods of the 21<sup>st</sup> century with changing climate. Referring to Table 7, while the 100-year flood peak discharge during the 2010-2054 period is 49 % higher than the channel capacity of 30,000cfs (44,800 cfs), the estimated 100-year flood peak discharge in the later period of the century is 91.2 % higher.

With the reconstructed historical flow conditions and the projected future flow conditions during 21<sup>st</sup> century along the main branch and tributaries of the Cache Creek by the calibrated and validated WEHY model hydrologic module, a comprehensive picture of the flow conditions in the Cache Creek watershed have been obtained in this project. Accordingly, the Milestones 1, 2, 3, 4, 5 and 6 of the project were accomplished successfully. Once concurrent flow-sediment-mercury field data that cover a range of flow conditions, are obtained at Rumsey station, then such data can be utilized to calibrate and validate the environmental module of WEHY model for Cache Creek watershed. Once the environmental module of WEHY model is calibrated and validated by field data, then it will be possible to achieve the remaining Milestones 7, 8 and 9 of the project to complete the sediment rating curve and to provide the comprehensive historical and future flow-sediment-mercury inflow data to CCSB.

### **7.1. Recommendations for future actions.**

Before simulating sediment load and mercury transport with the simulated flow discharge, it is necessary to calibrate and validate the WEHY-Environmental module over the Cache Creek watershed by means of concurrent flow-sediment-mercury data. However, as mentioned in

Section 4.3., the field data collected in various previous projects and in the current project at Cache Creek watershed are insufficient for utilization in the calibration and validation of WEHY environmental hydrology model, fundamentally due to lack of concurrent flow-sediment-mercury observations. There is an urgent need for a field-monitoring program at several locations, distributed over the watershed.

The desired sampling locations are shown in Figure 20. However, the substantial cost of realizing the desired sampling program is recognized. As such, if it is not possible to perform the monitoring at the 11 desired locations due to cost constraints, it is still absolutely essential to carry out a sampling program for sediment and mercury, simultaneously with the flow observations, at least at the Rumsey station. Accordingly, the following sampling data which should be collected simultaneously with streamflow data, are recommended as essential for the calibration and validation of the environmental hydrology module of WEHY model in order to produce reliable and scientifically defensible simulations of flow, sediment and mercury at the Yolo station in order to be able to reconstruct the portion of the sediment rating curve corresponding to flows above 13000 cfs, and in order to develop reliable flow-sediment-mercury inflow data for CCSB:

- **Instantaneous grab sampling data (suspended sediment, and mercury) concurrently with the flow discharge measurements**
  - At Rumsey station
- **Data on Mercury within the streambed (soil)**
  - At Rumsey station

## 8. References

Anthes, R. A., and Warner, T. T. (1978). Development of hydrodynamic models suitable for air pollution and other mesometeorological studies. *Mon. Wea. Rev.*, 106, 1045-1078.

Asner, G.P., Scurlock, J.M.O., and Hicke, J.A (2003). "Global Synthesis of Leaf Area Index Observations: Implications for Ecological and Remote Sensing Studies", *Global Ecology and Biogeography*, 12, 191-205.

Bosworth, D., and Morris, P. (2009). Bear Creek Mercury Inventory, Staff Report, Central Valley Regional Water Quality Control Board.

Canadell, J., Jackson, R.B., Ehleringer, J.R., Mooney, H.A., Sala, O.E., and Schulze, E.D. (1996). "Maximum Rooting Depth of Vegetation Types at the Global Scale." *Oecologia*, 108, 583-595.

CDM (2004a). Final technical Memorandum: Cache Creek Settling Mercury Study, Phase 1 - Existing Conditions. April, 2004.

CDM (2004b). Technical Memorandum: Cache Creek Settling Mercury Study, Phase 2 - Sediment Transport Modeling. July, 2004.

CDM (2007). Technical Memorandum: Cache Creek Settling Mercury Study, Phase 3 - Alternatives Evaluation. August, 2007.

Central Valley Regional Water Quality Control Board (2004). Cache Creek, Bear Creek, and Harley Gulch TMDL for Mercury, Staff Report. November, 2004.

Central Valley Regional Water Quality Control Board (2005). Amendments to

The Water Quality Control Plan for the Sacramento River and San Joaquin River Basins For The Control of Mercury in Cache Creek, Bear Creek, Sulphur Creek, and Harley Gulch, Staff Report. October, 2005.

Central Valley Regional Water Quality Control Board (2008). Mercury Inventory in Cache Creek Canyon, Staff Report. February, 2008.

Chen, Z. Q., Kavvas, M. L., Govindaraju R. S. (1993): Upscaling of Richards equation for soil moisture dynamics to be utilized in mesoscale atmospheric models. Exchange Processes at the Land Surface for a Range of Space and Time Scales, ed. by H.J. Bolle et al., IAHS Pub. No. 212, 125-132.

Chen, Z. Q., Kavvas, M. L., Tan, L., and Soong, S.-T. (1996): Development of a regional atmospheric-hydrologic model for the study of climate change in California. Proc., North American Water and Environment Congress, ASCE, Reston, Va. 1093-1098

Chen, Z. Q., Govindaraju, R. S., and Kavvas, M. L. (1994a): Spatial averaging of unsaturated flow equations for areally heterogeneous fields: Development of models. *Water Resour. Res.*, 30(2), 523-533.

Chen, Z. Q., Govindaraju, R. S., and Kavvas, M. L. (1994b): Spatial averaging of unsaturated flow equations for areally heterogeneous fields: Numerical simulations. *Water Resour. Res.*, 30(2), 534-544.

Chen, Z. Q., Kavvas, M. L., Yoshitani, J., Fukami, K., and Matsuura, T. (2004a): Watershed Environmental Hydrology (WEHY) model: Model application. *J. Hydrologic Eng.*, 9(6), 480-490.

Chen, Z. Q., Kavvas, M. L., Yoon, J. Y., Dogrul, E. C., Fukami, K., Yoshitani, J., Matsuura, T., (2004b): Geomorphologic and soil hydraulic parameters for Watershed Environmental Hydrology (WEHY) model. *J. Hydrologic Eng.*, 9(6), 465-479.

Chen, Z. Q., Ohara, N., Anderson, M., and Yoon, J. (2008): A Regional Hydroclimate Model For Water Resources Management Of The Tigris-Euphrates Watershed. World Environmental & Water Resources Congress. Honolulu, Hawaii. ASCE.

Cooke, J., Foe, C., Stanish, S., and Morris, P., (2004): Cache Creek, Bear Creek, and Harley Gulch TMDL for Mercury. Staff Report. Regional Water Quality Control Board Central Valley Region.

Domagalski, J.L., Alpers, C.N., Slotton, D.G., Suchanek, T.H., and Ayers, S.M. (2004): Mercury and methylmercury concentrations and loads in the Cache Creek watershed, California. *Science of the Total Environment*, 327, 215–237.

Dunne, T. (1978). Chapter 7: Field studies of hillslope flow processes. *Hillslope hydrology*, M. J. Kirkby, ed., 227–293.

Foe, C., and Bosworth, D. (2008): Mercury Inventory in the Cache Creek Canyon, Staff Report, Central Valley Regional Water Quality Control Board.

Gale, M.R., and D.F. Grigal. (1987): "Vertical Root Distributions of Northern Rree Species in Relation to Successional Status." *Can. J. For. Res.*, 17, 829-834.

Grell, G. A., Dudhia J. and Stauffer D.R. (1995): A description of the Fifth-Generation Penn State/NCAR Mesoscale Model (MM5). NCAR Technical Note, NCAR/TN-398+STR, 117pp.

Hirabayashi, Y., et al. (2008): "Global projections of changing risks of floods and droughts in a changing climate." *Hydrological Sciences Journal* **53**(4): 754-772.

Huntington, T. G. (2006): "Evidence for intensification of the global water cycle: Review and synthesis." *Journal of Hydrology* **319**(1-4): 83-95.

Kavvas M.L., Chen Z.Q., Tan L., Soong S.-T., Terakawa A., Yoshitani J. and Fukami K. (1998): A regional-scale land surface parameterization based on areally-averaged hydrological conservation equations, *Hydrological Sciences Journal* 43(4), pp. 611–631

Kavvas, M. L., Chen, Z.Q., Dogrul, E.C., Yoon, J.Y., Ohara, N., Liang, L., Aksoy, H., Anderson, M.L., Yoshitani, J., Fukami, K., Matsuura, T., (2004): Watershed environmental hydrology (WEHY) model, based on upscaled conservation equations: Hydrologic module. *J. Hydrol. Eng.*, 9(6), 450–464.

Kavvas, M.L., Yoon, J., Chen, Z.Q., Liang, L., Dogrul, E.C., Ohara, N., Aksoy, H., Anderson, M.L., Reuter, J., Hackley, S. (2006) “Watershed environmental hydrology model: Environmental module and its application to a California watershed”, *Journal of Hydrologic Engineering*, Vol.11, No.3, 261-272.

Kavvas, M.L., Chen Z.Q., Tan, L., Soong, S. T., Yoshitani, J., Masukura, K., Kaneki, M., Fukami, K. (2000): A Coupled Regional Hydrologic-Atmospheric Model for the Study of Hydroclimate over California”, Invited keynote paper, *Proceedings of the 4<sup>th</sup> International Conference on Hydro-Science and Engineering*, Vol. IV, Ed. By Yoon, Y.N., Jun, B.H., Seoh, B.H., Choi, G.W., Sept. 26-29, 2000, Seoul, Korea.

Kavvas, M.L., Chen, Z.Q., Ohara, N., Bin Shaaban, A.J., Amin, M.Z.M. (2007): Impact of climate change on the hydrology and water resources of Peninsular Malaysia”, In *Proceedings of International Congress on River Basin Management*, Antalya, Turkey, March 22-24.

Lustig, L.K. and Busch R.D. (1967): Sediment Transport in Cache Creek Drainage Basin in the Coast Ranges West of Sacramento, California. *Geological Survey professional paper*, 562-A.

McCuen, R.H., Rawls, W.J., and Brakensiek, D.L. (1981): “Statistical analysis of the Brooks-Corey and the Green-Ampt parameters across soil textures.” *Water Resour. Res.*, 2(4), 1005–1013.

Milly, P. C. D., et al. (2008): "Climate change - Stationarity is dead: Whither water management?" Science **319**(5863): 573-574.

Nakicenovic, N, and Swart, R. (Eds) (2000): Special Report on Emissions Scenarios: A Special Report of Working Group III of the Intergovernmental Panel on Climate Change. Cambridge University Press, Cambridge, U.K.

Ohara, N., Chen, Z.Q., Kavvas, M.L., Fukami, K., and Inomata, H. (2008): "Reconstruction of Historical Atmospheric data for Mekong River Basin by a Hydroclimate Model." World Environmental & Water Resources Congress. Honolulu, Hawaii. ASCE

Scurlock, J.M.O., Asner, G.P., and Gower, S.T (2001): "Worldwide historical estimates of Leaf Area Index, 1932-2000." Oak Ridge National Laboratory.

Superior Court of the State of California (1978): "Stipulation and consent to entry of judgment and decree." Order no.58122. County of Solano, California.

Shaaban, J.B., Chen, Z.Q., Ohara, N., and Amin, M. Z. M. (2008): Regional Modeling Of Climate Change Impact On Peninsular Malaysia Water Resources. World Environmental & Water Resources Congress. Honolulu, Hawaii. ASCE.

U.S. Army Corps of Engineers. 1987: Final General Design Memorandum No. 1, Cache Creek, California, Cache Creek Settling Basin. U.S. Army Corps of Engineers, Sacramento District. p. 3-20. January.

U.S. Army Corps of Engineers, Sacramento District. 1997: Sediment Deposition in the Cache Creek Training Channel. Memorandum for Chief, Western Region Section. Sacramento, California. March.

Wischmeier, W.H. and Smith, D.D. (1978): Predicting rainfall erosion losses – a guide to conservation planning. U.S. Department of Agriculture, Agriculture Handbook No. 537.

Yoshitani, J., Kavvas, M.L. and Chen, Z.Q. (2001): “Coupled regional-scale hydrological-atmospheric model for the study of climate impact on Japan”, In Soil-Vegetation-Atmosphere Transfer Schemes and Large-Scale Hydrological Models, Proceedings of International Symposium on S3: Soil-Vegetation-Atmosphere Transfer Schemes and Large-Scale Hydrological Models, during Sixth Scientific Assembly of the International Association of Hydrological Sciences (IAHS), 191-198

Yoshitani, J., Kavvas, M.L., and Chen, Z.Q. (2002): “Mathematical watershed models of large watershed hydrology: Chapter 7, Regional-Scale Hydroclimate Model .” Water Resources Publication, LLC.